Center for Biomedical Engineering and Physics
Medical University of Vienna

Austrian Society for Biomedical Engineering (ÖGBMT)
International FES Society (IFESS)

9th VIENNA INTERNATIONAL WORKSHOP ON FUNCTIONAL ELECTRICAL STIMULATION

Basics, Technology, Application

Krems, September 19th – 22nd, 2007

Krems Stein, Danube

PROCEEDINGS

ISBN 3-900928-08-8

Proceedings

of the

9^{th} Vienna International Workshop on Functional Electrical Stimulation

Krems/Danube, Austria
September 19^{th}-22^{nd}, 2007

Edited by

Manfred Bijak
Thomas Mandl
Johannes Martinek
Winfried Mayr
Melitta Pichler

Published by

Center for Biomedical Engineering and Physics
Medical University of Vienna, Vienna Medical School
AKH 4L
Waehringer Guertel 18-20
A-1090 Vienna
Austria

Tel.: +43-1-40400-1984
Fax: +43-1-40400-3988
http://www.fesworkshop.org

ISBN 3-900928-08-8

Contents

Keynote Lecture

Stanley Salmons

THE BENEFITS AND LIMITATIONS OF ELECTRICALLY STIMULATING MUSCLES WITH ESTABLISHED DENERVATION ATROPHY

Salmons S, Ashley Z, Sutherland H, Jarvis J

Department of Human Anatomy and Cell Biology, University of Liverpool, Liverpool L69 3GE, UK

Spinal cord injuries frequently involve damage to lower as well as upper motor neurones, and this can produce an irreversible loss of innervation in the corresponding limbs. The consequence is severe muscle atrophy and deleterious changes in bone, joints and skin. Until recently there were thought to be few therapeutic options for such patients. This position now needs to be reconsidered in the light of the finding that an intensive regime of electrical stimulation can produce marked improvements in the condition of the denervated limbs [1-3]. The clinical experience is now extensive and it raises a number of questions, to which we have sought the answers in an extensive animal-based investigation into the long-term effects of electrical stimulation in established denervation atrophy.

The success of intervention in patients depends crucially on initiating stimulation within the first twelve to eighteen months of the denervating injury. We established that the animal model of choice for this non-degenerative phase of the atrophic response was selective motor denervation in the rabbit [4]. We went on to use this model to investigate the extent to which activity induced by chronic electrical stimulation could restore the mass and contractile function of rabbit tibialis anterior (TA) muscles that had already undergone atrophy as a result of prolonged denervation.

Denervation was carried out in all animals by selectively interrupting the motor nerve branches to the ankle dorsiflexors in one hind limb. At the same time stimulators [5] were implanted, with electrodes on the superficial and deep surfaces of the denervated TA muscle. One group of rabbits was terminated 10 weeks later, at which time the mass and mid-belly cross-sectional area (CSA) of the denervated TA muscles had fallen to approximately 40% of normal. At this stage, stimulators in the other rabbits were activated for 1 hour/day to deliver 20-ms rectangular bipolar constant-current pulses of 4 mA amplitude at 20 Hz with a duty cycle of 1s ON/2s OFF, a total of 24,000 impulses/day. These animals were examined after a further 2, 6 or 10 weeks.

Stimulation restored the wet weight of the denervated muscles to values not significantly different to those of normal, innervated controls. It increased CSA from 39% to 66% of normal, with a corresponding increase in maximum isometric tetanic force from 27% to 50% of normal. Light and electron microscopic examination revealed a marked improvement in the size, packing, and internal organization of the stimulated-denervated muscle fibres. However, 10 weeks of stimulation failed to restore control levels of excitability, contractile speed, power, or fatigue resistance, and departures from normal structure remained. Similar results were found for muscles that had been denervated for 39 weeks and then stimulated for 12 weeks [6].

In a further series of experiments we examined the effect of calculated departures from the pattern of stimulation described above. Essentially we found no difference in outcome for patterns that delivered twice or twenty times the number of impulses, or the same number of impulses in two sessions per day, or the same number of impulses in 20 minutes rather than 1 hour per day (paper in preparation).

We conclude that long-term electrical stimulation does confer worthwhile benefits in the treatment of established denervation atrophy, but that these appear to stop short of a total restitution of the muscles, at least within the 10- to 12-week period of stimulation that was the maximum achievable under laboratory conditions. The increase in muscle mass has important secondary benefits for patients, which include better skin cushioning, with a reduction in the risk and severity of pressure sores, and enhanced appearance and self-esteem. If intervention is started early enough, the recovery of force generation can be sufficient to support regular short periods of standing and even walking between parallel bars. Such activity offers additional benefits: greater mobility, better blood supply to muscle and skin, improved cardiovascular fitness, and increases (at least in some cases) in bone mineral density.

Two important questions remain to be answered. First, what is the minimum amount of stimulation that will produce the observed changes in muscle mass and cross-section? Second, where there is a prospect of reinnervation, is it influenced by stimulating the denervated muscles, and if so is the eventual contractile function of the muscle better or worse?

Future efforts should focus on seeking answers to these questions, as well as continuing to develop the technology of stimulation in such a way as to make it accessible to the broadest possible cohort of patients.

Acknowledgements

This work was supported by European Commission Project "RISE", Contract Nr. QLG5-CT-2001-02191. We wish to record our warm appreciation of the contribution of other colleagues, particularly those recognized by their authorship of references [3-6] below.

References

[1] Kern H, Hofer C, Strohhofer M, Mayr W, Richter W, Stöhr H: Standing up with denervated muscles in humans using functional electrical stimulation. Artif. Org. 1999, 23, 447-452

[2] Kern H, Hofer C, Mödlin M, Forstner C, Mayr W, Richter W: Functional electrical stimulation of long-term denervated muscles in humans: clinical observations and laboratory findings. Basic Appl. Myol. 2002, 12, 293-301

[3] Kern H, Salmons S, Mayr W, Rossini K, Carraro U: Recovery of long-term denervated human muscles induced by electrical stimulation. Muscle Nerve 2005, 31, 98-101

[4] Ashley Z, Sutherland H, Lanmuller H, Russold MF, Unger E, Bijak M, Mayr W, Boncompagni S, Protasi F, Salmons S, Jarvis JC: Atrophy, but not necrosis, in rabbit skeletal muscle denervated for periods up to one year Am. J. Physiol. 2007, 292, C440-51

[5] Lanmüller H, Ashley Z, Unger E, Sutherland H, Reichel M, Russold M, Jarvis J, Mayr W, Salmons S: Implantable device for long-term electrical stimulation of denervated muscles in rabbits. Med. & Biol. Eng. & Comput. 2005, 43, 535-540

[6] Ashley Z, Salmons S, Boncompagni S, Protasi F, Russold MF, Lanmuller H, Mayr W, Sutherland H, Jarvis JC: Effects of chronic electrical stimulation on long-term denervated muscles of the rabbit hind limb. Submitted for publication, 2007

Author's Address

Prof. S. Salmons
Department of Human Anatomy and Cell Biology
The Sherrington Building
Ashton Street
University of Liverpool
Liverpool L69 3GE, UK
Email: s.salmons@liverpool.ac.uk

Session I

Denervated Muscle 1

Chairpersons
Stanley Salmons (Liverpool, UK)
Ugo Carraro (Padova, Italy)

COURSE OF DENERVATION AND EFFECTS OF ELECTRICAL STIMULATION IN LONG-TERM DENERVATED PIG MUSCLES

Weigel G[2], Bittner R[2], Mayr W[3], Unger E[3], Mickel M[1], Girsch W[1]

[1]Orthopaedic Hospital Speising, Vienna, Austria

[2]MUW, Center for Anatomy and Cell Biology, Vienna, Austria

[3]MUW, Center for Biomediacl Engineering and Phycics, Vienna, Austria

Abstract

Introduction:

An EU-Project named RISE was launched to investigate the process of long-term denervation of skeletal muscles and to investigate if Functional Electrical Stimulation (FES) can restore these muscles. The project consists of basic science, animal experiments, and clinical application in paraplegics.

Methods:

For the animal experiments we choose selective denervation of tibialis anterior muscle (TA) and extensor digitorum muscle (EDL) of the left leg as a model, trans-secting the ramus superficialis of common peroneal nerve, and keeping intact the peroneal branch responsible for the sensitivity of the foot. We applied our model to „Göttinger minipigs", weighing up to 90kg and therefore comparable with humans. Up to now 9 minipigs are under observation without complications, 5 pigs 28 months and 4 pigs 19 month after denervation procedure.

During the time course of the experiment routinely muscle biopsies were harvested and electrophysiological measurements were performed.

Results:

In TA and EDL of the pigs we noted signs of atrophy only within the first 6 months of denervation. Additionally signs of muscle degeneration occurred with increasing amount after that point, as a sign for long-term denervation,.

Discussion:

Our animal model allows to study long-term denervation of skeletal muscles in big animals for the first time. From the point of reconstructive microsurgery, especially muscle reinnervation and -transplantation it might be of great interest, that the course of denervation seems to run in two phases, first only muscle atrophy, second atrophy and degeneration. Our findings might contribute to the field of regeneration problems with long term denervated muscles..

SPONTANEOUS MYOGENESIS IN DENERVATED HUMAN MUSCLE AND FES-INDUCED MUSCLE MASS RECOVERY IN PARAPLEGICS WITH COMPLETE LOWER MOTOR NEURON LESION

Carraro U[1], Kern H[2]

[1] Translational Myology Lab, Interdepartmental Research Center of Myology, University of Padua, Italy

[2] Ludwig Boltzmann Institute, Department of Physical Medicine, Wilhelminenspital, Vienna, Austria

Abstract

In rodent long-term denervation repeated cycles of myofiber regeneration occur. We recently shown that this also takes place in humans by analyzing muscle biopsies from paraplegics submitted to a daily Functional Electrical Stimulation (FES) training. Enrolment in the EU Project RISE and follow-up of paraplegics with complete lower motor neuron lesion were performed in Wilhelminenspital, Vienna, Austria, analyses of muscle biopsies in Padova, Italy. The human long-term denervated muscle presents severe atrophy, and substitution of the muscle fibers with adipose and fibrous tissue (denervated degenerated muscle, DDM). Monoclonals against embryonic myosin show that regenerative events are present from 1- to 37-year post-spinal cord injury. In 2-year FES-trained muscles regenerative events are present, but at the same rate than in DDM. After2-year FES the muscles present larger round myofibers: the average diameter went from 15 to 27 μm, a 76% increase. We conclude that the Vienna FES-training of paraplegic muscles is safe and effective: the cosmetic and cushioning effects are granted. Supported by EU Commission Shared Cost Project RISE (Contract n. QLG5-CT-2001-02191) and Italian Ministry of University (MIUR) PRIN Project Contract n. 2004061452-002.

Introduction

Morphologic characteristics of the long-term denervated muscle in rodents suggest that some original fibers are lost and some of those seen are the result of repeated cycles of fiber regeneration [1-4]. Muscle biopsies from lower motoneuron denervated patients enrolled in the EU Project RISE show the characteristics of long-term denervation [5, 6]. From 3-5 years after complete Spinal Cord Injury (SCI) they present atrophic or severely atrophic myofibers dispersed among adipose and connective tissue (denervated degenerated muscle, DDM). Monoclonal antibody for embryonic myosin shows that regenerative events are present from 1- to 37-year post-SCI. In a pilot series of biopsies we previously showed that in 2-10 years FES-trained muscles regenerative events are present, but at a lower rate than in DDM [7].

In the EU Trial RISE the biopsies were performed in the same subjects before and after 2-year daily FES-training. In this series, morphometry of the muscle biopsies of subjects enrolled between 1 and 10 years after SCI, demonstrates that, in comparison to before-FES the after-FES biopsies show that: 1. the percentual content of regenerating myofibers remains constant; 2. the mean muscle fiber diameter display a 76% increase; 3. the increase is present in all subjects, but its clinical relevance is indirectly related to time from SCI. All together, the bioptic analyses show that conclude that the daily Vienna FES-training protocol of lower motor neuron denervated muscles in paraplegics is safe and that the cosmetic and cushioning effects are granted.

Material and Methods

Patients

The study included 28 subjects, who had experienced traumatic complete SCI, that affected the lower motor neuron pool of the thigh muscles. All subjects enrolled in the project were volunteers that had received detailed information and had signed an informed consent. Biopsies were obtained before and after a two-year daily FES treatment (five days per week). Age, sex, body weight, height, ethiology and level of spinal cord injury are reported in [8]. A detailed description of the FES training is reported in [5].

Experimental setting

Clinical and functional assessments, as well as follow-up and muscle biopsies, were performed at

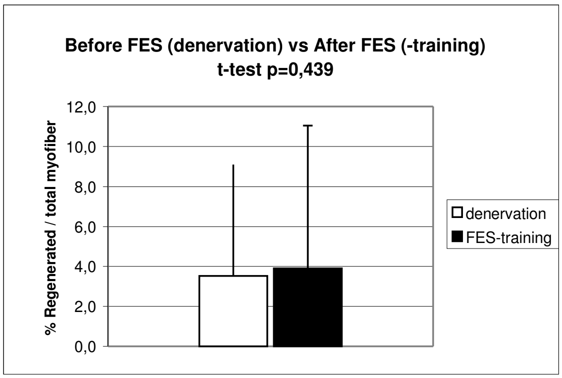

Fig. 1: EU RISE Trial: Percentual content of anti-MHCemb positive myofibers before and after FES. No changes are observed after two years of daily training.

the Wilhelminenspital, Vienna, Austria. Light microscopy on muscle biopsies were performed at the University of Padova, Italy.

Muscle Biopsy

Through a small skin incision (6 mm in diameter), needle muscle biopsies were taken from the right and left vastus lateralis muscles, as described in [5]. The resulting specimens were frozen in liquid nitrogen, overnight shipped in dry-ice to Italy and stored in liquid nitrogen until use.

Hematoxylin-eosin and morphometry

Three 10-µm-thick cryosections were collected on glass slides and stained with Hematoxilin and Eosin (H&E) using conventional techniques. Images were acquired using a Zeiss microscope connected to a Leica DC 300F camera at low magnification, under the same conditions that were used to photograph a reference ruler. The minimum transverse diameter of each muscle fiber was measured against the reference ruler. Morphometric analysis was performed with Scion Image for Windows version Beta 4.0.2 (2000 Scion Corporation), free software downloaded from the web site: www.scioncorp.com. Tissue type distribution (relative content of interstitial tissue and cumulative muscle fiber areas) was determined using the Adobe Photoshop software (Adobe Systems Incorporated, San Jose, CA). The details of fiber typing and morphometry are reported in [6].

Immunohistochemistry

Cryo-sections were labeled with antibodies: 1. anti-MHC-emb (from Novocastra, NCL-MHCd); 2. anti-dystrophin (C-terminus) (from Novocastra, NCL-DYS2); 3. anti-dystrophin (N-terminus) (from Novocastra, NCL-DYS3); 4. anti-NCAM (from Chemicon International); 5. anti-laminin (from Sigma), as described in [9-11].

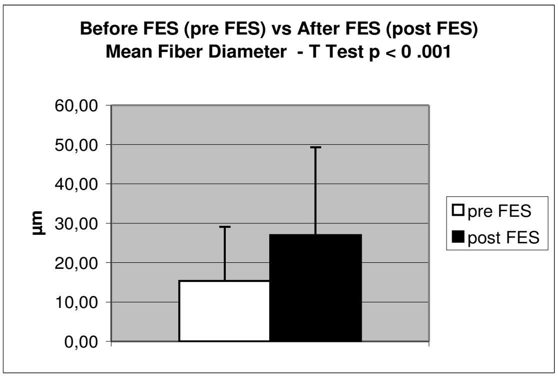

Fig.2: EU RISE Trial: Mean Fiber diameter before and after FES. Myofiber size change (76% increase) 2-year after FES-training is highly significant.

Results

No significant changes were observed after 2-year FES-training in the percentual content of anti-MHCemb positive myofibers (regenerating myofibers) in comparison to the before-FES results (Figure 1).

On the other hand, Figure 2 shows a highly significant increase of the myofiber size, that went from 15.4 (before-FES, empty bar) to 27.0, a 76% increase after 2-year daily FES (black bar).

In comparison to before-FES (blue symbols), all the biopsies presented larger myofibers after 2-year FES (red symbols), but the absolute values are in the range of normal adult muscle mainly in the subjects, who started FES two-three years after SCI (Figure 3).

The effects of 2-year FES-training on some immuno-histochemical characteristics of the *vastus l.* muscle is displayed in the exemplar case reported in Figure 4.

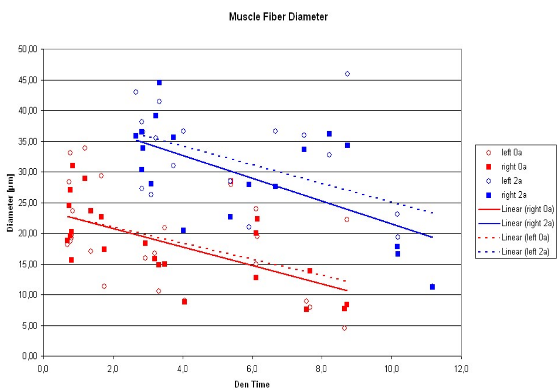

Fig.3: EU RISE Trial: Mean fiber diameter before (red symbols) and after (blue symbols) FES. Though all the subjects present larger myofibers after 2-year FES, the

absolute values are in, or near normal range mainly in the groups of subject, who started FES two-three years after SCI.

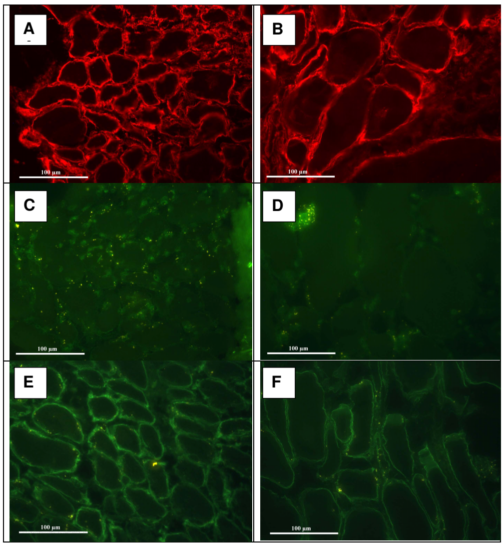

Fig.4: EU RISE Trial: Vastus lateralis muscle cryosections from a RISE patient, which started FES one-year after SCI (A, C, E) and trained for additional two years (B, D, F). A and B, anti-laminin stain; C and D, anti-dystrophin (C terminus); E and F, anti-dystrophin (N terminus). The absence of anti-dystrophin (C terminus) stain demonstrate that in spite of their large size the myofibers are denervated. Notice that the diameter of the myofibers increased to almost normal values (50 µm).

The RISE subject started FES one-year after SCI (A, C, E) and daily trained for additional two years (B, D, F). Notice that the diameter of the myofibers increased to almost normal values (50 µm).

Discussion

Functional electrical stimulation of human skeletal muscle is performed by surface electrodes, by transcutaneous needle electrodes or by epimisial or epineural implanted electrodes. Human lower motoneuron denervated muscles, from several months after SCI, are only activated by very large surface electrodes and very high currents. In spite of these difficulties, the Vienna protocol of therapeutic FES for human DDM paraplegia is achieving clinical acceptance on the grounds of sound experimental evidence [5-8, and present results]. Here we have reported that the muscle biopsies harvested two years after daily FES-training present myofibers larger than those in the biopsies collected before FES in the same subjects. Extent of changes correlated to time of SCI before training, strongly suggests an early starting of the therapeutic FES daily training. Both structural microscopic (here) and macroscopic (CT scan morphometry, in this Proceedings) analyses show much better results when the FES training starts earlier than 3-year from SCI.

In Fig. 4, panels A and B, the anti-laminin stain and the panels E and F, anti-dystrophin (N terminus) clearly show that the muscle fibers size had almost doubled. The absence of myofiber profiles in the muscle cryosections treated with anti-dystrophin (C terminus) antibodies demonstrates that in the before-FES biopsy, in spite of their relatively large size, the myofibers were denervated (they had lost the contact with the lower motor neuron) and that they were not reinnervated during the following two years of FES training(panels C and D of Figure 4). These results support other evidence of complete permanent denervation of the muscle fiber in the series of biopsies of the EU Trial RISE based on their ultrastructural features and on NCAM cytoplasmic expression ([11], and manuscript in preparation).

All together, the microscopic analyses here reported demonstrate that the daily Vienna FES-training protocol of lower motor neuron denervated muscles in paraplegics is safe and that the cosmetic and cushioning effects are granted.

References

[1] Carraro U, Morale D, Mussini I, Lucke S, Cantini M, Betto R, Catani C, Dalla Libera L, Danieli-Betto D, Noventa D. Chronic denervation of rat diaphragm: maintenance of fiber heterogeneity with associated increasing uniformity of myosin isoforms. J Cell Biol 100:161-174, 1985.

[2] Mussini I, Favaro G, Carraro U. Maturation, dystrophic changes and the continuous production of fibers in skeletal muscle regenerating in the absence of nerve. J Neurophatol Exp Neurol 46:315-33, 1987.

[3] Carraro U. Modulation of trophism and fiber type expression of denervated muscle by different patterns of electrical stimulation. Basic Appl Myol 12:263-272, 2002.

[4] Carlson BM, Borisov AB, Dedkov EI, Dow D, Kostrominova TY. The biology and restorative capacity of long-term denervated skeletal muscle. Basic Appl Myol 12:247-254, 2002.

[5] Kern H, Boncompagni S, Rossini K, et al. Long-term denervation in humans causes degeneration of both contractile and excitation-contraction coupling apparatus that can be reversed by functional electrical stimulation (FES). A role for myofiber regeneration? J Neuropath Exp Neurol 63:919-931, 2004.

[6] Kern H, Rossini K, Carraro U, Mayr W, Vogelauer M, Hoellwarth U, Hofer C. Muscle biopsies show that FES of denervated muscles reverses human muscle degeneration from permanent spinal motoneuron lesion. J Rehabil Res Dev 42:43-53, 2005.

[7] Carraro U, Rossini K, Mayr W, Kern H. Muscle fiber regeneration in human permanent lower motoneuron denervation: relevance to safety and effectiveness of FES-training, which induces muscle recovery in SCI subjects. Artif Organs 29:187-191, 2005.

[8] Modlin M, Forstner C, Hofer C, et al. Electrical Stimulation of Denervated Muscles: First Results of a Clinical Study Artificial Organs 29:203–206, 2005.

[9] Rossini K, Zanin ME, Podhorska-Okolow M, Carraro U. To stage and quantify regenerative myogenesis in human long-term permanent denervated muscle. Basic Appl Myol 12:277-286, 2002.

[10] Biral D, Jakubiec-Puka A, Ciechomska I, et al. Loss of dystrophin and some dystrophin-associated proteins with concomitant signs of apoptosis in rat leg muscle overworked in extension. Acta Neuropathol (Berl) 100:618-626, 2000.

[11] Rossini K, Biral D, Carraro U, Mayr W, Kern H. N-CAM and isomyosins of long-term denervated human muscle. Basic Appl Myol, in press.

Acknowledgements

This research was undertaken with the financial support of 1. Italian Ministry of Education (MURST) under the framework of PRIN Projects (PRIN 2004-2006 Program, Contract n. 2004061452-002); 2. The Italian C.N.R. funds and the Italian MURST funds (ex60%) to Ugo Carraro. This work was also supported by Research Funds from the Ludwig Boltzmann Institute for Electrostimulation and Physical Rehabilitation at the Institute of Physical Medicine and Rehabilitation (Wilhelminenspital, Vienna, Austria).

Author’s Address

Ugo Carraro
Translational Myology Lab, Interdepartmental Research Center of Myology, c/o Department of Experimental Biomedical Sciences, University of Padua, Viale G. Colombo 3, I-35122 Padova, Italy
eSkype: ugo.carraro

eMail: ugo.carraro@unipd.it

homepage: http://www.bio.unipd.it/bam/bam.html

ATROPHY AND DEGENERATION OF LONG-TERM DENERVATED HUMAN SKELETAL MUSCLE IS REVERSIBLE

Boncompagni S[1], Kern H[2], Rossini K[3], Hofer C[2], Mayr W[3], Carraro U[4], and Protasi F[1] .

[1]IIM - Interuniversitary Institute of Miology, CeSI - Center for Research on Ageing, University *G. d'Annunzio*, I-66013 Chieti, Italy.

[2]Ludwig Boltzmann Institute of Electrostimulation and Physical Rehabilitation, Department of Physical Medicine, Wilhelminenspital, A-1171 Vienna, Austria.

[3]Department of Biomedical Engineering and Physics, University of Vienna. A-1171 Vienna, Austria.

[4]C.N.R. Institute of Neuroscience, Laboratory of Applied Myology of the Department of Biomedical Science, University of Padova Medical School, I-35121 Padova, Italy.

Abstract

It is generally accepted that severe muscle atrophy as a result of a long-standing denervation injury (> 1 year) is irreversible in humans and thus no effective treatment has been available for patients that suffer from permanent denervation. Contrary to this belief, an innovative rehabilitation protocol of functional electrical stimulation (FES) has proven effective in reversing muscle atrophy in the lower extremities of spinal cord injury (SCI) patients with complete lesions of the *conus cauda*. FES treatment induced surprising recovery of muscle mass and force in the patients that could be effectively stimulated, even after prolonged denervation (up to 2 years). Here we report on the ultrastructural changes that accompany such recovery, in muscle biopsies (*vastus lateralis*) from patients treated with FES. These studies demonstrate that long-term denervated muscle can be rescued and/or maintained if appropriately stimulated, and may be of great importance for the rehabilitation and the general health of SCI patients.

Introduction

A still open question, which is especially important for the treatment of SCI patients, is whether or not muscle wasting caused by prolonged periods of denervation can be reversed in the absence of nerves. Functional electrical stimulation (FES) is currently used in the treatment of several patients affected by peripheral nerve damage, incomplete SCI, and when muscle of the extremities are still connected to motor neurons (1, 2). However, the clinical applications of FES is not effective in promoting muscle activity in patients that have lost their peripheral nerves and/or in rescuing muscle fibers that have undergone severe atrophy as a result of a long-standing complete denervation (3, 4). Because of this, paraplegic patients affected by complete lesion of the *conus cauda*, i.e. lacking any peripheral nerve endings in the lower extremities, usually do not receive any specific muscle treatment. Complete inactivity of muscle results in severe secondary complications caused the poor blood supply to the denervated areas (osteoporosis, pressure sores, decubital ulcers, etc.), and in several cases the life expectancy of these patients is shorter than normal (5, 6).

Recently, an innovative rehabilitation procedure based on functional electrical stimulation (FES) and specifically designed stimulators has been developed (7-10) with the specific aim of reversing muscle atrophy in paraplegic patients affected by complete lesion of the *conus cauda*. Experimental and clinical results show that muscle mass and function are substantially restored by this treatment. Unique human muscle biopsies from 5 FES treated patients who were trained for prolonged periods of time (2.4 to 9.3 years), gave us the great opportunity of studying recovery of fibers from severe atrophy and degeneration (up to 2 years of denervation) under the sole influence of muscle activity induced by external electrical stimulation. In the present work we report on the striking structural recovery, which interestingly follows a pattern mimicking in many aspects normal embryonal and postnatal muscle differentiation.

Material and Methods

Patients' characteristics and stimulation parameters. The 10 subjects (all males) had experienced complete traumatic *conus cauda* lesion and functional testing was performed as in Modlin et al., 2005. Details of the FES regimen are published elsewhere. (7-10).

Electron microscopy (EM). Needle muscle biopsies (0.5-1 mm diameter, 1-1,5 mm long, 2-5 mg) were harvested from both right and left *vastus lateralis* muscles at a single time point for each patient. Samples for electron microscopy were prepared and sectioned as in Boncompagni et al., 2006 (11). Sections were examined with a FP 505 Morgagni Series 268D electron microscope (Philips), equipped with Megaview III digital camera and Soft Imaging System (Germany).

Results

In electron micrographs, severely atrophic muscle fibers are identifiable based on recognizable remnants of contractile material and cell organelles, even though quite disarranged (Fig. 1).

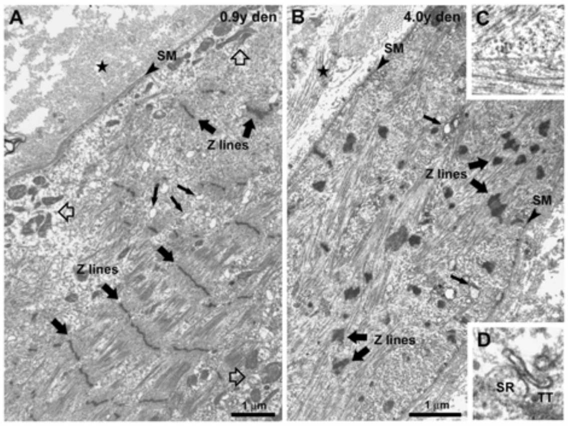

Figure 1. Effects of long-term denervation on skeletal fibers ultrastructure. A and B) Disarrangement of the internal structure of fibers starts from the periphery and results in severe atrophy and complete disruption of the internal organization. C and D) Two insets showing respectively an area with misoriented contractile filaments and an abnormal junction between a T-tubule and the SR. Empty arrows: mitochondria grouping; SM: surface membrane; small arrows: vesicled SR; stars: extracellular space.

The remaining myofibrils are reduced in size and usually discontinuous and/or completely missing from extended areas. Sarcomeres are often altered, with missing M lines and widened and/or streaming Z lines, a feature common to a wide variety of muscle diseases (12). The widened intermyofibrillar spaces contain an amorphous cytoskeletal network with scarce mitochondria, often found grouped in an abnormal fashion (Fig. 1A). The sarcoplasmic reticulum (SR) is incomplete and vacuolated, and transverse (T) tubules are hardly recognizable. Some T-tubule-like profiles are associated with elements of the SR to form triads or dyads, which are however misshapen (Fig. 1D). At shorter times of denervation, when some partial structure remains, the disorganization is always more severe in the subsarcolemmal region, suggesting that the degeneration of the contractile apparatus starts from the fiber periphery and proceeds toward the interior (Fig. 1A).

On the other hand, in muscle fibers from FES trained patients, cross striation covers the large majority of fiber area visible in the thin section. Myofibrils are quite well aligned with one another (Fig. 2A) and the hexagonal pattern of thin and thick filaments in cross section indicates a reorganization of the contractile proteins at the sarcomeric level (Fig. 2B).

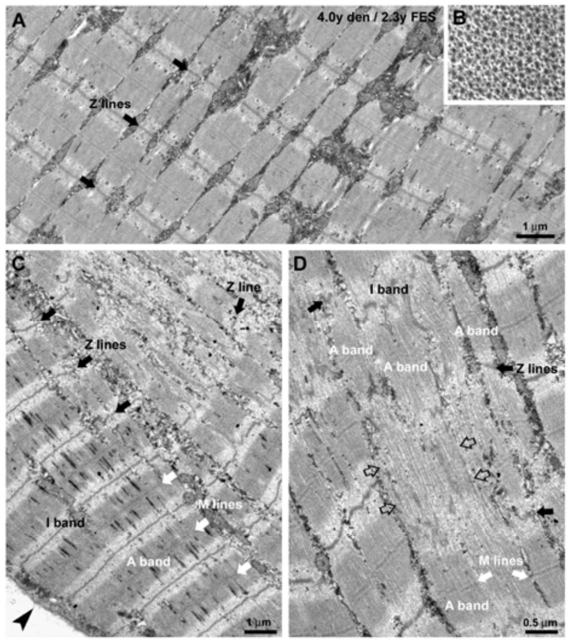

Figure 2. FES-induced ultrastructural restoration of myofibrils. A and B) Restoration of the myofibrils results in a transversal dark-pale striation (panel A) and, in cross sections, in a regular hexagonal pattern of thick and thin filaments (panel B). C) FES-induced restoration of the contractile apparatus usually starts at the fiber periphery (arrowhead, lower left corner). D) The formation of nascent myofibrils (empty arrows) resembles that of normal embryonal differentiation. Arrowhead: surface membrane; black arrow: Z lines; empty arrows: aligned myofilaments, which are not yet assembled into sarcomeres; white arrows: M lines.

Myofibril restoration is not always uniform throughout the cross section: in some fibers peripherally located reorganized regions co-exist with central areas in which myofibrils are not completely re-assembled (Fig. 2, C and D). The transition between more and less organized areas may be fairly abrupt in some areas and more gradual in others (Fig. 2C).

In *partially recovered* fibers (Fig. 2C), the presence of internal regions in which myofibrils are not fully re-organized may help to identify some of the possible steps that lead to restoration of the contractile apparatus. We know that the diameter of muscle fibers increases significantly as a result of FES (9). In addition, regions that are not completely restored are usually located in the fibers interior. These two observations taken together suggest that FES-induced restoration of the contractile apparatus likely starts from the fiber periphery and possibly proceeds towards the interior as the fibers grow in size. Furthermore, observing areas in which myofibrils are not completely restored, we may also try to outline possible steps in the reconstruction of myofibrils. Initially, thick filaments are parallel, but are not well aligned so that the edges of the A band are not well defined (Fig. 2D). In these early stages, the M lines are missing, and Z lines go through an intermediate *Z body* stage before fusing into the mature extended Z line, as in normal myofibril differentiation (13). An increase in the order of thin and thick filaments, appearance of an M line and better defined Z lines, which tend to align transversely, complete the assembly of the mature sarcomere (Fig. 2D). Interestingly, this reorganization of sarcomeres mimics the same general outline of myofibrillogenesis in myotubes (14).

Discussion

This study gave us a unique opportunity to gain additional understanding of the relationship between muscle activity in the complete absence of nerve input and differentiation/maintenance of muscle structure and function. Although it has long been known that activity influences significantly muscle properties (15-17), we believe that the results presented in this manuscript makes some important original contributions to the field.

Most importantly, the effects of long-term stimulation on severely atrophic muscles are largely unexpected: FES-induced activity can reverse muscle atrophy even after very long-lasting denervation/inactivity, when severe degenerative changes of muscle fibres have taken place. In fact, from the structural point of view, muscles from FES treated patients achieve an almost complete adult differentiation (Fig. 2), despite an extremely poor starting point due to long-lasting denervation (Fig. 1). These results are of interest both from a basic biological perspective, since this recovery occurs in the total absence of any neural trophic influence and, thus, presumably is due exclusively to activity. In addition they may be of importance from a clinical point of view, since in the field of muscle paralysis, the poor recovery of muscle tissue, which has been denervated for prolonged periods of time, has been a longstanding problem (3, 4).

An important open question is whether the structural rescue is due to: a) a *de novo* formation of fibers mediated by satellite cells; or to b) re-activation of the myogenic program in the existing severely atrophic fibers. Whether, and to what extent, in our samples satellite cells contribute to the rescuing of degenerating fibers could not be directly established in this study due to limitation in bioptic material. However, we do know from our previous studies in similar patients that *de novo* formation of fibers occurs at an extremely low rate after prolonged denervation (9). This is consistent with other scientific reports showing a drastic reduction of satellite cells number and activity after prolonged denervation (18). In addition, the presence of fibers that show a regenerating periphery together with an atrophic core (Fig. 2C), would argue in favor of the hypothesis b, i.e. the potential for recovery is an intrinsic property of the muscle fibres and suggest that FES is restoring muscle structure and function in the pre-existing and severely atrophic fibers. One other very important observation arising from the results presented in this manuscript is that the mechanisms by which the ultra-structure of myofibrils is rescued recapitulates in many aspects the normal process of fiber development/ differentiation, both in the apparent spread of events from the periphery to the center of the fiber and in various intermediate stages that lead to final organization of different apparatuses. The periphery-to-center differentiation gradient, the fusion of Z bodies into Z bands, the gradual alignment of myosin filaments into A bands are all steps that have been described in normal fiber differentiation in animal models *in vivo* and *in vitro* (13, 14).

The effectiveness of direct electrical stimulation in inducing muscle recovery in completely denervated extremities could represent a significant step forward in the treatment of SCI patients affected by complete lesions of the spinal cord (i.e. missing peripheral nerves). In fact, patients with this type of lesions usually do not receive any specific treatment of the denervated extremities. Complete inactivity and immobilization of the limbs causes poor blood supply to the denervated areas and a series of secondary complications (osteoporosis, pressure sores, decubital ulcers, etc.), which finally determines a decreases in their life expectancy (5, 6). Restoration of muscle function and mass is very encouraging for the patients and, with years of training, in 4 of the 5 patients included in the present study muscle function of the lower extremities was restored sufficiently to allow for supported standing up, standing, and even for a few steps to be taken. In addition, the beneficial effect of this daily training for the patients is not only limited, though, to the restoration of muscle mass: in fact, also blood circulation, skin and bone density is being closely monitored and several parameters showed a significantly improvement (results from these studies are currently being collected for publication). Moreover, all the patients reported beneficial psychological effect of being able to stand even for few seconds under stimulation.

FES treatment (1, 2) is currently not used in the standard treatment of patients which completely lack peripheral innervation, such as the ones studied in the present report. This is because of two main reasons: conventional FES devices delivers small currents which are unable to elicit muscle contraction in absence of nerve endings; current regulations do not allow the use the stimulation intensities employed in the present study. The studies presented in this work represented a unique opportunity offered by a European Union framework (see acknowledgments section), which allowed the development of new FES devices (7, 8) and the enrolment of SCI patients in this trial. The aim in the long-term is to extend FES treatment to all patients lacking peripheral innervation, with the main goal of avoiding secondary problems caused by prolonged inactivity (see above), improve the patients' quality of life, and possibly their life expectancy.

References

[1] Graupe, D. (2002) *Neurol. Res.* **24**, 431-442.

[2] Creasey, G. H., Ho, C. H., Triolo, R. J., Gater, D. R., DiMarco, A. F., Bogie, K. M. & Keith, M. W. (2004) *J. Spinal Cord Med.* **27**, 365-375.

[3] Bateman, J. E. (1962) in *Trauma to Nerves in Limbs*, Saunders, Philadelphia.

[4] Sunderland, S. (1978) in *Nerve and Nerve Injuries* (second edition), Churchill-Livingston, Edinburgh.

[5] DeVivo, M. J., Krause, J. S., & Lammertse, D. P. (1999) *Arch. Phys. Med. Rehabil.* **80,** 1411-1419.

[6] Strauss, D. J., Devivo, M. J., Paculdo, D. R., & Shavelle, R. M. (2006) *Arch. Phys. Med. Rehabil.* **87,** 1079-1085.

[7] Mayr, W., Bijak, M., Rafolt, D., Sauermann, S., Unger, E. & Lanmuller, H. (2001) *Med. Eng. Phys.* **23**, 53-60.

[8] Hofer, C., Mayr, W., Stohr, H., Unger, E. & Kern, H. (2002) *Artif. Organs.* **26**, 276-279.

[9] Kern, H., Boncompagni, S., Rossini, K., Mayr, W., Fanò, G., Zanin, M. E., Podhorska-Okolow, M., Protasi, F. & Carraro, U. (2004) *J. Neuropathol. Exp. Neurol.* **63**, 919-931.

[10] Modlin, M., Forstner, C., Hofer, C., Mayr, W., Richter, W., Carraro, U., Protasi, F. & Kern, H. (2005) *Artif. Organs.* **29**, 203-206.

[11] Boncompagni, S., d'Amelio, L., Fulle, S., Fanò, G., & Protasi, F. (2006) *J. Gerontol. Biol. Sci.* **61**, 995-1008.

[12] Engel, A. G. & Banker, B. Q. T. (2004) in *Myology (third edition)*, Engel A. G. & Franzini-Armstrong C., Eds., McGraw-Hill Med. Publish. Div., vol. **1**, chap. 31, pp. 749-887.

[13] Dabiri, G. A., Turnacioglu, K. K., Sanger J. M., & Sanger, J.W. (1997) *Proc. Natl. Acad. Sci. USA.* **94**, 9493-9498.

[14] Engel, W. K. & Horvath, B. (1960) *J. Exp. Zool.* **144**, 209.

[15] Salmons, S. & and Vrbova, G. (1969) *J. Physiol.* **201,** 535-549.

[16] Pette, D., Smith, M. E., Staudte, H. W., Vrbova, G. (1973) *Pflugher Arch*. **338,** 257-272.

[17] Lomo, T., & Westgaard, R. H. (1974) *Proc R. Soc. Lond. B.* **187,** 99-103.

[18] Dedkov, E. I., Kostrominova, T. Y., Borisov, A. B. & Carlson, B. M. (2001) *Anat. Rec.* **263**, 139-154.

Acknowledgements

We thank all the staff working in laboratories of Drs. H. Kern, W. Mayr, and U. Carraro, which with many years of dedicated work allowed the collection of these samples. This study was supported by: a) European Union Commission Shared Cost Project RISE (Contract n.QLG5-CT-2001-02191); b) Research Funds from the Ludwig Boltzmann Institute of Electrostimulation and Physical Rehabilitation at the *Institute for Physical Medicine and Rehabilitation* (Wilhelminenspital, Vienna, Austria); c) Research Funds from the Faculty of Sport Medicine to Feliciano Protasi; and d) Research Grant # GGP030289 from the Italian Telethon Foundation to Feliciano Protasi.

Author's Address

Feliciano Protasi
CeSI, Center of Research on Ageing
Università G. d'Annunzio of Chieti
Chieti, CH I-66013
Tel.: + 39 0871 541423
FAX: + 39 0871 541 423
E-mail: fprotasi@ unich.it
Homepage:
http://www.bams.unich.it/personale/protasi.html

IN VIVO FUNCTIONAL ELECTRICAL STIMULATION OF FELINE LATERAL RECTUS: RELATIONSHIP BETWEEN STIMULATION PARAMETERS AND EYE ROTATION IN DENERVATED MUSCLE

Isobe J[1], Velez F[2], Lee H[1], Patnode S[1], Judy J[1,3], Rosenbaum A[2]

[1] Biomedical Engineering IDP, University of California, Los Angeles, USA

[2] Jules Stein Eye Institute, Department of Ophthalmology, University of California, Los Angeles, USA

[3] Department of Electrical Engineering, University of California, Los Angeles, USA

Abstract

Complete sixth-nerve palsy results in esotropia and limits abduction of the affected eye. Existing treatments include extraocular vertical-rectus-muscle transposition in combination with weakening the medial-rectus (MR) muscle. However, this approach results in limited recovery of abduction and many patients require several surgical procedures to reach alignment in the primary position. It has been shown that direct electrical stimulation of denervated striate muscles can produce enough contraction to restore function. Our goal was to investigate the feasibility of functionally electrically stimulating the lateral-rectus (LR) muscle to recover more of its physiologic abduction ability.

A stimulator applied charge-balanced, biphasic, current-controlled stimulus varying frequency, amplitude, and cathodic pulse duration in the feline LR-muscle model. Denervated conditions were simulated by injection of botulinum toxin A (Botox). Minimum fusing frequency of the LR occurred at approximately 175 Hz. Although stimulation frequencies below 150 Hz were able to modulate eye rotation, higher frequencies produced very little gain in eye rotation. Current amplitude produced noticeable rotation throughout the tested range (0.2 to 9 mA). In the feline LR muscle, varying amplitude allowed greater eye rotation.

Introduction

Strabismus is the loss of bilateral eye alignment due to muscle paralysis, and can occur unilaterally or bilaterally. Strabismus affects approximately 2 to 4% of the population in the United States [1-3]. Causes of strabismus are many, some of which include congenital nerve miswirings, nerve injuries, and lesions on nerves.

The correction of strabismus is one of the most frequently-performed ophthalmic surgical procedures. Existing treatments for moderate to severe cases include extraocular vertical-rectus-muscle transposition in combination with weakening the medial-rectus (MR) muscle. However, this approach results in limited recovery of abduction and many patients require several surgical procedures to reach alignment in the primary position. We propose the use of direct-muscle functional electrical stimulation (FES) with a closed-loop control as an alternative solution to restore more physiologic eye-rotation ability.

Functional electrical stimulation (FES) has long been proposed as a potential treatment for restoring motor function of denervated motor systems such as those in paraplegia. Recent success has been noted in the ability of FES to allow paraplegics to gain the ability to stand [4]. The effectiveness of coordinating pairs of muscles using FES was proven in clinical research. Zealear *et al.* [5, 6] described a paced muscle stimulation where FES was applied to a laryngeal muscle (posterior cricoarytenoid) via input signals from its contralateral partner to help patients breathe, the feasibility of which has since been demonstrated in humans [7]. This approach can be modified to accommodate antagonistic muscle pairs such as those in the extraocular muscle system.

Extraocular muscles differ from other skeletal muscles in the body in many ways, some of which include the presence of multiply-innervated muscle-fibers, absence of muscle spindles, and high mitochondrial content [8-10]. Dmitrova *et al.* has conducted nerve stimulations of chemically-denervated LR muscles in cats [11]. We aim to demonstrate the feasibility to evoke adequate contractions from chemically-denervated LR muscles using direct-muscle FES.

For our investigation, we focused on patients with sixth-nerve palsy who have non-functioning LR muscles. In the study presented here, we characterized a chemically-denervated LR muscle's response to varying FES parameters. Our ultimate goal is to electrically excite the LR muscle to improve ocular alignment and enable horizontal pursuit movements using antagonist muscle activity in a closed-loop system.

Material and Methods

Surgical Preparation:

All procedures and protocols fulfilled human and animal research protection regulations of the University of California, Los Angeles. Two cats (Cat 4 and 5) were used in our chemically-denervated LR experiments. Surgery was performed under general anesthesia. Both eyes were prepped and draped for sterile ophthalmic surgery. An eyelid speculum was inserted. A limbal conjunctival incision was made next to the LR muscle. Five units of botulinum toxin A (Botox) was injected into each LR muscle using visual confirmation. The incision was sutured and closed. After waiting 4 weeks to allow time for degradation of the neuromuscular junction, another surgery was performed under general anesthesia. A limbal conjunctival incision was made next to the LR muscle. The incision was extended with two radial incisions. The LR muscle was exposed. A muscle hook was placed under the LR muscle. The LR muscle was cleaned from surrounding connective tissue. The lateral orbital wall was removed.

Stimulation and Data Recording

An automated protocol was developed in LabView 7.0 (National Instruments Corp., Austin, TX) to study LR response to various parameters of a biphasic pulse (Fig. 1). There were seven adjustable parameters: frequency [Hz], current amplitude [mA], cathodic pulse duration [msec], anodic amplitude [% cathodic amplitude], burst length [sec], rest between bursts [sec], and total stimulation time [sec]. The program automatically applied and delivered preset series of stimuli in a stimulation protocol. The parameters in the stimulation protocol were randomized to reduce the effect of statistical artefacts in muscle force readings from previous movements.

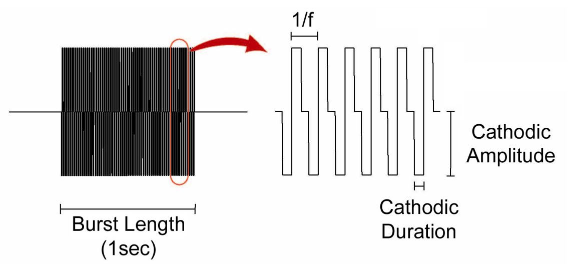

Fig. 1: Stimulus waveform. A biphasic waveform was used in our experiments to minimize fatigue and electrolyte diffusion.

A power supply (Hewlett-Packard 6205C, Palo Alto, CA) was used to supply ±38 V Direct Current (VDC) of input to the muscle stimulation circuit. This electrical current was controlled by the LabView software program running from a desktop computer with the following attributes: AMD Athlon 64 processor 3000+MMX (AMD Corp., Sunnyvale, CA), 1.8 GHz, 1024 MB RAM. This computer also served as the data acquisition system (DAQ).

The setup shown in Fig. 2 was constructed for stimulation and recording of feline LR muscle activity.

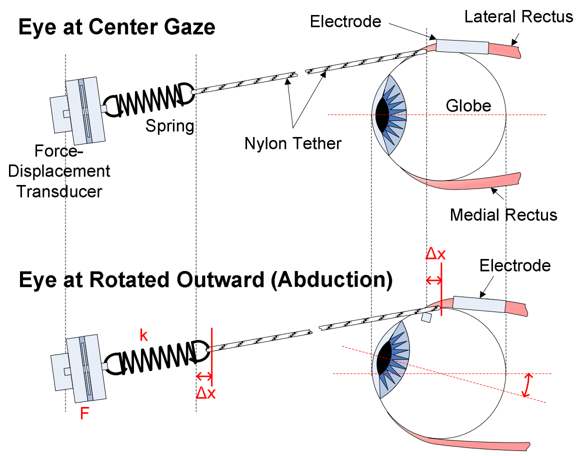

Fig. 2: Cat lateral rectus (LR) muscle force-recording setup. Eye movement was detected using a force transducer and spring with a known spring constant in series. A video camera also captured the movements against a ruler.

A force-displacement transducer (Grass Telefactor model FT03, W. Warwick, RI) was used in series with a spring (0.3 g/cm, Grass Telefactor, W. Warwick, RI) to measure the approximate isotonic forces generated by the stimulated LR. The force transducer (FT) was powered by a Vishay Measurements Group (Raleigh, NC), model 2160 power supply. Arclength displacement measurements were inferred using Hooke's Law. The FT measurement was compared against the physical displacement seen against a reference ruler on the recorded video camera image (JVC Everio GZ-MG21U, Yokohama, Japan).

Epimysial electrodes with a sleeve design (Fig. 3) were constructed from multi-stranded stainless steel Cooner wire (part no. AS633, Chatsworth, CA) stitched into Duralastic® silicone mesh material (Applied Biomaterial Technologies Corp 601-10, Silverdale, WA). The electrode was placed and sutured around the lateral rectus muscle posterior to the scleral insertion. The electrode was characterized using an impedance analyzer.

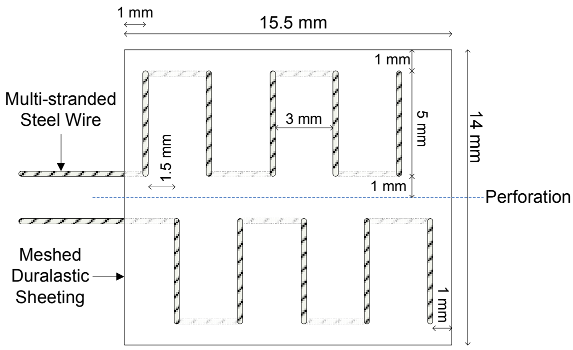

Fig. 3: The sleeve electrode design. In a trade study of different electrode configurations, this design offered the greatest and most stable force response from the stimulated muscle.

Results

Fig. 4 shows a comparison of two typical time-course plots obtained from the experiment. Stimulus was applied for 1 second between seconds 1 and 2. Each experimental run lasted at least 10 seconds. Higher frequencies produced more eye deflection; however, frequencies below 175 Hz did not produce a fused tetanus.

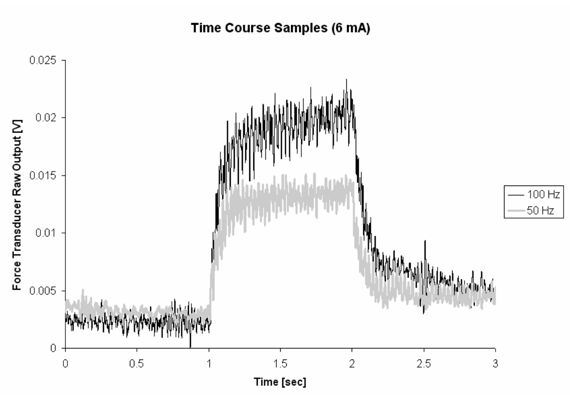

Fig. 4: Sample time-course plots of feline LR stimulation experiment (Cat 5). Plot shows 100 Hz and 50 Hz cases both at 6 mA: Force transducer raw output [V] vs. time [sec]. The higher frequencies produce more eye deflection, however, frequencies below 175 Hz produced unfused tetani.

Varying the asymmetry in the biphasic pulse showed no discernable trend in eye deflections (Fig. 5).

The combined data from Cat 4 is shown in Fig. 6. These plots were obtained by averaging the LR force measurement during the time stimulus was applied to the muscle. The same experiment was repeated for Cat 5 resulting in Fig. 7.

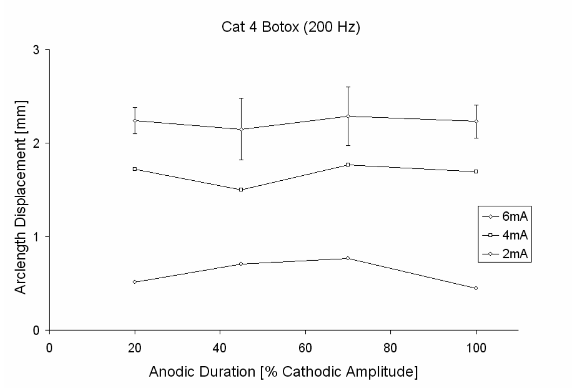

Fig. 5: Effect of asymmetry in the biphasic stimulation pulse in feline LR injected with Botox. Decreasing % cathodic amplitude (%CA) values signified increasing asymmetry in the biphasic pulse. For example, 100%CA yielded a symmetric biphasic pulse, whereas 50%CA had an ananodic phase of half the amplitude of the cathodic phase but twice the duration to maintain charge balance. There was no discernable trend in varying this parameter.

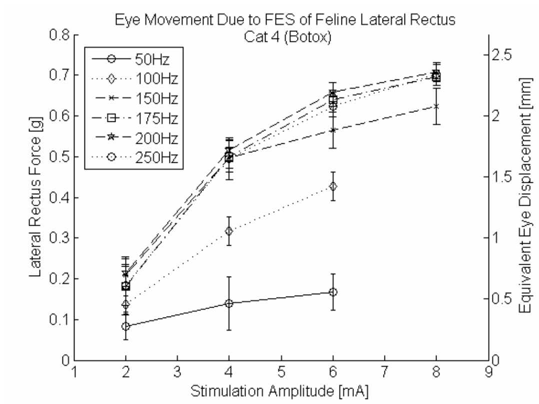

Fig. 6: Denervated feline lateral rectus (LR) response to FES (Cat 4, amplitude plot). Data was obtained 4 weeks subsequent to Botox injection to allow for neuromuscular junciton degradation.

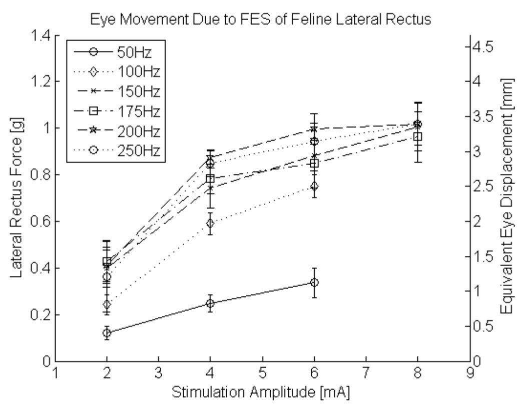

Fig. 7: Denervated Feline lateral rectus (LR) response to FES (Cat 5, amplitude plot). Variation in LR response between cats was noticed when comparing these plots.

Discussion and Conclusions

In our experiments, we have demonstrated the use of FES in evoking eye movements from feline LR artificially denervated by Botox injection.

Stimulation frequency and amplitude were the only parameters with statistically significant effects on evoked eye deflection. However, since frequencies below approximately 175 Hz did not produce a fused tetanus in normal feline LR (unpublished results), we conclude that varying stimulation amplitude will be the most effective way to control eye position using FES.

There was some variation in evoked forces between Cat 4 and Cat 5. This may be attributed to slight differences in the amount of tissue cleared from the LR, the way Botox was injected, or the penetration of Botox into the tissue. Also, individual subjects may naturally respond differently to Botox injection as seen in human patients in clinical practice.

Finally, we allowed a time of 4 weeks in our protocol for degradation of the neuromuscular junction. This length of time was chosen to allow a comparison between surgically-denervated muscle and chemically-denervated muscle in cases where denervation was more chronic. Although 4 weeks was well within the effective period of Botox in primates [12], Moreno-Lopez *et al.* [13] has shown at a lower Botox dose that feline LR is almost fully recovered from the effects of Botox by that time. There is a need to conduct more denervated feline LR experiments 1 to 2 weeks after Botox injection to validate the feasibility of this technology on denervated muscle.

Characterizing the LR muscle's response to direct-muscle FES was an important first step in our ultimate goal of developing a closed-loop system to improve ocular alignment and enable horizontal pursuit movements using antagonist muscle activity.

References

[1] NEI Congressional Justification FY2008, 2007.
[2] Hillis A, Flynn JT, Hawkins BS. The evolving concept of amblyopia: a challenge to epidimiologists. Am J Epidemiol, 118: 192-205, 1983.
[3] Preslan MW, Novak A. Baltimore Vision Screening Project. Ophthalmology, 103: 105-109, 1996.
[4] Kern, Hofer, Strohhofer, et al. Standing Up with Denervated Muscles in Humans Using Functional Electrical Stimulation. Artif Organs, 23: 447-452, 1999.
[5] Zealear DL, Rainey CL, Jerles ML, et al. Technical approach for the reanimation of the chronically denervated larynx by means of functional electrical stimulation. Ann Otol Rhinol Laryngol, 103: 705-712, 1994.
[6] Zealear DL, Rainey CL, Herzon GD, et al. Electrical pacing of the paralyzed human larynx. Ann Otol Rhinol Laryngol, 105: 689-693, 1996.
[7] Zealear DL, Billante CR, Courey MS, et al. Reanimation of the paralyzed human larynx with an implantable electrical stimulation device. Laryngoscope, 113: 1149-1156, 2003.
[8] Pachter BR. Fiber composition of the superior rectus extraocular muscle of the rhesus macaque. J Morphol, 174: 237-250, 1982.
[9] Porter JD, Baker RS, Ragusa RJ, et al. Extraocular muscles: basic and clinical aspects of structure and function. Surv Ophthalmol, 39: 451-484, 1995.
[10] Büttner-Ennever JA. Anatomy of the oculomotor system. Dev Ophthalmol, 40: 1-14, 2007.
[11] Dimitrova DM, Shall MS, Goldberg SJ. Short-term effects of botulinum toxin on the lateral rectus muscle of the cat. Exp Brain Res, 147: 449-455, 2002.
[12] Scott AB, Rosenbaum A, Collins CC. Pharmacologic Weakening of Extraocular Muscles. Invest Ophthalmol Vis Sci, 12: 924-927, 1973.
[13] Moreno-Lopez B, de la Cruz RR, Pastor AM, et al. Effects of botulinum neurotoxin type A on abducens motoneurons in the cat: alterations of the discharge pattern. Neuroscience, 81: 437-455, 1997.

Acknowledgements

The work presented here was supported by NIH grant R03 EY015247-01 awarded to Arthur L. Rosenbaum.

Authors' Addresses

Presenting Author:
Jun Isobe
University of California, Los Angeles
email: isobe@seas.ucla.edu
Website: www.judylab.org

Corresponding Author:
Arthur L. Rosenbaum, MD
100 Stein Plaza, UCLA
Los Angeles, California, 90095
Phone: (310)825-2872
email: rosenbaum@jsei.ucla.edu

A FINITE ELEMENT MODEL OF THE ELECTRICALLY STIMULATED HUMAN THIGH: CHANGES DUE TO DENERVATION AND TRAINING

Stickler Y[1], Martinek J[1,2], Hofer C[3], Rattay F[1]

[1] Institute for Analysis and Scientific Computing, Vienna University of Technology, Austria

[2] Center of Biomedical Engineering and Physics, Medical University of Vienna, Austria

[3] Ludwig Boltzmann Institute of Electrical Stimulation and Physical Rehabilitation, Institute of Physical Medicine and Rehabilitation, Wilhelminenspital, Vienna, Austria

Abstract

The complete denervation of muscles leads to changes in the muscle fibers as well as in the surrounding tissue. Concerning excitability the most important changes are reductions in fiber diameter, in muscle cross sectional area and in electrical conductivity of the muscle tissue. These changes can be partially reversed by intensive electrical stimulation.

Evaluation of a 3D finite element axial symmetric model of the human thigh shows that the training leads to a reduction in threshold values between 17 and 51 percent, depending on the position of the fiber in the thigh. Single parameter variation clarifies the influence of each of the different factors.

The electrode position was found to be most effective with the electrodes as far apart from each other as possible. Due to (i) comparatively higher changes in potentials at the distal electrode and (ii) variations in sodium channel dynamics, lowest threshold values can be reached with a hyperpolarizing first phase of the biphasic impulse at the distal electrode.

The tissue of the denervated muscle is known to be highly inhomogeneous. Therefore, effects of local tissue inhomogeneities on the fiber activation process were examined. Simulations demonstrate that the related irregularities in the field can actually initiate fiber activation.

Introduction

The complete denervation of muscles leads to changes in muscle fibers as well as in the surrounding tissue. Long disuse or immobilization causes fiber atrophy and a reduction of total muscle cross sectional area. Furthermore, the structure of the muscle fibers partially dissolves and the muscle gets enriched with fat and loose or fibrous connective tissue, which leads to a reduction in the electrical conductivity of the muscle tissue.

Intensive electrical stimulation with large surface electrodes can partially reverse these changes. Long disuse has lead to very poor excitability. Therefore, in the early stages of training very long impulses are needed to actually produce single twitches. After the excitability has improved due to the training, a tonus can be achieved with a train of shorter impulses. Finally force training starts.

During this training process, the mean fiber diameter of the trained muscles grows, the structure of the muscle tissue improves and the total cross sectional area of the muscle increases. After months of training patients can regain stand up function.

The following computer simulations should help to analyze the relations between geometry, muscle status, electrode placement and stimulus parameters.

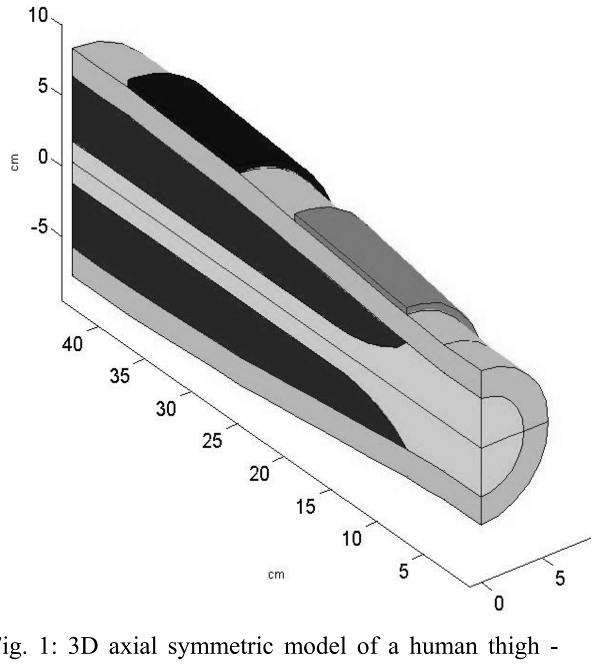

Fig. 1: 3D axial symmetric model of a human thigh - consisting of fat and skin, muscle and bone subdomains - with two large surface electrodes.

Material and Methods

A simplified 3D finite element model of the human thigh is created.

The thigh is assumed to be axial symmetric and to consist of bone, muscle tissue and a surrounding layer representing fat and skin (Fig. 1). Each of the regions has a different electrical conductivity.

For a poor trained long term denervated thigh, the muscle cross sectional area is assumed to be 40% of that of a healthy subject. A second model with 50 % more muscle mass than the first one represents an advanced stage of training.

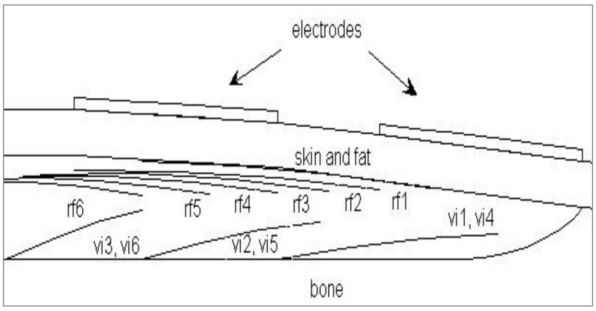

Fig. 2a: 2D-image detail with positions of selected muscle fibers.

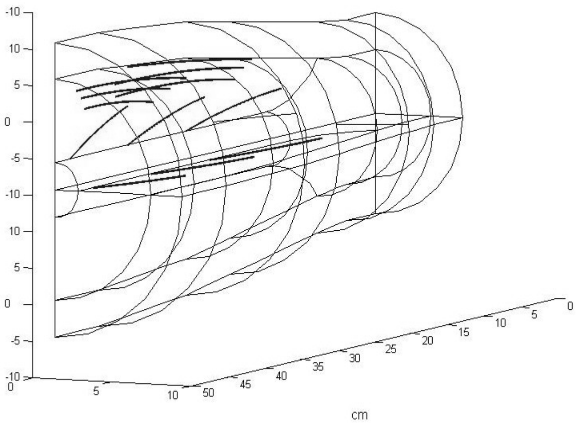

Fig. 2b: 3D-view of embedded and revolved fibers.

To simulate the improvement of muscle structure, the conductivity of the muscle tissue is increased in the second model.

The electrical stimulation is applied via two large surface electrodes. One of them is placed close to the knee, the other one on the uppermost part of the thigh. Biphasic rectangular impulses are applied and the voltage distribution is computed.

To study the effects of the field on a microscopic scale, several fibers located in the region of rectus femoris and vastus intermedius muscle were defined (Fig. 2a and 2b).

For these fibers threshold values were calculated with a muscle fiber compartment model. This was done by taking the exciting influence of the extracellular field, that is the activating function, as input into the compartment model.

Additionally, the effects of increased muscle fiber diameter due to the training are examined.

As current control is necessary to prevent skin damage, current/voltage-relationships are also computed.

Results

Figure 3 shows the potential distribution after an applied voltage square pulse of 0/1 Volt for the two models. The isopotential surfaces are plotted in seven 0.2 Volt steps from 0.1 to 0.9 V.

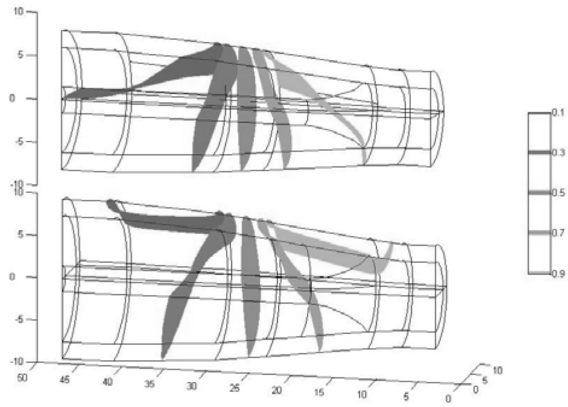

Fig. 3: Isopotential surfaces for the short term (top) and long term trained thigh (bottom). Applied voltage: 0 V left electrode, 1V right electrode. Note the enlarged diameter of the trained thigh.

Computed threshold values for muscle fibers in the poor trained and well trained thigh are given in Table 1. 'Not activated' means that activation is not possible within the voltage impulses up to the maximal allowed current value of 250 mA.

The training leads to a reduction in threshold values for all fibers. The improvement is of unequal amount, because the effects of the assumed changes depend on the position in the thigh.

Isopotential surfaces are shifted towards the electrodes in the well trained thigh, because the difference in fat and muscle electrical conductivity increases (Fig. 3). This effect lowers the threshold values for the fibers beneath the electrodes, but threshold values for fibers between the electrodes increase.

A higher conductivity means a higher current/voltage-relation. Taking into account the electrode current limits, lower voltage amplitudes have to be applied to the well trained thigh.

Due to the increase in muscle cross sectional area fibers in deeper regions have higher thresholds because of the greater distance to the electrodes.

rectus femoris	Volt (poor trained)	Volt (well trained)	Decrease in %
rf1	16	8	50.0
rf2	6	5	16.7
rf3	6	4	33.3
rf4	7	5	28.6
rf5	18	10	44.4
rf6	49	24	51.0
vastus intermedius			
vi1	9	7	22.2
vi2	6	5	16.7
vi3	not activated	not activated	
vi4	11	8	27.3
vi5	8	6	25.0
vi6	39	23	41.0

Table 1: Muscle fiber activation threshold values for the poor trained and well trained thigh for an applied biphasic rectangular voltage impulse of 5 msec per phase. Reduction due to training in percent.

The growth in fiber diameter has a large effect on the threshold value independent of the fiber location in the thigh. Assuming a diameter increase from 10 to 40 µm due to intensive training and ignoring other effects leads to app. 50% lower thresholds.

Charge balanced biphasic impulses are chosen as stimuli. Additionally, this pulse type has a positive effect on the activation process: Hyperpolarizing of the muscle fibers prior to depolarization leads to comparatively lower thresholds. This results from a different range in the time constants of the sodium channel gates. See Fig. 4 for details.

For that reason the most efficient electrode position is to start with a positive impulse at the electrode close to the knee, where the changes in potentials are higher.

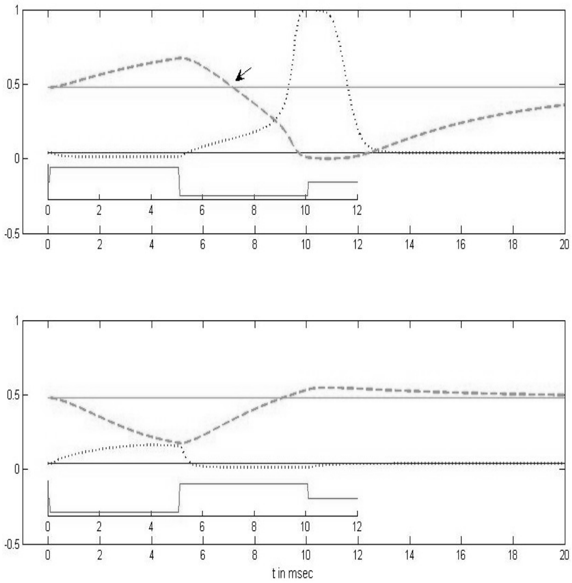

Fig. 4: Sodium channel dynamics of a single compartment responding to biphasic pulses:
Due to different time constants, the activation gate (dotted line) responds faster to changes in membrane potential than the inactivation gate (dashed line) and also gets back earlier to its resting potential level (solid lines).
When starting with a hyperpolarizing pulse (top) the inactivation gate gets back to resting potential level after hyperpolarization (marked with an arrow) not before the activation gate is already opened wide enough to trigger an action potential.
Starting with a depolarizing pulse (bottom) no action potential could be triggered when applying a voltage pulse of same amount.

The structure of the denervated muscle tissue is highly inhomogeneous (Fig. 5). Fat and connective tissue infiltrations get progressively larger after denervation.

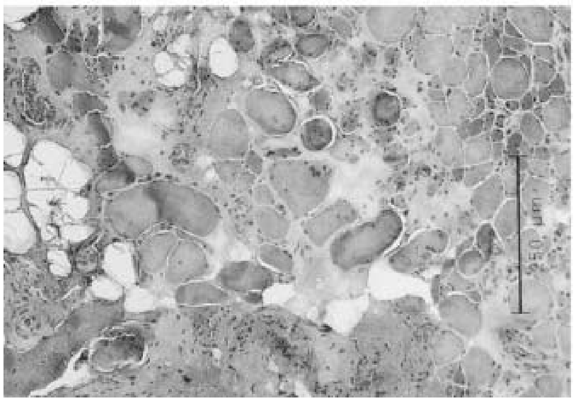

Fig. 5: Biopsy of a 1.3 year denervated thigh muscle, scale bar: 250 µm. From [3].

Our models take account of this phenomenon with a reduced mean conductivity for the tissue in the poor trained muscle. To study the effect of inhomogeneous tissue in detail, a fat infiltration modelled as a region of lower conductivity with diameter of a muscle fiber and of several millimeters of length is placed next to a muscle fiber in the rectus femoris (Fig. 6).

In the homogeneous surrounding, the action potential develops at the end of the fiber. The inhomogeneity in conductivity leads to changes in the field near the fiber and thus the fiber is activated there as well.

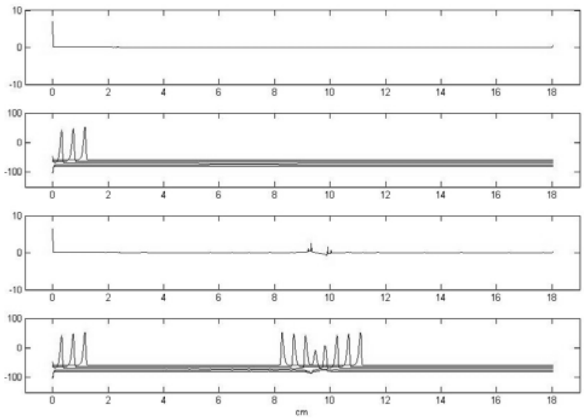

Fig. 6: Muscle fiber activating function and propagation along the fiber in homogeneous (top) and inhomogeneous tissue.

Discussion

3D finite element simulations provide a good overview on the potential distribution, structural relations and geometric effects in the human thigh. Such information cannot be attained from measurements. The possibility to study the effects of parameter changes independently enlightens our understanding concerning their effects on electrical stimulation. A larger muscle fiber diameter has a clearly positive effect on muscle fiber activation, whereas the effects of changes in muscle cross sectional area and conductivity depend on the muscle region.

On the other hand the computations need to make some simplifying assumptions, e.g. axial symmetry and a quasi-stationary field. Most importantly, local inhomogeneities of microscopic size, which were shown to have an important influence on fiber activation, cannot be taken into account on a larger scale.

It is well known, that denervation also leads to changes in the muscle fiber itself. Besides atrophy, alterations in dynamics and densities of the ion channels and structural variations in the excitation-contraction coupling process are important. These issues might also undergo changes due to the electrical stimulation and thus have an important influence on the training process. Modelling these changes is therefore an important task for future work.

References

[1] Rattay F, Electrical Nerve Stimulation (Theory, Experiments and Applications). Springer-Verlag Wien New York , 1990.

[2] Wallinga W, Meijer SL, Alberink MJ, Vliek M, Wienk ED, Ypey DL. Modelling action potentials and membrane currents of mammalian skeletal muscle fibres in coherence with potassium concentration changes in the T-tubular system. Eur Biophys J, 28: 317-329, 1999.

[3] Kern H, Hofer C, Mödlin M, Forstner C, Mayr W, Richter W. Functional electrical stimulation (FES) of long-term denervated muscles in humans: Clinical observations and laboratory findings. Basic Appl Myol , 12: 291-297, 2002.

[4] Kern H, Rossini K, Carraro U, Mayr W, Vogelauer M, Hoellwarth U, Hofer C. Muscle biopsies show that FES of denervated muscles reverses human muscle degeneration from permanent spinal moto-neuron lesion. J Rehabil Res Dev , 42(3) Suppl 1: 43-54, 2005.

[5] Midrio, M. The denervated muscle: facts and hypotheses. A historical review. European Journal of Applied Physiology, 98: 1, 1, 2006.

[6] Marshall MW, Ward MR, Anode-break excitation in denervated rat skeletal muscle fibers. J. Physiol., 236: 413-420, 1974.

Acknowledgements

This study was supported by the Austrian Science Fund (FWF) research project P18848-N13.

Author’s Address

DI Yvonne Stickler
Institute for Analysis and Scientific Computing,
Vienna University of Technology
Wiedner Hauptstraße 8-10
A-1040 Vienna, Austria
ystickler@osiris.tuwien.ac.at
http://www.asc.tuwien.ac.at

Session II

Denervated Muscle 2

Chairpersons
Jonathan Jarvis (Liverpool, UK)
Winfried Mayr (Vienna, Austria)

**THE EUROPEAN R&D PROJECT RISE -
USE OF ELECTRICAL STIMULATION TO RESTORE STANDING IN PARAPLEGICS
WITH LONG-TERM DENERVATED DEGENERATED MUSCLES (DDM)**

Mayr W. [1], Hofer C. [2], Kern H. [2], Bijak M. [1], Lanmüller H. [1], Rafolt D. [1], Stöhr H. [3], Unger E. [1]

[1] Center for Biomedical Engineering and Physics, Medical University Vienna, Austria

[2] Department of Physical Medicine and Rehabilitation, Wilhelminenspital Wien, Vienna, Austria

[3] Center for Biomedical Research, Medical University Vienna, Austria

Abstract

RISE was funded by the European Community within the 5th Framework Program. The consortium included 13 European partner institutions from Austria, United Kingdom, Italy, Slovenia, Germany and Iceland and additional six subcontractors from Austria and Germany. Nine out of the nineteen were spinal cord injury centres. The project started with November 1, 2001 and ended with May 31, 2006.

Within RISE a novel clinical rehabilitation method for patients suffering from long-term flaccid paraplegia with no chance of recovery of the nervous system, was developed. It restores their muscle fibres and mass, muscle function and thus their ability to rise and maintain a standing posture. Based on the results from animal experiments on rabbit and pig and a patient study the associated technology was developed and finally an initiative to gain compliance with current and future regulatory affaires was part of the project. One basic intension was to provide European industry with a novel product family to support a broad clinical application of the method that addresses the needs of about twenty new patients per million EU inhabitants per year. In addition to an appropriate stimulation equipment for home based training, suitable measurement equipment to support patient supervision by dedicated outpatient clinics was developed, to monitor the biomechanical and electrophysiological muscle conditions.

Introduction

Practically all established clinical FES applications are based on direct excitation of neural structures and - in case of muscle functions - indirect activation of the muscles. For reactivation of denervated and especially denervated degenerated muscles (DDM) the technical demands are completely different. Due to the absence of the neuromuscular junction and decomposition of motor units, muscular contractions can only be elicited by depolarizing the cellular membrane of each single muscle fibre.

There are few published studies that demonstrate in both animal and clinical experiments that functional reactivation of denervated muscles by FES is possible in principle and in the long-term even in case of severe degeneration [4, 8, 9]. This means that two important conditions are given: first remaining excitable structures in the DDM and second a sustained myogenetic capacity, that both improve in reaction to enhanced activity. Lomo et.al. [6] have demonstrated in a fundamental study on rats, that electrical stimulation is able to restore the electrical and electrochemical conditions of the muscle membrane from various degrees of degeneration to normal conditions not only once but repeatedly. In parallel they were able to show a similar restoration of muscle force and twitch characteristic. Carraro et.al. [2] have demonstrated also in a study on rats a low but sustained residual myogenetic activity in the denervated untreated muscle and a substantial increase of this activity after severe injury of the muscle. Similar myogenetic events were observed by the same research group in paraplegic patients with denervated lower extremities that had performed an intensive FES training of their quadriceps muscles.

All those experiments give strong evidence that FES is a powerful tool for regeneration, functional restoration and maintenance of denervated muscules. The technique obviously has the potential to serve as a novel rehabilitation method for patients with muscle denervations of various origins and especially after injury of the cauda equina. To work out a firm scientific basis for the later application was the main goal of the European project RISE, “Use of electrical stimulation to restore standing in paraplegics with long-term denervated degenerated muscles”. The project was funded by the European Union within the 5^{th} Framework Program and involved nineteen European partner institutions.

Excitability of the denervated muscles

The electrical membrane sensitivity strongly depends on the state of degeneration or recovery of the muscle cell, but in any case it is much lower than the sensitivity of a nerve cell. It requires impulse durations between 10 and 150 ms and after severe degeneration even up to 300 ms to elicit a depolarisation event in the muscle membrane at one location along the muscle fibre followed by formation of action potentials that travel in both directions towards the ends of the fibres. Consequently also the amplitude values are significantly higher than in nerve stimulation. The recruitment of a sufficient fibre population is depending on a homogenously distributed electrical field more or less concentrated on the target muscle. The later condition is essential to minimize unwanted co-contractions of adjacent other muscles and excitation of neural structures in the adjacent tissue. Useful impulse shapes are biphasic rectangular or in selected cases ramp shaped impulses. The rectangular form is more efficient in recruiting muscle fibres, the ramp shape provides the important advantage of reducing the excitation of neural structures in the immediate neighbourhood of the muscle. A severe problem that inhibits the application of FES on denervated muscles lies in the current too restrictive standards that regulate the specifications of stimulation devices. These limit the output energy to 300 mJ per impulse respectively for impulses above 100 ms limit the current to 80 mA. This is by far not enough to elicit functionally usable contractions in denervated muscles via surface electrodes, unless these muscles are very small and not severely degenerated.

Surface electrode based stimulation system for clinical use

During the past 15 years various clinical trials on patients with permanent complete denervation of the lower extremities were performed in Vienna. The work was carried out using non-invasive equipment with surface electrodes and different stimulator prototypes. The electrical parameters and training strategies were determined more or less by trial and error and very specific for the individual patients. The patients started the FES training between 1 and 30 years after denervation and consequently the state of degeneration differed in a wide range. Generally biphasic rectangular constant voltage (CV) impulses where used. The pulse width was varied between more than 150 ms in case of severe degeneration down to 40 ms with progress of training and muscle regeneration. In average a minimal amount of training of once 60 minutes or twice 30 minutes per day and muscle group was applied to restore and maintain the muscle function.

The study clearly showed that restoration and functional use of denervated muscles with FES is possible and muscle functions can be maintained on the long-term [4], though there remain open questions of optimal training strategies and parameters to be addressed [5]. Several patients were able to regain active standing up using their own muscle power. Other patients have achieved various states of improvements of their muscle conditions.

The applied stimulator in its recent development state [3] is a dual-channel stimulator that is capable of delivering charge balanced biphasic or monophasic CV impulses with amplitudes of up to +/- 80 V on an output load down to 300 Ω. To guarantee optimal patient safety the system is powered by rechargeable batteries, all output lines are decoupled via capacitors and patients´ access to adjust the parameters is reduced to an absolute minimum. The patient has access to up to nine pre-programmed stimulation sequences and to adjustment of the intensity in a limited amplitude range. All other parameters can only be adjusted by authorised personnel via laptop or PDA (Personal Digital Assistant) computer using an IrDa link. In addition to the rectangular impulses various alternative impulse shapes can be programmed to serve individual demands in case of incomplete or discomplete lesions. The pulse width is adjustable between 10 and 300 ms, the interpulse interval down to zero to allow optimal parameter adjustment in relation to the actual conditioning state of the muscle. The device records a compliance protocol containing date and time of use, chosen programs and intensity level. The surface electrodes are either conductive silicon-rubber types applied via a wet sponge layer or attached directly using electrode gel, or self adhesive hydro gel electrodes. The choice depends on skin condition and muscle training state respectively required electrical parameters. To minimise current density and optimise the electrical field distribution pairs of large electrodes with 200 to 250 cm2 for the quadriceps muscles and 100 cm2 for the hamstrings are essential. Accurate electrode application with equally distributed contact pressure and perfect electrode condition are indispensable to guarantee save operation of the system and avoid skin burn.

Actually the dual-channel stimulator is a bench version and the electrodes are attached one by one [3]. A second generation 4-channel belt version of the stimulator and prototypes of garments with integrated electrodes and cables, both to simplify donning and doffing of the equipment and to make its permanent use more reliable and attractive, where developed within the RISE project.

Implantable stimulator system for experiments

An implantable system for reactivation of denervated muscles potentially offers a number of advantages. It could be much more comfortable in daily handling than a surface electrode based system, provide a much higher selectivity in activating single muscles and avoid pain in applications where sensitivity is partly or completely intact. On the other hand many specific technological problems have to be solved in comparison to the usual implants for neural stimulation that make the development of this type of implant a complex task. Again long duration impulses between 10 and at least 150 ms have to be delivered in contrast to 0.1 to 1 ms for nerve stimulation. Consequently the charge flow across the electrode tissue interface is by far greater making it difficult to design a biocompatible and corrosion resistant electrode that is sufficiently flexible and mechanically resistant for long-term use. Alternative solutions are also required for the electronic circuitry, especially for the power supply and output stages, that have to deliver up 1500 fold the power of nerve stimulators, or for the decoupling capacitors, that have to guarantee charge balance for up to 1500 times longer impulses. All those constraints may explain, that no implantable equipment is available at least for clinical use.

One prototype solution was designed and tested in Vienna [7] that originated from a project aiming in development of an implantable solution for chronic bilateral recurrent nerve lesions. The animal study on sheep was dedicated to development of technological means including synchronisation with respiration, stimulation and training parameters for the denervated crycoarytenoid muscles, and a long-term feasibility study focused on the muscle condition under chronic stimulation. Implanted stainless steel (316L) electrodes and biphasic ramp-shaped constant current (CC) impulses with 30 ms per phase and a frequency of 10 Hz where applied.

The results were encouraging [1, 9]. Respiration synchronous stimulation could be demonstrated for periods of up to 18 months under full maintenance of the muscle function. The histological and biochemical investigations showed a transformation to a dominatingly slow type muscle with lack of atrophy and areas showing even hypertrophy, whereas now major signs of muscle damage where observed. The electrodes remained stable throughout the long observation period. The ramp-shaped impulses showed excellent selectivity in eliciting muscle contractions whilst avoiding the excitation of sensible and motor nerves in the surrounding tissue.

In conclusion the study demonstrated that it is possible to design and operate long-term stable implantable systems for FES of denervated muscles, which in addition to the specific application in the larynx may support various new therapeutic approaches.

The EU-project RISE

Based on the above mentioned work and addressing the open methodological problems the project RISE was established and funded by the European Community within the 5th Framework Program. The consortium included 13 European partner institutions from Austria, United Kingdom, Italy, Slovenia, Germany and Iceland and additional six subcontractors from Austria and Germany. Nine out of the nineteen were spinal cord injury centres. The project started with November 1, 2001 and ended with May 31, 2006.

RISE has aimed in developing a novel clinical rehabilitation method for patients suffering from long-term flaccid paraplegia (denervated degenerated muscles - DDM) with no chance of recovery of the nervous system, a problem that concerns about twenty new patients per million EU inhabitants per year. The project work was organised in 5 work-packages: an animal study on rabbits, a second one on pigs, a technical work-package on stimulation equipment, a second one on test- and measurement equipment and finally a patient study.

The rabbit experiments have provided us with new knowledge about the course of denervation in the rabbit tibialis anterior (TA) and extensor digitorum longus (EDL) over an observation period of up to one year. Comprehensive electrophysiological, biomechanical, histological and biochemical data of 70 rabbits were obtained. Various training strategies and safety issues were addressed.

The study on Göttinger Minipigs was performed in 9 animals and denervation periods of up to 3 years (isolated unilateral denervation of EDL and TA). Comprehensive data on histological electro-physiological and biomechanical changes were obtained, confirming that the model shows a very similar time course of post-denervation atrophy and later degeneration in comparison to humans. 4 of the animals where treated with patient stimulation equipment and protocols.

Technically and technologically we have developed stimulation and measurement equipment for the animal experiments and the patient study [10, 11]. An implantable battery powered stimulator including epifascial muscular electrodes, a versatile bench stimulator for both manual and PC-based control, measurement setups for both the rabbit experiments and the patient study, two generations of prototype stimulation equipment for pig and clinical experiments and various prototype garments for improved electrode application in the patient study are now available. A patent for a novel electrode minimizing the risk of skin burns is pending, an equipment transfer to industry under negotiation.

The patient study was completed with finally 20 patients. 5 of them achieved standing-up, 3 walking in mobile parallel bars up to 36m.

The data collected during the project have increased our knowledge about degeneration and regeneration of denervated degenerated muscle substantially. Especially the myogenetic events occurring in the muscle after denervation in a state of rest, after an injury and after electrical stimulation have become much clearer than available in literature. The data confirm, that there is a sustained myogenetic capacity of the denervated muscle even in the long-term and that the myogenetic activity is dramatically intensified by training - in our case FES based. The data help us to explain earlier clinical observations that a low amount of muscle substance is remaining even after 20 to 30 years after denervation and that restoration of a severely degenerated denervated muscle to a near normal muscle is possible in principle at least over periods of several years of intensive FES training.

Though the appearance of the FES restored muscle looks normal in many respects we have observed a remaining force and endurance deficit in experimental and clinical data. To explain this discrepancy and survey the underlying mechanisms will be main topics of our future work. For now – with the end of RISE – we are able to provide a clinical method and associated technology that is capable of reducing substantially the risk of pressure sores in patients with flaccid paraplegia and contributing to an improved quality of live for those patients.

References

[1] Carraro U, Catani C, Saggin L, Zrunek M, Scabolcs M, Gruber H, Streinzer W, Mayr W, Thoma H: Isomyosin changes after functional electrostimulation of denervated sheep muscle. Muscle Nerve 11: 1016-1028, 1988.

[2] Carraro U, Rossini K, Zanin ME, Rizzi C, Mayr W, Kern H: Induced Myogenesis in Long-Term Permanent Denervation: Perspective Role in Functional Electrical Stimulation of Denervated Legs in Humans. Basic Appl Myol 12 (2): 53-63, 2002.

[3] Hofer C, Mayr W, Stoehr H, Unger E, Kern H: A stimulator for functional activation of denervated muscles. Artif Organs 26(3):276-279, 2002

[4] Kern H, Hofer C, Strohhofer M, Mayr W, Richter W and Stöhr H. Standing up with denervated muscles in humans using functional electrical stimulation. Artif Organs 23(5):447-452, 1999.

[5] Kern H, Hofer C, Moedlin M, Forstner C, Raschka-Hoegler D, Mayr W, Stoehr H: Denervated muscles in humans - limitations and problems of currently used functional electrical stimulation training protocols. Artif Organs 26(3): 216-218, 2002

[6] Lomo T, Westgaard RH, Hennig R, Gundersen K: The response of denervated muscle to long-term electrical stimulation. in Carraro U, Angelini C, (eds): Cell Biology and Clinical Management in Functional Electro Stimulation of Neurons and Muscles. Padova, Italy, CLEUP Editore, 1985, pp 81-90.

[7] Mayr W, Bijak M, Rafolt D, Sauermann S, Unger E, Lanmueller H: Basic design and construction of the Vienna FES implants - existing solutions and prospects for new generations of implants. Medical Engineering and Physics 23:53-60, 2001

[8] Valencic V, Vodovnik L, Stefancic M, Jelnikar T. Improved motor response due to chronic electrical stimulation of denervated tibialis anterior muscle in humans. Muscle Nerve 9: 612-617, 1986.

[9] Zrunek M, Bigenzahn W, Mayr W, Unger E, Feldner-Busztin H. A laryngeal pacemaker for inspiration controlled direct electrical stimulation of denervated posterior cricoarytaenoid muscle in sheep. Eur Arch Otorhinolaryngol 1991, 248(8):445-448.

[10] Hofer C, Forstner C, Modlin M, Jager H, Mayr W, Kern H. In vivo assessment of conduction velocity and refractory period of denervated muscle fibers. Artif Organs. 2005 Jun;29(6):436-9

[11] Gallasch E, Rafolt D, Kinz G, Fend M, Kern H, Mayr W. Evaluation of FES-induced knee joint moments in paraplegics with denervated muscles. Artif Organs. 2005 Mar;29(3):207-11

Acknowledgements

This research was supported by **EU** Commission Shared Cost Project RISE (contract QLG5-CT-2001-02191) and the Austrian Ministry of Science.

Author's Address

Prof. Winfried Mayr
Center for Biomedical Engineering and Physics
Vienna Medical University
winfried.mayr@meduniwien.ac.at

RESTORING DENERVATED HUMAN MUSCLE BY FES: CLINICAL RESULTS OF THE EUROPEAN RESEARCH PROJECT RISE

Kern H[1,2], Vogelauer M[1], Forstner C[1], Mödlin M[1], Mayr W[3], Hofer C[2]

[1] Department of Physical Medicine and Rehabilitation, Wilhelminenspital Wien, Vienna, Austria

[2] Ludwig Boltzmann Institute of Electrical Stimulation and Physical Rehabilitation, Vienna, Austria

[3] Center for Biomedical Engineering and Physics, Medical University Vienna, Austria

Abstract

In the course of the European research project RISE we could demonstrate, by applying a highly intensive transcutaneous electrical stimulation protocol, a significant structural and functional regeneration of the long-term denervated, degenerated muscle (DDM). The method was not only capable of increasing the size of the denervated muscles as measured by CT-scans. It could also restore the capacity of the muscle to generate tetanic contraction, a precondition for inducing hypertrophy of the muscle. Training over a longer period of time made it first possible to induce knee extension by direct electrical stimulation of the denervated quadriceps muscle. Later with further improvement of muscle function 25% of the patients could perform stand up and walking exercises.

Introduction

The aim of the EU project RISE was to restore and maintain denervated human muscles in patients with total denervation of their lower limbs due to a complete conus – cauda lesion [1].

Denervation denotes the state that a muscle is deprived of the nerve normally activating it. Depending on the time elapsed since the accident, there is a vast muscle tissue degeneration with an extent that varies greatly, being influenced by secondary illness such as polytrauma, metabolic crisis, long comatose states or local destruction of muscle.

The absence of the motoneurone and the degeneration is the reason that long pulse durations and high intensities are necessary for activating the denervated muscle.

In the present work we demonstrate that it is possible to regenerate the long-term denervated, degenerated muscle (DDM) by applying a highly intensive transcutaneous electrical stimulation protocol.

Computed tomography, electrophysiological and functional assessment give evidence about significant structural and functional restoration.

Material and Methods

Patients:

Patients included in the EU project RISE [1] were recruited from spinal cord injury centres of Austria, Germany, Slovenia, and Italy according following criteria:

• epiconus or conus cauda lesion, traumatic or ischemic with resulting m. quadriceps denervation for 6-12 months and more,

• complete loss of sensation for touch and pinprick in the lumbar segments from L2 to L4,

• absent muscle hypertonia, Ashworth scale 0, and absent patellar tendon jerk,

• no volitional activity in the m. quadriceps group,

all studies subjects were otherwise healthy.

Stimulation procedure:

The long duration of the impulses needed for stimulation precluded the use of frequencies that would elicit tetanic contractions; training was therefore initiated with single twitches at 2 Hz and delivered for 15 min per day, 5 days per week.

After 4 months, excitability of the muscle fibres had recovered sufficiently for pulses of shorter duration to be used. At this stage, the protocol was augmented with an additional tetanic pattern consisting of pulses of 40 ms delivered at 20 Hz for 2 s on, 2 s off for 15 min daily, 5 days per week. The total amount of stimulation was then 30 min daily for each muscle [2]. The additional tetanic stimulation pattern produced more rapid and more forceful contractions, resulting in a progressive increase in knee extension torque.

Force measurement:

Measurement of FES-induced force was performed using a specifically designed chair, and activating the quadriceps m. by electrical stimulation. The force transducers connected as a bridge circuit are placed on the lever near the center of rotation. The isometric knee extension torque was measured in 90 degree knee flexion by activating the quadriceps muscle with a standardized stimulation program [3]. The stimulation parameters were: biphasic rectangular pulses with a duration of 40 ms, a stimulation frequency of 20 Hz and an maximum intensity of 160 V_{pp}.

CT scan:

The physiological shape of our upper leg muscle is never cylindrical but more or less spindle-shaped, therefore it is crucial for the CT - cut placement to be exact and well defined to reach relevant conclusions and so individual test results are comparable [Kern 95]. The patients were positioned that the top of the trochanter major of both femur bones were aligned in the same plane of the CT-scan. This served as reference plane for the three additional CT-scans 10, 20 and 30 cm below the trochanter major. To differentiate exactly between fat and muscle tissue we used a soft window frame (window 350, center 50). The complete cross section area of M. gluteus, M. quadriceps and hamstrings as well as their density (measured in Hounsfield unit, HU) were determined [2, 3].

Results

By using a protocol specifically adapted to the requirements for stimulating the denervated muscle by increasing number of stimuli per day, thus gradually increasing the amount of the muscle activity per day, we were able to improve the condition of the permanently denervated muscles.

The electrically induced isometric knee extension torque increased from almost zero (0.7 Nm) before stimulation therapy up to 10.4 Nm after 2 years of FES in patients who were denervated for more than 3 years. Less force was produced in patients who were denervated for a longer period of time (3 – 9 years) before starting FES training.

Restoration was further confirmed by measuring the muscle cross sectional area with computed tomography (CT) of the thigh, showing an increase of m. quadriceps area by 25.5%, that is in absolute values from 27.46 cm^2 up to 34.47 cm^2.

Being able to significantly reduce the stimulation pulse width in the course of the electrical stimulation training suggested that the excitability of the denervated muscle fibres was also increased. FES did not only not only increase or restore muscle size (mass), but induced also structural and metabolic changes of the muscle fibres. Ultrastructural analyses of muscle biopsies by electron microscopy confirmed the structural regeneration of the myofibres, e.g of the sarcolemma, sarcoplasmatic reticulum, and triads [4].

Functional outcome:

The FES training-induced improvements of the DDM allowed 25% of the participants to perform stand up and walking exercises with FES in parallel bars.

Two patients were even capable of walking outdoor with FES using a walker (Figure 1).

Figure 1: Patient with denervated lower limb muscles for 5 years performing walking exercises outdoor after 2 years of FES training. Left and right quadriceps muscles are switched on and off by the patient to induce stepping.

Discussion

Small increase in muscle mass and hypertrophy of the denervated muscle induced by electrical stimulation in both animals and humans has been previously demonstrated by other researchers [5, 6]. What is unusual in the present study is the extent of the changes produced in the long-term denervated and stimulated muscles. Furthermore the study provides evidence that the recovery process involves both hypertrophy as well as hyperplasia [4, 7].

The restored muscle regained the capability of FES induced tetanic contraction and thus the generation of sufficient force to enable a part of the patients to rise from the wheelchair.

To achieve these improvements in muscle structure, mass and function it is crucial to start the FES therapy of the denervated muscle not longer than 4 - 6 months after denervation.

References

[1] Mayr W, Hofer C, Rafolt D, Bijak M, Lanmüller H, Reichel M, Sauermann S, Unger E. The EU-Project RISE: General overview and engineering aspects. Proceedings of the 8th Vienna Inernational Workshop on Functional Electrical Stimulation 2004; ISBN 3-900928-07-9.

[2] Mödlin M, Forstner C, Hofer C, et al. Electrical Stimulation of Denervated Muscles – First Results of a Clinical Study. Artif Organs, 29(3):203-6, 2005.

[3] Kern H. Funktionelle Elektrostimulation paraplegischer Patienten. Österr. Z. Phys. Med. 5 , Heft 1 Supplementum, 1995.

[4] Kern H, Boncompagni S, Rossini K, Mayr W, Fanò G, Zanin ME, Podhorska-Okolow M, Protasi F, Carraro U. Long-term denervation in humans causes degeneration of both contractile and excitation-contraction coupling apparatus, which is reversible by functional electrical stimulation (FES): a role for myofiber regeneration? J Neuropathol Exp Neurol, 63(9):919-31, 2004.

[5] Eichhorn KF, Schubert W, David E. Maintenance, training and functional use of denervated muscle. J Biomed Eng, 6:205–211, 1984.

[6] Mokrusch T. LIB-stimulation (long impulse, bidirectional) improves reinnervation in patients with long term denervation. Proceedings of the 7th Annual Conference of the International Functional Electrical Stimulation Society, 144–146, 2002.

[7] Kern H, Salmons S, Mayr W, Rossini K, Carraro U. Recovery of long-term denervated human muscles induced by electrical stimulation. Muscle Nerve, 31(1):98-101, 2005.

Acknowledgements

This research was supported by **EU** Commission Shared Cost Project RISE (contract QLG5-CT-2001-02191) and the Austrian Ministry of Science.

Author's Address

Univ. Doz. Dr. Dr. Helmut Kern

Department of Physical Medicine and Rehabilitation
Wilhelminenspital Wien
Montleartstraße 37
A-1171 Wien, Austria

helmut.kern@wienkav.at

DESIGN OF A STIMULATOR TO ACTIVATE DENERVATED DEGNERATED MUSCLES

Bijak M[1], Unger E[1], Hofer C[2], Lanmueller H[1], Rafolt D[1], Mayr W[1]

[1]Medical University Vienna, Center for Biomedical Engineering and Physics, Vienna, Austria

[2]Ludwig Boltzmann Institute of Electrostimulation and Physical Rehabilitation, Department of Physical Medicine, Wilhelminenspital, Vienna, Austria

Abstract

Activation of muscles with electricity is well known for many decades.

In nearly all published FES applications only innervated muscles, muscles with intact lower motor neuron are addressed. In this cases tetanic contractions are achieved by activating the intact lower motor neuron usually with biphasic charge balanced rectangular pulses with a pulse width in the range of 10us up to several milliseconds, frequencies in the range of 20-70Hz and voltage amplitudes up to ±60V.

Contrary, in patients with denervated degenerated muscles (DDM) the muscle fibers have to be depolarised with pulse widths of up to 200ms and voltages up to ±100V. Those stimulation impulses conflict with the related EC regulations. In the scope of the EC-project RISE permission was given to apply those parameters on patients.

Stimulators for DDM must have a much higher output power than commonly used FES devices. Special care must be taken in developing the output stage for good energy efficiency, to keep the electrodes DC free and allow voltage levels down to 0V. A microprocessor was used to generate, in terms of parameters very flexible stimulation bursts and establish a connection to a Pocket PC via Bluetooth link. A first generation of stimulators is already used by 80 patients for ambulant FES training, while the second generation stimulator - currently in prototype stage – is intend for standing up and walking with patients suffering from lower motor neuron lesion.

Introduction

Restoration of lower limb function with the aid of Functional Electrical Stimulation (FES) is well known through decades. Lots of electrical stimulators, starting from simple one channel stimulators up to very complex PC controlled multi channel stimulators have been developed and applied to paraplegic patients with intact lower motor neuron [1].

Since those devices are intended to stimulate innervated muscles, muscles with intact lower motor neuron, typical stimulation parameters like pulse width of biphasic rectangular pulses 10µs … 2ms, 20-70Hz stimulation frequency and peak to peak voltage of ±60V are implemented and not conflicting with the safety regulations.

While research and technical development in various fields is going on for patients with intact lower motor neuron [2] no adequate rehabilitation methods for patients with long term denervated degenerated muscles (DDM) is available. To find a proper rehabilitation method for patients with DDM the European Union (EU) Commission Shared Cost Project RISE, with 9 project partners, 3 additional partners and 6 subcontractors all from 6 countries started in November 2001 to create a systematic body of basic scientific knowledge about the restorative effects of FES and related topics [3-5].

The RISE project showed that recovering and strengthening of DDM is possible but requires stimulation parameters far beyond the limits of current safety regulations [6]. So a special allowance was given and a stimulator for DDM had to be developed.

Recovering and strengthening of DDM starts with a single twitch training with stimulation pulses of up to 200ms at 2Hz with an amplitude of up to ±100V (±200mA), resulting in an energy of 4J per pulse delivered to the tissue (EC-standards: max. 300mJ). Following the training muscle excitability decreases and pulse duration can be shortened to 80-100ms. Finally burst stimulation can be performed with 40ms pulse width and at a frequency of 20Hz.

Material and Methods

Stimulation equipment was developed for 3 different applications. Firstly a simple to use device for home training of the patients, secondly a device for "scientific investigations" meaning, a stimulator which allows to change parameters in a wide range very easily and with a connection to Pocket PC or PC for semi-automated measurements and finally, as result of the experience gathered during the RISE project a miniaturised stimulator that can be worn on the

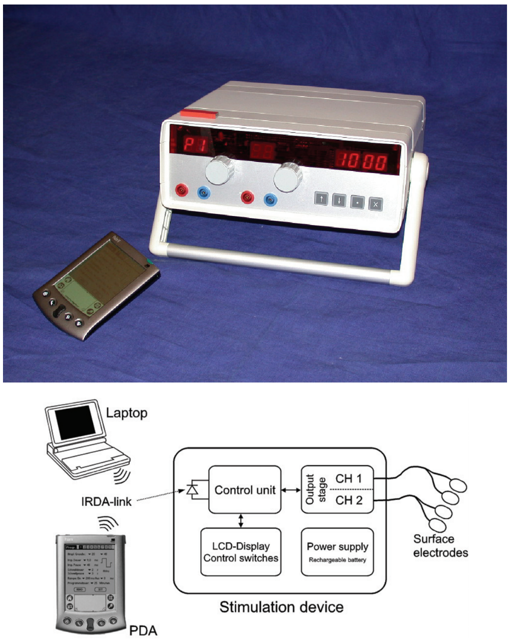

Fig. 1: Stimulator for home training

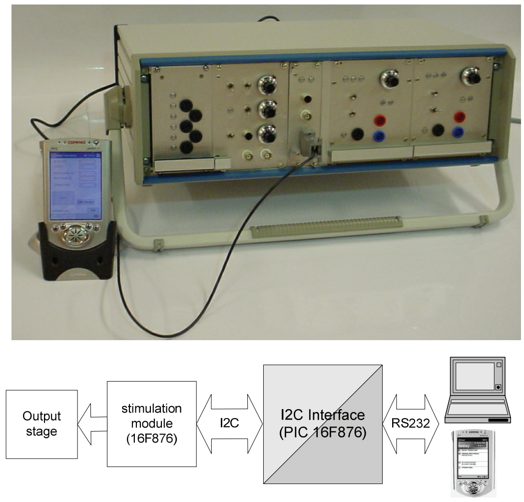

Fig. 2: "Bench" stimulator

body and which allows to program whole stimulation sequences as required for standing up, stepping and sitting down. A wireless link to PC or Pocket PC is a must for easy stimulation parameter changes during the stepping training.

Patient device

The patient device shown in figure 1 is a 2 channel device that can be programmed for different trainings protocols via infrared RS232 interface (IrDA). For safety reasons from the device itself only limited access is given to stimulation parameter changes. A handheld computer that is not given to the patient is used for comfortable parameter and protocol fitting.

Experimental stimulator ("Bench stimulator")

The "Bench stimulator" is a one channel device, and is built for scientific investigations, offering a wide range of stimulation parameters. It can be controlled completely "manually" by the built in buttons and remotely via RS232 link from a PocketPC or PC. The incoming data stream is converted to the I2C protocol which is hardware supported by the chosen microprocessor 16F876 (Microchip, Santa Clara, CA, USA). The output stage is controlled by one 16F876 which can generate a whole stimulation burst independently, avoiding real time problems that might occur from delays on the data link.

Single pulse stimulation and burst stimulation are available and can be triggered via an external signal. Burst stimulation can be freely defined as shown in figure 3 by positioning the four markers in the time-voltage space. For each of the resulting three burst parts pulse width and stimulation frequency can be independently set.

The output stage offers constant voltage mode and constant current mode. Selectable pulse shapes are biphasic rectangular and three types of biphasic triangular. Additionally any pulse shape defined by sixteen amplitude values can be programmed.

Special software developed for the Pocket PC and the PC (Microsoft Visual Studio C# 2003) supports burst and parameter adjustment, translates it for the stimulator and handles the serial data transfer. A connection to a Microsoft SQL database allows storage and management of stimulation sequences.

A modular concept with 19" racks is chosen that modules can be easily changed and adapted to specific requirements.

Portable stimulator (second generation)

The portable and latest stimulator generation is a further development of the "Bench stimulator". It is designed to fulfil the needs to stimulate DDM as well as to serve as a multipurpose experimental stimulator that is also suitable for stimulating

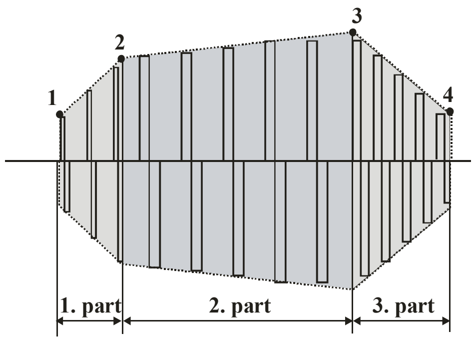

Fig. 3: Stimulation burst

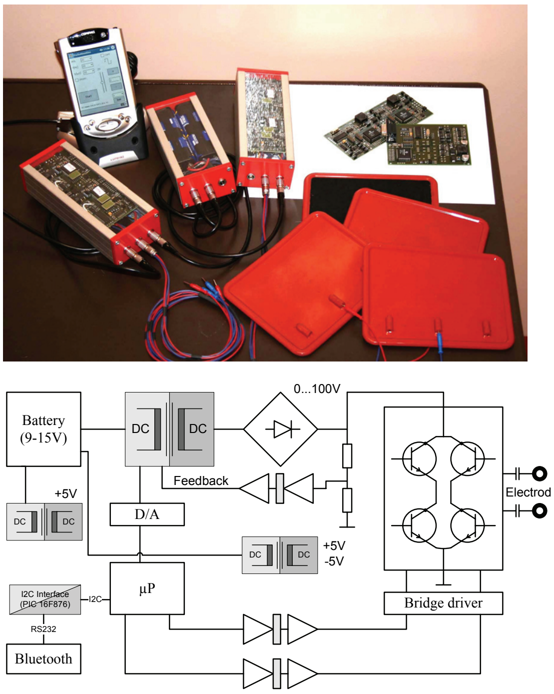

Fig. 4: Portable stimulator

muscles with intact lower motor neuron.

The whole stimulation system is packed into 3 cases, one holding the batteries and the two others the miniaturised electronic components for two independent stimulation channels each.

Figure 4 shows the stimulator and the block diagram of one stimulation channel with power supply and the Bluetooth connection. Battery and microprocessor circuitry are consequently galvanically decoupled from the output circuitry by DC/DC converters, analog and digital isolators. The stimulation voltage is produced by a with 500 kHz operating DC/DC converter. A controller takes care that the output voltage follows the desired value produced by the microcontroller. Since this controller is designed to act fast the pulse shape of a single stimulation impulse can be altered in real time giving the opportunity to deliver pulses of any shape. Output capacitors are used to keep the output signal DC free.

A much more powerful microprocessor (Microchip 18F4520) than previously used was implemented and the whole firmware was rewritten in C. The Compiler used is Hi-Tech Picc 18 (Hi-Tech Software, Acacia Ridge, Australia).

Also the stimulation parameter ranges have been extended. A stimulation burst (fig. 3) can now be built of n markers whereas n is only limited by the internal memory of the microprocessor. Further more each single impulse of a burst can be replaced with "nlets" as shown in figure 5 [7]. The number of nlet - pulses can be chosen, the polarity, the duration of the positive and negative pulse part independently, a time between the pulse with zero amplitude and the time between the nlet pulses.

The communication between PC / Pocket PC (iPaq hx2490, Hewlett Packard, Houston, TX, USA) and stimulator is done via Bluetooth serial port (RS232). In the stimulator the CE certified Bluetooth component WRAP THOR 2022-1 (Bluegiga, Espoo, Finland) is used. It implements all the Bluetooth requirements and offers a standard RS232 port to interact with the microprocessor. The iPaq hx2490 has a built in Bluetooth port, on the PC the USB / Bluetooth adapter DB-20 (D-Link, Mt. Herrmann, CA, USA) was used.

A related software library to control the stimulator was written in Visual Studio 2005 C# and is suitable for PocketPC and PC.

Results

The patient device was used within the scope of the RISE project by 80 patients for home training and also for standing up and stepping / walking in the clinic. For the latter quadriceps muscles where stimulated in an on/off manner. Additional activation of glutaeus muscles requires a second stimulator. Of course the stimulator(s) either had to be moved along with the patient (by a wheeled table) or very long electrode cables had to be used. Further more the possibility to optimise stimulation sequences like introducing ramps was desirable. The stimulation parameter range ±100V up to 250mA, pulse width of 1..300ms was sufficient in all patients for all phases of the rehabilitation process.

The "Bench stimulator" was used during animal experiments and special investigations on human

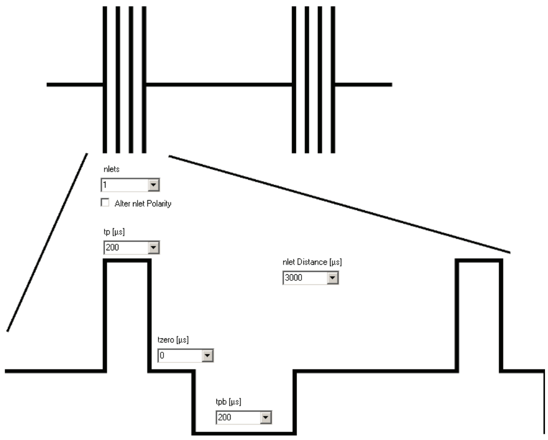

Fig. 5: nlet generation

subjects. Especially the modular concept with 19" racks made it easy to adapt the stimulator to specific experimental requirements. Stimulation parameter range is ±50V in constant voltage mode, ±50mA in constant current mode, pulse width from 50µs up to 100ms and stimulation frequencies from 1-200Hz. The output power is lower than in the patient device and therefore it would not be useful as training device in the first rehabilitation step. Nevertheless it fulfilled the other tasks sufficiently and can be, due to the selectable small pulse width, also be used when stimulating muscles with intact lower motor neuron.

The portable stimulator is now in prototype stage and is an agreement between size, weight and flexibility. The output amplitude is in the range of 0... ±60V (up to 180mA), the pulse width covers the range of 100µs up to 100ms with a power efficiency of 50%. The major limiter to the useful output parameter range is the output stage. While the microprocessor is able to produce pulses from microseconds up to seconds the output stage has to be optimised according to maximum voltage output, pulse width, slew rate and power efficiency. Other parameter ranges can be implemented by minor hardware changes.

In the beginning the Bluetooth / RS232 link caused troubles due to unpredictable delays up to 500ms in data transmission and some "byte pooling" - meaning, that sometimes a byte sent by the stimulator did not appear in the software on the PC until further bytes were sent. Those problems could finally be solved by optimising time outs and replacing the original MS-Windows Bluetooth driver with the Widcomm driver that came with the D-Link adapter.

Discussion

Designers of stimulators for denervated degenerated muscles have to deal with lots of conflicting requirements like stimulators shall be small and lightweight but long impulses and high stimulation amplitudes require large batteries for an acceptable usage time and large output capacitors for patient safety - leading compulsory to bigger devices. Energy efficiency is decreasing with higher output voltage. Further problems arise if stimulation parameters shall be built for both stimulation types, for muscles with intact lower motor neuron (smaller pulse width, smaller voltages, faster) and for DDM (long pulses, higher voltage, slower). All this requirements can be easily fulfilled from the point of software engineering because latest microprocessors have enough memory capacity and are fast enough. The bottle neck are the batteries, the output capacitors and in general the output stage, in which way it is optimised.

To summarise, during stimulator design it should be carefully evaluated: "what is really needed".

References

[1] Bijak, M., Mayr, W., Rakos, M.et al.: The Vienna functional electrical stimulation system for restoration of walking functions in spastic paraplegia. Artif. Organs, Vol. 26, No.3, 2002, pp 224-227.

[2] Bijak, M., Rakos, M., Hofer, C.et al.: Stimulation parameter optimization for FES supported standing up and walking in SCI patients. Artif. Organs, Vol. 29, No.3, 2005, pp 220-223.

[3] Carraro, U., Rossini, K., Mayr, W.et al.: Muscle fiber regeneration in human permanent lower motoneuron denervation: relevance to safety and effectiveness of FES-training, which induces muscle recovery in SCI subjects. Artif. Organs, Vol. 29, No.3, 2005, pp 187-191.

[4] Kern, H., Rossini, K., Carraro, U.et al.: Muscle biopsies show that FES of denervated muscles reverses human muscle degeneration from permanent spinal motoneuron lesion. J. Rehabil. Res. Dev., Vol. 42, No.3 Suppl 1, 2005, pp 43-53.

[5] Kern, H., Salmons, S., Mayr, W.et al.: Recovery of long-term denervated human muscles induced by electrical stimulation. Muscle Nerve, Vol. 31, No.1, 2005, pp 98-101.

[6] Modlin, M., Forstner, C., Hofer, C.et al.: Electrical stimulation of denervated muscles: first results of a clinical study. Artif. Organs, Vol. 29, No.3, 2005, pp 203-206.

[7] Karu, Z. Z., Durfee, W. K., and Barzilai, A. M.: Reducing muscle fatigue in FES applications by stimulating with N-let pulse trains. IEEE Trans. Biomed. Eng, Vol. 42, No.8, 1995, pp 809-817.

Acknowledgements

This project is supported by the Commission Shared Cost Project RISE (Contract no. QLG5-CT-2001-02191) and the Austrian Ministry of Science.

Author's Address

Manfred Bijak
Medical University of Vienna, Center for Biomedical Engineering and Physics
Waehringer Guertel 18-24/4L
A-1090 Vienna, Austria
Email: manfred.bijak@meduniwien.ac.at

TEST- AND MEASUREMENT EQUIPMENT FOR FUNCTIONAL ASSESSMENT OF DENERVATED MUSCLES

Rafolt D[1], Gallasch E[2], Krenn M[1], Mayr W[1]

[1] Center of Biomedical Engineering and Phyics, Med. Univ. Vienna, Austria
[2] Dep. Physiologie, Med. Univ. Graz, Austria

Abstract

One workpackage of the EU-project "RISE" was to develop biomechanical methods to evaluate effects of FES training of denervated degenerated thigh muscles.
Using a conventional knee dynamometer two problems have to be considered. First: the relatively low resolution of such devices at very low muscle forces typically produced at the beginning of the FES training of a long-term denervated muscle. Secondly: during electrical stimulation of quadrizeps muscles co-contractions of the hamstrings result in a reduced torque output of a FES activated knee extension. According to approved manual methods (palpation of the muscle belly, joint movements) to assess the strength of a contraction we developed objective methods to address the quadrizeps solely.
Palpation: As the hardness of a muscle reflects the force generation during contraction, a computer controlled sensor-actuator system was applied to the belly to palpate the muscle. The slope of the indentation force versus the measured displacement of the indented test pin shows the transversal muscle stiffness.
Oscillation tonometry: A manipulandum was connected to the knee joint to elicit gravity induced leg oscillations. Frequency and decay of the oscillations reflect the FES affected increase of stiffness and viscosity of the muscle. The pendulum test has been proved as the most sensitive method for low contraction levels.
Patella Tendometry: Twitch contractions due to single FES-pulses recorded at the patellar tendon reflects the force output of the quadriceps without superposition of the hamstrings activity.
Moreover the contour of the twitch responses at the patellar tendon and the m.rectus femoris were analysed to determine the dynamic properties of the quadrizeps muscles.
In 21 subjects measurements were performed before, after 1 and after 2 years respectively of FES training.

Introduction

To activate denervated thigh muscles by FES in general high stimulation amplitudes are necessary. [1]. Unfortunately the desired high electric field in the agonist (m. quadrizeps) is accompanied with a field in the antagonist (hamstrings). Therefore in order to evaluate the force output of a FES-stimulated muscle co-contraction of antagonistic muscles has to be considered. Depending on the type and state of the paralysis of the hamstrings, the torque output of an knee extension measured by a dynamometer therefore is reduced. In this case alternative methods must be applied to evaluate the training effect of FES in the target muscle (Quadrizeps).

Material and Methods

1. Palpation

A scanner galvanometer system with a lever and an exchangeable skin interface (spherical pin with

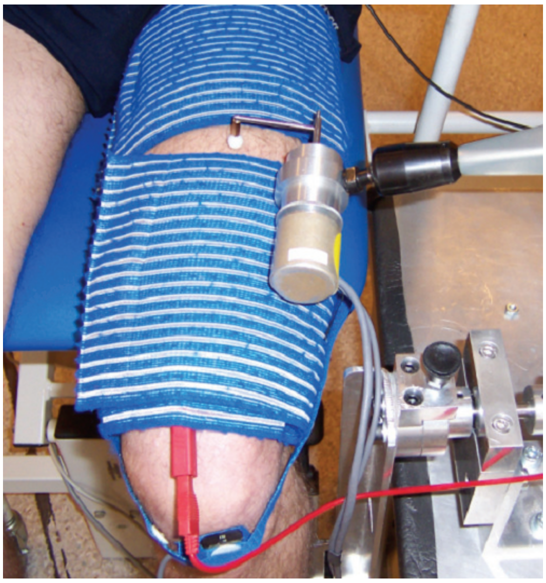

Fig.1 Galvanometer scanner at the m. rectus fem.

Additional to the indentation measurement the high dynamic range of the integrated angle sensor (26mm range, 200nm resolution with the 50mm lever) makes the device suited for high sensitive twitch recordings with adjustable preload [6].

10mm in diameter) was applied over the muscle belly (Fig.1). The actuator is driven by a PC-controlled constant current amplifier. Performing ramp force profiles (0-3N) the measured displacement of the skin shows typical compliance curves for biological tissues. The slope of the plot F=f(D) is defined as the transversal stiffness that steepen with FES. Adjusting a certain preload an optimum of the correlation between stiffness and force can be found [5]. The stimulation amplitude was increased up to 80V (160Vpp) in steps of 10% and the results were compared to the stiffness without stimulation.

2. Oscillation tonometry (pendulum test)

Apart from the problem of co-contraction in long term denervated muscles the force output is too small to be detectable by a conventional measurement technique at the beginning of FES training. A pendulum test was applied to evaluate FES induced joint moments. Former oscillation measurements were focused to the neuromuscular complex. For the clinical use and for a mobile application respectively two different pendulum systems were developed.

The active system [7] integrates a moment controlled torque motor that allows to compensate FES-induced output torques as well as the weight of the leg for knee angles greater then 90°.

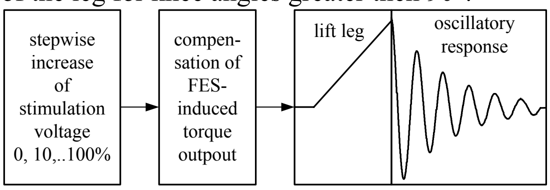

The mobile system is designed as a passive device where the oscillations are kicked on manually (Fig.2). The preferred application is focused at the beginning of FES training where the static output torque is very low.

Fig.2

In a second mode the lever arm is looked in a specific angle position in order to measure the isometric force output in a trained patient.

A 2nd order dynamical model was applied to extract the elastic and viscous moments from the recorded leg oscillations. This model provided an almost adequate description of the relaxed and FES contracted states.

$$J\ddot{\varphi} + D(\varphi,t)\dot{\varphi} + C(\varphi,t)\varphi + mgl_c \sin\varphi = 0 \quad (1)$$

In (1) J denotes the inertial moment of the leg and the manipulandum, D the lumped viscous moment, C the lumped elastic moment, m the mass of the lower leg, g the acceleration due to gravity and l_c the centre of mass from the knee axis. Parameters m, l_c and J are computed from an anthropometric model of leg and foot and the manipulandum mechanics.

3. Patella Tendometry:

Isometric twitch contractions recorded at the patellar tendon between their insertions at the patella and the tuberosity of the tibia respectively are determined by the force output of the quadriceps regardless of the hamstrings activity.

At the middle of the tendon the sinew is pressed toward the intrapatellar fat body (Fig.3). Due to this displacement a triangle of forces is built. The (longitudinal) force vector Fm in the tendon is represented by the transversal force component Ft.

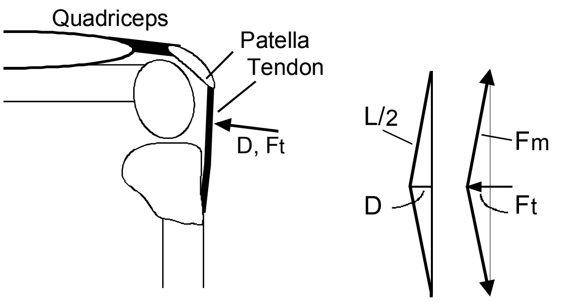

Fig. 3
In the presence of a tendon force **Fm** a transversal force **Ft** is necessary to produce a displacement **D**. With L is the length of the tendon: **Ft = Fm * 4D/L**

As L, the aponeurosis of the tendon and the underlying tissue (Connective tissue and fat that counteracts partly to Ft) vary from individual anatomical conditions, different preloads are necessary to obtain a certain value of D. Therefore this method is more focused on the dynamic properties analysing the shape of the force twitch rather then the absolute force amplitude. The twitch responses are elicited by a single electrical stimulation pulses with various amplitudes and pulse widths and can be measured either by a displacement sensor (e.g. galvanometer scanner) or a force transducer (lower part in Fig.1).

Long term denervation results in a slower contractility compared to healthy or FES-trained muscles. In order to classify the twitch responses a set of parameters are analysed.

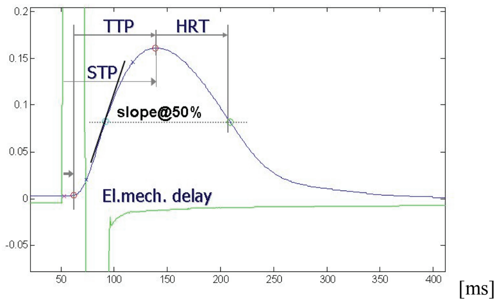

Fig.4. Electromechanical delay (EMD) from the FES stimulus to the onset of the twitch curve, Stimulus-to-Peak (STP), Time-to-Peak (TTP), Half-Relaxation-Time (HRT) and (normalised) slope of the force@50% are analysed from the contour of the twitch.

Recordings were made at stimulation amplitudes from 10-100% in steps of 10% (100%= 160Vpp, biphasic pulse) each with various pulse widths (1, 5, 10, 20, 40, 80, 120 160ms). The short pulses are used to detect possible re-innervations of the denervated muscle.

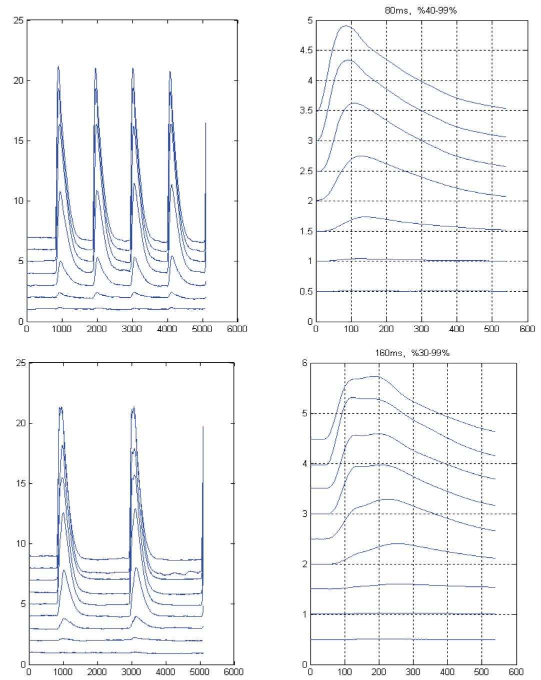

Fig.5 Twitch recordings from the patellar tendon: Typically force development (slope, TTP) becomes faster with higher stimulus amplitudes (upper trace). For very long pulses widths (>80ms) in contrast to the untrained muscle the maximum of the twitch of a FES-trained muscle may become separated into two peaks (lower trace). In this case the slope of the curve is the more better parameter then TTP to describe the muscle dynamic.

Results

Oscillation tonometry: the pendulum system showed very helpful to detect the weak contractile capacity of long term denervated and degenerated muscles. Some of the main findings with this system are:

- There is no contracture in passive degenerated muscle tissue
- FES rather results in muscle stiffening than in output torque at the beginning of the training
- Stiffening at low stimulation levels indicates disorientation of sarcomers
- Stiffening at high stimulation levels additionally induces co-contraction
- With denervation time muscle fatigue drastically increases

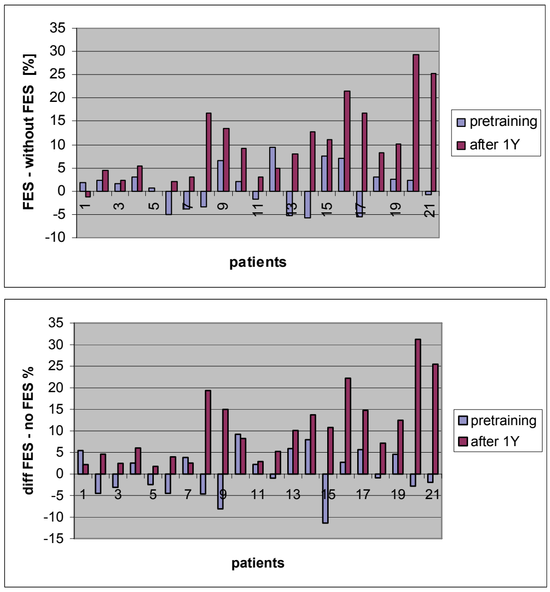

Fig. 6 Results of FES training for the pendulum test

The bars in Fig. 6 show relative changes (without FES – with FES) for muscle stiffness (upper diagram) and viscosity (lower diagram). The zero line represents the mean value of the pre training results (left bar). The right bars show the parameters after one year of FES training.

Twitch recordings: varying the pulse width of the stimulus the state of the degeneration or regeneration respectively can be elicited as the degenerated muscle needs much longer pulses than a trained one. Looking at the amplitude of the twitch we found, that in general for the FES trained patients the same twitch output was achieved with shorter pulses.

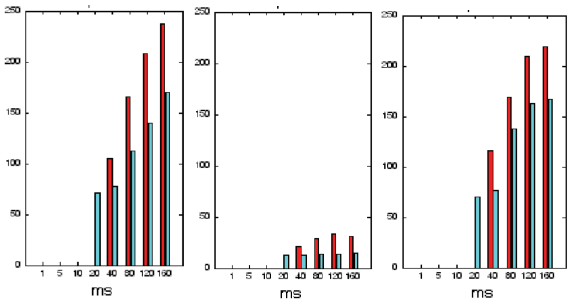

Fig.7 Typical values of TTP, EMD and HRT (from left to right) before training (left bars) and after one year FES (right bars) at different pulse width.

Discussion

A new test system based on the pendulum test was developed for the RISE-project. The application of the pendulum test showed very sensitive to detect FES-induced elastic and viscous moments, specifically in subjects from which no torque output was produced.
Comparing the results of the initial measurements [7] and the 1-Year control measurements it is obvious that the training of the quadriceps muscle by FES clearly increases joint stiffness and the viscosity. Here we could find that the viscosity is the more sensitive parameter.
Twitch responses at the patellar tendon became faster due to FES training indicating restructuring of the contractile apparatus in the denervated muscle.
The twitch response on the muscle belly often showed a change in the typical pulse contour. The reason is that in an isometric contraction task the change in the muscle diameter is not as clear as in a free contracting muscle. Depending on the anatomy and the stretch behaviour of the muscle, in some cases even inverse pulse were recorded. So in our investigations of the contraction dynamics we mainly are focused on the patella twitch.
The increase in the hardness of the muscle measured by palpation of the muscle belly was found in a good correlation with the evaluated static torque values. Most of the improvement happened during the first year of training.
In future data analysis we will also refer to the CT-scan pictures in order to model a relation between longitudinal (Patella), transversal (belly) twitches and transversal muscle stiffness.

References

[1] Mayr W., Hofer C., Bijak M., Lanmüller H., Rafolt D., Reichel M., Sauermann S., Unger E., Kern H.: EU-Projekt RISE, FES denervierter Muskulatur. Biomed. Technik 48 (Suppl.1), 2003, 52- 53

[2] Walsh E.G.: Muscles, Masses & Motion, Physiology of Normality, Hypotonicity, Spasticity & Rigidity. Mac Keith Press, USA, 1992

[3] Wartenberg R.: Pendulousness of the leg as a diagnostic test. Neurology 1, 1951, 18-24

[4] Badj T., Vodovnik L.: Pendulum testing of spasticity. J. Biomed. Eng. 6, 1984, 9-16

[5] Rafolt D., Gallasch E., Fend M., Bijak M., Lanmüller H., Mayr W.: FES Induced Surface Muscle Stiffness Captured by Computer Controlled Tonometry. Artificial Organs 26(3): 244-247, 2002

[6] Rafolt D, Gallasch E.: Surface myomechanical responses recorded on a scanner galvanometer. Medical & Biological Engineering & Computing Vol 40: p.594-599, 2002

[7] Gallasch E., Rafolt D., Fend M., Kern H., Mayr W..: Evaluation of FES-induced elastic and viscous moments in paraplegics with denervated muscles. Artificial Organs, 29 (3) 207-211, 2005

Acknowledgements

Supported by the European Union, Grant RISE EC/QLG5-CT-2001-02191

Author's Address

Dietmar Rafolt, PhD
Center of Biomedical Eng. and Physics,
Medical Univ. Vienna,
dietmar.rafolt@meduniwien.ac.at
www.bmtp.meduniwien.ac.at

CHANGES IN CONDUCTION VELOCITY AND RECOVERY OF DENERVATED MUSCLE FIBERS

Hofer C[1], Forstner C[2], Mödlin M[2], Mayr W[3], Kern H[1, 2]

[1] Ludwig Boltzmann Institute of Electrical Stimulation and Physical Rehabilitation, Vienna, Austria

[2] Department of Physical Medicine and Rehabilitation, Wilhelminenspital Wien, Vienna, Austria

[3] Center for Biomedical Engineering and Physics, Medical University Vienna, Austria

Abstract

Long-term denervation of a muscle after conus cauda or cauda equina lesion causes structural, electrophysiological and biomechanical changes of the muscle.

To assess changes of the electrophysiological properties of long-term denervated muscle fibres, conduction velocity and shortest inter-stimulus interval were studied using needle stimulation (single and double pulses) and needle EMG recording.

In the examined patients a markedly decreased muscle fibre conduction velocity (MFCV, 1.0 – 2.1 m/s) compared to healthy muscle (3.5 m/s) was measured before start of electrical stimulation training. After two years of training with functional electrical stimulation MFCV was increased but not reaching standard values (2.2 – 2.4 m/s). The shortest inter-stimulus interval (ISI) showed a decrease (from 4.0 – 8.0 ms to 3.3 – 3.0 ms). This indicates that the muscle fibre membrane recovers faster after depolarisation, when having been stimulated for a prolonged period of time.

The findings give evidence that therapy of denervated muscle with electrical stimulation is able to reverse denervation related changes in the electrophysiological parameters MFCV and shortest ISI after denervation to near normal values.

Introduction

Studies of muscle fibre conduction velocity (MFCV) have been conducted by several research groups in the last decades. In contrast to nerve conduction studies and invasive electromyography (EMG), measurement of MFCV is not routinely used as diagnostic tool in neuromuscular disorders. One reason might be that usually used techniques are time consuming and difficult to handle. Nevertheless the influence of several neuromuscular diseases on MFCV has been studied [1, 2, 3, 4].

There are non-invasive and invasive methods used for measuring the MFCV. To determine MFCV by non-invasive methods, surface recording electrodes are placed above the investigated muscle and the patient is asked to contract the muscle voluntarily [1, 5]. Invasive measurement is performed by using single fibre needle electrodes [4, 6, 7, 8], monopolar needles [9] or concentric needle electrodes [1, 10]. This technique can be carried out with voluntary activation of the muscle or with intramuscular electrical stimulation.

The measurement setup using intramuscular electrical stimulation permits the determination of a second parameter, the shortest inter-stimulus interval (ISI) of double pulse stimulation, where still a response to the second stimulus is elicitable [4]. This shortest ISI provides information about the electrophysiological recovery of the muscle fibre membrane after discharge by an action potential.

In this work we investigate MFCV as well as shortest ISI in patients with chronic denervation of the quadriceps muscle due to a lesion of the conus cauda or cauda equina before and after 2 years of training with functional electrical stimulation (FES).

Material and Methods

Patients

Three patients with permanent lower motor neuron lesion and completely denervated thigh were selected from the patient group participating in the RISE study [11]. The patients were examined at the time of inclusion in the RISE study before application of any stimulation training and again after two years of regular FES training.

FES training of the quadriceps muscle was performed by the patients five times a week for 20 – 30 min per day. At the beginning biphasic rectangular impulses of up to 150 ms were used that were later - with improved excitability of the denervated muscle - gradually reduced down to a pulse width of 40 ms. In this later phase a stimulation frequency of 20 Hz was achievable to elicit tetanic contractions. The patients carried out the FES training at their homes [12].

Before onset of the stimulation training the patients were denervated for 0.8, 1.2 and 3.2 years.

The study was approved by the local ethical committee (vote no.: EK-02-068-0702) and all examinations were performed after obtaining informed written consent from the patients.

Measurement method

To study MFCV and ISI in the paralysed muscle an invasive needle based technique was chosen. The method used is similar to the one v. d. Hoeven used in the biceps muscle [1]. Accurate needle placement was crucial and sometimes not easy to achieve because of the severe muscle atrophy. The recordings were conducted with the patient lying in supine position with the legs extended. In each patient stimulation and recording needle electrodes were repositioned three times in order to examine different parts of the muscle.

Stimulation

In order to deliver the stimulus to the denervated muscle fibres a monopolar needle with an active area at the tip of 5 mm^2 (Medtronic, Skovlunde, Denmark, Ref. No. 9013R0232) was inserted into the vastus intermedius muscle. The needle was positioned about 10-15 cm proximal to the upper edge of the patella on the connection line between the spina iliaca anterior superior and the centre of the patella. The indifferent stimulation electrode with a size of 3 x 3 cm was placed 2 cm proximal to the needle electrode on the thigh surface. For activating the muscle fibres in the immediate vicinity of the needle tip symmetric biphasic rectangular impulses with a duration of 100 µs (50 µs each phase) were applied with a constant voltage stimulator. MFCV and shortest ISI were measured by applying single pulses and double pulses with inter-stimulus intervals between 15 and 1 ms, shortened stepwise by 1 ms (Fig. 1).

Recording

A concentric recording needle electrode (Medtronic DCN37, Ref. No. 9013S0031) was inserted into the muscle about 3 cm distally to the stimulation needle electrode. Placement of both needles perpendicular to the skin and parallel to each other is crucial to obtain valid MFCV data. After inserting the recording electrode the stimulator delivered single stimuli with a frequency of 1 Hz, whereas the recording needle was repositioned until reproducible polyphasic potentials were recorded. The recorded signals were pre-amplified (v = 100) and bandpass filtered (13 Hz – 11 kHz) before being digitised via 12 bit A/D-converter at a sample rate of 50 kHz and stored for off-line analysis.

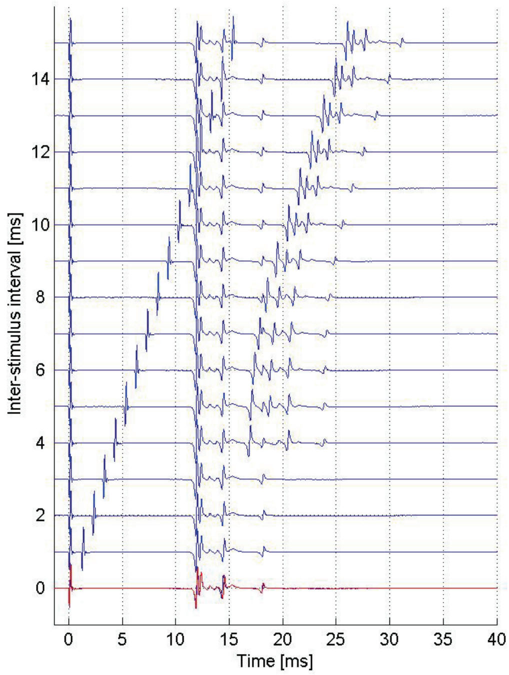

Fig. 1: Recording sequence to determine the shortest inter-stimulus interval (ISI). From top to bottom trace the ISI between the double pulses is stepwise reduced from 15 to 1 ms. The last trace shows two superimposed recordings of responses to a single stimulus. In this example recorded in a patient denervated for 0.8 years the shortest effective ISI is 4 ms.

Results

MFCV was assessed by measuring the latency between the initial slope of the stimulus and the positive peak of each individual recorded action potential (AP) larger than 50 µV. For each recording the maximum, minimum and the mean MFCV of all recorded fibres (APs) were calculated (Fig. 2).

MFCV and ISI before FES training

At the time of inclusion into the RISE study without prior FES training the patients showed a mean MFCV of 2.14 m/s, 1.97 m/s (0.8 and 1.2 years denervated) and 1.0 m/s (3.2 years denervated). The shortest ISI with second response was 4 ms, 4.2 ms (0.8 and 1.2 years denervated) and 8 ms (3.2 years denervated).

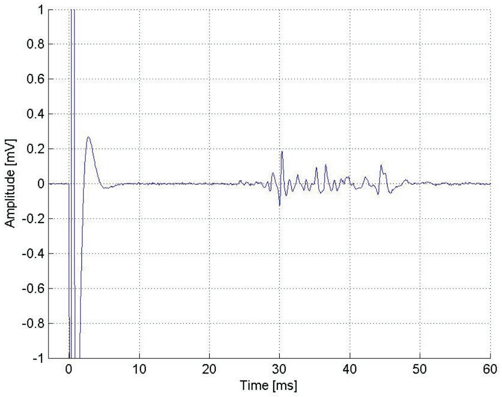

Fig. 2: Response to a single stimulus from a patient denervated for 3.2 years at the time of inclusion into the study prior to stimulation training. The first spike at 0 ms is the stimulus artefact. Mean MFCV of all recorded fibres was 1.0 m/s. Distance between stimulation and recording electrode was 34 mm.

MFCV and ISI after 2 years of FES training

After two years of FES training according to the therapy protocol of the RISE study the patients were examined again. Mean MFCV post FES training was 2.44 m/s, 2.26 m/s and 2.01 m/s (0.8, 1.2 and 3.2 years denervated before start of FES training). The shortest ISI was 3.3 ms, 3.2 ms and 3.0 ms (Table 1).

Patient			P1	P2	P3
Denervation Time		yrs	0.8	1.2	3.2
before FES	MFCV				
	mean	m/s	2.14	1.97	1.00
	max.	m/s	2.34	3.65	1.18
	min.	m/s	1.53	1.12	0.77
	ISI	ms	4.0	4.2	8.0
after FES	MFCV				
	mean	m/s	2.44	2.26	2.22
	max.	m/s	3.19	3.20	3.05
	min.	m/s	1.77	1.02	1.59
	ISI	ms	3.3	3.2	3.0

Table 1: Results of the measurements before and after 2 years of stimulation training. Denervation time is defined as the period between onset of denervation and start of FES training. Data of three patients from the RISE study.

Discussion

MFCV and ISI are two additional parameters characterising denervation related alterations in the skeletal muscle. Measurement of these parameters by stimulation needle EMG allows to monitor electrophysiological changes in the muscle fibre membrane that occur and develop after denervation that are strongly influenced by regular FES training.

In contrast to other studies [1, 6] placement of the recording needle was not guided by a visible or palpable muscle twitch because the few activated fibres are lying underneath a thick layer of subcutaneous fat and the contractions elicitable by needle stimulation are mostly too weak for reliable palpation tests (Fig. 3).

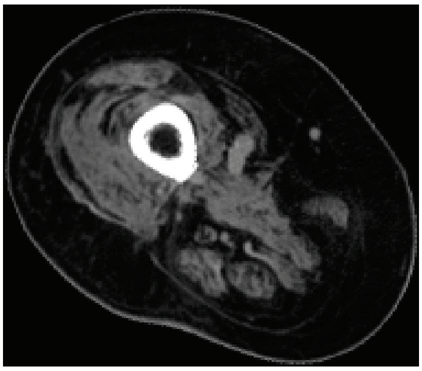

Fig. 3: CT-scan showing the cross section of the right thigh 20 cm distal to the trochanter major. The patient was denervated for 3.3 years.

Sometimes movement of the stimulation needle indicates the fibre orientation and helps to position the recording needle.

The inter-individual differences in MFCV and shortest ISI before FES training are most probably caused by the different periods of denervation (0.8, 1.2 and 3.2 years). Apart from electrophysiological parameters like the resting membrane potential [2], the muscle fibre diameter is the major influence on the conduction velocity [12], suggesting that the degree of muscle atrophy and the conduction velocity are closely related.

Furthermore it seems plausible that mainly the progressive changes of the muscle fibre membrane properties after denervation are responsible for the slow recovery of the muscle fibre after depolarisation. This leads to a prolonged refractory period of the muscle fibre which is reflected in the increase of the measured shortest effective ISI.

After two years of electrical stimulation training the patients showed improvements in almost all measured parameters. This gives evidence that electrical stimulation therapy is effective to reverse the denervation related degenerative changes in the human skeletal muscle at least in part.

References

[1] van der Hoeven JH, Zwarts MJ and van Weerden TW. Muscle fiber conduction velocity in amyothrophic lateral sclerosis and traumatic lesions of the plexus brachialis. *Electroenceph Clin Neurophysiol,* 89: 304-10, 1993.

[2] Gruener R, Stern LZ and Weisz RR. Conduction velocities in single fibers of diseased human muscle. *Neurology,* 29: 1293-7, 1979.

[3] Cruz-Martinez A, Arpa J. Muscle fiber conductionvelocity in situ (MFCV) in dernervation, reinnervation and disuse atrophy. *Acta Neurol Scand,* 100: 337-40, 1999.

[4] Mihelin M, Trontelj JV and Stålberg E. Muscle fiber recovery functions studied with double pulse stimulation. *Muscle Nerve,* 14: 739-47, 1991.

[5] Sollie G, Hermens HJ, Boon KL, Wallinga-de Jonge W, Zilvold G. The measurement of the conduction velocity of muscle fibers with surface EMG according to the cross-correlation method. *Electromyogr Clin Neurophysiol,* 25: 193-204, 1985.

[6] Cruz Martinez A. Conduction velocity in human muscle fibers in situ. Study in upper and lower limbs in healthy adults. *Electromyogr Clin Neurophysiol,* 29:363-8, 1989.

[7] Trontelj JV and Stalberg E. Responses to electrical stimulation of denervated human muscle fibres recorded with single fibre EMG. *J Neurol Neurosurg Psychiatry,* 46:305-309, 1983.

[8] Troni W, Cantello R and Rainero I. Conduction velocity along human muscle fibers in situ. *Neurology,* 33:1453-9, 1983.

[9] Chino N, Noda Y and Oda N. Conduction study in human muscle fibers in situ- A useful technique for diagnosing myopathies. *Electromyogr Clin Neurophysiol,* 58:513-6, 1984.

[10] Buchthal F, Guld C and Rosenfalck P. Propagation velocity in electrically activated muscle fibers in man. *Acta Physiol Scand,* 34:75-89, 1955.

[11] Mayr W, Hofer C, Rafolt D, Bijak M, Lanmüller H, Reichel M, Sauermann S, Unger E. The EU-Project RISE: General overview and engineering aspects. Proceedings of the 8th Vienna Inernational Workshop on Functional Electrical Stimulation 2004; ISBN 3-900928-07-9.

[12] Mödlin M, Forstner C, Hofer C, et al. Electrical Stimulation of Denervated Muscles – First Results of a Clinical Study. *Artif Organs,* 29(3):203-6, 2005.

[12] Håkansson CH. Conduction velocity and amplitude of the action potential as related to circumference in the isolated fibre of frog muscle. *Acta Physiol Scand,* 37:14-34, 1956.

Acknowledgements

This research was supported by **EU** Commission Shared Cost Project RISE (contract QLG5-CT-2001-02191) and the Austrian Ministry of Science.

Author's Address

Christian Hofer

Ludwig Boltzmann Institute of Electrical Stimulation and Physical Rehabilitation
Wilhelminenspital Wien
Montleartstraße 37
A-1171 Wien, Austria

christian.hofer@wienkav.at

COMPARISON OF FEMUR BONE DENSITY, MUSCLE SIZE AND MECHANICAL PROPERTIES BY DENERVATED AND DEGENERATED THIGH MUSCLES

Helgason T[1], Gargiulo P[1], Vatnsdal P[1], Ingvarsson P[2], Gudmundsdottir V[2], Knutsdottir S[2], Yngvason S[2]

[1] Dep. of Research and Development, HTS, Landspitali-Uni. Hosp., Reykjavik, Iceland

[2] Dep. of Rehabilitation Medicine, Landspitali-Uni. Hosp., Reykjavik, Iceland

Abstract

The purpose of this work is to compare density changes of the femur bone with changes in thigh muscle size and their mechanical properties in paraplegic patients with denervated and degenerated muscles treated with electrical stimulation.

In a European project RISE (QLG5-CT-2001-02191) a novel method for treating denervated degenerated muscles has been developed. Muscle fibres are directly stimulated electrically with higher current intensities than are recommended in international standards and are available in current commercial simulating devices.

To monitor this treatment, that is changes in muscle, bone and other tissue volume, shape and density a method has been developed using spiral computer tomography (CT). Thereby the thigh is scanned from the hip joint to the knee joint with 1,25 mm thick slices. The three Icelandic patients participating in the RISE project are scanned regularly every four months during electrical stimulation therapy. From this information a three dimensional models of muscles, bones and other tissue are made. Comparing the models the tissue changes can be detected.

A second method to monitor the electrical stimulation therapy of the DDM thigh muscles is using the pendulum test. A second order model is developed for the knee joint with associated thigh muscles. From that model parameters are evaluated for each patient from measurement taken at the same time as the CT scans, that is three times a year during the electrical stimulation therapy. Changes in the parameters show therapy progress.

The results show that changes in bone mineral density correlate with changes in muscle size and force. In areas where mechanical strain in the bone can be expected from muscle activity a slight increase in bone density is measured in the most compliant patient. In the other patients this cannot bee seen and the bone remains unchanged or continues to loose density.

Three patients, with different therapy compliance where measured over a period of three years. Results indicate that a change in muscle activity correlate with changes in bone mineral density.

Introduction

Spinal cord injured (SCI) patients with a lower motor neuron lesion suffer from degeneration of muscles below the injury. This is due to inactivity, as the muscles are never contracting. In comparison paraplegic patients with an intact lower motor neuron tend to develop spasm, activated through the motor neuron and the muscles do contract but without control. This muscle activity means that they do not degenerate to the same extent, as do the denervated muscles. Blood flow and metabolism are also enhanced. Because of the total inactivity of the denervated and degenerated muscle (DDM) other tissue types suffer. Thinner skin, lower capillary density, lower bone mineral density is the consequence. One side effect of this is decubitus ulcer with a high risk of infection, which in turn is one of the causes for a high mortality in the population of SCI people. Another side effect is bone fracture. Due to lower bone mineral density (BMD) the strength of the bones in the sublesional area is diminished and risk of fracture is increased substantially. The risk is further increased through the absence of sensibility and inability to react on mechanical interrupts. Bone fracture in turn can have severe consequences for the patient's health including inflammatory processes. Since the incidence of SCI is most frequent by young people and the survival rate in accidents has become much higher in recent decades, raising these patients quality of life is highly motivated. Up to now there is no treatment for DDM patients that restore their muscle mass or bone strength or reverses the process of degeneration of this tissue types. Drug therapies of muscle or of bone remain deficient. Physiotherapeutic treatment also does not stop or reverse the degeneration. The main treatment of these patients addresses the side effects like ulcer or bone fracture. These can be very difficult to treat because of low blood flow and in general low metabolism in the degenerating area. It is not unusual that a decubitus ulcer is open for several years.

In the RISE project a new method has been developed for DDM patients based on electrical stimulation [3, 4]. Since the lower motor neuron is not intact anymore and there is no connection to neural tissue the muscle fibbers are directly stimulated. Skeletal muscle tissue is normally not as sensible to electrical stimulation as is the motor neuron and by DDM sensibility is further reduced. The average diameter of the muscle fibber population is reduced, some fibbers seemed to be without contractile elements and need higher current density in order to depolarise the muscle fibber membrane. This requires current intensities that are two or three order of magnitude higher than used by normal neuromuscular stimulation.

The RISE therapy has shown that a DDM can regain its former size and force [1, 4]. The capillary density in the skin increases and its appearance becomes healthier. This has a great psychological effect on the patient. In this work we compare changes in femur bone density with changes in muscle size and changes in mechanical properties of the knee joint during electrical stimulation therapy over the past 3 years.

Material and Methods

Subjects

Three patients where treated in the RISE project in Iceland. Table 1 gives an overview of them. Time from accident to therapy beginning is called degeneration time and time from start of therapy to date is called the therapy time, not subtracting therapy stops. Both are given in years and months.

Table 1: Subject overview

Pat.	Born	Lesion	Time of accident	Therapy beg.	Deg. time	Ther. time
P1	1973	L1	Feb. 2003	Des. 2003	10m	3y, 2m
P2	1979	ThXI-ThXII	July 1999	Oct. 2003	4y 4m	3y, 5m
P3	1949	ThXII-LII	Jan. 1996	Oct. 2003	7y, 11m	3y, 5m

Patient 1 had the shortest time from accident to treatment and was therefore the one with the least degenerated muscles at therapy beginning. He was and is a hard worker and was very muscular at the beginning.

Patient 2 had severe atrophy at the beginning of therapy. He is of a corpulent type and not very muscular.

Patient 3 has the longest time from accident to therapy. He was a hard worker before but that could not be bee seen anymore on his thigh muscles.

Therapy

The patients are electrically stimulating for about two hours a day six days a week. In every session there are three different stimulation protocols done, one for warming up, one for tetanic training and one for small muscle fibre training. The quadriceps muscle group is each stimulated with two electrodes covering most of the skin area of the upper part of the thigh.

Therapy compliance is varying and complications come up that have stopped the therapy fore some weeks each time. This is the case for P1 and P3. P1 has stopped two times for 12 weeks; first summer 2005 and again summer 2006. P3 stopped for 12 weeks in the beginning of 2004, again autumn 2004 and the third time for some weeks in the beginning of 2005. P3 is very compliant but P1 and P2 are not up to now.

CT scan

A spiral CT scan is made three times a year, which is every four months to monitor the tissue changes. The scan starts above the femur head and continues down below the knee joint, with both legs covered by one scan. The scans are taken with a 0,625 slice increment resulting in about 750 to 1000 slices, depending on the patient’s size. Each slice has 512 x 512 pixels, and each pixel has a grey value in the Houndsfield scale of 4096 grey scale values, meaning that it is represented with a 12-bit value. A total data set from a single scan is therefore 512 x 512 x 750 x 12 = 2.36 GBit or around 300 MB. This data set gives a complete three-dimensional description of the tissue, including the muscles and bones in both upper legs.

The scans are made with 140 kV or 120 kV on the X-ray tube. For calibration a phantoms are used. It contains hydroxyapatite rods equivalent to 0, 75 and 150 mg/cm³ of calcium and solid and water filled plastic rods are used.

Processing of data

Each spiral CT scan gives one data set showing the tissue situation at the time scanning. From every data set the Femur bones and the Rectus Femoris Muscle for both legs are segmented (Software: Mimics from Materialise, Leuven, Belgium).

For the Femur bone a region of interest (ROI) is chosen as the area between a line 140 mm below the femur head and 100 mm above the knee joint.

The ROI is then processed. This area is segmented according to six Houndsfield unit intervals as shown in figure 1. This segmentation corresponds to going from the inside of the bone, with 150 HU for the trabecular bone with the lowest density, to the outside of the bone, with 1536 HU for the cortical bone with the highest density.

The volume of the Rectus Femoris Muscle is measured and its shape is evaluated. Figure 3 shows the results.

Knee Joint Mechanics

The mechanical properties of the thigh muscles where accessed with measurements of pendulum movements of the lower leg around the knee joint as described in [5] and [6]. The patient is sitting on a table with their lower leg hanging down ideally making a 90º angle to the upper leg. The lower leg is raised to about 20º from the equilibrium state and released to oscillate freely. This is done both without and with stimulation. The oscillation is recorded with a video recorder and processed in movement analysis software (KineView). For these oscillations a damping (B) and stiffness coefficients (K) are calculated. Results can bee seen in figure 2. They represent properties of the muscles and other tissue connected to the knee joint. During the therapy they change and give a tool to monitor the state of de- and/or regeneration of the muscles in the thigh.

Results

Fig. 1 through 4 shows some of the results from patient 2, as an example. In figure 1 it can be seen that the bone tissue with the highest density is increasing in the same time as the bone tissue with the next highest density is decreasing.

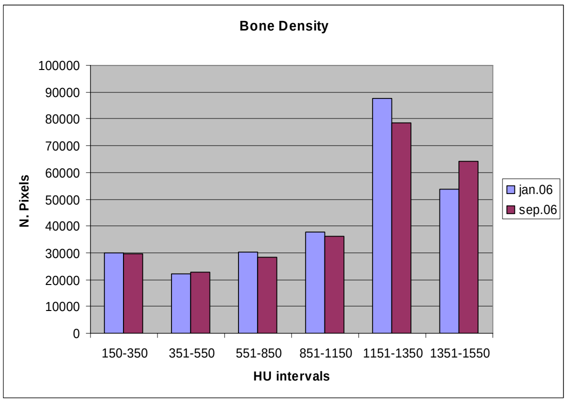

Figure 1: Number of pixels in six different HU intervals representing the femur bone is compared for the datasets taken in Jan. 2006 and Sept. 2006 for patient 2. They clearly show that almost no changes are in amount of bone tissue in the lower HU densities but that in the interval from 1151 to 1350 HU the amount of tissue is reduced and in the interval 1351 to 1550 the amount of tissue is increased.

Figure 2 shows an unchanged damping (B) of the oscillation around the knee joint but at the same time a rise in the stiffness (K) of about 10%.

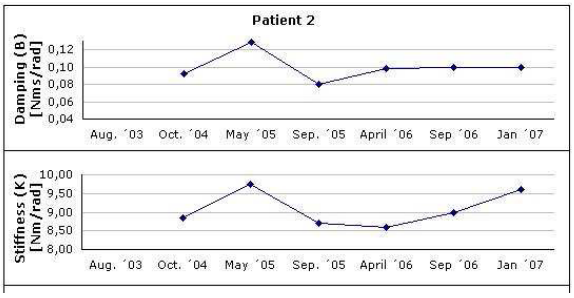

Figure 2: The damping factor (B) and the stiffness (K) knee joint of patient 2 recorded without stimulation. In the period of the last two years there is no change in damping but stiffness is constantly rising.

Figure 3 shows a 35% increase in the volume of Rectus Femoris in the year 2006 in respect to 2005. This is about the same time period as the results in figure 1. Patient 2 is relatively therapy compliant in this period as shown in figure 4. Figure 3 also shows an 85% increase in the volume over the whole therapy time form 2003 to 2007.

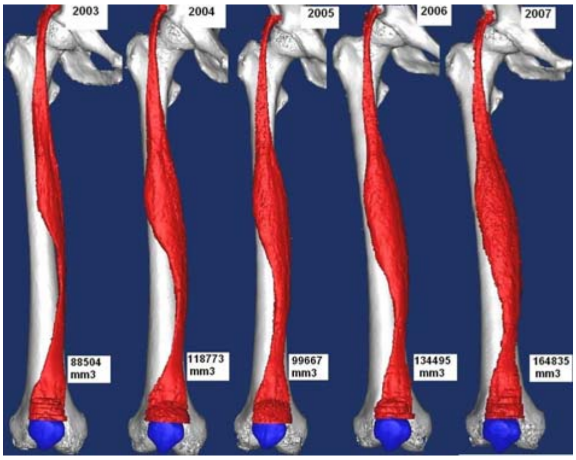

Figure 3: The left Rectus Femoris of patient 2 in front of the Femour bone. The increase in volume and changes in shape can clearly bee seen. The otherwise almost straight muscle between its fastening points forms a curve towards medial as a consequence of inactivity. The electrical stimulation therapy counteracts this development as can bee seen comparing the shape in the year 2003 with the one in 2007.

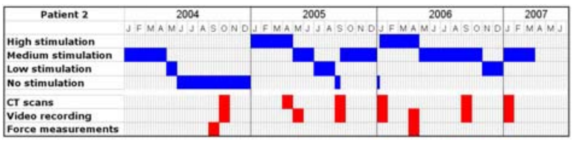

Figure 4: The therapy compliance of patient 2. High stimulation indicates that the stimulation scheme was applied 5 times or more in a week, medium stimulation

3-4 times, low stimulation 1-2 times and no stimulation 0-1 time a week. Red marks measurements instances.

Discussion

The data available from the three Icelandic patients has not all been processed. Anyway the results up to now and presented here give reason to the following thoughts.

The results shown in figure 1 suggest that some of the tissue that where in interval of 1151 – 1350 Hu before the therapy has increased its density and is after the therapy time in the interval 1351-1550 Hu. The increase of the later interval is as high as the decrease of the former. Increase in the cortical bone density by this therapy suggests that either a relatively little mechanical stimulus is sufficient for the increase or other factors also play a rule in this.

The increase in stiffness shown in figure 2 suggests that contractile elements, actin and myosin, connected to the knee joint are increasing as they account for the stiffness of the joint. This is confirmed by the results presented in figure 3 showing a big increase in volume of the Rectus Femoris Muscle and a change in shape towards a normal straight lined muscle. It can be expected that both factors contribute to the increased stiffness.

The Rectus Femoris Muscle lies nearer to the stimulating electrodes than the other muscles of the thigh. They did not increase their volume as much. The reason is the greater distance and fat tissue between them and the electrodes shunt some of the stimulating current making the therapy inefficient. This effect has to be considered in the future design of electrode geometry.

Figure 3 clearly demonstrates the effect of the stimulating therapy. The volume of the denervated and degenerated muscle increases 85% in four years by a patient that is not always compliant to the therapy as can be seen in figure 4.

The fact that not all the thigh muscles are experiencing an increase in volume and are some even degenerating further gives a good reason to reconsider the stimulating technique.

As a summary it can be said that due to the RISE therapy muscles grow in volume and force, their mechanical properties indicate this increases, there are evidences that bone density increases and all these things correlate in time.

References

[1] Kern H, Hofer C, Mödlin M, Forstner C, Mayr W, Richter W.: Functional electrical stimulation (FES) of long-term denervated muscles in humans: clinical observations and laboratory findings. Basic Appl Myol, 12: 291–9, 2002.

[2] Helgason T, Gargiulo P, Jóhannesdóttir F, Ingvarsson, P, Knútsdóttir S, Gudmundsdóttir V, Yngvason S.: Monitoring Muscle Growth and Tissue Changes Induced by Electrical Stimulation of Denervated Degenerated Muscles with CT and Stereolithographic 3D Modelling. Artificial Organs, 29(6): 440–443, 2005.

[3] Mayr W, Hofer C, Bijak M, et. al.: Functional electrical stimulation (FES) of denervated muscles: existing and prospective technological solutions. Basic Appl. Myol, 12: 287-90, 2002.

[4] Kern H, Boncompagni S, Rossini K, et. al.: Long-term denervation in humans causes degeneration of both contractile and excitation-contraction coupling apparatus, which is reversible by functional electrical stimulation (FES): a role for myofiber regeneration? J Neuropath Exp Neurol, 63: 919, 2004.

[5] Gallasch E, Rafolt D, Kinz G, Fend M, Kern H, Mayr W: “Evaluation of FES-Induced Knee Joint Moments in Paraplegics with Denervated Muscles”, Artificial Organs, 29 (3), pp 207-11, 2005.

[6] Palsdottir JL: “Design and Testing of a Method for Monitoring Treatment of Denervated Degenerated Muscles”, Master Thesis, University of Iceland, 2006.

Acknowledgements

This work was supported by:

Health Techonlogy Venue - HTV, The Icelandic Centre for Research, The Technical Innovation Fund – Rannis, The Research Fund of Landspitali, The Icelandic Student Innovation Fund,

Author’s Address

Dr. Thordur Helgason
Dep. of Research and Development,
Landspitali – University Hospital, Eiriksgata 5,
101 Reykjavik, Iceland
E-mail: thordur@landspitali.is
Home page: www.landspitali.is

DENERVATED DEGENERATED MUSCLE GROWTH INFLUECED BY FES: A NOVEL MONITORING METHODOLOGY BASED ON MUSCLE SEGMENTATION

[1]Gargiulo P, [1] Helgason T, [2] Ingvarsson P, [2] Yngvason S

[1]Department of Research and Development, HTS, Landspitali-University Hospital, Reykjavik - Iceland

[2]Department of Rehabilitation Medicine, Landspitali-University Hospital, Reykjavik – Iceland

Abstract

This paper describes a new method to monitor growth of fully denervated and degenerated muscles (DDM) treated with electrical stimulation (ES) in the lower extremities.

In the frame of the EU-funded RISE project three patients with a complete spinal cord injury of flaccid type are stimulated. The aim is to stop degeneration and enable muscle growth.

To monitor muscle growths a method based on muscle segmentation is developed. Spiral CT from the hip joint down to the knee joint is used to gather 3D data on the upper leg tissue. CT data are processed with special image processing software. A method to segment different muscle areas on the thigh was developed. In a certain region of interest the muscles bellies are represented by different 3 Dimensional masks. Selective follow up of muscle behaviour is made measuring mask volume and density estimation for every patient during the therapy.

The results demonstrates that degeneration stops in all muscle bellies when the stimulation therapy is carried out continuously and uninterrupted. Beside data shows that Rectus Femoris muscle is the most sensible to the stimulation.

The new technique allows a better monitoring of the RISE therapy providing qualitative and quantitative information on the muscle behaviour otherwise hidden.

Introduction

In the frame of the EU-funded RISE project, patients with lower motor neuron lesion and denervated and degenerated muscles are treated with electrical stimulation, with the aim of restoring muscle mass and force. It has been shown to be possible to build up mass, force, and function of long-term denervated and degenerated muscles with the use of electrical stimulation [1, 3].

Using large surface electrodes, quadriceps muscles from long term denervated patients are treated with functional electrical stimulation [5].

The goal of the electrical stimulation is to restore muscle fiber, mass and function. Moreover the developed muscle force should enable the legs to bear the patients weight allowing him to stand up and maintaining the standing posture, e.g., in bars, with the aid of electrical stimulation.

In order to reach and maintain these results, muscles are stimulated for up to two hours per day, six days a week, always.

As part of the RISE project, in Iceland, three paraplegic patients with fully denervated and to a great extent degenerated muscles in the lower extremities are treated with electrical stimulation. These patients with long-term flaccid paraplegia have no hope of regaining their muscle function. Traditional treatment only aims at side effects of the injury. Moreover, in comparison with patients with a spastic paraplegia, they often suffer more from several severe complications, e.g., decubitus ulcers, reduced bone density with a high risk of fractures, severe muscle atrophy with decreased circulation, lower metabolism, etc. Beside the clinical work, different monitoring methodologies are developed and applied to measure the therapy effects in quantitative and qualitative way. The treatment effects on the patients are monitored, e.g., by morphological and histochemical analysis of muscle biopsies as well as by clinical neurological, neurophysiological mechanical, and radiological methods [2, 3]. To follow changes in size and shape of the quadriceps muscle, computer tomography (CT) scans are taken at 10 cm intervals from the trochanter major to the knee [1]. A comparison of two scans taken at two different times at the same position shows the muscle growth in that specific place during the time period between the two scans. Comparing five scans, taken at 10 cm intervals, yields to estimate the total muscle growth and changes in fat and bone tissue. However, it does not show the growth of the whole muscle and is not enough to make a three-dimensional model of the muscle, bone, or other tissue.

In this paper a different approach to monitor muscle growth is described. A segmentation methodology was developed to monitor selectively muscle bellies. Repeated serial CT scans and special image processing software are used to create three-dimensional masks representing muscles bellies. Changes of muscle shape, volume and density are measured very accurately [4].

Material and Methods

CT scan

Every four months a spiral CT was taken of the RISE Study's Icelandic subgroup of three patients with a complete spinal cord injury of flaccid type.
The spiral CT scan starts above the head of the femur and continues down to the knee joint, both legs being covered by one scan. They are taken with a distance of 0.625 mm between slices, resulting in a total of about 750-900 CT slices, depending on the patient's size. Each slice has 512 $\times$ 512 pixels, and each pixel has a grey value in the Hounsfield scale of 4096 grey scale values, meaning that it is represented with a 12-bit value.
A total data set from a single scan is therefore 512 $\times$ 512 $\times$ 750 $\times$ 12= 2.36 GBit, approximately 300 MB. This data set gives a complete three-dimensional description of the tissue, including the muscles and bones in both upper legs.

Segmentation

CT scan data are imported into a special image processing and editing computer program called MIMICS [6]. In this software environment CT scan images are imported, organized and segmented. After importing the images, left and right legs are divided in two different projects and processed separately. This operation optimizes computer memory and processing capacities.
The muscles in the thigh are segmented in a defined region of interest. This is where the muscles are expected to be intensively influenced by the electrical stimulation. It starts 140 mm below the head of the femur and ends 100 mm above the knee joint.
CT scanned objects are coded in the Hounsfield scale which is a quantitative scale for describing X-ray attenuation properties of the tissue. Different HU values are ascribed to air, water, fat, bone and muscle. To isolate the muscle tissue from other tissues a threshold based on the HU values is defined: individual pixels are marked if their value is included in a certain HU interval. The HU interval chosen to allow clear differentiation and visualization of muscle volumes is [-37, 129] HU. A different threshold is defined to monitor number of voxels with normal muscle tissue density. Since the mean HU value for muscle is 40 HU, the interval chosen to measure and compare number of voxels with normal muscle tissue density is [20, 60] HU.
To allow selective and accurate monitoring of muscle changes the cross sectional area of the thigh is segmented in fours so called "Masks" (Fig 1, Left). The Masks are set of pixels with certain HU value. In the Region of Interest the four Masks represent the muscle bellies. To create these masks the muscles need to be isolated from each other. The main difficulty is given from the continuity between the muscles. Without a remarkable difference in terms of HU values, conventional segmentation tools are useless. The segmentation process is semi-automatic, based on the direct reorganization of the muscle bellies on the CT-Scan slide.
The different Masks are created in the following way: the initial slice is selected. A contour is drawn manually around the first muscle directly on the cross sectional area of the thigh. This operation allows isolating the muscle belly from the surrounding. Then all pixels having HU value inside a defined threshold interval and present in the muscle bellies area are marked. The shape created is projected on the next slice. If the muscle contour from the previous slice is not fitting the new one, a new shape is drawn around the muscle. All pixels are marked again and the contour projected forward. This process continues until all cross sections in the region of interest are covered.
The results from the segmentation on the thigh are four Masks (called M1, M2, M3 and M4) representing vastus lateralis and intermedius with M1, vastus medialis with M2, rectus femoris with M3 and the antagonist muscles with M4. (See Fig.1)

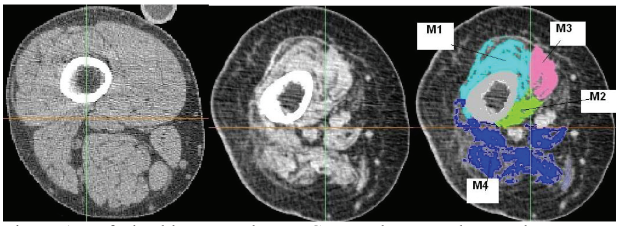

Figure 1: Left: healthy musculature. Centre: denervated musculature. Right: coded masks of muscle bellies.

3- Dimensional reconstruction of the thigh and visualization of the muscle bellies in the Region of interest is made for the three Icelandic RISE patients. (Fig. 2)

Measurement

Muscles are segmented at different point of time during the RISE therapy.

In every data set the volume from the four masks is measured. Changes are compared from time to time and correlate to patient compliance. Special attention is dedicated to measure and monitor the volume changes in Rectus Femoris because it is, generally, the muscle most influenced by FES. Fig

3 shows volume changes in Rectus Femoris during the therapy for the three patients.

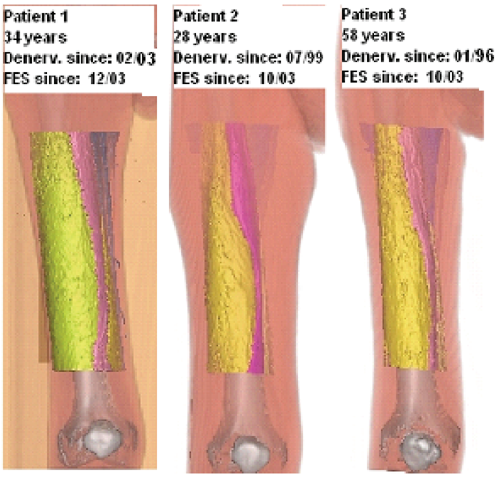

Figure 2: Patient Right leg, Volume Rendering

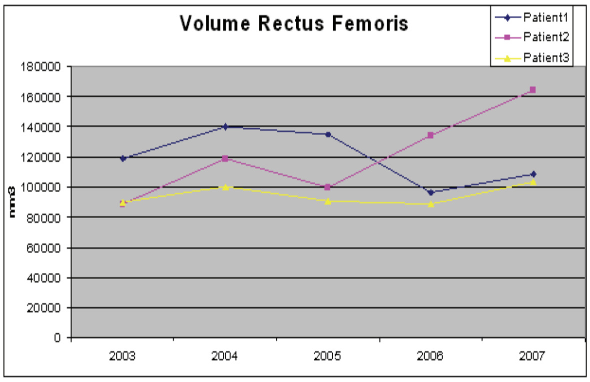

Figure 3: Volume changes in Rectus Femoris

To evaluate changes of density inside the muscles, the numbers of voxels in a certain HU interval are counted. The mean HU value for the muscle tissue is normally around 40 HU. Therefore the HU interval which is chosen to represent the denervated muscle tissue is [10, 60] HU. Finally the muscle density is evaluated by counting the number of voxels in this different mask.

Fig 4 shows the number of voxels, counted as described above, as an estimation of muscle density changes, in one patient, in comparison to the volume changes in Rectus Femoris during the therapy time.

Furthermore Rectus Femoris was completely isolated from other muscle bellies and reconstructed in three dimensions, then morphological changes were monitored during the FES treatment. In Fig. 5 a series of pictures shows the Rectus Femoris muscle at different point of time demonstrating the development of the shape from time to time due FES.

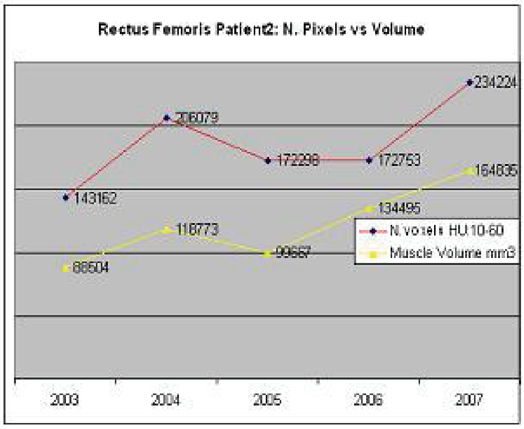

Figure 4: Patient 2. Rectus Femoris Volume vs N. of pixels

Results

The methodology developed in this work demonstrates to be a powerful tool for muscle monitoring. The result is a method which allows quantitative and qualitative measure on the degenerate muscle otherwise hidden.

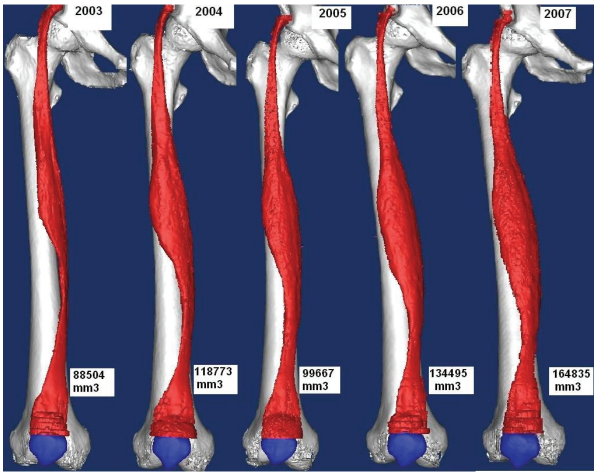

Figure 5: Patient 2, morphological changes in Rectus Femoris

The main achievement is the possibility to isolate and measure the whole muscle belly. The new method validates the RISE therapy thoroughly allowing correlation between volume, density and changes of muscle morphology. Beside it demonstrates that muscle growth is accompanied to the restoration of normal muscle shape (Fig.5).

The results from the measurement show that degeneration for denervated muscle can be stopped by electrical stimulation and even be reversed so that muscle mass increases.

The muscle growth depends strongly from the patient compliance. This fact is demonstrated clearly in Fig.6 where muscle growth is correlated with patient compliance. The therapy time is sorted out in three regime of stimulation: High stimulation regime where patient stimulates 5-6 times a week, Medium stimulation 3-4 times a week and Low stimulation 1-2 times a week. It important to notice how rapidly volume reduces when muscles are not stimulated or poorly stimulated.

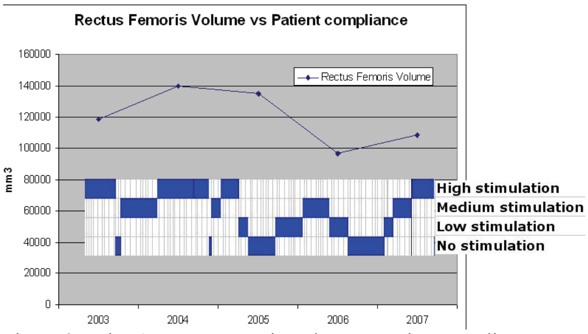

Figure 6: Patient1, Rectus Femoris Volume vs Patient compliance.

Due patient compliance and clinical history, the muscle growth is very different among patients. Following is a summary of the results:

1. Total muscle volume changes in the thigh in the period between December 2003 and January 2007 are: -16% for Patient 1, +20% for Patient 2 and +8% for Patient 3.

2. The total Volume changes in Rectus Femoris in the period between December 2003 and January 2007 are (see also trend line in Fig.3): +4% for Patient 1, +84% for Patient 2 and +20% for Patient 3.

3. In compliant patients the volume growth is accompanied with the restoration of muscle fiber which means muscles with higher counts of voxels in normal range of Hu values. This result is demonstrated in Fig.4 where volume and counts of normal voxels double during the therapy time.

- Number of Pixel from 143162 to 234224
- Volume from 88504 mm3 to 164835 mm3

Discussion

FES stops muscle degeneration and allow muscle growth in the regions where it is applied.
The new technique described in this paper improves monitoring of the RISE therapy and allows measures of volume and density selectively on the muscle bellys. The 3-dimensional reconstruction of the muscle, the measurement of volume and density estimation provides qualitative and quantitative information on the behaviour of the muscle in therapy otherwise hidden.
CT data from the three Icelandic RISE patients were processed with a new method. The results of this work clearly demonstrate muscle growth, both in term of volume and counts of voxels with normal density, and also the tendency of the muscle to restore a normal muscle shape.
In three years of stimulation, rectus femoris in patient most compliance has almost doubled its volume and voxels with normal density. The results from patient 2 show that though the stimulation is applied using large electrodes on the skin surface above musculus quadriceps the volume of rectus femoris has increased more than that of the other muscles. The explanation can be that the fat layer surrounding the other quadriceps muscles keeps a larger distance to the electrodes and decreases the stimulation effectiveness.
The muscle growth rate is of course influenced by patient compliance and by possible clinical problems affecting the patients during therapy. For instance, having to stop the stimulation for a few weeks can lead to the loss of a muscle mass previously gained over several months. It is crucial to correlate stimulation and muscle changes in order to understand how denervated musculature grows. Changes in volume and density at different regimes of stimulation should be measured for the same reason (Fig. 6). Segmentation of muscles can be a highly useful tool to perform such investigations.
Information from muscle segmentation contributes to the adjustment and improvement of the stimulation protocol, in changing electrode position or stimulation patterns. Furthermore this information on muscle behaviour is an important basis for new development such as: stimulator, electrodes and implantable devices.
Finally the segmentation process and monitoring methodology developed in this work is an accurate tool to validate the RISE therapy and provide a better understanding of denervated muscle behaviour.

References

[1] Kern H, Hofer C, Mödlin M, Forstner C, Mayr W, Richter W: Functional electrical stimulation (FES) of long-term denervated muscles in humans: clinical observations and laboratory findings. Basic Appl Myol 2002; 12: 291–9.

[2] Mayr W, Hofer C, Bijak M, et al.: Functional electrical stimulation (FES) of denervated muscles: existing and prospective technological solutions. Basic Appl Myol 2002; 12: 287–90.

[3] Kern H, Boncompagni S, Rossini K, et al.: Long-term denervation in humans causes degeneration of both contractile and excitation-contraction coupling apparatus, which is reversible by functional electrical stimulation (FES): a role for myofiber regeneration? J Neuropath Exp Neurol 2004; 63: 919–921

[4] Helgason T, Gargiulo P, Jóhannesdóttir F, Ingvarsson, P, Knútsdóttir S, Gudmundsdóttir V, Yngvason S: Monitoring Muscle Growth and Tissue Changes Induced by Electrical Stimulation of Denervated Degenerated Muscles with CT and Stereolithographic 3D Modeling. Artificial Organs 29(6) 2005:440–443

[5] Kern H., 1995. Funktionelle Elektrosimulation Paraplegischer Patienten, Österr. Z. Phys. Med. Heft 1, Supplementum

[6] Web site: www.materialise.com

Acknowledgements

This work has been supported by Health Technology Venue, Rannís – The Icelandic Centre for Research and The Icelandic Student Innovation Fund

Author's Address

Paolo Gargiulo, Biomedical Engineer.
Department of Research and Development, Landspitali University Hospital of Iceland
Ármuli 1a, 105 Reykjavik, Iceland.
e-mail: paologar@landspitali.is.
Gsm phone: 003548245384

FES OF LONG TERM DENERVATED, DEGENERATED HUMAN SKELETAL MUSCLE: ESTIMATING ACTIVATION USING T2-PARAMETER MRI METHODS

T. Mandl[1,2], M. Meyerspeer[1,2], M. Reichel[1], H. Kern[3], C.Hofer[3], W. Mayr[1], E. Moser[1,2]

[1]Center for Biomedical Engineering and Physics, Medical University of Vienna

[2]MR Centre of Excellence, Medical University of Vienna

[3]Ludwig Boltzmann Institute of Electrostimulation and Physical Rehabilitation, Department of Physical *Medicine, Wilhelminenspital Vienna*

Abstract

FES of long-term denervated, degenerated human skeletal muscle has proven to be a suitable method for improving a number of physiological parameters. The underlying mechanisms of activation of a denervated muscle fiber can be described with suitably modified and extended Hodgin-Huxley type models, coupled with 3D finite element models of the surrounding electrical field. Regions of activation within a muscle can be determined using a 3D computer model. However, simulation results have not yet been validated experimentally. During and immediately after exercise, muscle shows increased T2-relaxation times. It is thus possible to estimate muscle activation non-invasively and spatially resolved with the MRI method of T2-mapping, which was, therefore, chosen as a suitable validation approach. Eight patients were scanned prior to FES training with a MSME-sequence at 3 Tesla and then asked to perform one of their regular daily training-sessions (leg extensions). Subjects were then repositioned in the MR-scanner and two to five post-exercise scans were recorded. Pre- and post exercise scans were co-registered and T2-parameter maps were calculated. ROIs were drawn manually around quadriceps femoris and its antagonists. Activation was detected in all patients. In well trained patients, activation in the quadriceps was found to be considerably higher than in its antagonists.

Introduction

FES and Modeling

Paraplegic patients with degenerated, denervated muscle (DDM) have been successfully treated with Functional Electrical Stimulation (FES) in Vienna's Wilhelminenspital for more than a decade [1,2]. To establish better understanding of the underlying mechanisms of direct activation of denervated muscle fibers and to answer a number of optimization questions regarding FES parameters, a computer model of FES has been developed [3-5]. Results of the computer simulations are activation patterns showing where activation would occur, i.e. at locations of fiber endings and along the entire length of a fiber. Experimental validation of these results, however, has not yet been established.

T2-Mapping

The effect of an acute increase in human muscular transverse relaxation time (T2) immediately after exercise has been known for about two decades [6]. It has been used to study activation patterns in rehabilitation and sports medicine [7]. The exact underlying mechanisms mediating the effect are not entirely understood, however, a number of responsible factors have been identified and the individual T2-increase has been shown to correlate well with exercise intensity quantified as peak force or power. Increased T2 is observed under ischemic conditions [7] and can thus not be solely attributed to increased perfusion or blood oxygenation in exercising muscle regions. Both, changed osmolarity and pH due to the presence of metabolic end products and the shift of water between muscle compartments are considered the main contributors to the observed rise in T2-times [7]. T2-times are elevated for about 30-40 minutes after exercise and show approximately exponential decay towards T2 of resting muscle. MRI-methods allow the computation of T2-maps, showing the spatially resolved distribution of T2-times in the imaged volume.

T2-mapping has thus been chosen as a suitable means to study the activation patterns of FES of degenerated, denervated human skeletal muscle.

Material and Methods

The experimental protocol was submitted to and approved by a local ethics committee. Patients provided fully informed, written consent prior to the study.

Subjects and Protocol

Eight male paraplegic patients with DDM were included. For each patient, one pre-exercise scan was acquired. Then patients were asked to perform one of their regular daily training sessions in the magnet room. Immediately after exercise, patients were carefully repositioned (as exactly and quickly as possible) and 2-5 post-exercise scans were acquired. In total patients spent about 3 hrs at the MR-facility for one measurement session.

FES

Two large surface electrodes were placed over qudriceps femoris (QF). The electrodes were connected to a custom designed stimulator for denervated muscle [9]. Patients were sitting on the patient bed of the MR device at the farthest possible distance from the magnet bore, performing 6-7 sets of 15 leg extensions with 2-4 kg weights around the ankle. Leg extensions lasted for 2 s followed by a 2 s rest period. Stimulation frequency was 20 Hz with a (bi-)phasic pulse duration of 40 ms and 10 ms pulse pause.

MR Imaging

MR-images were acquired on a 3T Bruker Medspec whole-body NMR scanner (Bruker Biospin, Ettlingen, D) with a multi-slice multi-echo (MSME) sequence. Acquisition parameters were TE=25/50/75/100/125/150 ms, TR=3 s, 14 axial slices, 96x128 matrix size. A birdcage head-coil was used, covering about two thirds of the length of the thigh. To allow exact repositioning for the post-exercise scans, patients' positions relative to both, the coil and the patient bed were marked with a felt-tip pen. A MR-visible marker was used to record the electrode's center position on the patient's thigh and two external references with known T2 were included in the field of view. The tubes containing the reference material made no direct contact with patients' skin to avoid any temperature depending T2-increasing effects.

Post-processing and Analysis

The reconstructed multi-echo images were transferred to a desktop PC for further processing. Post-processing included a linewise background subtraction to correct for ghosting artifacts and a co-registration procedure using the minc-tools software (McConell Brain Imaging Center, McGill University, Montreal, Canada). Assuming mono-exponential decay, T2-times were fitted to the mutli-echo images on a pixel-by-pixel basis with a simplex-algorithm, producing T2-maps of the imaged region. Regions of interest (ROIs) were then drawn manually in the anatomical images for the muscles of QF and its antagonists and used for estimation of activation. Care was taken to exclude non-muscle pixels. No threshold for activation was defined; rather percentage change of T2 was used to estimate training effects. All post-processing steps were performed with either MATLAB or `ImageJ`.

Results

Elevated mean T2 values in post exercise scans were found in muscle ROIs. Increase in mean T2 was observed neither in the external references nor in fatty tissue. Fig. 1 shows axial T2-maps in one axial slice of one single patient in the pre-exercise and two post-exercise scans before co-registration.

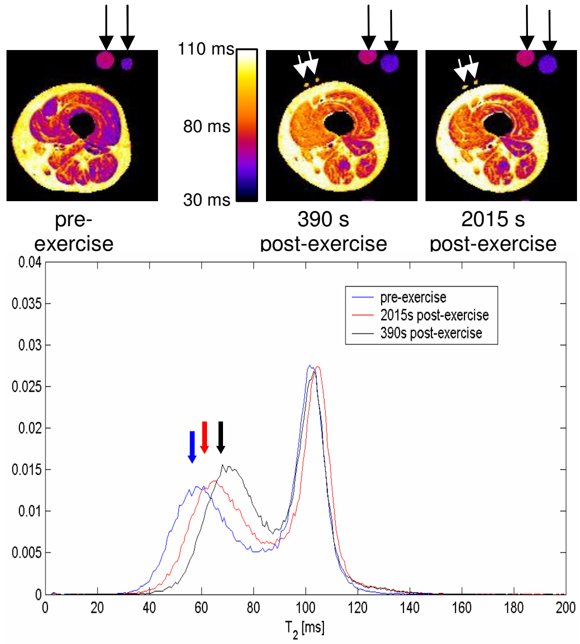

Fig. 1: One axial slice of one pre- and two post-exercise T2-maps of a male patient and the T2-histograms of the entire scans. The color-coded maps show T2-values between 30 and 110 ms, all other values are not shown (black). In the post-exercise scans both the markers for the electrode (white arrows) and the two external references (black arrows) can be seen. The histograms show a shift of the muscle peaks relative to resting muscle (blue). The position of the muscle peak in the second post-exercise scan (red) indicates the relaxation of elevated T2-times toward resting state.

The images also show the external references (black arrows) and, in the post-exercise scans, the marker for the electrode's central position (white arrows). The histograms calculated for the entire data-sets demonstrate the shift of the muscle peak, whereas the peak at about 105 ms, corresponding to T2 of fat, is unchanged between pre and post-exercise scans as well as between post-exercise scans. Mean T2 increase in QF was found to be in the range of 10 and 40 %. Fig 2 shows activation levels in rectus femoris (RF) along the length of the thigh in the first post-exercise scan.

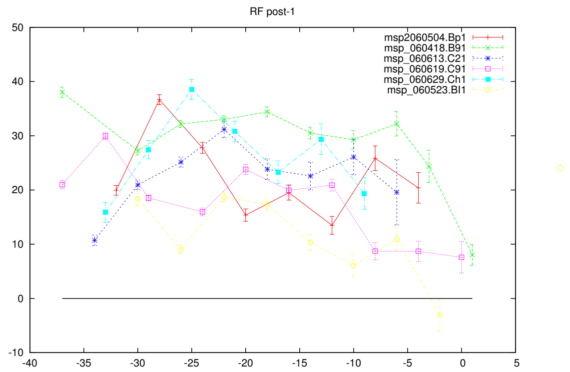

Fig. 2. First post-exercise scan activation levels [%] in RF across subjects along the length of the thigh. Profiles are aligned to contain the electrode marker at position x =0.

Mean T2 increase in the hamstrings was found to be in the range between 5 and 20 %. The activation profiles of biceps femoris (BF) along the length of the thigh in the first post-exercise scan are shown in Fig 3.

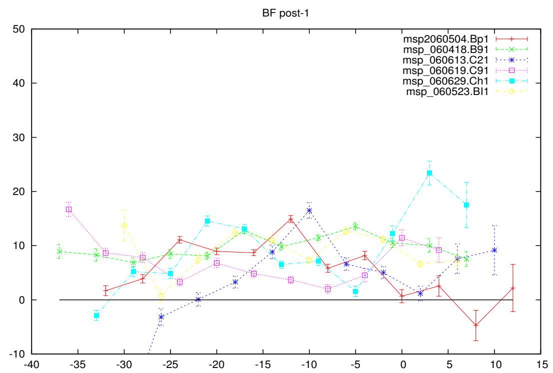

Fig. 3. First post-exercise scan activation levels [%] in BF across subjects along the length of the thigh. Profiles are aligned to contain the electrode marker at position x =0.

Discussion

We have used the method of high-field MR T2-mapping to estimate activation levels in degenerated, denervated human skeletal muscle. We could show that the effect of an acute increase of transversal relaxation time immediately after exercise is present in DDM after FES. Patients performed leg extensions exercises between pre- and post-exercise scans, which is reflected by the fact that activation levels in the leg extensor muscles are higher than those in the hamstrings. It has been observed before that knee-torque of well trained patients declines with an increase in amplitude due to co-contractions of the quadriceps' antagonists, an effect which is also present in our data, as activation could be detected in the hamstrings.

References

[1] Kern H, Funktionelle Elektrostimulation paraplegischer Patienten, Österr. Z. Phys. Med. Heft 1, Supplementum, 1995.

[2] Kern H, Hofer C, Mödlin M, Forstner C, Raschka-Högler D, Mayr W, Stöhr H, Denervated muscles in humans: limitations and problems of currently used functional electrical stimulation training protocols. Artif Organs 26: 216–218. 2002

[3] Reichel M, Funktionelle Elektrostimulation denervierter Skelettmuskulatur – Modellbildung und Simulation, (in German), Dissertation TU-Wien, 1999.

[4] Reichel M, Breyer T, Mayr W, Rattay F, Simulation of the three dimensional electric field In The course of functional electrical stimulation. Artificial Organs 26:252-255, 2001.

[5] Martinek J, Stickler Y, Reichel M, Rattay F, Analysis of Calculated Electrical Activation of Denervated Muscle Fibers in the Human Thigh, Artifical Organs 29; 444-447. 2005

[6] Fleckenstein AL, Canby RC, Parkey RW, Peshock RM. Accute effects of exercise on MR imaging of skeletal muscle in normal volunteers. Am J Roentenol 151:271–237. 1988

[7] P. Carolynn, M. Ronald A. and J. L. Fleckenstein. Seminars in Musculoskeletal Radiology, 7:297, 2003.

[8] Fisher MJ, Meyer RA, Adams GR, Foley JM, Potchen EJ. Direct relationship between proton T2 and exercise intensity in skeletal muscle MR images. Invest Radiol 25:480–485. 1990

[9] Hofer C., Mayr W.Stöhr H., Unger E., Kern H. A Stimulator for Functional Activation of Denervated Muscles. Artificial Organs 26:276-279, 2002

Acknowledgements

Phillipp Drewniak, Stefan Löfler, Claudia Forstner, Michaela Mödlin for patient handling during experiments and interesting discussions.

The support of the Austrian Science Fund (FWF) under grant number FWF-TRP L36 B15 is gratefully acknowledged.

Author's Address

Thomas Mandl
Center of Biomedical Engineering and Physics,
Medical University of Vienna
thomas.mandl@meduniwien.ac.at

Keynote Lecture
Paul Meadows

IMPLANT TECHNOLOGY AND USABILITY

Meadows, PM[1]

[1] Advanced Bionics Corporation, Valencia, California, USA

Abstract

Implanted electrical stimulation technology has changed greatly in the roughly five decades of its existence. Many factors determine the viability of the technology and whether the systems and products developed ultimately go on to help the target patient population. This paper describes the successful introduction of an implanted system and the challenges to implanted system development, acceptance and usability of these systems by the patient and clinical communities.

Introduction

Functional electrical stimulation was first described as a therapy by Liberson in 1961 [1] when he described a method to treat drop-foot in the hemiplegic patient. Using a footswitch to sense when the heel of a patient lifts at the initiation of the swing phase of gait, a stimulator would deliver electrical pulses to the nerves of the calf muscles causing the knee and ankle to flex which then allowed the toe to clear the floor as the patient would advance their limb. This simple system has assumed numerous forms over the years but was first converted into a commercial implantable device by Medtronic in 1969 and described by Waters [2] and has been implanted in thousands of hemiplegic patients.

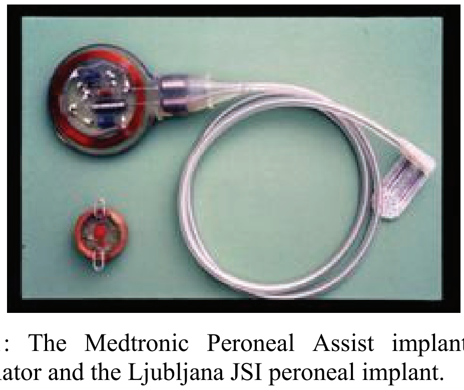

Fig 1: The Medtronic Peroneal Assist implantable stimulator and the Ljubljana JSI peroneal implant.

The implanted portion of this system was extremely simple by today's standards, consisting of an epoxy encased passive receiver and pulse shaping circuitry, silicone encased platinum leads terminating in a cuff electrode that was sutured around the peroneal nerve.

In 1973 Jeglic and Vavken [3] of Ljubljana, Slovenia, described a much smaller implanted receiver/stimulator with integrated electrodes that was placed directly upon the nerve to be excited and which was improved upon by Strojnik et al at the Josef Stefan Institute [4]. This reduced the likelihood of lead breakage which was a common problem for the Medtronic device as it crossed over the knee joint on its way to the peroneal nerve from its implant site in the medial thigh. It alsoeliminated the need to tunnel the lead the significant distance required previously and significantly reduced surgery time.

Implanted stimulation technology continued to develop over the next decade, with an increase in the number of contacts available and ever smaller package sizes per contact. Very few systems ever enjoyed the commercial, but limited, success of the Medtronic implant for peroneal assist, but one such device, introduced in the early eighties, did. Giles Brindley et al [5] developed a sacral nerve root stimulator with an integrated three channel "book" electrode that was implanted to stimulate the sacral roots to treat urinary incontinence in the spinal cord injury population. In this population few options other than catheterization were available for the daily and necessary function of bladder voiding. Over a thousand patients have been implanted with this device and up until a few years ago the system was available as the VOCARE system offered by NeuroControl of Cleveland, Ohio.

Other examples of non-commercial implanted stimulation systems include multi-channel systems for the restoration of grasp (Smith et al [6]), for walking (Thoma et al [7], Donaldson et al [8]), visual cortex stimulation systems for the restoration of vision (Brindley, et al [9]), cochlear stimulation for restoration of hearing (Merzinich et al [10]), and countless other systems too numerous to adress here. One common thread among all of these systems is the architecture of the technology employed to deliver the stimulation: all of these devices are powered and controlled through a radio-frequency link and all except the visual cortex and cochlear implants use a single pulse generator that is multiplexed to the various electrodes which interface to the nervous system. Many of the applications were directed at a very small patient population that presented many challenges to the clinical application.

Even with their limited success only one of these devices significantly penetrated the market in terms of percentage of candidate patients implanted – the cochlear implant. This can probably be attributed to the narrow scope of the implant methods, the size of the patient population, and the limit of other complicating conditions that must be addressed in these patients. Most of the systems described in the literature have never seen broader application than their initial clinical trials, and thus have helped only a limited patient population. Only a few of these systems have been brought to market and of those, still fewer have stood the test of time as a valid and profitable medical treatment. Why is it that so many organizations have developed sophisticated and well-intentioned devices but so few have been commercialized? Conversely, what are the features of an implantable stimulation system that enables it to become a commercial success and go on to help the lives of countless patients? In this presentation I will attempt to describe the process by which our company choses an application of electrical stimulation, how we analyzed the existing marketplace, technologies, and environments for the application of implanted device utilization and how we successfully entered and rapidly reached a position of market leadership and commercial success in a very short period of time.

Materials and Methods

The first step in formulating a new business model is to study the market. This requires the evaluation of potential patient populations and applications, the complexity of the approach needed to treat the patient, the existence of competing technologies to treat the disability, and the sustainability of a business model over time. It has been our approach to enter an underserved market that has been well established by another company with a significant patient population and reimbursement structure, and then bring disruptive change to that market with advanced technology. The neuromodulation market at the time of our initial exploration in 1998 was determined in our own review of the data as depicted in Table 1 below.

Advanced Bionics was already a market leader in cochlear stimulation and desired to expand its coverage in the growing neuromodulation market. The markets already being addressed by commercial implantable stimulators included chronic pain, angina, urinary incontinence, and Parkinson's Disease. Of these, the simplest market and the one which could most readily benefit from a dramatic change in technology was chronic pain.

Condition	Prevalence	Treatment
Chronic Pain	1,000,000	Spinal Cord Stim
Angina	900,000	Spinal Cord Stim
Cancer Pain	500,000	Drug Pump
Migraine	2,800,000	Occiptal Stim
Profoundly Deaf	1,300,000	Cochlear Stim
Urinary Incon.	360,000	Sacral/Pudendal Stim
Parkinson's	380,000	Deep Brain Stim
Movement Dis.	5,000,000	Deep Brain Stim
Epilepsy	440,000	Vagus, Deep Brain
Severe Depression	300,000	Vagus, Deep Brain
Morbid Obesity	12,000,000	Gastric, Deep Brain

Table 1: Conditions, prevalence and best treatment of potential patient populations with most direct intervention, Sources: NIH, Lazard Capital Markets Research, Advanced Bionics internal analysis.

Spinal cord stimulation was first described as a treatment method for chronic pain by Shealy and Mortimer in 1967 [11]. The Gate Theory of Melzack and Wall [12] hypothesized that there is a gate in the circuitry of the spinal cord that controls the flow of pain signals to the brain. Electrical stimulation of the nerve fibers in the dorsal columns can activate these gates and replace the pain sensation with a tingling sensation or paresthesia. Compared to drug therapy or the non-reversible procedures of radio frequency ablation the prospect of utilizing electrical stimulation was appealing because of its control, its ease of application and because of its reversible nature.

Chronic pain was served in 1998 principally by two manufacturers: Medtronic and Advanced Neuromodulation Systems (ANS). Medtronic was the market leader with a well designed but simple architecture: a single voltage source multiplexed to four or eight contacts with battery powered or RF powered implants. ANS had only RF powered implants but used a current source rather than a voltage source and later introduced battery powered devices. Very few improvements were made over the course of 25 years of market presence and due to the multiplexed nature of the designs optimal stimulation patterns and thus pain relief were rarely achieved.

Advanced Bionics looked at the existing products, their limited design approach, the science of neurostimulation, and leveraged its multiple independent current source design technology of its cochlear implant product and brought the first multi-contact independent current source rechargeable implantable pulse generator to the market. This system revolutionized the optimal fitting of stimulation patterns to address the complex pain conditions of this broad patient population, extended the anticipated life of a battery powered implant from the typical 1-3 years to well over ten years, and it is still the smallest device available on the market to this day.

Bringing this new technology to the market presented numerous design challenges. The dominant system architecture of a single pulse generator source and simple multiplexer or switches is a very simple design but which compromises the precise delivery of current required for consistent control of nerve excitation. Only independent current sources for each contact would result in this control, but it meant that for each contact a complete current controlled pulse generator would be required, greatly increasing the complexity of the circuitry required. In order to provide adequate treatment options at least 16 current sources were required and resulted in a custom integrated circuit (IC) measuring roughly 13x15mm. Providing timing for four independent groups with no pulse overlaps and control of jitter required a custom timing IC, and all operations were controlled by another custom IC containing an 8086 core and support circuitry. Most revolutionary about the design was a custom hermetically sealed lithium ion battery with a zero volt recovery property allowing complete depletion of charge with little or no impact on battery capacity.

The greatest change brought about by this advanced technology introduction was the increase in usability by the patient and the clinician. By virtue of its independent current sources, a sophisticated clinicians programming system, and by allowing the patient to help to control the distribution of current amongst the electrical contacts of the leads, patients achieved unprecedented pain relief in a very brief programming session with the clinician and patient using intuitive controls. This translated to much improved pain relief and an expansion of the market. The patient's control over their implant was greatly enhanced with a remote control that could be used at a comfortable distance from the implant, rather than relying on a magnet or controllers placed directly over the implant (often in difficult to reach positions for the patient) to control only rudimentary functions of their device.

Results

Advanced Bionics introduced its Precision Spinal Cord Stimulation system in April, 2004. With 34 patients in the first trial period, 3 patients were implanted that month. In that first year 366 patients were implanted. In 2005 2,769 patients were implanted, in 2006 5,200 patients, and at the month end in May, 2007, only three years later, almost 10,800 patients had been implanted by over 665 physicians. In a little over two years Advanced Bionics Corporation was able to capture approximately 25% of the market share and became the number two manufacturer - Medtronic and St. Jude Medical (formerly ANS) are expecting slower growth rates and are losing market share as Advanced Bionics succeeds in the market. Medtronic has dropped from 55% share in 2005 to an expected 48% share in 2007 and St. Jude Medical is predicting a 2007 annual growth from 3-8% versus their 17% growth rate from 2005 to 2006.

Fig. 2: The Precision IPG and Linear lead, Remote Control, cordless Charger and External Trial Stimulator.

Spinal Cord Stimulation is the largest component of the Neuromodulation market and is growing at an annual rate of approximately 20%. In 2005 total sales of SCS systems were approximately \$434M and by 2009 it is expected to exceed \$1B and Advanced Bionics will have a growing share of this market.

One of the benefits of the advanced technology introduced into the market was an actual expansion of the types of patients that could benefit from spinal cord stimulation. Failed Back Surgery Syndrome (FBSS) and lower back pain are two of the most difficult types of pain to treat, and often with older technology based spinal cord stimulation systems these patients could realize little if any benefit from electrical stimulation. Because of the independent current control, ease of programming and rechargeable design of the Precision IPG these patients can now receive substantial pain relief with the result that the whole pain market patient population has increased.

A final benefit of the introduction of the Advanced Bionics Corporation Precision system is that the entire field of products has seen recent improvements. Dominated for 25 years by Medtronic with essentially two implanted stimulator system designs, and secondly by ANS with similar “me-too” designs, the market has suddenly seen the introduction of rechargeable IPGs with more contacts available from these two sleeping giants with rechargeable devices expected to provide more than 80% of the market in the next few years. Innovation has prodded the market leader and once second largest player in the market to improve upon their designs with the result that the patient now has more options and better choices for their treatment. The disruptive introduction of this new technology has broken the cycle of incremental minor improvements to the market and changed the landscape of neuromodulation for all and the path chosen by Advanced Bionics has ensured it market share and continued support for its implanted patients.

Discussion

The decision to produce an implanted medical device clearly demonstrates the commitment to help patients suffering serious disease or dysfunction not well addressed by any other medical procedure. The type of device developed and population served must reflect sound research and decision making or the result will be a tremendous amount of development expense, limited deployment, and eventual disappearance from the market and at worst, abandonment of the patients implanted. In order to serve the greatest number of patients and to morally and ethically produce a device for treatment it must be reasonably expected that the product developed will be accepted and reimbursed, produce a profit for the company, and that the company will survive to support the patient for the life of the product. Many of the implanted electrical stimulation devices developed in the past have targeted small patient populations, had poor or no reimbursement strategy, and often required complex surgical implantations and associated procedures. This made the transfer of the device to the commercial environment extremely difficult as only a very small number of clinical environments were able to deliver a working system for their patients. It cannot be overstated that simplifying the procedures, designing tools and methods that are readily understood, reliable, and fault-tolerant, are mandatory for a successful implementation and cannot be after-thoughts. It is only when all of these conditions are considered that the patient is truly served and an impact can truly be made by the introduction of any new medical technology.

References

[1] Liberson WT, Holmquist HJ, Scot D, Functional Electrotherapy: Stimulation of the peroneal nerve synchronized with the swig phase of the gait of hemiplegic patients, Arch. Phys. Med., 4:3, 1957.

[2] Waters RL, Mcneal D, Perry J, Experimental Correction of Footdrop by Electrical Stimulation of the peroneal Nerve, J. Bone and Joint Surg., 57-A(8): 1047-1054, 1975.

[3] Jeglic A, Vavken E, Benedik M, Implantable muscle-nerve stimulator as a part of an electronic brace, Proc 3rd Int. Symp. External Control of Human Extremities, pp. 594-603, 1970.

[4] Strojnik P, Acimovic R, Vavken E, Simic V, Stanic U, Treatment of drop foot using an implantable peroneal undernee stimulatork, Scand. J. Rehab. Med., 19: 37-43, 1987.

[5] Brindley GS, An implant to empty the bladder or close the urethra, J. Neurol. Neurosurg. Psychiatry, 40: 358-369, 1977.

[6] Smith B, Peckham PH, Keith MW, Roscoe DD, An Externally Powered, Multichannel, Implantable Stimulator for Versatile Control of Paralyzed Muscle, IEEE Trans. On BME, 34(7): 499-508, 1987.

[7] Thoma H, Gerner H, Holle J, Kluger P, Mayr W, Meister B, Schwanda G, Stohr H, The Phrenic Pacemaker: Substitution of Paralyzed Functions in Tetraplegia, ASAIO, 10(3): 472-479, 1987.

[8] Donaldson PEK, Sayer E, A technology for implantable hermetic packages, Part 1: Design and Materials, Med. & Biol. Eng. & Comput., 19: 398-402, 1981.

[9] Brindley GS, Lewin WS, The sensations produced by electrical stimulation of the visual cortex, J. Physiol, 196: 479-493, 1968.

[10] Michelson RP, Merzenich MM, Pettit CR, Schindler RA., A cochlear prosthesis: further clinical observations; preliminary results of physiological studies, Laryngoscope, 83(7): 1116-22,1973.

[11] Shealy CN, Mortimer JT, Reswick JB, Electrical inhibition of pain by stimulation of the dorsal columns: preliminary clinical report, Anesth. Analg. Curr. Res. 46: 489-491, 1967.

[12] Melzack R, Wall PD, Pain mechanism: a new theory, Science, 150: 971-979, 1965.

Author’s Address

Paul Meadows, MS.
Advanced Bionics Corporation, Inc.
25129 Rye Canyon Loop
Valencia, CA 91355 USA
E-Mail: paul.meadows@bionics.com
Homepage: www.advancedbionics.com

Session III

Implant Technology & Applications

Chairpersons
Paul Meadows (Valencia, USA)
Hermann Lanmüller (Vienna, Austria)

DESIGN OF AN IMPLANT FOR PREVENTING INCONTINENCE AFTER SPINAL CORD INJURY

Donaldson N, Perkins TAP, Pachnis I, Vanhoest A, Demosthenous A

University College London, London, UK

Abstract

The Healthy Aims Conditional Neuromodulator *for urinary incontinence is very challenging for the designers. The novel battery, battery charger and neural amplifier are described.*

Introduction

Arranging a satisfactory system of bladder-management is a high clinical priority after spinal cord injury (SCI). The well-established and highly successful Finetech-Brindley sacral anterior root stimulator[1] is one method of treatment. This is implanted at the same time as a posterior rhizotomy is performed to disable the bladder-emptying reflex that causes incontinence. The stimulator is used to empty the bladder. Although about 3000 of these devices have been implanted, many people with SCI and their urologists are reluctant to cut nerves. They sometimes argue that their chances will be reduced when the *cure* for spinal cord injury becomes available. However dubious this argument, these patients must still be treated and a neuroprosthetic method that does not require a rhizotomy is attractive.

Kirkham *et al.* have shown that neuromodulation, stimulating the pudendal nerve pathway, can suppress bladder contractions [1]. Kurstjens *et al.* have shown that small neural signals can be detected when the bladder contracts [2]. These signals might be used to trigger the neuromodulation, what we call *conditional neuromodulation.*

Given that there were already partners contributing Medical Implant Communication System (MICS) radio know-how (Zarlink Semiconductor Ltd) and Saft/CEA developing an implantable rechargeable battery, when the *Healthy Aims* consortium asked for tenders for the design of an incontinence device, it seemed a good opportunity to tackle the design and make a prototype system. This should comprise a controller that would kept in a pocket or wheelchair, a charger, and an implant that uses neural signals as inputs, and stimulates to suppress bladder contracts or so as to intentionally empty the bladder.

Three aspects of this design will be outlined here.

Rechargeable Battery

The specification for the re-chargeable implant battery was written before we joined *Healthy Aims* and was for battery of dimensions 5×10×22 mm, a capacity of 35 mA.hr when discharged at C/10 rate (i.e. 3.5 mA), and life of 4000 cycles. The assumption was that this would be recharged every day, and therefore they would have a life of about ten years.

Whether we could use it conveniently therefore depended on how much charge we would need every day. We can only estimate the charge needed for stimulation: assuming neuromodulation might be active for 100 minutes per day, its average current would be 9 μA; other stimulation (e.g. bladder-emptying, high intensity) might add a further 65 μA. However, these are small compared to the probable current required by the neural signal amplifier which we expect to be about 500 μA. The total charge expected is therefore ~14 mA.hr, neglecting current used by the microcontroller and the MICS chip. We see that the amplifier dominates the energy requirement. Because of the amplifier, recharging will be necessary nearly ten times more often than would be required for stimulation alone and recharging will probably be necessary every day or every few days.

Fortunately, the Li-ion battery that Saft/CEA have developed has a greater capacity than the original specification, at least when new. Batteries received by us have a nominal capacity of ~50 mA.hr, and capacities were measured at about 48 mA.hr (but see below). The terminal voltage changes between 3 and 4 during charge/discharge; they weigh 2.5 gm (Fig. 1, Fig 2))

[1] http://www.finetech-medical.co.uk

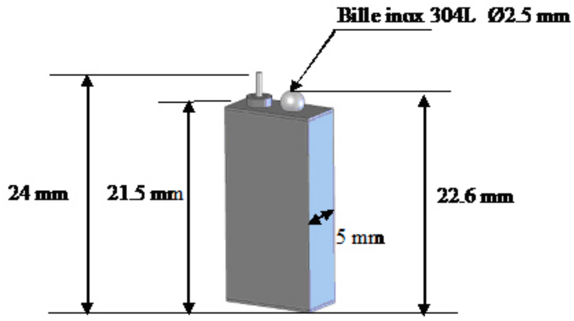

Figure 1: Dimensions of the battery

Figure 2: Photograph

Battery Charger

There seemed to be two important considerations when deciding how to re-charge the battery: how to maximise the life of the battery, and the convenience of the patient.

Saft/CEA have shown that the capacity of their battery depends on the charge rate. Furthermore, the capacity decreases with time. Thus, if the battery is charged and discharged at the so-called C/7 rate, its capacity is likely to decrease about 20% over 1000 charge cycles. At the higher rate of C/2, it may be expected to have lost 50% capacity by this time. It appears that this is not a harmful effect of fast charge and discharge: if, after a long period of rapid charging and discharging, the rate is reduced, the capacity rises to where it would have been if slow charging and discharging had always been used. This means that if rapid charging is sometimes necessary, no harm will be done, but usually the battery should be charged slowly, which means taking seven hours or more.

The only convenient way to charge for seven hours every day seemed to be to do so while the patient is in bed. We have therefore made an *Under-mattress Charger* (UMC) comprising a large coil and its drive circuit that will be placed between their mattress and the bed. The Class E driver [3] excites the coil at ~100 kHz and is self-oscillating, which means that changes in resonant frequency do not strongly affect the power consumption.

The coil is a 1 m diameter pancake made of Litz wire (Fig. 3).

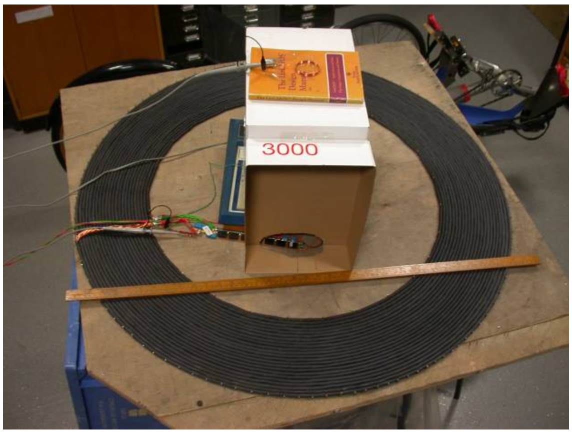

Figure 3: first UMC coil and driver circuit. The receiver coil can be seen on top of the data book.

Effect of Receiver Coil Position

For charging to occur, the voltage across the receiver coil must exceed a threshold of 12 $V_{p\text{-}p}$ when connected to a load resistance of 430 Ω. With the driver set so that it was drawing 12.7 W, this threshold was reached at the positions shown in Table 1. This should enable charging for most positions of the patient so long as the surgeon who implants the device knows whether he sleeps mostly on his side or his back, and implants accordingly.

Distance (cm)		Rotation from parallel (degrees)
Axial	Radial	
35	0	45
35	23	0
30	47	0
30	33	45

Table 1

Power Dissipation

The charger was tested to see how susceptible it is to pieces of metal, placed in the magnetic field: would this increase the power consumption giving a risk of fire? A rectangle of metal, 20×30 cm, was moved about just above the coil. The greatest increase was from 12.7 to 20W – still much less than the heat loss from the patient.

Conclusion

Patients would probably need a portable charger, as well as a UMC, for use when away from home. This would not be technically difficult, but how they would use is not obvious. The UMC seems to be technically feasible and should be quite convenient (switched on and off by a clock). Despite the dramatic-sounding fact that the coil will have about 2.5 kV across it, the heat dissipation is small. Because the patients may still have incontinent events, water-proofing the coil and the drive electronics will be important.

EMG Neutralisation

Ideally, the *Conditional Neuromodulator* will detect bladder contraction from the neural signal in the pudendal pathway. Whether this is practicable is unknown because no one has tried it. Kurstjens *et al.* [2] made intra-operative recordings and found very small amplitude changes (~ 0.1 μV). In non-anaesthetised people, the bladder signal will be mixed up with neural signals from the rectum and cutaneous afferents and there will also be interference and noise. The interference will be of two types: common-mode and gradient.

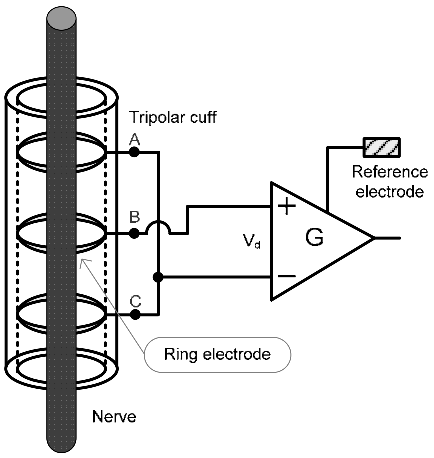

Figure 4: tripolar recording

Figure 4 shows the usual method of recording from three electrodes that encircle the nerve within a recording cuff. In this arrangement (sometimes known as a '*quasi tripole'*), the outer electrodes are connected together (A to C). The neural signal appears between B and AC across the amplifier input. Common-mode interference is due to potential differences that may occur between the reference electrode and the cuff electrodes (A, B, C). As in other biomedical amplifiers, this interference may be kept small, seen at the amplifier output, if the amplifier's CMRR is high and its common-mode input impedance is also high [4].

Gradient interference is due to potential difference between the cuff ends. We call it *'EMG'* interference because it is likely to be due to muscle activity near the cuff. In principle, because the cuff is cylindrical, the potential gradient inside will be constant and therefore, if the electrodes are equally-spaced and open-circuit, the potential at the middle electrode will be half way between the potentials of the end electrodes. The tripolar cuff should, therefore, have zero sensitivity to external fields [5]. However, real cuffs will have some sensitivity because of manufacturing tolerance and the tissue within the cuff being non-uniform.

For the quasi-tripole, the situation is more complicated. Because the outer electrodes are connected together, the impedance of the end electrodes can not be neglected. The situation can be represented as a Wheatstone Bridge (Fig. 5).

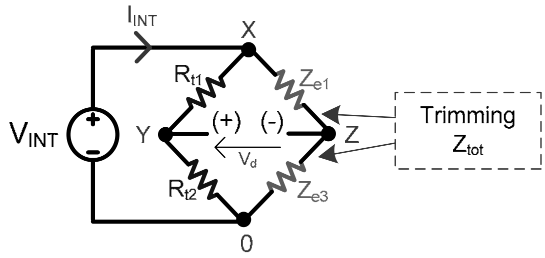

Figure 5: R_{t1} and R_{t2} represent the tissue resistances from A to B and from B to C respectively. Z_{e1} and Z_{e2} represent the impedances of electrodes A and C. The impedance of electrode B can be neglected because it is connected only to an amplifier input (high impedance).

To avoid EMG interference, we would like this bridge to be balanced so that $\frac{V_d}{V_{INT}} \approx 0$. Struijk and Thomsen [6] suggested that this could be done by placing a potentiometer between and A and C with its wiper connected to the amplifier input. However, this ignores the fact that Z_{e1} and Z_{e2} are reactive. To balance this bridge, with the least additional resistance, impedance must be added at one side of node Z. Unfortunately, it also means that the bridge can only be balanced at one frequency.

Two decisions must be made:

(i) if the added impedance comprises a resistor and a capacitor, should they be in series or parallel?

(ii) at what frequency should the bridge be balanced?

We found [7] that parallel connection is better, because the impedance and R and C in parallel changes with frequency more like the electrode impedance than the series combination. The bridge should be balanced at a low frequency for two reasons. First because this gives less interference across the whole frequency band, and because EMG lies at the bottom of the ENG spectrum and this is the interference that one wants to remove.

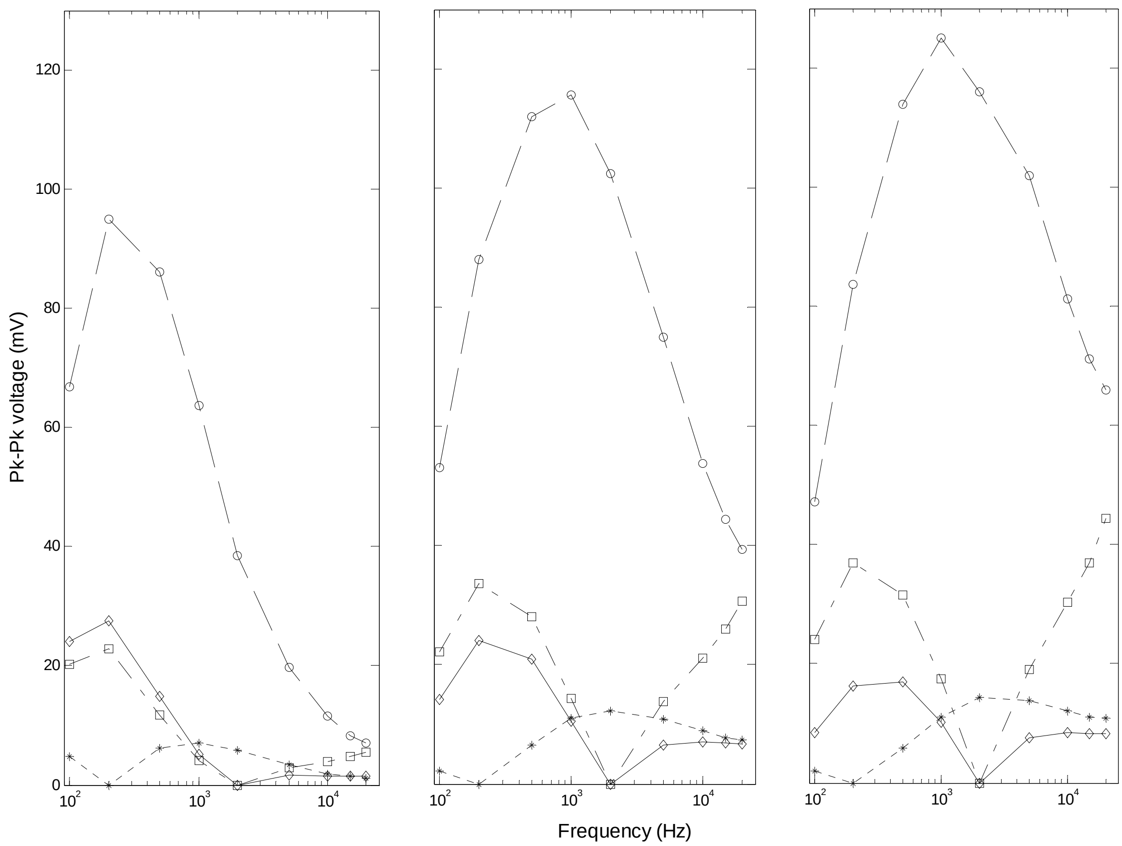

Figure 6: interference spectra for three electrodes in saline of three conductivities, 1.6, 8.5 and 15.5 mS/cm. Symbols: o no trim; ◊ parallel trim at 2 kHz; □ series trim at 2 kHz; + parallel trim at 200 Hz (which is the best).

Conclusion

This passive method gives complete neutralisation of EMG interference at one frequency. In this tank test, with a geometrically-asymmetric cuff, a worst-frequency of about 10-fold at all frequencies is possible. No extra power is needed and the additional noise is minimal.

References

[1] Kirkham AP, Knight SL, Craggs MD, Casey AT, Shah PJ. Neuromodulation through sacral nerve roots 2 to 4 with a Finetech-Brindley sacral posterior and anterior root stimulator. Spinal Cord, 40(6): 272-81, 2002.

[2] Kurstjens M, Borau A, Rodriguez A, Rijkhoff NJ, Sinkjaer T. Intraoperative recording of electroneurographic signals from cuff electrodes on extradural sacral roots in spinal cord injured patients. J Urol., 174: 1482-87, 2005.

[3] Troyk PR, Schwan MA. Closed-loop class E transcutaneous power and data link for microimplants. IEEE Trans. BME, 39: 589-99, 1992.

[4] Casas O, Pallas-Areny R. Optimal Bias Circuit for Instrumentation Amplifiers. Proc. XIV Imeko World Congress, 6: 143-8, 1997.

[5]Donaldson N, Zhou L, Perkins TA, Munih M, Haugland M, Sinkjaer T. Implantable Telemeter for Long-Term Electroneurographic Recordings in Animals and Humans. *Med. & Biol. Eng. & Comput.*, 41: 654-64, 2003.

[6] Struijk JJ, Thomsen M. Tripolar Nerve Cuff Recording: Stimulation Artifact, EMG, and the Recorded Nerve Signal," IEEE-EMBS, 1105-1106, 1995

[7] Pachnis I, Demosthenous A, Donaldson N. Passive neutralisation of myoelectric interference from neural recordin tripoles. IEEE Trans BME, 54:1067-1074, 2007.

Acknowledgements

We acknowledge financial support from EU Framework VI, within the Integrated Project *Healthy Aims* (IST-2002-1-001837).

Author's Address

Prof. Nick Donaldson
Implanted Devices Group
University College London
nickd@medphys.ucl.ac.uk

INTRABODY NETWORK FOR ADVANCED AND EFFICIENT FUNCTIONAL ELECTRICAL STIMULATION

Souquet G.[1,2], Andreu D.[1], Guiraud D.[1]

[1] LIRMM CNRS-UM2, Montpellier and INRIA Sophia-Antipolis, France

[2] MXM, Vallauris, France

Abstract

We have developed the first hardware and software elements to provide an implanted FES system based on networked stimulation units. They embed advanced analogue circuits to provide multi-polar and multi-phasic stimulation profiles, and numeric circuits to ensure safety, to locally execute programmed profiles, to support remote configuration and control (communications). This architecture needs only for a 2-wire bus to communicate whatever the number of poles of the driven electrode is. Moreover the bus will provide energy. This structure is then easy to implant in the way that a single 2-wire cable needs to be linked from one unit to the next. The configuration can evolve adding new stimulation units in further surgical sessions. In the same time each unit will offer a wide variety of stimulation profiles on multipolar electrodes opening a wide research and application areas.

Introduction

Implanted functional electrical stimulation (FES) applications need for more advanced neuroprostheses that leads to mainly increasing the complexity of the hardware design: multipolar neural electrode to gain selectivity, and increasing number of stimulation and measurement sites. A centralized architecture can no more be used due to the wiring [1][2]. The architecture we have developed is different from existing electrical-stimulation architectures as it is not a centralized one. Centralized architectures often rely on a central implant to which each stimulation site (electrode) is connected by several wires. Consequently, the use of multipolar neural electrodes, required for selectivity and efficiency [3], increase this number of wires and so the surgery complexity and risks.

Our approach, based on a distributed architecture, requires only a 2-wire data and energy bus and is independent from the number of poles of the electrode. The paper focuses on network issues, both the protocol description and the first validation on prototypes.

Material and Methods

Functional electrical stimulation architecture

Each stimulation site has an electronic part implanted near the electrode: this electronic device corresponds to a Distributed Stimulation (or Measurement) Unit [4]. These units are connected together and with an implanted controller (CTR), by means of an asynchronous intrabody network (Fig. 1). This architecture is then easy to implant in the way that a single 2-wire cable needs to be linked from one unit to the next (according to a bus topology, and not a physical ring), and not from a centralized implant.

To exchange (small) packets of data each node of this network embeds a specific protocol stack, we will later present as we focus on data and not energy.

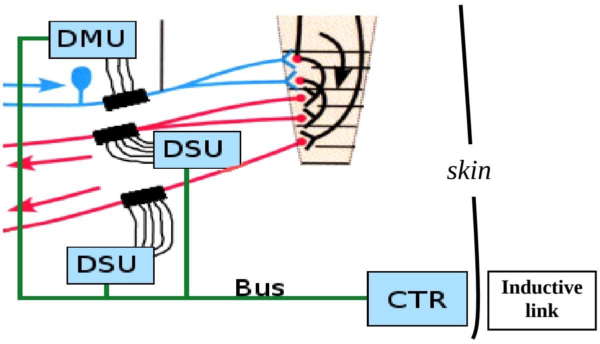

Fig. 1: Example of intraboby network architecture

The link between intrabody architecture and extrabody device(s), for data and energy transmission, is ensured by means of an inductive link. In this architecture the (stimulation) controller also ensures the “relay” between those two worlds.

Distributed implantable units

The implantable architecture relies on two kinds of distributed units; those for activating (Distributed Stimulation Units, DSU) and those for monitoring (Distributed Measurement Units, DMU) the peripheral nervous system. Each unit is a device composed of digital and analogue parts, the latter being connected to the multipolar electrode used to stimulate or record (ENG) the neural activity. We only detail DSU units in this paper; Fig. 2 gives a schematic representation of the internal architecture of a DSU.

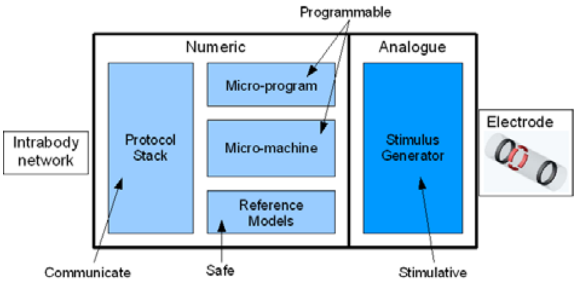

Fig. 2: Schematic representation of DSU's internal architecture.

A DSU embeds:

• A stimulus generator (6 mm² ASIC, for a 0.8 µm technology) which creates the analogue stimulus to be applied to the nerve [5], from numeric commands sent by the micro-machine.

• A micro-machine (3.5 mm² ASIC, for a 0.35 µm technology), a kind of specific very small processor, which executes a micro-program representing the stimulation profile that must be applied to the nerve. The micro-program is coded using a specific reduced instruction set [6]. This micro-program is downloaded by the master controller. The micro-machine is assisted by reference models that monitor the stimulation resulting from the micro-program execution. They are able to stop any stimulation if any physiological constraints violation is detected. The micro-machine can be remotely controlled:

• A communication module (5 mm² ASIC, for a 0.35 µm technology) composed by a 3-layer protocol stack according to the reference given by the structure of the OSI model. These layers are the Application layer, the Medium Access Control layer (MAC) and the Physical layer.

The protocol stack

Each node of the implanted network embeds the 3-layer protocol stack; doing so, the modularity of the protocol stack allows to easily modify any layer. On this network, we use two types of logical addresses, allowing unicast, multicast and broadcast communications: individual addresses (one for each DSU) and group addresses (for different groups of DSU, and all DSUs). These addressing modes are necessary since the controller can communicate for example with a single DSU, to program it, or with a group of DSU to start stimulation, or all DSUs to stop any stimulation. The notion of group is significant in our context. In case of movement control, for example, at a given instant of time the control only concerns a subset of muscles and thus a subset of DSU (those associated to these muscles). This implies that it is possible to dynamically impose to a DSU to subscribe/unsubscribe to one or several groups.

The three layers of the protocol stack are briefly described according to a top-down approach:
• The Application layer. The application protocol is mainly dedicated to the management of the micro-machine by modifying micro-programs (download, modify, upload, erase) and by piloting the activity of the micro-machine (start, stop, rearm, commute). It also allows « real-time » (on-line) modification of the parameters of the stimulation profile (pulse width, pulse amplitude, pulse frequency).

• The MAC layer. The basic role of the MAC layer is to filter incoming packets, since at the physical layer we systematically broadcast frames on the bus, and to manage subscription/unsubscription to groups. But the most important role of the MAC layer is the control of the medium access. A simple deterministic medium access is ensured by the master-slave model of cooperation, the controller being thus the master. Doing so, we can be sure that no DSU will emit any frame if not authorized to do so. However this model of cooperation is not really efficient when dealing with a group of slaves (DSU) as it requires to poll slaves, i.e. to individually communicate with each slave. To limit energy consumption and the bandwidth need, communications and quantity of data must be limited. We defined and patented [7] a method based on the master/slave model which has been modified for performance considerations.
It obviously allows basic individual master-slave and slave-master communications, but offers a way to manage the communications with a group of slaves without polling all the members of the group. This MAC method allows a deterministic exploitation of the medium and favours the reactivity of the distributed architecture [8].

• The Physical layer is the lowest level of the DSU. It permits to receive bit-frames coming from the 2-wire physical medium, ensuring the validity of the received frame (start and stop delimiters, bit coding). Data contained in the frame are then extracted and transmitted to the upper layer. It can also emit data coming from the upper layer, ensuring a correct encoding of the frame.

Intrabody network

The specific intrabody asynchronous network we developed is based on a medical 2-wire cable (35N

LT metal based implantable 2-wire cable) on which data transit with a differential mode. Encoding is achieved with a synchronous clock encoding technique, a pseudo Manchester code. Each bit of data is signified by two voltage levels (and transitions) separated by impedance phases (Fig. 3). So, we get a self-clocking encoding and we limit energy consumption on transitions, ensuring moreover to keep DC-balance (a null average tension on the network). The encoding of each bit on the two wires is given in Tab 1.

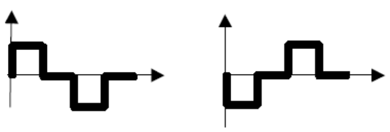

Fig. 3: Bit coding according to a differential view

	Rest	Positive pulse	Negative pulse	Forbidden value
Bus +	Vdd (HZ)	Vdd (HZ)	0	0
Bus -	Vdd (HZ)	0	Vdd (HZ)	0
IO+ (RD & WR)	1	1	0	0
IO- (RD & WR)	1	0	1	0

Tab. 1: Bit coding on the 2-wire bus

A frame (bit sequence) generation is shown on Fig. 4 (left side). A XOR between the data to emit and the serial clock permits to obtain the tension to which the signal «bus-» must be set while the clock is on a high state. We only need to invert this value to obtain the tension to which the signal «bus+» must be set.

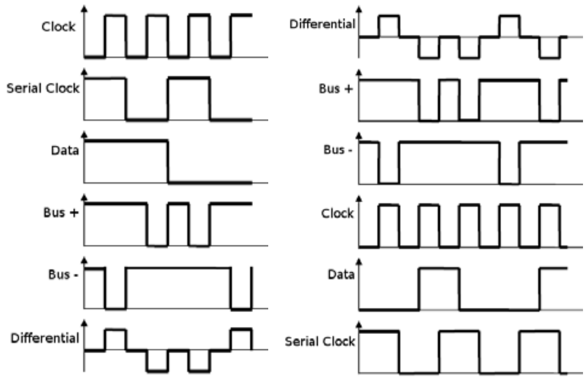

Fig. 4: Frame encoding (left) and decoding (right)

Decoding a frame is simple to perform as it is easy to recover the clock used for encoding (the encoded signal containing frequent level transitions). It is done using a NAND between the two signals (wires) of the bus as we can see Fig. 4 (right side). Then data extraction is done, at the frequency of the recovered clock.

To encode start and end delimiters of a frame, we use patterns that can not appear in a correctly encoded data equivalent bit sequence. These patterns are given on Fig. 5.

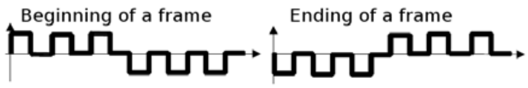

Fig. 5: Start and Stop frame delimiters

Results

Prototype

We developed prototypes of the advanced intraoperative neural stimulator corresponding to the DSU which has been presented. This prototype is based on an ASIC for the analogue part of the DSU (part B on Fig. 6) and a FPGA that embeds the numerical part (part A on Fig. 6). This stimulator can communicate over different media like the presented 2-wire bus (the medium coupler being plugged on the stimulator, part C on Fig. 6).

Fig. 6: Prototype of intraoperative stimulator (Stim3D)

Experimentation of communication over the 2-wire bus

Several DSUs have been connected according to a bus topology. We captured a frame over the 2-wire bus; the frame start delimiter can be recognised on Fig. 7. This frame has been encoded with a 2 MHz clock. The medium bandwidth is then 1 Mbps (the maximum bandwidth is 7 Mbps, beyond 14 MHz the signal being strongly attenuated).

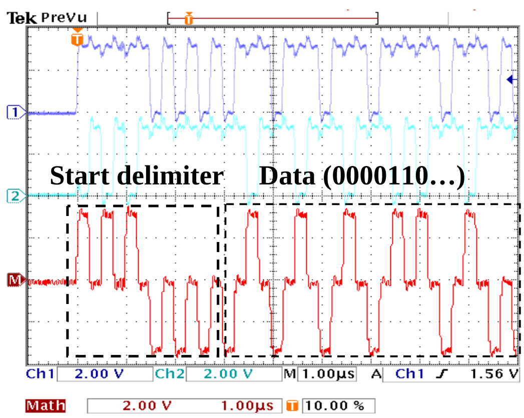

Fig. 7: Frame capture over the 2-wire bus

A bandwidth of 500 kbps is sufficient as, on this distributed architecture, we only send short packets (usually 4 to 10 bytes packets) except when downloading micro-programs (more complex ones can contain up to 200 bytes). The stimulus shown on Fig. 8 (left side), applied to a 5 poles electrode (4 cathodes and 1 anode), corresponds to a micro-program of 17 instructions; the corresponding packet contains 75 bytes. This packet must be send only once, at the initial phase of the stimulation, except when dynamical programming of the DSU is required.

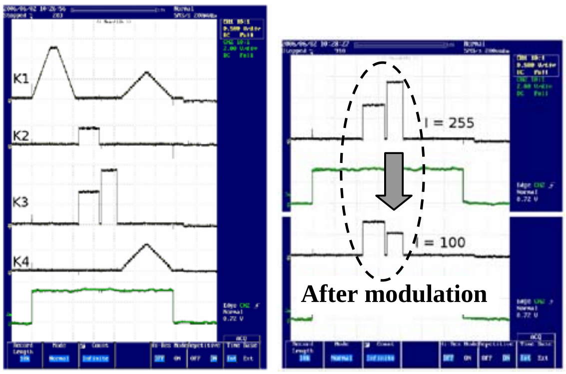

Fig. 8: Examples of illustrative complex stimulation profile (left) and network based stimulus amplitude modification (right). Both are real stimulation traces captured at the output of our intraoperative stimulator.

When performing "real-time" (i.e. on-line) stimulus modification, the packet size depends on the number of parameters (amplitude, width, number of steps in case of a ramp-like stimulus, etc.) to be modified on the given real-time instruction of the micro-program. For the example shown on Fig. 8 (right side), the amplitude modulation of the second pulse requires to transmit a packet of 7 bytes (so a transmission time of 56 µs).

Conclusion

Complex implanted FES applications will need for: i) an increasing amount of wires between electronics and electrodes, ii) embedded computation facilities both for measuring and stimulating the peripheral nervous system. A centralized architecture is thus no more useable but distributed units linked with the minimum wiring are suitable. On the other hand, for complete wireless systems, such as Bion technology [9], the energy transfer is not completely solved. Then, we developed an intermediate solution based on the minimal bus configuration needed to transport data and energy: a 2-wire bus. We also specified a dedicated protocol that may also be used on wireless medium. We designed the numeric and analogue parts of a distributed stimulation unit to test the ability of the DSU to activate a quadri-polar electrode, and to communicate with the master controller using our protocol stack. Results show that the protocol stack is robust, efficient and answers to the requirements in term of reactivity, addressing, and data bit rate. Further work will be carried out on energy transport and then implantable system will be developed and validated through in vivo experiments.

References

[1] K. von Wild, P. Rabischong, G. Brunelli, M. Bénichou, K. Krishnan, *Computer Added Locomotion by Implanted Electrical Stimulation in Paraplegic Patients (SUAW)*, Acta Neurochir, Vol. 79, p99-104, 2001.

[2] D. Guiraud,T. Stieglitz, K.P. Koch, J.L. Divoux, P. Rabischong, *An implantable neuroprosthesis for standing and walking in paraplegia: 5-year patient follow-up*, J. Neural Eng., vol. 3, pp 268-275, 2006.

[3] Sweeney J.D., Crawford N.R., Brandon T.A *Neuromuscular stimulation selectivity of multiple-contact nerve cuff electrode arrays*. Medical and Biological Engineering and Computing, Vol. 33, p418-425, 1995.

[4] Andreu D., Techer JD., Gil T., Guiraud D. *Implantable Autonomous Stimulation Unit for FES.* 10th Annual Conference of the International Functional Electrical Stimulation (IFES'05), Montréal, Canada, July 5-9, 2005.

[5] Bernard S., Techer JD., Cathébras G., Bertrand Y. and Guiraud D. *Electrical Performances of a New Multipolar Micro- Stimulator*. 10th Annual Conference of the International Functional Electrical Stimulation (IFES'05), Montréal, Canada, July 5-9, 2005.

[6] Andreu D., Guiraud D., Souquet G. *Stimulation Electro-Fonctionnelle : vers une architecture distribuée de stimulation neurale.* Journal Européen des Systèmes Automatisés, "Robotique et Handicap", vol. 41, pp. 159-177, 2007.

[7] Guiraud, G., D. Andreu, G. Cathebras, Y. Bertrand, S. Bernard, J. Galy and J.D. Techer. *Dispositif de répartition de courant entre des cathodes d'une électrode multipolaire, notamment d'un implant*, Patent Number FR0409351 2004-09-0.

[8] Godary K., Andreu D., Souquet G. *Sliding Time Interval based MAC Protocol and its temporal validation*. 7th IFAC International Conference on Fieldbuses and nETworks in industrial and embedded systems (FET'07), Toulouse, France, November 7-8-9, 2007. Paper submitted.

[9] G. E. Loeb, R. A. Peck, W. H. Moore, K. Hood, *BIONtm system for distributed neural prosthetic interfaces*, Medical Engineering and Physics, vol. 23, pp 9-18, 2001.

Author's email

author-name@lirmm.fr

TROUBLESHOOTING FOR DBS PATIENTS BY A NON-INVASIVE METHOD WITH SUBSEQUENT EXAMINATION OF THE IMPLANTABLE DEVICE

Lanmüller H[1], Wernisch J[2] and Alesch F[3]

[1] Department of Biomedical Engineering and Physics, Medical University of Vienna, Vienna, Austria
[2] Institute of Solid State Physics, Technical University of Vienna, Vienna, Austria
[3] Department of Neurosurgery, Medical University of Vienna, Vienna, Austria

Abstract

Multichannel devices are used for deep brain stimulation in patients suffering from Parkinson's disease. A non invasive method to inspect each single output of these devices was applied in 12 patients. The clinician programmer indicates an electrode impedances beyond standard values in these patients or a non explainable loss of the therapeutic effect was given. A small device was developed to measure and display the stimulation impulse via surface electrodes. The results from the measurement pointed at an incorrect measurement by the programmer in 9 cases, broken electrode leads in 2 patients and an IPG failure in 1 patient. Leads and IPG was exchanged and inspected by light or electron microscopy. Each failure prognosis was confirmed by these examinations. The non invasive measurement of the stimulation pulse via surface electrodes turned out as an easy and accurate method for the detection of incomplete IPG malfunctions.

Introduction

Deep brain stimulation (DBS) has proven to be an efficient therapy in patients with late complications of medical treatment of Parkinson's disease. Battery-powered multichannel devices are used for this FES application and the durability and lifetime had been increased to a high level.

Nevertheless, a complete or partial loss of the therapeutic effect could occur and it is essential to identify if there is a medical or technical cause. In some cases this separation is not obviously and the diagnostic features provided by the programmer or the implantable pulse generator (IPG) are not sufficient. By this instance additional technical examinations had to be carried out in cooperation between medical and technical experts.

In this paper we present a non invasive method to inspect each single output of the IPG and examples from the analysis of the explanted faulty components.

Material and Methods

The stimulation output of each channel could be inspected directly on the patient's skin. The voltage drop driven by the IPG is proportional to the stimulation current and the tissue impedance. A small device was developed to measure and display this value via surface electrodes. The device consists of an instrumentation amplifier, a trigger unit, a sample & hold circuit, an A/D converter and a LCD panel. The voltage drop caused by the stimulation pulse is sampled 10µs after the rising slope and averaged above 100 pulses. The complete time course could be displayed and stored additionally by the use of a laptop computer.

To enable an easy handling during an ambulant or intra operative measurement the forehead above the nose and the cranial end of the sternum was selected as our measuring points. The common reference electrode was placed optional on neck or shoulder. The functional test for one IPG with eight channels takes less then five minutes. Each output was activated against the implant case with an amplitude of 1V which was usually below the sensitivity level. In case of faultless results only the single values were recorded for subsequent tests. The complete time course was stored If a failure was detected.

The examination of an explanted lead was done by light microscopy (model SZH10, Olympus Hamburg Germany). The technical examination of a presumed faulty IPG was started with a functional test followed by a destructive inspection. If possible, amplitude, pulse width and frequency on each output channel of the IPG were measured in the functional test. In a second step the titanium case of the IPG was opened by laser cutting. This technology was chosen to minimize any additional mechanical stress during the opening procedure. A Nd:YAG laser (model LPM300, Lasag AG, Thun Switzerland) was used with a pulse repetition rate of 60Hz, a pulse width of 0,2ms and a voltage of 450V. The titanium case was cut in a shape like a semicircle above the electronic circuit. The semicircle was lifted and the metal sheet was bended back over the battery side of the IPG. The opened window allows a view to the thick film hybrid which holds the electronic components and the connection to the battery. Details could be inspected by light microscopy and electron microscopy (model XL 30 ESEM, Philips, Eindhoven, The Netherlands).

Results

A non invasive inspection of the IPG function was carried out, if the clinician programmer indicates electrode impedances beyond standard values or after a complete or partial loss of the therapeutic effect. 12 patients were examined up till now. Broken electrode leads were found in 2 patients, an IPG failure in 1 patient. In all other cases an incorrect measurement by the programmer could be verified. The measured voltage between forehead and sternum was minimal 28mV and maximal 55mV in these patients. In the case of broken leads the voltage was below 8mV and increases back to normal values after lead replacement. The subsequent examination of the leads by light microscopy confirmed the non invasive measurements (see Fig. 2).

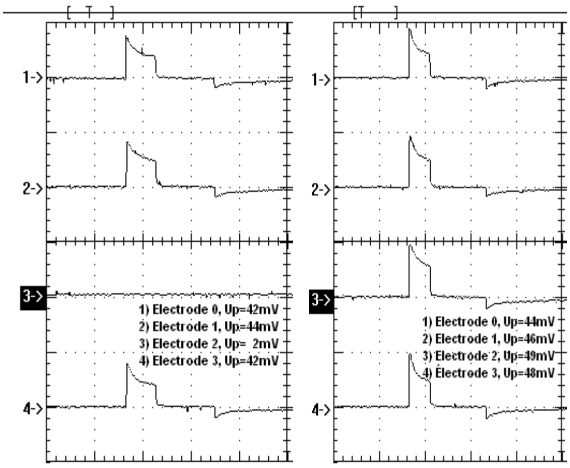

Fig. 1. Time course of the stimulation pulse measured via surface electrodes. Trace 3 (marked) indicates the failed channel
left: output channel 0-3 before electrode replacement (amplitude 1V, pulse duration 120µs),
right: output channel 0-3 after electrode replacement (amplitude 1V, pulse duration 90µs)

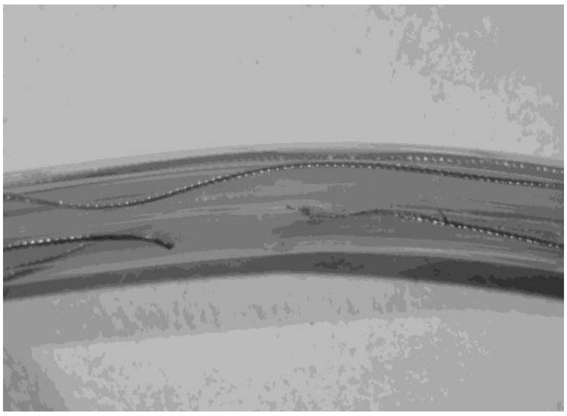

Fig. 2. Fracture of the lead by light microscopy

The examination of the failed IPG showed fractures in the battery connection. Two bond wires in parallel for each battery pole had been used for the connection to the thick film hybrid. Hairline cracks could be found in one bond of the minus pole and in both bonds of the plus pole.

At higher magnification by electron microscopy the cracks seemed to spread through the whole bond wire. By applying a bond pull test (model Micropull III, Unitek Eapro B.V. Helmond Netherlands) both wires from the plus pole could be lifted with 0g-force, both wires from the minus pole passed the test with 5g-force. Summarizing, the connection to the minus pole was functioning, but both wires to the plus pole turned out as broken and the electrical connection to the battery was given just by the elasticity of the wires.

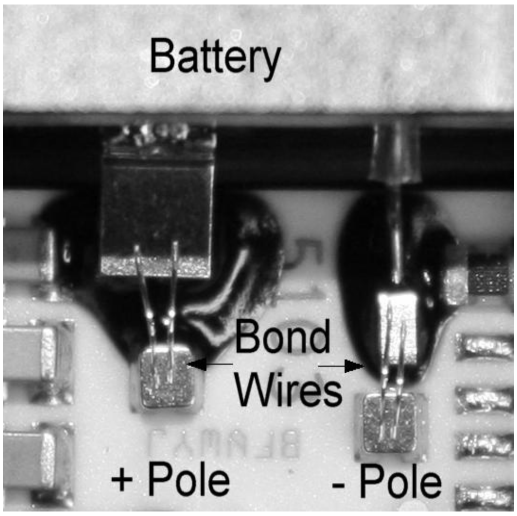

Fig. 3. Electrical connections between implant battery and thick film hybrid

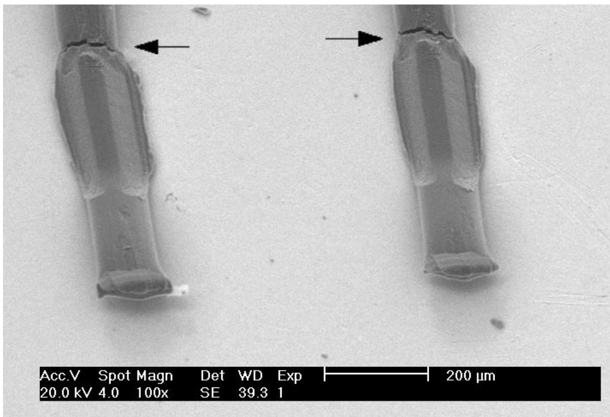

Fig. 4. Images made by electron microscopy showing the connection between the battery minus pole and the thick film hybrid. Hairline cracks through the whole bond wire marked by arrows.

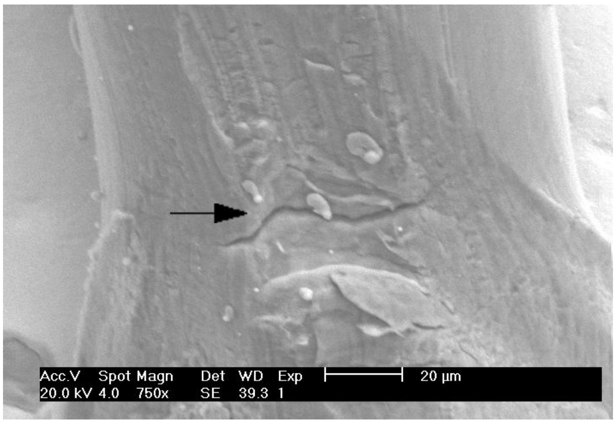

Fig. 5. Connection between the battery minus pole and the thick film hybrid, hairline crack starting from the surface of the bond wire.

Discussion

The non invasive measurement of the stimulation pulse via surface electrodes turned out as an easy and accurate method for the detection of incomplete IPG malfunctions. The function of each single output could be inspected. Each failure prognosis was confirmed by the subsequent IPG examination. In 12 patients two broken leads and one IPG failure had been verified.

Interestingly, we could not found a description of this method in literature. Maybe it had been used without publishing or remarked in passing without explanation.

Further investigations are planed to locate the position of a lead interruption. A fracture of a lead or a contact failure in the connector should be identified. This will shorten and simplify the operation.

Author's Address

Lanmüller Hermann
Department of Biomedical Engineering and Physics, Medical University
Vienna, Austria
hermann.lanmueller@meduniwien.ac.at

A Cuff Electrode dedicated to ENG Recording with Multipolar Configuration for both Efficient Sensitivity and High Rejection of EMG Parasitic Signals

Gouyet L, Cathébras G, Bernard S, Guiraud D and Bertrand Y
LIRMM, Université Montpellier II - CNRS - INRIA, Montpellier, France

Abstract—**To be able to perform a closed loop control in Functional Electrical Stimulation (FES) system, an attractive idea consists in using natural sensors available in the body. In this context the main difficulties are to be able to discriminate the sensory information from the full ENG signal generated by all the axons included in the nerve and to perform measurement with high rejection of interference signals. For this purpose, we propose a new configuration of the cuff electrode with a large number of poles laid-out in an hexagonal tessellation. Using seven adjacent contacts as a directive antenna, we get better spatial selectivity and gain than the standard tripolar cuff. Moreover, this gain enhancement doesn't debase significantly the rejection of EMG parasitic signals. Last, but not least, the large number of poles will allow enough channels in order to apply source separation signal processing on the ENG.**

I. Introduction

In a context of neural system pathologies such as spinal cord injury, Functional Electrical Stimulation (FES) techniques are the possible alternatives to restore lost sensory or motor abilities. These techniques consist in generating artificial contraction by electrical stimulation. In FES system a direct opened loop control doesn't allow efficient stimulation. In order to provide a loopback control we need sensory information (force, contact…) [1]. An attractive solution consists in using the natural sensors. The sensory information is propagated by associated afferent fibers. But unfortunately, in peripheral nerves the complete nerve activity due to the large number of axons makes the extraction of the studied signal particularly hard. Moreover the sensory signal seen throught the nerve is a very low amplitude signal compared with the amplitude of parasitic signals. For instance, on a monopolar recording, EMG created by muscle activity have amplitude about three orders of magnitude higher than the ENG. In this context, the two main objectives to be able to exploit natural sensors are:

- to find a solution to separate the useful information from the complete ENG signal;
- to reject the parasitic external signals.

The classical solution consists in using multipolar electrodes, but from tripole [2] to nine pole electrode [3], [4], the selectivity of the neural information is not efficient enough to be suitable in closed loop FES system. In this paper, we consider a new configuration of the cuff electrode with a large number of poles laid-out in an hexagonal tessellation. Because of the very low level of processed signals we propose to perform the maximum of signal processing as close as possible to the nerve. Therefore, in this configuration, a group of seven poles can behave, with suitable low level analog signal processing, like a kind of a directive antenna. Moreover, the large number of poles will allow enough channels in order to apply source separation signal processing on the ENG. Of course, the directivity of the sensor relies on the quality of the subsequent low-level analog signal processing.

In section II we present the architecture of the proposed multipolar cuff electrode and the modeling equations used to evaluate its performances. The results of these evaluations are presented in section III and perspectives for this work are detailed in section IV. Finally, section V gives some concluding remarks.

II. Material and methods

A. Electrodes

Cuff electrodes have been the most used in the last ten years [5]–[7]. They are relatively easy to implant, they are not invasive for the nerve and implantation is very stable and thus allows chronic experiments. ENG can be recorded as the potential difference created on the electrodes by the charges associated to the action potentials (AP)

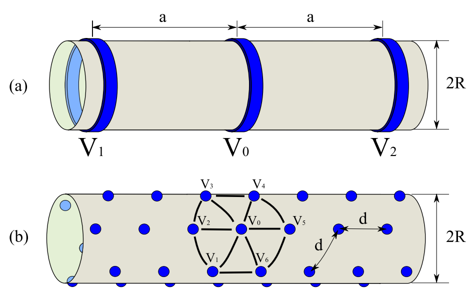

Figure 1. Tripolar cuff (a) and hexagonal electrode (b) models

propagating along the nerve fibers. Fig. 1-a shows a typical tripolar cuff electrode. When recording with this kind of electrode, a classic method to reject parasitical signals consists in calculating the average of the potential differences between the central pole and each of the outer poles [8], [9]:

$$V_{rec} = \frac{(V_0 - V_1) + (V_0 - V_2)}{2} = V_0 - \frac{V_1 + V_2}{2} \quad (1)$$

With the aim of obtaining more localized measures, we propose to use a structure with a large number of poles in an hexagonal configuration (Fig. 1-b: 42 poles). Let us call this an *hexagonal cuff*. On this electrode, poles will be gathered in hexagonal *patches*. On each patch, we calculate the mean of the potential differences between the central pole and each of the peripheral poles:

$$V_{rec} = \frac{1}{6}\sum_{i=1}^{6}(V_0 - V_i) = V_0 - \sum_{i=1}^{6}\frac{V_i}{6} \quad (2)$$

B. Action Potential modelling

In order to evaluate the performances of our electrode, we need a model for the extracellular electric field created by an action potential. Let us consider a $10\,\mu$m diameter myelinated axon. Its Ranvier nodes are $1\,\mu$m long, while their diameter is $6\,\mu$m and their spacing is $1\,$mm. Let us call Ω the centre of the Ranvier node. When the AP is present at this node, we can model it as a $6\,\mu$m diameter circle, perpendicular to the axon axis, with a positive charge $+q$ at its centre (Ω) and a negative charge $-q$ spread on the circle. The potential created at a point M of the space by this AP can be approximated by:

$$V(M) = \frac{qa^2}{8\pi\varepsilon_0\varepsilon_r r^3}\left(1 - \frac{3}{2}\sin^2\psi\right) \quad (3)$$

In this expression, a is the radius of the ranvier node ($3\,\mu$m), r is the distance between Ω and M, while ψ is the angle between the axe of the axon and $\overrightarrow{\Omega M}$. This approximation, valid for $r \gg a$, is in good accordance with measurements. In particular, we can see that $V(M)$ is negative for $\psi = \pi/2$ [10, page 81]. Last, q can be easily estimated from the characteristics of the Ranvier node. For this study, we took $q \simeq 20\,$fC and $\varepsilon_r \simeq 80$.

The model given by equation 3 was used to evaluate the sensitivity of the electrodes to action potentials occurring inside the nerve. For the evaluation of the rejection of parasitic signals, we must first recall that EMG are also action potentials, creating the same kind of electric field. But, in this case, we cannot make any assumption on the value of ψ. So, to evaluate the external sensitivity of electrodes, we chosen to use only a $1/r^3$ model, unable to give voltages, but sufficient to compare the sensitivities of various electrodes.

C. Measurements

Given the position of a single AP we can easily calculate the induced potential on each pole of the hexagonal cuff, since they are very small. For the tripolar cuff, we need to average the potential on each ring. This lead to an elliptic integral we have solved using numerical methods.

In the following, we compare a tripolar cuff electrode, whose diameter is $2R = 3\,\mathrm{mm}$ and ring spacing is $a = 4R$, with one patch of our hexagonal cuff. To get comparable results, this hexagonal cuff has the same diameter ($2R = 3\,\mathrm{mm}$) and the spacing between poles is $d = R$. Since this patch is partially wrapped around the nerve, we considered also another patch perfectly flat.

For all the calculations, the coordinates were fixed as follow: the origin O is at the centre of the cuff electrode. The Ox axis is the axis of the nerve (and, obviously, of the cuff). The Oy axis passes by the centre of the considered patch (which is perpendicular to this axe). Last the Oz axe is placed to form a direct trihedron with Ox and Oy.

III. Results

A. Internal sensitivity

Figure 2 shows the radial sensitivities of the three electrodes (tripolar cuff, planar hexagonal patch and wrapped hexagonal patch) that we compare. The vertical axis is the value of V_{rec} (in dB$\,\mu$V) calculated for an AP placed on the Oy axis, at abscissa yR. The graph shows clearly that while the sensitivity of the tripolar cuff is quasi constant on the section of the nerve, the sensitivity of the

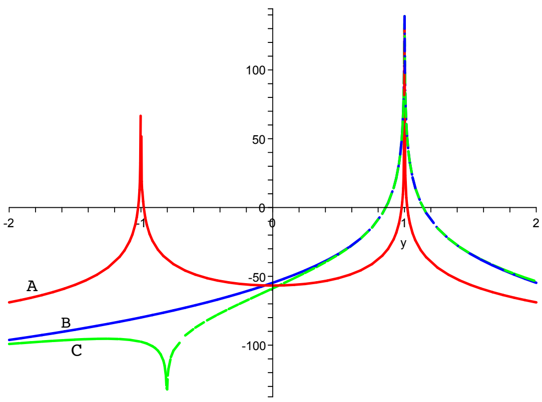

Figure 2. Radial sensitivities of (A) a tripolar cuff electrode, (B) a planar hexagonal patch and (C) a bent hexagonal patch. The vertical axis is in dB$\,\mu$V and the unit for the horizontal axis is the radius R of the electrode.

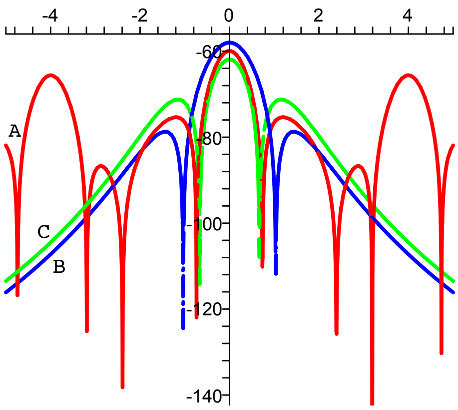

Figure 3. Longitudinal sensitivities on the axe of (A) a tripolar cuff electrode, (B) a planar hexagonal patch and (C) a bent hexagonal patch. The vertical axis is in dB μV and the unit for the horizontal axis is the radius R of the electrode.

hexagonal patch is far higher (up to 30 dB) when considering an AP located between the centre of the patch and the centre of the cuff.

Figures 3 and 4 show the longitudinal sensitivities of the three considered electrodes. On figure 3, the sensitivity is computed for an AP placed on the Ox axe, while, on figure 4, the AP is placed on a line, parallel to Ox, cutting Oy at abscissa $0.8R$. On this later figure, we can see an increase of sensitivity of the tripolar cuff in the vicinity of the rings, but this remains far lower than the sensitivity of any of the hexagonal patches.

B. External sensitivity

The figure 5 show the external sensitivities of our three electrodes for an AP placed on the Ox or on the Oz axis of the electrode. As stated above, the quantity plotted is not a voltage, but is homogeneous to the reciprocal of the cube of a distance. Nevertheless, we can see on these two

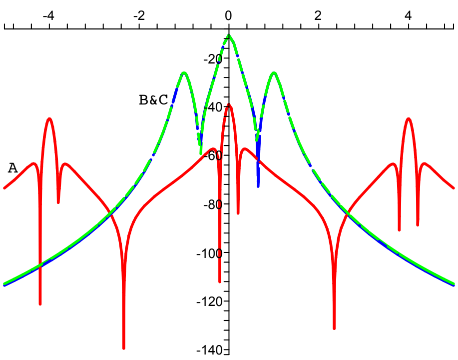

Figure 4. Longitudinal sensitivities on an off-centre (80 % of R) axis of (A) a tripolar cuff electrode, (B) a planar hexagonal patch and (C) a bent hexagonal patch. The vertical axis is in dB μV and the unit for the horizontal axis is the radius R of the electrode.

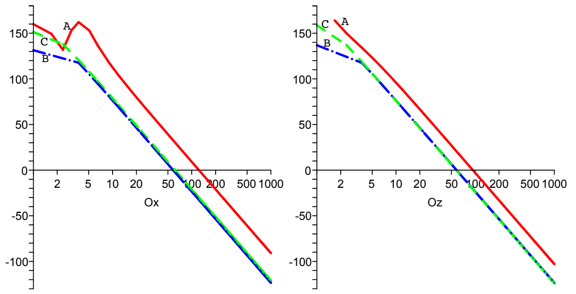

Figure 5. External relative sensitivity along Ox and Oz axes for (A) a tripolar cuff electrode, (B) a planar hexagonal patch and (C) a bent hexagonal patch. The vertical axis is in dB and the unit for the horizontal axis is the radius R of the electrode.

graphs that the hexagonal patches exhibit a better rejection of parasitic signals than the tripolar cuff. This improvement is of 32 dB for Ox and 20 dB for Oz.

Unfortunately, the same study conducted along the Oy axis (figure 6) show that, while the planar patch continue to have the better rejection of parasitic signals, the wrapped hexagonal patch has a sensitivity decreasing too slowly along this Oy axis. In particular, we can see that the bent hexagonal patch as a larger sensitivity than the tripolar cuff for action potentials placed at more than fifty times the radius of the cuff, i.e. approximately 7 cm…

IV. Perspectives

The results presented here show that the hexagonal patches allow to have better sensitivity, better spatial selectivity and higher rejection of parasitic signals than the classical tripolar cuff.

To facilitate the signal post-processing on the recording system, we need a maximum of neural data. A tripolar electrode cuff [11] provides only one recording which is the superposition of all action potentials "seen" by the electrode at a given moment. The use of several hexagonal patches on

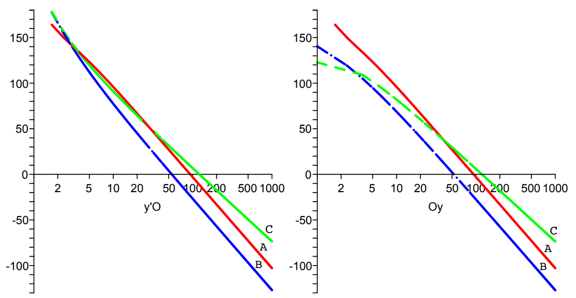

Figure 6. External relative sensitivity along the two halves of the Oy axis for (A) a tripolar cuff electrode, (B) a planar hexagonal patch and (C) a bent hexagonal patch. The vertical axis is in dB and the unit for the horizontal axis is the radius R of the electrode.

a cuff electrode (see Fig. 1-b) could allow us to record more signals and thus increase the quantity of neural data.

Furthermore, references [4], [12] show that it is possible to extract the direction and the speed of the signal propagation of AP by using several successive poles. This principle is still relevant for our electrode and would thus allow us to obtain more accurate pieces of information about the direction and the speed of AP propagations.

V. Conclusion

We have presented here a comparison between the classical tripolar cuff electrode for ENG recording and a new cuff electrode using a large number of poles using an hexagonal layout.

Simulations have shown that this new structure is very promising in terms of sensitivity and selectivity, allowing to envisage the use of source separation techniques to process ENG signals.

References

[1] M. Djilas, C. Azevedo Coste, K. Yoshida, and G. Cathébras, "Interpretation of ENG signal for FES closed-loop control," in *IFESS'06: 11th Annual Conference of the International Functional Electrical Stimulation Society*, Miyagi-Zao, Japan, 12-15 Sep. 2006, pp. 85–87.

[2] A. Ramachandran, J. Sacristan, N. Lago, T. Dörge, M. Osès, K. Koch, and K. Hoffmann, "Multipolar cuff electrodes with integrated pre-amplifier & filter to interface peripheral nerves for FES application." in *10th Annual Conference of the International FES Society*, Montreal, Canada, Jul. 2005. [Online]. Available: http://ifess.org/ifess05/Poster\%20Session\%201/Ramachandran\%20A.pdf

[3] J. Winter, M. Rahal, N. Taylor, N. Donaldson, and J. Struijk, "Improved spatial filtering of ENG signals using a multielectrode nerve cuff," in *5th Annual Conference of the International Functional Electrical Stimulation Society*, Aalborg, Denmark, Jun. 2000. [Online]. Available: http://www.ifess.org/ifess00/Poster\%20Session\%204/Winter.pdf

[4] J. Taylor, N. Donaldson, and J. Winter, "Multiple-electrode nerve cuffs for low-velocity and velocity-selective neural recording," *Medical and Biological Engineering and Computing*, vol. 42, no. 5, pp. 634–643, Sep. 2004.

[5] M. K. Haugland, J. A. Hoffer, and T. Sinkjaer, "Skin contact force information in sensory nerve signals recorded by implanted cuff electrodes," *IEEE Transactions on Rehabilitation Engineering*, vol. 2, no. 1, pp. 18–28, 1994. [Online]. Available: http://dx.doi.org/10.1109/86.296346

[6] W. Jensen, T. Sinkjaer, and F. Sepulveda, "Improving signal reliability for on-line joint angle estimation from nerve cuff recordings of muscle afferents," *IEEE Transactions on Neural Systems and Rehabilitation Engineering*, vol. 10, no. 3, pp. 133–139, Sep. 2002.

[7] L. N. S. Andreasen and J. J. Struijk, "Signal strength versus cuff length in nerve cuff electrode recordings," *IEEE Trans. Biomed. Eng.*, vol. 49, no. 9, pp. 1045–1050, Sep. 2002.

[8] J. J. Struijk and M. Thomsen, "Tripolar nerve cuff recording: stimulus artifact, EMG and the recorded nerve signal," in *Engineering in Medicine and Biology Society, 1995. IEEE 17th Annual Conference*, vol. 2, Montreal, Que., Sep. 20–23, 1995, pp. 1105–1106.

[9] C. Pflaum, R. R. Riso, and G. Wiesspeiner, "Performance of alternative amplifier configurations for tripolar nerve cuff recorded ENG," in *Engineering in Medicine and Biology Society, 1996. Bridging Disciplines for Biomedicine. Proceedings of the 18th Annual International Conference of the IEEE*, vol. 1, Amsterdam, Oct. 31–Nov. 3, 1996, pp. 375–376.

[10] R. B. Stein, *Nerve and Muscle*. Plenum Press, 1980.

[11] A. Demosthenous and I. F. Triantis, "An adaptive ENG amplifier for tripolar cuff electrodes," *IEEE J. Solid-State Circuits*, vol. 40, no. 2, pp. 412–421, Feb. 2005.

[12] R. Rieger, M. Schuettler, D. Pal, C. Clarke, P. Langlois, J. Taylor, and N. Donaldson, "Very low-noise ENG amplifier system using CMOS technology," *IEEE Transactions on Neural Systems and Rehabilitation Engineering*, vol. 14, no. 4, pp. 427–437, Dec. 2006.

VI. Authors's Address

All authors are with the Laboratoire d'Informatique, Robotique et Microélectronique de Montpellier :

LIRMM,
Univ. Montpellier 2 – CNRS – INRIA
161 rue Ada
34392 Montpellier, France.

Emails:

- Lionel.Gouyet@lirmm.fr
- Guy.Cathebras@lirmm.fr
- Serge.Bernard@lirmm.fr
- David.Guiraud@lirmm.fr
- Yves.Bertrand@lirmm.fr

MINIMALLY-INVASIVE INTRAMUSCULAR MASSIVE MUSCLE STIMULATION

Carraro U[1], Mayr W[2], Lanmüller H[2], Rigatelli GL[1], Biral D[1], Adami N[1], Vindigni V[3], Kern H W[4]

[1] Translational Myology Lab, Interdepartmental Research Center of Myology, University of Padua, Italy

[2] Center of Biomedical Engineering and Physics, Medical University of Vienna, Austria

[3] Unit of Plastic Surgery, Interdepartmental Research Center of Myology, University of Padua, Italy

[4] Ludwig Boltzmann Institute, Department of Physical Medicine, Wilhelminenspital, Vienna, Austria

Abstract

Functional electrical stimulation of skeletal muscle is performed by cutaneous surface electrodes, by transcutaneous needle electrodes or by epineural/intramuscular implanted electrodes. From several months after injury, denervated muscle can only be electrostimulated by very large transcutaneous surface electrodes, that need very high currents or by implanted perimisial electrodes.We are exploring the hypothesis that customized endovascular electrodes may be inserted via veins into the denervated muscle capillary network. In spite of the success of the endocardial electrostimulation for cardiac pacing, problems/risks of this approach are related to the: i) lower excitability of the denervated muscle in comparison to innervated tissue or myocardium; ii) thrombogenesis and embolism, iii) muscle trauma related to muscle contraction against the inserted electrodes. Some of these risks ask for new materials and technologies (possibly, nano- or micro-technologies) and therefore of new concepts and methods. On the other hand, we will show that, standing on sound biological bases, preliminary studies in rabbits demonstrate the feasibility of the approach. Plasticity of muscle tissue and of its vascular bed grants further testing and development of the new concept.

Introduction

Skeletal muscle tissue-based cardiac-bio-assists may be better designed and developed if the muscle tissue may be set free from neurovascular constrains, using direct muscle electrical stimulation to provide the needed activation of the device. Based on our experience on paraplegic muscles, we are wondering if a new stimulation approach would be possible for the cardiac-bio-assists. Functional electrical stimulation of human skeletal muscle is performed by surface electrodes, or by intramuscular or epineural implanted electrodes. From several months after permanent contact with the lower motoneuron, human denervated muscle can only be electrostimulated by implanted perimisial electrode or by very large transcutaneous surface electrodes, the latter needing very high currents. We are exploring the hypothesis that customized soft endovascular electrodes may be inserted via veins up to the capillary network of denervated muscle We here show that preliminary tests in rabbit grant feasibility of the concept for innervated thigh muscles.

Material and Methods

Animals, endovascular electrodes implantation and stimulation protocols:

Adult male rabbit (4 kg) were anesthetized with Zoletil (Virbac, France), 0.2 ml/Kg. The Vienna implantable stimulator used for animal experiments was implanted as described in [1-3]. A large reference electrode was implanted on the back muscles of the rabbit, while a 0.8 mm stainless teflon-coated wire was inserted 2 cm in the safena vein of both thighs using a human pediatric catheter (24G Jelco, Johnson&Johnson Medical). Four-day after implantation the muscle was activated with bidirectional inpulses at 2.52 mA, 1.00 msec, 50 Hz; 1 sec ON, 2 sec OFF bursts, 300 min, daily. At stated time the rabbits were euthanized, thigh vessels and muscles were isolated, immediately frozen in liquid nitrogen and stored at –80°C until use. Cryosections of frozen tissues were stained with Hematoxilin-Eosin, using conventional techniques as described by Rossini et al. [4]. Images were acquired using a Zeiss microscope connected to a Leica DC 300F camera at low magnitude under the same conditions that were used to acquire a reference ruler. Morphometric analysis was performed with Scion Image for Windows version Beta 4.0.2 (by 2000 Scion Corporation), free software downloaded from the web site:

www.scioncorp.com. Figures were mounted and labeled using Adobe Photoshop® v6.0.

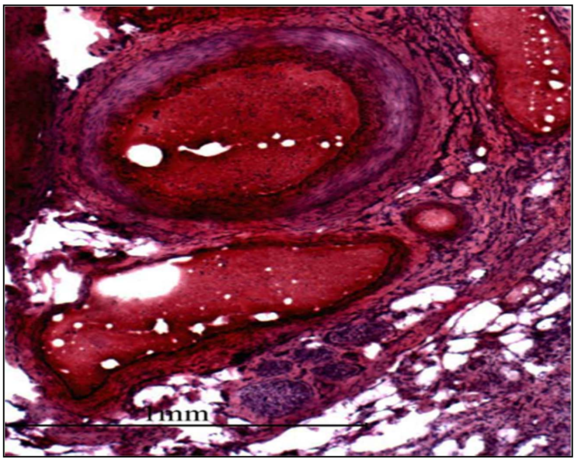

Fig. 1: Femoral vessels of an endovascular electrostimulated rabbit

Results

Figure 1 shows that the endovascular electrodes (and the electrical stimulation) do not modify the structural characteristics of the vessels. At the end of a sub-acute experiment (30-day stimulation) the vessels were patent.

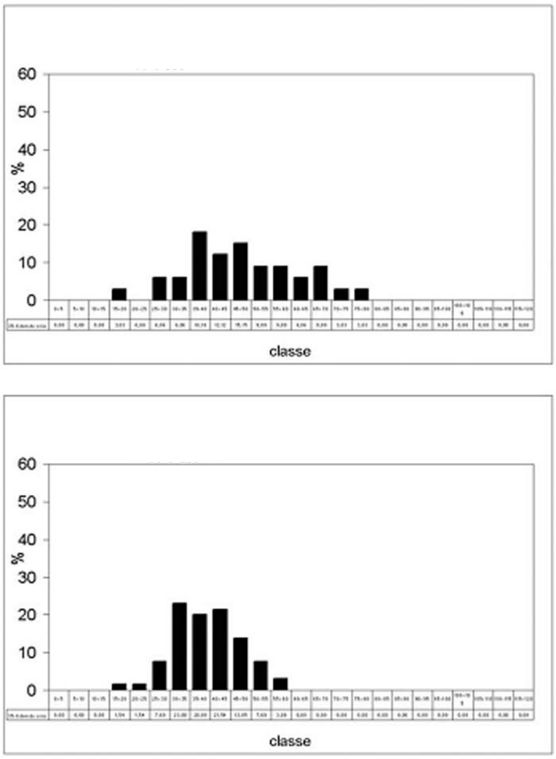

Fig.3: Endovascular electrostimulation of rabbit muscle: Fiber size distribution of contralateral (Upper panel) and endovascular electrostimulated muscle (Lower panel). After 30-d electrostimulation the myofibers are of uniformely smaller size.

The left upper panels of Figure 2 shows an H&E stain of a transverse section of the unstimulated leg rabbit muscle, that is characterized by well-packed

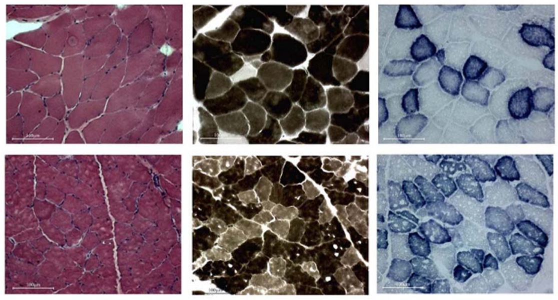

Fig.2: Endovascular electrostimulation of rabbit muscle: Left panels, Hematoxilin-Eosin; Central panels: Myofibrillar ATPase, pH 9.4; Right panels: SDH activity. Upper panels: Contralateral leg. Lower panels: Endovascular electrostimulated muscle. Myofibers are of uniformely smaller size. SDH and ATPase activities indicate a shift towards more oxidative-slow type myofibers.

muscle fibers of variable size (see also upper panel of Figure 3). The muscle fibers show three levels of myofibrillar ATPase staining and seldom present high SDH activity (fast-type prevalence).

Lower panels of Figure 3 show that after 30-day endovascular electrostimulation (300 min daily, 1 sec ON and 2 sec OFF), the muscle fibers are of uniformly smaller size, the larger of the normal range being absent (Figure 2, lower panel). ATPase staining shows a shift towards intermediate-type myofibers, that more often present high SDH activity, a mithocondrila marker, peculiar of fatigue-resistent myofibers.

Discussion

Skeletal muscle tissue-based cardiac-bio-assists or other more usual clinical applications of muscle transfer in Plastic&Reconstructive Surgery (e.g., sfincter or bladder reconstruction) may be better designed and developed if the muscle tissue may be set free from neurovascular constrains, using direct muscle electrical stimulation to provide the needed activation of the device. Standing on our experience with FES of denervated paraplegic muscles [5-10], we are wondering if a new stimulation approach would be possible for those other promising clinical applications.

Functional electrical stimulation of human skeletal muscle is performed by surface electrodes, by transcutaneous needle electrodes or by epimisial or epineural implanted electrodes. From several months after injury, human lower motoneuron denervated muscles are only electrostimulable by implanted perimisial electrode or by very large surface electrodes, the latter needing very high currents. We are exploring the hypothesis that customized endovascular electrodes may be inserted via veins into the capillary network of denervated muscle. In spite of the success of the endocardial electrostimulation for cardiac pacing, risks of this approach are related to the: i) lower excitability of the denervated muscle in comparison to innervated tissue or myocardium, and ii) muscle trauma related to muscle contraction against the inserted electrodes.

Some of these risks ask for new materials and technologies (possibly, nano- or micro-technologies) and therefore of new concepts and methods. On the other hand, we are showing that, standing on sound biological bases, preliminary studies in rats [11] and rabbits (present results) demonstrate the feasibility of the approach. Plasticity of muscle tissue and of its vascular bed grants further testing and development of the new concept.

References

[1] Ashley Z, Sutherland H, Lanmuller H, et al. Determination of the chronaxie and rheobase of denervated limb muscles in conscious rabbits. Artificial Organs, 29: 212-215, 2005.

[2] Lanmüller H, Ashley Z, Unger E, et al. Implantable device for long-term electrical stimulation of denervated muscles in rabbits. Medical & Biological Engineering & Computing, 43: 535-540, 2005.

[3] Ashley Z, Sutherland H, Lanmuller H, et al. Atrophy, but not necrosis, in rabbit skeletal muscle denervated for periods up to one year. American Journal of Physiology, in press.

[4] Rossini K, Zanin ME, Podhorska-Okolow M, Carraro U. To stage and quantify regenerative myogenesis in human long-term permanent denervated muscle. Basic Appl Myol 12:277-286, 2002.

[5] Kern H, Boncompagni S, Rossini K, et al. Long-term denervation in humans causes degeneration of both contractile and excitation-contraction coupling apparatus that can be reversed by functional electrical stimulation (FES). A role for myofiber regeneration? J Neuropath Exp Neurol 63:919-931, 2004.

[6] Carraro U, Rossini K, Mayr W, Kern H. Muscle fiber regeneration in human permanent lower motoneuron denervation: relevance to safety and effectiveness of FES-training, which induces muscle recovery in SCI subjects. Artif Organs 29:187-191, 2005.

[7] Modlin M, Forstner C, Hofer C, et al. Electrical Stimulation of Denervated Muscles: First Results of a Clinical Study Artificial Organs 29:203–206, 2005.

[8] Rossini K, Biral D, Carraro U, Mayr W, Kern H. N-CAM and isomyosins of long-term denervated human muscle. Basic Appl Myol, in press.

[9] Carraro U. Modulation of trophism and fiber type expression of denervated muscle by different patterns of electrical stimulation. Basic Appl Myol 12: 263-273, 2002.

[10] Kern H, McKay WB, Dimitrijevic MM, Dimitrijevic MR. Motor control in the human spinal cord and the repair of cord function. Curr Pharm Des 11:1429-1439, 2005. Review.

[11] Carraro U, Rossini K, Adami N, et al. Endovascular electrostimulation of rat muscles. Basic Appl Myol, in press.

Acknowledgements

This research was undertaken with the financial support of 1. Italian Ministry of Education (MURST) under the framework of PRIN Projects (PRIN 2004-2006 Program, Contract n. 2004061452-002); 2. The Italian C.N.R. funds and the Italian MURST funds (ex60%) to Ugo Carraro. This work was also supported by Research Funds from the Ludwig Boltzmann Institute for Electrostimulation and Physical Rehabilitation at the Institute of Physical Medicine and Rehabilitation (Wilhelminenspital, Vienna, Austria).

Author's Address

Ugo Carraro
Translational Myology Lab, Interdepartmental Research Center of Myology, c/o Department of Experimental Biomedical Sciences, University of Padua, Viale G. Colombo 3, I-35122 Padova, Italy
eMail: ugo.carraro@unipd.it
homepage: http://www.bio.unipd.it/bam/bam.html

Session IV

Upper Extremity

Chairpersons
Thierry Keller (Zurich, Switzerland)
Dejan Popovic (Aalborg, Denmark)

FINGER AND WRIST TORQUE MEASUREMENT SYSTEM FOR THE EVALUATION OF GRASP PERFORMANCE WITH NEUROPROSTHESES

Lawrence M[1,2,3], Gross G[1], Keller T[1,2,3]

[1] Electrical Stimulation Group, ETH Zurich, Zurich, Switzerland

[2] Spinal Cord Injury Centre, University Hospital Balgrist, Zurich, Switzerland

[3] Sensory and Motor Systems Laboratory, ETH Zurich, Zurich, Switzerland

Abstract

New multi-channel neuroprotheses have been developed which can significantly improve grasping function by allowing selective stimulation of the finger and wrist flexors and extensors. A new isometric measurement system was therefore developed to enable assessment of finger forces and wrist torques generated using multi-channel techniques.

Finger forces (from the middle phalanxes) were recorded using five load cells (range ±100N) mounted on a 'grasp handle' that can be arbitrarily positioned in space. The hand and the grasp handle were rigidly mounted to a six degree of freedom load cell (±1000N, ±100Nm), and the forces and torques about the wrist recorded. A vacuum cushion was used to comfortably fixate the forearm. The position and orientation of the forearm, wrist, fingers and handle were recorded using a new 3-dimensional position measurement system (accuracy <±1mm).

A mathematical model was used to provide an estimate of the joint centres, enabling the finger and wrist torques to be calculated. Analysis of the model indicated that small movements of the hand (<2mm) would confine the measured force error to less than 5%. Actual measurements during maximum voluntary contractions indicated small drifts (±1N, ±0.1Nm), however, a good repeatability (error < ±1N) could still be achieved.

The measurement system was integrated into a real-time multi-channel transcutaneous electrode environment which is able control multiple activation regions across both the flexors and extensors. Using the combined system it is possible to optimise configurations for selective activation of the finger and wrist flexors and extensors. The technology can be used to configure and assess new multi-channel neuroprostheses for grasping.

Introduction

Selective finger and wrist movements can be generated by electrical stimulation using multiple activation regions distributed across transcutaneous electrode arrays placed above the extrinsic forearm flexors and extensors [1]. To further investigate the effects of multiple activation regions, a measurement system was required which can simultaneously record isometric finger forces and wrist torques.

Isometric finger forces were previously recorded during dynamic wrist motion [2]. Five load cells were mounted on a custom adjustable handle, and used to record isomeric finger flexor forces at different wrist positions (flexion / extension and ulnar / radial deviation). Constant torque loads could be generated against which the wrist had to flex / extend. However isometric wrist torques were not recorded.

Wrist torques and prehensile grasp forces were previously recorded using force dynamometers mounted onto a six degree of freedom load cell [3]. Wrist torques were recorded while volunteers performed 'pulp pinch', 'key pinch' and 'power grip' tasks. However finger and wrist synergies could not be investigated as only a single force was recorded for grasp.

Joint torque synergies were extensively investigated for different finger angles [4]. The hand, wrist and forearm were fixed in a rigid cast; with the distal finger tip mounted in the centre of a 6-dof load cell. Joint torques were generated using intramuscular stimulation of extrinsic flexors. The ratio of recorded joint torques was found to vary significantly with joint angles; although the values were associated with the metacarpal joint.

A new measurement system was developed which enables investigation of finger and wrist forces and torques. The system can be used to investigate finger and wrist synergies produced by transcutaneous stimulation of the forearm flexors and extensors.

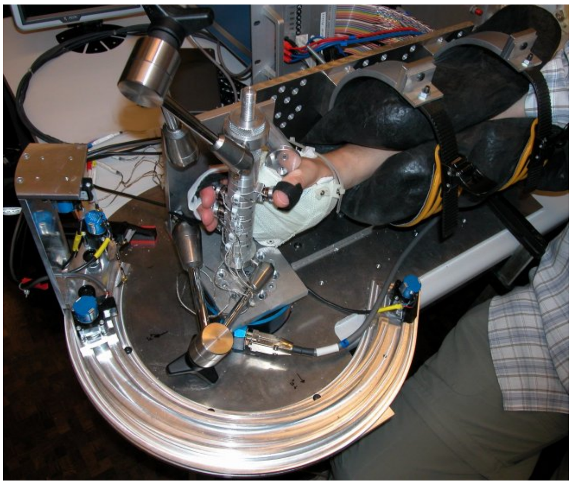

Fig. 1: Photo of the grasp and wrist assessment system

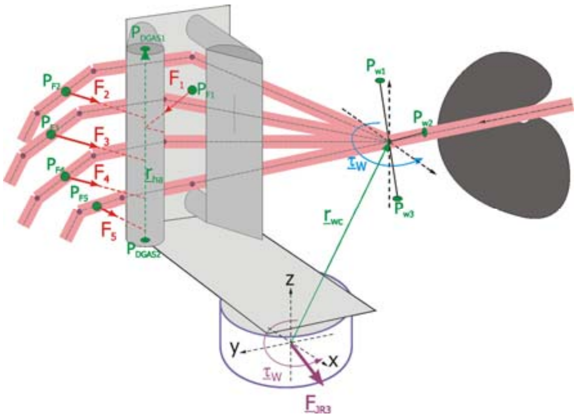

Fig. 2: Schematic model showing orientation of JR3 axis; (left hand rule) applied torques and measurement points for calculating orientation of applied thumb and finger forces (P_{F1} to P_{F5}) with respect to axis of the measurement handle (P_{DGAS1} and P_{DGAS2}). The wrist center ($\underline{r}_{wc}$) and rotation angles were estimated from the projection of vectors $P_{W3} \rightarrow P_{W2}$ onto $P_{W3} \rightarrow P_{W1}$. Flexion of the wrist and fingers produce positive forces and torques.

Materials and Methods

System overview

The new grasp and wrist assessment system (Fig. 1) was developed by adapting an existing grasp handle [2] and combining it with a six degree of freedom load cell (JR3 45E15AU760, JR3 Inc, Woodland CA). Five sub-miniature load cells (BL321 Honeywell, ±100N) were integrated into the modified grasp handle, with fingers attached using Velcro™ straps mounted through custom aluminium plates [5]. Each BL321 was mounted on a custom ring, with its measurement axis aligned perpendicular to the axis of the handle (the thumb was mounted at 70°). Each ring could be independently rotated and locked around the grasp handle. Two lockable articulated arms (Fisso G13, Baitella CH) were used to fixate the grasp handle to the JR3.

The forearm was held in place using a modified vacuum cushion (Summit-Rehab, DE) fixated using adjustable snowboard bindings and aligned parallel to the Y axis of the JR3. The palm of the hand was mounted against an aluminium plate orientated perpendicular to the index finger. Scotchcast (3M) was used to ensure a rigid connection of the hand to the plate, with screws mounted to allow the hand to be removed and re-secured. The plate was connected to the JR3 and mounted such that the hand remained in 30° extension.

A novel 3D position system [5] was used to record anatomical landmarks. The system uses trilateration [6] to calculate the 3D intersection of three wire-draw sensors (WDS750MKII, Micro-Epsilon, DE). The three sensors were mounted onto a cart which could be rotated around the outside of the measurement system, with the angle recorded using a fourth WDS750. The coordinate system was aligned along the axis of the JR3; with the [0,0,0] point defined as the centre of the JR3.

Joint centres and finger force orientations were estimated using vector projection between three measured points; e.g. (1)

$$\underline{r}_{WC} = P_{W2} + \frac{(P_{W3} - P_{W2}) \cdot (P_{W1} - P_{W2})}{\left|(P_{W1} - P_{W2})\right|} \qquad (1)$$

Metacarpal joint centres were estimated using [7] and aligned along the projection of the index finger (F_3) from the wrist joint ($\underline{r}_{wc}$).

Measurement data from the load cells and wire draw sensors was sampled at 100Hz using a 12bit data acquisition card (6024E National Instruments, USA) embedded into the Virtual Electrode Environment [8]. Custom xPC Simulink models (The Mathworks, USA) were used to sample and store data; before being uploaded to Matlab for filtering (median filter n=10) and offset subtraction.

Wrist Torque Model

A schematic model of the system (Fig. 2) was developed to show the orientation of the measured points and applied force vectors and torques. For simplicity the wrist was assumed to be a spherical joint, localised at the distal wrist crease [7].

Wrist torques and forces were assumed to be transmitted entirely through the hand plate and cast. Internal forces generated between the grasp handle and hand cast were assumed to have no

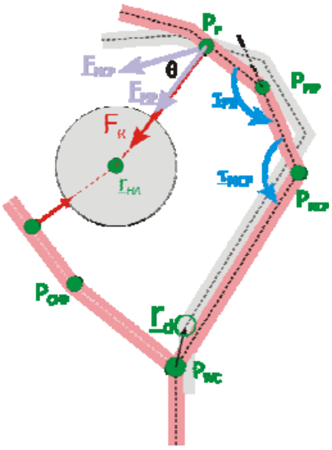

Fig. 3: Schematic model indicating forces $\underline{F}_{MCP}$ and $\underline{F}_{MCP}$ generated by torques $\underline{\tau}_{MCP}$ and $\underline{\tau}_{PIP}$ about the metacarpal (MCP) and proximal inter-phalange (PIP) joints. The measured force F_R acts along the unit vector $\hat{\underline{F}}_R$ defined from the point P_F to the intersection with axis of the grasp handle $\underline{r}_{HA}$

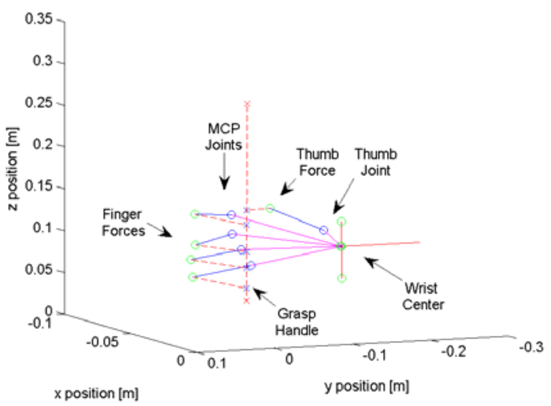

Fig. 4: Recorded and calculated locations of joint centers (blue circle) and orientation of finger forces (green circles) with respect to the grasp handle (red / blue cross).

affect on JR3 measurements. Wrist torques $\underline{\tau}_w$ were calculated using a Jacobian representation of (2) with cartesian rotation matrices (R_z,R_y and R_x) applied to rotate and translate the forces and torques to the actual orientation of the hand and wrist joint.

$$\underline{\tau}_w = R_z R_y R_x \left(\underline{\tau}_{JR3} - \underline{r}_{wc} \times \underline{F}_{JR3} \right) \qquad (2)$$

Finger Forces

The metacarpal (MCP) and proximal inter-phalange (PIP) joints were assumed to be simple flexion / extension hinge joints with no additional degrees of freedom. Activation of the extrinsic flexors and extensors was assumed to produce torques $\underline{\tau}_{MCP}$ and $\underline{\tau}_{PIP}$ about the MCP and PIP joints. Thumb forces were assumed to be generated from the carpometacarpal (CMP) joint.

The resultant grasping finger force F_R measured by the BL321 is formed from the components $\underline{F}_{MCP}$ and $\underline{F}_{PIP}$ (3) where the angle $\theta\cdot$is that of the PIP joint.

$$F_R = \left|\underline{F}_{PIP}\right| + \left|\underline{F}_{MCP}\right| \cos\theta\cdot \qquad (3)$$

The production of finger joint torques can generate displacement of the hand $\underline{r}_d$; altering the relative finger angles. Using anatomical data and simple geometric models; the error on the measured finger force F_R was found to be less than 5% for displacements $\left|\underline{r}_d\right|$<4mm [5]. Rigid hand was therefore considered essential.

Results

The system was calibrated and verified by applying known forces and torques using spring balances (Pesola, CH). Mean and standard deviation (SD) values were recorded before, during and after application of the loads. Typical SD values were <0.5N for the BL321 load cells; and <0.6N and <0.1Nm for the JR3. Forces applied between the finger sensors and hand cast generated no forces or torques about the JR3. Similarly external forces and torques generated no forces on the finger sensors.

A volunteer placed his right arm in the system, with anatomical landmarks and sensor orientations recorded. Joint centers were calculated according to (1) and [7] (Fig 4). Finger forces and wrist torques were recorded during individual voluntary finger flexion, and wrist extension and flexion. Measurements were repeated 5 times, with mean and standard deviations recorded.

Voluntary flexion of the thumb and fingers produced forces of 3.43±0.11N 4.07±0.41N 7.45±0.16N, 4.62±0.24N and 5.0±0.48N respectively. Net wrist torques were below 0.2N±0.1Nm flexion and 0.1±0.02Nm ulna deviation. Thumb flexion generated small wrist extension torques <0.1±0.02Nm and larger ulna deviations ~0.2±0.3Nm. Voluntary wrist extension produced net torques of -2.86±0.22Nm with maximum coupling of –0.93 ±0.14N (0.07±0.01Nm) on the ring finger. Voluntary wrist flexion produced net torques of 2.25±0.07Nm; with coupled thumb and finger forces of -1.3±0.12N, 1.37±0.11N, 0.58±0.08N, 0.75±0.08N and 3.05±0.11N respectively.

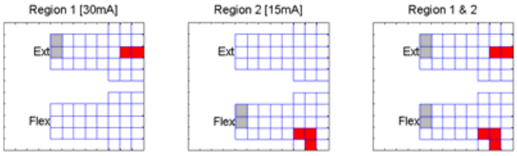

Fig. 5 Locations of activation regions (red) and compensating electrodes (grey) for stimulation of the wrist and finger extensors (region 1, 30mA) and finger flexors (region 2, 15mA).

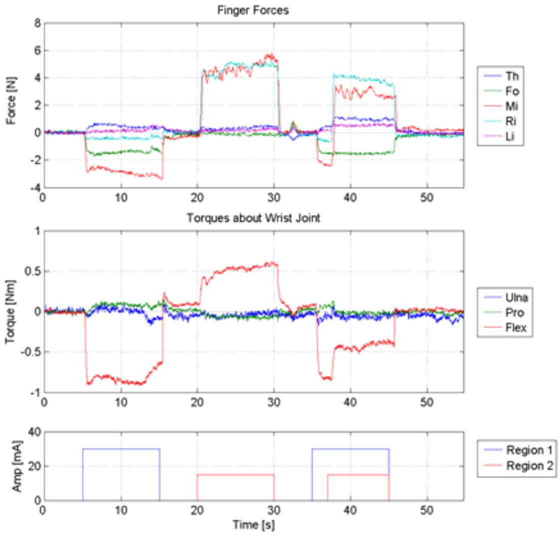

Fig. 6: Finger forces and wrist torques recorded during wrist extension, finger flexion and functional grasp. Flexion is taken as positive; with extension negative.

Electrically stimulated functional grasp

New custom transcutaneous electrode arrays [1] were placed above the wrist extensors and finger flexors. Asymmetric biphasic pulses (length 250ms) were applied to activation regions chosen for wrist and finger extension and finger flexion (Fig 5). Finger forces and wrist torques were recorded for wrist extension; middle and ring finger flexion and functional grasp; i.e. simultaneous activation of wrist extensors and flexors.

Wrist extension (-0.88±0.02Nm) produced a maximum middle finger force of -2.81±0.04N. Middle and ring finger flexion (4.49±0.2N, 4.85±0.03N) produced a wrist torque of 0.52±0.08Nm. A net wrist extension (-0.42±0.04Nm) could be maintained during electrically stimulated functional grasp producing middle and ring finger forces of 2.87±0.26N and 3.87±0.14N.

Discussion

A new measurement system has been developed which enables isometric finger forces and wrist torques to be recorded. Validation measurements indicated that internal forces on the grasp handle are decoupled from external forces and torques.

The net torques from the MCP and PIP joints could be estimated from the measured grasping force F_R and the projected joint centers [7]. However [4] found that the orientation of the resultant force vector was dependant upon the relative activation of the different extrinsic muscles. Since this change in orientation cannot be measured only the grasping force F_R is recorded.

During functional grasp, a net wrist extensor torque can be maintained whilst the middle and ring fingers are flexed. By measuring the finger forces and wrist torques for different activation regions, it will be possible to investigate and improve electrically stimulated functional grasp.

References

[1] Keller T., Lawrence M., Lang M, Kuhn A., Textile Neuroprosthesis Garment for Functional Electrical Stimulation. Proceedings of Vienna International Workshop on FES, 2007

[2] Dumont C.E., Popovic M. R., Keller T., Sheikh R. Dynamic force-sharing in multi-digit task. Clinical Biomechanics, 21, 138-146, 2006

[3] Greig M., Wells R.. Measurement of prehensile grasp capabilities by a force and moment wrench: Methodological development and assessment of manual workers. Ergonomics, 47(1): 41-58, 2004

[4] Kemper D. G., Fischer H. C., Cruz E., G. Impact of finger posture on mapping from muscle activation to joint torque. Clinical Biomechanics 21, 361-369, 2006

[5] Gross; G-P. Selective Control of Wrist and Finger Flexors for FES grasping, Masters Thesis, Automatic Control Lab, ETH Zurich, April 2007.

[6] Thomas F., Ros L., Revisiting Trilateration for Robot Localization. IEE Trans. Robotics, 21(1), 93-101, 2005.

[7] Buchholz B., Armstrong T. J., A kinematic model of the human hand to evaluate its prehensile capabilities. J. Biomechanics, 25(2) 149-162, 1992.

[8] Lawrence, M., Brunschweiler A., Keller T., Multi-channel Transcutaneous Electrical Stimulation Environment. Proceedings of 11th IFESS, Zao Japan, 210-212, 2006

Acknowledgements

The project was supported by the Swiss National Centre of Competence of Research for Neural Plasticity and Repair.

Author's Address

Marc Lawrence, Electrical Stimulation Group,
ETH Zurich, www.control.ethz.ch/~fes

EXPERIMENTAL RESULTS IN ASSESSING THE GRIP FORCE CONTROL IN STROKE PATIENTS DURING THE FES-BASED REHABILITATIVE TREATMENT

Ştefan Marius Ciprian[1], Poboroniuc Marian[1], Livinț Gheorghe[1]

[1] Faculty of Electrical Engineering / "Gh. Asachi" Technical University of Iaşi, Iaşi, Romania

Abstract

The aim of the paper is to present the results obtained after using a tracking system for the assessment and training of the grip force control on patients with neuromuscular diseases. In conjunction with other known hand tests the Grip Force Tracking System proved to be an effective tool for assessing hand dexterity and to quantify the hand rehabilitation process at stroke patients which use devices based on Functional Electrical Stimulation (FES) for regaining the upper limb mobility.

Introduction

Stroke is a leading cause of serious, long-term disability, fact that inspired the scientific and medical community in finding the best rehabilitation methods for treatment and assessing the patients during the post-stroke recovering process. The World Health Organization estimates for the year 2001 that there were over 20.5 million strokes worldwide from which 5.5 million of these were fatal [1].

In Romania, stroke is the second most common cause of death. In UK, approximately 100,000 first ever strokes occur each year [2]. Generally, half of all acute stroke patients starting rehabilitation will have a marked impairment of function of one arm and only about 14% of these will regain useful function [3].

According to the National Stroke Association: 10% of stroke survivors recover almost completely, 25% recover with minor impairments, 40% experience moderate to severe impairments that require special care, 10% require care in a nursing home or other long-term facility, 15% die shortly after the stroke and approximately 14% of stroke survivors experience a second stroke in the first year following a stroke [4].

Stroke is affecting all kind of people in different ways, depending on the type of stroke, the area of the brain affected and the extent of the brain injury. Paralysis with weakness on one side of the body is a common after effect. Within the physical therapy, the rehabilitation process aims to help the patient to regain its ability to walk and the mobility of the affected upper limb as it was before the unwished event.

The improvement or restoration of lost sensory-motor function is one of the major issues in the rehabilitation of subjects with neurological disorders, such as those caused by spinal cord injury (SCI), stroke or head injury [5]. These subjects can become more independent and improve their physical and psychological situations through a rehabilitation program based on functional electrical stimulation (FES). Different methods of rehabilitation and therapy, including FES, can help such people regain a certain degree of functionality in their hands [6].

Assessing the hand and overall functionality of the upper limb it is more difficult. Some tests assessing the range of motion & sensation, strength and dexterity have been proposed. The Jebsen-Taylor test has been proven to be an objective test of hand functions commonly used in activities of daily living [7].

After the stroke patient regains some movement over the shoulder and elbow, hand dexterity and grip force have to be assessed. Some grip strength measurements are mainly focused on the evaluation of the maximal voluntary grip force, but it is important to assess the capacity to control the grip strength of sub-maximal forces which are engaged during grasping and manipulation of different objects.

This paper presents some experimental results obtained throughout the assessment and training of stroke (CVA) patients while performing classic hand exercises along with FES based rehabilitative treatment within the Rehabilitation Hospital of Iasi, Romania.

Material and Methods

Grip Force Tracking System:

The Grip Force Tracking System (GFTS) involves biofeedback training methods and consists of two grip-measuring devices of different shapes (cylinder and thin plate), as shown in figure 1. The cylindrical device allows assessment of grip forces up to 360 N with the accuracy of 0.02% over the entire measuring range. The other device is made from two metal parts which shape into a thin plate at the front end it is being used for assess or train fingers pinch task. It can measure forces up to 360N with the accuracy of 0.1%. The output given by the two grip-measuring devices is sampled through an interface box, consisting of an amplifier with supply voltage stabilizer and an integrated 12-bit A/D converter. The interface box it is connected to the parallel port of a personal computer, and used for data acquisition and visual feedback.

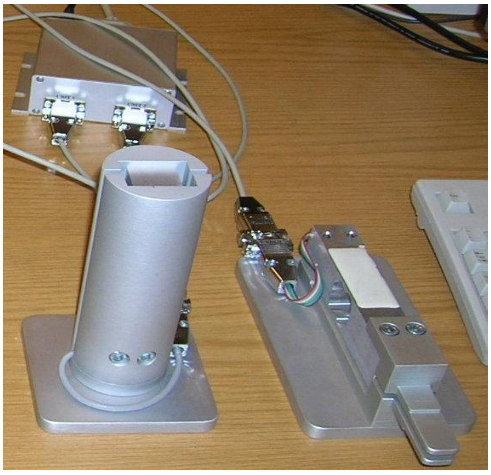

Fig. 1: The Grip Force Tracking System (GFTS)

The tracking task, as part of the biofeedback training, requires the patient to track an on-screen presented target by applying the appropriate grip force to the end-object of the grip-measuring device. The computer screen shows a blue ring which modifies its vertical position according to a target signal. The voluntary applied grip force is associated to a red spot which moves upwards when the force is applied to the measuring object and returns to the initial position when the grip is released. The aim of the tracking task is to continuously track the position of the blue ring by dynamically adapting the grip force to the measuring unit.

Participants:

The investigation of the grip force control was made on two stroke (CVA) patients (see table 1) and for evaluation reasons two healthy subjects also participated.

Patient	Age [years]	Gender	Time post stroke [months]	Hemiparesis
P1	24	Male	3	Right
P2	26	Male	8	Left

Table 1. CVA patients

The first healthy subject (S1) is 30 years of age and a left hand dominant, while the second (S2) is 35 years old and right-handed.

The first patient P1 started the usual physiotherapy treatment after only one month from stroke, showing a strong recovery potential. The second one P2 started the rehabilitation program two months after the trauma. In December 2006, after three months of physiotherapy he introduced also FES based therapy in his program. Devices like Microstim2 or O4CHS surface stimulators were used in the rehabilitative process [8].

The Microstim2 is a two channel device training such muscles as wrist and finger extensors in the upper extremities, quadriceps or dorsiflexor group in the lower limbs. It allows choosing between three frequencies 10 Hz, 20 Hz and 40 Hz, while the pulse width is fixed at 300 μs. The output can be continuous, alternate or simultaneous with a rest period. The O4CHS is a four channel stimulator with similar parameters to the Microstim2 but with two additional channels of stimulation for when more muscles are required.

Before the investigation, the subjects gave their informed consent. All the investigations have been made at the Neurology Clinic from Rehabilitation Hospital of Iasi under the supervision of physicians and kinetotherapists.

Data analysis:

Objective and accurate assessment is needed to monitor and quantify patient's progress during the therapy and to validate the effects of the treatment [9]. The majority of hand function tests use qualitative or semi-quantitative measures to evaluate patient's functional state of the hand [7], [10]. Some tests lack the objectivity and accuracy to be able to detect small changes in performance, reducing in this way the ability to more specifically adjust the therapy to the current condition of the patient [11].

The performance of the GFTS sinus task has been assessed by calculating the relative root mean square error (RRMSE) between the target force and the measured output force over the trial time [12]. The tracking error was normalized by the maximal value of the target signal to allow the evaluation among the results obtained in different grips and patients. A lower tracking error suggests better activation control of the corresponding muscles and improved hand functionality.

Results and Discussion

Stroke patients have been assessed during their hospitalization when they are performing classical hand exercises along with FES treatment within the Rehabilitation Hospital of Iasi, Romania. Because of the reduced time (three weeks) of hospitalization during the rehabilitation period of stroke patients, the GFTS has been proven more effective as an assessment tool than a training tool.

The P1 patient that performed the grip force sinus tracking test showed a RRMSE=2.47 while the mean maximal force was 18 N, having difficulty with releasing the grip.

The P2 patient has performed a test for the right hand (the unaffected side of the body), that can be used as reference data for the affected hand during the rehabilitation process. The results are shown in figure 2 where a RRMSE=0.57 has been calculated while a maximal force of 340 N can be exerted.

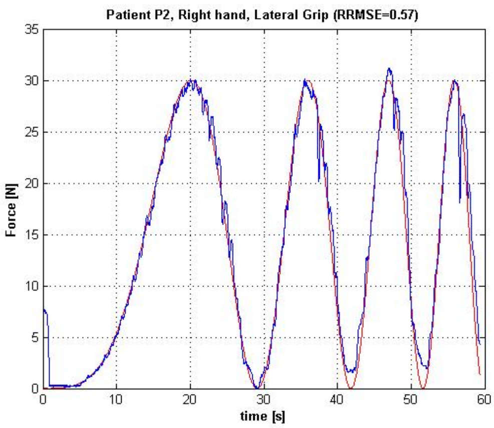

Fig. 2: P2 tracking results for the right hand

The same tasks were performed by patient P2 for the left hand showing a RRMSE=2.45 and a mean maximal force of 61 N. In figure 3 we can observe that the patient had difficulty with releasing the grip being difficult to reach the minimum picks of the sinus, the same as the P1 patient.

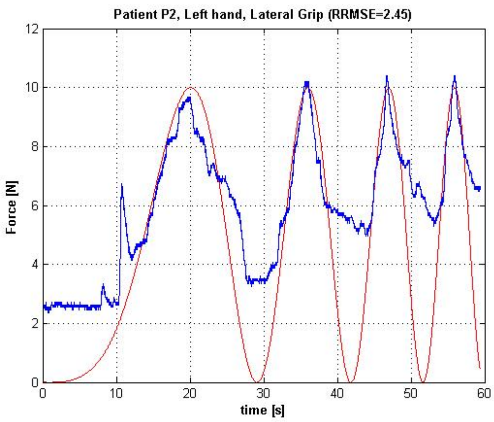

Fig. 3: Tracking results of the P2 CVA patient

After another three months of classical physiotherapy combined with FES based therapy a new assessment was performed. The patient P2 achieved a RRMSE=1.085 with a mean maximal force of 218 N. The tracking results in figure 4 show relevant improvements in grip force control as revealed by the RRMSE values. After the FES-based training the patient shows much better control while releasing the grip force (big improvements in reaching the minimum picks of the sinus).

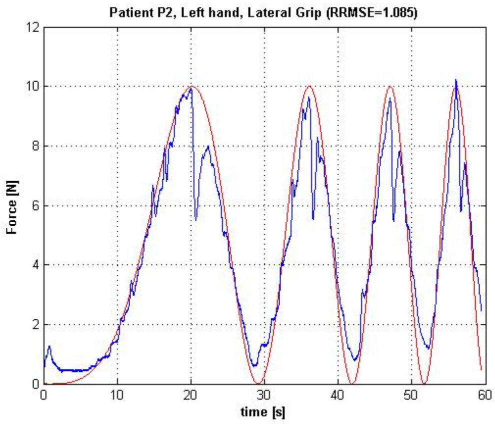

Fig. 4: Tracking results of the P2 patient, 3 months later

For the same tasks the healthy subject S1 achieved a RRMSE=0.44 with a mean maximal force of 360 N while S2 achieved a RRMSE=0.62 with a mean maximal force of 348 N.

The results suggest that the FES based rehabilitative treatment during the first 6 months after stroke would benefit better the patient in terms of a faster recovery of the hand dexterity, if compared with one that starts much more intense after that period.

Conclusions

The results of our tests in stroke patients show that treatment started at few months after stroke is more effective and a faster recovery can be achieved.

The GFTS proved to be an effective tool for assessing hand dexterity and to quantify the hand rehabilitation process at stroke patients which use devices based on FES for regaining the upper limb mobility and will be further used also as a training tool.

As future work we proposed to use transcranial magnetic stimulation (TMS) in association with the GTFS device. A trial will be conducted to emphasize the improvement that can be achieved following the TMS sessions.

References

[1] The Internet Stroke Center at www.strokecenter.org.

[2] Burridge JH, Mann GE, Malone L, et al. A Randomised Controlled Pilot Study to Investigate the Effect of Neuromuscular Electrical Stimulation on Upper Limb Function and Hand Sensation Following Stroke. Proceedings of the 7th Annual Conference of the International Functional Electrical Stimulation Society, 243-245, 2002.

[3] Wade DT, Langton-Hewer R, Wood VA, et al.The hemiplegic arm after stroke: measurement and recovery. Journal of Neurology, Neurosurgery and Psychiatry, vol 46: 521-524, 1983.

[4] Stroke: Conventional Treatments for Stroke at www.holistic-online.com.

[5] Popovic D, Sinkjaer T. Control of movement for the physically disabled. Springer-Verlag, 2000.

[6] Peckham PH, Keith MW and Kilgore KL. Restoration of upper extremity function in tetraplegia. Topics in Spinal Cord Injury Rehab., vol 5: 33-43, 1999.

[7] Jebsen RH, Taylor N, Trieschmann RB, et al. An objective and standardised test of hand function. Arch of Physical Medicine and Rehabilitation, vol 50(6): 311-319, 1969.

[8] Medical Physics and Biomedical Engineering Department, Salisbury District Hospital, UK. Available: http://www.salisburyfes.com.

[9]McPhee S. Functional hand evaluations: A review. American Journal of Occupational Therapy, vol 41: 158-163, 1987.

[10] Fugl-Meyer AR, Jaasko L, Leyman I, et al. The post-stroke hemiplegic patient: I. A method for evaluation of physical performance. Scandinavian Journal of Rehabilitation Medicine, vol 7: 13-31, 1975.

[11] Marx RG, Bombardier C and Wright JG. What do we know about the reliability and validity of physical examination tests used to examine the upper extremity. Journal of Hand Surgery, vol 24A: 185-193, 1999.

[12] Jones RD. Measurement of sensory-motor control performance capaities: tracking tasks. The Biomedical Engineering Handbook 2nd ed, vol II, 2000.

Acknowledgements

The authors gratefully acknowledge the financial support of the Romanian Ministry of Education and Research and Republic of Slovenia Ministry of Education, Science and Sport. The work has been supported within the frame of the Slovene-Romanian Bilateral Scientific and Technological Cooperation Project: “Standing-up motion augmentation in paraplegia by means of FES and robot technology” and the Romanian Grant CNCSIS 41 contract no. 33GR/2007 research theme 40.

Author’s Address

Name: Ştefan Marius Ciprian
Affiliation: Faculty of Electrical Engineering / “Gh. Asachi” Technical University of Iaşi, 53 D.Mangeron Blvd., Iasi, Code 700050, Romania
eMail: ciprian.stefan@gmail.com
homepage: http://www.ee.tuiasi.ro/~euedia

HAND CAPABILITY AUGMENTATION BASED ON FES ASSISTED FORCE TRACKING

Perdan J[1], Kamnik R[1], Obreza P[2], Bajd T[1], Munih M[1]

[1] Faculty of Electrical Engineering, University of Ljubljana, Ljubljana, Slovenia

[2] Institute for Rehabilitation, Republic of Slovenia, Ljubljana, Slovenia

Abstract

The aim of our paper is to present FES system for augmenting the sensorimotor abilities of the hand. The system is designed for training of the finger flexor and extensor muscles by accomplishing the force tracking task in isometric conditions. The system allows full voluntary force control of hand opening or closing, while the FES is added to facilitate the voluntary contributions of the patient. The FES is closed-loop controlled according to the difference between the desired and actual force. Actual forces are acquired by a specially designed adjustable measurement device instrumented by two force sensors. The visual feedback about tracking performance is provided to the patient. The system was evaluated in experimental training study with two incomplete tetraplegic patients. The patients trained with the system in addition to regular therapeutic treatment over a period of four weeks. The results show that both patients have strengthened finger extensor and flexor muscles and reduced tracking error, implying the improvement of sensorimotor abilities of the hand.

Introduction

Grasping and manipulating of objects requires versatile control of grip forces. Neuromuscular disease, stroke or an injury to a central nervous system (CNS) can result in loss of sensory and motor functions in upper extremities which than reduces the hand functionality. Due to such impairment, patients have trouble or are incapable of grasping and manipulating objects [1]. Patients with spastic finger flexors after stroke or incomplete spinal cord injury usually preserve control over finger flexion; however, due to spasticity and weakness of finger extensor muscles, they commonly have difficulties with voluntary hand opening [2]. As a result, they are normally able to hold an object, but are incapable of grasping or releasing already grasped object.

Assessment of hand function is important for therapists to evaluate the condition of lesion and to monitor the progress of therapy. Tracking tasks proved to be suitable for measurement of sensorimotor capability of the hand [3]. During tracking, subjects have to track the target as closely as possible by voluntary controlling the force applied to (or position of) a selected sensor. During the task, visual feedback about their performance is provided to the patients. Beside the evaluation, the tracking systems can also be used as a training tool. It was shown that the force tracking training improved accuracy of grip force control and increased grip strength [4].

In addition to conventional therapy the functional electrical stimulation (FES) can be used during rehabilitation period. Surface FES is suitable for use during rehabilitation, because it is practical for usage and noninvasive. The majority of FES systems used in clinical practice are open-loop controlled by therapist or patient. Specific and fixed tasks can be achieved with pre-programmed stimulation patterns. On an experimental level the closed-loop controlled FES systems have being developed and tested. Closed-loop FES systems demonstrated better input-output linearity, repeatable system response, and better disturbance rejection. Sensors that provide feedback information about the force and/or joint position are required in closed-loop FES systems.

The aim of our research was to develop and evaluate a system for training of finger extensors and flexors that combined the force tracking task with FES. System comprises the visual feedback display, the hand force measuring device, and the closed-loop controlled FES. The system was evaluated during experimental training. In addition to their regular treatment, two patients were trained using the system over a period of four weeks. The hardware and the software of the system are presented in the next section along with the training protocol. In the results section, the training outcomes are outlined. In the final section, the results are discussed and conclusions are presented.

Material and Methods

Training system

The conceptual scheme of the training system for hand capability augmentation is presented in Fig.

1. The core of the system is a personal computer (PC) that is used for reference force generation, actual grip force acquisition, visual presentation of reference and grip force, and stimulation control. The software application for controlling the system was developed in C++ programming language. During training, the patient has to track the desired force represented by the target signal as closely as possible by adjusting his grip strength. The system is designed to allow full voluntary control of hand opening or closing in isometric conditions; FES was added to facilitate the patients' voluntary contribution.

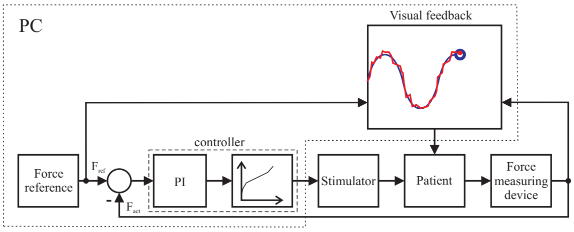

Fig. 1: Conceptual scheme of the training system

The device for measuring isometric hand force is built out of aluminium strut elements. Two JR3 force/torque sensors (50M31A-I25; JR3, Inc., Woodland, USA) and forearm support are mounted on a mechanical support. First sensor is aimed at measuring the thumb force. The thumb is fixated to the force sensor by means of finger support and Velcro strap. The second sensor is used for measuring force of other four fingers. The finger fixation is made out of two parallel aluminium profiles, that fully constrain finger motion in the direction of flexion and extension. All finger supports are padded with neoprene material to prevent unpleasant sensations. The finger fixation enables the acquisition of isometric forces of hand opening and closing. To ensure the proper position and to prevent the arm and wrist from moving during training, forearm is fixated to the arm support by Velcro straps. The use of the strut profiles enables arbitrary positioning of the sensors and forearm support. In this way, the measuring setup can be adjusted to each individual, as well as to assess either the right or the left hand. A PCI board is used for data acquisition from sensors. The data are sampled with frequency of 100 Hz and then filtered in real time using on-board integrated filter with the cut-off frequency of 31.25 Hz and delay of approximately 32 ms.

Force reference signal is composed of four periods of sinusoidal signal with superimposed DC component. Between the periods, 15-s rests are inserted. The amplitude of the reference signal ranges from zero to maximum positive value for training hand closing and from zero to maximum negative value for training hand opening. During the tracking task the reference and actual grip forces are displayed on the monitor screen for providing visual feedback to the patient. The difference between the momentary values of both forces serves as an input to the proportional-integral (PI) controller. The inverse approximation of muscle recruitment curve is added to the final stage of controller to cancel the nonlinearity of the muscle response. The output of the controller is directly proportional to the width of the stimulation pulse, while the pulse amplitude is kept constant throughout a single training session. The stimulation parameters are sent to the stimulator via RS-232 serial connection with the frequency of 33 Hz, determining the width of each pulse. Two channel stimulation was utilized stimulating the finger flexors and finger extensors independently.

Participants

Two incomplete tetraplegic patients participated in evaluation of the system. Patient AD was 28-years-old male who had a spinal chord injury at the C5/C6 level almost 4 years earlier. He had strong but spastic finger flexors, which caused him difficulties with hand opening. Patient AS was 15 years old; he had incomplete tetraplegia at the C3/C4 level due to an injury 8 months earlier. He preserved considerable voluntary control over finger flexor and extensor muscles. Both participants used the system in addition to their regular treatment at the Institute for Rehabilitation, Republic of Slovenia.

Training protocol

The experimental training using the system for hand capability augmentation lasted for four weeks, one session per working day. In both patients the dominant right hand was treated. The training was supervised by experienced physiotherapist.

During training, the patient was seated behind the desk in front of a computer screen (see Fig. 2). The physiotherapist positioned the surface electrodes on his right forearm in such a way that the maximal flexion/extension of index, middle, ring and little finger without flexion/extension of wrist was obtained. After placement of electrodes, the fingers and forearm were fixated onto the force sensors and forearm support, respectively. The maximal amplitude of stimulation pulse was determined by manually increasing the pulse amplitude up to the level where the patient felt that the stimulation was uncomfortable. During testing, the stimulation pulse width was set to maximum value of 500 µs. The pulse amplitude determined during this initial testing was then used throughout the training session. For tuning the PI controller, i.e., setting the gains K_P and K_I, the model of muscle in isometric condition was built. The muscle was represented by Hammerstein model, which consists of the static recruitment nonlinearity and linear discrete-time transfer function. To identify the recruitment curve of isometric muscle response, linearly increasing stimulation was applied to the muscles, lasting for 1.5 s and increasing pulse width in a range from 0 to 500 μs in increments of 10 μs. Five identification trials were accomplished and the results averaged to obtain approximation of muscle recruitment, which represents the nonlinear relationship between the pulse width and the finger force. In the next step of muscle response identification, the response to pseudo-random binary signal (PRBS) was measured for identification of the linear discrete-time transfer function. The measured response of finger forces and the stimulation values were used in identification procedure.

Fig. 2: Patient during training.

For the PI controller tuning, the discrete model was built in Matlab-Simulink simulation environment. The simulation model comprised the model of closed-loop FES system and the model of muscle. Parameters K_P and K_I were defined with the optimization procedure minimizing the tracking error. Simulink Response Optimization toolbox was used for this purpose.

After successful adaptation of the system to an individual, the maximal force that the patent was able to voluntarily achieve was acquired. On the basis of measured value, the maximal amplitude of reference force signal was determined as 50% of the maximal voluntary force. The training consisted of tree repetitions of two tracking tasks: *Task A* and *Task B*. In *Task A*, the patient had to accomplish tracking task only with his voluntary activity, while in *Task B*, the FES was added to facilitate patient's voluntary effort. The training consisted of repetitions of *Task A*, followed by *Task B*. During tracking, the reference and actual force signal and the stimulation output were sampled with the frequency of 100 Hz and saved in a file. The training procedure was accomplished for training in isometric hand closing and opening. For assessing the tracking performance the relative root mean square error (rrmse) was calculated for each tracking task.

Results

In Fig. 3, an example of the tracking performance of *Task A* and *Task B* during hand closing is presented. Large deviations can be observed during *Task A* (Fig. 3a), especially when the patient sustains the grip force for a longer time; better tracking is observed for the shortest period of the reference force. The tracking performance in *Task B* is presented in Fig. 3b and shows that FES considerably improved force tracking performance. The stimulation intensity during *Task B* is shown in Fig. 3c.

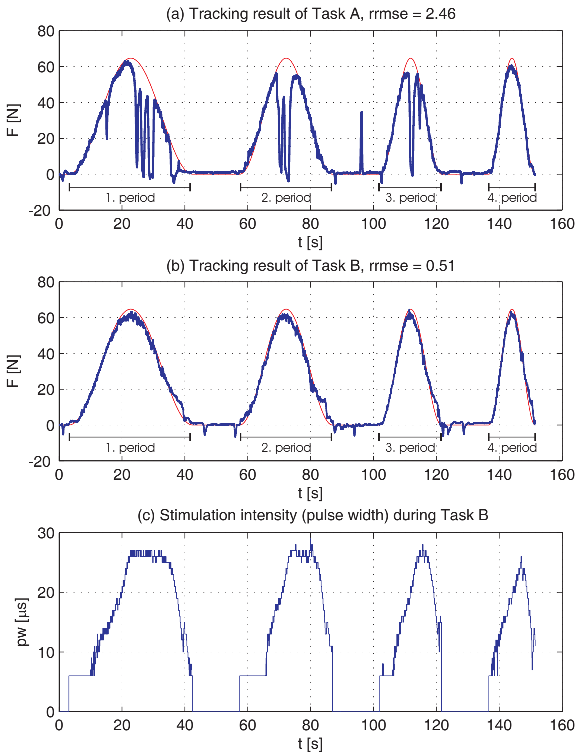

Fig. 3: Tracking of patient AD (a) Task A, (b) Task B, (c) output of the controller during Task B.

Fig. 4 shows the progression of hand strength during training. In both patients, the maximal voluntary hand opening and closing forces are shown in the top and the bottom graphs, respectively, for comparison.

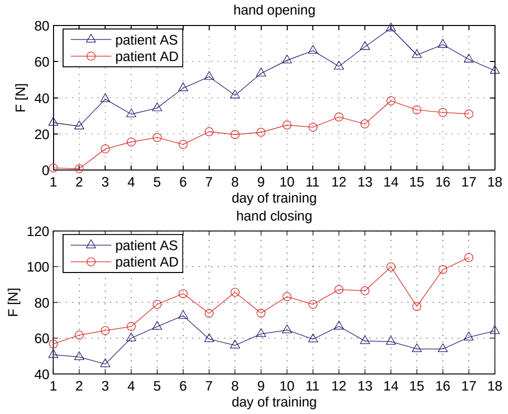

Fig. 4: Maximal voluntary hand force for both patients through training days.

Patient AD had steady improvement of maximal voluntary hand force on hand closing and opening during the training period. At the beginning of training, he had difficulty with hand opening in the maximal voluntary hand force test. Wrist flexion occurred when he tried to achieve finger extension. After the first two days of training, the patient was able to activate his finger extensor muscles more selectively and, thus, achieve greater hand opening forces. Patient AD had better control of, as well as stronger, finger flexor muscles. Nevertheless, his grip strength improved considerably during training.

Patient AS also had steady improvement of maximal voluntary force on hand opening. The strength of his finger extensor muscles more than doubled, while the maximal voluntary force of hand closing quickly improved during the first days of training and then remained relatively constant.

Tracking error results show that patient AD achieved steady and good overall tracking performance, for both hand opening and closing tracking tasks, which is comparable to a tracking of a healthy person. His average rrmse in hand opening tasks was less than 0.35 and average rrmse in hand closing tasks less than 0.4, except for two successive days where rrmse was higher than 1. He usually performed better without help of the FES.

The tracking results for patient AS were more inconsistent; however, a trend to improvement was observed. At the beginning his tracking error was rrmse > 2, and at the end of training more than halved, with rrmse < 1. Addition of FES significantly increased his tracking performance, resulting in lower tracking error.

Discussion and Conclusion

A novel system for training finger flexor and extensor muscles under isometric conditions was developed and evaluated. The system combines tracking tasks and closed-loop controlled FES to facilitate patient's voluntary control.

Based on the results, training with a combination of tracking task and FES appears to improve a patient's voluntary control and increases hand strength. Furthermore, FES seems to be more beneficial for patients with less voluntary control over finger flexors and extensors, i.e., larger tracking error. The results are thus promising with respect to augmentation of the sensorimotor abilities of the hand, especially in training of finger extensor muscles.

References

[1] Popovic MR, Thrasher TA, Zivanovic V et al. Neuroprosthesis for retraining reaching and grasping functions in severe hemiplegic patients. Neuromodulation, vol: 8, 58–72, 2005.

[2] Hines AE, Crago PE, Billian C. Hand opening by electrical stimulation in patients with spastic hemiplegia. IEEE Trans Rehabil Eng, vol: 3, 193–205, 1995.

[3] Kurillo G, Zupan A, Bajd T. Force tracking system for the assessment of grip force control in patients with neuromuscular diseases. Clin Biomech, vol: 19, 1014–10221, 2004.

[4] Kurillo G, Gregoric M, Goljar N et al. Grip force tracking system for assessment and rehabilitation of hand function. Technol health care, vol: 13, 137–149, 2005.

Acknowledgements

The authors acknowledge the financial support from the Slovenian Research Agency. The authors would also like to thank both patients for participating in experimental training.

Author's Address

Name: Jernej Perdan
Affiliation: Faculty of Electrical Engineering, University of Ljubljana
eMail: jernej.perdan@robo.fe.uni-lj.si
homepage: http://robo.fe.uni-lj.si/

A HYBRID SYSTEM FOR UPPER LIMB MOVEMENT RESTORATION IN QUADRIPLEGICS

Varoto R[1], Barbarini ES[1], Cliquet Jr A[1,2]

[1] Biocybernetics & Rehabilitation Engineering Laboratory (LABCIBER), Electrical Engineering Department, University of São Paulo (USP), São Carlos, Brazil

[2] Orthopedics Department, Faculty of Medical Sciences, State University of Campinas (UNICAMP), Campinas, Brazil

Abstract

Generally, individuals having upper limb motor dysfunctions present difficulties to perform object manipulation, which is essential for activities of daily living (ADLs). Towards satisfactory manipulation, reach and grasp movements must be performed with voluntary control by the spinal cord injured individual, and for that, grasp force feedback is essential. A hybrid system aiming at partial upper limb sensorymotor restoration for quadriplegics was built. Such device is composed of an elbow dynamic orthosis, a static wrist orthosis and neuromuscular electrical stimulation (NMES); an instrumented glove allows grasping force feedback. Voice control of the entire system (elbow dynamic orthosis and electrical stimulator) is performed by the patient himself through pattern recognition of keywords, using artificial neural networks.

Introduction

According to the spinal cord injury levels, there are two types of paralyses – paraplegia and quadriplegia. Paraplegia refers to impairment or loss of motor and/or sensory function in the thoracic, lumbar or sacral segments of the spinal cord. Quadriplegia refers to impairment or loss of motor and/or sensory function in the cervical segments of the spinal cord. This results in impairment of function in the arms as well as in the trunk, legs and pelvic organs [1]. This dysfunction makes it difficult for the quadriplegic, to reach for, grasp and release an object, tasks that are essential for the individual.

These impairments can be overcome with the use of Neuromuscular Electrical Stimulation (NMES), which consists of the artificial activation of the skeletal muscle thus generating muscular contraction [2]. However, some physiologic restrictions exist in relation to NMES, such as the traumas or pathologies that affect the motor neuron, in other words, the presence of denervated skeletal muscles that restrict the movement restoration with NMES [3].

Thus, for these cases other techniques can be used towards providing impaired limb movements. In this attempt, the use of orthoses is indicated.

In relation to movements, the orthoses can be classified as statics, which provide appropriate positioning of the limb; and as dynamics, where the mobile parts are used to restore movements [4]. When orthoses are combined with NMES, they are called hybrid systems [5].

This work presents a hybrid system triggered by voice command that provides elbow extension and flexion, with forearm support; grasp movements and grasping force feedback.

Material and Methods

The hybrid system is composed of an elbow dynamic orthosis, a wrist static orthosis and NMES; and an instrumented glove. The dynamic orthosis provides elbow flexion/extension with forearm support, while grasping is generated by NMES. The instrumented glove allows grasping force feedback. This system, along with the user, forms a closed-loop system (Fig. 1).

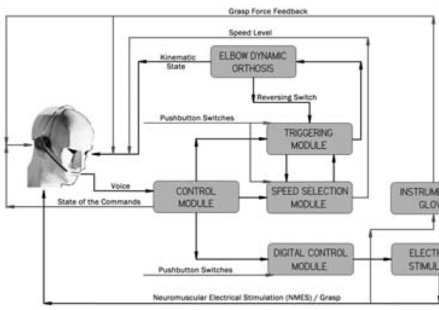

Fig. 1: Closed-loop system.

Elbow Dynamic Orthosis

According to the function of the orthotic device, the transmission method for the movement between actuator and limb was determined. The method used was a crossed axes gearbox with transmission by cylindrical endless screw and cogwheel [6].

Towards dimensioning the actuator, knowledge about upper limb anthropometrical measurements was made necessary. With these data, it was therefore possible to determine a value for minimal moment that should be provided by the mechanism responsible for movement.

The orthosis' components are shown in Fig. 2.

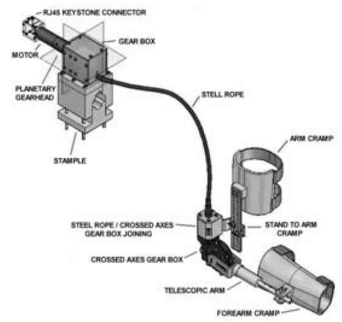

Fig. 2: Design of an elbow dynamic orthosis.

The electrical circuit comprises 4 modules, called: Triggering, Control, Speed Selection, and Range Limit Circuit.

The Control Module is responsible for voice pattern recognition of the user, whereby a function can be called using a keyword. In this way, 6 words were recorded to control the orthosis: master word – orthosis; slave words – flexion, extension, stop, more, and less (to increase or decrease the speed, respectively).

The first test was performed with a healthy individual. The goals were to measure the rotation speed and real-time angular variation of the Telescopic Arm (and subject's forearm). For real-time angular variation measurement, a Fiber Optics S700 Joint Angle Shape Sensor® (sample rate of 120Hz) was used. Voice control was also used.

On the following test, the same procedure was accomplished. In this case, five quadriplegic subjects used the orthosis operating in maximum speed (level 6) (Fig. 3). Table 1 presents the subjects' data. The range limitation sensors were responsible for the direction inversions.

Fig. 3: Patient with elbow dynamic orthosis and Fiber Optics S700 Joint Angle Shape Sensor®.

Table 1: Subjects' data

Subject	Age (year)	Body Mass (kg)	Height (m)	Lesion
Healthy Individual	26	70	1.80	-
A	36	60	1.71	C5
B	40	45	1.60	C8
C	33	58	1.75	C6
D	42	64	1.82	C5
E	29	71	1.77	C6

Instrumented Glove

The Instrumented Glove for sensory feedback during palmar or lateral grasp has 2 user interface modes: visual or audio, which may be selected by a switch. In the visual mode, the instrumented glove indicates the intensity of the applied force by the fingers through 10 Lighting Emissor Diodes (LED). The larger the force, more LEDs are lit. Already in the audio mode, the larger the force, the sharper it is the sound emitted by the buzzer.

The force transducer used was the Force Sensing Resistor (FSR®). Five sensors were used, fixed on a cloth glove at the middle and distal phalanges of the index and middle fingers, and the distal phalange of the thumb.

The bench tests' goal was to verify the functionality of the Instrumented Glove in both interface modes. On the visual mode, the FlexiForce's Economical Load & it Forces (ELF) System® was used for real-time force values measurement.

Neuromuscular Electrical Stimulation

Similar to the elbow dynamic orthosis, the voice command control was coupled to a conventional 2 channels electrical stimulator developed and used in previous work (Fig. 5A). This electrical stimulator presents the following parameters: bipolar monophasic square wave, signal frequency of 25 Hz and adjustable amplitude from 0 V to 150 V (1kΩ load). Thus, NMES was used to perform grasp. Surface electrodes were positioned over the finger flexor and the thumb adductor muscles for lateral grasp, and over the lumbricalis and thumb abductor muscles for palmar grasp. The wrist static orthosis developed (7) was used towards maintaining the wrist in the functional position (30^o of flexion) during NMES (Fig. 5B).

Fig. 5: Neuromuscular electrical stimulation. (A) 2 channels electrical stimulator. (B) Wrist static orthosis.

The Digital Control Module developed allows the complete control of electrical stimulator by voice through the same Control Module used with the orthosis, and it offers 15 levels of stimulation intensity. In this case, the master word is stimulator and the slave words are start, stop, more and less, to increase and to decrease the stimulation intensity.

The bench test was based on the determination of the amplitude value for each stimulation intensity level.

For this, 1kΩ load was used. Each level was determined by voice.

Results

The mechanical structure, the Triggering Module, the Control Module, the Speed Selection Module, the microphone and the earphone made up the final configuration of the Elbow Dynamic Orthosis (Fig. 6).

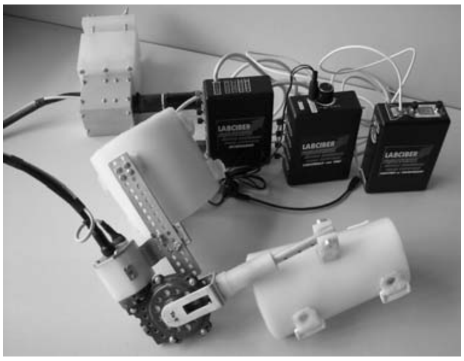

Fig. 6: Elbow Dynamic Orthosis.

With a healthy individual, the angular average speed and maximum angular variation for the forearm in relation to the arm, for one total extension-total flexion-total extension cycle, using the orthosis (limited range by the reed switches) can be seen in Table 2.

Table 2: Speed levels

Speed Level	Average Angular Speed (^{o}/s)	Maximum Angular Variation (^{o})
1	7.2	113.0
2	8.6	113.3
3	9.1	112.9
4	9.3	113.5
5	9.8	113.1
6	13.2	113.4

Using voice command, the following commands were given: 1-“extension”, 2-“stop”, 3-“flexion”, 4-“extension”, 5-automatic range limit rotation direction inversion, 6-“extension”, 7-“stop”, 8-“flexion”, 9-“stop”, 10-“extension”, 11-“stop”, 12-“extension” and 13-“stop”, and the orthosis’ behavior may be seen on Fig. 8.

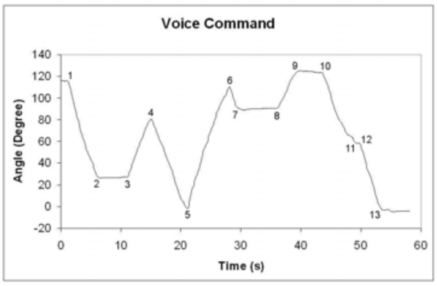

Fig. 8: Elbow movements.

Figure 9 shows real-time angular and speed variations for the forearm in relation to the arm of a quadriplegic subject.

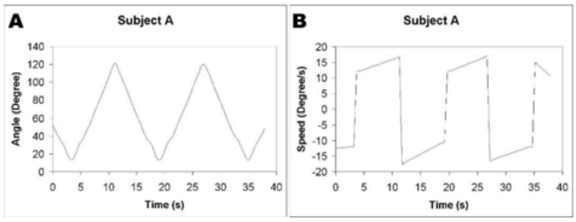

Fig. 9: (A) Angular variation, where valleys correspond to total extension and peaks correspond to total flexion. (B) Speed variation.

Table 3 presents the average angular speed and maximum angular variation for the forearm of each quadriplegic subject.

Table 3: Results with quadriplegic subjects

Quadriplegic Subject	Average Angular Speed (^{o}/s)	Maximum Angular Variation (^{o})
A	13.4	107.4
B	14.4	100.4
C	14.3	103.2
D	10.6	82.0
E	13.5	103.5

Figure 11 shows the actual Instrumented Glove developed.

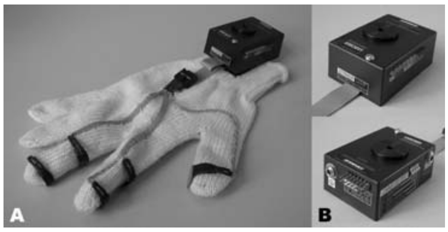

Fig. 11: (A) Instrumented Glove. (B) Interface Module.

The bench tests for the Instrumented Glove do show relations between lit LEDs and applied forces for visual interface and between emitted sound frequencies and applied forces for audio mode (Fig. 12).

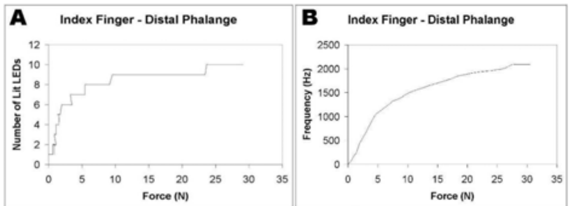

Fig. 12: (A) Visual and (B) Audio interface modes.

The conventional 2 channel electrical stimulator and the Digital Control Module constitute the portable NMES system. For each voice command given, one stimulation level increased/decreased, resulting in the amplitude values (1 kΩ load) shown in Fig. 14.

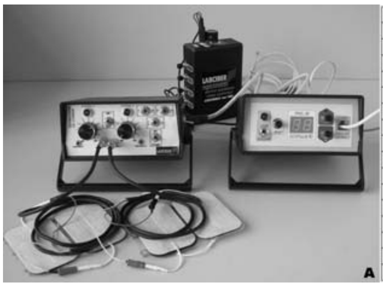

Level	Amplitude Value (V)
0	0
1	12.0
2	14.4
3	16.8
4	18.4
5	20.0
6	20.8
7	21.6
8	26.4
9	35.2
10	42.4
11	45.0
12	49.6
13	53.6
14	58.4
15	126.0

B

Fig. 14: (A) Portable NMES system. (B) Stimulation amplitude value.

Discussion

On the tests with healthy individual and quadriplegic subjects, the Elbow Dynamic Orthosis performed movements effectively regarding electrical circuit and mechanical structure.

The values of angular variation obtained during elbow flexion/extension movements match the positions of the range limit switches (120º between reed switches). The differences presented are potentially due to skin artifact relating to orthosis fixation, and operation of reed switch only by the magnet approach. Already the variation of average angular speed for each volunteer is due to the load being moved and maintained by the orthosis, in this case the volunteers' right forearm.

In relation to voice command, the orthosis responded correctly to most of the given commands. There was no case of misinterpretation by the system.

The functionality of the Interface Module of the Instrumented Glove was verified. And in relation to the sound, the frequency range used by Interface Module is compatible with the frequency range perceived by the human sense of hearing that is from 20 Hz to 20 kHz [7].

The portable NMES system based on conventional 2 channels of electrical stimulation, used to perform grasp, presented the same parameters in regard to wave type and frequency of the NMES signal; amplitude being adjustable through levels determined by voice.

The functional movement restoration of quadriplegic upper limbs has been investigated by several authors. Besides the movement restoration, another important aspect is that dynamic orthoses, as mechatronic devices, can be used as a possible treatment, denominated therapy aided by robot [8].

Conclusions

This work shows the availability of the Hybrid System for reach movement restoration in quadriplegics, because the Elbow Dynamic Orthosis provides enough conditions for movement during ADLs, without causing discomfort. The voice command control provides voluntary control of the reach and grasp movements, and it responds to the commands given by the user with efficiency, so far orthosis as electrical stimulator. In relation to fingers grasping force feedback, the Instrumented Glove is efficient in both interface modes. The Hybrid System represents an alternative for partial upper limb sensorymotor restoration in quadriplegics.

References

[1] Maynard Jr. FM, Bracken MB, Creasey G, Ditunno JF, Donovan WH, Ducker TB, Garber SL, Marino RJ, Stover SL, Tator CH, Waters RL, Wilberger JE, Young W. International Standards for Neurological and Functional Classification of Spinal Cord Injury. Spinal Cord, 35: 266-274, 1997.

[2] Castro MCF, Cliquet Jr. A. An artificial grasping evaluation system for the paralysed hand. Med Biol Eng Comput, 38: 275-280, 2000.

[3] Salmons S, Ashley Z, Sutherland H, Russold MF, Li F, Jarvis JC. Functional electrical stimulation of denervated muscles: basic issues. Artif Organs, 29: 199-202, 2005.

[4] Rahman T, Sample W, Seliktar R, Alexander M, Scavina M. A body-powered functional upper limb orthosis. J Rehabil Res Dev, 37: 675-680, 2000.

[5] Jaeger RJ. Stimulating Steps. TeamRehab Report, 19-23, 1994.

[6] Lima GF, Varoto R, Paolillo AR, Paolillo FR, Cliquet Jr. A. Restauração artificial do movimento de membros superiores de tetraplégicos: um sistema homem-máquina. Proceedings of the III Congresso Latino-Americano de Órgãos Artificiais e Biomateriais; 2004 Jul 27-30; Campinas, Brazil. 2004;150-150.

[7] Beranek LL, eds. Acoustics. New York: McGraw-Hill, 1993.

[8] Volpe BT, Krebs HI, Hogan N, Edelstein L, Diels C, Aisen M. A Novel Approach to Stroke Reabilitation: Robot-Aided Sensori-Motor Stimulation. Neurology, 54:1938-1944, 2000.

Acknowledgements

The authors thank the support of the State of São Paulo Foundation for Research – FAPESP.

Authors Addresses

R.Varoto , DSc student

rvaroto@yahoo.com.br

A Cliquet Jr. , Professor

cliquet@fcm.unicamp.br

cliquet@sel.eesc.usp.br

TEXTILE NEUROPROSTHESIS GARMENT FOR FUNCTIONAL ELECTRICAL STIMULATION

T. Keller[1,2,3], M. Lawrence[1,2,3], M. Lang[1,2], A. Kuhn[1,2,3]

[1] Automatic Control Laboratory, ETH Zurich, Switzerland
[2] Spinal Cord Injury Center, University Hospital Balgrist, Zurich, Switzerland
[3] Sensory Motor Systems Laboratory, ETH Zurich, Switzerland

Abstract

We have developed a new embroidered multi-channel transcutaneous electrical stimulation (TES) electrode garment for neuroprosthetic applications. The multi-layered construction includes a fabric electrode layer and a skin interfacing layer. The fabric electrode layer contains embroidered electrode pads and electrode wiring. It was designed such that short circuits between the embroidered wiring and the skin cannot occur.

The multi-channel stimulation electrodes are integrated in a glove-like garment. Three sets of TES electrodes consisting of a total of 64 pads allow activation of the muscles for finger and wrist extension, finger and wrist flexion, and thumb articulation

To allow stimulation currents to be equally distributed into the body, a skin contacting material is used; e.g. hydrogel or our new skin interface material. The skin interface material was designed to have a higher impedance than skin. This helps maintain a better current distribution despite skin inhomogeneities. Furthermore, the high impedance enables us to use a single interface layer across multiple electrode pads without disturbing the current distribution, whilst ensuring current flow through the skin rather than the interface layer.

In functional tests we used the multi-channel electrode garment with our developed virtual electrode stimulation environment. Using the combined system we were able to demonstrate selective finger and wrist articulation. Future developments are aimed at developing a miniaturized multi-channel electrical stimulator for the control of the multi-channel electrode garment.

Introduction

Neuroprostheses based on TES consist of an external electrical stimulator and a controller unit, (both can be contained in one device) and a set of stimulation electrodes [1]. Either multiple self-adhesive electrodes, or electrodes integrated in a hard shell are used. A good knowledge of arm anatomy [2] is required when placing multiple self adhesive electrodes for upper extremity neuroprostheses.

In the case of the a hard shell neuroprosthesis such as the Ness Handmaster (now called Bioness H200), the electrode placement is done once by the experienced person that sets up the device. Electrode foils and a watered tissue layer are positioned and integrated into the orthotic shell. This concept is simple to use, however flexibility in repositioning of electrodes is very limited, as may be required when the subject improves his/her gasp function. In addition, a hard shell neuroprosthesis/orthosis is bulky to wear and limits movements in some directions, in this case pronation/supination. For wear comfort a soft tissue neuroprosthesis like the Bionic Glove [3] is preferred. To overcome the electrode placement problem multi-channel TES systems were proposed by different groups. Systems that compensate foot eversion/inversion using a multi-channel approach as well as systems for selecting a subset of electrodes for grasping were presented [4,5,6].

We have developed a textile neuroprosthesis garment for hand grasp and wrist control using our multi-channel array technology [6,7]. In this paper we present first results obtained with this garment that allows us to stimulate single finger movements in a controlled wrist position.

Material and Methods

Textile garment construction

The neuroprosthesis garment for hand grasp is made from stretchable textile in the shape of a long sleeve glove. The glove opens along the ulna from processus styloideus to olecran and is closed by three integrated Velcro™ straps. Embedded in the sleeve are semi-flexible plastic straps that stiffen the construction. Three sets of array configured multi-channel TES electrode cushions are placed inside the garment and fixed by Velcro™. The three electrode sets allow selective activation of the extrinsic muscles for finger and wrist extension, finger flexion, and thumb articulation. The wrist is not stiffened as in most of our previous gloves [8] and the Bioness H200. This helps perform a more natural grasp with active or FES articulated wrist movements.

Fig. 1: Prototype of a multi-channel textile neuroprosthesis: Multi-layer structure comprises electrode cushions positioned for finger and wrist articulation.

Multi-channel TES electrode cushions

Two multi-channel electrode cushions were built; one for stimulating the flexor muscles of wrist and fingers and one for stimulating the extensor muscles. The thumb will be articulated with four electrodes, not yet implemented.

Each cushion is made from polyester (PES) fabric that holds 30 embroidered electrode pads and the associated embroidered wiring. The pads are arranged in a T-shape made from two arrays of 3x5 elements (see Fig. 3). The electrode wiring had to be designed free of crossings. All 30 wires at the terminal have a 200 mil spacing to fit to a standard ribbon cable connector. The embroidered electrode wiring was insulated with three layers of painted Latex. The PES fabric was folded as illustrated in Fig. 2 to form a cushion.

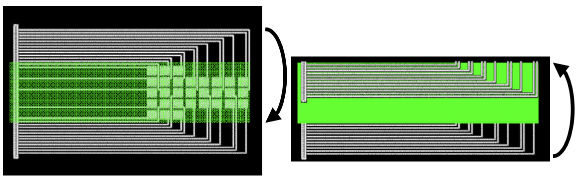

Fig. 2: Folded PES fabric forms electrode cushion comprising 30 electrode pads and the integrated wiring.

For the skin interface layer we used different types of electrode hydrogels, as well as a conductive polymer developed in collaboration with EMPA St. Gallen. The skin interface layer preferably has a higher impedance that the skin itself. Thus skin inhomogeneities no longer dominate the path of electrical current flow into the body. A second big advantage is that a single high impedance skin interface material can be used to cover multiple electrode pads without impacting the current distribution formed by the active electrode pads.

Multi-channel electrical stimulation system

A Compex Motion [9] electric stimulator and a 64 channel analog multiplexer [10] containing an embedded xPC target (Mathworks Inc.) was used to control the stimulation current delivered to the neuroprosthesis. The multiplexer can switch a subset of pads between the anode or cathode of each of the four stimulation channels of the electric stimulator. The stimulation intensity (current), pulse duration and active pad configurations can be controlled from pulse to pulse in real-time. Four different stimulation regions can be active at the same time.

Selective finger force and wrist torque measurements

Isometric finger force and wrist torques were measured using the GAWAS [11], a newly developed grasp assessment platform. The subject's forearm was fixated with a deflatable surgical cushion, which kept the arm at rest. The wrist was fixated to a JR3 (JR3 Inc., Woodland, CA) 6 DOF load cell using a cast. For the exact fixation procedure refer to [11]. Three activation regions for wrist extension with balanced ulnar/radial deviation, flexion of digit 3, and flexion of digit 4 were determined using an automated detection procedure [10]. An activation region is defined by a set of electrode pads that elicits a certain movement with minimal activation of other movements. The electrode pads used for selective activation are depicted in Fig. 3.

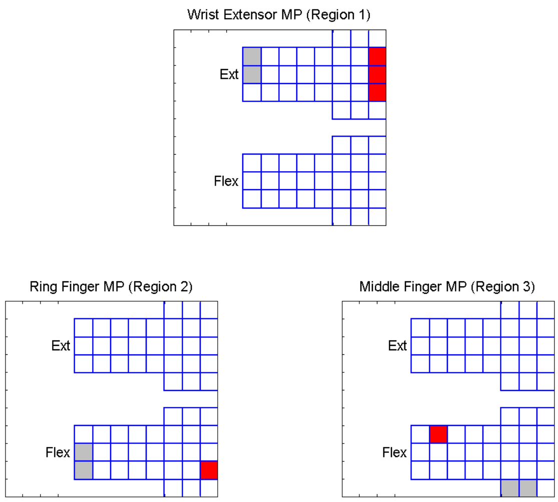

Fig. 3: The found activation regions (cathode) for decoupled wrist extension and finger flexion of the middle finger (digit 3) and the ring finger (digit 4) are shown with dark color. Light colored are the positions of the anodes.

Each activation region was stimulated in a healthy subject consecutively for five times with a stimulation pattern shown in the third plot of Fig.

4. The stimulation amplitudes were 23 mA for wrist extension, 23 mA for flexion of digit 3, and 18 mA for flexion of digits. For all activation regions the stimulation pulse duration was 200 µs and the stimulation frequency was 25 Hz. Between the selective activations a pause of 1 minute was introduced to avoid muscle fatigue. In a second part of the testing the three activation regions were combined to investigate coupling effects when activating multiple regions at the same time. We were mainly interested if we can stabilize the wrist in an extended position while performing finger flexion stimulation. During all tests the subject was asked not to interfere with voluntary muscle contractions.

Data was recorded at 100 Hz with a median filter (n=10) used to smooth the data. Offsets in the 6 DOF load cell data were subtracted before the wrist torques were calculated.

Results

For single region activations we could obtain selective activation of wrist extensor muscles with little coupling with finger extensors. A wrist extension torque of 1.48±0.26 Nm could be achieved with small finger extension couplings of 3.55±0.26 N and 1.24±0.29 N for digits 3 and 4, respectively. All values are mean values and standard deviation of a 200ms time window around the maximum force or torque for five trials with same stimulation amplitude applied to the region.

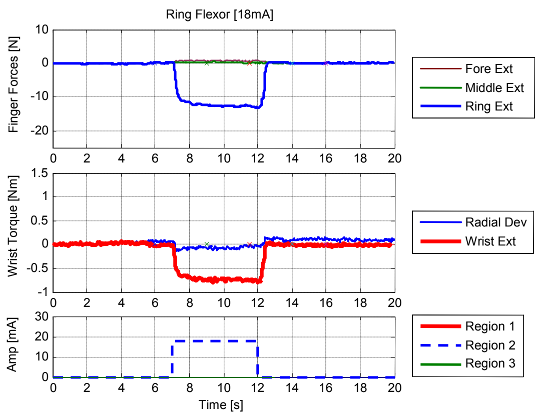

Fig. 4: Stimulation of activation region 2 produced a nicely decoupled middle finger flexion with some coupling at the wrist in flexion direction.

We could observe stronger coupling of finger flexor muscles with wrist flexion for digits 3 and 4, as can be seen in Fig. 4 for digit 4. The values were 12.67±0.98 N finger flexion force (digit 4) and 0.69±0.07 Nm wrist flexion torque for activating region 2 and 11.03±2.01 N finger flexion force (digit 3) and 0.46±0.09 Nm wrist flexion torque for activating region 3. Digits 1 and 2 were not activated in the presented trials. For all stimulation sequences the wrist kept its neutral position in radial/ulnar direction.

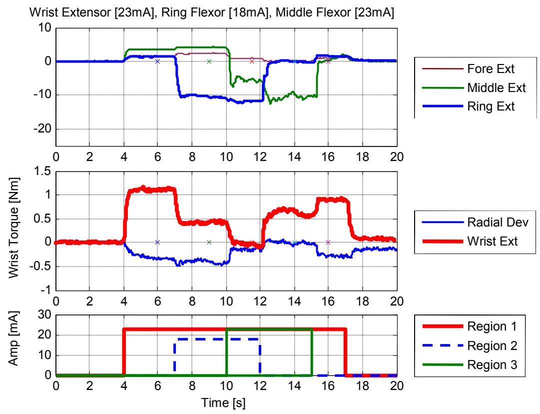

Fig. 5: Coupling and interference when activating multiple regions are plotted in these graphs. First only the region that activates wrist extension is stimulated. After 3 seconds ring finger flexion is activated and after 6 seconds middle finger flexion is added. Ring finger stimulation is stopped after 8 seconds and middle finger stimulation after 11 seconds.

We measured finger forces and wrist torques during the activation of multiple regions. In Fig. 5 we can see as an example how stimulation of finger flexors acts on the wrist when wrist extensors are stimulated. With moderate amplitudes a net wrist extension torque can be produced when fingers are not activated. The activation of the finger flexors during wrist extension reduces the net wrist extension torque. With our multi-channel garment neuroprosthesis we could obtain grasp forces of 5 N and 10 N in digits 3 and 4 without generating a wrist flexion net torque. This can be seen in Fig. 5 in the middle panel between 10 to 12 seconds where the wrist net torque was neutralized.

Discussion

We have developed a multi-channel TES electrode garment for hand grasp. Embroidered multi-channel textile electrode cushions are fixed inside a garment glove. With a real-time multiplexer and a Compex Motion electrical stimulator, up to four activation regions can be simultaneously stimulated. The activation regions as well as stimulation parameters can be changed dynamically.

In isometric recordings using the GAWAS we could show that it is possible to generate finger flexion forces and at the same compensate wrist flexion torques by co-contraction of the wrist extensors. The activation region for wrist extension could be found such that finger extensors were not affected. It is easily possible to activate radial and ulnar deviations such that the wrist can be properly controlled during gasping tasks. Wrist flexion torques were always present then finger flexors were stimulated. With small activation regions of 1.21 cm^2 we could produce decoupled finger flexion of digit 3 and 4. Digits 4 and 5 were always coupled. Decoupled activation of digit 2 could be achieved, however only at higher amplitudes that produce some discomfort in healthy subjects.

In the current stage all measurements were performed in a fixed arm and hand position. Since the wrist is stabilized through co-contraction we assume that wrist stability can also be kept in a dynamic situation and with different light objects as loads. When we find out in future tests that different arm and hand configurations lead to changed muscle activations, these can be compensated by changing the stimulation parameters and the positions of the activation regions. This will be addressed in future research.

References

[1] Popovic M.R., Popovic D.B., Keller T.: Neuroprostheses for grasping. Neurol Res, 24(5), 2002, 443-452.

[2] Nathan R.H.: Functional electrical stimulation of the upper limb: charting the forearm surface (joint moments). Med Biol Eng Comp 6, 1979, 729-736.

[3] Prochazka A., Gauthier M., Wieler M., Kanwell Z.: The bionic glove: an electrical stimulator garment that provides controlled grasp and hand opening in quadriplegia. Arch Phys Med Rehabil, 78, 1997, 1-7.

[4] Popovic-Bijelic A., Bijelic G., Jorgovanovic N., Bojanic D., Popovic D.B., Popovic M.B.: Multi-field surface electrode for selective electrical stimulation, Proc. 8th Vienna Int. Workshop on Functional Electrostimulation, 195-198, 2004.

[5] Elsaify A., Fothergill J.C., and Peasgood W.: A portable FES System incorporating an electrode array and feedback sensors, Proc. 8th Vienna Int. Workshop on Functional Electrostimulation, Vienna, Austria, 191-194, 2004.

[6] Lawrence M., Kirstein T., Keller T.: Electrical stimulation of finger flexors using 'virtual electrodes', Proc. 8th Vienna Int. Workshop on Functional Electrostimulation, Vienna, Austria, 187-190, 2004.

[7] Keller T., Kuhn A., Lawrence M., Morari M.: New multi-channel transcutaneous electrical stimulation technology for rehabilitation, IEEE Engineering in Medicine and Biology Conference, New York, USA, 28, 184-187, 2006.

[8] Mangold S., Keller T., Curt., A., Dietz V.: Transcutaneous functional electrical stimulation for grasping in subjects with cervical spinal cord injury. Spinal Cord 43(1), 2005, 1-13.

[9] Keller T., Popovic M.R., Pappas I.P., Muller P.Y.: Transcutaneous functional electrical stimulator "Compex Motion". Artif Organs, 26(3), 2002, 219-223.

[10] Keller T., Hackl B., Lawrence M., Kuhn A.: Identification and control of hand grasp using multi-channel transcutaneous electrical stimulation, Proc. 11th IFESS Conference, Zao, Japan, 29-31, 2006

[11] Lawrence M., Gross G., Keller T.: Finger and wrist torque measurement system for the evaluation of grasp performance with neuroprostheses, Proc. 9th Vienna Int. Workshop on Functional Electrostimulation, Krems, Austria, 191-194, 2007.

Acknowledgements

This work was supported in part by the Commission for Technology and Innovation CTI under Grant 7735.1 DCS-LS, the Swiss National Science Foundation under Grant 205321-107904 and the National Center of Competence NCCR: Plasticity and Repair. The authors would like to thank Bischoff Textile AG, St. Gallen, Switzerland, Compex Medical SA, Ecublens, Switzerland, and the EMPA St. Gallen, Switzerland for the materials and manufacturing of the array electrode

Author's Address

Dr. Thierry Keller
Automatic Control Laboratory
ETH Zentrum, ETL K 24
Physikstrasse 3
CH-8092 Zurich
e-mail: kellert@control.ee.ethz.ch
home page: www.control.ethz.ch/~fes

POST-STROKE HEMIPARESIS: SURGICAL IMPLANTATION OF 5-7 MICROSTIMULATORS FOR UPPER LIMB REHABILITATION

Davis R[2], Sparrow O[1], Cosendai G[2], Burridge J[1], Turk R[1], Wulff C[1], Schulman J[2]

[1]School of Health Professions and Rehabilitation Sciences, University of Southampton, and Southampton University Hospital, Southampton, UK

[2]Alfred Mann Foundation, Valencia, CA, USA

Abstract

For post-stroke upper limb paresis, surface electrical stimulation has been shown to improve function; however, implanted nerve stimulators are now shown to provide finer control. At the School of Health Professions and Rehabilitation Sciences, University of Southampton, UK, a feasibility study of 7 post-stroke Subjects (4 males, 3 females: age:49yr+/-11yrs) with upper limb paresis was undertaken; their strokes occurred within 1.1 to 10.5yrs (mean:3.9 yrs). 43 radio-frequency controlled microstimulators (RFM; 5-7 per Subject; Alfred Mann Foundation, Valencia, CA) were inserted on affected radial nerve branches or their individual muscle motor-points using AMF implant tools. Each RFM (2.4mm x 17mm) received controlled activation commands via a 2 MHz RF-inductive link from an external coil connected to the Control Unit. Pre-operatively, implantation sites were identified by needle EMG studies.

Using local anesthesia, implantation needed a 5 mm incision. Each targeted nerve/motor-point (N/M-P) was found using an inserted probe with stimulation. An introducer tool was passed over the probe to the target site; the probe was withdrawn and the RFM inserted with an ejection tool. If necessary, RFMs were retrieved during surgery and re-implantation for stronger contractions; one on a triceps motor-point moved post-operatively from the target, necessitating a later implantation. Implantation time was 4.7 hrs (range:3.5-5.5hrs). Mean thresholds of 2.2 µC/cm2/phase were recorded, indicating the RFM's cathodes are within 1-2mm from their target sites (our sheep studies). Complications were minimal with no infections. Intra-operative pain experienced differing little from the pre-operative expectations of each subjects.

Programmed stimulation did extend the elbow, wrist and fingers for functional reach and grasp activities. Over the last 1-2 years, the motor thresholds have remained low and stable. RFMs have not failed, only minor correctable problems have occurred with the external control units and coils. The system has proven reliable and is functioning in further stimulation programs.

POST-STROKE UPPER LIMB REHABILITATION USING 5-7 IMPLANTED MICROSTIMULATORS: A CASE STUDY OF CHANGES IN FUNCTION, SPASTICITY AND MOTOR CONTROL

Burridge J[1], Turk R[1], Davis R[4], Cosendai G[4], Sparrow O[2], Roberts H[3]

[1]School of Health Professions and Rehabilitation Sciences, Southampton, UK

[2]School of medicine, University of Southampton, Southampton, UK

[3]Southampton University Hospital Trust, Southampton, UK

[4]Alfred Mann Foundation, Valencia CA, USA

Abstract

Purpose

For post-stroke patients with impaired upper limb function, surface-applied stimulation has shown therapeutic effects, enhanced by stimulation associated with voluntary effort. We propose that implanted systems may avoid these problems of surface electrodes, provide finer functional movements and with triggered open-loop control greater functional benefit may results.

Method

5-7 microstimulators were implanted into the upper and forearms of seven chronic post-stroke participants, and were powered via an external inductance coil joined to a control unit to stimulate opening of the hand and extension of the wrist and elbow. Activity sequences, set up to assist functional reach and grasp activities, were practiced daily at home for 12 weeks in Phases 1. In Phase 2, programmes at the Laboratory used sensors (electro-goniometer, button and pressure mat) and provided a responsive, triggered open loop system. Phase 3 was duplicated at home. Pre- and post-phase measures included: Action Research Arm Test (ARAT), Fugl Meyer, motor control (target tracking task) and spasticity (electromyographic response to passive stretch of wrist flexors).

Results

All participants completed Phase 1. Six participants are now undergoing Phase 3. Results are presented (N=7) in terms of mean (SD) and % changes in ARAT 4.9 (7.89) 21% and Target tracking 57.3 (48.65) 70% during Phase 1. Results for one subject who completed Phase 3 (Table) will be described in detail.

Outcome measures at each time point for Participant 52

Assessment	*B1*	*B2*	*End 1*	*Start 3*	*End 3*
ARAT	*9*	*8*	*17*	*27*	*38*
Fugl-Meyer	*27*	*29*	*37*	*36*	*42*
Tracking	*25.97*	*61.52*	*146.33*	*129.45*	*171.88*
*Stretch Index**	*3.03*	*9.01*	*0.37*	*1.03*	*2.31*

** Decrease in score = improvement*

Conclusion

The study shows a mean improvement across all participants during Phase 1. Results in Phase 3 may indicate greater improvement.

Keynote Lecture

Janez Rozman

SELECTIVE STIMULATION OF AUTONOMIC NERVES AND RECORDING OF ELECTRONEUROGRAMS IN A DOG MODEL

Rozman J, Pečlin P *(Student)*

ITIS d. o. o. Ljubljana, Centre for Implantable Technology and Sensors, Lepi pot 11, 1102 Ljubljana, Republic of Slovenia

Abstract

Electroneurograms (ENGs) from superficial regions of the left vagus nerve of a dog were recorded with a multielectrode spiral cuff having thirteen groups of three electrodes (GTE 1-13). Their relative positions on the nerve were identified with stimulating pulses individually delivered to all thirteen GTEs. Only when the stimuli were delivered to GTE 9, the heart rate began to fall and only when the stimuli were delivered to GTE 4 the rate of breathing decreased. To test the selectivity of recording the abovedefined groups GTEs 4 and 9 and randomly chosen GTEs 1 and 7 were simultaneously used as recording GTEs while cardio-vascular or respiratory systems were stimulated by carotid artery compression, epinephrine injection and non-invasive, positive end-pressure ventilation. Results showed that power spectrum of the ENG recorded with GTE 9, contained frequencies belonging to the neural activity elicited by compression of the carotid artery and injection of epinephrine. The power spectrum of the ENG recorded with GTE 4, contained frequencies belonging to the neural activity elicited by non-invasive, positive end-expiratory pressure ventilation.

Introduction

Sensing of neural signals could be used to control FES devices (3, 10, 11). Published results demonstrate that limitations of most recently developed techniques can be circumvented by using tripolar nerve cuffs (4, 6, 8, 9). When recording an ENG from nerve fibres one must exclude EMG activity as well as other noise sources. It was shown (13) that tripolar cuffs assist in the additional reduction of interference from sources outside the cuff. The electrode separation is one of the important parameters that determines signal amplitude (12). Another important factor that determines signal amplitude is the volume of extracellular fluid surrounding the nerve segment inside the cuff. The cuffs implanted on cutaneous nerves provided useful and reproducible whole-nerve recordings (1, 2, 6). However, these whole-nerve recordings provide only one channel of information from the aggregate activity of many nerve fibres. Information recorded selectively with a multi-electrode spiral cuff could be used for closed loop control in stimulation of the nerves innervating the heart (5, 7). The purpose of this study was to examine the feasibility of using the cuff for selective recordings of cardio-vascular output modulated by compression of the carotid artery at the carotid sinus and by neurally mediated syncope (NMS), induced by intravenous injection of epinephrine and to examine the feasibility of using the cuff for recordings of respiratory output in anaesthetized and artificially ventilated dogs.

Material and Methods

A spiral cuff was made by bonding two silicone sheets together (5). The lectrodes (0.6 mm X 1.5 mm) were made of 50 μm thick platinum ribbon and connected to the insulated lead wires. Afterwards, a matrix of 39 openings arranged in three parallel groups each containing 13 positions at a distance of 0.5 mm were made in the third silicone sheet. The distance between the three groups was 6 mm. Each of 39 electrode-lead wire compositions was then inserted into one of rectangular openings and fixed with adhesive. Back side of the silicone sheet with the matrix of electrodes was then bonded on the inner side of the mechanically opened cuff. Lead wires were connected to a common connector to be implanted within the lateral subcutaneous tissue for the time between the experimental sessions. As a result, thirteen GTEs, in a longitudinal direction were formed. The cuff was then trimmed to a length of 20 mm as shown in Fig. 1.

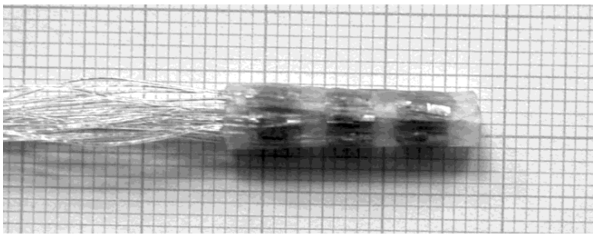

Fig. 1. 39-electrode spiral cuff.

The experiment was performed on an adult Beagle dogs according to the protocol approved by the ethics committee of the Veterinary Administration of the Republic of Slovenia, Ministry of Agriculture, Forestry and Food.

The first recording was performed two months after implantation. At one end of the cable to connect common connector and stimulator was a switching module designed to fit the pins of the common connector. The switching module permitted each GTE to be connected to the amplifier individually or in combination with other GTEs.

The relative positions of GTEs closest to the regions innervating the heart and the respiratory muscles were determined by delivering stimulating pulses to all 13 GTEs within the cuff (biphasic, charge balanced, current pulses, 1.3 to 2 mA, 20 Hz). Stimulation with GTE 9 elicited a sharp fall in blood pressure and heart rate and also a minor disturbance in ventilation rate as shown in Fig. 2a. To validate changes in heart rate, the ECG was recorded via the hypodermic needles inserted in the animal's limbs. Simultaneously, arterial blood pressure was measured using a catheter inserted into the dorsal metatarsal artery. Then the ECG and blood pressure signals were delivered to a differential amplifier and to a DigiPack 1200 (Axon Instruments) data acquisition system connected to a PC.

When the stimuli were delivered to the GTE 4 that was in contact with the region innervating the respiratory muscles, the rate of respiration decreased as shown in Fig. 2b. Stimulation with GTE 4 abolished ventilation during stimulation but did not affect the heart rate or blood pressure. To validate the changes in the rate of respiration, variations of the circumference of the thorax were measured by a force transducer. Then the signals were delivered to a bridge amplifier and to a data acquisition system connected to the PC.

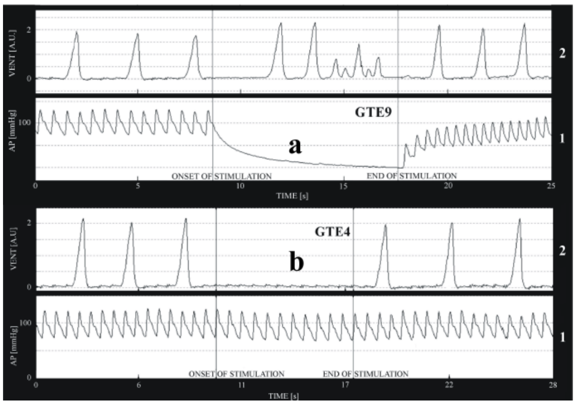

Fig. 2. a) The effect of selective stimulation of the left vagus nerve with GTE9 on respiration (trace 2) and blood pressure (trace 1), b) The effect of selective stimulation of the left vagus nerve with GTE4 on respiration (trace 2) and blood pressure (trace 1).

The electrodes in each of the two indicated GTEs 4 and 9, and randomly chosen GTEs 1 and 7, were then connected to the ENG preamplifier. The recorded ENGs were fed to the data acquisition system and sampled at 20 kHz. Heart rate and blood pressure were modulated by two interventions: (1) manual compresion of the carotid artery at the neck for 15 s and (2) a single i.v. bolus of epinephrine (0.1 ml/kg, 1:200). Non-invasive, positive end-expiratory pressure ventilation (10 cm of H_2O) delivered to the lungs through a mouthpiece connected to a respirator was used to modulate respiration.

Changes in ENG, recorded by each GTE within the defined region of the nerve, that were elicited by abovementioned interventions were evaluated by calculating the power spectra of corresponding ENGs. For this purpose a fast Fouriere transformation (fFt) using Matlab 6.5 was performed.

Results

Unilateral compression of the left carotid artery decreased blood pressure and had a significant effect only on the ENG power spectrum recorded by GTE 9. A mean arterial pressure (MAP) decreased from 100 mmHg (systolic pressure 120 mmHg, diastolic pressure 80 mmHg) to 50 mmHg (systolic pressure 70 mmHg, diastolic pressure 30 mmHg). Carotid artery compression did not influence the heart rate (103 bpm before and after compression). Only the GTE 9 ENG power spectrum showed frequencies which could be attributed to changed superficial nerve activity due to compression of the carotid artery as shown in Fig. 3a.

The effect of epinephrine on the heart rate and blood pressure is presented in Fig. 3b. Epinephrine injection caused a significant decrease in MAP and bradycardia. MAP decreased from 100 mmHg (systolic pressure 120 mmHg, diastolic pressure 80 mmHg) to 25 mmHg (systolic pressure 45 mmHg, diastolic pressure 5 mmHg) and heart rate decreased from 117 bpm to 40 bpm. Only the ENG power spectrum recorded with GTE 9 showed frequencies which could be attributed to changed superficial nerve activity due to the injection of epinephrine.

Non-invasive positive end expiratory pressure ventilation elicited a significant change in the ENG power spectrum recorded with GTE 4, situated close to the nerve region innervating the lungs

(Fig. 3c.). Namely, only the ENG power spectrum recorded with GTE 4 showed frequencies which could be attributed to changed superficial nerve activity elicited by non-invasive, positive end-pressure ventilation.

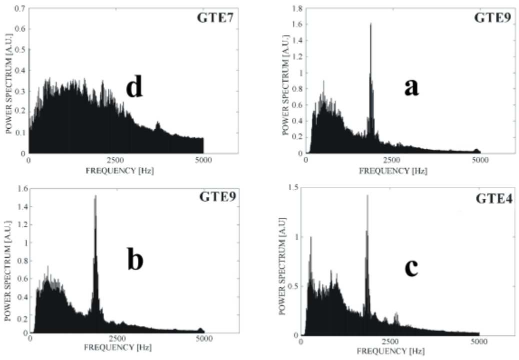

Fig. 3. a) The effect of unilateral compression of the left carotid artery on the ENG power spectrum of GTE 9, b) The effect of a single i.v. dose of epinephrine on the ENG power spectrum of GTE 9, c) The effect of non-invaisive, positive end-expiratory pressure ventilation on ENG power spectrum recorded by GTE 4. The effect of either intervetion on ENGs power spectrum recorded by GTE 7.

Discussion

Natural sensory activity in superficial regions of the left vagus nerve of a dog innervating the heart and the lung, arising most probably from their receptors such as barroreceptors and recorded selectively with a chronically implanted cuff, potentially contains useful information about the visceral function. It was shown that the heart and the lung ENGs contained frequencies that can be attributed to communicating activity between the aforementioned organs and the central nervous system. In the presented study the activity of the left vagus nerve rose immediately after carotid artery compression, non invasive positive end-expiratory pressure ventilation and i.v. epinephrine administration. However, afferent and efferent activities could not be distinguished. Multi electrode spiral cuffs on peripheral autonomic nerves could be used for stimulation and recording of nerve activity. ENGs recorded selectively with a multi-electrode cuff could be useful as a potential feedback signal for control of visceral function of different internal organs and glands.

References

1. Haugland, K.H. and Hoffer, J.A. Slip information provided by nerve cuff signals: Application in closed-loop control of functional electrical stimulation. IEEE Trans. Rehabil. Eng. 2:29–36, 1994.

2. Haugland, M.K. and Sinkjær, T. Cutaneous whole nerve recordings used for correction of footdrop in hemiplegic man. IEEE Trans. Rehabil. Eng. 3:307–317, 1995.

3. Lichtenberg, B.K. and DeLuca, C.J. Distinguishability of functionally distinct evoked neuroelectric signals on the surface of a nerve. IEEE Trans. Biomed. Eng. 26:228–237, 1979.

4. Metting van Rijn, A.C., Peper, A. and Grimbergen CA. High–quality recording of bioelectric events (Part 1 Interference reduction, theory and practice). Med. Biol. Eng. Comput. 28:389–397, 1990.

5. Naples, G.G., Sweeney, J.D. and Mortimer JT (inventors). Implantable cuff, method and manufacture, and method of installation. US Patent 4602 624, 29 July 1986.

6. Nikolić, Z.M. Instrumentation for ENG and EMG recordings in FES systems. IEEE Trans. Biomed. Eng. 41:703–706, 1994.

7. Pelletier, C.L., Clement, D.L. and Shepherd JD. Comparison of afferent activity of canine aortic and sinus nerves. Circ. Res. 31:557–568, 1972.

8. Popović, D.B., Stein, R.B., Jovanović, K.L., Dai, R., Kostov, A. and Armstrong WW. Sensory nerve recording for closed-loop control to restore motor functions. IEEE Trans. Biomed. Eng. 40:1024–1030, 1993. 9. Sahin, M., Durand, D.M. and Haxhiu, M.A. Chronic recordings of hypoglossal nerve activity in a dog model of upper airway obstruction. J Appl Physiol. 87:2197-2206, 1999.

10. Stein, R.B., Charles, D., Davis, L., Jhamandas, J., Mannard, A. and Nichols TR. Principles underlying new methods for chronic neural recording. Can. J. Neurol. Sci. 2:235–244, 1975.

11. Stein, R.B., Nichols, T.R., Jhamandas, J., Davis, L. and Charles D. Stable long term recordings from cat peripheral nerves. Brain Res. 128:21–38, 1977.

12. Taylor, J., Donaldson, N. and Winter J. Multiple-electrode nerve cuffs for low-velocity and velocity-selective neural recording. Med. Biol. Eng. Comput. 42:634–643, 2004.

13. Triantis, I.F., Demosthenous, A. and Donaldson, N. On cuff imbalance and tripolar ENG amplifier. IEEE Trans. Biomed. Eng. 52:314–320, 2005.

Acknowledgements

This work was supported by the Ministry of Higher Education and Science, Republic of Slovenia, research programme P3-0171.

Author's Address

Janez Rozman, Ph. D., ITIS d. o. o. Ljubljana, Centre for Implantable Technology and Sensors, Lepi pot 11, 1102 Ljubljana, Republic of Slovenia, Tel.: +386 41 415 268, Fax.: +386 1 470 19 39, E-mail: janez.rozman@guest.arnes.si

Session V

Autonomic Nervous System

Chairpersons
Janez Rozman (Ljubljana, Slovenia)
Dietmar Rafolt (Vienna, Austria)

PROCEDURE FOR REAL-TIME OPTIMIZATION OF CARDIAC CONTROL THROUGH VAGAL NERVE STIMULATION

Tosato M[1], Yoshida K[1,2], Toft E[1], Struijk JJ[1]

[1] Center for Sensory-Motor Interaction, Dept of Health Science and Technology, Aalborg University, Fredrik Bajers 7D, DK 9220 Aalborg Øst, Denmark

[2] Biomedical Engineering Department, Indiana University-Purdue University Indianapolis (IUPUI), 723 W. Michigan St. SL164, Indianapolis, IN 46202, USA

Abstract

Vagal Nerve Stimulation (VNS) has proved successful in regulating the heart rate. Model-based custom regulators may work better than standard algorithms used so far, as similar Functional Electrical Stimulation (FES) studies suggest. In two acute animal experiments, a novel identification and control strategy was applied to the cardiac vagal control. A battery of system identification steps was applied on the vagus-heart system and modeling attempted. Then custom controllers were built, based either on minimal stability requirements (stable) or given dynamic specifications (optimal). They were compared to standard proportional-integral-derivative (PID) algorithms. The results show the feasibility of this new real-time procedure. In both experiments, the performance of the custom controllers was similar to that of the general purpose ones. The best dynamic and overall performance was that of the optimal controllers, whereas the general purpose ones were somehow slow and robust. Further understanding of the complex cardiovascular effects of the stimulation of the intact vagus is needed to improve and speed up the regulator design procedure implemented in the present study.

Introduction

The stimulation of the vagus nerve (VNS) is beneficial in heart failure [1]. Although the beneficial effects may be independent from those on the heart rate [2], the use of VNS for controlling the heart is still worthy for further investigation. Functional electrical stimulation (FES) takes advantage of closed-loop control to compensate for the limitations of the physiological model and for the unforeseeable disturbances [3]. To date, most VNS models are based on experiments where nerves have been cut, so they give only part of the picture [4]. So far the closed-loop regulators used for external cardiovascular control were general purpose ones, since they don't require previous knowledge of the system for their design [5-8]. Other studies have shown that a better model of the system leads to regulators with higher performances [9]. When applying automatic control theory to physiological systems, one has to recognize the intrinsic limitations due to the lack of precise information and the non-linear and time-varying nature of these systems.

The vagus-heart system is not controllable in a strict sense [10]. None of its states (e.g. heart rate and mean blood pressure) can be controlled completely, and many cannot be observed or controlled at all (ACh at nerve endings, parasympathetic and sympathetic interaction in the cardiac ganglia). So it is important to understand the intrinsic limitations of any external control on such a system. Depending on the species and the circumstances, stimulation of the vagus nerve will result in a variation of heart rate ranging from 1% to 100% [11-12]. The ability of stabilizing such a variation decreases with its magnitude. Nevertheless, the better the closed-loop regulator used, the biggest the controllability set and the stability range.

In the first two steps of the optimization of closed-loop VNS control on the heart, the cardiac and side effects were characterized and used for deciding the best stimulation and feedback strategies [13]. As final step, presented here, it was attempted to improve the dynamic response of the system, by building simple adhoc models and using them to design custom regulators in real-time.

Material and Methods

Surgery and Setup:

Two minipigs, age 3 years, were sedated, intubated and anaesthetized with isoflurane. During positive pressure ventilation, the bladder was catheterized and an ear vein used for continuous fentanyl IV injection (Fentanyl "Hameln", 50µg/ml). A catheter terminating in a balloon was inserted in the esophagus. The balloon was filled with saline and it was connected to a pressure transducer (Namic Morse Compensator Manifold, Boston Scientific Inc.). Arterial blood pressure was measured through another strain-gauge transducer

(Namic Manifold) connected to a cannula in the saphenous artery.

After a midline incision in the neck, the left vagus was identified and isolated from surrounding tissue for 10 cm. Two silicone cuffs, each containing 3 platinum ring electrodes, were carefully wrapped around the nerve [14]. The proximal was used for recording vagal ENG, the distal was connected to a controlled current source stimulus (NoxiSTIM, JNI Biomedical, Aalborg, Denmark) isolator which received voltage pulses from the PC (through an ADC Card) and converted them into current pulses. As part of the protocol, a temporary block of the vagus was attempted using Lidocaine: the drug was applied around the nerve trunk and a passive 5mm silicone cuff was loosely wrapped around the application area. Suprathreshold stimulation pulses were used to assess the efficacy of the block, by monitoring the ENG and measuring the reduction of VCAP components. To remove the block, the cuff was removed and the area was rinsed and soaked with saline. Typically it took 20 minutes to achieve the desired threshold and 30 minutes to be reversed.

Throughout these automatic control experiments, VNS is regarded as input to the system, while RR interval duration measured through surface electrodes in the standard lead 2 configuration was the output signal. The system itself is the in situ living preparation of vagus, autonomic nervous system (ANS), heart and circulatory system.

Acquisition and Analysis

All signals were filtered and amplified using Cyberamp 380 (Axon Instruments, USA). They were acquired to the PC through its ADC acquisition card (National Instruments). Acquisition and real-time computation and control routines were written in Labview (National Instruments). On-line model identification and control design routines were written in Matlab (Mathworks). Performances were computed off-line in Matlab.

Identification Protocol

First the allowed ranges of the stimulation parameters were found. Typical values eliciting cardiac effects and reducing side-effects are: 1-5 pulses, 3-7 mA and 0.2-0.6 ms. One parameter was selected for automatic control, while the others were fixed. Each stimulation trial was 5 minutes long, with an initial off-phase, then on, then off again.

The identification procedure is explained in Fig. 1. The lidocaine block is an approximation of cutting the nerve. The complex effect of intact VNS on the heart should resemble the sum of the outputs from the proximal and distal models (Fig. 1).

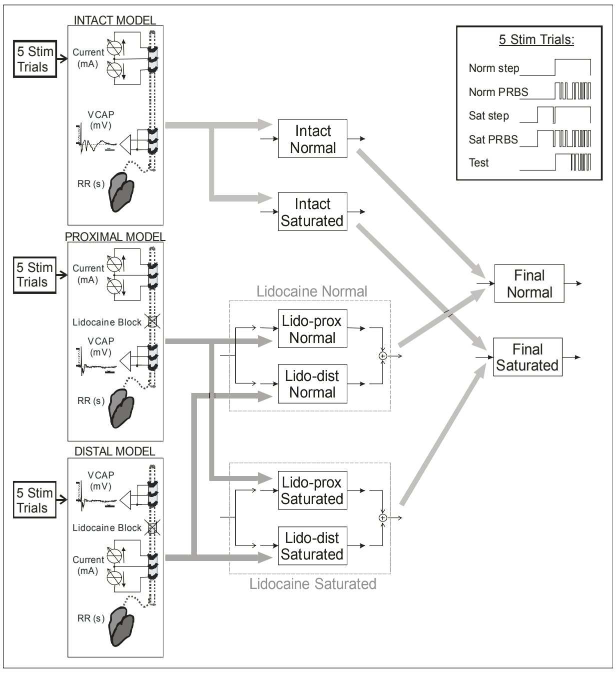

Fig. 1: Identification protocol

Fifteen identification trials were conducted in each animal. They consisted of 3 sets of 5 inputs. The inputs were: 1) unit step, 2) unit pseudo random binary sequence (PRBS) [15], 3) a short step and a normal step, 4) a step and a PRBS, and 5) a short combination of step and PRBS. These five stimulation types were randomly applied in 3 conditions: the intact vagus first, then on the proximal end of the blocked nerve and on the distal end at last.

The first 4 inputs were for building the models, the fifth was for testing them and select the best. The step response was used for building a black-box model in the time-domain while the PRBS was used for one in the frequency domain. They were then both tested on the short combination trial and the best performing one saved as intact normal. Performance was assessed in the time domain, as best fit between predicted and real output, given the test input.

The third and fourth stimulation types were like the first two plus 40 second step stimulation. This was done to simulate the case when the system is nearly saturated and its response varies. The third and fourth trials were again used for time-domain and frequency-domain analysis respectively, and then tested on the same short combination stimulation. The best performing was saved as intact saturated. For normal stimulations the on-phase was one minute, for the saturated cases, the total was 100 seconds.

Next, a lidocaine block was applied. When the B elevation in the VCAP was reduced to 30% of its initial amplitude (inset in Figure 1), the procedure was repeated, for the proximal model first and the distal one afterwards. The models obtained were labelled respectively as: proximal normal, proximal saturated, distal normal and distal saturated. These last four models were combined, in pairs, in a grey-box model resulting from the combination of two independent vagal pathways to the heart: the efferent and the afferent. The proximal normal was used for the afferent subsystem and the distal normal was the efferent subsystem of the total lidocaine normal model. The other two were used accordingly to form the lidocaine saturated.

Finally, the two intact and two lidocaine models were compared and the best two were used, one as normal, the other as saturated.

Regulation Protocol

While the lidocaine block wore off (single VNS pulses were used to monitor the restoration of the VCAP), the models were used to design custom regulators. For each model, two regulators were designed: the stable, for the quickest stable response – phase margin (PM) = 60º – and the optimal, for optimal performance. The optimal performance was defined as: PM = 60º, steady-state error down to zero, settling time (within 5% 7 ddof the final value) below 5 seconds and overshoot below 5% of the final value.

In random order, the following controllers were used for closed-loop VNS: Stable Normal, Optimal Normal, Stable Saturated, Optimal Saturated, multiple model adaptive controller (MMAC) and a standard proportional-integral-derivative (PID). Our simplified version of the MMAC was an algorithm that switched between a normal and a saturated controller when a decision variable crossed a threshold value. The decision variable was the combination of tracking error and stimulation time. The switching threshold of the MMAC had to be tuned manually.

Results

Controllers' performances are summarized in Table I. In both experiments, the performance of the custom controllers was similar to that of the general purpose ones. The best dynamic and overall performance was that of the optimal controllers.

The controllability range of the state variable RR was found by hand and it depended on the animal. In the first experiment, the RR interval could be set to 25% of its baseline value (Fig. 2), although only 10% was used for regulators comparison. In the other experiment, up to 10% was possible, but 5% targets were used.

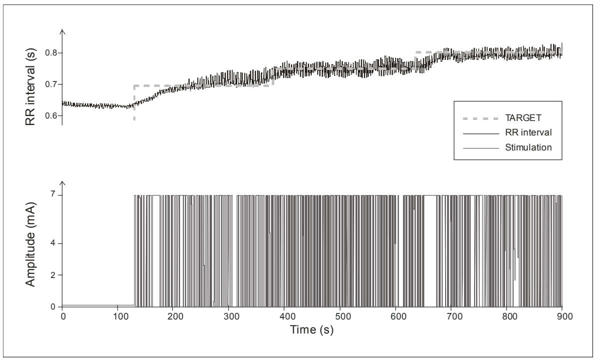

Fig. 2: MMAC keeps RR around 25% of its initial value

Models built from PRBS inputs were always inferior to Step ones, probably because the signal length was too short for frequency characterization and the cut-frequency of the input filters may have been too low, removing high frequency information. Fig. 3A shows a comparison between two of the models from the first experiment. Below the graphs, the models and regulators from the first experiment are shown. The controlled input parameters in the two experiments were current amplitude and number of pulses respectively.

Since the vagus-heart system is intrinsically stable, the Stable controllers were typically simple gains. The Optimal ones were designed with the pole-placement technique, with zeros equal to the poles of the system and poles placed *adhoc* to meet the performance specifications. Usually one pole was placed in the origin, since the integrative action is the only certain way to meet the target. Fig. 3B shows the behaviour of the Saturated Optimal regulator, both for the simulated best saturated model and for the real system. It also gives a graphical explanation of the values reported in Table I.

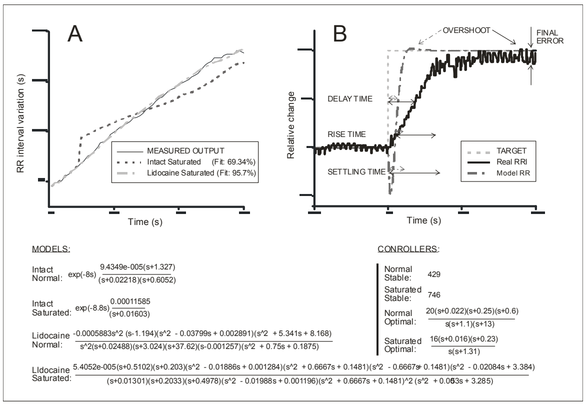

Fig. 3: A. Comparison between Intact Saturated and Lidocaine Saturated to choose the best model. B. Regulator is Sat Opt, comparing real and Final Sat.

Controller:	Norm Stable		Norm Optimal		Sat Stable		Sat Optimal		MMAC		PID	
Experiment	1	2	1	2	1	2	1	2	1	2	1	2
Final Error	0.018	0.031	0.012	0.003	0.012	0.006	0.005	0.008	0.014	0.029	0.007	0.001
Overshoot	0.001	0.027	0.003	0.003	0.003	0.001	0.001	0.001	0.011	0.055	0.007	0.004
Delay Time	18.1	6.1	16.9	17.4	16.5	23.3	18.7	13.9	23.3	6.0	19.4	21.5
Rise Time	30.3	13.9	28.2	43.5	28.1	83.6	33.7	45.8	36.4	9.35	99.9	56.9
Settle Time	36.6	17.2	32.2	49.3	33.2	97.9	57.3	50.7	59.1	12.4	117.3	66.3

Table 1: Controllers performance

Discussion

The present preliminary results suggest that a real-time procedure for building simple models and regulators for the vagus-heart system may be used. Although real responses of the system did not precisely match those predicted by the models (Figure 3), this is a first step towards an optimization of the cardiac-VNS control. In particular, better dynamics are needed for minimizing reaction times for new targets or overcoming disturbances. The aim of the real-time procedure was not to build precise models, but to design custom regulators, which could be further optimized manually. It is expected that with careful design, model-based regulators will outperform general purpose ones. For example, one of the limitations of the present study is that models and controllers were linear, whereas they shouldn't be. The pole in the origin drives the control to enormous values, which of course were not possible since the controls had a tiny allowed range (1-5 pulses or 3-7 mA).

After a lengthy procedure, two final models were selected: Normal and Saturated. The former was for normal operations, at the beginning of VNS, or for short sessions. The response of the system is fast, and the controllability set is maximal. That is the RR interval can be pushed to virtually any target value, the heart may even be stopped for a few seconds [12]. After some time, depending on many factors, the system saturates. Saturation can be either ACh depletion at the vagal postganglionic nerve endings or sympathetic compensation of the artificial increase of vagal activity [16]. The response of the system is slower, high targets can't be reached anymore and holding the RR duration stable even at low targets becomes difficult.

Each model served the design of two regulators. The first (Stable) is only proportional, and its goal is to maximize the speed of the response keeping the system within the stability range. The second (Optimal) replaces the system's poles and sets faster dynamics. Typically, the Stable regulator for the saturated model had a higher gain than for the normal, and the Optimal saturated had lower dominant poles.

Both optimal regulators were better than the stable ones. In general, the Optimal Normal and Saturated regulators showed the best dynamic performances, although the saturated was slightly better. That may be because these comparisons were at the end of the experiment, and the system might have drifted to the saturation region.

The MMAC algorithm is very promising, especially for prolonged stimulation sessions (the MMAC in Figure 2 is switching between Normal Stable and Saturated Optimal). It combines two or more models, and for this reason it needs further optimization – for the choice of switching variable and threshold. Its main advantage over the other regulators is that its intrinsic non-linear time-varying nature matches well any physiological system [17].

Many other studies dealt with the autonomic control of the cardiovascular system, from black box [18] to grey [19] to white box ([20]). Their goal was to build a model to investigate and further understand the physiological system. None has attempted using the models for designing the controllers. The goal of the present study was the latter: optimizing the dynamic performance of closed-loop control, using regulators based on a model of the system. The idea was that for the high variability among animals, the best would be building a model for each single animal. This was only a first step, and although it has proved feasible, the inherent procedure is too long and too stressing for the nerve, especially for clinical use. Using available data to build a simple grey-box model off-line will enable us to shorten the system identification procedure. More precisely, if the structure of the model is previously validated, then only parameters identification would be necessary. A few stimulation trials would suffice to find an initial guess for the parameters and an iterative procedure would correct and update them. Then a MMAC or a simpler algorithm could be used, where the parameters of the controller or the model would be continuously adapted to the real system [21].

References

[1] Li M, Zheng C, Sato T, et al. Vagal nerve stimulation markedly improves long-term survival after chronic heart failure in rats. Circulation, vol: 109, 120–124, 2004.

[2] Pavlov VA, Tracey KJ. The cholinergic anti-inflammatory pathway. Brain Behav Immun, vol: 19(6), 493–9, 2005.

[3] Popovic D, Sinkjær T. Control of Movement for the Physically Disabled. (I ed) Springer, 2000.

[4] Dokos S, Lovell NH, Celler BG. Review of ionic models of vagal-cardiac pacemaker control. J Theor Biol, vol: 192(3), 265–74, 1998.

[5] Zhang YH, Mowrey KA, Zhuang SW, et al. Optimal ventricular rate slowing during atrial fibrillation by feedback AV nodal-selective vagal stimulation. American Journal of Physiology-Heart and Circulatory Physiology, vol: 282, H1102–1110, 2002.

[6] Waninger MS, Bourland JD, Geddes LA, et al. Electrophysiological control of ventricular rate during atrial fibrillation. Pace-Pacing and Clinical Electrophysiology, vol: 23, 1239–1244, 2000.

[7] Leor R, Bobrovsky BZ, Eliash S et al. Heart rate control by the computerized infusion of isoproterenol. Computers in Cardiology, vol: 24, 517–519, 1997.

[8] Peters TK, Koralewski HE, Zerbst E. The principle of electrical carotid sinus nerve stimulation: a nerve pacemaker system for angina pectoris and hypertension therapy. Ann Biomed Eng, vol: 8(4), 445–58, 1980.

[9] Ferrarin M, Palazzo F, Riener R et al. Model-based control of FES-induced single joint movements. IEEE Trans Neural Syst Rehabil Eng, vol: 9(3), 245–57, 2001.

[10] Kuo B. Automatic Control Systems. (6th ed) Prentice Hall, 1991.

[11] Binks AP, Paydarfar D, Schachter SC, et al. High strength stimulation of the vagus nerve in awake humans: a lack of cardiorespiratory effects. Respiration Physiology, vol: 127, 125–133, 2001.

[12] Matheny RG, Shaar CJ. Vagus nerve stimulation as a method to temporarily slow or arrest the heart. Annals of Thoracic Surgery, vol: 63, S28–S29, 1997.

[13] Tosato M, Yoshida K, Toft E et al. Optimization of vagal nerve stimulation with respect to cardiac- and side-effects. unpublished.

[14] Haugland M. A flexible method for fabrication of nerve cuff electrodes. Proc. 18th Annual Int. Conf. IEEE Engineering in Medicine and Biology Society, Amsterdam, vol: 1, 359–360, 1996.

[15] Ljung L. System identification: Theory for the user. (2nd ed) Prentice-Hall, 1999.

[16] Kawada T, Ikeda Y, Sugimachi M et al. Bidirectional augmentation of heart rate regulation by autonomic nervous system in rabbits. American Journal of Physiology-Heart and Circulatory Physiology, vol: 40, H288–295, 1996.

[17] Khoo MCK. Physiological Control Systems: Analysis, Simulation and Estimation. IEEE Press, NJ, 2000.

[18] Warner HR, Cox A. A Mathematical Model of Heart Rate Control by Sympathetic and Vagus Efferent Information. Journal of Applied Physiology, vol: 17, 349–355, 1962

[19] Ursino M, Magosso E. Short-term autonomic control of cardiovascular function: a mini-review with the help of mathematical models. J Integr Neurosci, vol: 2(2), 219–47, 2003.

[20] Dokos S, Celler BG, Lovell NH. Vagal control of sinoatrial rhythm: a mathematical model. J Theor Biol, vol: 182(1), 21–44, 1996.

[21] Martin JF, Schneider AM, Smith NT. Multiple-model adaptive control of blood pressure using sodium nitroprusside. IEEE Trans Biomed Eng, vol: 34(8), 603–11, 1987.

Acknowledgements

The authors thank the Danish Heart Foundation for financial support and the staff of the Animal Lab at the Institute of Pathology, Aalborg Hospital, for their technical help and friendly support.

Author's Address

Marco Tosato:
Center for Sensory-Motor Interaction, Dept of Health Science and Technology, Aalborg University, Fredrik Bajers 7D, DK 9220 Aalborg Øst, Denmark
e-mail: marco@smi.auc.dk
homepage: http://www.smi.hst.aau.dk

BLOOD PRESSURE RESPONSES IN PARAPLEGIC SUBJECTS DURING FES-INDUCED WALKING: PRELIMINARY FINDINGS.

Russold M[1], Menezes L[1], Nightingale J[2], Middleton JM[3], Raymond J[1], Crosbie J[2], Davis GM[1]

[1] Rehabilitation Research Centre, Discipline of Exercise and Sport Sciences, University of Sydney, Australia

[2] Discipline of Physiotherapy, University of Sydney, Australia

[3] Rehabilitation Studies Unit, University of Sydney, Australia

Abstract

FES-assisted walking by paraplegic subjects has been a focus of research for several decades. Numerous studies have found that symptoms of orthostatic hypotension during upright stance often could be reduced by FES-evoked muscle contractions. The aim of our study was to investigate the severity of orthostatic hypotension and whether progressive-intensity FES training might alter its clinical presentation. Assessments were performed during passive stepping and during FES-assisted gait with and without a walking frame. All gait experiments lasted for up to 60-min or until fatigue-related knee-buckle limited walking safety. These preliminary findings proceed from the first 3 subjects of a group undergoing FES exercise and gait training.

Results from the first cohort prior to treadmill training revealed a mildly reduced blood pressure (S1), a severe drop in blood pressure (S3) and an increase in blood pressure (S2) in one patient each. Following 8 weeks of increased-intensity FES gait training, S1 demonstrated a slightly increased blood pressure, while the response of S2 and S3 remained essentially unchanged, although the occurrence of (severe) orthostatic hypotension in S3 was delayed when compared to pre-training. These data suggested that patients suffering from severe orthostatic hypotension might not achieve FES-assisted ambulation for extended periods of time, even after high-intensity task-specific gait training. In contrast, patients afflicted by mild orthostatic hypotension during exercise might be able to overcome this with training.

Introduction

The principle of FES walking systems has been established for some time now. But only recent innovative developments in biomedical engineering have made small, user-friendly functional electrical stimulation (FES) devices to restore upright mobility after spinal cord injury (SCI) possible [1-3]. Recently, individuals with SCI ranked standing and walking as their top two priorities for using a FES system, with 23% and 66% of respondents who were surveyed requesting these functional outcomes, even if high cost or extensive neurosurgery were required to achieve them [4]. Several centres worldwide are developing technologies for individuals with SCI that enable standing and stepping by means of FES systems. An overwhelming majority of this research and development is focused upon bioengineering and motor control aspects to restore and improve functional mobility. In contrast, there is only limited investigation into the concomitant physiological adjustments that accompany such activities.

Upright posture is particularly challenging for those with SCI. The absence of an effective lower limb muscle pump, an impaired thoraco-lumbar pump and deficient sympathetically mediated vasocons-triction below the lesion affect maintenance of central blood volume and blood pressure. Considering these deficits, it is not surprising that orthostatic hypotension is frequently observed in people with SCI [5]. FES-induced muscle contractions in the lower limbs may attenuate the effects of gravity by improving venous return and increasing diastolic and systolic blood pressures [6-9]. While these studies offer support for the idea that FES may overcome the gravitational load imposed by upright posture, this may not be the case during upright mobility with added upper body workload. Anecdotal reports of SCI-subjects exist, detailing acute episodes of light-headedness and discontinuation of training programs due to orthostatic hypotension. It is possible, that some individuals may not be able to tolerate FES-assisted upright posture, thus limiting their participation in standing and stepping activities.

The aim of our study was to establish changes in blood pressure responses in sensorimotor complete paraplegics before and after an intense progressive-intensity FES-gait training program. This preliminary report will present findings from our first cohort of individuals who completed the study. We will primarily focus on tests in which subjects walked with FES and a walking frame (*FES + frame*), as it resembles gait by SCI-subjects within their home and/or occupational environments.

Material and Methods

Subjects:

Six subjects with sensorimotor complete (ASIA A) SCI were recruited for this study, of which 3 males have completed the assessment protocols before and after gait training. Five more individuals were initially recruited, but left the study without completing any measurements, mainly due to changed personal circumstances. Subjects were recruited from an existing pool of patients that had expressed interest to participate in research studies in the past. All patients were screened for sufficient bone integrity by means of a DEXA scan and underwent a clinical assessment by an experienced physician. Furthermore, subjects underwent a screening procedure whereby their response to electrical stimulation was assessed. The study was approved by the Human Research Ethics Committee of the University of Sydney and all subjects undersigned written informed consent prior to their participation.

Training:

Subjects were first trained on an isokinetic exercise cycle incorporating electrical stimulation (iFES-LCE) at a cadence of 15rev•min^{-1} [10]. Once a subject was able to stand for at least 3min by means of FES, gait training commenced. Subjects were then trained between parallel bars over level ground. Once sufficient balance and control had been achieved, they were familiarised with a walking frame on level ground, before finally commencing treadmill gait training. Then subjects underwent an 8-week progressive-intensity training programme employing speed- and incline-titrated treadmill walking. Subjects were trained 3 times a week throughout the whole programme.

For FES-induced walking we used either the ExoStim™ or Vienna FES 8-channel walking systems [2, 11]. During training and assessments patients wore a safety harness system that provided overhead support in case of a fall.

Measurements:

Testing was conducted before and after the 8-week training protocol. In each block of testing the following tests were performed.

- *Passive*: Subjects were suspended in a harness system and received no FES during 60-min of passive stepping.
- *FES only*: Subjects received FES and were asked to use minimal arm support during gait.
- *FES + frame*: Subjects received FES and used a walking frame for upper body support during walking.

All tests were performed on a treadmill at a speed of 0.04m•s^{-1}. Foot placement was provided by a trained physiotherapist in all tests. Tests were continued for up to 60-min, or until either appearance of pre-syncope or knee-buckle occurred even at maximum stimulation amplitude. Tests were also terminated at a drop in systolic blood pressure >20mmHg or when heart rate exceeded the age-predicted maximum.

Heart rate was measured continuously with an electrocardiogram (Portascope CR55, Cardiac Recorders, UK) using the CM5 electrode configuration. Blood pressure was measured at discrete time-points using an automated sphygmomanometer (Tango Blood Pressure Monitor, SunTech Medical Instruments, USA) and continuously by means of a Portapres 2 system (TNO-TPD Biomedical Instrumentation, Netherlands). Syncopal symptom scores were acquired together with blood-pressure readings.

Subjects were instructed to avoid additional exercise for 24h preceding each assessment, to abstain from caffeine and cigarettes for 12h and not to eat for the 2h immediately prior to testing. Subjects were also asked to empty their bladder and bowel prior to testing. Regular medication was not limited during training and testing.

Results

Table 1 shows all walking times achieved under the three assessment conditions. Walking times were improved in most tests. It was interesting to note, that in post-testing S3 during *Passive* and S2 during *FES + frame* walked for shorter periods of time when compared to pre-testing.

	Passive		***FES only***		***FES + frame***	
	PRE	**POST**	**PRE**	**POST**	**PRE**	**POST**
S1	60:00	60:00	12:45*	18:06*	9:57*	22:16*
S2	60:00	60:00	4:15*	6:45*	8:18*	5:45*
S3	15:30§	14:00§	10:45§	15:25§	4:00§	8:46§

Table 1: Walking times (in min:sec), for all subjects and tests. Times marked with (§) were terminated because of syncopal symptoms. Tests marked with (*) were stopped because knee-buckle could no longer be prevented.

We have observed that although subjects performed consistently, day-to-day performance was still somewhat variable, even after gait-training and this could have caused the shorter duration of walking during *Passive* in S3. The shorter duration achieved by S2 during *FES + frame* was most likely linked to improved technique with less use of his arms and subsequently earlier onset of knee buckle. All tests of S3 had to be terminated early because of signs of pre-syncope. FES experiments of S1 and S2 were terminated because knee-buckle could no longer be averted. S1 and S3 showed a marked improvement in their walking abilities, and walking durations under the *FES + frame* condition more than doubled in both subjects. Although walking duration for the *Passive* test of S3 was slightly shorter during post-testing, all FES related post-training tests recorded longer walking times.

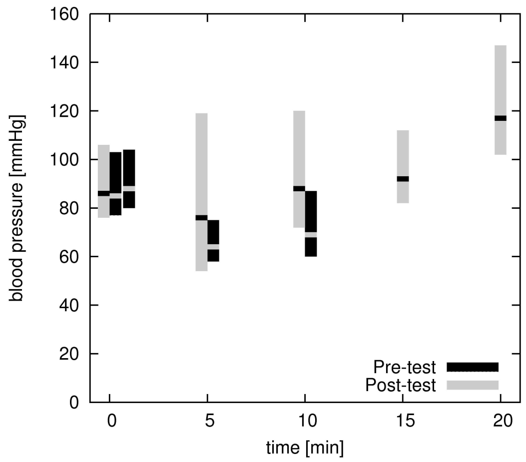

Fig. 1: Blood pressure responses (mmHg) of S1 during FES-induced gait with a walking frame. Bars represent systolic and diastolic blood pressure with MAP as the cross-line.

S1 showed a mildly reduced blood pressure (Figure 1, “Pre test”), while S3 showed a severe drop in blood pressure (Figure 2, “Pre test”) during pre-testing, respectively. In contrast to S1 and S3, S2 showed an increase in blood pressure.

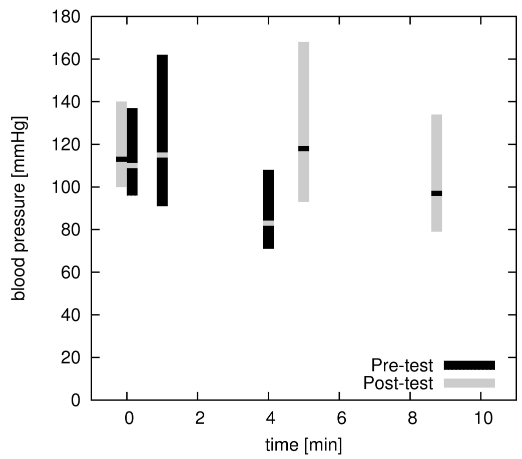

Fig. 2: Blood pressure responses (mmHg) of S3 during FES-induced gait with a walking frame. Bars represent systolic and diastolic blood pressure with MAP as the cross-line.

After 8-weeks of progressive-intensity training, S1 demonstrated a slightly increased blood pressure compared to pre-training, while MAP was elevated by 10-15 mmHg prior to termination of the test (Figure 1, “Post test”). Individual S3, who had experienced severe symptoms of orthostatic hypotension during pre-testing showed similar symptoms even after 8-weeks of progressive-intensity training, albeit with a delayed clinical presentation (Figure 2, “Post test”).

As S2 demonstrated a rise in blood pressure during all experiments we have not portrayed his data herein due to manuscript space limitations.

Discussion

It has long been known that FES may be used successfully to ablate symptoms of orthostatic hypotension in paraplegics during upright posture [7-9]. But all of these previous studies investigated upright stance, not FES-induced mobility. The impact of added upper body effort during FES-gait has not yet been established.

During our study we found it difficult to develop sufficient muscle strength to achieve walking times that would allow us to compare our results to those presented in the studies mentioned earlier. S3, for example, had a longest walk of close to 20-min during training, but under test-conditions only managed 8:46min and 15:25min respectively. We believe that the longer setup and the measurement equipment required for the testing days might have negatively influenced S3’s results when compared to his training results.

Subject S1 showed a slight drop in blood pressures compared to seated rest during pre-testing at 5-min and a small rise in blood pressure by 10-min (which was also the longest duration S1 was able to walk during pre-testing). Notably, the 10-min changes of blood pressures were still below resting levels (Figure 1). During post-testing, blood pressures were again reduced, albeit less compared to resting conditions at 5-min, and these had fully recovered to resting levels by 10-min, and rose further thereafter. Thus it seems possible that the augmented blood pressure responses of S1 could have been associated with his ability to walk for a longer duration. A similar response might have been observed during pre-testing if he could have walked for a longer period of time.

However, we believe this was not the case and that we observed a real change in blood pressure response after gait training, as data collected during the *FES only* condition also revealed an increased mean arterial pressure during post-testing compared to pre-testing. If the blood-pressure response was essentially unchanged for S1 and increased pressures during the *FES + frame* condition were simply a function of a longer duration of walking, then the *FES only* test should have shown a similar response in pre- and post-testing. The changed response during the *FES only* test thus supported the hypothesis that real physiological changes have been triggered by the progressive intensity training.

Subject S3 revealed a similar decrease of blood pressures compared to seated rest (Figure 2), but of greater magnitude and strongly associated with the onset of pre-syncope symptoms. During the pre-training assessments his mean blood pressure fell by 25% at 4:00 min – the longest duration of his walking ability, limited by severe orthostatic hypotension and symptoms of light-headedness and nausea. After 8-weeks of FES gait-training he demonstrated a reduced hypotension (14% fall of mean blood pressure compared to seated rest) associated with a longer walking duration (8:46 min). Yet, his clinical symptoms were not ablated after training. So for S3, improved blood pressure control during upright mobility was a good indicator of his walking ability, but the underlying mechanisms for this are uncertain and the clinical sequelae adverse.

In conclusion, our data suggested that subjects suffering from severe orthostatic hypotension might not achieve FES-assisted ambulation for extended periods of time, even after high-intensity task-specific gait training. In contrast, patients afflicted by mild orthostatic hypotension might be able to overcome this with training. If similar results were obtained from our next subjects, it might allow us to establish guide-lines for patient selection for FES assisted walking in the future. Interestingly, the 'dip' of blood pressures observed at the onset of FES treadmill walking until 5-min was longer than is usually observed for voluntary exercise onset in able-bodied individuals.

We feel that the fact that we have observed three distinctly different patterns of blood pressure response during FES-walking warrants further investigation. We currently have 3 more subjects in training. Unfortunately the long-term commitment (3 days/week for up to 1 year) required to complete this study limits the number of participants.

References

[1] Kralj A and Vodovnik L. Functional electrical stimulation of the extremities: part 2. J Med Eng Technol, 1(2): 75-80, 1977.

[2] Bijak M, Mayr W, Rakos M et al. The Vienna functional electrical stimulation system for restoration of walking functions in spastic paraplegia. Artif Organs, 26(3): 224-7, 2002.

[3] Klose K J, Jacobs P L, Broton J G et al. Evaluation of a training program for persons with SCI paraplegia using the Parastep 1 ambulation system: part 1. Ambulation performance and anthropometric measures. Arch Phys Med Rehabil, 78(8): 789-93, 1997.

[4] Brown-Triolo D L, Roach M J, Nelson K et al. Consumer perspectives on mobility: Implications for neuroprosthesis design. J Rehab Res Develop, 6(39): 659-670, 2002.

[5] Mathias C J and Frankel H L. Cardiovascular control in spinal man. Annu Rev Physiol, 50: 577-92, 1988.

[6] Faghri P D, Yount J P, Pesce W J et al. Circulatory hypokinesis and functional electric stimulation during standing in persons with spinal cord injury. Arch Phys Med Rehabil, 82(11): 1587-95, 2001.

[7] Chao C Y and Cheing G L. The effects of lower-extremity functional electric stimulation on the orthostatic responses of people with tetraplegia. Arch Phys Med Rehabil, 86(7): 1427-33, 2005.

[8] Sampson E E, Burnham R S, and Andrews B J. Functional electrical stimulation effect on orthostatic hypotension after spinal cord injury. Arch Phys Med Rehabil, 81(2): 139-43, 2000.

[9] Elokda A S, Nielsen D H, and Shields R K. Effect of functional neuromuscular stimulation on postural related orthostatic stress in individuals with acute spinal cord injury. J Rehabil Res Dev, 37(5): 535-42, 2000.

[10] Fornusek C and Davis G M. Maximizing muscle force via low-cadence functional electrical stimulation cycling. J Rehabil Med, 36(5): 232-7, 2004.

[11] Simcox S, Davis G, Barriskill A et al. A portable, 8-channel transcutaneous stimulator for paraplegic muscle training and mobility-A technical note. J Rehabil Res Dev, 41(1): 41-52, 2004.

Acknowledgements

This research was jointly supported by Australian National Health and Medical Research Council Project Grant #302013 and an Outgoing International Fellowship from the European Commission.

Author's Address

Michael Russold
Rehabilitation Research Centre, Discipline of Exercise and Sport Sciences, University of Sydney, Australia
michael@russold.at

Session VI

Lower Extremity

Chairpersons
Friedrich Russold (Sydney, Australia)
Manfred Bijak (Vienna, Austria)

ITERATIVE LEARNING CONTROL FOR CORRECTION OF DROP-FOOT USING BIO-IMPEDANCE AS SENSORY INFORMATION

Nahrstaedt H[1], Schauer T[1], Hesse S[2], Raisch J[1,3]

[1] Technische Universität Berlin, Control Systems Group, Berlin, Germany

[2] Charité - University Hospital Berlin, Dept. of Neurological Rehabilitation, Berlin, Germany

[3] Max Planck Institute for Dynamics of Complex Technical Systems, Magdeburg, Germany

Abstract

Automatic control of ankle-joint angle for the correction of drop-foot has been investigated using Bio-Impedance (BI) for measuring the joint angle and Iterative Learning Control (ILC) for adjusting the stimulation profile.

A customised four-channel measurement system (50 kHz) was used to assess bio-impedance changes caused by ankle-joint motion. Two current excitation electrodes were placed below the patella on the shank and on the dorsum of the foot. Voltage detection electrodes were attached to the posterior surface of lower leg below the calf and on the M. tibialis anterior close to its origin. A demodulation circuit determines changes in the absolute value of the BI from the measured and amplified voltage. All circuits are protected against stimulation artefacts so that the recording of BI is possible while muscle stimulation is active. Calibration of the angle measurement was performed by positioning the ankle joint at three known angles. Reference measurements were taken with a marker-based optical system. Dorsiflexion of the unconstrained ankle joint was achieved by stimulation of the M. tibialis anterior. First-order ILC was applied to realise a pre-defined angle profile in a cycle-to-cycle manner. The new stimulation intensity profile will be an update of the last profile taking tracking errors of the last cycle into account. Preliminary experiments were conducted with one able-bodied subject.

An almost linear correlation between ankle-joint angle and bio-impedance was found for the angle range applicable during gait. The chosen angle trajectory (sine half-wave from the resting foot to 0 degree) was realised by the ILC within 3 cycles. The final root mean square tracking error was below 5 degree.

Automatic control of ankle-joint angle by ILC is feasible when using bio-impedance as sensory information. Experiments under real walking conditions and with stroke patients must be conducted in future.

Introduction

Stroke is a major cause for disability and death in the Western countries. Many people have walking deficits after stroke. Ineffective dorsiflexion during swing (drop-foot) is present in 20 percent of the population with partial recovery [2]. A conventional treatment is an ankle-foot orthosis (AFO). Electrical stimulation for correction of drop-foot was introduced by Liberson in 1961 [1]. The stimulation was applied via surface electrodes and was synchronised to the gait phases by using a simple heel switch inside the shoe below the foot sole. Electrical stimulation was active during the swing phase when the heel was not in contact with the floor. Many drop-foot stimulators have been developed since Liberson's first study. Most commercially available stimulators still use a heel switch [3]. Other approaches such as the use of miniature inertial sensors for detection of gait phases have been investigated (e.g. [4]).

Closed-loop control of the stimulation intensity is not satisfactory solved until now and requires a discreet sensor for measuring the ankle-joint angle or the angle of the foot with respect to the ground. Latter can be estimated by mounting an inertial sensor to the shoe [4].

This work introduces Bio-Impedance (BI) as a tool to measure directly the ankle-joint angle. The use of real-time bio-impedance measurements to determine joint angles was initially proposed in [5]. The feasibility of employing such angle measurement for automatic control of the ankle-joint angle will be demonstrated here. Iterative learning control can be applied to update the stimulation profile from step to step during gait to realise a desired angle trajectory (adaptive feedforward controller). ILC was already used successfully for control of the electrically stimulated upper limb by Dou et al. [6].

Material and Methods

Bio-impedance Measurement

The passive electrical properties of tissue are summarised as bio-impedance. The bio-impedance

Z is measured by the voltage drop U caused by a constant sinusoidal current flow I through the tissue:

$$Z(\omega) = \frac{|U(\omega)|}{|I(\omega)|} e^{j(\phi_U(\omega) - \phi_I(\omega))}, \quad (1)$$

where ω is the frequency of the used current and $\phi_U(\omega) - \phi_I(\omega)$ is the phase shift between voltage and current. BI can be measured by a two-channel device which uses the same electrodes for applying the current and for measuring the voltage drop, or by a four-channel device which has two electrodes for measuring the voltage and two separate electrodes for applying the current. BI is usually measured at a frequency of 50 kHz. Here, a four-channel device was chosen to avoid the voltage drop from the skin-electrode-impedance, which cannot be neglected at this frequency.

Bio-impedance varies over time caused by changes of the investigated tissue. The measured voltage will be proportional to the amplitude- and phase-modulated Bio-Impedance Change (BIC):

$$u(t) = |Z(\omega, t)||I| \cos(\omega t + \angle Z(\omega, t)). \quad (2)$$

Thus, temporal changes in BI are mapped to a higher frequency range which is determined by the frequency of the applied current. Consequently, a high-pass filter can remove all low frequency disturbances which are caused by EMG and movement artefacts from the measured voltage without losing the BIC information. After high-pass filtering the remaining signal is demodulated to extract the BIC. Only the absolute value of the BI has to be considered to determine the joint movement. Therefore the signal is amplitude demodulated using an envelope detector in order to extract the absolute value of the BI.

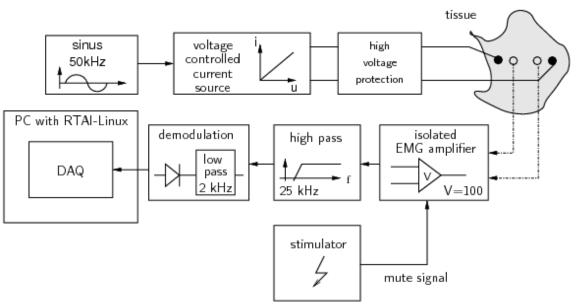

Fig. 1: Bio-impedance measurement.

The structure of the BI-device is shown in Fig. 1. Because of the high voltage stimulation pulses, the input of the EMG pre-amplifier (Neurolog System by Digitimer, UK) is muted during stimulation pulses and the output of the current source is protected by z-diodes which can divert the high voltage drop on the current electrodes.

Only the BIC caused by ankle-joint movements should be measured. Good electrode positions for measuring this angle can be found in [5]. In Fig. 2 the used electrode positions for recording the ankle-joint angle are illustrated.

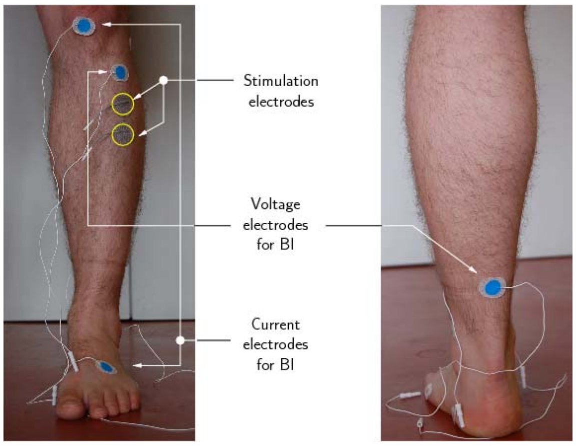

Fig. 2: Electrode positions.

As figured out in [5] the correlation between BI and joint angle is almost linear.

Reference Measurement System

A webcam with USB-interface was used to film the joint-angle movement with 30 fps and a resolution of 320x240 pixels. Four passive markers were placed on the foot and on the shank as shown in Fig. 3. The ankle-joint angle is then calculated from the angles defined in Fig. 3 by

$$\phi_{angle} = \phi_{34} - \phi_{12} + 90°. \quad (3)$$

The recorded videos were analysed offline by using a custom-made program to track the marker positions and to calculate the joint angle. For video processing the OpenCV Library[1] was utilised.

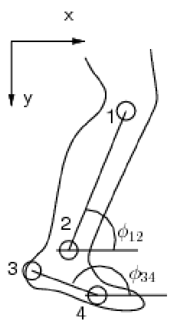

Fig. 3: Marker positions.

[1] http://sourceforge.net/project/opencvlibrary

Iterative Learning Controller

The control problem is to realise a pre-defined angle trajectory for the ankle joint by stimulation of the muscle tibialis anterior. System output y is the angle and control action u is the stimulation intensity (pulsewidth). Walking is a cyclic movement. This fact can be exploited when finding the optimal stimulation intensities. The idea is to apply a fixed stimulation intensity profile during a step and to measure the resulting angle profile. Then, in the next step an updated stimulation profile will be applied which brings the angle trajectory closer to the desired one. The error of the previous step is used to obtain the right update of the stimulation intensity. The repeated application of such control strategy is called iterative learning control.

It is assumed that the system can be described as a linear transfer function G_c for non-saturated control inputs:

$$y_k(t) = G_C(q)u_k(t), \tag{4}$$

where q is the time-shift operator, $t \in [0,T]$ is the time and T is the length of one movement cycle. The sampling time is defined by the stimulation frequency. With the desired angle trajectory $r(t)$, the tracking error is given as

$$e_k(t) = r(t) - y_k(t) \tag{5}$$

which should be minimized. The index k of y, u and e is called iteration index and indicates how many times the cyclic motion has been repeated. ILC algorithms use iterative search methods to find the optimal input to the system. In the ideal case it means to find the signal $u(t) = G_C^{-1}(q)r(t)$. One possible approach to an ILC updating formula is given by

$$u_{k+1}(t) = Q(q)\left[u_k(t) + L(q)e_k(t)\right], \tag{6}$$

where $L(q)$ and $Q(q)$ are linear discrete-time filters. If it can be assumed that the initial condition is reset every cycle and that $G_C(q)$ is invariant, a sufficient condition for the error to decrease is that

$$\left|1 - G_C(e^{i\omega})L(e^{i\omega})\right| < \left|Q^{-1}(e^{i\omega})\right|. \tag{7}$$

If the knowledge about the system is reduced to only the time delay δ of the system, a heuristic approach can be used to find $L(q)$ and $Q(q)$ [7]. The $Q(q)$ filter should be chosen as low-pass filter with cut-off frequency such that the bandwidth of the learning algorithm is sufficient. $L(q)$ is set to κq^{δ}, where δ is chosen as the time delay and a good chosen positive κ keeps the ILC system stable.

Stimulation Device

For stimulation of the dorsiflexor muscle the current-controlled stimulator Rehastim by the German company HASOMED was employed.

Software Interface

The scientific platform SCILAB/SCICOS (http://www.scilab.org) was used to build the real-time program for data acquisition, signal processing and iterative learning control. The programming was done graphically over the block diagram editor SCICOS which allows C-code generation for the real-time Linux extension RTAI (http://www.scilab.org). Customised SCICOS blocks for the used hardware interfaces and the ILC have been generated by inclusion of C-code. The COMEDI interface (http://www.comedi.org) was employed for accessing the data acquisition card.

Experimental Procedure

The experimental procedure should demonstrate the feasibility of controlling the ankle joint using BI as sensory information. Experiments were conducted with one neurologically intact subject. The experimental procedure consisted of the 3 following steps:

1st step - calibration: The foot was positioned at three different joint angles whereas bio-impedance and reference measurements were taken for calibration of the BI-readings.

2nd step - sensor validation test: The active movement of the unconstrained ankle-joint was recorded by BI and webcam while the subject was sitting on a table or standing on a pillar with the other leg.

3rd step - ILC test: In the standing position (one leg on a pillar) the ILC controller had to track a sine half-wave reference for the joint-angle by stimulation of tibialis anterior.

Results

The results of the sensor validation test are shown in Fig 4. The upper graph shows the measurements for the sitting subject whereas the lower graph represents the data obtained for the standing subject. The root mean square error for both tests is 2.8 and 4.5 degree respectively after the time delay was removed from the BI measurements.

Fig. 5 illustrates the result of the ILC test. The reference trajectory is shown in upper graph (dashed line) together with the controlled angle (BI-measurement, solid line).

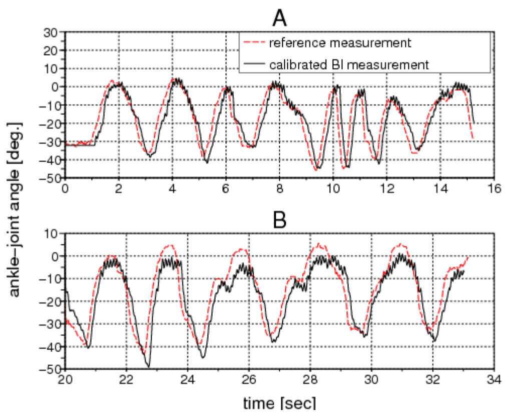

Fig. 4: Results of the sensor validation test. A: Subject sits on a table with the shank and foot free to swing. B: Subject stands with one leg on a pillar while the other leg is free to swing.

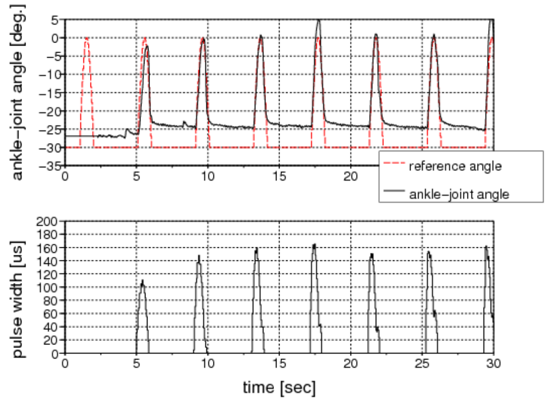

Fig. 5: Results of ILC test ($L(q)=4q^3, Q(q)=1$).

The tracking error has been calculated for the time periods where the reference is above the resting ankle-joint angle. From the third stimulation cycle on, the root mean square error is between 2 and 5 degree. The stimulation intensity (pulsewidth) is shown in the lower graph. Constant current amplitude of 40 mA and frequency of 20 Hz were applied.

Discussion and Conclusions

These first results indicate that bio-impedance may be a good tool to measure the ankle-joint angle in a controlled drop-foot stimulator system. The measurement is accurate enough for the considered application and reliable for at least two hours. Longer tests were not performed. Variations in the knee-joint angle influence the ankle-joint measurement only very slightly. The phase shift (time delay) in the BI-measurement is mainly caused by the signal-processing within the BI-measurement system. In adaptive feedforward control schemes such as iterative learning control no disadvantages arise from a delayed measurement. The iterative learning controller tracks the desired joint angle within 3 stimulation cycles.

Normally, the cycle time T in ILC is fixed, but for gait the step durations differ. Instead of time gait cycle percentage should be considered as new “time” variable t.

The obtained results must be verified with stroke patients and under real walking conditions in future. A disadvantage of the presented approach is large number of electrodes to attach. An elastic stocking with integrated stimulation and BI-electrodes would be desirable.

References

[1] Liberson W, Holmquest H, Scot D et al. Functional Electrotherapy:Stimulation of the Peroneal Nerve Synchronized with the Swing Phase ofthe Gait of Hemiplegic Patients. Archives of Physical Medicine and Rehabilitation, 21:101-105, 1961

[2] Burridge JH, Taylor PN, Hagan SA et al. The effects of common peroneal stimulation on the effort and speed of walking: a randomized controlled trial with chronic hemiplegic patients. Clin. Rehabil., 11: 201-210, 1997.

[3] Lyons G, Sinkjær T, Burridge J et al. A Review of Portable FES-Based eural Orthoses for the Correction of Drop Foot. IEEE Trans.. Neural. Syst. Rehabil. Eng., 10: 260-279, 2002.

[4] Negård N, Schauer T, Raisch J, et al. Control of FES-assisted gait training after stroke using inertial sensors. Proc. of the 11th Annual Conference of the International Functional Electrical Stimulation Society (IFESS 2006), Pages 74-76, 2006.

[5] Song CG, Kim SC, Nam KC et. al. Optimum electrode configuration for detection of leg movement using bio-impedance. Physiol. Meas., 26:59-68, 2005.

[6] Dou H, Tan K, Lee T et al.. Iterative learning feedback control of human limbs via functional electrical stimulation Control Engineering Practice, 7:315-325, 1999.

[7] Norrlöf M, Iterative Learning Control. Analysis, Design, and Experiments. PhD thesis, Linköpings universitet, 2000.

Author’s Address

Thomas Schauer
Technische Universität Berlin
Fachgebiet Regelungssysteme (EN-11)
Einsteinufer 17, 10587 Berlin, Germany
schauer@control.tu-berlin.de
http://www.control.tu-berlin.de

COMBINATION OF PASSIVE ROBOTIC ARM AND SENSORY-DRIVEN FES IN TREADMILL WALKING TRAINING – FEASIBILITY STUDY

Cikajlo I, Obreza P, Šavrin R, Matjačić Z

Institute for rehabilitation, Ljubljana, Slovenia

Abstract

In this paper we present a novel approach and technology for treadmill gait training that combines a passive robotic arm and sensory-driven FES of peroneal nerve. Passive robotic arm was designed to help in controlling and stabilizing the pelvis movement in such a way that holding on the parallel bars is not necessary. In this way the training subject can practice maintenance of balance in true bipedal conditions. Simultaneously, a sensory driven FES of peroneal nerve is applied to facilitate the movement of a swinging leg where the level of stimulation amplitude depends on current performance. In this feasibility study we tested whether a selected incomplete SCI subject in chronic stage can make successful use of both systems at the same time. The results show that a combined use of both systems may be possible. Further clinical studies are needed to explore the viability of the proposed approach.

Introduction

Impaired walking abilities are common consequence of a neurological disease or injury that frequently persists in chronic stage. Efficient walking necessitates reciprocal lower limb movement that provides adequate support during stance phase and efficient swing during swing phase, generation of propulsive forces and efficient balance of the overall body. Treadmill walking as a part of rehabilitation procedures is well established treatment modality [1]. Reciprocal lower limb movement on a treadmill can be facilitated either by manual assistance of a therapist, therapist triggered FES provoking movement of lower extremities [1,2] or by use of robotized gait trainers [3,4]. Propulsive forces and balance are predominantly maintained by the walking subject using arm to hold on parallel bar support. The above methodology is well suited for treatment of patients in the sub-acute phase where an emphasis is on a physical support during training. Different situation arises in subjects in chronic condition where repetitive practice may also bring further functional improvement. However, more refined treatment modalities challenging residual central nervous system to improve functional skills are needed.

In our past work we have developed a sensory-driven functional electrical stimulation (FES) gait re-education system that automatically adjusts the amplitude of stimulation of the common peroneal nerve according to swing performance of a walking subject who was holding on parallel bars, thus maintaining balance and concentrating only on the task of accomplishing adequate reciprocal leg activity [5,6]. A case study has demonstrated feasibility of the proposed approach. We also developed a passive robotic arm that allows walking on a treadmill without using arm support thus facilitating improvement in balancing abilities [7]. The feasibility of this approach has also been demonstrated in a case study. A natural step forward would be application of both systems at the same time, thus allowing for simultaneous training of adequate reciprocal leg activity, maintenance of balance and consequently also propulsion.

The aim of present feasibility study was to test whether a combination of the two previously developed approaches can be successfully applied simultaneously in treadmill walking training in a subject with incomplete spinal cord injury (SCI) in chronic stage.

Materials and methods

Devices

Figure 1 shows a subject with an incomplete spinal cord injury walking on a treadmill. The subject is equipped with a sensory-driven FES system and assisted with a passive robotic arm.

The core of the passive robotic arm is a helical spring that is housed within a steel cylinder. Between the walls of the steel cylinder and the spring a resistance adjustment ring with handle is located. By displacing the adjustment ring vertically we are able to change the stiffness of the spring. The higher is the position of the adjustment ring, the shorter is the bending length of the spring, thus making it stiffer. Conversely, with lowering the position of the adjustment ring also the action of the spring is more compliant. The spring is connected to a vertical rod that is coupled to the horizontal rod via a simple hinge joint that allows rotation in the sagittal plane, which is the plane of progression. At the other end of the horizontal rod there is another hinge joint that is coupled to a leader pelvic belt via a foam rubber disc. The foam rubber disc is very compliant thus allowing pelvic tilt, list and rotation within the physiological ranges that occurs during normal walking (± 8 degrees). If the subject, who is walking on a treadmill, leans forward or backward or to the side a passive stabilizing force acts upon the pelvis in the transverse plane with a magnitude that depends on the position of the adjustment ring. The level of the supportive force should be selected to provide just enough support to allow a subject to walk without using arms for holding onto the parallel bars or handles and should therefore depend on the current balancing abilities of each particular subject. Detailed description on the system is provided in [7].

The sensory-driven FES gait re-education system comprises a sensory system (two dual-axis accelerometers and a gyroscope), an auditory system providing a cognitive feedback to a walking subject and a single-channel electrical stimulator stimulating the common peroneal nerve, thus facilitating swinging of lower extremity. During the swing phase of gait the shank acceleration is assessed by the sensory system and stored into a buffer. At the terminal swing the stored acceleration time-course is compared with the reference that is captured during the initial treadmill assessment and considered to be adequate. The comparison output is termed as ’swing quality’. Based on the quantitative value of the real-time correlation the information is classified into levels - ’good’ (correlation coefficient above the pre-set value of 0.4), ’satisfactory’ (correlation coefficient above the pre-set value of 0.2) and ’poor’ (correlation coefficient below the pre-set value 0.2). After each step a cognitive feedback in a form of auditory signal is provided (high-pitch tone for a good swing and a low-pitch signal for a satisfactory or a poor swing). If the subject is able to perform a pre-set number of consecutive swings, classified as ’good’, the FES intensity is decreased for 10 % and in the case of ’poor’ classification increased for 10%. The user can pre-set a number of the consecutive classified swings required to adjust the stimulation amplitude. In the case of ’satisfactory’ classified swing no action is taken and the ’swing counter’ is reset. The peroneal nerve FES is triggered at heel-off and stopped at the heel-on. Detailed description on the system is provided in [5,6].

Subject and treatment procedures

The subject participating in testing was a chronic incomplete SCI (Th-10, ASIA D classification) with more impaired right extremity. His Berg Balance Scale score was 44, he was using crutches and could cover a distance of 10 meters within 13 seconds and could cover the distance of 420 meters in a 9-minutes walking test. His main deficiencies during walking were poor swing when not assisted by FES and poor balance which required use of crutches. The subject was a well-trained FES user (right lower extremity peroneal nerve stimulation). The subject was equipped with sensory-driven FES system and fitted with the passive robotic arm as shown in Fig. 1. An experienced therapist adjusted an adequate level of electrical stimulation (frequency 25 Hz, pulse duration 150 µs, pulse amplitude 0-50 mA). The subject underwent three training sessions in three consecutive days, each lasting to app. 30 minutes with a treadmill belt speed adjusted to 0.7 km/h. Shank angular velocity, FES intensity and swing quality were monitored and stored.

Results

Figure 2 shows walking performance of the subject in the first and the last session. The performance on the first day shows that the subject was not able to perform required swing quality. This was predominantly because the subject was not holding onto the handles but was forced to rely on the passive robotic arm support, which created challenging training conditions, thus forcing the subject to share his attention between paying attention to auditory feedback signals as well as co-ordinating lower limb movement and trunk in order to maintain balance during walking. However, within the next two sessions the subject became comfortable with the passive robotic arm balancing support and could perform both tasks in a much better way. It can be clearly seen that the subject was able to make use of sensory-driven FES system as the level of pre-set intensity of stimulation could be successfully reduced to 50% of the initially selected intensity.

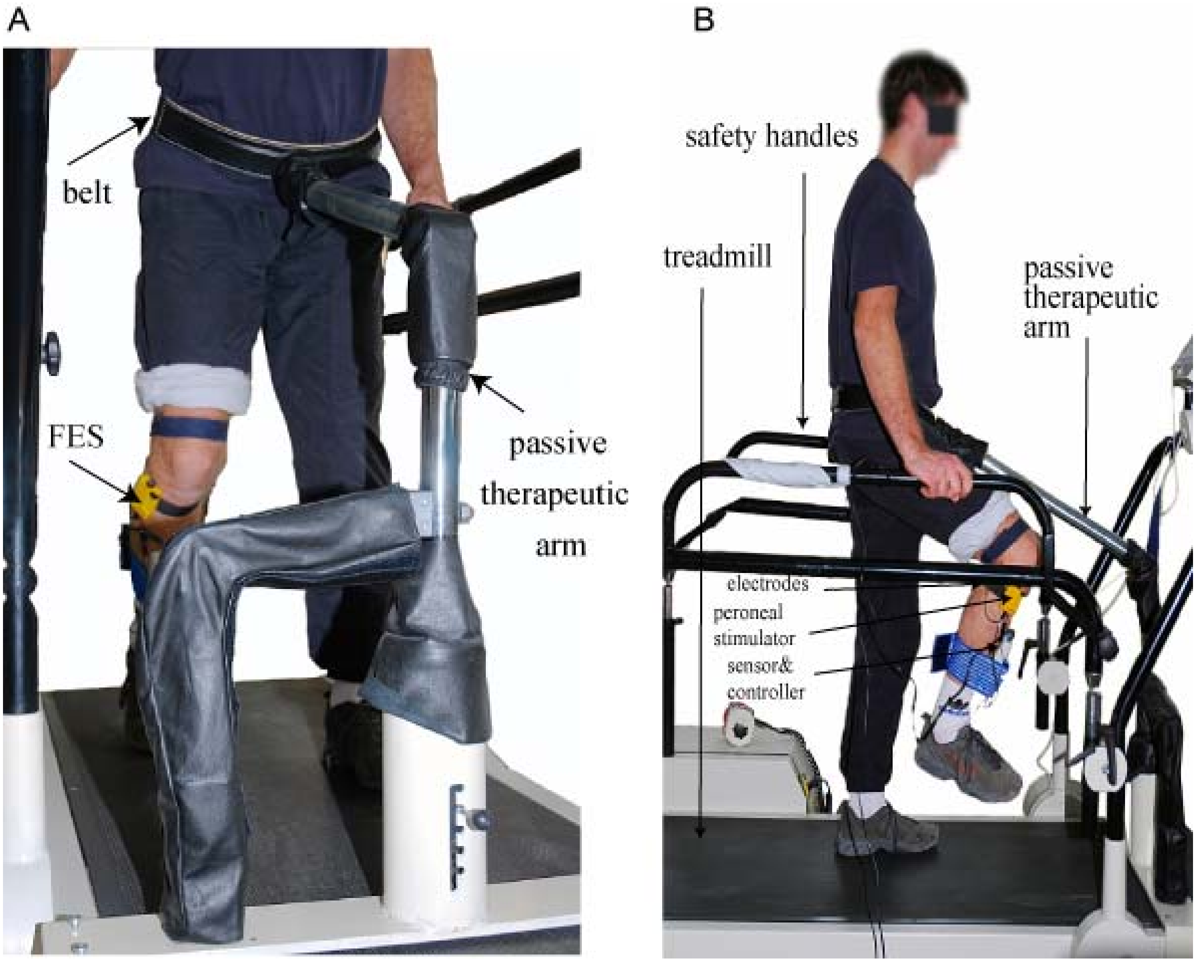

Figure 1. Subject walking on a treadmill while being supported by a passive robotic arm and a sensory-driven FES system. A. Frontal view. B. Side view.

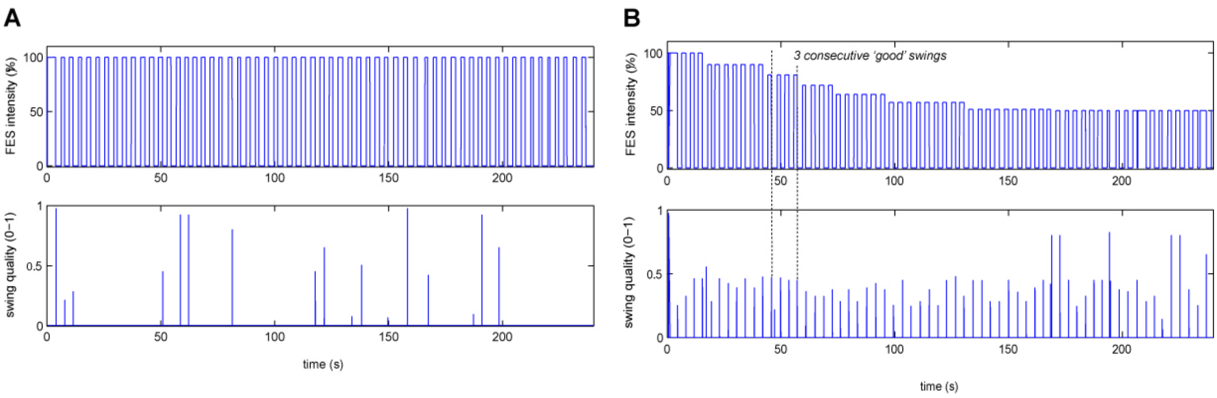

Figure 2. Resulting quality of swing and level of FES intensity. A. The first day of training. B. The third day of training.

Discussion

The main aim of this study was to test feasibility of introducing a combination of passive robotic arm, facilitating development of walking balance abilities, and sensory-driven FES gait re-education system, facilitating development of appropriate control of leg muscles that produce adequate swing phase into treadmill walking. The results of the study show that a combination of both technological solutions can be successfully implemented in a treadmill walking training in the selected incomplete SCI subject. By combining the two approaches a walking subject becomes an active participant in the gait re-education process, which can be judged from diminished support from sensory-driven FES system, while maintaining and improving the level of swing quality. Another advantage of such an approach is a continuous inflow of rather rich sensory information that is generated by physiological system and inputs to the spinal neural circuits and brain [1]. It is currently believed that it is this continuous and repetitive sensory inflow that facilitates re-organisation of movement patterns, leading to functional improvement. We can conclude that the proposed treadmill walking training supported by the introduced technical systems is feasible treatment modality. Further clinical trials are warranted to further explore this promising approach.

Acknowledgements

The authors express their gratitude to the volunteer subject and acknowledge financial support of Agency for Research, Republic of Slovenia.

References

[1] EC. Field-Fote, Combined Use of Body Weight Support, Functional Electric Stimulation, and Treadmill Training to Improve Walking Ability in Individuals With Chronic Incomplete Spinal Cord Injury, *Arch. Phys. Med. Rehabil.*, vol. 82, 2001, 818-824.
[2] S. Hesse, M. Maležič, A. Schaffrin and KH Mauritz, Restoration of gait by combined treadmill training and multichannel electrical stimulation in non-ambulatory hemiparetic patients, *Scand. J. Rehabil.Med.*, vol. 27, 1995, pp 199-204.
[3] G. Colombo, M. Joerg, R. Schreier, V. Dietz, Treadmill training of paraplegic patients using a robotic orthosis, *J. Rehab. Res. Dev.*, vol. 37, 2000, pp 693-700.
[4] S. Hesse, Th. Sark die-Gyan, D. Uhlenbrock, Development of an Advanced Mechanised Gait Trainer, Controlling Movement of the Centre of Mass, for Restoring Gait in Non-ambulant Subjects, *Biomed. Technik*, vol. 44, 1999, pp 194-201.
[5] I. Cikajlo, Z. Matjačić and T. Bajd, Development of a gait re-education system in incomplete spinal cord injury, *J. Rehabil. Med.*, vol. 35, 2003, pp 213-216.
[6] I. Cikajlo, Z. Matjačić, T. Bajd and R. Futami, Sensory supported FES control in gait training of incomplete spinal cord injury persons, *Artif. Organs.*, vol. 29, 2005, pp 459-461.
[7] Z. Matjačić, Apparatus for dynamic balance training during treadmill walking , *J. Rehabil. Med.*, vol. 39, 2007, pp 91-94.

Author's Address

Dr. Imre Cikajlo
Institute for rehabilitation
Linhartova 51, SI-1000 Ljubljana
Slovenia
e-mail:imre.cikajlo@mail.ir-rs.si

CONTRASTING DESIGN ISSUES FOR UPPER AND LOWER LIMB NEUROPROSTHETIC SYSTEMS

Nathan R H

Mechanical Engineering Department, Ben Gurion University of the Negev, Beer Sheva, Israel

and

NESS Ltd., Raanana, Israel

Abstract

The NESS H200 (Handmaster) upper limb surface neuroprosthesis is today established in clinical practice in several countries. The design and development process has recently been completed of a lower limb surface neuroprosthesis for dropfoot correction in hemiplegia (the NESS L300), and it has been introduced to the market. Twelve years separated the development of the two devices. Although the two neuroprosthetic systems were developed on the basis of the same technological platform, the various parameters characterizing the design requirements resulted in two substantially differing system designs.

Introduction

Neuroprosthesis systems for restoring limb movement have been developed since the pioneering work of the 1960's. This has resulted over the last 10 years in a first generation of commercial systems which have reached clinical practice. Based on a platform technology comprising an orthosis with surface electrodes arrayed over the interior surface, two neuroprosthetic systems were developed (NESS H200 upper limb neuroprosthesis and the NESS L300 lower limb neuroprosthesis). Both systems are now in clinical practice in Israel, Europe and the USA.

The Platform Technology

Basic research on activating the human limb with FES covered aspects relating to microprocessor control of multichannel FES, and surface electrode design and placement [1-8], led to the development of the electrode-arrayed orthosis. The electrodes are confined to be moveable within a set region which allows adjustment during initial device set-up by the clinician for the individual patient. This adjustable electrode arrangement combined with other innovations such as the use of modular inserts in a standard size of orthosis allowed a mass-produced off-the-shelf device to be disseminated to a large patient population. Clinician and patient expertise required to deal with the system technology has been minimized, while system set-up time has been reduced to a few seconds.

The orthosis component has built-in flexibility and rigidity to meet the requirements of the body site activated.

This technology concept has been applied to prototype devices for five body limb segments. Two applications based on the technology have further been developed to commercial devices. It is the design of these two devices that are compared here.

The Design Process

The technology development process was initiated at Ben-Gurion University of the Negev by the author in 1975, carrying out research into multichannel computer-controlled surface FES.

In 1985 the research group transferred its activities to the Neurological Rehabilitation Centre at Tel Hashomer Hospital in Tel Aviv where the technology was directed towards applications for the upper limb. The first upper limb neuroprosthesis prototypes were developed in 1987 and beta-site tested in the homes of SCI subjects.

On founding the NESS company in 1991 development of the Handmaster was initiated and during the final 8 month period the author led a design development team comprising a plastics and manufacturing engineer, a rehabilitation physician, an industrial designer, and an electronic engineer, completing the design process in 1994.

During the technology transfer phase from 1994 to 2000 the NESS engineering team next carried out an engineering debugging process and developed the injection-molded industrial model of the Handmaster.

Commercial sales were initiated in Holland in 2000, and in the USA in 2006, where the device was renamed the NESS H200. A large size model was developed over a period and introduced to the market in 2006. Several prototype children's Handmasters have also been produced for ages down to 3 years old.

The Leg device was also developed in the initial stages by the author from 1998 to 2000 and the first alphasite prototype was batch produced and betasite tested at home by 50 adults and children.

The industrial model was designed by a team comprising staff from NESS and several participating companies, and this 14 month phase was completed in 2006.

Contrasting Design Issues

Orthosis Stability:

The lower limb orthosis was designed to hold the electrodes against the limb surface, applying an even and adequate pressure during conditions of changing body surface topography, and for stability during high dynamic inertia forces due to hip and knee rotations and polar rotations especially at heelstrike. The lower limb orthosis takes the form of a light cuff, having no requirements to stabilize the distal body joint.

In contrast the upper limb during use of the device is comparatively static. The orthosis mechanically stabilizes the wrist joint and is designed to support considerable stresses, whilst having the flexibility to hold the surface electrode array on to two limb segments during dynamic changes in limb topography. A spiral orthosis form was developed for the upper limb extending to the hand segment, electrodes activating muscles in both the forearm and intrinsics of the hand segment. The orthosis design allows unimpeded upper limb movement except for wrist flexion.

Donning/Doffing:

Surface orthoses require accurate but simple and fast means of positioning, carried out using one hand only (in hemiplegia). The upper and lower limbs presented totally different challenges to solving this problem, but location of the orthosis on to underlying bone features allowed the positioning of both devices within an accuracy of a few millimeters, important for activating correctly the target muscles.

Technology Evolution:

Available technologies strongly influenced the design. For example development of off-the-shelf RF transmitter/receiver chips during the twelve years separating the design processes of the two devices influenced the design, making low-cost off-the-shelf wireless communication between the system components a more attractive option than cable connection used in the earlier upper limb device.

This in turn affected the stimulator design. Wireless communication between the device components necessitated the stimulator being housed on the orthosis itself (fig. 1) controlled with a hand-held remote controller (inset), the stimulator in particular was miniaturized in mass and moment of inertia. This was not a requirement for the upper limb device. Here a large, clear, and simple control panel design was adopted for the stimulator unit (figure 2).

Electrode Technology:

Electrode technology was similar in the two devices, the improvement in the newer lower limb device resulted from eventually solving technological problems. The cloth pad dampened with tap water, used as the interface between the metal electrode and the skin in the earlier upper limb device was replaced by a hydrogel layer between the metal electrode and skin surface which was assessed during the 1980's but only successfully implemented after mechanical problems had been finally solved many years later in the design process for the leg device.

Figure 1:
The NESS L300
Dropfoot System
(Remote Control inset)

Figure 2: The NESS H200 Upper Limb System

Control Aspects:

The intended use of the device influenced the design of the control regime for the two systems. The upper limb neuroprosthesis restores grasp, hold and release of objects and was found to be best operated in open-loop, in contrast to the lower limb neuroprosthesis applied to gait modulation which required a sensor to synchronize device activation in closed-loop with the gait cycle.

Marketing the devices:

The upper limb device is perceived as a therapeutic device with functional capabilities while the dropfoot device is a functional device with therapeutic benefits. As such the use and benefits of the lower limb device are immediate, self-evident, and well-known and the technology transfer process straightforward.

The carry-over therapeutic improvements in the upper limb often take some weeks to become evident and are little known and sceptically accepted in the rehabilitation field. This becomes a marketing headache when most clinical centres and national healthcare bodies require to be convinced individually of the efficacy of the device. The technology transfer process has been time-consuming, expensive and difficult.

Conclusions

A wide variety of factors have influenced the design of the upper limb and lower limb neuroprosthetic systems, resulting in a number of similarities and differences between the two devices.

References

1. Nathan, R.H., *Electrical stimulation of the upper limb: charting the forearm surface*, Med & Biol Eng & Comp, 17, pp 729-736, 1979.
2. Nathan, R.H., *Functional electrical stimulation of the upper limb: the motor nerve prosthesis*, Artificial Organs, 5(A), pp 51, 1981.
3. Nathan, R.H., *Functional electrical stimulation: closed loop digital control of the isometric joint moment in multi-degree of freedom joint*, 3rd Mediterranean Conf on Med and Biol Eng, Portoroz, Yugoslavia, 1983.
4. Nathan, R.H., *The development of a computerized upper limb electrical stimulation system*, Orthopaedics, 7:7, pp 1170-1180, 1984.
5. Nathan, R.H., *FNS of the upper limb: targeting the forearm muscles for surface stimulation*, Med. & Biol. Eng.& Comp, 28:3, pp 249-256, 1990.
6. Nathan, R.H., *The isometric action of the muscle drives of the wrist joint,* ASME J of Biomech Eng, 114, pp 162-169, 1992.
7. Nathan, R.H., *Control strategies in FES systems for the upper extremities*, CRC Crit Rev in Biomed Eng, 21:6, pp 485-568, 1993.
8. Sagi, A., Prutchi, D., Nathan, R.H., *3-D current density distributions under surface stimulation electrodes*, Med & Biol Eng & Comp, 33, pp 403-408, 1995.
9. Triolo, R., Nathan, R., Handa, Y., Keith, M., Betz, R., Carroll, S., Herbison, G., Kantor, C., *Challenges to clinical deployment of upper extremity neuroprostheses*, J of Rehab Res & Dev, 33:2, pp 111-122, 1996.
10. Nathan, R.H., Weingarden, H., Katz, D., Dar, A., *The Handmaster NMS1: an upper limb external neuroprosthesis*, in The 8th World Congress of the International Rehabilitation Medicine Association (IRMA VIII), eds. Ueda, S., Nakamura, R. Ishigami, S.,Monduzzi Editore, pp 237-243, 1997.

Author's Address

Prof. Roger Nathan

Mechanical Engineering Department, Ben Gurion University of the Negev, POB 653 Beer Sheva 84105, Israel

email: roger@ness.co.il

Homepage:

http://eng2.bgu.ac.il/engineering/profile.aspx?id=eVMeueij

DESCRIPTION OF POSTURAL COORDINATION PATTERNS DURING FES-ASSISTED STANDING IN COMPLETE PARAPLEGIA

Azevedo-Coste C[1], Pages G[1], Maimoun L[2], Fattal C[2], Delignières D[3], Guiraud D[1]

[1] DEMAR LIRMM/INRIA, Montpellier, France

[2] PROPARA, Montpellier, France

[3] EDM UMI, Montpellier, France

Abstract

We investigate the postural organization of external FES-assisted sit to stand and standing in patients suffering from complete spinal cord lesion. The protocol was to stand in between parallel bars and to maintain postural balance by aligning head, pelvis and ankles with minimum arm support. In order to help patients to adopt the correct posture, visual feedback assistance was provided: a screen was set up in front of the patients where they could see their own profile. A video motion analysis system recorded the positions of reflective markers placed on relevant body points. Force sensors mounted to handles fixed on the parallel bars recorded arm support efforts. Insoles, fitted in the patient's shoes, recorded plantar pressure distribution. This study aimed at determining whether or not sensors placed on a walker could be sufficient to inform about patient posture and be used to trigger stimulation and observe fatigue evolution. The results are promising as they show that a large amount of knowledge concerning valid movements can be obtained through the proper analysis of arm support. Concerning fatigue of lower limbs, additional sensors are needed; pressures insoles could be used, which remains practically acceptable for a daily use of the system.

Introduction

Functional electrical stimulation (FES) is a mean to perform standing in complete paraplegic patients. Benefits of an active verticalization are both psychological and physiological. FES creates a split-body situation where the lower body is controlled externally, whereas the upper body remains under the voluntary influence of the central nervous system. Several issues remain to be solved before making **long term arm-free standing** achievable. We address two of these issues here: **fatigue** and **sit to stand transfer**. Muscle contractions induced by FES tend to result in rapid muscle fatigue, which greatly limits standing. Some solutions to reduce fatigue are now appearing but the problem of detecting and evaluating fatigue remains opened. The idea is to investigate the possibility of producing relevant feedback to FES controller using an instrumented walker associated to pressure insoles; the goal being to develop a safe, simple and practical system for the patients. We do not intend to propose a complex control law, based on accurate modelling of dynamics, but to propose solutions which can be directly implanted on our existing stimulation system (PROSTIM™). Classically, studies investigate the use of body mounted sensors in order to provide feedback to FES controllers [4]. They have the advantage of providing accurate information but are not very practical from a patient's view. The standing-up manoeuvre in paraplegia, considering the body supportive forces as a potential feedback source in functional electrical stimulation FES-assisted standing-up, has been previously studied [3]. Arm, feet, and seat reaction signals were used to reconstruct the centre-of-mass trajectory, the use of a sensory system incorporating a six-dimensional handle force sensor and an instrumented foot insole was recommended. We extended the use of this type of sensors to fatigue estimation. As suggested in [2] force sensors can give a feedback to the patients so that they should "feel" that their leg muscles are tiring and be able to voluntary modify his posture in order to indirectly relieve efforts on the fatigued muscle.

Material and Methods

Patient selection and training to FES

15 volunteer complete paraplegic patients (T5-T12) were selected to participate in our study. All the patients gave their informed consent prior to the experiment. The patients went through a muscle mapping session during which we first tested the compatibility with surface electrical stimulation. We investigated only muscles involved in standing: quadriceps vastus medialis, hamstring biceps femoris, gluteus maximus and tibialis anterior. But we had to be flexible on the target muscles: in some patients ankle flexion was not controllable and quadriceps vastus lateralis was stimulated instead. Concerning tibialis anterior, one group of patients received muscle stimulation

whereas the other received peroneal nerve stimulation. The muscles have been selected to allow knee and ankle locking. The second aspect of mapping session consisted in testing muscles separately in order to evaluate threshold current amplitudes: contraction initiation, diffusion to other muscles, joint locking and contracture onset. MRC (Medical Research Council) grades were also evaluated. Stimulation frequency and pulse width were respectively 25Hz and 300µs (this stands for all the study).

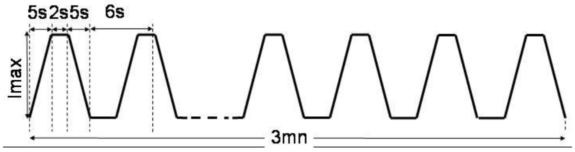

Fig. 1: Training session stimulation sequences.

5 patients could not be included in our protocol. 1 patient presented flaccidity, 1 patient had unpleasant sensation to stimulation, 1 patient had over-spasticity and the last 2 patients had non stimulable gluteus maximus. 10 patients were finally selected for the next phases of the study. Muscular reinforcement, to prepare muscles to verticalization, consisted in 4 training sessions. The session consisted, for each muscle, in 3mn stimulation sequence application followed by 3mn rest, 4 times. Stimulation sequences were composed of ramp-hold-ramp cycles as presented in (Fig. 1). The maximum current amplitude was increased over the sessions to improve joint locking. One patient decided to quit the protocol after one training session. The 9 remaining patients presented large inter-variability in terms of lesion level and injury occurrence.

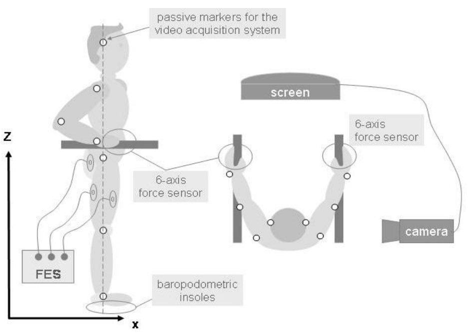

Fig. 2: Description of the experimental protocol.

FES-assisted verticalization protocol

Two sessions of five trials were performed: a first session to adjust the stimulation parameters and for the patient to get familiarized with the protocol, a second session where kinematics and dynamics information were recorded. The protocol was to stand in between parallel bars and maintain postural balance by **aligning head, hips and ankles** with **minimum arm support**. In order to help patients to adopt the correct posture, visual feedback assistance was provided: a screen was set up in front of the patients where they could see their own profile. A video motion analysis system recorded the positions of 16 passive markers. Six-degrees of freedom force sensors were mounted to handles fixed on the parallel bars in order to record upper limbs efforts. Insoles were fitted in the patient's shoes to record plantar pressure distribution (Fig. 2). 1 group of 4 patients received tibialis anterior (TA) stimulation whereas the others not. The goal was to evaluate the contribution of ankle locking during arm supported standing.

Results

We present in this section some typical recordings which sound relevant to better understand the FES-assisted verticalization issues. Patient #2 training did not succeeded in functional verticalization, only a few seconds of standing was possible. Patient #5 received additional training session as the first verticalization was not successful. Patients performed 5 to 6 tries-out (duration=45sec ±12). No relevant difference was found when comparing the group of patients who received TA stimulation (ankle lock) and the other one.

Body alignment

8 patients out of 9 were able to achieve a vertical trunk orientation. This was true despite the fact that in 3 patients legs were not straight. 1 patient was not able to keep his hips on the alignment of his ankles without help (this patient also presents some overweight).

Arm support vs. foot support

We measured the total efforts applied to the handles and the ground during sit-to-stand transfer and standing (Fig. 3). As expected in all the patients, transfer (phase ❶) is mainly ensured by arm support. During early standing (phase ❷) some patients (#1, #3, #6) managed to ensure the gravity compensation by supporting their weight mainly through ground reaction forces. When fatigue starts to take place (phase ❸) and when fatigue really occurs (phase ❹) the contribution of foot support decreases in favour of arm support. In some patients (#5) joint lock is not good enough and from phases ❷ to ❹ the support forces are constantly transferred between arms to feet. 4 patients never succeeded in supporting themselves mainly on their legs (#7, #8, #9), arm support being predominant. Patient #4 almost completely supported himself through his arms.

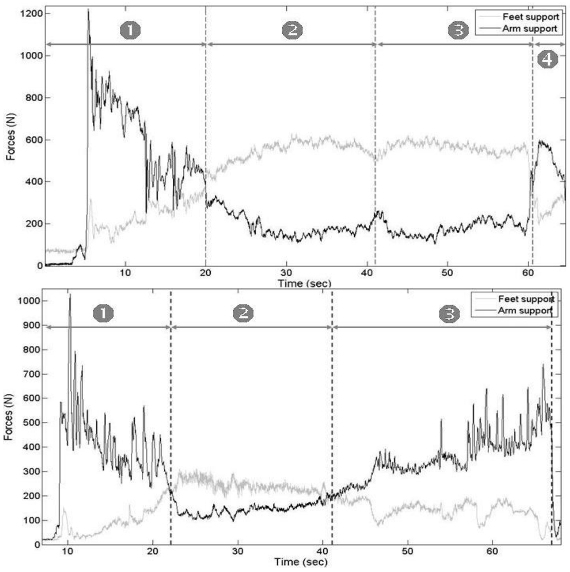

Fig. 3: Feet and arm support evolution. ❶ sit to stand phase, ❷ + ❸ standing, ❹ knee flexion. + **Top:** Patient #3, trial 6. **Bottom:** Patient #9, trial 3.

Fatigue

It is well known that one main issue with FES is the fatigue it induces. Indeed, patients could not maintain a long term upright position. The longest standing we managed was 73sec. Muscle fatigue implies that the torques initially generated by stimulation decrease if no update of parameters occurs. To counteract the effects of fatigue the patient's only solution is to increase arm support, if not, the "weak" leg flexes. We could observe visually that fatigue appears early after verticalization: it affects slightly the posture maintenance over the trial and the joint may suddenly unlock. Fatigue occurs earlier and is more important when the trials are repeated. In order to describe fatigue, we present the evolution of knee joint over time after sit to stand in Fig. 4.

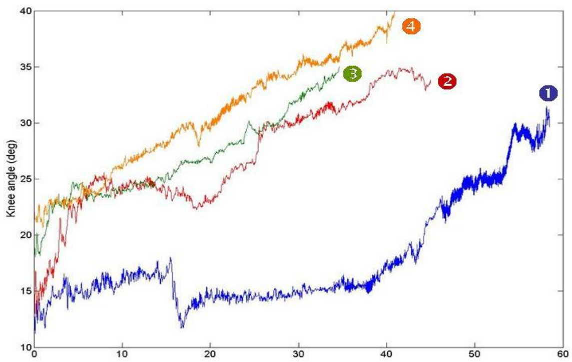

Fig. 4: Patient #1, Right knee flexion evolution over 4 trials (0° corresponds to legs stretched).

4 trials are illustrated. The angle increases (leg flexes) slowly along the trial. The leg is also less and less straight after the sit to stand transfer over the different trials. In this patient the slope of the angle variation remains the same (20° over 40sec).

In Fig. 5, we plotted the corresponding arm and foot support variations. The patient maintains a constant effort on the handles and an identical repartition between left and right sides, while the force repartition tends to become asymmetrical when the leg is fatigued.

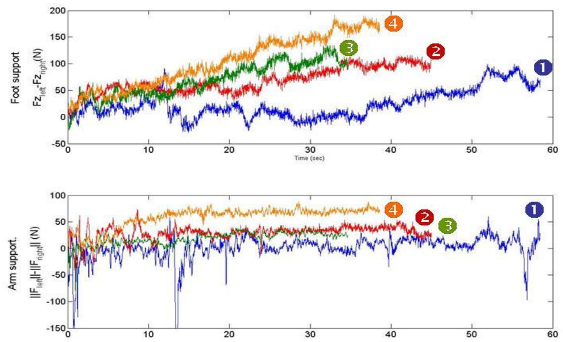

Fig. 5: Patient #1, Difference between recorded forces over 4 trials from left and right supports. Top: Foot support; bottom: arm support.

Sit to Stand

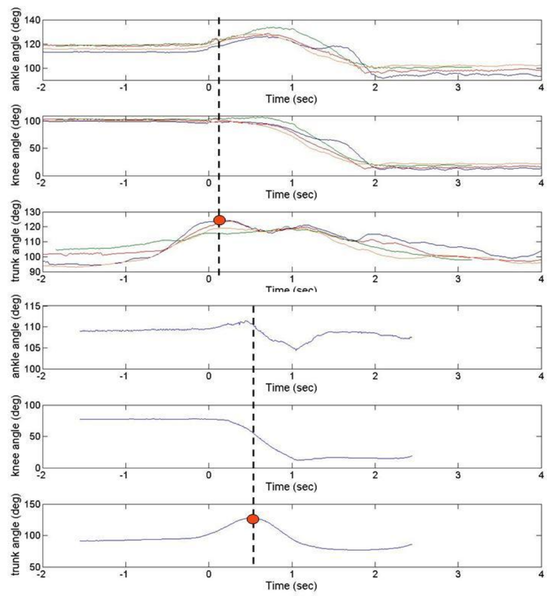

Fig. 6: Posture coordination during sit to stand. **Top:** Patient #1, over 4 trials, **Bottom:** valid subject. The red dot indicates the maximum trunk bending.

In Fig. 6, we plotted the evolution of trunk, knee and ankle angles during the sit to stand transfer. We give instruction to the patients to bend their trunk in preparation to the chair rising. A first important observation is the low intra-variability between trials of one given patient. On the contrary, inter-variability between patients is important. A main difference between valid subjects and patients is the onset of leg movement in regards to trunk bending (fig. 6). To be efficient, trunk bending forward should start before and last during knee and ankle movement. This was never the case in our trials on FES-assisted standing.

Discussion

One main issue when working with paraplegic patients is the important differences which exist between patients such as lesion level, time since lesion occurred, presence of spasticity and available range of joint motion. These elements have an impact on the stimulation levels needed to contract muscles and therefore on muscle fatigue.

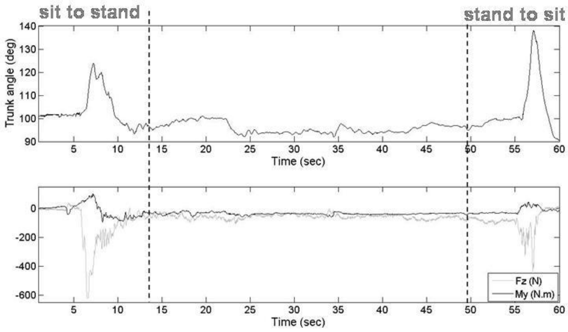

Fig. 7: Correspondence between trunk angle and handle information. Patient #1, Trial 1. **Top:** angle, **Bottom:** right side vertical force and momentum around hip axis.

This inter-variability implies that training should be adapted individually. In our study all the patients received the same set of training sessions regardless their initial capacities (except patient #5 who received additional training). Performance should be carefully evaluated from the beginning and followed up till they are satisfactory to allow verticalization. Joint locking should be sufficiently efficient for reasonable stimulation levels. The stimulation levels used during muscle reinforcement should: 1) be as low as possible to reduce fatigue during verticalization and 2) leave a margin to increase levels for, and during, standing in order to cope with fatigue. A critical problem is that patients can not feel fatigue before it affects importantly their posture and thus does not ensure gravity compensation by arm support (Fig. 5). Observing knee and ankle angles show a continuous evolution before unlock occurs. This evolution is also observable from insoles measurement where the force repartitions evolves towards asymmetrical efforts when one leg becomes weaker (Fig. 5). Adapting stimulation parameters along asymmetry increase may lead to longer standing. Security margins on this asymmetry may also prevent risks of unexpected sudden unlock.

Sit to stand in valid persons implies a complex coordination between upper and lower limbs. Minimizing arm support help is possible only if trunk inertia is used [1]. This implies a good triggering of muscle contraction regarding limb movements. Trunk behaviour can be indirectly observed by analyzing efforts applied by arm support (Fig. 7) [5]. Indeed, normal force decreases (pulling) while momentum around transversal axis increases. A proper threshold detection based on these signals could be used to initiate the leg stimulation and improve greatly the sit to stand. The same may be used for stand to sit as shown in Fig. 7. Anticipated postural adjustments should also be artificially created in order to prepare the actual standing, instead of switching from no stimulation to maximum levels of current.

References

[1] Héliot, R., Azevedo C., Espiau B., David D. Early detection of postural modifications and motion monitoring using micro attitude sensors Adaptive Motion in Animals and Machines AMAM Conference, Ilmenau, Germany, 2005.

[2] Donaldson Nde N., Yu CH. FES standing: control by handle reactions of leg muscle stimulation (CHRELMS). IEEE Trans Rehabil Eng. 1996 Dec;4(4):280-4, 1996.

[3] Kamnik R., Si J.Q., Murray-Smith R., Bajd T. Nonlinear modeling of FES-supported standing-up in paraplegia for selection of feedback sensors. IEEE Trans Neural Syst Rehabil Eng. 13(1):40-52, 2005.

[4] Williamson R, Andrews BJ. Sensor systems for lower limb functional electrical stimulation (FES) control. Med Eng Phys. June; 22(5):313-25, 2000.

[5] Pages G., Ramdani N., Fraisse P., Guiraud D. Upper body posture estimation for standing function restoration. IEEE Int. Conf. on Robotics and Automation, Roma, Italy, 2007.

Acknowledgements

The authors would like to specially thank all the patients for giving so much of their time, making this study possible.

Author's Address

Christine Azevedo-Coste, PhD.
DEMAR LIRMM/INRIA, Montpellier, France
Christine.Azevedo@lirmm.fr

Gaël Pages, PhD.
DEMAR LIRMM/INRIA, Montpellier, France

Laurent Maïmoun
PROPARA, Montpellier, France

Charles Fattal, MD PhD.
PROPARA, Montpellier, France

Didier Delignières, PhD.
EDM UMI, Montpellier, France

David Guiraud, PhD.
DEMAR LIRMM/INRIA, Montpellier, France

Session VII

Modeling, Simulation, Virtual Reality

Chairpersons
Tadej Bajd (Ljubljana, Slovenia)
Martin Reichel (Vienna, Austria)

LOWER EXTREMITIES TRAINING BY THE USE OF VIRTUAL ENVIRONMENT AND FUNCTIONAL ELECTRICAL STIMULATION

T. Koritnik[1], T. Bajd[1], P. Obreza[2], Z. Matjačić[2], M. Munih[1]

[1] University of Ljubljana, Faculty of Electrical Engineering, Ljubljana, Slovenia

[2] Institute for Rehabilitation, Republic of Slovenia, Ljubljana, Slovenia

Abstract

We designed a virtual mirror – a large screen which shows a human figure in virtual environment, displaying the patient's lower extremity movements in real time. Another figure – a virtual instructor, also included in the display, shows the reference movements to be tracked by the patient as accurately as possible. This approach includes patient's visual feedback interactively in the training process. The system was first evaluated in a group of healthy persons. Afterwards, we investigated training abilities of an incomplete tetraplegic patient, undergoing a rehabilitation process, two years after an accident. He was instructed to track the virtual instructor's stepping-in-place movements as performed by a healthy person. In the second part of the investigation, functional electrical stimulation triggering flexion reflex in the less able of the lower extremities was included. The virtual mirror provided a tight temporal coordination between the patient and the experienced therapist who triggered the stimulation, delivering better results of the patient's reference tracking performance, compared to non-stimulated execution of the same task.

Introduction

In our recent studies [1] we have proposed a neurorehabilitation system for reeducation of walking, consisting of three subsystems: actuation, sensory, and cognitive feedback. The actuation system was represented by surface functional electrical stimulation (FES) of knee extensors during the stance phase of walking and triggering of a flexion response by peroneal stimulation during the swing phase of walking. The aim of our first neurorehabilitation system was to provide reliable foot contact and to reduce the duration of the double stance phase in completely paralyzed paraplegic persons. The sensory system consisted from hand pushbuttons, knee goniometers, and foot-switches. Cognitive feedback was represented by sensory electrical stimulation signal delivered to the patient's upper arms. The sensory signal was considered as a "reward" for the patient, indicating successful transition from swing into stance phase of walking.

Better success of FES gait reeducation was expected in incomplete spinal cord injured (SCI) patients when training early after the accident. The aim of our second neurorehabilitation system was to achieve efficient swing phase of walking [2]. A multisensory system was developed consisting of four accelerometers and a gyroscope attached to the shank and estimating the quality of the swing phase by comparing the signals from a more affected extremity to those assessed in less paralyzed limb. Cognitive system was represented by an audio signal of high frequency when there was poor correlation of right and left leg signals and low frequency during satisfactory swinging of the leg.

In this paper we are presenting the third version of a neurorehabilitation system which is based on visual feedback information. Patient is training stepping-in-place (SIP) movements in front of a virtual mirror where he can see his own lower leg movements superimposed on the movements of a virtual instructor (fig. 1).

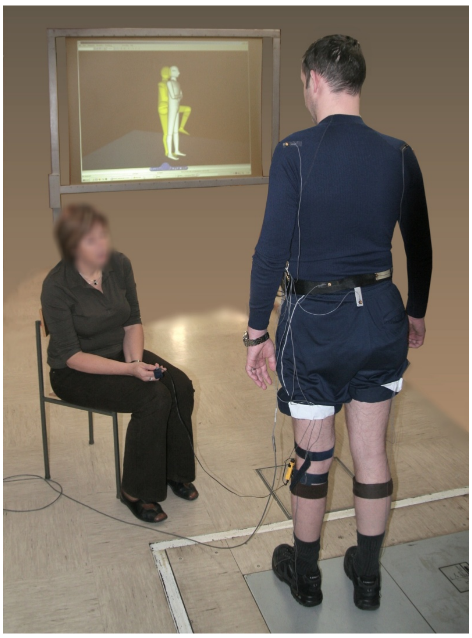

Fig. 1: Virtual mirror

OPTOTRAK system with 11 active markers was used as the sensory subsystem. Stepping-in-place movements were enhanced by using peroneal electrical stimulation.

Methods

Virtual Mirror

A kinematic model of the human body was developed in order to visualize the human motion in the virtual environment [3]. The complexity of the model was adjusted to the predominant movement of lower extremities resulting in an overall of 19 degrees of freedom, whereas segment ratios were adopted from statistical anthropometry [4]. We used OPTOTRAK system for movement assessment. 11 active markers were placed on the ankle joints, knees, pelvic area, and shoulders in order to obtain position and angular data.

These kinematic data were used to animate the motion of the human figure in the virtual environment. The movements of the figure corresponded to the movements of the subject at a 35-Hz refresh rate without detectable lag, thereby enabling a convincing perception of the virtual mirror. We used VRML 2.0 (Virtual Reality Modeling Language) to visualize the movements of the figure. The position of the body was represented by the position coordinates of the pelvic center. It was expressed as a percentage of the subject's body height in order to allow comparisons among subjects and enabling the use of the same virtual figure for all subjects.

Prior to the SIP training, a calibration of the virtual figure was performed. This was done by instructing the subject, with markers in place, to remain still for 3 s in a quiet stance, with the knees fully extended and the feet oriented in parallel.

During the SIP training, the subject would see the figure of a virtual instructor besides his own in the virtual mirror. The additional figure was semi-transparent and a different color. Both figures were superimposed onto each other (fig. 2). The motion of the virtual instructor had been preprogrammed with stepping movements, and presented a reference that the subject was instructed to follow. Ideally, both figures should have been perfectly aligned at all times, thereby indicating that the subject was performing the SIP in unison with the virtual instructor.

The semi-transparency allowed the subject's figure to be seen even when it was behind the virtual instructor. In order to provide the subject with the desired view of his performance, it was possible to set the viewing angle and distance of the virtual camera arbitrarily. It was also possible to switch the image in the virtual mirror between the real and mirror views.

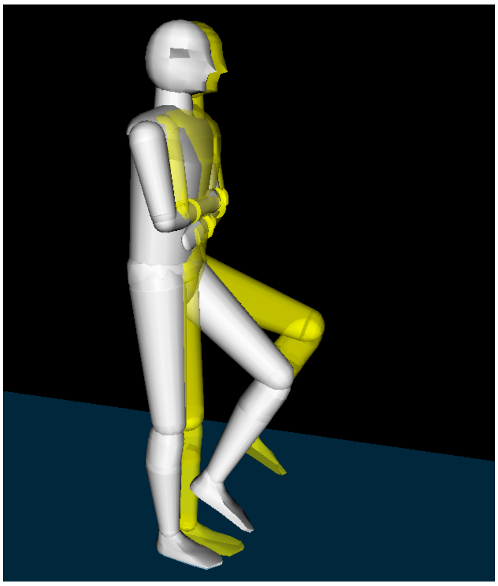

Fig. 2: Subject's figure and virtual instructor.

Stepping-in-place task

We chose SIP for training of the lower-extremities movements. The movements of the virtual instructor were obtained by capturing the steps of a healthy male subject (aged 25 years), who was well familiarized with the virtual mirror. In our previous study [3] we established the level of adaptation during SIP performance among the healthy male population. In the present experiment we have included an incomplete tetraplegic patient (spinal cord injury level C5, two years after an accident). He was instructed to follow the stepping movements of the virtual instructor at the cadence 60 beats per minute (BPM) and hip angle 90°. These values were in accordance with the previous study to enable comparison between the patient and healthy subjects.

In the second part, an FES stimulator triggering the flexion reflex of the left (less able) extremity was added. Trigger signal to the stimulator device was administered manually by an experienced therapist at the moment of each step initiation. The amplitude of electrical stimuli was adjusted by the therapist as well. Both patient and therapist were observing the patient's figure and the virtual instructor in the virtual mirror and were therefore provided with the same reference of the desired and actually achieved movements.

Results

The patient's performance was evaluated in comparison with healthy population's results [3]. We observed kinematic adaptation (hip angles) and temporal adaptation (swing durations). Fig. 3 shows the patient's hip goniograms (solid line) with the reference to be tracked (dashed line). The subject was able to catch up with the virtual instructor in the second step which did not differ significantly from the healthy subjects' average. However, it can be observed that angle peaks of the left leg did not reach the reference values and were significantly lower than in healthy subjects ($p < 0.005$). Right extremity performed better and no significant difference compared to healthy population was observed.

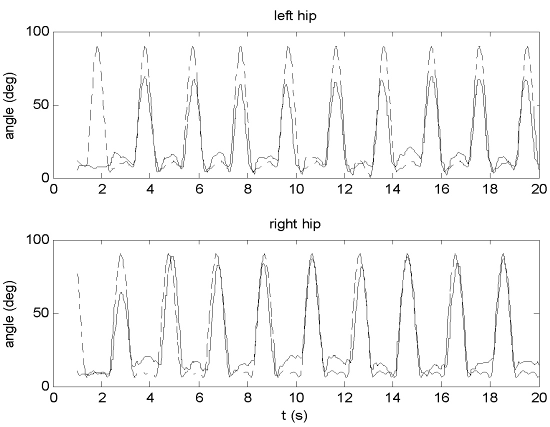

Fig. 3: Left and right hip goniograms.

Fig. 4 shows hip goniograms of the same task with added FES in the left extremity. Peak values of the left hip improved significantly from the first run ($p < 0.005$) but were still worse than healthy subjects' performance ($p < 0.005$). The improvement suggests that the same visual reference for both patient and therapist was beneficial in terms of providing a precise temporal coordination between the patient's voluntary control and the therapist's FES signal timing. Swing durations during both repetitions of the stepping task showed no significant difference from healthy subjects, indicating that the patient was able to track the cadence of the task without any substantial difficulties.

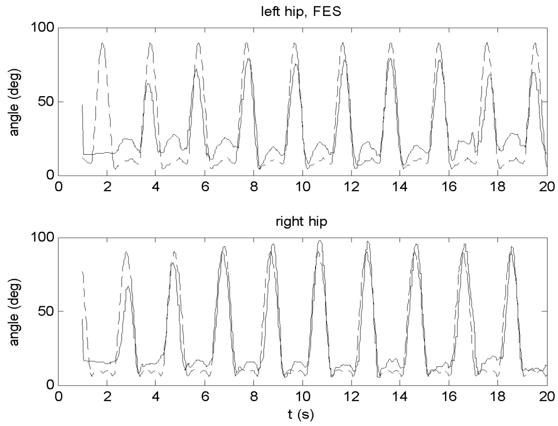

Fig. 4: Left and right hip goniograms with FES.

Discussion

In our preliminary studies virtual mirror was used in conjunction with a simple SIP test. The adaptation to the virtual instructor was predominantly evaluated in a group of healthy persons [3]. In our further studies it is our aim to expand the approach to body weight supported treadmill training of walking. Here, the stepping of the severely paralyzed incomplete SCI patients can be enhanced by either manual or robotic assistance or usage of FES. Similar outcomes across the three training approaches were obtained in a preliminary comparative study [5]. Detailed statistical analyses suggested even a trend for greater improvement in the patients that were trained with FES. With the use of FES, a step can be triggered either by afferent eliciting of flexion response or by efferent FES of several flexor muscle groups. Afferent stimulation input may be associated with the central pattern generator for locomotion and can thus provoke beneficial neural changes [6]. From the other point of view, the flexor reflex is highly variable and subject to rapid habituation. In this respect direct muscle stimulation can have greater rehabilitative potential than the stimulation of reflexes [7].

Surface FES in incompletely paralyzed SCI patients is predominantly used for therapeutic purposes. In therapeutic applications, the goal is to produce a functional benefit that lasts beyond the application of the stimulation itself. The question is arising, how FES can produce a "carry over" effect in incomplete SCI patients. Rushton [8] is proposing a hypothetical answer that FES combined with coincident voluntary effort could help to promote restorative synaptic modifications at segmental level. Patient's voluntary effort is efficiently increased while introducing the virtual mirror into the FES neurehabilitation gait reeducation system.

References

[1] Bajd T. Neurorehabilitation of standing and walking after spinal cord injury. In: Rosh PJ (ed.), Markov, MS (ed.). Bioelectromagnetic medicine. Marcel Dekker, 439-459, 2004.

[2] Cikajlo I, Matjačić Z, Bajd T. CNS reorganization during sensory supported treadmill training, In: Akay M (ed.) Handbook of Neural Engineering. Wiley - Interscience, 509-518, 2007.

[3] Koritnik T, Bajd T, Munih M. Stepping in place training in front of a virtual mirror. Gait & Posture, accepted for publication.

[4] De Leva P. Adjustments to Zatsiorsky-Seluyanov's segment inertia parameters. J. Biomech., 29: 1223-1230, 1995.

[5] Field-Fote EC, Lindley SD, Sherman AL. Locomotor training approaches for individuals with spinal cord injury: A preliminary report of walking-related outcomes, J. Neurophysiol., 29: 127-137, 2005.

[6] Postans NJ, Hasler JP, Granat MH, Maxwell DJ. Functional electrical stimulation to augment partial weight-bearing supported treadmill training for patients with acute incomplete spinal cord injury: A pilot study, Arch. Phys. Med. Rehabil., 85: 604-610, 2004.

[7] Thrasher TA, Flett HM, Popovic MR, Gait training regimen for incomplete spinal cord injury using functional electrical stimulation, Spinal cord, 44: 357-361, 2006.

[8] Rushton DN. Functional electrical stimulation and rehabilitation-an hypothesis. Medical Engineering & Physics, 25: 75-78, 2003.

Acknowledgements

The authors acknowledge the financial support from the state budget by the Slovenian Research Agency (program No. P2-0228).

Author's Address

Tomaž Koritnik
University of Ljubljana, Faculty of Electrical Engineering
tomazk@robo.fe.uni-lj.si
http://robo.fe.uni-lj.si

A MODEL FOR TRANSCUTANEOUS ELECTRICAL STIMULATION USING ACTIVATION VOLUMES TO DESCRIBE THE INFLUENCE OF THE ELECTRODE PLACEMENT AND SIZE

Kuhn A[1,3], Keller T[1,2,3]

[1] Automatic Control Laboratory, ETH Zurich, Switzerland

[2] University Hospital Balgrist, Zurich, Switzerland

[3] Sensory-Motor Systems Laboratory, ETH Zurich, Switzerland

Abstract

Transcutaneous electrical stimulation (TES) enables functional movements of human limbs by applying electrically generated pulses to pairs of electrodes placed on the skin surface. New TES technology uses multi-channel configurable electrodes that can dynamically distribute the stimulation current across the skin surface. Such systems require a quantitative understanding of the spatial and temporal activations of underlying neural structures. We have developed a versatile TES simulation framework that calculates nerve activation using a transient finite element model combined with a nerve model. Activation volumes (AVs) are used to describe regions where nerves are activated. Post processing using computer graphics methods enables the comparison of AVs produced for different model parameters.

In this paper the TES simulation framework was used to investigate the influence of electrode size and position on spatial nerve activation. Isometric force measurements were performed on three human volunteers to validate the findings.

Using AVs we determined the relationship between electrode size and activation depth for constant current densities. We found that for smaller electrodes the current density has to be increased to keep nerves at a particular depth stimulated. This is particularly important for new multi-channel configurable electrodes which use small sized electrodes (~ 1cm^2). Further, the simulations and experiments confirmed that the placement of the anode has a minor influence on nerve activation (less than 2mm spatial change of AVs and less than 15% in experiments) if the anodes and cathodes are more than 0.5 cm apart.

Introduction

Transcutaneous electrical stimulation (TES) can be used to enable functional movements of human limbs. In TES, surface electrodes are used to apply electrical current pulses to the human body in order to stimulate motor nerves. New multi-channel configurable electrodes that can dynamically change the size and position of virtual electrodes across the skin surface were developed [1]. In order to better understand and quantify the effect of changing electrode sizes and positions new modeling methods are required. Current TES models [2, 3] lack a description and quantification of spatial activation changes. We use activation volumes (AVs) to describe the volume enclosing all locations where nerves are possibly activated. AVs enable a quantitative analysis of the influence of model parameters (e.g. electrode size, fat thicknesses, bulk resistances …) on spatial nerve activation. A similar approach was used to represent neural activation in deep brain stimulation [4]. The rotational symmetry of needle electrodes was utilized to calculate the volume of tissue activated from a 2D activation distribution. Because no symmetries are readily available for arbitrary electrode configurations we calculate the AVs directly from the 3D activation distribution. In this paper we used AVs to investigate whether certain electrode sizes require a lower current to stimulate nerves at a specific depth. We were interested in finding appropriate electrode sizes for stimulating certain regions on the human body. The influence of the anode position on activation underneath the cathode was also investigated to find out how close the cathode and anode can be on multi-channel configurable electrodes.

Methods

Simulation Tool for TES (ArmSimP):

The simulation framework used to model TES consists of three elements: A finite element (FE) model describing the potential distribution within the bulk tissues, a nerve model describing the activation distribution depending on the potential distribution, and a postprocessing module that calculates quantitative values from the activation distribution. We developed a software environment that combines the three elements (volume conductor, nerve model, postprocessing) into one tool (ArmSimP). ArmSimP provides a GUI to configure and store the model parameters, it sends batch jobs to different simulation environments (FE, nerve model) and it can be used to perform the postprocessing (see Fig. 1).

ArmSimP was developed in C++ with Qt libraries (Trolltech Inc.). The current version interfaces to Ansys (EMAG, Ansys Inc., Canonsburg, PA), Neuron [5], Matlab (The Mathworks Inc., Natick, MA), and Paraview (Kitware Inc., NY). Ansys is a FE modeling software that is used to calculate the transient 3D potential distribution in the bulk tissues based on the resistivities and permittivities. In Neuron and Matlab different nerve models (single axon models and nerve bundles) were implemented to describe nerve activation based on the 3D potential distribution. Paraview is an open-source visualization application based on VTK (Kitware Inc., NY) that added the functionality to create AVs and to calculate quantitative measures from the simulation results.

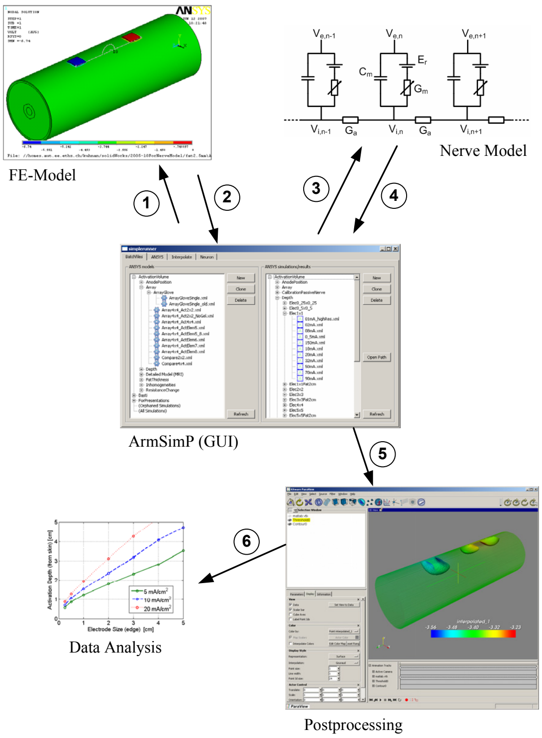

Fig. 1: Standard procedure for TES modeling. 1. Send parameters to FE software, 2. Receive computed potential distribution, 3. Send potential distribution to nerve model, 4. Receive activation distribution, 5. Perform postprocessing on activation distribution, 6. Analyze Data

TES Model

The TES model consisted of a volume conductor representing the human forearm, and a passive nerve model describing the time dependent evolution of the nerves' transmembrane potential (TP). The volume conductor comprised of electrodes, the electrode-skin interface, skin, fat, muscle, cortical bone, and bone marrow in a multiple layer cylindrical setup (see Fig. 2). The potential distribution was calculated by Ansys using the given electrode configuration and the applied current (different pulse amplitudes with 0.2msec pulse duration).

Passive axon models (derived from MRG-model [6] by replacing non-linear resistance with a linear resistance, diameter 11µm) were placed within the volume representing the muscle and oriented in the axial direction of the cylinder (see Fig. 2). Passive nerve models can be used to detect nerve activation by determining when the TP exceeds a threshold Th_P [7]. The passive nerve model was used as it provides spatial information about activation, whereas active models only show "activation" or "no activation" for each axon. Hence, at every node of the nerve model the value of the TP at the end of the applied pulse was stored yielding the 3D activation distribution, from which the AV was calculated.

Activation Volume (AV)

The goal of AVs is to describe quantitatively the locations where axons experience activation. We used the activation threshold Th_P to build an iso-surface in the 3D activation distribution with the marching cubes algorithm [8] in Paraview. This surface separates activated locations from locations that are not activated. The volume that contains the activated nodes is denoted AV. Axons which pass through the AV generate action potentials and those that fully lie outside the AV are not activated.

AVs obtained from simulations with different model parameters (e.g. electrode configuration, fat thickness, …) have different sizes, shapes, and positions. Computer graphics methods were used in order to quantify these spatial changes of activation. We propose two measures: The mean distance (MD) and the activation depth (AD). For every point on the surface representing volume 1, the shortest distance to the surface representing volume 2 was calculated; the average defines MD. The AD is defined as the distance from the center of the stimulation electrode to the deepest point on the AV.

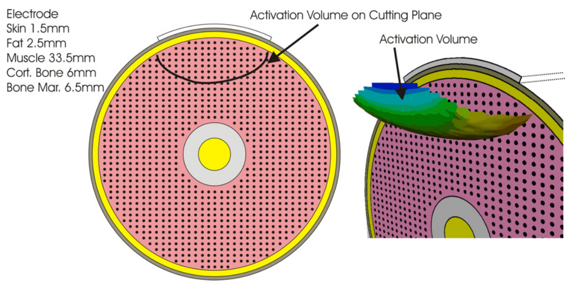

Fig. 2: Cylindrical arm model. Each point in the muscle represents a line on which the electrical potential was interpolated. The interpolated potentials were the input

to the nerve models which calculate the activation distribution, from which the AVs were calculated.

Electrode Size and Anode-Position of Simulations and Experimental Measurements

ArmSimP was used to calculate the AD for different square electrode sizes and fat thicknesses with an applied fixed current density. Further, the threshold stimulation current densities required to activate a 11µm axon at 1cm and 2cm depth were determined. The threshold current densities were compared for different electrode sizes and fat thicknesses in order to find out if certain electrode sizes use less current density to stimulate an axon at a certain depth.

Both the cathode and the anode can be arbitrarily placed on a multi-channel electrode, and we investigated if certain configurations are beneficial to TES. Cathode to anode distances (0.5, 1, 2, 4, and 6cm) and rotations (0, 45, 90, and 180°) of the anode around the arm model were investigated for two electrode sizes (1 and 5cm edge length) and two fat thicknesses (0.25 and 1cm).

Isometric force measurements were recorded in four subjects with the Dynamic Grasp Assessment System (DGAS) [9]. The cathode was placed on the arm over the finger flexor of finger 4 (ring) and the anode was placed distally at the same distances and rotations that were investigated in the simulations. The forces of finger 4 were measured for the different electrode configurations.

Results

The AD versus electrode size for fixed current densities of 5, 10 and 20mA/cm^2 is shown in Fig. 3. The AD increased approximately linearly for larger electrode sizes.

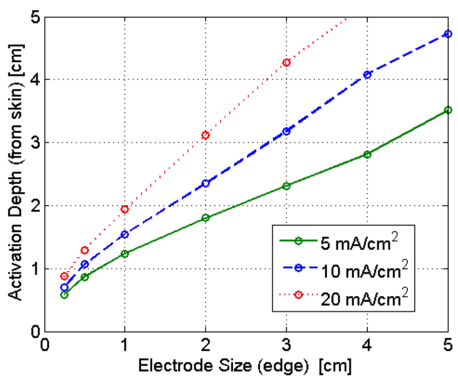

Fig. 3: AD vs. electrode size for constant current densities (fat thickness 0.25cm).

The slope was larger for higher current densities; an increase of the electrode size from 1 to 2cm, increased AD by 0.6cm for 5mA/cm^2, whereas at the higher current density (20mA/cm^2) AD was increased by 1.2cm. Further, larger electrodes increased the range of ADs, which were reached with the tested current densities. For example with a 3cm electrode, ADs between 2.3 and 4.3cm were reached for the tested current densities, whereas for a 1cm electrode a smaller range between 1.2 and 1.9cm was reached for the tested current densities.

Fig. 4 and 5 show the threshold current densities that were required to stimulate an axon at a certain depth. For smaller electrodes and bigger fat thicknesses, exponentially higher current densities were necessary to stimulate an axon at a certain depth. Furthermore, the curves for different fat thicknesses in Fig. 5 were closer together compared with Fig. 4 indicating that for the stimulation of deep nerves the influence from bigger fat thicknesses was smaller.

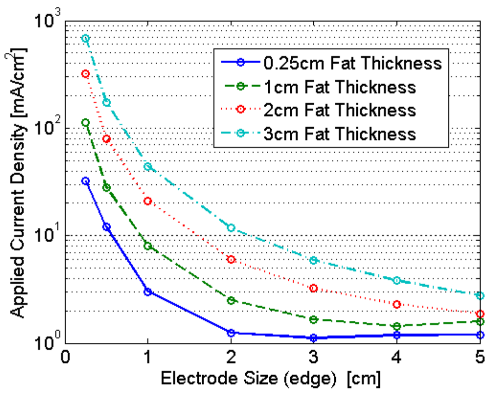

Fig. 4: Current density required to stimulate 11µm axon in 1cm depth (AD).

The influence of the anode position on nerve activation underneath the cathode was investigated with different AVs. For the tested cathode to anode distances the MD between AVs was always below 2mm. For the tested rotations the MD was always below 1mm. In general the influence was bigger for smaller anode-cathode distances and for bigger fat layers.

Isometric force measurements were performed on three human volunteers for different anode positions. The influence on the force of finger 4 in all configurations was below 15%.

Discussion and Conclusion

A simulation tool for TES (ArmSimP) was developed that describes the spatial nerve activation with AVs depending on the applied stimulation pulse and various model parameters. The influence of the electrode size and the anode position on spatial nerve activation was investigated.

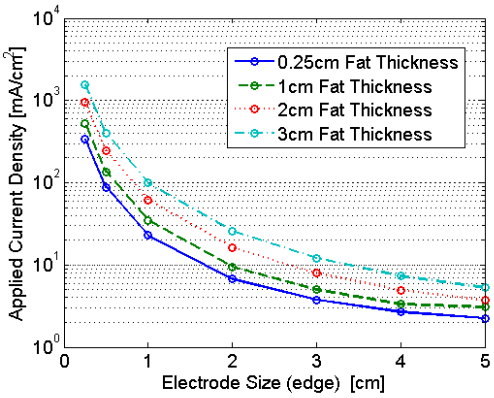

Fig. 5: Current density required to stimulate 11µm axon in 2cm depth (AD).

The results showed that the AD increased for bigger electrodes when the current density was fixed, and this increase was larger for higher current densities (Fig. 3). As a consequence larger electrodes allow stimulation of deeper nerves with lower current densities. However, when using larger electrodes adjacent muscles can be co-activated due to the decreased selectivity larger electrodes have. This suggests that depending on the stimulated nerve depth the size of the electrode should be adapted in order to achieve an optimal trade off between a low current density (big electrode) and a good selectivity (small electrode).

In Fig. 4 it can be seen that when bigger fat layers are present, higher current densities are needed in order to activate nerves at the same depth. However, in real applications the current density is restricted to certain tolerable levels. Therefore, the fat thickness can limit the use of small electrodes because high current densities would increase pain.

Both the simulation results and the results from the experimental measurements showed a small influence of the anode position on nerve activation underneath the cathode. This indicates that the positioning of the anode in real applications is not crucial for anode-cathode distances above 0.5cm.

In conclusion, we present a simulation tool that enables us to describe the locations where nerves are activated using AVs. Quantitative measures (MD, AD) on AVs enable us the analysis of the influence of model parameters on spatial nerve activation. This allows to better understand and to optimize certain aspects of TES. We showed that the same current density on differently sized electrodes does not activate nerves at the same depth and that the positioning of the anode in TES is not critical. Quantitative measures for selectivity and stimulation comfort based on the AV will help to balance between selective stimulation with small electrodes and more stimulation comfort, using larger electrodes.

References

[1] T. Keller, M. Lawrence, A. Kuhn, and M. Morari, "New multi-channel transcutaneous electrical stimulation technology for rehabilitation," presented at Annual International Conference of the IEEE Engineering in Medicine and Biology Society (IEEE Cat. No. 06CH37748), 2006.

[2] A. Kuhn and T. Keller, "The influence of capacitive properties on nerve activation in transcutaneous electrical stimulation," presented at International Symposium on Computer Methods in Biomechanics and Biomedical Engineering, Antibes, France, 2006.

[3] M. Reichel, J. Martinek, W. Mayr, and F. Rattay, "Functional Electrical Stimulation of Denervated Skeletal Muscle Fibers in 3D Human Thigh - Modeling and Simulation," presented at Proc. of 8th Vienna International Workshop on Functional Electrical Stimulation, 2004.

[4] C. R. Butson and C. C. McIntyre, "Role of electrode design on the volume of tissue activated during deep brain stimulation," J Neural Eng, vol. 3, pp. 1-8, 2006.

[5] www.neuron.yale.edu, "NEURON."

[6] C. C. McIntyre, A. G. Richardson, and W. M. Grill, "Modeling the excitability of mammalian nerve fibers: influence of afterpotentials on the recovery cycle," J Neurophysiol, vol. 87, pp. 995-1006, 2002.

[7] E. N. Warman, W. M. Grill, and D. Durand, "Modeling the effects of electric fields on nerve fibers: determination of excitation thresholds," IEEE Trans Biomed Eng, vol. 39, pp. 1244-54, 1992.

[8] W. E. Lorensen and H. E. Cline, "Marching Cubes: A High Resolution 3D Surface Construction Algorithm," presented at International Conference on Computer Graphics and Interactive Techniques, 1987.

[9] T. Keller, M. R. Popovic, M. Amman, C. Andereggen, and C. Dumont, "A System for Measuring Finger Forces During Grasping," presented at International Functional Electrical Stimulation Society Conference, Aalborg, Denmark, 2000.

Acknowledgements

This work was supported by the Swiss National Science Foundation (SNF) No. 205321-107904/1. We would like to thank Marcel Baschnagel for his contribution to the development of ArmSimP and Eva Wentink for conducting the experimental measurements.

Author's Address

Andreas Kuhn
ETH Zurich, Automatic Control Laboratory
Physikstrasse 3, CH-8092 Zurich
kuhnan@control.ee.ethz.ch
http://control.ee.ethz.ch/~fes/

A FE MODEL TO IDENTIFY ELECTRODE INFLUENCE ON CURRENT DISTRIBUTION IN THE SKIN

Sha N [1], Kenney LPJ [1], Heller BH [2], Barker AT [3] Howard D [1], Moatamedi, M [4]

1. CRHPR, University of Salford, Salford, UK
2. Centre for Sport and Exercise Science, Sheffield Hallam University, Sheffield, UK
3. Dept of Medical Physics, Royal Hallamshire Hospital, Sheffield, UK
4. Institute for Materials Research, University of Salford, Salford, UK

Abstract

Discomfort experienced during surface functional electrical stimulation (FES) is thought to be partly a result of localised high current density in the skin underneath the stimulating electrode. This paper describes a finite element (FE) model to predict skin current density distribution in the region of the electrode during stimulation and its application to the identification of electrode properties that may act to reduce sensation. The FE model results showed that the peak current density was located in an area immediately under the stratum corneum (SC), adjacent to a sweat duct. Simulation of stimulating with a high resistivity electrode resulted in a reduction in the peak current density, when compared with that predicted with a low resistivity electrode.

Introduction

Functional electrical stimulation (FES) via surface-located electrodes can be used to partially restore motor function lost as a result of, for example, a stroke, spinal cord injury, or cerebral palsy [1, 2]. However, FES is still used by relatively small numbers in niche application areas. One aspect contributing to the low uptake is the discomfort experienced when current is passed through the skin [2]. Approaches to reduce the discomfort have been widely examined, including stimulus waveform and pulse width [3, 4]. However, relatively little work has been carried out on the effects of electrode properties on sensation and this paper examines this area in detail.

The stimulation targets of surface FES are motor neurons. However, sensory receptors located in the skin lie between the electrodes and motor neurons and also respond to stimulation, leading to sensation and often discomfort. The skin is covered by the highly resistive stratum corneum (SC) on the top of the epidermis and traversed by skin appendages such as hair follicles and sweat glands. It is believed that stimulus current will tend to flow through the skin via the low resistive skin appendages, acting as “current pores”, possibly creating areas of high current density in their vicinity [5]. However, there has been little previous research to examine this effect in detail, or how the electrical properties of electrodes might influence this current distribution.

This paper describes the development of a finite element based skin model that represents the anatomical structures in the skin and uses this model to explore the effect of a high impedance layer between the skin and the electrode. It is hypothesised that introduction of such a layer between the skin and the electrode would increase the impedances of all possible current pathways, reducing the effect of impedance differences and hence current flow differences between pathways.

Methods

Prior to developing the model a preliminary study was carried out to verify the assumption described above. A pin array was constructed of discrete current paths, most of which were highly resistive, but with a single low impedance path. This experiment proved that a high impedance layer between the current source and the pins would reduce the ratio of current through the low impedance path to that through the high impedance paths [8].

A 2D axi-symmetric skin FE model, centred on a sweat pore, was produced, using a FE package (Ansys 10.0, Ansys, Inc, USA), as shown in figure 1. The skin, fat and muscle were modelled as flat media and the skin was divided into SC and the rest of the skin (RS). As the current flow in the vicinity of the current pore was assumed not to be influenced by the presence of any other current pores, only one current pore (a sweat duct) was included in this FE model. It traversed through the skin, fat and muscle. Representative values for the thickness of each component, together with the width of the current pore were taken from the literature [6, 7]. Bone, blood vessels and sensory nerves were assumed to have negligible effect on the parameters of interest and were not explicitly included in the model. A foil stimulating electrode was modelled overlying a hydrogel layer on the skin surface. As stimulation of a nerve is not a temporal summation and only varies with stimulation intensity, DC current was used in the model. The bottom of the muscle was assumed to be at zero voltage. Differentiation between the materials in the model was achieved through assigning appropriate resistive properties (table 1) to the elements representing the different media. Apart from the SC, the other tissue properties are dominated by resistivity. To account for the capacitive properties of the SC, an equivalent resistivity was calculated, including its resistive and capacitive properties. A convergence study was carried out to ensure the mesh-density was sufficiently fine.

Current density gradient is the measure of stimulation function. However, current density is a reasonable approximation to this in areas where nerves terminate or are convoluted, such as the skin [4]. Current density was thus used in this model to describe the stimulation intensity.

Components	Resistivity (Ωm)
Foil electrode	1.5E-7
Hydrogel	$10\text{-}10^5$
SC	5300
RS	4.5
Fat	63
Muscle	2 on X, 4 on Y
Sweat	1.4-45

Table 1: resistivities of the biological tissues [9, 10]

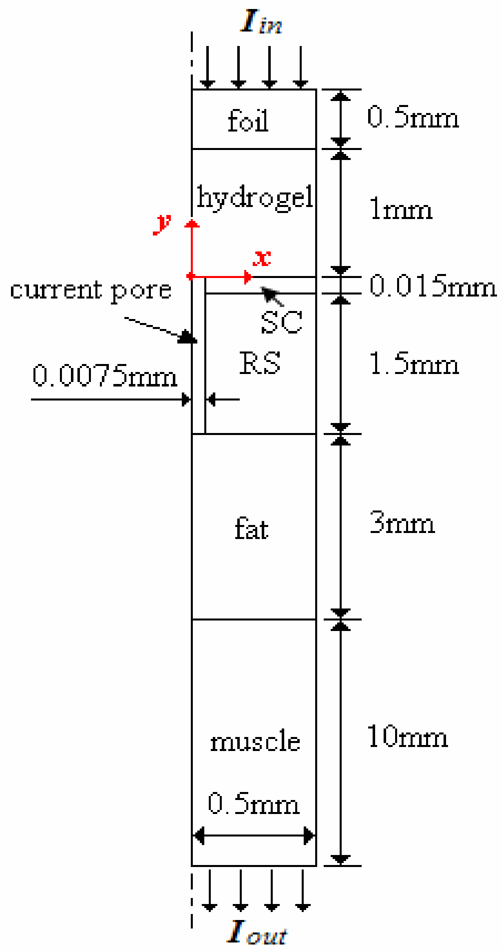

Fig 1: Schematic of the standard skin FE model

Results

As sensory receptors are normally located in the dermis in the skin, the current density distribution in the RS was assumed to determine the sensation. The skin FE model predicted that the peak current density (hot spot) in the RS was located in the top corner of the RS layer, adjacent to the SC and sweat pore (see figure 2). The non-uniformity of current distribution was quantified using a current hogging coefficient (CHC), which was the ratio between the peak current density in the RS and the mean current density in the same area. Effects of four variables (hydrogel resistivity, hydrogel thickness, sweat duct resistivity, SC thickness) on CHC were predicted by the skin FE model, as shown in figures 3, 4 and 5. Four different hydrogels were modelled, corresponding to commercially available samples (see tables 2 and 3), and their effects on CHC were plotted in figure 6.

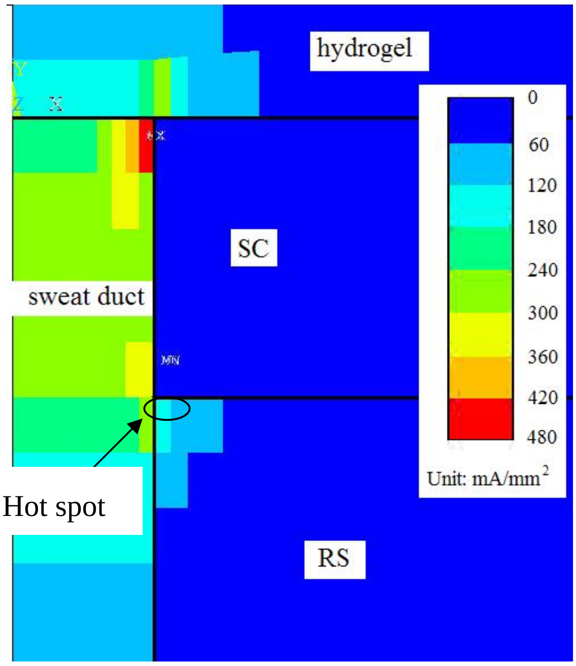

Fig 2: Current density distribution and the hot spot in the RS

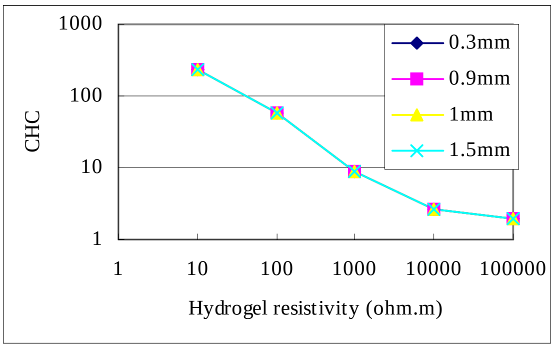

Fig 3: Effect of hydrogel thickness and resistivity on CHC (all lines and markers overlie)

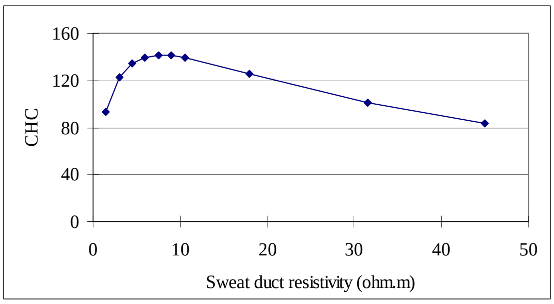

Fig 4: Effect of sweat duct resistivity on CHC

Hydrogel name	Approx thickness (mm)	Resistivity
Hydrogel 703	0.9	55
Hydrogel 803	0.9	206
Hydrogel ST	0.5	1363
Hydrogel AG	0.3	25185

Table 2: Properties of the hydrogel samples

Hydrogel name	Product code	Suppliers
Hydrogel 703	AG703	Axelgaard manufacture Co., Ltd. USA
Hydrogel 803	AG803	Axelgaard manufacture Co., Ltd. USA
Hydrogel ST	SRBZAB-0 5SB	Sekisui Plastics, Co., Ltd. Japan
Hydrogel AG	AG3AM03 M-P10W05	Sekisui Plastics, Co., Ltd. Japan

Table 3: the suppliers of the selected hydrogel

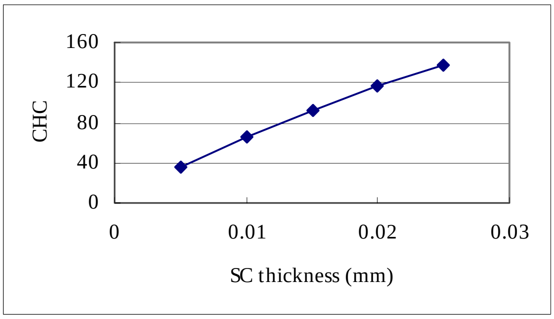

Fig 5: Effect of SC thickness on CHC

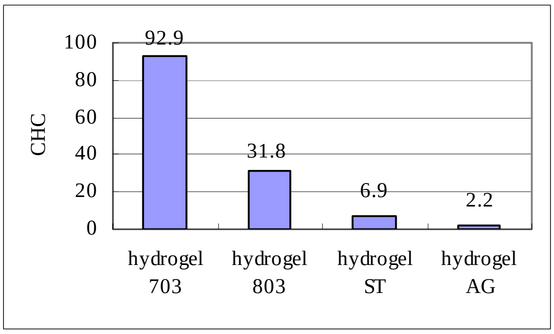

Fig 6: Effect of hydrogel samples on CHC

Discussion

Figure 3 shows that hydrogel with higher resistivity will lead to a more uniform current distribution in the vicinity of the current pore. However, hydrogel thicknesses from 0.3mm to 1.5mm have very little influence on current hogging, and therefore hydrogel resistivity dominates within the range of hydrogel thickness.

The resistivity of the sweat duct can be assumed to vary with the amount of sweat in the duct. Figure 4 suggests that current hogging peaks when the resistivity of the sweat duct is similar to that of the rest of the skin. Hence sweaty skin or dry skin would be associated with more uniform current distribution in the RS during electrical stimulation.

Figure 5 shows that the thinner the SC the less current hogging occurs in the vicinity of a current pore. This suggests that reducing the thickness of the SC before stimulation will not only reduce the skin impedance, but also improve the uniformity of current distribution.

The model's prediction on the effect of high impedance hydrogels on CHC (see figure 6) is consistent with a recent experimental study on the effects of sensation of a high impedance electrode [11].

The study limitations are as follows. First, it has only examined current flow in the vicinity of a current pore and does not consider other mechanisms by which high current density can result, such as the edge effect [4]. Second, no in-vivo validation of the model is possible.

Conclusions

The model describes current density distribution in the skin due to the current pore effect during electrical stimulation. It predicts the non-uniformity of the current density caused by anatomical effects (SC thickness and sweat duct resistivity) and electrode effects (hydrogel thickness and resistivity). It also suggests that a stimulating electrode with high resistivity could reduce the discomfort associated with transcutaneous electrical stimulation, in agreement with our experimental results [11].

References:

[1] Peckham, P. H. and Knutson, J. S., Functional electrical stimulation for neuromuscular applications, *Annual Review of Biomedical Engineering*, vol. 7, pp. 327-60, 2005.

[2] Burridge, J., Does the drop-foot stimulator improve walking in hemiplegia?, *Neuromodulation*, vol. 4, pp. 77-83, 2001.

[3] Prausnitz, M. R., The effects of electric current applied to skin: A review for transdermal drug delivery, *Advanced Drug Delivery Reviews*, vol. 18, pp. 395-425, 1996.

[4] Reilly, J. P., *Applied bioelectricity: from electrical stimulation to electropathology*. New York: Springer-Verlag, 1998.

[5] Cullander, C. and Guy, R.H., Visualization of iontophoretic pathways with confocal microscopy and vibrating probe electrode. *Solid State Ionics* Vol. 53-56, pp. 197-206, 1992.

[6] Bannister L.H., Berry M.M., Collins P., Dyson M., Dussek J.E., Ferguson, W. J., *Gray's Anatomy*, Pearson Professional Limited. 1995.

[7] Odland, G. F., *Structure of the skin*. Biochemistry and Physiology of the Skin. L. A. Goldsmith, editor. Oxford University Press, Oxford. 1983.

[8] Sha, N., *Development and evaluation of a drop foot stimulator using an electrode array*. PhD thesis in progress, University of Salford.

[9] Gabriel, S., Lau, R.W., Gabriel, C., The dielectric properties of biological tissues: III. Parametric models for the dielectric spectrum of tissues. *Physics in Medicine and Biology*, vol. 41, pp. 2271-2293, 1996.

[10] Yamamoto, T. and Yamamoto, Y., Electrical properties of the epidermal stratum corneum *Medical and Biological Engineering*, pp. 151-158, March 1976.

[11] Sha N., Kenney L.P.J., Heller B.H., Barker A.T., Howard D., Wang W., The effect of the impedance of a thin hydrogel electrode on sensation during functional electrical stimulation, *Medical Engineering and Physics* – in review.

Author's Address

Ning Sha, CRHPR, University of Salford, Salford, UK; n.sha@salford.ac.uk

Laurence Kenney, CRHPR, University of Salford, Salford, UK; l.p.j.kenney@salford.ac.uk; http://www.seek.salford.ac.uk/viewPersonalProfile.jsp

DEVELOPMENT OF MODELING FUNCTIONAL ELECTRICAL STIMULATION IN DENERVATED MUSCLE

Reichel M[1], Martinek J[1,2], Mandl T[1,3], Mayr W[1], Rattay F[2]

[1] Center of Biomedical Engineering and Physics, Medical University of Vienna, Austria

[2] Department of Analysis and Scientific Computing, Vienna University of Technology, Austria

[3] MR Centre of Excellence, Medical University of Vienna (MUW)

Abstract

Activating denervated muscle fibers by Functional Electrical Stimulation (FES) to create tetanic contraction has been shown very well in the last 25 years. In a rather empiric way stimulation parameters (amplitude, pulse widths and shape), and electrode parameters (material, shape and position) have been optimized. The stimulation process can be observed by applying stimulation current and measuring e.g. knee extension torque due to contraction of m. quadriceps but modeling and simulation give better insights for optimizing stimulation and electrode parameters.

Nerve fiber models and the theory of Hodgkin & Huxley are adapted for denervated muscle fibers by fitting membrane dynamics and by adding active or passive membrane currents for the T-system. The extracellular activation of the muscle fiber is found in a two step procedure: (i) modeling the extracellular electrical field and (ii) extracting the driving effect to the fiber membrane called activating function (AF). The adaptation process from nerve to muscle fiber model was investigated from a line model with simplified T-system up to a 3D model of the fiber. A 3D model including anisotropy of muscle tissue was developed for the human thigh.

The coupling of field and fiber leads to two theories of the AF one is the well known classic AF and the other is the so called terminal AF which effects only at muscle fiber endings. The improvement of the fiber model leads to more realistic behavior in excitation evaluated by comparing chronaxy and rheobase from animal studies. The development of the field model shows an improvement of realistic 3D results but saves also computation time.

Activation of denervated muscle fibers can be calculated individually for each subject with arbitrary electrode and stimulation parameters. For validation of these results, a currently running project uses T2-parameter MRI methods to estimate activated regions in human skeletal muscle.

Introduction

In Functional Electrical Stimulation (FES) of the denervated human thigh we can separate the clinical view and the modeling view. From the clinical view knee extension torque, selectivity, fatigue, electrode handling and safety are very important points [1]. The modeling side is trying to investigate these clinical issues by calculating muscle activation influenced by stimulation and electrode parameters [2].

In order to optimize the FES process in denervated muscles we used two coupled models. One is the model of the denervated muscle fiber and the other is the model of the surrounding electrical field in the human thigh induced via surface electrodes [3]. The models are coupled by the activating function AF [4, 5] which quantifies the driving effect for muscle fiber excitations as consequence of their membrane depolarizations.

The muscle fiber model is developed from a compartment line model of Hodgkin-Huxely type (HH) [4], but their nerve fiber model has to be extended considering the current flow into the transverse tubular system (T-system) [6, 7]. Calculation of chronaxy and rheobase showed that without T-system the model cannot be fitted to results from animal studies. Currently the investigation of a 3D model of the fiber including all results from the line model is in progress.

The electrical fields in human thighs can be calculated both with finite element and finite difference methods. These calculations can be done either in two and three dimensions and with consideration of isotropy or anisotropy of conductivity [8]. The geometric information can be obtained from CT or MRI data.

The AF depends on the path of fiber and the endings of the fiber lying in the electrical field. The classic AF can calculate the exciting effect along the fiber path and the terminal AF is used to calculate the activation at the two ending points of the fiber.

Material and Methods

Fiber-Model:

A muscle fiber is a cylindrical cell which essentially consists of the sarcolemma, the transverse tubular system (T-system), the myofibrils and the intracellular fluid. The electrical excitation of a target fiber is simulated with a classical compartment model for a nerve fiber that is extended to include the current flow into the T-system (symbols are explained in Table 1)

$$i_{T,n} = \frac{V - V_{T,a}}{r_a} \tag{1}$$

The main equation depends on the compartment position along the fiber and consequently we have to consider two cases: (i) for the central compartments of the fiber the current balance reads as (symbols are explained in Table 1)

$$\frac{a}{2\cdot\rho_i}\left[\frac{V_{n+1}-2\cdot V_n+V_{n-1}}{\Delta x^2}+\frac{V_{e,n+1}-2\cdot V_{e,n}+V_{e,n-1}}{\Delta x^2}\right]=c\frac{dV_n}{dt}+i_{ion,n}+i_{T,n} \tag{2}$$

and (ii) at the ending of the fiber

$$\frac{a}{2\cdot\rho_i\cdot\Delta x}\cdot\left[\frac{V_{N-1}-V_N}{\Delta x}+\frac{V_{e,N-1}-V_{e,N}}{\Delta x}\right]=c\cdot\frac{dV_N}{dt}+i_{ion,N}+i_{T,N} \tag{3}$$

Note that we get different difference quotients of the extracellular potential V_e as driving terms.

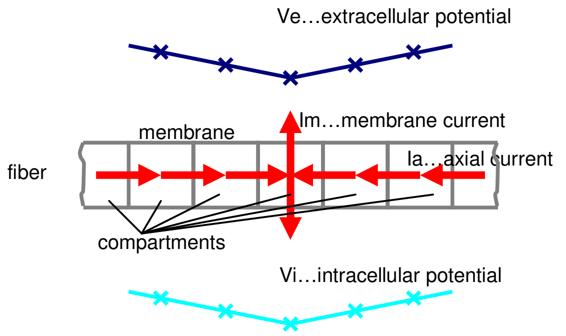

Fig. 1: Intracellular current flow (I_a) in a muscle fiber driven by the extracellular potential (V_e) at the center of the fiber.

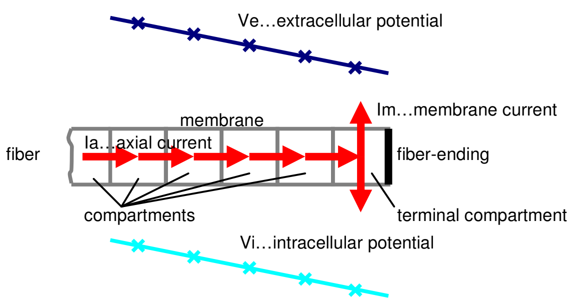

Fig. 2: Intracellular current flow (I_a) at one ending of a muscle fiber driven by the extracellular potential (V_e).

To illustrate Equ. 2 and Equ. 3 the current flow in a fiber is shown with two examples (Fig. 1 and Fig. 2). Fiber excitation occurs at the position of current flow across the membrane resulting from the intracellular current which is driven by the extracellular electrical field. In Fig. 1 there is no fiber ending involved and therefore the extracellular potential along the fiber has to be inhomogeneous to enforce local differences in axial currents which result in a radial current depolarizing the membrane according to Ohm's law. In the case of Fig. 2 the fiber ending works like a barrier for the axial current and the whole amount of axial current flows through the membrane very close to the fiber ending.

For that reason the classic AF is directly proportional to the 2nd derivative (Equ. 1) and the terminal AF to the 1st derivative (Equ. 2) of the extracellular electrical field along the fiber. The calculation of the fiber models and the AF has been implemented by MATLAB.

Field-Model:

The geometric information is available as a number of CT or MRI cross-sections from patient data. The MATLAB application FES-FIELD provides an input filter for DICOM format. The entire Hounsfield or gray scale can be segmented by threshold values into several groups where each group stands for a type of tissue. The potential distribution can be calculated in different ways depending on questions have to be answered.

A very simple way is to calculate the 2D field of a point source or to extend this method to a line source which may be assumed to be superposed by several point sources. A further step can be the calculation of the 2D field by using the partial equation toolbox (PDE) of MATLAB, where e.g. a length section of the human thigh can be drawn and calculated by defining regions of different conductivity, boundary conditions and positions of current sources.

A more complex way is to build up a 3D model and to calculate the electrical field by the finite difference method implemented by MATLAB. Moreover, the 3D geometry can be imported into the simulation tool FEMLAB and there the field can be calculated by finite element method.

Results

With the knowledge of the difference concerning the AFs, a very simple 2D example has been set up. FES of human denervated thigh is performed with large electrodes covering almost the entire thigh above the m. quadriceps. This situation leads to an electrode configuration shown in Fig. 3 by neglecting areas of different conductivities and boundary conditions. Below the two electrodes a fiber path is drawn to give either the position of an entire fiber or the possibility of positions of fiber endings.

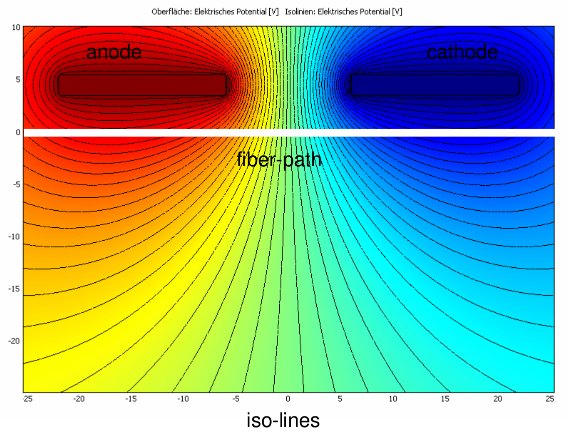

Fig. 3: 2D Electrical field applied by two electrodes (anode, cathode) above a fiber path.

From the electrical field in Fig. 3 the extracellular potential and the classic and terminal AF can be calculated (Fig. 4).

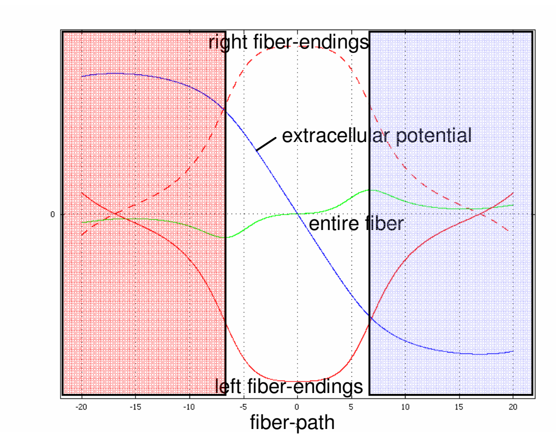

Fig. 4: Extracellular electrical potential along the fiber path of Fig. 3 and calculated classic (green) and terminal AF for possibility of right and left endings; left: anode area, right: cathode area

The calculation of the classic AF shows that the activation is highest at the inner edges of the electrodes but it is very small in comparison to the activation value of the terminal AF.

For further investigation of the differences of the AFs a more realistic 3D example has been built from CT data (Fig. 5). The data were segmented by threshold of Hounsfield units. Different volumes of conductivity have been determined, like fat, muscle, bone, skin and electrode material. Biphasic stimulation pulses with the pattern of either 80V / 20ms per phase or 200V / 100ms per phase have been applied to the electrodes. For the resulting electrical field the classic AF and the terminal AF have been calculated in the entire volume of muscle tissue. The same phenomenon as in the 2D example can be observed. With the pattern of 80V/20ms, which is the common pattern for well trained denervated patients, only activation by terminal AF can be seen. But with the non realistic stimulation with 200V/100ms activation by classic AF is observed.

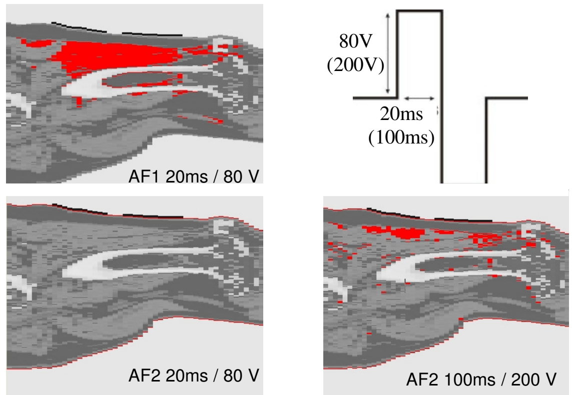

Fig. 5: Example of a 3D model of the human thigh stimulated by biphasic pulses of 80V/20ms and 200V/100ms. Estimated terminal AF (AF1) and classic AF (AF2) is shown under the electrodes in a chosen length section.

Fig. 6 shows the terminal AF of the 3D example at several cross sections.

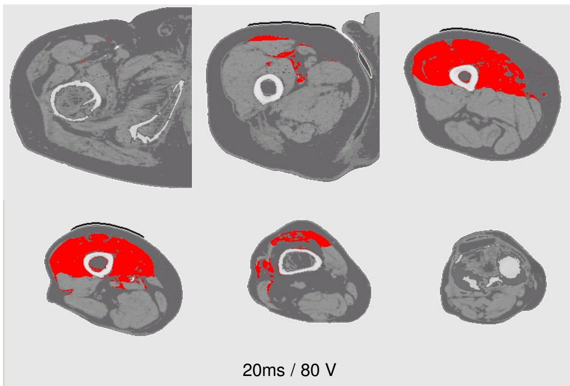

Fig. 6: Cross sections of the human thigh showing estimated areas of activation calculated by the terminal AF from stimulation pulses of 80V/20ms.

Discussion

Examples of 2D and 3D models show, that the classic AF along the muscle fiber is mostly very low because of a more or less homogeneous electrical field surrounding the fiber. The electrode configuration can alter field characteristics to gain activation at regions where no fiber endings are present. The examples also show that the activation occurs mainly at the fiber endings. The activation due to the terminal AF can only be an estimation because it assumes that at each position (voxel, volume compartment) of calculation a fiber ending is present, but this will not be effective when no muscle fibers within this voxel has an ending.

In an ongoing project simulation results are to be validated with T_2-MRI methods. The effect of an increased transversal relaxation time (T_2) immediately after exercise correlates well with exercise intensity [9] and can be used to calculate activation maps. It has been shown that the effect is present in denervated muscle [10] and thus suitable to reveal the spatial distribution of muscle activation during FES.

A new approach of simulating and analyzing the effects of FES is to use the Software FEMLAB [11, 12]. This should allow a new point of view investigating the activation and the effects of different geometries, pulse shapes and fiber parameters.

symbol	**description**
V, V_n, V_{n+1}, V_{n-1}	membrane potential (n…compartment)
$V_{e,n}, V_{e,n+1}, V_{e,n-1}$	extracellular potential (n…compartment)
$V_{T,a}$	tubular membrane pot. in outermost sphere
$i_{T,n}, i_{T,N}$	tubular current (N…terminal comp.)
$i_{ion,n}, i_{ion,N}$	ionic membrane current (N…terminal comp.)
a	fiber radius
r_a	access resistance to tubular system
ρ_i	intracellular resistivity
c	membrane capacity
Δx	length of compartment

Tab. 1: Symbols of Equ. 1-3.

References

[1] Kern H, Funktionelle Elektrostimulation paraplegischer Patienten, Österr. Z. Phys. Med. Heft 1, Supplementum, 1995.

[2] Reichel M, Funktionelle Elektrostimulation denervierter Skelettmuskulatur – Modellbildung und Simulation, (in German), Dissertation TU-Wien, 1999.

[3] Reichel M, Breyer T, Mayr W, Rattay F, Simulation of the three dimensional electric field In The course of functional electrical stimulation. Artificial Organs 26 (3):252-255, 2001.

[4] Rattay F, The basic mechanism for the electrical stimulation of the nervous system. Neuroscience 89, 335-346, 1999.

[5] Reichel M, Mayr W, Rattay F, Simulation of Exitation Effects at the Muscle-Tendon Junction in Denervated Muscle Fiber. Proc. of 7th Ann. Conf. International Functional Electrical Stimulation Soc. (IFESS), 152-154, 2002.

[6] Henneberg KA, Roberge FA, Simulation of propagation along an isolated skeletal muscle fiber in an isotropic volume conductor, Ann. Biomed. Eng. 25: 15-28 , 1997.

[7] Adrean RH and Peachey LD, Reconstruction of Action Potential of Frog Sartorius Muscle. J. Physiol. Lond. 235:103-131, 1973.

[8] Martinek J, Stickler Y, Reichel M, Rattay F, Analysis of Calculated Electrical Activation of Denervated Muscle Fibers in the Human Thigh, Artifical Organs 29(6); 444-447. 2005

[9] P. Carolynn, M. Ronald A. and J. L. Fleckenstein. Seminars in Musculoskeletal Radiology, 7:297, 2003.

[10]T. Mandl, M. Reichel, M. Meyerspeer, H. Kern, E. Moser, W. Mayr. Estimation of Muscle Activation in Denervated Patients after FES by mfMRI. Proceedings Gemeinsame Jahrestagung der Deutschen, Österreichischen und Schweizerischen Gesellschaft für Biomedizinische Technik; ISSN 0939-4990

[11] Martinek J, Stickler Y, Reichel M, Rattay F, A new Approach to simulate Hodgkin-Huxley like Excitation with Femlab, Proceedings of 9th. FES Workshop. 2007

[12] Stickler Y, Martinek J, Hofer C, Rattay F, A finite element model of the electrically stimulated human thigh: changes due to denervation and training, Proceedings of 9th. FES Workshop. 2007

Author's Address

FH-Prof. DI Dr. Martin Reichel
Center of Biomedical Engineering and Physics,
Medical University of Vienna
martin.reichel@meduniwien.ac.at
www.meduniwien.ac.at/zbmtp/bmt/home.htm

A NEW APPROACH TO SIMULATE HODGKIN – HUXLEY LIKE EXCITATION WITH COMSOL MULTIPHYSICS (FEMLAB)

Martinek J[1,2], Stickler Y[1], Reichel M[2], Rattay F[1]

[1] Institute for Analysis and Scientific Computing, Vienna University of Technology, Austria

[2] Center of Biomedical Engineering and Physics, Medical University of Vienna, Austria

Abstract

A proof of concept for the evaluation of nerve and muscle fiber excitation with COMSOL Multiphysics software is presented. Partial differential equations of the Hodgkin-Huxley type simulate the membrane kinetics along the fiber. Such 1D models of nerve or muscle fibers are embedded in a volume conductor where the electric field is calculated with finite element methods. The presented bidomain model includes the interaction between electrode currents and trans-membrane currents during the excitation process. Especially for direct muscle fiber stimulation (cardiac muscle, denervated muscle) the effects from secondary currents from large populations of excited fibers seems to be significant. The method has many applications, e.g. the relation between stimulus parameters and population size can be analyzed.

Introduction

When Hodgkin and Huxley published their mathematical theory of the gating mechanisms in giant squid axons [1], they started a new period of understanding and modeling the processes that lead to action potentials, muscle contraction etc. [2]. Later these models where refined and adapted to many other problems of modeling like the denervated muscle fiber [3]. Most of these models were based on compartment models, where first the electrical field and then as a result of the field, the action potential was calculated [4, 5, 6]. In these models it is often difficult to integrate geometrical aspects on the one hand, and a time dependency on the other hand.

As a consequence of the EU Project RISE there is a lot of data of long time denervated patients that were stimulated with surface electrodes [7]. Analyzing this data new questions arose concerning the correlation between the propagation of the electrical field and the development of action potentials.

Material and Methods

The Hodgkin-Huxley Model - ODE:

The Hodgkin-Huxley Model (HHM) describes the voltage-current relation for the membrane of a fiber (e.g. a nerve or a muscle fiber). The "original" HHM was described using the following system of ODEs (Ordinary Differential Equation):

$$C_m \frac{\partial V}{\partial t} = g_{NA} m^3 h (V_{Na} - V) + g_K n^4 (V_K - V) + g_L (V_L - V)$$

C_m *... capacitance of membrane*
$g_{Na}, g_K, g_L, \ldots$ *conductance of Natrium, Potassium and Leakage*

Equ. 1: Hodgkin-Huxley ODE [1]

with

$$\frac{\partial w}{\partial t} = \alpha_w (1 - w) - \beta_w w \quad (w \text{ is } m, n \text{ or } h)$$
$$\alpha_m = \frac{2.5 - 0.1V}{e^{2.5-0.1V} - 1} \quad \beta_m = 4e^{-\frac{V}{18}}$$
$$\alpha_n = \frac{1 - 0.1V}{10(e^{1-0.1V} - 1)} \quad \beta_h = 0.125e^{-\frac{V}{80}}$$
$$\alpha_h = 0.07e^{-\frac{V}{20}} \quad \beta_h = \frac{1}{e^{3-0.1V} + 1}$$

Equ. 2: Parameters and gating variables for the Hodgkin-Huxley Model [1]

The resting state conditions where defined by:

$$V(0) = 0, \quad m(0) = 0.05, \quad n(0) = 0.32, \quad h(0) = 0.6$$

This ODE System was derived from space clamp experiments where the membrane potential does not depend on the spatial location within the clamped experiments.

The Hodgkin-Huxley Model - PDE:

If instead of space clamping, one allows the voltage across the membrane of the axon also to vary along the axon with longitudinal distance x then the membrane potential satisfies a PDE (Partial Differential Equation). This PDE is similar to the ODE case (Equ. 1):

$$C_m \frac{\partial V}{\partial t} = \frac{r}{2\rho} \frac{\partial^2 V}{\partial x^2} + g_{NA} m^3 h (V_{Na} - V) + g_K n^4 (V_K - V) + g_L (V_L - V)$$

C_m *... capacitance of membrane*
r *... radius of axon*
ρ *... resistance of intracellular space*
$g_{Na}, g_K, g_L, \ldots$ *conductance of Natrium, Potassium and Leakage*

Equ. 3: Hodgkin-Huxley PDE [1]

Using the HHM PDE (Equ. 3) it is possible to calculate and simulate the voltage along the membrane in reference to the location along the fiber and to the time.

Bidomain Model

Simulating the characteristics of a muscle or nerve fiber, and especially the membrane of the fiber, it is necessary to simulate two different potential distributions. On the one hand the “macroscopic”, extracellular potential distribution in the area around the fiber, and on the other hand the “microscopic”, intracellular potential distribution inside the fiber (Fig. 1).

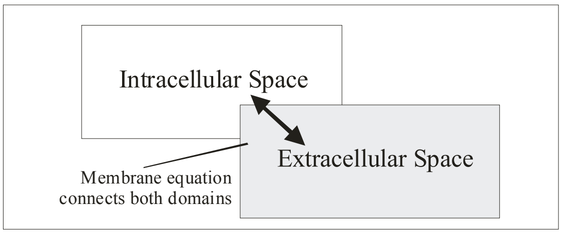

Fig. 1: Simplification of the bidomain model and the connection between the two domains.

Knowledge of the potential distribution in both domains is necessary for calculating the propagation of action potentials along the fiber. It is difficult to simulate this problem in one model because of the complexity of the problem. Therefore it is useful to divide the area of interest in two domains and to calculate each domain on its own [8, 9]. The two domains are connected by their boundary conditions.

Comsol Multiphysics (FEMLAB)

Comsol Multiphysics (Fig. 2), formerly known as FEMLAB, is a PDE software to create 1D, 2D and 3D spatial models and to simulate their time dependent behaviour. Even it is possible to couple multiple problems, e.g. the extracellular potential and the propagation of HH-like action potentials, and thereby to generate bidomain models.

1D model of fiber

Using the HHM PDE (Equ. 3) a 1D bidomain model of a fiber was implemented.

$$d_a \frac{\partial V_e}{\partial t} - \nabla(c \nabla V_e) = 0$$

Equ. 4: PDE to calculate extracellular potential

The extracellular potential was calculated by Equ. 4. The two domains are coupled by:

$$V = V_i - V_e - V_{Rest}$$

Equ. 5: V_i – intracellular potential; V_e – extracellular potential; V_{Rest} – resting voltage of the cell.

The model (Fig. 2) represents a simplified fiber. It was primary used to evaluate the model and to analyze the effects of different stimulation or fiber parameters.

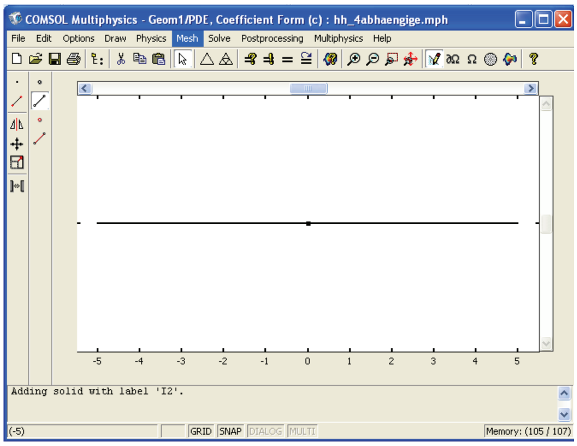

Fig. 2: Comsol Multiphysics with 1D model of fiber. The bidomain model was implemented using Equ. 3, Equ. 4 and Equ. 5.

1D fibers in 2D area

Two 1D fiber models were embedded in a 2D domain (Fig. 5). The potential in the 2D domain was calculated using Equ. 4. The rectangular stimulation impulse was applied by a point-like source at the top of the 2D domain. The two embedded fibers where coupled to the potential in the 2D area by using Equ. 5.

To simulate the influence of action potentials along the fiber to the extracellular space there is also a coupling between the potentials along the fiber and the extracellular potential.

1D fibers in 3D area

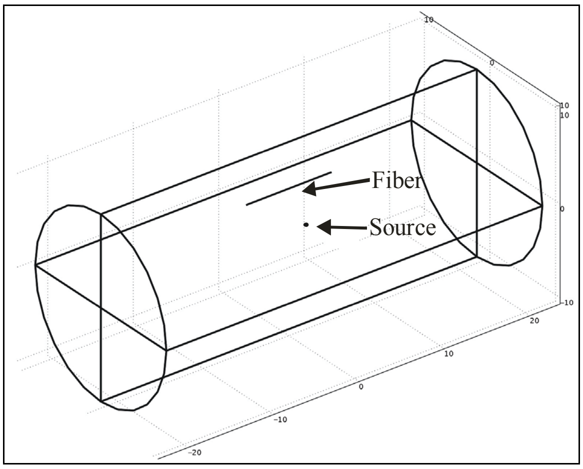

Fig. 3: 1D fiber model embedded in a 3D area

At last one 1D fiber model was embedded in a 3D cylindrical area, to analyze the effects of a 3D area surrounding the fiber (Fig. 3). The rectangular stimulation impulse was applied on a point like source.

Results

1D model of fiber

The 1D model of the fiber was first used to evaluate the model and to study the influences of different stimulation and fiber parameters.

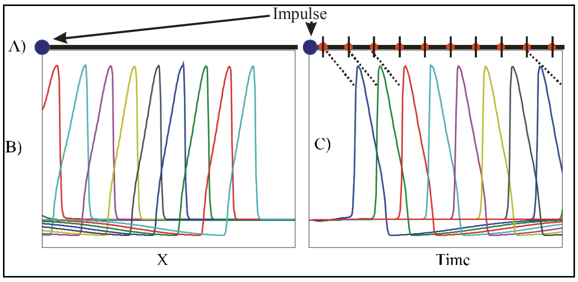

Fig. 4: A) 1D fiber: injected stimulation impulse at the left end of the fiber; B) propagation of the action potentials along the fiber (every line represents a snapshoot of transmembrane voltage along the fiber); C) change of action potential over the time at different places.

Figure 4 shows the excitation process of a fiber as response to single current pulse injection at the left fiber ending. These presented test results are in accordance with Hodgkin-Huxley standard compartment model (lumped circuit model) evaluations based on space discretization with constant Δx [2].

1D fibers in 2D area

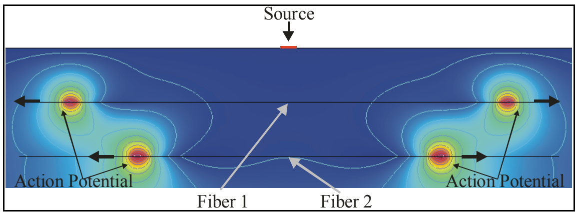

Fig. 5: Two 1D fibers with HH dynamics embedded in a 2D area. At the source a rectangular 5ms pulse is applied. The resulting action potentials and their moving direction are shown at time = 20ms. Note the delayed response of the more distant fiber which needs more time to reach the threshold.

Simulating 1D fibers in a 2D area the intracellular potential and the HH-like excitation is comparable to the simple 1D model (Fig 4). The interesting part is the "recoupling" of the intracellular potential to surrounding area (Fig. 5).

The influence of the intracellular potential of the fiber model to the extracellular potential can be seen on the one hand by action potentials propagating along the fiber. On the other hand, the influence can also be observed by changes of the potentials in the surrounding area (Fig. 6).

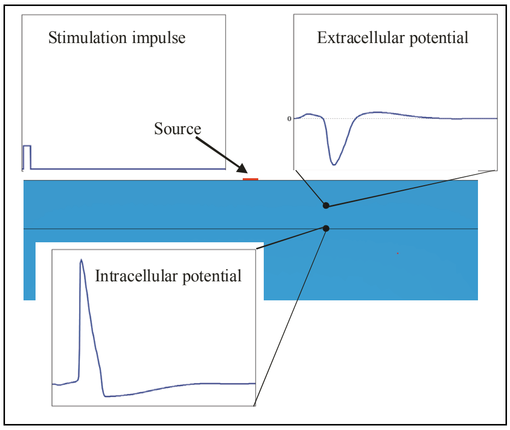

Fig. 6: intracellular and extracellular potential of a 1D fiber model. A square stimulation impulse was applied at the source.

1D fiber in 3D area

Embedding the fiber in a 3D volume and calculating the potential distribution in the extracellular space and the currents across the fiber demonstrate comparable results to the 2D case (Fig. 7).

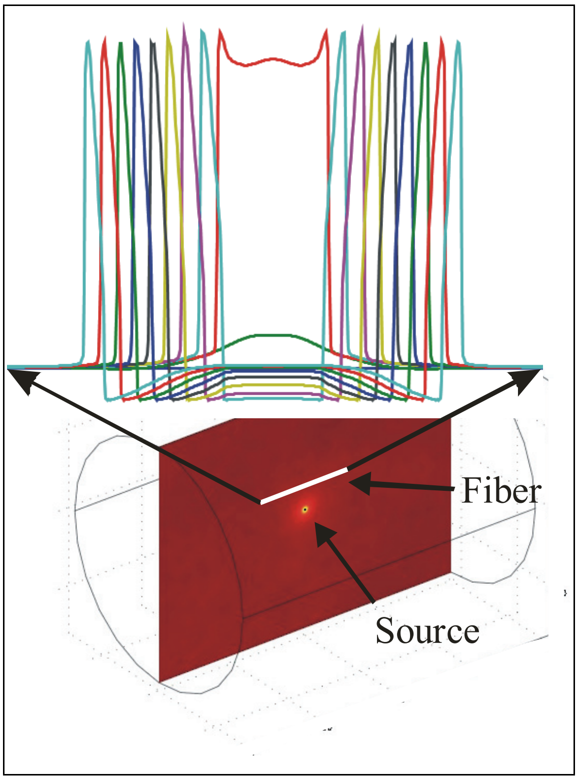

Fig. 7: 1D fiber model embedded in a 3D area. A stimulating square pulse was applied at the source. The propagation of the action potential along the fiber is shown.

Discussion

Using Comsol Multiphysics, formerly known as FEMLAB, it is possible to easily calculate Hodgkin-Huxley like potentials in different geometries and with a different set of parameters. Once the model is implemented into the software it can be easily adapted to different geometries and parameters of fibers and extracellular areas.

The big advantage of using bidomain model PDEs is that the time dependent distribution of the stimulation potential and the resulting action potentials can be calculated at the same time. Therefore it is possible to calculate the coupling between fiber and the surrounding area in one calculation step. So far calculations of action potentials had to be done in two steps: first the calculation of the extracellular potential distribution. Using this distribution the excitation of the fiber was calculated with a compartment model.

The coupling between the two domains can be calculated in both directions. On the one hand the extracellular potential, the area outside the fiber, affects the membrane potential and the development of action potentials. On the other hand the membrane potential, especially the action potential, has an influence on the extracellular potential. With the presented technique the influence on the extracellular area can also be used to create models of EMG or EEG measurements. Such modeling studies will be a major step to enlighten many measurements and experiments that were made in the past [10].

References

[1] Hodgkin A.L., Huxley A.F. A quantitative description of membrane current and its application to conduction and excitation in nerve. J. Physiol. (London), 117: 500-544, 1952.

[2] Rattay F. Electric nerve stimulation (theory, experiments and applications). Springer-Verlag Wien, 1990.

[3] Reichel M. Funktionelle Elektrostimulation denervierter Skelettmuskulatur – Modellbildung und Simulation. (In German) Doctor Thesis. Vienna University of Technology, 1999.

[4] Grotz B. Simulation der Funktionellen Elektrostimulation an denervierter Skelettmuskulatur im anisotropen 3-D Modell des menschlichen Oberschenkels. (in German). Master's Thesis. Vienna University of Technology, 2002.

[5] Martinek J. Analyse der Aktivierung von denervierten Muskelfasern im menschlichen Oberschenkel bei Funktioneller Elektro-Stimulation. (in German). Master's Thesis. Vienna University of Technology, 2003.

[6] Martinek J. et al. Analysis of Calculated Electrical Activation of Denervated Muscle Fibers in the Human Thigh, Artifical Organs 29(6); 444-447, 2005.

[7] Mödlin M. et al. Electrical Stimulation of Denervated Muscles: First Results of a Clinical Study. Artifical Organs 29(3); 203-206, 2005.

[8] Tung L.A. A bidomain model for describing ischemic myocardial d.c. potentials. Ph.D. Dissertation. M.I.T., Cambridge, MA, 1978.

[9] Miller W.T., D. B. Ceselowitz. Simulation studies of the electrocardiogram. Circ. Res., vol. 43; pp. 301-315, 1978.

[10] Hofer C. et al. In vivo assessment of conduction velocity and refractory period of denervated muscle fibers. Artifical Organs 29(6); 436-439. 2005.

Acknowledgements

This study was supported by the Austrian Science Fund (FWF) research project P18848-N13.

Author's Address

DI Johannes Martinek
Institute for Analysis and Scientific Computing,
Vienna University of Technology
Wiedner Hauptstraße 8-10
A-1040 Vienna, Austria
johannes.martinek@technikum-wien.at
http://www.asc.tuwien.ac.at/

PULSE-SHAPE ENERGY MINIMIZATION FOR MAGNETIC STIMULATION SYSTEMS

Jezernik S[1], Sinkjaer T[2], and Morari M[3]

[1] Altran Switzerland, Technology / Engineering / Innovation Consulting, Zürich, Switzerland

[2] Center for Sensory-Motor Interaction, Aalborg University, Aalborg, Denmark

[3] Swiss Federal Institute of Technology (ETH Zürich), Zürich, Switzerland

Abstract

In magnetic stimulation of nervous tissue, a time-varying magnetic field is generated by a time-varying stimulation current flowing through a hand-held stimulation coil. Current magnetic stimulation systems require very high stimulation currents in the order of 1000 Amperes, large stimulator circuit components, and often suffer from coil overheating which limits the speed of application of magnetic stimulation (limited repetition frequency of magnetic stimulation pulses or pulse trains). Therefore, it is of interest to reduce the amplitude of required currents/power and electrical energy.

In this work, the energy-minimal magnetic stimulation pulse waveform is mathematically derived. Energy-minimal waveform could overcome problems mentioned above as it reduces power requirements for magnetic coil stimulation. The derivation of energy-minimal magnetic stimulation waveform necessitated a special mathematical problem treatment, namely that of a singular continuous optimal control. The solution is a pulse-waveform that is a rising exponential. Its time-derivative that induces electrical fields that excite the nervous tissue is growing with time (rising exponential as well) vs. falling in case of the decaying exponential that is used in the commercial magnetic stimulation systems . In the stimulation case treated in this article, the non-optimal stimulation needed an energy that was 56.1% greater than the optimal waveform energy. With an exponentially rising energy-optimal waveform, large energy savings are thus possible that will reduce the stimulation coil heating and allow higher stimulation repetition rates.

Introduction and Methods

Nervous tissue can be excited by electrical or magnetic stimulation systems. An example of a magnetic stimulation system/device is shown in Fig.1. The physics of magnetic stimulation is different from physics of electrical stimulation, since with the magnetic stimulation tissue activation is achieved by means of electromagnetic induction, whereas with electrical stimulation, the activation is caused by direct volume conduction of the stimulation current. In magnetic stimulation, a time-varying magnetic field is generated by a time-varying stimulation current flowing through the stimulation coil (coil current is generated by a special electronic circuit that can be modeled by a circuit consisting of a capacitor connected to a series resistance and inductance, see e.g. [1]; see also Fig.1 below). The electro-magnetic pulse then propagates through the air, enters the body, and induces electric fields in the tissue that (can) cause depolarization of the nerve membrane and - if of sufficient amplitude - generation of action potentials.

Fig. 1: A commercially available magnetic stimulation system with electronics housing and stimulation coil. Courtesy of: Medtronic Inc.

The induced electric fields can be calculated by the use of quasi-stationary approximation of Maxwell equations for electrodynamics [2,3]. According to these calculations, the induced electric field is a product of a time-dependent function and a spatial, time-independent function that reflects the problem geometry as well as geometry and some other properties of the used magnetic coil (function $\hat{C}(x)$ in eq.1 below) [2,3]. The time-function is the derivative of the stimulation coil current, di/dt(t). The electric field therefore enters the nerve excitation model via its spatial gradient [2]. The magnetic stimulation waveform energy-optimization problem can be formulated within the optimal control theory framework (see next section) as was done for waveform energy-optimization of electrical stimulation systems in our earlier work [4,5]. However, a special problem treatment is required in the case of magnetic stimulation, as the magnetic stimulation problem represents a singular optimal control problem. The theory for this type of problems is described for example in [6,7]. Pulse-waveform energy optimization is motivated by the fact that current stimulation systems need most energy for the actual tissue excitation – this energy is thus delivered to the tissue [8]. If it would thus be possible to excite nervous tissue with less delivered energy (i.e. reaching the excitation threshold with an energy-minimal stimulation waveform), the desired stimulation effect will still be the same, but achieved at lower energy/power levels.

The derivation of the energy-minimal magnetic stimulation pulse-waveform is presented in the next, *Results* section. Article is concluded with a *Discussion and Conclusion* section.

Results

Modeling and problem treatment:

Our problem treatment basis is the nerve membrane excitation equation in case of magnetic stimulation that can be written in the following way (with nerve membrane capacitance, Cm, conductance, gm, and nerve membrane voltage, Vm; Ga is the axonal conductance and i(t) the stimulation current waveform):

$$C_m \frac{dV_m}{dt} = -g_m V_m + G_a \frac{\partial^2 V_m}{\partial x^2} + \hat{C}(x)\frac{di}{dt} \qquad (1)$$

Approximated optimization problem with minimization of the square of the stimulation current functional (which is proportional to energy in case of constant load impedance) reads then:

$$C_m \frac{dV_m}{dt} \approx -g_m V_m + \hat{C}(x)\frac{di}{dt}$$
$$J[i(t)] = \int_{t=0}^{t_F} i^2(t)dt \rightarrow \min \qquad (2)$$

When translated into the optimal control theory framework, the problem reads (with u(t)=di/dt):

$$\frac{dx_1}{dt} = -\frac{g_m}{C_m}x_1 + \frac{\hat{C}}{C_m}u(t) \qquad \frac{dx_2}{dt} = u(t)$$
$$J[u(t)] = \int_{t=0}^{t_F} x_2(t)^2 dt \rightarrow \min \qquad (3)$$

The corresponding system Hamiltonian H equals:

$$H[x(t),\lambda(t),u(t)] = x_2^2 + \lambda_1 \cdot (-g_m / C_m x_1 + \hat{C} / C_m u) +$$
$$+ \lambda_2 \cdot u \qquad (4)$$

Since ∂H/∂u is not a function of u(t) and thus ∂^2H/∂u^2=0, the energy-minimal magnetic stimulation problem is a singular optimal control problem (singular arcs form a part of the solution). The optimal control solution is obtained by a procedure as described in [6]. The first set of optimality conditions yield:

$$\lambda_1(t) = K \cdot e^{\frac{g_m}{C_m}t} \qquad \lambda_2(t) = -\lambda_1(t)\frac{\hat{C}}{C_m}$$
$$\frac{d\lambda_2(t)}{dt} = -x_2 \qquad (5)$$

Time derivatives conditions on ∂H/∂u yield:

$$\frac{d}{dt}[\partial H / \partial u] = \lambda_1 \frac{g_m}{C_m}\frac{\hat{C}}{C_m} - 2x_2 = 0$$
$$\frac{d^2}{dt^2}[\partial H / \partial u] = \lambda_1 \frac{g_m^{\ 2}}{C_m^{\ 3}}\hat{C} - 2u = 0 \qquad (6)$$

From the latter expression, optimal u(t)=di/dt is determined as an exponentially rising waveform (u(t) is proportional to λ_1(t)). By the evaluation of the boundary condition V(t_F)=Vthr and by integration of di/dt we finally arrive to the optimal magnetic stimulation current waveform:

$$i^*(t) = \frac{V_{THR}C_m}{\hat{C}\sinh(g_m / C_m \cdot t_F)} e^{g_m / C_m \cdot t} \qquad (7)$$

For optimality we also need to check the generalized Legendre-Clebtsch condition with Qm [7], which is satisfied since –Q_2=-(-2)=2 > 0 and thus –Q_2 is positive definite as required for a minimum. The energy-optimal magnetic stimulation current waveform is thus up to a linear scaling the same as the energy-optimal electrical stimulation waveform [4,5]. The associated minimal energy (integral of the squared current) equals:

$$E_{MAG-STIM-OPT-ENERGY} = \int_{t=0}^{t_F} i^*(t)^2 dt = \frac{V_{THR}^{\ 2}(C_m / \hat{C})^2}{\sinh^2\left(\frac{g_m t_F}{C_m}\right)} \cdot \frac{\left(e^{\frac{2g_m}{C_m}t_f} - 1\right)}{\frac{2g_m}{C_m}} \qquad (8)$$

Presently, the magnetic stimulation circuit consists of a charged capacitor that is discharged via the stimulation coil by means of a semiconductor switch [1]. The electric equivalent scheme for magnetic pulse generation is thus a capacitor C discharged by a series connection of a coil resistance R and coil inductance L. The resulting current has – in the overdamped case - the following form [2]:

$$i_{MAG-STIM}(t) = V_{C,0} \cdot C \cdot \left[\left(\frac{\omega_1}{\omega_2}\right)^2 - 1\right] \cdot e^{-\omega_1 \cdot t} \cdot \sinh(\omega_2 \cdot t) \qquad (9)$$

with ω_1=R/(2L) and ω_2=sqrt(ω_1^2-1/(LC)). This waveform has a decaying exponential characteristics, however starting at i(0)=0 due to the *sinh* term. However, the term driving the nerve membrane depolarization is the time-derivative of the applied coil current. Fig.2 shows both, the current waveforms (bottom graph) and their time-derivatives (top graph) in case of typical magnetic stimulation current presently used (light dashed lines, eq.9) and the energy-optimal magnetic stimulation (dark solid lines, eq.7). We note that the time-derivative of the rising exponential is growing with time vs. falling in case of the decaying exponential. From the bottom graph in Fig.2 it is already clear that the energy in the energy-optimal case will be lower. In fact, the total energy for the energy-optimal magnetic stimulation for stimulation durations of t_F=0.1 and 0.5 ms equals 13.818 and 13.157 respectively (which is also close to the asymptotic value for large t_F). The response of the nerve membrane to energy-optimal magnetic stimulation current waveform is shown in Fig.3 (light line = di/dt; dark line = membrane voltage with maximum depolarization Vthr=5 mV that is reached at t= t_F =0.1s).

The maximum depolarization with the decaying exponential *sinh* current is not reached at the end of the stimulation interval, but at a time t=0.057 ms < $t_{I\text{-}MAX}=1/\omega_2 \cdot \mathrm{atanh}(\omega_2/\omega_1)$=0.1504 ms (see Fig.4). Longer commonly used magnetic stimulation pulses will thus only increase the needed and delivered energy, but will not cause greater membrane depolarization. The corresponding energy value for t_F =0.1 and exponentially decaying sinh current equals 21.57 (with maximal depolarization equal to 5 mV) and 32.89 (with boundary V(tF)=Vthr=5 mV and maximal depolarization that equals 6.174 mV). Even in the former case, the non-optimal stimulation energy is by 56.1% greater than the energy needed for the energy-minimal waveform stimulation. The energy value for t_F=0.5 ms equals 151.87.

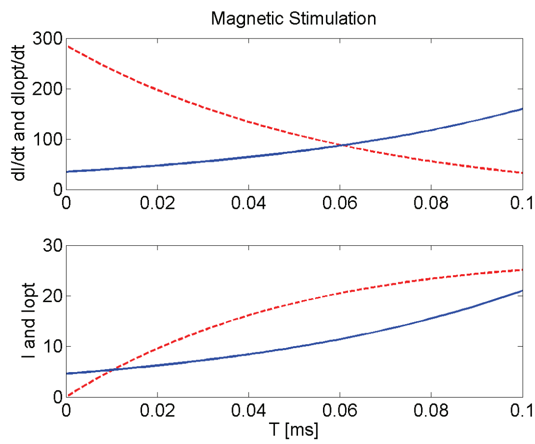

Fig. 2: Bottom graph: energy-optimal (dashed) and non-optimal (solid line), typically used stimulation coil current waveforms. Top graph: corresponding time-derivatives of the stimulation currents.

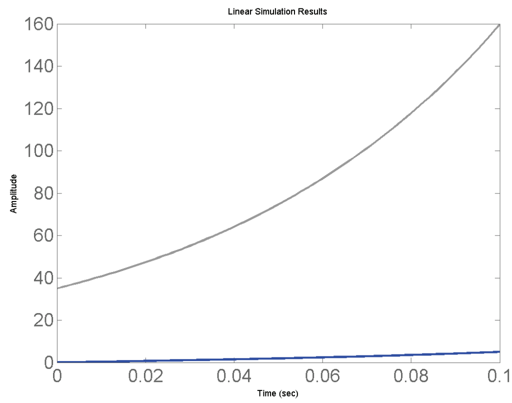

Fig. 3: Top line: energy-optimal stimulation coil current derivative, di/dt. Bottom line: resulting nerve membrane depolarization reaching the end level of 5 mV (target/desired value).

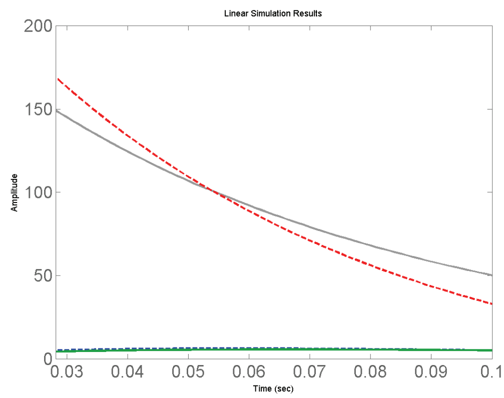

Fig. 4: Top two lines: time-derivatives of the stimulation coil current – non-optimal current waveforms. Bottom two lines: corresponding nerve membrane voltage depolarization levels peaking at about t=0.057 ms at about a 5 mV depolarization level.

Discussion and Conclusion

In spite of some early research into energy optimization of cardiac pacemakers and defibrillators via optimization of stimulation waveforms, the research in the last 2 decades focused on optimization and miniaturization of electronics and minimization of associated power consumption. Due to the advancements made, we have reached a technological developmental stage where current best devices on the market consume most of the energy due to stimulation itself [8], i.e. due to energy that is delivered via stimulation electrodes and/or magnetic stimulation coil. It is then clear that the focus on minimization of energy should thus again shift to the optimization of the stimulation waveforms, which was done in this article and in [4].

In conclusion, new theoretical results concerning energy-minimal pulse-waveform for magnetic stimulation systems were derived. With an exponentially rising energy-optimal waveform, large energy savings are potentially possible that will reduce the stimulation coil heating and allow higher stimulation repetition rates. More sophisticated solid-state inverters (power electronics, IGBT or MOSFET stages) and current-controllers are needed to allow the required current-waveform control. However, such systems have been state of the art in control of electric drives for more than 15 years. Their design and implementation is straightforward.

Next step in our research will be experimental validation of the described results. It is planned to perform stimulation studies with elicited reflexes and H-reflex measurements that will allow direct comparison of needed stimulation energy based on energy and reflex threshold measurements.

References

[1] Davey K and Epstein CM. Magnetic Stimulation Coil and Circuit Design. IEEE Trans Biomed Eng; vol. 47(11):1493-1499, 2000.

[2] Roth BJ and Basser PJ. A Model of the Stimulation of a Nerve Fiber by Electromagnetic Induction. IEEE Trans Biomed Eng; vol. 37(6):588-597, 1990.

[3] Carbunaru R and Durand DM. Toroidal coil models for transcutaneous magnetic stimulation of nerves. IEEE Trans Biomed Eng; vol. 48(4):434-441, 2001.

[4] S. Jezernik and M. Morari. Energy-Optimal Electrical Excitation of Nerve Fibers. IEEE Transactions on Biomedical Engineering; vol. 52(4): 740-743, 2005.

[5] S. Jezernik and T. Sinkjaer. Finite Element Modeling Validation of Energy-Optimal Electrical Stimulation Waveform. In: Proceedings of the 10th Annual IFESS Conference, Montreal, Canada; 346-348, July 2005.

[6] Bryson AE and Ho Y-C. Applied Optimal Control. Halsted Press/John Wiley & Sons, New York; revised edition, 1975.

[7] Robbins HM. A Generalized Legendre-Clebsch Condition for the Singular Cases of Optimal Control. IBM Journal of Research & Development; vol. 11(4):361-372, 1967.

[8] Sarpeshkar, R., C. Salthouse, J.J. Sit, M. Baker, S. Zhak, T. Lu, L. Turicchia, and S. Balster. An Ultra-Low-Power Programmable Analog Bionic Ear Processor. IEEE Transactions on Biomedical Engineering; vol. 52(4):711-727, 2005.

First Author's Address

Dr. Sašo Jezernik
Altran Group / BERATA AG
Hardturmstr. 105
CH-8005 Zürich, Switzerland
eMail: saso.jezernik@berata.ch
homepage: control.ee.ethz.ch/~jezernik

Keynote Lecture

Milan Dimitrijevic

CLINICAL PRACTICE OF FES: FROM “YESTERDAY” TO “TODAY”

Dimitrijevic MR[1,2,3]

[1] Department of Physical Medicine and Rehabilitation, Baylor College of Medicine, Houston, Texas

[2] Foundation for Movement Recovery, Oslo, Norway

[3] Ludwig Boltzmann Institute of Electrical Stimulation and Physical Rehabilitation, Vienna, Austria

Abstract

FES is an accepted treatment protocol for upper motor neuron paresis, paralysis in the neurological condition after spinal cord, head injury, stroke and other neurological upper motor neuron disorders. At the beginning FES worked like an electrophysiological brace for the correction of drop foot of ambulatory patients after stroke. When analyzing the FES accomplishments of its early period of the first two decades, it becomes evident that technology, biomedical engineering, cybernetics, feedback loops were dominating the understanding of neurocontrol of movement in individuals with upper motor neuron paralysis. Nevertheless, with better understanding of pathophysiology, spasticity and neurocontrol of altered movement due to upper motor neuron dysfunction, FES is advancing from an electrophysiological brace to a treatment modality for the improvement of control of the muscle, neuron-augmentation of residual movements and supportive procedure for the so called “spontaneous recovery” of the motor control.

In this lecture we shall illustrate barriers which delayed the clinical practice of FES in neurorehabilitation from “Yesterday” until “Today” and discuss the importance of the already present trend to apply FES during early onset of neurological condition in order to prevent the effect of disuse of non-injured portions of the CNS. Moreover, FES can have a significant role in the supporting processes of neuroplasticity in the subacute phase of the upper motor neuron dysfunction in the recovery.

Therefore if FES of “Yesterday” was an electrophysiological brace, “Today” this brace provides correction of missing neuromuscular function and at the same time it is an active external device during correction of the motor deficits interacting with the somatosensory-motor integration. Thus “Yesterday” and “Today” of the same technological approach can be very different thanks to a different understanding and assessment of “external” and “internal” components of human motor control.

FES of “Yesterday”

The begin of “Yesterday’s” FES was the effort to obtain an immediate functional muscle movement in response to electrical stimulation that started with Giaimo as early as in 1951, by the use of so called “faradic current” built from coils and relays, even before portable transistorized stimulators became available [1]. The pioneering work of the functional electrical therapy later renamed functional electrical stimulation for correction of upper motor neuron motor deficits was done by Wladimir T. Liberson. He described in his autobiography how critical for his pioneering work was his neurophysiological education gained from leading Russian neuroscientists, the opportunity to work with distinguished French neuroscientists in the field of electrical stimulation and finally the technological development of transistorized stimulators and in 1960 the availability of portable electrical stimulators for functional electrical stimulation [2].

Let us quote a description by Liberson of his discovery of peroneal FES in 1960 from his autobiography: *“With the help of Dr. Franklin Offner, a manufacturer of EEG equipment, I was able to demonstrate my idea on limited scale. I took for a model, the drop foot of a hemiplegic patient. I placed a switch in the shoe. Each time the patient would lift his leg from the floor a current would be initiated and would stimulate the tibialis anticus and peroneal muscles. The tibialis anticus elicits dorsi-flexion of the foot and its shoes. Thus a closed loop was created and an automatic correction of the hemiplegic gait was achieved.”* [3].

Before Liberson discovered “FES for correction of the drop foot” he worked in the Laboratory of Nikolai Wedensky (1852-1922), a Russian neurophysiologist in the end of the 19th century. He was introduced while working in Salpêtrière, Paris to electro diagnosis by Lapicque and Bourguignon. Liberson’s educational and research path and his physician practice supported by technological electronic development clearly illustrates the development of “Yesterday’s” FES towards new solutions for medical problems by integrating contemporary neurophysiology and technology. Liberson developed consequently other systems for the improvement of locomotion: an electromechanical brace for the stimulation of soleus and gluteus maximus activities in 1966 and "reflex walking" in paraplegic patients in 1973.

From 1963 onwards new groups appeared in addition to Liberson's pioneering work about clinical application of FES. These groups were oriented more towards medical and biological engineering, technology and cybernetics than towards neurophysiology. In their publications we can read about (1) information processing in the central nervous system, (2) proportionally controlled functional electrical simulation of the hand, (3) information content of myo-control signals for orthotic and prosthetic systems, (4) indirect and direct effects of electrical currents on pathological neuromuscular systems, (5) the effect of stimulation parameters on the modification of spinal spasticity, (6) rigidity in the parkinsonism characteristics and influences of passive exercise and electrical stimulation, (7) improved motor response due to electrical simulation of the denervated tibialis anterior muscle in humans and (8) muscle force recovery after continuous direct current stimulation of a crushed nerve. Thus, FES research and clinical practice interests moved on to a variety of dysfunctions of upper and lower motor neurons from the previous restricted interests in the development of functional movements by electrical stimulation of the corresponding nerve trunk of paralyzed or paretic muscle groups [4]. However, in this period from 1963 to 1999 further technological and clinical improvements of single and multisite FES systems for upper and lower limbs with surface and implanted electrodes continued to be the area of ongoing projects in Vienna, Ljubljana, Cleveland and some less defined but active laboratories in Sweden, Poland, Los Angeles, USA, Netherlands, Belgrade and Denmark.

This was a brief outline of "Yesterday's" FES with its characteristic origin in the early development of electrophysiology in the end of 19th and the beginning of 20th century making FES to become a clinical reality thanks to new technologies of transistorized stimulators. After this success FES advanced to a more sophisticated clinical system together with studies of upper and lower motor neuron properties of trophic and increased excitability conditions in the 60ies and 70ies of the 20th century. Let us conclude where we have been with "Yesterday's" FES and what we have been expecting from "Today's" FES by using another quotation of Liberson from his autobiography: *"Whatever will be accomplished now will be little in comparison with the progress to be expected in the future. So my younger colleagues will have a great deal to expect during their scientific lifetime".*

FES of "Today"

Where are we today and how different is the progress achieved in comparison to FES from "Yesterday"? When reviewing programs of recent International FES congresses, symposia and workshops common topics are the following: (1) denervated muscles, (2) paraplegia, upper motor neuron lesion, (3) FES cycling (4) implant technology and application, (5) command and feedback signals, stimulation parameters, (6) stimulation and closed loop control, (7) drop foot, functional restoration, (8) drop foot stimulators (9) upper extremity, functional restoration. All these examples are taken from the Vienna FES workshop series [5]. In a way we are "Today" giving priority to new developments of FES systems to solve problems of the FES clinical practice from "Yesterday" and expend the clinical practice of FES.

"Despite the high promise of functional electrotherapy and *functional electro-stimulation for improving walking of hemiplegic and paraplegic people it is still unusual to see plegic patients walking around with stimulators instead of walkers and other mechanical prosthesis, even in the nineties."* This observation of Liberson is still holding in the first decennium of the 21st century.

What we shall do "Today" to bring FES closer to the clinical practice of the so called "electrophysiological bracing" of impaired movement? I think we are already on the right track by the beginning of modest industrial interests for new technological systems and by teaching professionals involved in the rehabilitation medicine programs. Nevertheless we should not forget that the majority of users of FES systems expect ultimately an improvement of their control and force of otherwise weak movements and after some time of regular use of electrophysiological bracing they replace them by classical mechanical braces. Therefore we shall move the application of FES clinical protocols to the early onset, early phase of upper motor neuron disorders (as well as in some conditions of the lower motor neuron) in order to prevent effects of disuse and to support neuroplasticity and recovery processes.

Finally we should ask ourselves, where neurophysiology of the electrical stimulation is now at the beginning of the 21st century in comparison to the one at the end of the 19th century, which contributed so significantly to the early development of FES clinical practice, the FES of “Yesterday”? In this first decennium of the 21st century the knowledge about the generation of movements and control, the motor control of volitional, automatic and reflex activity becomes a part of our practice of FES “Today”. Advancements in the conduction and processing nervous system mechanisms are not only available in scientific publications but also in laboratories for studies of motor control in humans by application of non-invasive neurophysiological methods. Shall we ask why the pace of advancements of clinical practice of FES from “Yesterday” to “Today” is so slow in the past 50 years? Is it because the development depends from so many different professions and expertise and we did not learn how to integrate necessary knowledge, sciences and technologies towards one common achievable goal?

References

[1] Reswick JB. A brief history of functional electrical stimulation, in Neural Organization and its Relevance in Prosthetic. Fields WS and Leavitt LA (eds). Intercontinental Medical Book Corporation. New York 1973, 3.

[2] Liberson WT. Brains, Nerves, Muscles and Electricity: My Life in Science. Cohen R (ed). Smirna Press, ISBN-10: 0918266386, June 1999.

[3] Liberson WT, Holmquest ME, Scott D, Dow M. Functional electrotherapy: stimulation of the peroneal nerve, synchronized with the swing phase of gait of hemi-paraplegic patients. Arch Phys Med, 42: 101-105, 1961.

[4] Vodovnik L. Collected Works. Miklavcic D (ed). Ljubljana. ISBN 961-6371-55-X, 2003.

[5] Proceedings of the 7th Vienna International Workshop on Functional Electrical Stimulation. Mayr W, Bijak M, Jancik C (eds). ISBN 3-9000928-05-3. 2001.

Acknowledgements

The author would like to acknowledge the support of the Foundation for Movement Recovery, Oslo, Norway

Author’s Address

Milan R. Dimitrijevic
Department of Physical Medicine and Rehabilitation, Baylor College of Medicine,
6550, Fannin Suite 1421,
Houston, Texas 77030, USA
e-mail: naissus.milan@gmail.com

Session VIII

Spinal Cord Stimulation

Chairpersons
Milan Dimitrijevic (Houston, USA)
Christian Hofer (Vienna, Austria)

MODIFICATION OF MONOSYNAPTIC RESPONSES TO TRANSCUTANEOUS LUMBAR POSTERIOR ROOT STIMULATION IN MULTIPLE LOWER LIMB MUSCLES BY SUPRASEGMENTAL MOTOR TASKS IN HEALTHY SUBJECTS

Hofstoetter U[1], Minassian K[1], Persy I[1], Hofer C[1], Rattay F[2], Dimitrijevic MR[3], Kern H[1]

[1] Ludwig Boltzmann Institute of Electrical Stimulation and Physical Rehabilitation, Vienna, Austria

[2] TU-BioMed Association for Biomedical Engineering, Vienna University of Technology, Vienna, Austria

[3] Department of Physical Medicine and Rehabilitation, Baylor College of Medicine, Houston, Texas

Abstract

Dynamic task-dependent regulation of reflexes controlled by the central nervous system plays an integral part in neurocontrol of locomotion. Such modifications of somatosenory transmission can be studied by conditioning a test reflex with specific motor tasks. To elicit short-latency test reflexes we applied a novel transcutaneous stimulation technique depolarizing large-diameter posterior root afferents. These responses, termed posterior root-muscle reflexes (PRM reflexes), are equivalent to the H reflex but can be evoked in several muscles simultaneously. We elicited PRM reflexes in quadriceps, hamstrings, tibialis anterior, and triceps surae in healthy subjects. During three different conditioning-test paradigms in a standing position, i.e. unilateral single- and multi-joint lower limb movements and leaning forward/backward, we recorded characteristic movement-induced modulations of the PRM reflexes in the thigh and leg muscle groups. We could thus demonstrate that monosynaptic PRM reflexes in functional extensor and flexor muscles of thighs and legs can be elicited in upright standing subjects and can be modulated during the execution of postural maneuvers. Transcutaneous posterior root stimulation allows extending H reflex studies of a single muscle to the assessment of the synaptic transmission of two-neuron reflex arcs at multiple segmental levels simultaneously.

Introduction

The central nervous system control of somatosensory transmission is an essential element of neural control of locomotion, since successful limb movement depends on an effective interaction of specific sensory flow with motor plans. In human studies, conditioning-test paradigms utilizing the H reflex have commonly been used to assess the synaptic transmission between the afferents and motoneurons and how its gain is modulated by central neural mechanisms [1]. Due to the location of the posterior tibial nerve at the popliteal fossa, the possibility to stimulate large-diameter afferents selectively to some degree, and the state of central excitability of the corresponding two-neuron reflex arc, the H reflex of the soleus muscle is the one most commonly studied in the human lower limb. Equivalents of the H reflex can be evoked also in other lower limb muscles by peripheral nerve stimulation, however, some require special conditions and are in any case difficult to be obtained selectively from a methodological point of view, especially during movement at the stimulation site.

While in the lower limbs peripheral nerves are widely separated in numerous branches to supply all muscles, tendons, joints, and cutaneous and subcutaneous tissues, the respective axons leave or enter the lumbosacral cord via the posterior roots within a small longitudinal extent of only approx. 5 cm in humans. Thus, it appears plausible that stimulation at that site allows eliciting reflex responses at multiple segmental levels to study how the central nervous system controls the reflex gain of several lower limb muscles simultaneously.

We have demonstrated that muscle twitch responses in multiple bilateral lower limb muscles can be evoked by epidural lumbar cord stimulation [2]. These responses are initiated in large-diameter afferents within the posterior roots, are of reflex nature, and were thus termed posterior root-muscle reflexes (PRM reflexes) [3]. PRM reflexes elicited by stimulation at low frequencies (e.g. 2 Hz) are independent, segmental monosynaptic reflexes initiated within group Ia muscle spindle afferents. Thus, monosynaptic PRM reflexes are assumed to be equivalent to the H reflex, both elicited within the same afferents, either within the posterior roots or the tibial nerve trunk.

In our recent studies we have shown that PRM reflexes can also be elicited non-invasively via surface electrodes at sites corresponding to the rostro-caudal level of the lumbar cord [4].

Within this manuscript we shall demonstrate that PRM reflexes can be used to assess the central gain control of short-latency reflexes at multiple segmental levels simultaneously. In particular, we will focus on the modification of PRM reflexes by different volitional lower limb movements during the postural task of upright standing.

Material and Methods

Subjects

Transcutaneous spinal cord stimulation (tSCS) for eliciting reflex responses was conducted on three men. Subjects were numbered according to their height, with subject 1 being the tallest. The examination protocol used in this study was approved by the local ethics committee.

Stimulation and recording set-up

For eliciting PRM reflexes, single stimuli were applied through self-adhesive surface electrodes placed over the T11-T12 vertebral levels with the indifferent electrodes over the abdomen. The aim of positioning the paravertebral electrodes was to elicit motor responses simultaneously in quadriceps (Q), hamstrings (H), tibialis anterior (TA), and triceps surae (TS) bilaterally. A constant-current stimulator was used to generate symmetric, biphasic rectangular pulses with widths of 2 ms. For details see [4].

Electromyographic (EMG) activity was recorded with pairs of surface electrodes placed over the bellies of the corresponding muscles. The EMG signals were amplified using Phoenix amplifiers (EMS-Handels GmbH, Korneuburg, Austria) with a gain of 502 over a bandwidth of 10–1000 Hz and digitized at 2048 Hz per channel.

Study protocol

Three different conditioning-test paradigms were conducted on subjects standing upright: unilateral dorsi- and plantar flexion of the foot; unilateral hip and knee flexion-extension; leaning forward and backward. For each maneuver, five control responses were elicited before conditioning the responses. Stimulus intensities were adjusted to elicit control responses symmetrically in bilateral Q, H, TA, and TS with amplitudes > 100 μV. While adjusting the intensity, pairs of stimuli with interstimulus intervals of 50 ms were applied to test the occurrence of depression of the second response and thereby to verify that all responses were PRM reflexes. For the conditioning-test paradigms, only single pulses were applied.

First, subjects were asked to perform volitional unilateral dorsi- and plantar flexion, while standing on the contralateral lower limb on the edge of a small podium. To support posture, subjects could rest gently on a table with one hand. The cycle duration was approximately 6 seconds. Excessive EMG activity during voluntary innervation was avoided. Five conditioned responses were elicited with constant intensity during arbitrary segments of the two phases of the movement.

Secondly, volitional unilateral hip and knee flexion-extension movement was performed, with the joint angles being approximately 90° at the end of the flexion phase. Again, subjects used a table to stabilize equilibrium. Stimuli were applied during the actual extension and flexion movements when the lower limb was unloaded.

During the third task subjects were asked in separate trials to lean forward and backward from neutral standing, and test responses were elicited in the respective phases. In particular, subjects were asked to alter only the ankle joint angle without movements at knees and hip.

Data analysis and definition of significance

The amplitudes of the five control and the five conditioned responses were calculated and averaged for each muscle. The mean conditioned responses were normalized to the corresponding control values.

Due to the small number of subjects, we used the following criteria for a result being "significant": Since unilateral conditioning–test paradigms were conducted on both sides in separate trials in 3 subjects, arranging "left" and "right" muscle groups into "ipsilateral" and "contralateral" groups (with respect to the conditioned side) resulted in 6 values for each studied muscle. Results of these tests are only reported, if at least 5 out of these 6 responses showed the same sign of modification, i.e. either suppression or facilitation with respect to control. In case of the postural motor task testing both limbs simultaneously, categorization was not needed. A result was only taken as "significant" if being qualitatively the same (i.e. suppression or facilitation) in at least 5 of the 6 right and left muscles.

The data were analyzed off-line using Matlab 6.1 (The MathWorks, Inc., Natick, MA, USA).

Results

PRM reflexes could be elicited in all three studied subjects in a standing position. In each subject, a single pulse was effective to evoke responses bilaterally in all recorded muscles with stimulus intensities of 31-39 V, varying interindividually.

Volitional unilateral dorsi- and plantar flexion

Figure 1 shows a characteristic example of the conditioning effect of volitional unilateral single-joint movements in a standing position on PRM reflexes elicited in multiple muscles. Ankle dorsiflexion led to suppression of the ipsilateral H and TS responses and facilitation of the ipsilateral Q response, respectively. Normalized mean peak-to-peak amplitudes derived from the 3 subjects amounted to H, 0.7 ± 0.5; TS, 0.3 ± 0.2; and Q, 1.5 ± 0.8. PRM reflexes showed modifications during ankle plantar flexion without an overall tendency towards either facilitation or suppression. However, magnitudes of reflexes in H and TS were always smaller during dorsiflexion than plantar flexion. This was a consistent finding in all subjects with the mean normalized response amplitudes of H and TS being larger by the factor 0.29 and 5.36 during plantar flexion than dorsiflexion, respectively.

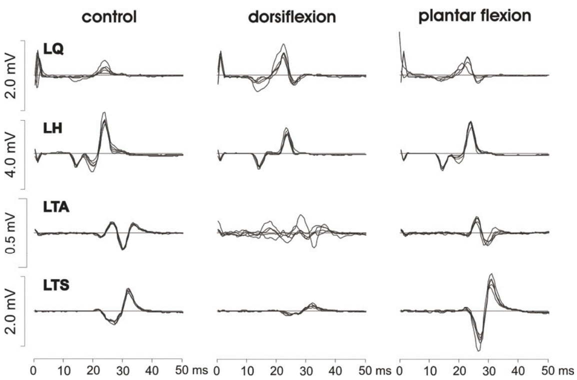

Fig. 1: PRM reflexes of Q, H, TA, and TS elicited with tSCS at 34 V in subject 1; left to right columns: controls, conditioned by dorsiflexion and plantar flexion; five stimulus-triggered responses displayed superimposed.

Volitional unilateral multi-joint movement

Figure 2 illustrates the effect of unilateral volitional multi-joint movements performed in a standing position on PRM reflexes.

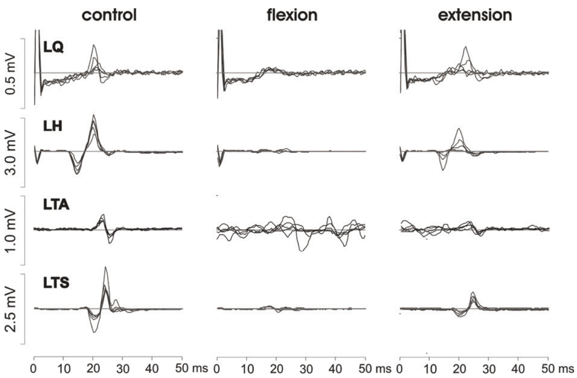

Fig. 2: PRM reflexes of Q, H, TA, and TS elicited with tSCS at 31 V in subject 3; left to right columns: controls, conditioned by hip and knee flexion and extension movements, respectively. EMG interference pattern in the LTA trace is the background EMG activity during muscle contraction.

Ipsilateral H and TS responses were suppressed during both flexion and extension phases in all subjects. Mean normalized magnitudes of responses were H, 0.2 ± 0.3 (flexion phase) and 0.4 ± 0.3 (extension phase); and TS, 0.1 ± 0.1 (flexion phase) and 0.3 ± 0.1 (extension phase). Again the attenuation was stronger during flexion than extension phases.

Postural motor tasks

Figure 3 displays the conditioning effect of postural motor tasks on the gain of PRM reflexes. Leaning forward resulted in bilateral facilitation of H, TA, and TS in all subjects with normalized amplitudes being H, 1.4 ± 0.6; TA, 1.3 ± 0.2; and TS, 2.1 ± 0.8. Leaning backward, on the other hand, reduced the H and TS response magnitudes. The same motor task led to facilitation of bilateral Q. The group results for conditioning the responses with leaning backward were Q, 2.1 ± 1.0; H, 0.5 ± 0.4; and TS, 0.5 ± 0.3.

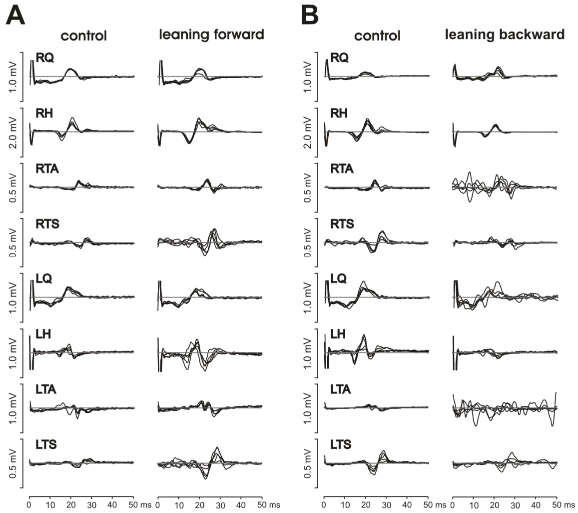

Fig. 3: PRM reflexes of right and left Q, H, TA, and TS elicited with tSCS at 39 V in subject 2; A: control responses and test responses conditioned by leaning forward. B: controls and test responses conditioned by leaning backward.

Discussion

We have applied a novel technique based on surface electrode stimulation of lumbar posterior roots for studying the motor control of monosynaptic reflexes in several lower limb muscles simultaneously. The test responses were PRM reflexes, monosynaptic muscle reflexes initiated within the posterior roots [4]. Within the present work we have shown that these test reflexes could be elicited bilaterally in four key muscles of the lower limbs in upright standing healthy subjects. We have further demonstrated that the magnitudes of the PRM reflexes could be characteristically modified by volitional motor acts during the postural task of upright standing.

The result of slight voluntary dorsiflexion of the foot was suppression of the PRM reflexes in TS just as voluntary dorsiflexion was shown to depress the monosynaptic soleus H reflex to tibial nerve stimulation [5]. This methodology allowed extending the information about reflex modification also to other muscles of the lower limbs: In addition to the reflex attenuation in TS, response amplitudes were also reduced in H and at the same time facilitated in Q. A suppression of PRM reflexes of H and TS by conditioning with unilateral voluntary dorsiflexion was also found in our previous study that was conducted on healthy subjects in a supine position [4]. Volitional unilateral movements at the hip and knee joints led to reduction of the H and TS magnitudes during both flexion and extension movements while the limb was unloaded. Although stimuli were applied at moments when the hip angle was approx. 135° during both flexion and extension, different degrees of attenuation were observed when this angle was passed in opposite directions. Leaning backward from an upright standing position requires automatic contraction of Q and TA to counteract perturbation of stance. Our tests revealed facilitation of the central excitability of the Q reflexes. PRM reflexes of H and TS, two muscles that are quiescent during this particular motor task, were suppressed at the same time. Leaning forward, on the other hand, is normally accompanied by activation of H and TS to avoid falling. This mechanism might explain the increased magnitudes of the reflexes elicited in these muscles. In addition, we also found facilitation of TA responses. The common increase of the excitability of the antagonists TA and TS might be due to the necessity to increase the effective stiffness of the ankles.

In this preliminary study, results of conditioned TA responses when superimposed with EMG background activity due to voluntary contraction were not reported since the averaging procedure to remove the background would have required more samples. Results from the side contralateral to the conditioning were not yet considered because of variability in the supporting limb while counteracting postural perturbations. Future study protocols should therefore be designed to limit movements other than relevant to the investigated tasks, either by supporting equilibrium or constraining the degrees of freedom of movements.

Conditioning test-paradigms utilizing the classical H reflex depend on the elicitation of M waves to monitor variations in stimulation efficacy due to relative movements between stimulation electrode and target nerve. Transcutaneous stimulation at the rostro-caudal level of the lumbar cord as applied in the present report did not elicit direct efferent responses (M waves). However, significant movement-related changes of the conditions at the stimulation site during the tests are not expected. Furthermore, changes of the reflex amplitudes during the motor tasks were different for the different muscles, and could be even different regarding the sign of modification. Moreover, reflexes were modified in a way to functionally meet the requirements of a particular motor task.

This approach opens a new avenue to assess the supraspinal and sensorimotor control of multiple segmental levels in both able-bodied subjects and those with different neurological disorders.

References

[1] Schieppati M. The Hoffmann reflex: a means of assessing spinal reflex excitability and its descending control in man. Prog Neurobiol, 28: 345-376, 1987.

[2] Murg M, Binder H, Dimitrijevic MR. Epidural electric stimulation of posterior structures of the human lumbar spinal cord: 1. muscle twitches - a functional method to define the site of stimulation. Spinal Cord, 38: 394-402, 2000.

[3] Minassian K, Jilge B, Rattay F, et al. Stepping-like movements in humans with complete spinal cord injury induced by epidural stimulation of the lumbar cord: electromyographic study of compound muscle action potentials. Spinal Cord, 42: 401-416, 2004.

[4] Minassian K, Persy I, Rattay F, et al. Posterior root-muscle reflexes elicited by transcutaneous stimulation of the human lumbosacral cord. Muscle Nerve, 35: 327-336, 2007.

[5] Crone C, Nielsen J. Spinal mechanisms in man contributing to reciprocal inhibition during voluntary dorsiflexion of the foot. J Physiol (Lond), 416: 255-272, 1989.

Acknowledgements

Wings for Life Spinal Cord Research Foundation. Proj.Nr. WFL-FR-001/06

EU Project Interreg III A: ”Grenzenlos bewegen” – Verbesserung der Mobilität bei postoperativer Funktionsstörungen (= funktionelle Lähmung) bei älteren Patienten mit Kniegelenksersatz. Proj.Nr. 349 / 2005

Author’s Address

Ursula Hofstoetter
Ludwig Boltzmann Institute of Electrical Stimulation and Physical Rehabilitation,
Wilhelminenspital der Stadt Wien,
Montleartstrasse 37, 1160 Vienna, Austria
ursula.hofstoetter@wienkav.at

CLASSIFICATION OF SACRAL ROOT NERVE SIGNALS WITH SIGNAL-DEPENDENT WAVELETS

Kurstjens G.A.M., Rijkhoff N.J.M., Sinkjaer T, and Farina D.

Center for Sensory-Motor Interaction (SMI), Department of Health Science and Technology, Aalborg University, Denmark.

Abstract

Traditional nerve cuff electrodes record an aggregate signal and thus provide only one channel of information. However, since most peripheral nerves innervate multiple structures, greater selectivity is needed if nerve signals are to provide sensory feedback or control signals in neuroprosthetic devices. In this study we apply a pattern recognition approach based on signal-dependent wavelets to classify sacral root nerve signals generated from mechanical stimulation of the bladder, rectum and skin. Nerve signals from the skin were discriminated from those from bladder and rectum with misclassification rates ranging 29.4-34.5% and 23.3-36.5% respectively. Discrimination between nerve signals from the bladder and rectum was more difficult (40.1-44.4% error). Doubling the length of signals used decreased the classification error for all pairs of classes (bladder-rectal: 36.6-43.8%; bladder-skin: 24.5-28.2%; rectal-skin: 12.8-28.8%). The results indicate that signal projection on optimized wavelet functions is promising for discrimination between different types of sacral root sensory nerve signals of relative short duration. Future work should include a more sophisticated classifier and extension to multi-class comparisons.

Introduction

Nerve cuff electrodes are extraneural electrodes that can provide a stable neural interface for long-term recording of peripheral nerve activity [1,2]. Recording sensory nerve signals from peripheral nerves has therefore become a realistic alternative to artificial sensors to provide feedback or control signals in neuro-prosthetic devices [3]. Such neural signals have been used in neural prosthesis systems to correct foot drop [4] and restore hand grasp [5]. In these applications, onset or changes in skin contact is detected from increases in whole nerve activity recorded from distal and purely cutaneous nerves. In other applications, electrode implantation on more proximal nerves may be necessary because of e.g. anatomical reasons or safer electrode application. For example, in case of a neural prosthesis to treat neurogenic bladder overactivity in patients with spinal cord injury, the sacral nerve roots are of interest for chronic electrode application [6]. As the sacral nerve roots provide a combined sensory and motor innervation of multiple end organs, increases in whole nerve activity can be recorded when activating mechanoreceptors in the bladder, rectum or relevant skin areas [7,8,9]. Information from the bladder can therefore only be extracted if the contribution from the bladder afferent fibers can be distinguished from the other contributing sources.

The traditional nerve cuff electrode provides only a single channel of information, but the amplitude and frequency spectrum of the recorded signals depend on the contact spacing as well as the nerve conduction velocity [1,2]. Different signal components can therefore be enhanced using appropriate filtering techniques [10] and the modality of sensory nerve signals can be determined based on the spectral properties [11]. However, the frequency bandwidths of the signal components largely overlap making classification more difficult.

Recorded nerve activity is a summation of signals of compact support (the nerve fiber action potentials) that occur at random time intervals. Traditional Fourier transformation can therefore lead to a poor representation, and other basis functions that use compact support waveforms may be preferred. The discrete wavelet transform (DWT) is an example of transformation in compact support functions, called wavelets. In the present study, a pattern recognition method based on DWT [12] was applied to nerve signal classification.

Material and Methods

Acquisition of nerve signals

Whole nerve signals were recorded intra-operatively from the extradural S3 sacral roots in spinal cord injured patients who underwent implantation of an extradural FineTech-Brindley Bladder System [9]. Afferent nerve activity was evoked by mechanical stimulation of the bladder (rapid saline bolus infusions), rectum (rapid balloon distensions), and skin (tapping and stroking the appropriate dermatome by hand).

In this study, only data from two representative patients were used. Following re-sampling from tape (20 kHz), the nerve signals were band-pass filtered (300 Hz - 3 kHz) and signal portions exceeding 2*SD the mean baseline activity were selected and split into epochs of 512 samples. Three classes of nerve signals were formed: bladder (B), rectum (R) and skin (S). The number of epochs used for training and validation of the different data sets is shown in table 1.

	Patient 1		**Patient 2**	
	Training	*Test*	*Training*	*Test*
Bladder	420	336	472	448
Rectum	120	80	240	200
Skin	120	120	60	60

Table 1: Number of signal epochs per data set and class.

Discrete wavelet decomposition

The discrete dyadic wavelet transform (DWT) is the decomposition of the signal in a set of basis functions, formed by scaling and translation of unique function of compact support (the wavelet):

$$\Psi_{j,k}(t) = 2^{-j/2}\,\Psi\left(2^{-j}t - k\right) \qquad j,\ k \text{ integer}$$

where j indicates the scaling and k the shift of the mother wavelet [13]. The DWT can be performed through the application of a bank of FIR filters within the framework of the multiresolution analysis (MRA) [13]. In the MRA a scaling function $\phi(x)$ generates the approximation spaces and the wavelet function the detail spaces. These two functions satisfy the two-scale equations:

$$\phi(x/2) = \sqrt{2}\sum_n h(n)\phi(x-n)$$

$$\psi(x/2) = \sqrt{2}\sum_n g(n)\phi(x-n)$$

where $h(n)$ and $g(n)$ are the scaling and wavelet filter coefficients, which are the impulse responses of a discrete low-pass and high-pass filter, respectively. In case of orthonormal wavelets, $g(n)$ can be obtained from $h(n)$:

$$g(n) = (-1)^{1-n}h(1-n)$$

The entire decomposition is thus obtained from h(n).

Wavelet parameterization

The scaling filter should satisfy some constraints to be associated to orthogonal wavelets. For a length L, there are L/2+1 conditions on the filter coefficients [14] and thus L/2-1 degrees of freedom.

Classification

The signals were decomposed using the DWT. The N (signal length) wavelet coefficients $c_x(j,k)$ were normalized to make the representation space insensitive to the waveform occurrence time instants, and a set of the normalized marginals $\mathbf{F}_m = [m_x(1),\ldots, m_x(J)]$ of the DWT was calculated. This vector provides information on the distribution of the wavelet coefficients over J bands, giving a representation of the energy distribution over different dyadic scaled frequency bands when using a particular wavelet shape. Filter lengths of 4 and 6 were chosen for the scaling filter, thus leading to one ($\theta = [\alpha]$) or two ($\theta = [\alpha\ \beta]$) free parameters.

The parameters that defined the wavelet were optimized for discrimination between classes. Let ω_i be the training signals for the class Ω_i, with $i = 1,\ldots, I$, where I is the total number of classes. The representative $R^F_{\omega i}$ of class ω_i was then calculated as the average vector of the feature spaces $\mathbf{F}_{\omega i}$ computed for training signals of that class. In this study, only a relative simple classifier based on the rule of nearest representative was used. Two types of distance measures were tested: Euclidian distance and the Kullback distance.

The probability of classification error, as estimated from the training set, was used as quality criterion to optimize the classification of the nerve signals using the feature space computed from the DWT. The parameter defining the optimum wavelet was that corresponding to the minimum classification error estimated from the training set. A test set separated from the training set was used to provide the results on the misclassification rate (table 1).

Results

Single component design parameter

Fig. 1 shows the probability of classification error estimated for the learning sets when attempting to separate nerve signals (L = 512) from the bladder and rectum of patient 1 based on the Euclidian distance between feature spaces. With using only one component for the design parameter, $\theta = [\alpha]$, the misclassification can be seen to vary significantly for different mother wavelets constructed by α. The value of α resulting in a minimum of the average of the two error probabilities defined the optimum wavelet for decomposition of this particular training set and was used for classification of the signals in the test sets to obtain the final error probability. Classification was also performed for the data set pairs of bladder-cutaneous (B-C) and rectum-cutaneous (R-C), and for the same signals but with length 2L (but for only N/2 signals), see table 2A. Results obtained when using the Kullback distance between feature spaces for the same classifications are given in table 2B.

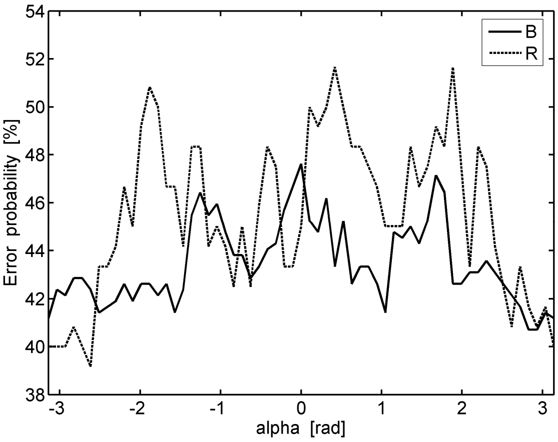

Fig. 1: Probability of error [%] estimated from the training sets for varying θ = [α] values when classifying nerve signals from the bladder (B) and rectum (R) of patient 1 (Euclidian distance, L = 512).

A	**Patient 1**		**Patient 2**	
	L = 512	*L = 1024*	*L = 512*	*L = 1024*
B–R	41.6 (40. 6)	36.3 (35.4)	44.4 (43.4)	41.8 (40.4)
B–C	33.4 (28.9)	27.5 (22.3)	34.0 (23.5)	24.6 (11.8)
R–C	30.8 (28.3)	24.2 (21.2)	23.3 (20.6)	12.8 (9.6)

B	**Patient 1**		**Patient 2**	
	L = 512	*L = 1024*	*L = 512*	*L = 1024*
B–R	40.1 (38.9)	36.9 (34.5)	42.4 (43.3)	44.0 (40.5)
B–C	31.9 (27.1)	25.0 (21.0)	29.4 (20.5)	25.6 (15.6)
R–C	36.5 (25.8)	28.8 (16.7)	26.5 (17.7)	19.0 (12.1)

Table 2: Misclassification rates [%] for classification of the nerve signals in the test (training) sets for optimum θ = [α] and based on the Euclidian (**A**) and Kullback (**B**) distance between feature spaces.

The misclassification rates obtained for the training sets were lower than for the test sets in both patients. Furthermore, the misclassification rate decreased when increasing the length of the signal, and thereby increasing the resolution of the wavelet decomposition. Finally, although in most cases the lowest misclassification rates on training set were obtained using the Kullback distance, the final misclassification rate on the validation sets was often smaller when the Euclidian distance measure was used.

Two component design parameter

Enlarging the design parameter to a two-component vector θ = [α β] increases the complexity of the mother wavelets, increasing the variation in misclassification rate obtained for different values of θ (Fig. 2). This lead to lower minimum probabilities of misclassification in all training sets, see table 3. However, when using the optimal training values on the test sets, no improvement was found compared to the results when using a single component θ only.

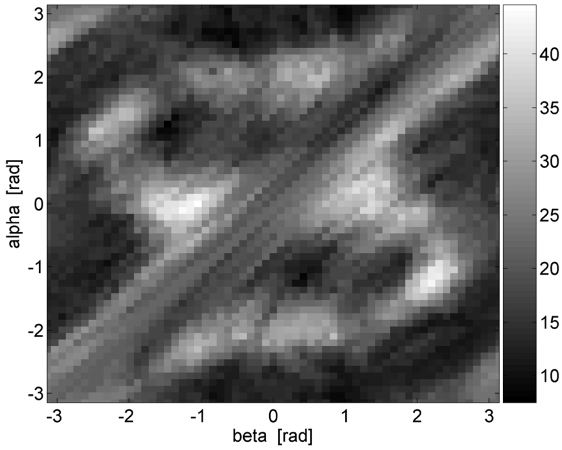

Fig. 2: Probability of error [%] estimated from the training sets for varying θ = [α β] values when classifying nerve signals from the rectum and skin of patient 2 (Kullback distance measure, L = 1024).

A	**Patient 1**		**Patient 2**	
	L = 512	*L = 1024*	*L = 512*	*L = 1024*
B–R	44.6 (37.8)	43.3 (35.0)	41.3 (41.4)	38.9 (38.7)
B–C	34.5 (28.0)	27.6 (18.5)	32.2 (19.2)	28.2 (9.7)
R–C	29.8 (25.0)	23.8 (17.5)	27.3 (17.1)	19.5 (7.9)

B	**Patient 1**		**Patient 2**	
	L = 512	*L = 1024*	*L = 512*	*L = 1024*
B–R	41.6 (27.8)	37.9 (32.1)	42.5 (41.3)	41.7 (35.9)
B–C	35.7 (26.0)	27.7 (17.4)	33.1 (17.3)	24.5 (11.4)
R–C	32.7 (24.2)	25.0 (14.2)	25.3 (15.2)	24.5 (7.5)

Table 3: Misclassification rates [%] for classification of the nerve signals in the test (training) sets for optimum θ = [α β] and based on the Euclidian (**A**) and Kullback distance (**B**) between feature spaces.

Discussion

The signal-dependent wavelet classification method was originally developed for classification of surface electromyogram signals and was based on the observation that these signals are composed of compact support waveforms which are scaled depending on the conduction velocity of intracellular muscle action potentials and on the depth of the muscle fibers forming the motor unit [12]. Signals recorded from cuff electrodes show a large resemblance to this observation as they depend on the geometry and diameter of the cuff electrode and the nerve conduction velocity [1,2]. This resemblance suggested that wavelet decomposition could also provide a natural representation for neural signals recorded from cuff electrodes and therefore form a suitable feature space for classification.

The results in this study demonstrate that sacral root nerve signal from the bladder, rectum and sacral dermatome can be classified based on a feature space obtained by the discrete wavelet transformation. Mother wavelets found optimal for the set of training signals were however not that optimal for the test set. Both data sets were assumed to contain signals from the same source but the actual signals were different, thus the information content was not exactly the same. Furthermore, despite normalization of the wavelets coefficients, the misclassification rate seemed consistently smaller for signals with larger difference in SNR and nerve signals from the bladder/rectum versus the cutaneous nerve signals. Although some degree of cross talk cannot be excluded because both organs are mechanically connected, this would suggest that both organs are innervated by population of nerve fibers with similar diameter distributions.

A previous study used relatively long signals (1.25 s) to classify sacral root nerve signals based on their autocorrelation function [11]. The current study demonstrates that classification based on wavelet decomposition of considerably shorter signals is possible; doubling the epoch lengths used in this study would further decrease the probability of misclassification more whilst still using signals that are ten times shorter. Lower classification errors could also be obtained using non-filtered data. Band-pass filtering removes information from certain decomposition levels leading to a smaller feature space. Alternatively, feature spaces based on different methods and a more sophisticated classifier could be tested.

Finally, only two-class comparisons were made in the present study, but for signals from peripheral nerves that proximal as the sacral roots, it is important to consider all sources the neural activity could originate from. Future work should therefore extend to the multi-class case, also allowing a direct comparison of the current method with previously used classification methods, as well as data from a larger patient group.

References

[1] Stein RB, Nichols TR, Jhamandas J. Stable long-term recordings from cat peripheral nerves. Brain Res, 128: 21-38, 1977.

[2] Hoffer JA. Techniques to study spinal-cord, peripheral nerve, and muscle activity in freely moving animals. Neurometh, 15: 65-145, 1990.

[3] Sinkjaer T, Haugland M, Struijk JJ, and Riso R, Long-term cuff electrode recordings from peripheral nerves in animals and humans. In: Windhorst U and Johansson H (eds) Modern techniques in neuro-science, Springer Verlag, p 787-802, 1999.

[4] Haugland M and Sinkjaer T, Cutaneous whole nerve recordings used for correction of footdrop in hemiplegic man. IEEE Trans Rehabil Eng, 3: 307-15, 1995.

[5] Inmann A, Haugland M, Haase J, Biering-Sorensen F, and Sinkjaer T, Signals from skin mechanoreceptors used in control of a hand grasp neuroprosthesis. Neuroreport, 12: 2817-20, 2001.

[6] Rijkhoff NJ, Wijkstra H, van Kerrebroeck PE, and Debruyne FM, Urinary bladder control by electrical stimulation: review of electrical stimulation techniques in spinal cord injury. Neurourol Urodyn, 16: 39-53, 1997.

[7] Jezernik S, Wen JG, Rijkhoff NJ, Djurhuus JC, and Sinkjaer T, Analysis of bladder related nerve cuff electrode recordings from preganglionic pelvic nerve and sacral roots in pigs. J Urol, 163: 1309-14, 2000.

[8] Jezernik S, Grill WM, and Sinkjaer T, Detection and inhibition of hyperreflexia-like bladder contractions in the cat by sacral nerve root recording and electrical stimulation. Neurourol.Urodyn, 20: 215-30, 2001.

[9] Kurstjens GA, Borau A, Rodriguez A, Rijkhoff NJ, and Sinkjaer T, Intraoperative recording of extradural sacral roots in spinal cord injured patients. J Urol, 174: 1482-7, 2005.

[10] Jezernik S and Grill WM. Optimal filtering of whole nerve signals. J Neurosci Methods, 106: 101-10, 2001.

[11] Jezernik S, Grill WM, Sinkjaer T. Neural network classification of nerve activity recorded in a mixed nerve. Neurol Res, 23: 429-34, 2001.

[12] Maitrot A, Lucas MF, Doncarli C, Farina D. Signal-dependent wavelets for electromyogram classification. Med Biol Eng Comp, 43: 487-92, 2005.

[13] Mallat SG. A Theory for Multiresolution Signal Decomposition - the Wavelet Representation. IEEE Trans Pattern Anal Mach Intell, 11: 674-93, 1989.

[14] Lawton WM. Necessary and sufficient conditions for constructing orthonormal wavelet bases. J Math Phys, 32: 57-61, 1991.

Author's Address

Mathijs Kurstjens
Dept. Health Science and technology
Aalborg University
Fredrik Bajers Vej 7, D3
DK-9220 Aalborg
Denmark
eMail: mku@hst.aau.dk
homepage: www.hst.aau.dk

Keynote Lecture

Glen Davis

CARDIORESPIRATORY, METABOLIC AND BIOMECHANICAL RESPONSES DURING FES LEG EXERCISE: HEALTH AND FITNESS BENEFITS

Davis GM, Hamzaid NA and Fornusek C

Rehabilitation Research Centre, Discipline of Exercise and Sport Sciences, University of Sydney, Australia

Abstract

Functional electrical stimulation (FES) - induced leg exercise offers the potential for individuals with lower-limb paralysis to otherwise gain some benefits conferred by leg exercise. Although its original intent was to re-activate the leg muscles to produce functional upright mobility, as a rehabilitation therapy FES-evoked exercise increases whole body metabolism of an individual with SCI so that they may gain general and localized health and fitness benefits. The physiological and psychosocial responses during FES-evoked cycling, standing, rowing, leg extension or stepping have been extensively explored for over 20 years. Some of the advantages of such exercise include augmented cardiorespiratory fitness, promotion of leg blood circulation, increased activity of specific metabolic enzymes or hormones, greater muscle volume and fibre size, enhanced functional exercise capacity such as strength and endurance, and altered bone mineral density. Positive psychosocial adaptations have also reported amongst SCI individuals who undergo FES-exercise. This paper presents a position review of the available literature on the effects of FES-evoked exercise since the earliest date until 2007, to warrant a conclusion about the current status and potential of FES-evoked exercise for paralysed people.

Introduction

Exercise has proven beneficial not only for the able-bodied population, but also for people affected by spinal cord injury (SCI). SCI can lead to moderate-severe muscle paralysis, loss of lower limb functionality and usually results in lower levels of aerobic fitness. Consequently, individuals with SCI have significant reduction in their fitness and health due to a restricted movement capacity as a wheelchair user.

Since the 1960's, functional electrical stimulation (FES) – induced muscle contractions have been widely used as a rehabilitation therapy or an exercise regimen for the paralysed lower-limbs of people with SCI. With FES, paralysed legs can be artificially evoked to produce otherwise unattainable dynamic movements, such as cycling, rowing, knee extension, standing and stepping

Despite some periodic literature reviews [1- 5], there has not been a careful systematic review investigating the possible benefits of FES-evoked exercise after SCI. In this current position review, the authors have employed 'systematic techniques' to investigate the hypothesis that FES-evoked lower-limb exercise might promote certain health and fitness benefits amongst its users.

Material and Methods

A systematic search of published sources was performed in common electronic databases within the date range 1900-February 2007. In addition, relevant journal and conference proceedings were hand searched. Studies were limited to human research, but could be in any language, as long as English abstract translations were available. A preliminary search was conducted to identify the types of FES-evoked exercise that were accessible to SCI individuals, as well as the available outcomes of the activities. This preliminary search also generated the inclusion criteria keywords utilised in the systematic search of databases.

The collective conclusions of the obtained RCTs and quasi-RCTs were not sufficient to position the status of the topic under question. The authors finally included other non-randomised or controlled studies, which mainly comprised clinical trials, to encompass all available scientific evidence pertaining to FES-induced exercise.

Health and fitness outcomes were divided into six broad domains: (i) skeletal muscle morphology and biochemistry, (ii) cardiovascular and haemodynamic responses, (iii) generalised metabolic responses, including aerobic fitness, (iv) bone mineral density and stiffness, (v) functional changes in exercise capacity, and, (vi) psychosocial outlook.

Only two of the categories will be reported herein due to restrictions of manuscript length, but all are reported in detail in a full-length manuscript under peer-review.

Results

From over 865 potentially relevant publications, 177 fulfilled the primary inclusion criteria. Only one study was a randomised-controlled trial (RCT), and 31 quasi-experimental investigations were identified. The remainder were cross-sectional or cross-over research designs, which included clinical trials and patient surveys.

Discussion

Skeletal muscle morphology and biochemistry:

Six primary studies, meeting the inclusion criteria, collectively suggested that FES-exercise may reverse or ameliorate muscle atrophy, and that muscle fibres can shift their morphological characteristics towards that of sedentary, able-bodied people. Baldi and colleagues [6], demonstrated via a randomized-controlled trial, that 6-months of FES-cycling could prevent muscle atrophy, compared to FES-isometric muscle contractions or no exercise at all. SCI individuals who performed regular cycling realised no reductions in their lower-limb and glutei lean mass after 3-months of training and after six months had significantly increased these measures of muscularity. Similar results were found by other authors in controlled and quasi-experimental studies.

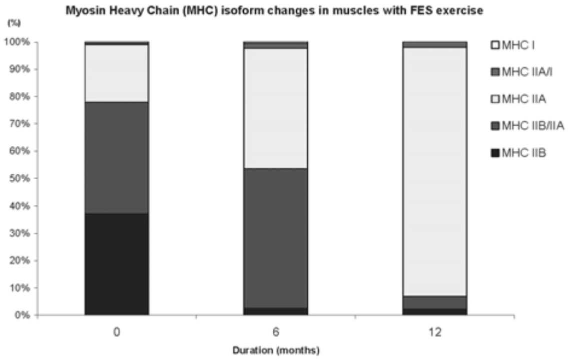

Fig 1: Muscle fibre composition changes following FES-evoked cycling. [8]

Factors that affect muscle properties during FES exercise include external loading and neuromuscular stimulation frequencies. A controlled study by Crameri and co-workers [7] revealed that isometric FES-training, with a high external loading, significantly increased muscle fibre cross-sectional areas, and produced a shift towards Type I (slow twitch oxidative) fibres with higher aerobic enzyme activity and muscle oxygenation. Other authors have shown this to be particularly effective for low-frequency FES isometric training in terms of improving fatigue resistance. In general, a number of reports have demonstrated that muscle morphology and biochemistry, sampled through needle biopsy, are significantly altered after FES-exercise training towards characteristics of able-bodied individuals. With regular FES cycling exercise, muscle fibre shifts towards greater fatigue resistance (i.e. from equal amounts of type IIB and type IIA fibres to a majority of type IIA) [8]

In summary, one randomized-controlled study, either randomized or controlled investigations and quasi-experimental evidence all generally support positive muscle sequelae in adherents to FES-exercise training programs. These data lend support to our position statement that such exercise programmes promote peripheral muscle health and fitness benefits for the SCI population.

Generalised metabolic responses, including aerobic fitness:

In general, the metabolic responses to FES-evoked leg exercise are different to an analogous form of exercise performed voluntarily. These differences of physiological responses may be explained by two principle underlying factors. First, significant muscle atrophy and fibre type shift to predominantly fast-twitch morphology (i.e. IIA, IIB, IIX) and the biochemical adaptations that accompany these yields working muscles that are smaller and less able to engender aerobic metabolism during exercise. Second, lack of central neural drive to below the spinal lesion results in usual control of local blood flow being absent or attenuated (i.e. predominantly sympathetic vasoconstriction to inactive vascular beds).

Nevertheless, six primary studies meeting the inclusion criteria of randomized, controlled or randomized-controlled designs clearly demonstrated enhanced aerobic metabolism after variable periods of FES-exercise training. In general there is a trend for these improvements of exercise metabolism to be greater in individuals with lower initial aerobic fitness levels (e.g. tetraplegics, older SCI). For example De Carvalho and Cliquet [9] performed a controlled study whereby subjects with tetraplegia undertook either FES-treadmill training (with partial body weight support) or no exercise for 6-mo duration. Following training the FES-training group had increased their oxygen uptake ($l \bullet min^{-1}$) and exercise metabolism ($j \bullet kg^{-1} \bullet s^{-1}$) by 36% and 33%, respectively, during treadmill gait. In contrast, the control group realised only a small increase of their oxygen uptake and no change of metabolism during FES-evoked knee extension exercise.

In a previous study, Hooker and co-workers [10] observed that sedentary paraplegics and tetraplegics increased their peak oxygen uptake by 10% after only twice-weekly FES-cycling over 19 weeks. Additionally, the authors observed a significant decrease in markers for anaerobic metabolism accompanying a trend to lower lactate-driven expired ventilation during submaximal effort cycling exercise – these presume a shift to higher aerobic leg metabolism accompanying the fibre-type changes noted by other researchers [7, 8].

There is strong evidence that FES-induced leg exercise when combined with voluntary arm effort ("hybrid" exercise) is a potent stressor to evoke changes of aerobic fitness and metabolism. During arm exercise with concurrent FES-cycling or FES-rowing oxygen uptake is higher that arm or leg exercise alone. In a non-randomized controlled trial, Mutton and colleagues [11] demonstrated that FES-cycling alone increased aerobic fitness after SCI, but when combined with arm cranking, peak oxygen uptake was further incremented (Fig. 2). Interestingly, there was a trend for arm exercise peak oxygen uptake to be augmented after hybrid exercise (Fig 2; ▲-▲), but not after FES-leg cycling alone (Fig. 2; ♦-♦), indicating there is no "cross transfer of training effect" (a.k.a. cross-training) from leg exercise to arm performance in SCI individuals. In other quasi-experimental findings and a randomized study similar results have been noted for hybrid exercise comprising rowing, cycling and stepping.

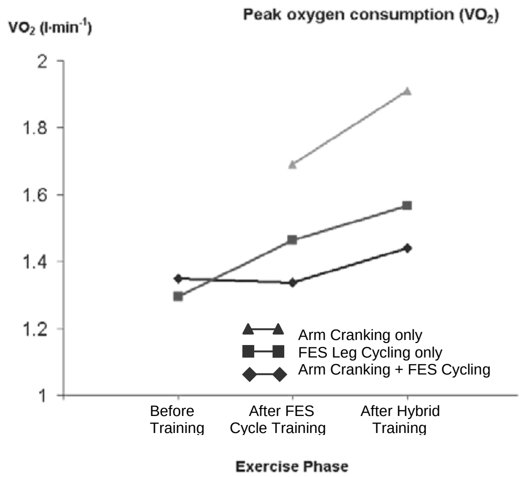

Fig. 2: Peak oxygen uptake before FES-Leg cycling, after FES-leg cycling only, and after hybrid leg cycling + arm crank training. [11]

Generally, all literature surveyed lends support to the view that FES-evoked leg exercise promotes positive metabolic responses and enhances aerobic fitness for people with SCI. Randomized and controlled investigations and quasi-experimental evidence of different modes of FES-evoked exercise conditioning all contribute to the same conclusion.

Biomechanical Considerations:

Recent evidence has emerged that some of the major physiological adaptations that transpire after FES-evoked exercise may be related to biomechanical factors. In particular, both external load on the muscle [7] and the rate/cadence of exercise [12, 13] contribute to altered muscle forces, morphological adaptation and external power production.

Fornusek and colleagues [12, 13] have shown that the 'force-velocity' relationship of voluntarily-activated muscle is also evident for muscles stimulated via FES. In a randomized study, the authors demonstrated higher pedal torques at slower FES-cycling cadences (Fig 3; left panel). In contrast, greater power outputs were observed at higher cycling cadences (Fig 3; right panel). In another randomized investigation, Fornusek and Davis [12] observed differing rates of fatigue over 35-min of leg cycling between torque production and power output. Whether higher muscle forces or greater external power outputs are more important for beneficial physiological adaptations to emerge is currently unknown. One of the authors will report some preliminary findings pertaining to this question at this meeting.

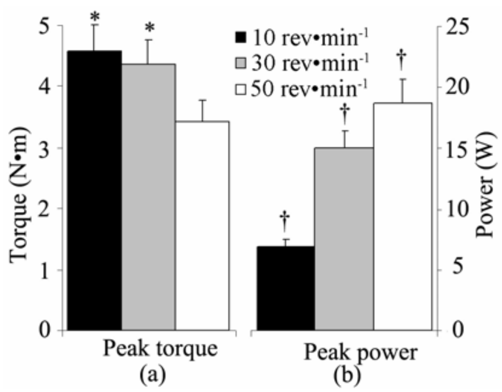

Fig. 3: Instantaneous peak torque and peak power during constant-velocity FES-cycling at 10, 30 and 50 rev•min^{-1}. Symbols * and † denote different than 50 rev•min^{-1} and 10 rev•min^{-1}, respectively ($p<.05$) [12].

Another biomechanical consideration is which mode of exercise (e.g. cycling, rowing, knee extension or stepping) has then greatest 'dose potency' to elicit beneficial adaptations to muscle, general metabolism, bone and psychosocial outcomes? While some of these modes lend themselves to hybrid arm and leg exercise to a greater degree, and thereby might augment aerobic fitness more, there is not sufficient evidence currently to recommend one as superior over the others.

Irrespective of the FES exercise mode, by producing artificially-evoked movement of their paralysed legs, people with SCI can improve their health and fitness. Figure 4 illustrates one model illustrating the interrelationships of some of the primary health and fitness outcomes after FES-evoked exercise.

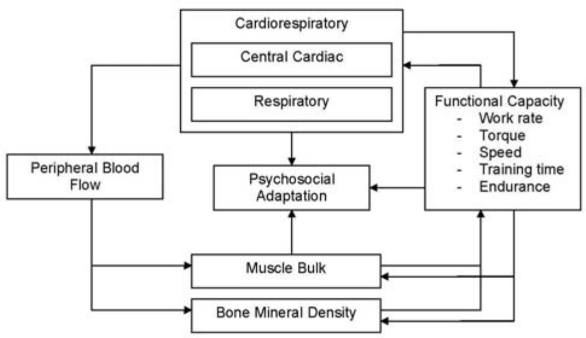

Fig. 4: Relationship between Health and Fitness Outcomes following FES-evoked Exercise [14]

In the two domains of health and fitness outcomes reported herein, positive effects of FES-evoked exercise were identified. Even though increments of health and fitness were lower than observed for age-matched able-bodied cohorts performing voluntary exercise, there were significant trends for altered skeletal muscle size and morphology, enhanced metabolism, including aerobic fitness, greater functional exercise capacity and improved psychosocial outlook. Less consistently observed were positive changes of bone mineral density and stiffness after FES-training.

References

[1] Glaser RM. Functional neuromuscular simulation. Exercise conditioning of spinal cord-injured patients. Int J Sports Med, 15:142-148, 1994

[2] Andrews BJ, Wheeler GD. Functional and therapeutic benefits of electrical stimulation after spinal cord injury. Current Opin Neur, 8:461-466, 1995

[3] Janssen TWJ et al. Clinical efficacy of electrical stimulation exercise training: Effects on health, fitness and function. Top Spinal Cord Inj Rehabil, 3:33-49, 1998

[4] Raymond J, Crameri R. Electrical stimulation for individuals with spinal cord injury. Am J Med Sports, 4:209-222, 2001.

[5] Wilder RP et al. Functional electrical stimulation cycle ergometer exercise for spinal cord-injured patients, J Long term Eff Med Implants, 12:161-164, 2002.

[6] Baldi JC, Jackson JC, Moraille RD, Mysiw WJ. Muscle atrophy is prevented in patients with acute spinal cord injury using functional electrical stimulation. Spinal Cord, 36: 463-469, 1998.

[7] Crameri RM, Cooper P, Sinclair PJ, Bryant G, Weston A. Effect of load during electrical stimulation training in spinal cord injury. Muscle Nerve, 29:104-11, 2004.

[8] Andersen JL, Mohr T, Biering-Sorensen F et al. Myosin heavy chain isoform transformation in single fibres from m. vastus lateralis in spinal cord injured individuals: effects of long-term functional electrical stimulation (FES). Pflugers Arch, 431:513-518, 1996.

[9] De Carvalho CL, Cliquet A. Energy expenditure during rest and treadmill gait training in quadriplegic subjects Spinal Cord , 43:658-663.2005.

[10] Hooker S, Scremin E, Mutton DL et al. Peak and submaximal physiologic responses following electrical stimulation leg cycle ergometer training. J Rehabil Res Develop, 32:361-366, 1995

[11] Mutton DL, Scremin AM, Barstow TJ et al (1997) Physiologic responses during functional electrical stimulation leg cycling and hybrid exercise in spinal cord injured subjects. Arch Phys Med Rehabil, 78:712-718, 1997.

[12] Fornusek C, Davis GM. Maximising muscle forces via low cadence FES-cycling. J Rehabil Med, 36:232-237, 2004.

[13] Fornusek C, Sinclair PJ, Davis GM. The force–velocity relationship of paralyzed quadriceps muscles during functional electrical stimulation cycling. J Neuromodulation, 10:68–75, 2007.

[14] Hamzaid NA, Davis GM. Health and fitness benefits of functional electrical stimulation-evoked leg exercise on leg-paralysed individuals. International Sports Science Conference 2006, Malaysia.

Acknowledgements

A portion of this work has been drawn from a systematic review conducted by the second author, as a component of her PhD studies. The second author received funding from a JPA Malaysian Government Scholarship. This research was also supported by a NSW Ministry of Science and Medical Research Program Grant.

Author's Address

Glen Davis
Rehabilitation Research Centre, Discipline of Exercise and Sport Sciences, University of Sydney, Australia
g.davis@usyd.edu.au

Session IX

Sports and Fitness

Chairpersons
Glen Davis (Sydney, Australia)
Nick Donaldson (London, UK)

REAL-TIME PCR TO FOLLOW THE RESPONSE OF MUSCLE TO TRAINING

Moore L[1], Coulson J[1], Salmons S[1], Jarvis J[1]

[1]Human Anatomy and Cell Biology, Liverpool, UK

Abstract

Considerable progress has been made over the last few decades in understanding the response of healthy skeletal muscle to changes in activity pattern or loading. Such responses can be followed by measuring parameters directly related to whole muscle function - mass, force, power, speed and fatigue resistance. It is, however, difficult to make such measurements sequentially in animal models, and complex to do so in exercising or stimulated human subjects. This is partly because the response of fibres to changes in activity develops slowly: it takes several weeks for a new equilibrium to be attained in terms of myosin isoform shifts, muscle growth or atrophy, or changes in the volume of mitochondria.

At the level of gene expression, on the other hand, changes in response to activity take place within hours. Such changes could provide an early indication of the eventual functional outcome of particular exercise or stimulation regimes.

We have searched for sequences in the rat and mouse genomes suitable for use in primer design for quantitative PCR. Our aim is to evaluate the level of expression of the myosin isoforms 1, 2A, 2X and 2B, whose relative abundance determines muscle contractile speed and power, and of IGF1 and myostatin, whose expression affects the balance between protein synthesis and degradation and thus the mass of a skeletal muscle.

Some published primer sequences are inappropriate for quantitative PCR according to the latest sequence data for rat. Our new primers have been tested in standard PCR and shown to produce single bands on agarose gels stained with ethidium bromide. The sizes of the PCR products are appropriate for use in quantitative PCR and should therefore enable us to measure the response of muscle to controlled changes in activity or loading in terms of the expression of our targeted genes. Sufficient mRNA for quantitative PCR can be extracted from a few hundred milligrams of tissue. Quantitative PCR of small needle biopsy samples should therefore allow us to predict at an early stage the direction of changes resulting from a training regime, and if necessary, to follow the long term effect by minimally-invasive re-sampling.

THE EFFECTS OF A LONG TERM PROGRAMME OF FUNCTIONAL ELECTRICALLY STIMULATED CYCLING ON MUSCLE PROPERTIES AND POWER OUTPUT IN SPINAL CORD INJURED PEOPLE.

Duffell LD[1], Donaldson N de N[2], Newham DJ[1]

[1] Division of Applied Biomedical Research, King's College London, London, United Kingdom

[2] Implanted Devices Group, University College London, London, United Kingdom

Abstract

Functional electrical stimulation (FES) for cycling has the potential to substantially improve health and quality of life for people with spinal cord injury (SCI).

We recruited 11 SCI people (9 male) aged 41.8 ± 2.3 years (mean ± SEM) >2 years post injury to train for one hour 5 times weekly for one year. Muscle properties were measured at three monthly intervals and explosive PO was measured at the end of training. Comparative measurements were made in able bodied (AB) subjects.

Muscle strength and fatigue resistance improved progressively and significantly (P <0.05). Paradoxically, muscle speed tended to increase. Fatigue resistance was greater in SCI people after training than in AB however muscle strength and PO remained modest.

Although long term intense training substantially improved fatigue resistance, PO generally remained inadequate for outdoor recreational cycling. Nevertheless, SCI people were able to cycle for long periods on a smooth flat surface allowing them to participate in indoor sporting events. The training intensity used was probably the maximum practical limit for SCI people, thus additional variables must be optimised to improve PO during FES cycling.

Introduction

A complete spinal cord injury (SCI) results in the absence of motor and sensory function below the lesion level, which has substantial implications on the individual's health and well being. There is a reduction in the size [1, 2] and strength [2, 3] of paralysed muscles as well as a slow-fast fibre type transformation [1, 4]. Reduced physical activity results in an increased susceptibility to cardiovascular diseases, obesity, type II diabetes [5] and pressure sores [6] within this population.

Functional electrically stimulated (FES) cycling has been used as a means to reduce or reverse some of the physiological complications of SCI [7] and gives SCI people the opportunity to participate in recreational and sporting activities. Electrically stimulated (FES) exercise has been shown to increase muscle size [1] and strength [3, 8] although SCI people remained substantially weaker than able bodied (AB) people [3]. Fibre type transformation from type IIx to IIa has also been demonstrated following FES training [9] but not to slow type I fibres [3, 9]. Studies that have used measures of contractile speed have provided contrasting results [1, 2]. Increased blood flow [9, 10] and aerobic capacity [1, 9] have also been demonstrated following FES training, resulting in increased fatigue resistance [3, 8].

Relatively low levels of FES training (30 minutes, 3 per week) have been reported to improve power output (PO) during FES cycling [9]. However the PO remained low, below 50 Watts, even after a year [11]. It is important to use a regimen that induces a combination of improved contractile speed, power and fatigue resistance. High frequency, long duration sessions appear to be most effective for improving both PO and endurance [12]. The effects of an intense, long term and high frequency FES training programme on muscular adaptations and PO during FES cycling have not been investigated previously.

We studied the effects of an intensive year-long FES cycle training programme at 50Hz on muscular properties of SCI people. We measured the isometric strength, contractile speed and fatigue resistance of quadriceps before and at three-monthly intervals during training as well as explosive PO during FES cycling after training.

Material and Methods

Subjects:

Eleven volunteers (9 male) with complete SCI <T3 for 10.7 ± 2.1 years (mean ± SEM) were recruited from three centres (London, Nottwil and Glasgow). Their age was 41.8 ± 2.3 years, height 175.6 ± 2.3 cm and body mass 73.6 ± 4.2 kg. The study was approved by local ethics committees.

Training

Each subject was given a Stanmore Stimulator and taught correct electrode placement and skin care. Initial training involved FES of 4 muscle groups. Once subjects were able to turn the pedals of the trike for 10 mins they progressed to cycle training.

For cycle training, the glutei, quadriceps and hamstring muscles were stimulated bilaterally in all subjects. Calf stimulation was also used in 6 of the 11 SCI subjects. Subjects were requested to perform cycle training for a total of 52 weeks using a commercial tricycle (Trice, Inspired Cycle Engineering Ltd, UK), which was set up and maintained in the subjects' homes. Three weekly sessions were performed for the first 8 weeks, 4 during the subsequent 8 weeks and 5 thereafter giving a total of 236 scheduled sessions.

Subjects were asked to maintain a cadence of 45-55 rpm using a stimulation frequency of 50 Hz. Initial training duration was set according to individual ability. The target duration was increased to 60 min as endurance capacity permitted and subjects were requested to maintain this duration thereafter, if possible. Resistance at the pedals was adjusted by a combination of a trainer resisting the back wheel and the gears.

Laboratory Tests

Quadriceps isometric contractile properties were measured on all 11 subjects before and at 3 monthly intervals during training. Quadriceps maximal strength (3 monthly) and explosive PO during FES cycling (12 months) was also measured on 5 of these subjects (London). For comparative purposes 10 healthy, untrained AB people subjects (aged 30.6 ± 3.2 years, height 172.6 ± 1.8 cm, body mass 69.4 ± 3.1 kg) were assessed once for the strength of a maximal voluntary contraction (MVC), contractile properties and explosive power output.

For quadriceps strength and contractile properties subjects were seated on a dynamometer in isometric mode with the knee at 90º flexion and the ankle strapped to the dynamometer lever arm. Square wave pulses of 200μs duration were delivered through electrodes (12 x 12 cm) bandaged onto the anterolateral aspect of the thigh. The analogue torque was recorded on a personal computer for subsequent analysis.

For maximal strength in SCI people, the stimulation intensity at 50Hz was increased incrementally until the torque either reached a plateau or declined. To avoid risk of bone fracture the frequency was reduced to 20Hz when 50Nm force was attained and the equivalent strength at 50Hz was estimated using the 20:50Hz ratio. AB people performed three MVCs of 2-3 s duration with a 10 s rest between each and the highest value was recorded.

The stimulation intensity was then reduced to that which generated 20-30% of the maximal strength for both SCI and AB subjects for subsequent tests (contractile properties and fatigability). Where maximum strength was not measured (Glasgow and Nottwil), subsequent tests were carried out at an intensity that generated a visible contraction.

The force:frequency characteristics were assessed by stimulation at 1 Hz for 5 s and 10, 20, 50 and 100 Hz for 2 s each, with a 2s interval between each burst. The torque generated by each frequency was expressed as a percentage of that at 100 Hz. Relaxation rate was measured as the time taken for the force to fall from 80 to 40 % of plateau stimulation force at 100 Hz.

Fatigability was measured over 3 min of stimulation at 40 Hz for 250 $ms.s^{-1}$ [13]. The percentage of force loss at 1, 2 and 3 min was calculated.

The peak explosive PO was measured after training in SCI people and once in AB people. For the SCI people the FES was ramped up to maximum intensity over 10 seconds and maintained for 10 min. AB people were given verbal encouragement to cycle voluntarily at their maximum ability for 30 seconds.

One way analysis of variance assessed changes throughout the training programme. If a significant change was identified, post-hoc analysis was carried out using the Students T-Test for paired data. SCI subjects were compared with AB using the Students T-test for unpaired data ($\alpha = 0.05$).

Results

Training

As judged by the diaries, compliance was good with the subjects taking an average of 57 weeks (range 51-69 weeks) to complete the programme. Average compliance for each quarter was 100, 85, 78 and 76 % throughout training (85% overall). Average session duration was 51.0, 56.7, 59.1 and 61.5 minutes for each quarter of training.

Laboratory Tests

The maximal strength of the SCI group (5 subjects) increased progressively and significantly throughout (P =0.012; Fig. 1).

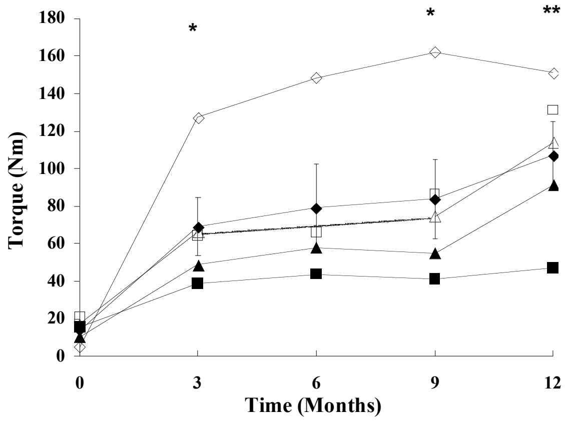

Fig. 1: Maximal strength in 5 SCI people throughout the training programme (significant change from baseline *P <0.05; **P <0.01).

SCI people initially had a higher 1:100Hz ratio than the AB (P<0.01) but otherwise there were no significant differences between groups. The relative forces at the three lower frequencies tended to drop progressively, shifting the force:frequency relationship of SCI people towards that of AB. The only significant change was a reduction in the 1:100Hz ratio at 6 months (P<0.02). The relaxation rate before training tended to be slower in SCI than AB people (35.4 *vs* 30.9 ms) though not significantly (P> 0.05). After 3 months, the relaxation rate had become slightly, but not significantly, faster in SCI people (29.8 ms; P>0.05) and thereafter remained unchanged.

After three months of training, quadriceps fatigue resistance had improved significantly (P<0.001; Fig. 2) and continued to do so until 9 months of training (P<0.001). After 9 months of training SCI people were less fatigable than AB (P<0.05).

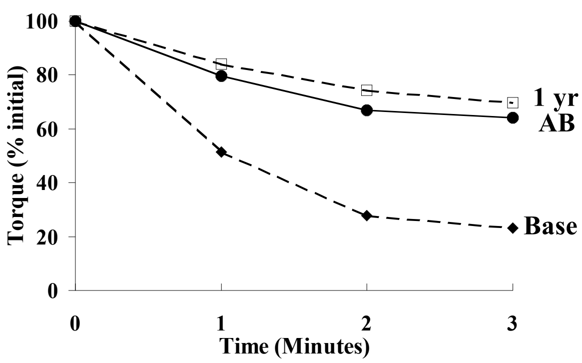

Fig. 2: Force loss over 3 minutes of stimulation for SCI people before (Base) and after (1 yr) training, also for AB subjects.

After training maximal strength and explosive PO were 33 and 13% that of AB people, respectively (Fig. 3). Despite greater than normal fatigue resistance, the SCI subjects fatigued rapidly during FES cycling (Fig. 4) attaining an average steady state of 13.5 (SEM 3.6) Watts.

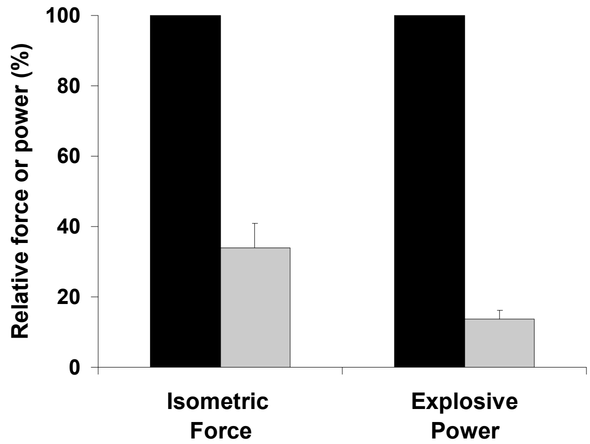

Fig. 3: Isometric force and explosive PO for SCI people after training (grey), relative to AB values (black).

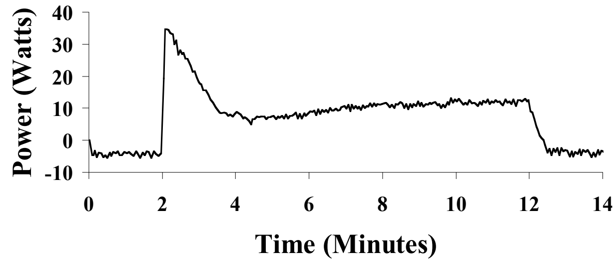

Fig. 4: PO during 10 minutes FES cycling at 100% stimulation intensity for one SCI subject after the training programme.

Discussion

FES cycle training significantly improved quadriceps muscle strength however, despite the high stimulation frequency (50Hz), high intensity (up to 5 hours per week) and long duration (1 year) of the training programme, both muscle strength and explosive PO remained modest after training. This was disappointing although the subjects could participate in indoor sporting events for several hours[1]. The contractile speed of the quadriceps paradoxically increased but became closer to AB values and fatigue resistance improved becoming greater than AB people.

Before training, maximal torque was low (13.8 ± 2.8 Nm) and increased throughout the training period, but remained significantly less than that of AB. AB people are able to voluntarily activate virtually all their motor units, which is not the case with this method of stimulation. Additionally the

[1] http://www.medphys.ucl.ac.uk/research/impdev/fits/

training carried out by SCI people was perhaps more likely to increase endurance than strength and the use of a greater resistance might be a better stimulus for hypertrophy [14].

Before training, relative force generation at low frequencies (1 and 10Hz) was high, which reduced with FES cycle training, as reported previously in shorter term studies [3]. Relaxation rate was slow at the start of training and became faster. This is paradoxical because one would expect a fast-slow fibre conversion The reason for the observed reduction in contractile speed is unclear but could be due to increased oxidative metabolism [3, 8] and muscle blood flow [10]. Changes in tendon properties due to immobility and training might also have influenced these results.

Quadriceps fatigue resistance was significantly less in untrained SCI than AB subjects, which had significantly improved after only 3 months training, as reported previously [2, 3]. This was due presumably to increased blood flow [10] and capillary:fibre ratio [9]. Fatigue resistance continued to improve until 9 months when SCI people were more fatigue resistant than AB. This is a suprising result, probably due to the long-term programme involving high frequency and long duration training sessions inducing a more pronounced conversion towards oxidative fibre types. Indeed, a transformation from Type IIx towards Type IIa fibres has been reported to occur to a greater extent after 12 months training [4]. It has also been reported that FES exercise carried out two hours per day, 5 days per week results in progressive increases in the number of fibres containing the mRNA transcript for MHC I [17].

After training SCI people attained explosive PO that was 13% that of AB and fatigued rapidly, sustaining an average PO of 13.5 Watts. The reasons for this rapid fatigue and low PO are unclear, and deserve further investigation.

In conclusion, a long-term intensive programme of FES cycling can increase muscle strength and improve fatigue-resistance to a level comparable with AB people. However PO remains low, limiting the recreational and health benefits of this form of exercise. Future work should aim to optimise PO during FES cycling.

References

[1] Rochester LBM. Influence of electrical stimulation of the tibialis anterior muscle in paraplegic subjects. 2. Morphological and histochemical properties. Paraplegia, 33:514-522, 1995.

[2] Gerrits HL, de Haan A, Hopman MTE, et al. Contractile properties of the quadriceps muscle in individuals with spinal cord injury. Muscle & Nerve, 22:1249-1256, 1999.

[3] Rochester LBM, Chandler CS, Johnson MA, Sutton RA, Miller S. Influence of electrical stimulation of the tibialis anterior muscle in paraplegic subjects. 1. Contractile properties. Paraplegia 1995a; 33:437-449.

[4] Andersen JL, Mohr T, Biering-Sorensen F, et al. Myosin heavy chain isoform transformation in single fibres from m. vastus lateralis in spinal cord injured individuals: effects of long-term functional electrical stimulation (FES). Pflugers Archive, 431:513-518, 1996.

[5] Myers J, Lee M, Kiratli J. Cardiovascular disease in spinal cord injury: an overview of prevalence, risk, evaluation, and management. American Journal of Physical Medicine and Rehabilitation, 86:142-152, 2007.

[6] Johnson RL, Gerhart KA, McCray J, et al. Secondary conditions following spinal cord injury in a population-based sample. Spinal Cord, 36:45-50, 1998.

[7] Petrofsky JS, Phillips CA, Heaton HH, et al. Bicycle ergometer for paralyzed muscle. Journal of clinical engineering, 9:13-19, 1984.

[8] Gerrits HL, Hopman MTE, Sargeant AJ, et al. Effects of training on contractile properties of paralyzed quadriceps muscle. Muscle & Nerve, 25:559-567, 2002.

[9] Crameri RM, Weston A, Climstein M, et al. Effects of electrical stimulation-induced leg training on skeletal muscle adaptability in spinal cord injury. Scandinavian Journal of Medicine and Science in Sports, 12:316-322, 2002.

[10] Gerrits HL, de Haan A, Sargeant AJ, et al. Peripheral vascular changes after electrically stimulated cycle training in people with spinal cord injury. Archives of Physical Medicine and Rehabilitation, 82:832-839, 2001.

[11] Mohr T, Andersen JL, Biering-Sorensen F, et al. Long term adaptation to electrically induced cycle training in severe spinal cord injured individuals. Spinal Cord, 35:1-16, 1997.

[12] Sutherland H, Jarvis JC, Kwende MMN, et al. The dose-related response of rabbit fast muscle to long-term low-frequency stimulation. Muscle & Nerve, 21:1632-1646, 1998.

[13] Burke RE, Levine DN, Salcman M, et al. Motor units in cat soleus muscle: physiological, histochemical and morphological characteristics. Journal of Physiology, 238:503-514, 1974.

[14] Crameri RM, Cooper P, Sinclair PJ, et al. Effect of load during electrical stimulation training in spinal cord injury. Muscle & Nerve, 29:104-111, 2004.

Acknowledgements

We gratefully acknowledge funding from the EPSRC and INSPIRE.

Author's Address

Dr. Lynsey Duffell, Division of Applied Biomedical Research, Kings College London, UK. Lynsey.duffell@kcl.ac.uk

Effect of FES Cycling Cadence on Muscle Girth, Strength, and Endurance after SCI: Preliminary Results

Fornusek C, Russold M, Davis GM

Rehabilitation Research Centre, Discipline of Exercise and Sports Sciences, University of Sydney, Sydney, Australia

Abstract

The aim of this study was to investigate the effects of FES cycling training cadence on muscle hypertrophy, strength, and endurance. Three untrained subjects with paraplegia (T4-T11) performed six weeks (18 sessions, 30 min each leg) of training on an isokinetic FES cycle ergometer. One leg was randomized to be trained at 10 rev•min^{-1} and the other at 50 rev•min^{-1}. Pre- and post tests were performed on each leg using a Biodex isokinetic testing system to measure isometric strength and endurance. Thigh circumferences were also assessed. The cycling performance of each leg was also measured during 30-min of cycling at each pedalling cadence. Results indicated that cycle training led to increased thigh girth (hypertrophy), enhanced isometric strength, and improved cycling performance at both cadences. Trends from the data also suggest that training at 10 rev•min^{-1} resulted in greater hypertrophy, muscle strength, and isometric endurance than at 50 rev•min^{-1}. Additionally, there was a trend for cycling performance improvement being greater for the legs trained at the slower cadence. The data collected to date suggest that if muscle strength and girth are desired from FES cycling, then low cadence training should be considered.

Introduction

FES cycling is a common and popular exercise mode for persons with spinal cord injury (SCI). During FES cycling, a computer system electrically stimulates paralyzed leg muscles to produce a repetitive cycling motion.

Regular FES cycling can be used for both health benefits and recreation [1]. The health benefits bestowed to the paralysed limbs by FES cycle training include increased muscle strength and mass, augmented blood flow, and improved muscle oxidative capacity.

Due to the large muscle mass employed, FES cycling has the potential to induce significant cardiovascular health benefits. However, current FES cycling protocols only improve fitness in highly deconditioned individuals (i.e. high level tetraplegics, older SCI). This is probably because the intensity of FES cycling is not sufficient to induce continuous gains, causing patients' performances to plateau within six months of training.

One limitation of FES cycling is that the muscle forces produced are low resulting in modest strength and hypertrophy gains compared to other FES exercises [2, 3]. With some success, FES cycling research has improved exercise intensity by focusing on training protocols, stimulation patterns, and biomechanical analysis. However, little research has investigated the effect of FES training cadence on muscle force; most likely because until recently the majority of FES cycles were based on an early prototype with a restricted cadence range (i.e. 35-50 rev•min^{-1}).

Recent FES cycle ergometers can produce isokinetic FES cycling over a wide range of cadences (i.e. 5-60 rev•min^{-1}) [4]. Preliminary studies have shown that low cadence FES cycling can produce larger muscle forces than traditional cadences (35-50 rev•min^{-1}). Therefore, low cadence FES cycling should produce greater strength and hypertrophy.

The purpose of this research was to compare the muscle strength, hypertrophy, and endurance improvements bestowed by FES cycling at low versus high cadences.

Material and Methods

Subjects:

Three subjects with paraplegia participated in this study. All of the subjects were at least 5 years post injury. All were sedentary and none of the subjects had performed FES exercise within the last two years. The sex, age, injury level, ASIA classification, and medication of each subject are shown in Table 1.

Table 1: Subject Characteristics

Subject	Sex	Age (y)	ASIA Grade	SCI Level
1	F	42	A	T4
2	M	39	A	T4
3	M	53	C	T11

The stimulation-evoked strength of the muscles ranged from very weak (subject 2, no anti-gravity) to weak (subject 1 & 3, antigravity). Subject 2 had a Baclofen intrathecal pump implant which eliminated muscle spasm activity below the level of his injury. Consequently his muscles were very atrophied and weak. Subject 3 had very weak voluntary control of knee extension and hip flexion.

Training protocol:

Training consisted of 6 weeks of FES cycling (30 min per session, 3 times per week). One leg was randomized to train at 10 rev•min^{-1} and the other at 50 rev•min^{-1}. Each leg was trained separately and the order of training was reversed each day. The muscle stimulation angles for cycling at 50 rev•min^{-1} were adjusted to be 30° earlier than during cycling at 10 rev•min^{-1}; this accounted for the force rise time of the muscle contractions.

FES cycling training and testing equipment:

A Custom designed FES cycle was used [5]. The components of the cycle were an isokinetic Motomed Viva2, a DS2000 muscle stimulator (University of Sydney), and a Laptop computer (Pentium II MMX). The DS2000 Stimulator delivered 250 μs pulses at a frequency of 35 Hz. Stimulation amplitude was initially set to 70 mA and linearly ramped to reach 140 mA after 10 min. Stimulation was held at 140 mA for rest of training session. Stimulation was delivered via pre-gelled self-adhesive electrodes.

Pre and post training measurements:

Thigh girth

As a measure of muscle hypertrophy, thigh circumference was measured at 2 positions (10 and 20 cm above the top of the patella).

Quadriceps strength and endurance

Isometric quadriceps contractions were performed on a Biodex 2000 Isokinetic Dynamometer (Biodex Medical Systems, Shirley, NY) with the knee extended at 90°. The contractions were elicited by an ExoStim™ neuromuscular stimulator that delivered monophasic square wave pulses at 35 Hz with a pulse width of 250 μs. Stimulation amplitude was ramped from 0 to 125 mA in 5 s then held at 125 mA for 50 s. The following variables were measured from the resulting torque data: peak torque, torque integral, and the torque 50 seconds after peak stimulation was reached. Endurance was calculated as torque at 50 s divided by peak torque and represented as a percent.

Cycling performance

The average power output that could be produced during a 30 minutes FES cycling was tested with each leg at both cadences (10 & 50 rev•min^{-1}). For subject 1, only the left quadriceps was stimulated in the cycling test. This was so that quadriceps cycling performance could be correlated with the quadriceps isometric tests. However, considering the untrained state of the muscles and the very small forces that subject 2 could generate, it was decided that for remaining subjects quadriceps, gluteals, and hamstrings should be stimulated during the cycling tests. The stimulation protocol used during testing was similar to that used in the training sessions, that is, muscle stimulation amplitude was ramped from an initial value of 70 mA up to 140 mA over the first 10 min.

Results

Leg circumference

Consistently larger gains in girth were obtained by the leg trained at the slower cadence of 10 rev•min^{-1} (Table 2). Overall, the circumference of the legs trained at slow speed gained around 5% (ΔGirth$_1$ 5.4 ± 1.5%, ΔGirth$_2$ 5.0 ± 1.7%) whereas the legs trained at 50 rev•min^{-1} only gained around 2.5% (ΔGirth$_1$ 2.6 ± 1.3%, ΔGirth$_2$ 2.8 ± 1.7%).

Table 2: Thigh girths pre & post training

Training Cadence (rev•min^{-1})	Subject	Girth 1 (cm) Pre	Girth 1 (cm) Post (%Δ)	Girth 2 (cm) Pre	Girth 2 (cm) Post (%Δ)
10	1	36	39 (+8.3%)	43.5	47 (+8.0%)
	2	38	39.5 (+3.9%)	43.5	44.5 (+2.2%)
	3	37.5	39 (+4.0%)	40.5	42.5 (+4.9%)
50	1	37.5	39.5 (+5.1%)	44.5	47.2 (+6.1%)
	2	38	38.5 (+1.3%)	43	43.5 (+1.2%)
	3	38.5	39 (+1.3%)	44	45 (+1.0%)

Quadriceps isometric strength and endurance

Table 3 shows quadriceps performance during the isometric strength testing for subject 1 and 2; subject 3 experienced spasms and hip flexion during measurements making it very difficult to analyze the data; therefore isometric strength tests for subject 3 are not shown. Isometric strength gains were found in all legs of subjects 1 and 2. The trend was for larger gains in the leg trained at 10 rev•min^{-1}. Endurance (indicated by % of maximum torque produced after 50 s of contraction) was increased by training a 10 rev•min^{-1} but decreased by training at 50 rev•min^{-1}. Torque time integral (not shown) was increased by both cadences, but more so by low cadence training.

Table 3: Muscle strength and endurance

Training cadence (rev•min^{-1})	**Subject**	**Max Torque (Nm)**		**%Max at 50 s**	
		Pre	**Post** (%Δ)	**Pre**	**Post** (%Δ)
10	1	16.1	25.4 (+58%)	35.4	50.7 (+43%)
	2	4.0	8.3 (+109%)	60	46.9 (-22%)
50	1	16.7	21.3 (+28%)	27.3	32 (+17%)
	2	1.7	3.5 (+106%)	2 7.4	12.3 (-45%)

Cycling performance

Six weeks of FES cycling increased the power output at both the trained and the non-trained cadence. The average power outputs produced by each leg at the two different pedalling cadences are displayed in table 4. In general, power output increased more for the leg which was trained at low cadence (i.e. 10 rev•min^{-1}).

Table 4: Cycling Performance

Training cadence (rev•min^{-1})	**Subject**	**Mean Power$_{10rpm}$**		**Mean Power$_{50rpm}$**	
		Pre	**Post (%Δ)**	**Pre**	**Post (%Δ)**
10	1*	0.41	1.55 (+280%)	0.77	3.30 (+329%)
	2	†	0.38	†	0.96
	3*	1.34	2.01 (+50%)	1.56	3.4 (+118%)
50	1	0.37	1.20 (+222%)	0.88	2.91 (+230%)
	2	†	0.19	†	0.76
	3	1.82	2.24 (+23%)	3.2	4.0 (+20%)

* results for this subject represent quadriceps data, † power output could not be measured due to weakness of subject.

Discussion

The trends in these data suggest that slow cadence cycling induced greater muscle hypertrophy, and improved isometric strength and endurance. Cycling training improved performance at the trained cadence but also demonstrated a 'crossover effect' by improving cycling performance at the untrained cadence.

Isometric contractions

The strength and hypertrophy data are fairly consistent with prior research: 1) larger forces are produced during slow cadence FES cycling [4] and 2) larger muscle forces result in increased strength and hypertrophy gains for paralyzed muscle [3]. Similar to our results, Crameri and colleagues [3] found that higher force isometric contractions produced greater hypertrophy than cycling at 50 rev•min^{-1}.

These preliminary findings suggest that isometric endurance was increased by 10 rev•min^{-1} FES-cycling but reduced by 50 rev•min^{-1} FES-cycling. This is not surprising considering that at 10 rev•min^{-1} quadriceps contractions last 1.5 seconds each whereas at 50 rev•min^{-1} the duration of contraction is only 300 ms. The much longer (i.e. 5-fold) contractions at 10 rev•min^{-1} might be expected to condition the muscles for long duration isometric contractions more than the very brief contractions at 50 rev•min^{-1}. Relative endurance may have decreased in the legs trained at 50 rev•min^{-1} because strength (and energy demand) increased but the capacity to supply energy during long isometric contractions has not increased at the same rate.

Cycling performance

Cycling performance was increased by both cadences, but the trend indicates that training at 10 rev•min^{-1} may have enhanced performance more. The performance of the leg trained at 10 rev•min^{-1} probably increased more due to a greater improvement in muscle strength [6].

At 50 rev•min^{-1} the rapid intermittent stimulation results in rapid fatigue [4]. It is possible that a portion of the performance improvements for the leg trained at 50 rev•min^{-1} could be due to greater fatigue resistance to intermittent stimulation. If this was the case, then training with a combination of slow and fast cadences could result in the greatest improvements at 50 rev•min^{-1}.

Clinical applications

The principle benefits of FES cycling are that it; 1) can exercise a large muscle mass which induces a large cardiorespiratory response, and, 2) can be used for recreation. Traditionally, FES cycling has been employed at higher cadences. The drawback of using higher cadences is that muscles forces are low due to a high fatigue rate [4]. Lower cadence training should assist with improving and accelerating gains from FES cycling training. In the past leg extension with weighted cuffs has often been used to prepare subjects for FES standing. However, the accelerated strength and isometric endurance gains due to low cadence FES cycling could also make it a suitable precursor for FES activities which require significant muscle strength like standing and walking.

The subjects used in this study were spinally injured. However, these results should be applicable to other subject populations who can perform FES cycling exercise, for example persons with stroke.

The limitations of this research are that only a few subjects have been completed and these subjects possess a wide range of muscle strengths. Six weeks is not a very long training program. A longer training program and greater subject numbers should clarify any differences present.

Conclusions

Further subjects need to be trained and tested to confirm the trends seen in this data from only a few subjects. Slow cadence cycling resulted in greater hypertrophy, and isometric strength and endurance. Depending on the training goals, slow cadence FES cycling could play an important role in optimising FES training for a particular individual.

References

[1] Raymond J, Crameri R. Electrical Stimulation for Individuals with Spinal Cord Injury. Am J Med Sports, 228:209-222, 2001.

[2] Dudley GA, Castro MJ, Rogers S, Apple DF, Jr. A simple means of increasing muscle size after spinal cord injury: a pilot study. Eur J Appl Physiol Occup Physiol, 80:394-396, 1999.

[3] Crameri RM, Cooper P, Sinclair PJ et al. Effect of load during electrical stimulation training in spinal cord injury. Muscle Nerve, 29:104-11, 2004.

[4] Fornusek C, Davis GM. Maximizing muscle force via low-cadence FES cycling. J Rehabil Med, 36:232-237, 2004.

[5] Fornusek C, Davis GM, Sinclair P, Milthorpe B. Development of an isokinetic functional electrical stimulation cycle ergometer. Neuromodulation, 7:56-64, 2004.

[6] Petrofsky JS, Laymon M. The effect of previous weight training and concurrent weight training on endurance for functional electrical stimulation cycle ergometry. Eur J Appl Physiol, 91:392-398, 2004.

Acknowledgements

The authors are grateful to Miss Anna Lauffer and Mrs Luciola Menezes for their assistance in this project. This research is supported by a NSW Ministry of Science and Medical Research Program Grant.

Author's Address

Ché Fornusek

Rehabilitation Research Centre
Exercise, Health, and Performance
Faculty of Health Science
University of Sydney

cfornuse@mail.usyd.edu.au

QUANTITATIVE COMPARISON BETWEEN DIFFERENT STIMULATION STRATEGIES DURING CYCLING BY SPINAL CORD INJURED PATIENTS

<u>Pella A.</u>[1], Ferrante S.[1], Duffell L.[2], Pedrocchi A.[1], Perkins T.[3], Newham D.[2], Donaldson N.[3]

[1]Bioengineering Department, Politecnico di Milano, Milan, Italy

[2]Applied Biomedical Research Group, Kings College London, London, UK

[3]Implanted Devices Group, Department of Medical Physics, University College London, London, UK

Abstract

Spinal cord injured (SCI) people are able to produce cyclical leg motion by means of functional electrical stimulation (FES).

The aim of our study was to compare 3 stimulation strategies already developed in literature called Perkins, Nitlab and Munich, in order to identify an optimal pattern in terms of power output (PO) and metabolic effort.

Three SCI subjects performed three days of trials of FES cycling, each day using one of the test strategies.

Mechanical and metabolic data were acquired and blood samples were taken to analyze the presence of lactate.

An index for each subject was defined to normalize the outcome measurements (PO and energetic effort) in order to make the different sessions comparable.

The metabolic readings were within normal ranges.

A non parametric statistical test showed significant differences between the strategies in the intra-subject analysis.

The results showed that patients trained and familiar with one strategy (Perkins) could obtain optimal performance with it.

In patients that had trained with an alternative FES protocol (rowing), the Nitlab strategy produced on average 15% and 23% more PO per revolution than Perkins and Munich, respectively.

A comparative analysis of the PO expressed during the exercise and of the metabolic cost represents a first step toward understanding how the optimal strategy depends on the subject's characteristics and their training goals.

Introduction

SCI people are able to produce cyclical leg motion by means of controlled functional electrical stimuli. Many studies have clearly shown that a period of regular cycling exercise induces physiological adaptation [1]. However, this artificial exercise has started to be used not only in rehabilitation but also for sport and competitions (http://www.medphys.ucl.ac.uk/research/impdev/fits/index.htm).

Efficiency is defined as the ratio of the work produced to metabolic energy input [2]. Glaser *et al.* suggested that FES cycling is an inefficient exercise [3]: the efficiency obtained by SCI patients was about 5% while the efficiency produced by able-bodied subjects performing cycling under volitional control was about 20%.

The major effort in optimizing efficiency of FES cycling was directed toward defining an optimal stimulation strategy [4, 5, 6]. The term stimulation strategy refers to the ranges of crank angles over which stimulation is applied to the various muscle groups.

The 3 strategies chosen were called Perkins, Nitlab and Munich. The first one, Perkins, is the strategy developed and used in the University College of London [4]. This strategy focused on the maximization of PO and has been used in competitions. The second strategy was conceived in the Nitlab laboratory of the Politecnico of Milan [5]. It was defined as a biomimetic strategy based on the muscle activation patterns of healthy persons cycling. It aimed at rehabilitation to maintain exercise for as long as possible. The third strategy was called Munich because it was representative of the method used by Szecsi *et al.*in that Bavarian city [6]. This strategy was used to train SCI athletes for competitions, and was chosen because two of those performed very well (including fastest over 1km). Even though this strategy should be optimized for each athlete, we decided to use fixed ranges for all our subjects, assuming that the anthropometrical data of these patients were quite similar.

The aim of this study was to compare the 3 selected strategies used in cycling exercise on SCI people. Our performance measures were: PO; metabolic efficiency, and stimulation efficiency (work out of stimulus charge in).

Material and Methods

Subjects

The programme was approved by the Kings College London Ethics Committee and the subjects provided written informed consent prior to participation. Three SCI subjects with a complete lesion took part to the study. Anthropometric data are shown in Table 1.

	Age	Lesion	YPI	H [cm]	W [Kg]
S1	48	T9	7	167	54
S2	60	T4	12	173	85
S3	51	T5	8	171	72

Table 1: Details for the subjects who participated in the study. YPI=Years Post Injury; H=Height; W=Weight.

These subjects were trained and regularly carried out long (endurance based) training sessions. S1 and S2 were trained with FES cycling since 2004 and 2005, respectively, both using the Perkins strategy. S3 was trained as a rower for more than 2 years. FES rowing involved only the quadriceps and hamstrings.

Experimental setup

The experimental setup consisted of a motorized recumbent tricycle modified for FES cycling with a shaft encoder to measure the crank angle and with orthoses mounted on the pedals to fix the ankles. An SRM sensor measured the torque between the crank shaft and the cycle chain. The tricycle was mounted on a home trainer and the system was connected to a PC running Matlab Simulink for data acquisition and control over the motor and the stimulation sequence (stimulation ranges for each muscle in respect to the crank angle). The motor is controlled via a cadence controller [2]. An 8 channel stimulator (Stanmore Stimulator®) was used and quadriceps, hamstrings, gluteal and calf muscle groups were stimulated through surface electrodes. Metamax 3B™ was employed for the gas exchange readings. A Super GL *Easy*™ was used to analyze the amount of lactate in blood.

Protocol

Each subject attended three sessions at Kings College London. During the initial session stimulation parameters for each muscle group were set. The current amplitude was fixed for all subjects at 130 mA.

To set the PW value we stimulated each muscle during isometric conditions while measuring the force produced. During the trial the PW was increased in steps of 10 μs until the peak of the muscle force output was reached.

Once the patient was seated on the tricycle an initial hardware test was carried out in order to check the setup. Then, the mask was attached to the subject for the gas exchange readings and the ECG electrodes were attached.

A description of a single session is reported in Fig.1. To reach steady state of metabolic readings, we started each session with a period of rest (at least 3 minutes, r in Fig. 1) and a period of passive cycling (at least 4 minutes, p_I in Fig. 1) at a constant velocity of 30 rpm. The duration of these periods was dependent on attaining stable values of gas exchange.

The first 2 minutes of FES cycling consisted of a warm up in which the Perkins strategy, taken as the reference strategy, was delivered with a ramp PW profile ranging from 0 to 100% of the chosen value. Then, the subject was stimulated for 5 minutes with the reference strategy (ref_I in Fig.1), 20 minutes with the test strategy (Perkins, Nitlab or Munich, test in Fig. 1) and again for 5 minutes with the reference strategy (ref_II in Fig.1). The session was completed with 5 minutes of passive cycling (p_II in Fig.1). During all sessions the velocity was maintained at 30 rpm.

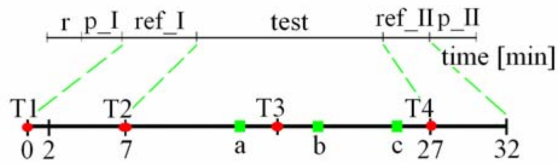

Fig. 1: Description of the different phases of a single session: r indicates the period of rest and p the period of passive cycling. T1-4 indicate the instants in which a blood sample was taken from a finger. a, b, c represent the points across which gross efficiency was evaluated.

To analyze the lactate concentration blood was taken from a finger with a capillary tube in the instants indicated as T1-4 in Fig. 1.

Heart rate was monitored continuously and registered as an instant value every minute.

For each subject, we used the same stimulation parameters and electrode placement and we replicated exactly the subject placement on the tricycle across all 3 sessions.

The 3 stimulation strategies are reported in Fig. 2. While the Perkins and Munich strategies combined the stimulation ranges with an ON-OFF profile of PW, the Nitlab strategy provided a sinusoidal PW profile. This aimed to generate a smoother activation of the muscles. The Munich strategy did not involve the calves.

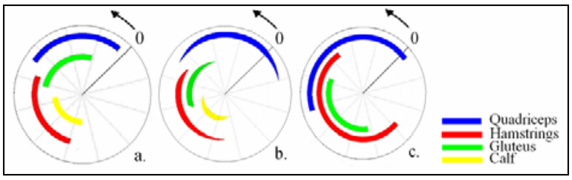

Fig. 2: Stimulation ranges versus crank angle for the muscle groups of the left leg (a.Perkins; b.Nitlab; c.Munich), as derived from the literature. The 0 reference of the crank angle corresponds to the maximal flexion of the left hip.

Data analysis

We computed the active PO (aPO) as the difference between the PO produced during the FES exercise and the passive cycling during p_I.

Starting from this signal, we analyzed two mechanical parameters:

- the mean value of the aPO per revolution.

- the ratio (Z) between the area under the aPO and the stimulation cost (SC) per revolution. SC was the area delimited by the PW profile of all the muscles, and was defined as follows:

$$Z = \frac{\int_{0}^{360^\circ} aPO d\alpha}{SC}; \qquad SC = \sum_{i=1}^{8} PW_i d\alpha$$

where α = crank angle and with i = number of stimulator channel.

Metabolic data analysis included concentration of lactate in blood, heart rate, gas exchange measurements and their combination with values of PO for the calculation of gross efficiency (GE) as proposed by [3]. GE was evaluated over periods of 1 minute during steady state exercise, as indicated by a, b, c in Fig. 1.

The problem of repeatability

The trend during the first few minutes of stimulation (ref_I) was very similar for all the subjects (see Fig. 3). Considering the mean PO per revolution, there was initially a ramp, then the PO profile attained a peak, that represented the maximal power the subject could express during the session. As the muscle fatigued, PO achieved a lower steady state, depending on the initial conditions and the effect of the stimulation on the muscles.

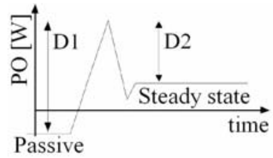

Fig. 3: Detail of the warm up of the power diagram

Considering Fig. 3, we introduced R as the ratio between D1 and D2. R seemed to be repeated by each patient across different days. Indeed, for each patient, the mean value of R was constant with a standard deviation always lower than 4% of the mean value.
R was used to normalize the mechanical results obtained with the test strategy in order to make the results independent of the initial conditions of the single session and to allow an intrasubject comparison between the strategies.

Statistical analysis

Since the data related to the aPO were not normally distributed, a Kruskal-Wallis non-parametric test ($p=0.05$) was carried out to compare the performance of the 3 stimulation strategies for each subject. The analysis was completed with a post-hoc Dunn-Sidak test. The asterisks in Fig. 4 and Fig. 5 indicate that the Dunn-Sidak test produced a significant difference ($p < 0.05$) between the strategies.

Results

Mean of the aPO per revolution

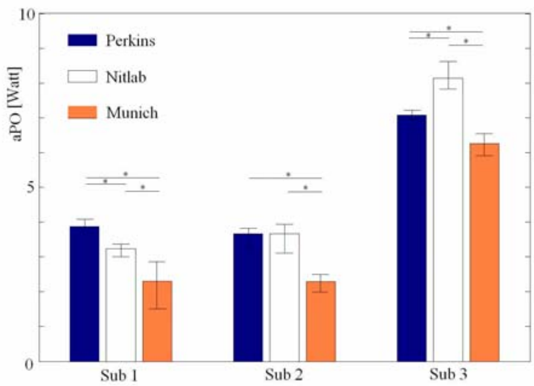

Fig. 4: Comparison of the performance obtained by the 3 strategies in terms of the median and the quartiles of the mean aPO per revolution obtained by the subjects.

In terms of mean aPO (Fig.4) produced in each revolution, Perkins strategy was the best for S1 and Nitlab strategy gave the best outcomes for S3. S2 produced similar power with Nitlab and Perkins, and always more than Munich.

Ratio Z between the area under aPO and SC.

The Nitlab strategy gave greater Z values than Perkins and Munich both for S2 (10% and 57% respectively) and S3 (23% and 47% respectively).

S1 manifested by far the best power with Perkins and consequently the Z value was similar to Nitlab.

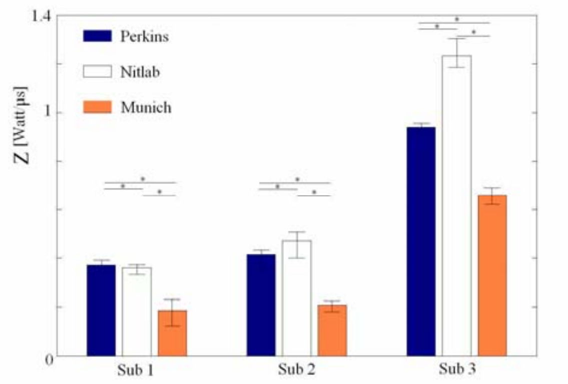

Fig. 5: Comparison by Z of the 3 strategies: the medians and the quartiles are shown.

Gross Efficiency, GE:

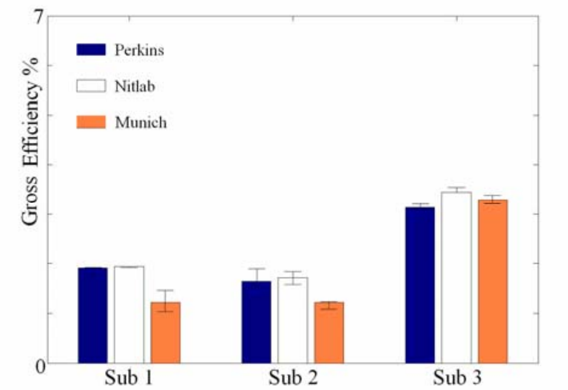

Fig. 6: Comparison of the GE produced by the 3 strategies: the median and the quartiles are shown.

GE (Fig. 6) were found to be within normal ranges [3], no evidence of reduction of efficiency imputable to fatigue emerged. The small population of data, being instant measurements, did not allow us to carry out a statistical analysis.

Discussion

It was noticed that the performance were well maintained for all the sessions. We could conclude that our subjects were all well trained with FES, and also that they were able to sustain sessions of stimulation that last more than half an hour.

S3 was the only patient not trained to FES cycling and produced the best performance with Nitlab strategy both in terms of mean aPO and of Z. This result was unexpected, because as seen the aim of Nitlab strategy was not to maximize the PO but to stress muscles as little as possible. Since sinusoidal profile of PW gives less quantity of current to muscles than a sudden switch off – on, this case represents the best result: the best outcomes with the lowest quantity of stimulation. Since all the subjects were well trained, it should be important to quantify how a long training programme with a strategy could influence results. S1 and S2 were cyclists, trained with the Perkins strategy, and S1 showed the best outcomes with Perkins. Concerning S2 the results obtained by Perkins and Nitlab were quite comparable.

Results obtained by the Munich strategy were probably affected by the fact that we did not customize activation angles for each patient. Moreover, this strategy had very long angular intervals of co-contraction of agonist and antagonist muscles. Even if eccentric contractions produce more strength and less fatigue [7], the risk of induced spasms is increased.

This study illuminates the importance of different strategies used in cycling, and the value of analysing their advantages and disadvantages. This paper represents a first approach to choosing optimal stimulation patterns.

References

[1] Mohr T, Andersen JL, Biering-Soerensen F, et al. Long term adaptation to electrically induced cycle training in severe spinal cord injured individuals. Spinal cord 35, 1-16, 1997.

[2] Hunt KJ, Ferrario C, Grant S, et al. Comparison of stimulation patterns for FES-cycling using measures of oxygen cost and stimulation cost. Medical Engineering & Physics 28 710–718, 2006.

[3] Glaser RM, Figoni SF, Hooker SP, et al. Efficiency of FNS leg cycle ergometry. Proc. 11th Ann. Int. Conf. IEEE Eng. Med. Biol. Soc. 1989. p. 961–3.

[4] Perkins T, Donaldson N, Fitzwater R, et al. Leg powered paraplegic cycling system using surface functional electrical stimulation. Proc. 7th Vienna International Workshop on FES, 2001, pp. 36–39.

[5] Ferrante S. Neuroprostheses for the rehabilitation of neurological patients: from control strategies design to clinical applications. Ph.D. Dissertation, Politecnico of Milan, 2003-2006.

[6] Szecsi J, Krause P, Krafczyk S, et al. Functional output performance in paraplegic cycling propelled by leg stimulation with middle frequency alternating current. 11th annual conf. of the international FES society September 2006- Zao, Japan

[7] Pasquet B. Muscle fatigue during concentric and eccentric contractions. Muscle nerve 23: 1727–1735, 2000.

Acknowledgements

We wish to thank the three people who took part to the experimental trials. The research project was supported by the Italian Institute of Technology (IIT) and by INSPIRE.

Author's Address

Andrea Pella; Bioengineering Department, Politecnico di Milano, Milan, Italy. andrea.pella@googlemail.com

OUT-OF-THE-SADDLE FES-CYCLING BY PARAPLEGICS

J. Szecsi*,**, A. Straube*

*Dept. of Neurology, Ludwig Maximillians University Munich, Germany
**Hospital of Neurology, Bad-Aibling, Germany

Abstract

Reinforcing muscular and cardiovascular training as well as improving standing and walking are important goals of rehabilitation after SCI. While standard recumbent FES-cycling is considered a means to improve muscle condition, it is not adequate for achieving efficient balance control and intense cardiopulmonal training.

In this study a new method of FES- propelled cycling is presented, called upright or standing cycling, resembling out-of-the-saddle cycling of healthy cyclists climbing a hill.

Using a single subject with complete paraplegia Th9, this study investigated the technical feasibility and biomechanical and physiological characteristics of training using an upright FES-cycle.

It could be shown that upright FES-cycling is technically straightforward to realize and combines the advantages of intense cardiovascular (power, peak O_2 uptake, PCI), orthostatic and balance training.

Introduction

A minimum amount of generated mechanical output force and work is required to initiate cardiovascular adaptation processes with functional electrical stimulation (FES) ergometer training or to cover useful distances with FES cycling. As a rule this is not yet possible. While FES-propelled pedaling always uses recumbent cycles, one must remember that able-bodied subjects produce more mechanical work and cardiovascular load using upright cycles(Astrand P.O. 1989).

In the same line of ideas, improvement of impaired walking ability could be an important goal of the rehabilitation of incomplete and complete paraplegics. Walking implies the existence of the gait components: cyclical generation of propulsive forces of the legs and maintaining balance and upright posture of the upper body. Standard, recumbent FES-cycling as gait training addresses only the first component and not the second. Therefore, it is questionable whether recumbent cycling optimally triggers the spinal pattern generator to re-learn the skills necessary for bipedal walking. Thus, it would be advantageous to complement the training of bilateral cyclic activity of both legs provided by today's FES-cycle systems with the possibility to maintain and control the balance and posture of the trunk and body

The purpose of this study was to investigate (1) the technical feasibility of "out-of-the-saddle" FES cycling and to determine (2) whether more mechanical power and cardiopulmonary load can be produced with it than with standard recumbent cycling.

Material and Methods

Methods: A prototype of a stationary step cycle ergometer (inclination of the crank axis-hip axis line = 82°) was built (Fig.1), which allowed pedaling in the sitting or out-of-the-saddle position. The cycle was combined with a pneumatic weight-lifting system (Cosmos GmbH Traunstein, Germany) that reduced the effective weight and ensured an upright position. Standard 20 Hz biphasic, rectangular pulse stimulation was applied to six muscle groups (quadriceps, gluteus, hamstrings). Individual isometric torque profiles of the muscle groups (Perkins TA 2001) of the patient were collected in the sitting position and extrapolated to the upright out-of-the-saddle posture. Next, upright seated cycling was practiced (Fig.1, upper right) and finally the seat was removed and out-of-the-saddle cycling (upright standing cycling) was performed (Fig.1,upper). A handrail provided additional arm support during dynamic movements. A spirometer (Renaissance, Puritan-Bennett,Hounslow,UK) was used to measure maximal O_2 uptake. The physical cost index was calculated using the formula: PCI= blood pressure difference (activity-rest)/cadence/crank radius.

Results

Despite the multiple degree of freedom movement in case of out-of-the-saddle cycling, the stimulation pattern determined in the sitting position on the basis of Perkins' method(Perkins TA 2001) was successfully applied to cycling in an upright posture.

Fig. 1. Patient with complete paraplegia on an upright FES-cycle: Upper left: The components of the upright cycle Upper right: Patient pedaling in a sitting position on the upright cycle. Lower: Patient pedaling in a standing position on the upright cycle

Biomechanical and physiological parameters of ergometric experiments are given in Fig.2. Upright seated cycling and upright standing cycling were performed for time periods of 180-310 s and 375-440 s respectively. Braking resistance was fixed at 5.1 Nm in both cycling modes because of the necessity of limiting cadence at 50 rpm in the out-of-the-saddle situation.

A comparison of the isometric torque (15.6 Nm ± 4.1) and mechanical power (22.7 W ± 9.7) generated during "cycling out-of-the-saddle" with the power and torque collected in a previous study during recumbent cycling

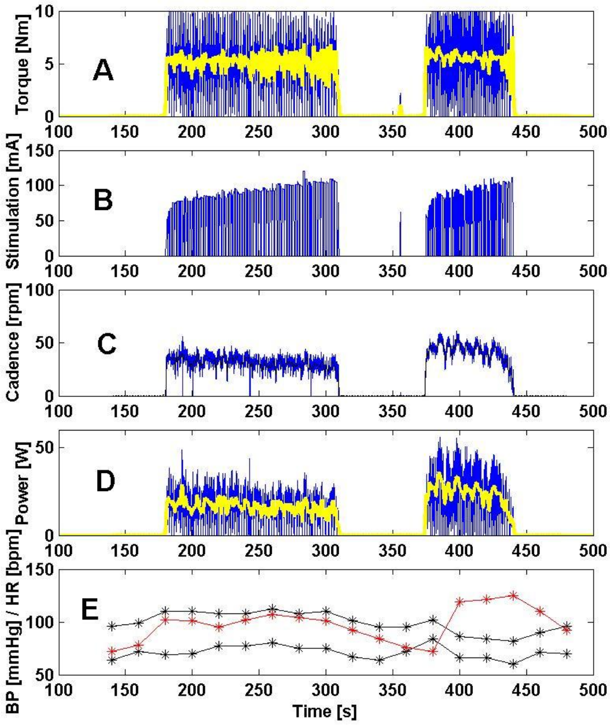

Fig. 2. Patient with complete paraplegia riding the upright FES-cycle on sitting(left) and standing position(right). A: Braking torque (blue:raw, yellow: averaged). B: Stimulation intensity. C: Cadence. D: Power (blue: raw, yellow: averaged). E: systolic and diastolic blood pressure (black), heart rate (red).

revealed differences of < 5%. Comparing seated cycling with standing cycling in Fig. 2, cadence increased during standing cycling (51 vs. 41 rpm), leading to greater mean power(25 vs. 20w). However, endurance (cycling time until standstill) was greatly reduced (-65%), and peak O_2 uptake (1.1 l/min vs. 2.1 l/min) was greatly increased (+88%) during upright standing pedaling.

A slight decrease in systolic blood pressure (105 vs. 82 Hgmm) and a considerable increase in heart rate (125 vs. 95 bpm) was recorded.

Considering that resting heart rate is 75 bpm, the physical cost index amounts to (95-75)/30/0.6= 1.11 and (125-75)/45/0.6= 1.8 in the upright seated and upright standing cycling situation respectively.

Discussion and conclusion

FES-propelled cycling of paraplegics in an upright posture can be considered an alternative to walking or stair climbing (Fig 3). Movement is not restricted to the sagittal plane, as in the case of robotic training devices like(Colombo et al. 2000). Moreover, lateral movement of the pelvis is possible (Fig. 1,lower right) and warranted for weight

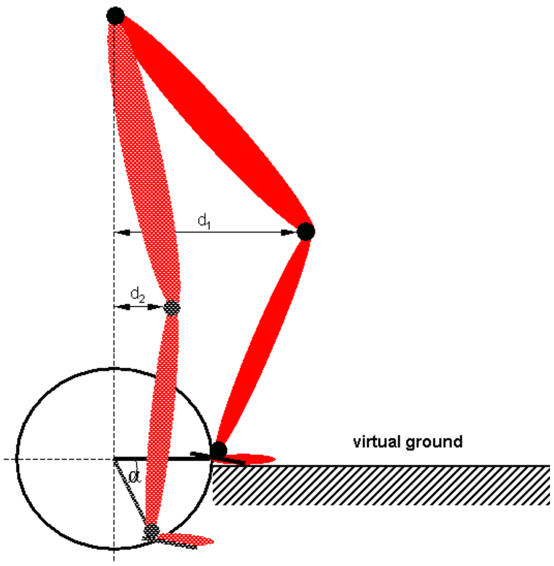

Fig. 3. Analogy of upright standing cycling to stair climbing

shifting to train body balance control.
The stimulation pattern used for the multijoint movement is straightforward and easy to calculate. Feedback control relies only on the crank angle.
The cardiopulmonary load (as peak O_2 uptake and PCI) achieved during upright standing FES-cycling was much higher than during standard recumbent FES-cycling Mechanical power output increased and endurance decreased, as expected during standing cycling.
Further therapeutical studies have to be done to evaluate the long-term effects of the proposed method of training. In conclusion, FES-propelled out-of-the-saddle cycling of paraplegics can be proposed as a cheap and easily realizable alternative to treadmill-walking.

Acknowledgements

This work was supported by the Else-Kröner-Fresenius Foundation.

References

Astrand P.O. RK (1989) Textbook of Work Physiology. McGraw-Hill Book Company, New-York

Colombo G, Joerg M, Schreier R, Dietz V (2000) Treadmill training of paraplegic patients using robotic orthosis. Journal of rehabilitation research and development 37: 693-700

Perkins TA DN, Fitzwater R, Phillips GF, Wood DE. (2001) Leg powered paraplegic cycling system using surface functional electrical stimulation. IFESS Proceedings of the 7th Vienna International Workshop on Functional Electrical Stimulation, Vienna, Austria, pp. 36-39

Author’s Address

Johann Szecsi, MD
Department of Neurology
University of Munich
D-81377 Munich, Marchioninistr. 23
e-mail: jszecsi@nefo.med.uni-muenchen.d

DEVELOPMENT OF A HYBRID FES TRICYCLE

Berkelmans R.[1], Duysens J.[2], van Kuppevelt D.[3], Hopman M.[4]
[1]BerkelBike BV, Nijmegen, The Netherlands
[2]Rehabilitation dept. UMC St Radboud, Nijmegen, The Netherlands
[3]Sint Maartenskliniek Research, Development and Education, Nijmegen, The Netherlands
[4]Physiology, UMC St Radboud, Nijmegen, The Netherlands

Abstract

Purpose: To develop a Functional Electrical Stimulation tricycle that is suitable for the largest part of the Spinal Cord Injury population, including those with incomplete lesions. In addition it has to be practical as well in speed, range, reliability and physiological response. Methods: The BerkelBike is a combination of voluntary arm and FES leg cycling. There are 3 different models; The BerkelBike Pro which is a complete tricycle, the BerkelBike Classic which the user can attach or detach to their own wheelchair and the BerkelBike Home which is designed for SCI in an electrical wheelchair. The first two types are developed to ride outdoors but can be used as a stationary bike as well. The Home version however can only be used as a stationary bike. Results: The Classic and the Pro are favored for SCI with lesions from C8-T12 because of the fact that they allow the possibility to ride outdoors. The home version is most suitable for C5, C6, C7. Almost half of the current BerkelBike owners use their BerkelBike without FES. These are mostly incomplete SCI, MS and stroke patients, who still have some power left in their legs but merely not enough for riding on leg power alone. The only defined problem so far occurred with injuries of joints due to rapid increase of training load. We now have a more moderate training protocol.

Introduction

Since the early 80's, a lot of research has been conducted about the effects of Functional Electrical Stimulation (FES) with people who suffer from a Spinal Cord Injury (SCI). Especially riding a stationary bike seemed a very good method to obtain physiological effects. Local effects of riding this bike provides better blood circulation [1-3] hypertrophy [1, 4-8] of stimulated muscles and alteration of muscle fiber types [6]. Cardiac output [9-12] maximum oxygen intake [11, 13, 14] hormone metabolism [15-17] and psychological effects[17] are the more general benefits. It has been determined that combining FES biking with voluntary arm cranking has a greater impact on the general benefits [18, 19]. Considering the life expectancy of SCI patients still being remarkably lower than non-patients [20, 21], it is understandable that there have been multiple attempts to make FES cycling more attractive by developing an outdoor bike [22-27]. Our goal was to develop a FES tricycle that is suitable for the largest part of the SCI population, including the spinal cord injured with an incomplete lesion. For this purpose, it has to be practical in speed, range, reliability and physiological response as well.

Methods

The patented BerkelBike is a combination of voluntary arm and FES leg cycling. Spinal cord patients produce a power with their stimulated legs between 0 – 50 W. They are able to produce between 20 – 200 W with their arms. The average speed goes up from 5 km/h to 15 km/h by combining the arm and leg power. It also makes it possible to handle moderate slopes.

Spinal cord patients are not aware that their FES muscles are getting fatigued. If they cycle only with their legs they could be faced with sudden lack of power resulting in not being able to finish their trip. However with combined leg and arm cycling they can experience fatigue in their arms to which they can respond by shortening their trip. In addition, their voluntary muscles are more powerful and more fatigue resistant. Even if these patients overestimate themselves they always are able to arrive at their destination.

Our first model BerkelBike Classic was designed for paraplegics. The user can attach and detach their BerkelBike to and from their own wheelchair. This way their wheelchair transforms into a tricycle (Photo 1). There are two big advantages to this system: The bike itself is relatively small which makes it easy to store and to transport into a car. The second advantage is that the user always has access to his or her own wheelchair. This is mostly necessary if they want to enter a building at their destination.

Photo 1: BerkelBike “Classic” the front part is attached to the patients wheelchair.

There was one aspect we overlooked regarding the adaptation of the bike in rehabilitation centers. Physiotherapists have a very limited time to adjust the bike to a new patient. When their patients differ much in height it was not always easy to quickly adjust these bikes to each individual patient. Therefore it was necessary to design an additional concept, the BerkelBike Pro (Photo 2). This bike has the same front part as the Classic but it is a complete tricycle. The chair is wide enough to accommodate all patients and it is adjustable forwards as well as backwards by turning a crank

Photo 2: BerkelBike “Pro” a complete tricycle.

Because we received a lot of questions from quadriplegics and because they benefit the most from this concept, we also made the BerkelBike Home (Photo 3). This bike has almost the same front as the other two bikes, however it is a stationary bike placed on a aluminum plate. This allows people in electrical wheelchairs to use this system.

Photo 3: BerkelBike “Home” free standing system for SCI with a high lesion. White box is previous stimulator. Small blue box on the arm cranks is the controler for the Tacx software which has to be installed on a personal computer. The arm cranks are normally synchrone but in this example we tried asynchrone.

To make the stationary ride as attractive as possible we used bicycle trainers from Tacx (www.Tacx.com). With this system the BerkelBike Classic and Pro can also be used as a stationary bike. Tacx BV specially adapted frames so we could place the 16” front wheel of the BerkelBike in it. They have virtual reality software and provide different types of analytic features.

All the bikes can be equipped with a FES 8 channel stimulator (Impulsbox 3.0 BerkelBike BV, Photo 4) with a maximum of 180 mA, 180 V, 70 Hz. The duration of the positive and negative pulse and the interpulse can be programmed separately. This stimulator also has EMG and EEG measuring inputs.

Before the patients could use FES they had to put on shorts with 12 inbuilt electrodes (Bioflex Inc. Columbus, Oh, USA) or they had to place 12 adhesive surface electrodes on their quadriceps, hamstrings and the gluteal muscles.

For cycling we normally used maximum 150 mA, 150 V, 35 Hz, 0,4 mS positive and 0,4 mS negative pulse. We did not use an interpulse. In each stimulator we preprogrammed 5 different stimulation programs. Most of the times, they only differ in timing of the muscle stimulation. The subjects can chose their own favorable program and adjust the stimulation intensity with a plus and minus button.

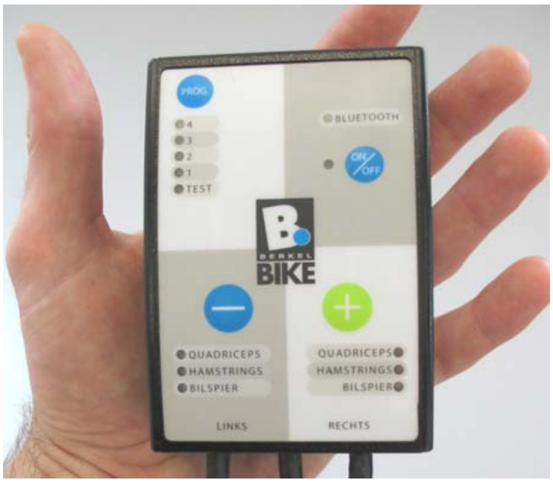

Photo 4: 8 channel FES stimulator for cycling.

Results

The Classic and the Pro are favored for SCI with lesions from C8-T12 because of the fact that they allow the possibility to ride outdoors. If the tricycle is solely used for training and if there is enough storage room, the Pro is favored more than the Classic. If people prefer to use the tricycle for visits and/or they lack storage space, then the Classic is favored more over the Fixed frame. The home version is most suitable for C5, C6, C7. Eleven of the 21 privately owned BerkelBikes are used without FES. These patients have an incomplete SCI, MS or stroke. They still have some power left in their legs but merely not enough for riding on leg power alone. The only defined problem so far occurred with injuries of joints due to rapid increase of training load. We now have a more moderate training protocol.

Discussion

The biggest problem for people with a C5-C6 or C7 lesion to operate the Classic or de Pro, is not being able to use the hand break. This is caused by the fact that this group of patients has lost the functionality of their hands. To prevent their hands from gliding off the handle bars, the hands are being firmly secured by means of special safety grips (Photo 3). Currently we are working on a back pedal brake for the arm cranks. With this special feature, it is no longer necessary to let go of the handles while braking. However it is more difficult to realize this with the BerkelBike than with a regular hand bike because the pedal axis of the legs also serve as an in-between-axis.

When patients no longer have their hand functionality, they always require assistance when preparing to use the bike: for example when putting on the stimulation pants or when attaching the electrodes. Similarly, attaching or detaching the bike will be almost impossible. When patients have limited use of their triceps, delivering output with their arms will be significantly decreased. This can create problems when riding up moderate slopes.

Conclusion

Adding arm cranking to the FES tricycle has practical as well as physiological advantages. We were able to develop a well functioning outdoor bike with or without the use of FES. The device can be beneficial for a large patient population. Attaching and detaching to and from one's own wheelchair is experienced as a great advantage by most SCI patients.

References

[1] Chilibeck PD, Jeon J, Weiss C, Bell G, et al. Histochemical changes in muscle of individuals with spinal cord injury following functional electrical stimulated exercise training. Spinal Cord, 37:264-268, 1999.

[2] Gerrits HL, de Haan A, Sargeant AJ, et al. Peripheral vascular changes after electrically stimulated cycle training in people with spinal cord injury. Arch Phys Med Rehabil, 82:832-839, 2001.

[3] Thijssen DH, Ellenkamp R, Smits P, et al. Rapid vascular adaptations to training and detraining in persons with spinal cord injury. Arch Phys Med Rehabil, 87:474-481, 2006.

[4] Baldi JC, Jackson RD, Moraille R, et a. Muscle atrophy is prevented in patients with acute spinal cord injury using functional electrical stimulation. Spinal Cord, 36:463-469, 1998.

[5] Bremner LA, Sloan KE, Day RE, et al. A clinical exercise system for paraplegics using functional electrical stimulation. Paraplegia, 30:647-655, 1992.

[6] Crameri RM, Weston A, Climstein M, et al. Effects of electrical stimulation-induced leg training on skeletal muscle adaptability in spinal cord injury. Scand J Med Sci Sports, 12:316-322, 2002.

[7]. Hjeltnes N, Aksnes AK, Birkeland KI, et al. Improved body composition after 8 wk of electrically stimulated leg cycling in tetraplegic patients. Am J Physiol, 273:R1072-9, 1997.

[8] Scremin AM, Kurta L, Gentili A, et al. Increasing muscle mass in spinal cord injured persons with a functional electrical stimulation exercise program. Arch Phys Med Rehabil, 80:1531-1536, 1999.

[9] Faghri PD, Glaser RM, Figoni SF: Functional electrical stimulation leg cycle ergometer exercise: Training effects on cardiorespiratory responses of spinal cord injured subjects at rest and during submaximal exercise. Arch Phys Med Rehabil, 73:1085-1093, 1992.

[10] Figoni SF, Rodgers MM, Glaser RM, et al. Physiologic responses of paraplegics and quadriplegics to passive and active leg cycle ergometry. J Am Paraplegia Soc, 13:33-39, 1990.

[11] Hooker SP, Figoni SF, Rodgers MM, et al. Physiologic effects of electrical stimulation leg cycle exercise training in spinal cord injured persons. Arch Phys Med Rehabil, 73:470-476, 1992.

[12] Hooker SP, Figoni SF, Glaser RM, et al. Physiologic responses to prolonged electrically stimulated leg-cycle exercise in the spinal cord injured. Arch Phys Med Rehabil, 71:863-869, 1990.

[13] Barstow TJ, Scremin AM, Mutton DL, et al. Changes in gas exchange kinetics with training in patients with spinal cord injury. Med Sci Sports Exerc, 28:1221-1228, 1996.

[14] Hooker SP, Scremin AM, Mutton DL, et al. Peak and submaximal physiologic responses following electrical stimulation leg cycle ergometer training. J Rehabil Res Dev, 32:361-366, 1995.

[15] Bloomfield SA, Mysiw WJ, Jackson RD. Bone mass and endocrine adaptations to training in spinal cord injured individuals. Bone, 19:61-68, 1996.

[16] Hjeltnes N, Galuska D, Bjornholm M, et al. Exercise-induced overexpression of key regulatory proteins involved in glucose uptake and metabolism in tetraplegic persons: Molecular mechanism for improved glucose homeostasis. FASEB J, 12:1701-1712, 1998.

[17] Twist DJ, Culpepper-Morgan JA, Ragnarsson KT, et al. Neuroendocrine changes during functional electrical stimulation. Am J Phys Med Rehabil, 71:156-163, 1992.

[18] Hooker SP, Figoni SF, Rodgers MM, et al. Metabolic and hemodynamic responses to concurrent voluntary arm crank and electrical stimulation leg cycle exercise in quadriplegics. J Rehabil Res Dev, 29:1-11, 1992.

[19] Mutton DL, Scremin AM, Barstow TJ, et al. Physiologic responses during functional electrical stimulation leg cycling and hybrid exercise in spinal cord injured subjects. Arch Phys Med Rehabil, 78:712-718, 1997.

[20] National spinal cord injury statistical center, The 2006 Annual Statistical Report for the Model Spinal Cord Injury Care System. 1-121; 2006.

[21] Strauss DJ, Devivo MJ, Paculdo DR, et al. Trends in life expectancy after spinal cord injury. Arch Phys Med Rehabil, 87:1079-1085, 2006.

[22] Gfohler M, Loicht M, Lugner P: Exercise tricycle for paraplegics. Med Biol Eng Comput, 36:118-121, 1998.

[23] Hunt KJ, Stone B, Negard NO, et al. Control strategies for integration of electric motor assist and functional electrical stimulation in paraplegic cycling: Utility for exercise testing and mobile cycling. IEEE Trans Neural Syst Rehabil Eng, 12:89-101, 2004.

[24] Petrofsky JS, Smith J: Three-wheel cycle ergometer for use by men and women with paralysis. Med Biol Eng Comput, 30:364-369, 1992.

[25] Perkins TA, de N Donaldson N, Hatcher NA, et al. Control of leg-powered paraplegic cycling using stimulation of the lumbo-sacral anterior spinal nerve roots. IEEE Trans Neural Syst Rehabil Eng, 10:158-164, 2002.

[26] Pons DJ, Vaughan CL, Jaros GG: Cycling device powered by the electrically stimulated muscles of paraplegics. Med Biol Eng Comput, 27:1-7, 1989.

[27] Szecsi J, Fiegel M, Krafczyk S, et al. The electrical stimulation bicycle: A neuroprosthesis for the everyday use of paraplegic patients. MMW Fortschr Med, 146:37-8, 40-1, 2004.

Acknowledgements

This work was supported by the Dutch National Rehabilitation Foundation.

Author's Address

Rik Berkelmans
BerkelBike BV
Info@BerkelBike.nl
www.BerkelBike.nl

FES ROWING AND SCULLING AFTER SPINAL CORD INJURY

Andrews B.J[1], Hettinga D[2], Gibbons R[3], Goodey S[4], Wheeler GD[5]

[1] School of Technology and the Nuffield Department of Surgery, Oxford UK, [2] School of Health and Social Care, Brunel University, London, UK, [3] ASPIRE National Training Centre, Stanmore, London, UK, [4] London Regatta Centre, London, UK, [5] MS Society and the Steadward Centre, Alberta, Canada.

Abstract

FES Rowing has been successfully demonstrated on the indoor ergometer, the powered rowing tank, the rowing simulator and on-water in male and female SCI volunteers ranging from ASIA (A/B) C4/5 to T12 using at least 4 channels of surface electrical stimulation.

Paraplegic and quadriplegic FES rowers have competed alongside able-bodied rowers over the Olympic distance of 2,000 meters at the British Indoor Rowing Championships (BIRC) in 2004, 2005 and 2006 and at the World Indoor Rowing Championships (CRASH-B's – 2006 in Boston, USA). The best performance to date has been achieved by a 23yr male, T12 ASIA(A), in 10 min 28 sec.

A range of exercise intensities can be achieved ranging from recreational to levels of VO_2 in excess of 35 ml/kg/min. High volumes have also been achieved and we expect that such high levels may help some to achieve significant reductions in the risks to their health, particularly where a dose-response relationship exists, for example in cardiovascular disease.

Introduction

Although individuals with SCI regard exercise as important and clearly can benefit from proper exercise, there are several hurdles to overcome. Most importantly, it has been suggested that an exercise intensity of at least 6 METs (i.e., oxygen consumption of 21 ml/kg/min) is required to lower the relative risk for coronary heart disease (Tanasescu et al. 2002) and to significantly improve blood lipids volumes of at least 1200-2200 kcal/week (Durstine et al 2001). However, many persons with SCI can have difficulty achieving these levels (Manns et al. 1999). Even though some can achieve moderately high peak oxygen consumptions using their upper body muscles alone, maintaining sufficient aerobic power with small muscle mass exercise is difficult. Exercise performance may be limited by local fatigue of the highly stressed arm musculature despite adequate systemic responses.

The solution may be FES of the paralyzed lower limbs to increase the amount of metabolically active muscle mass. However, FES exercise alone is not of sufficient intensity for many of the beneficial adaptations associated with aerobic exercise. Therefore, hybrid FES exercise that involves both innervated upper body and electrically stimulated lower body, has been explored and has been shown to produce significantly greater aerobic power and peak oxygen consumption than FES exercise alone. Wheelchair propulsion and arm-cranking ergometry have been associated with shoulder pain (Jacobs 2004). Pulling actions have been proposed as therapy for chronic shoulder pain in wheelchair users (Jacobs 2004). In chronic wheelchair users, this may help prevent upper limb overuse injury (Olenik et al. 1995). FES rowing involves pulling actions and participants in report it to be better tolerated than standard upper body exercise, even though the latter was conducted at a lower absolute VO_2 (Wheeler et al. 2002).

FES-rowing Technology

<u>Indoor Rowing</u> Andrews and colleagues have developed FES rowing (www.FESrowing.org) with exercise intensities in excess of 35ml/kg/min with volumes greater than 2,000 kcal/week have been achieved by some ASIA(A) SCI who have competed in international rowing competitions over the Olympic 2,000m distance alongside able-bodied rowers (Hettinga & Andrews 2007). In Nov 2004 two paraplegics (Fig 1(b), subjects 1 and 2 in the table) using the 4-channel (quads plus hamstrings controlled using a change-over switch mounted on the handle) FES rower shown in Fig 1(a), successfully competed along with over 2,500 able-bodied rowers in Birmingham at the British Indoor Rowing Championships (BIRC) http://www.concept2.co.uk/birc/ – this event and the FES equipment is the subject of a permanent exhibit at Rowing Museum http://www.rrm.co.uk/ Since then, paraplegics and quadriplegics (controlled by changeover switch operated either by the attendant or self-controlled by the rower by positioning the switch so as to allow operation by wrist extension movements with/out velcro closed mitts around the handle grip) have competed in the annual BIRC and the World Indoor Rowing Championships (WIRC or CRASH-B's). Their data are summarized in the table

Subject	**1**	**2**	**3**	**4**	**5**	**6**
Age (years)	50	34	44	28	18	22
Weight(kg)	70	65	77	52	51	90
Lesion, ASIA	T4 (A)	T8 (A)	T6 (A)	C7/8 (A)	C4 (A)	T12 (A)
Since injury yrs	5	5	6	13	2	2
FES-rowing training duration	18 months	12 months	3 months	14 months	7 months	12 months
FES before rowing	3 months of muscle conditioning	>1 year FES-cycling and muscle conditioning	1 month of muscle conditioning	1 month of muscle conditioning	1 month of muscle conditioning	3 months of muscle conditioning
BIRC						
2004	12:02	13:59	na	na	na	na
2005	11:11	13:58	11:39	na	na	na
2006	11:12	na	10:35	na	25:13	10:28
WIRC 06	11:37	14:01	12:00	16:55	na	na

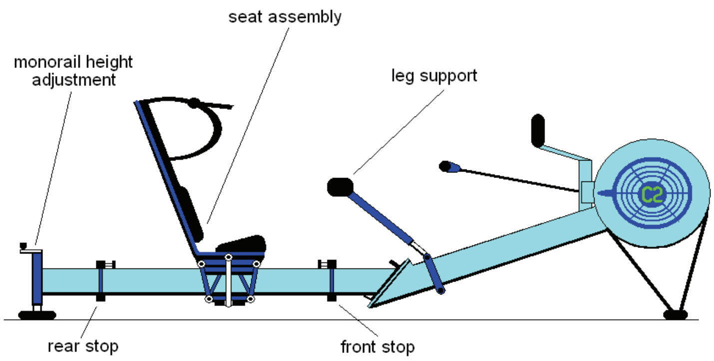

Fig. 1a Schematic of adapted rower

Fig 1b Paraplegic rowers at BIRC '04, foreground, co-author RG and subject 1.

On-Water Sculling Recently, we have further developed FES rowing in the tank and on-water. The Alden 16 (single) and Alden 18 (double) recreational rowing shells were chosen (http://www.rowalden.com/) for stability and the removable stateroom module fig 2(b). A bungee cord was attached to the custom sliding seat to assist recovery as shown in figure 2(b). To facilitate laboratory training and development a sculling simulator was developed based on the Alden stateroom module. Regular carbon fibre oars were cut down to remove the spoons and coupled to two 2-state hydraulic cylinders (2-state to closely simulate rowing i.e. minimal resistance during RECOVERY and adjustable resistance during DRIVE) as show in Figure 2(a). In the simplest arrangement 4-ch surface stimulation was used (as with the indoor rower) with the control switch mounted on the oar handle. Training in the simulator followed a similar protocol to that used for rowing on the adapted Concept II shown in Fig 1(a).

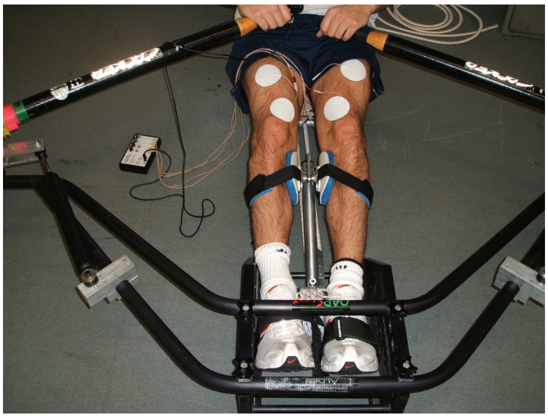

Fig 2(a) The FES rowing simulator: comprising an Alden boat stateroom and fitted with hydraulic cylinders for laboratory training and development.

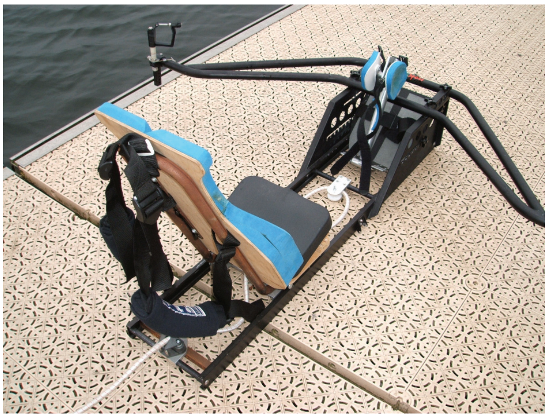

Fig 2(b) The Alden (16 & 18) detachable state room with modified seat, padded shoulder straps and bungee cord, pully and cam cleat to allow adjustment of bungee cord tension. The telescopic leg stabiliser is similar to that used on the indoor rower.

Following at least two one hour sessions on the rowing simulator and prior to rowing on-water, FES rowing is undertaken in a powered rowing tank with the water flow rate set to simulate a boat speed of 2.3 m/s. In addition to 2 or 3 one hour FES ergo-rowing/week, a further one hour per week of FES rowing is undertaken in an adapted station in the turbine powered rowing tank at the London Regatta Centre (McLean 2002).

<u>Case report FES sculling</u> subject (6), shown in figure 2(c), has successfully demonstrated FES sculling. He had two 1 hour sessions on the simulator followed by five 8 minute pieces with 5 minute rest periods in the tank. Initial on-water training began following the second tank session using the Alden 18 double with the coach in the bow seat. After three 30 minute sessions with the coach he began single sculling in the Alden 16, shown in Fig 2(d). He now regularly sculls on-water in typical rowing pieces exceeding 1,000m.

Fig 2(c) The adapted stateroom module shown in figure 2(b) is shown installed into the Alden 16 shell. Subject (6) is shown dockside with the leg stabiliser in place, testing the control switch fixed to the oar handle.

Discussion

We have observed that all the FES rowers progressively increased their strength and endurance of rowing, beginning with distances of a few tens of meters to many thousands of meters. For example, subject 1 began in June 2004 and only able to attain a few hundred meters before quadriceps were fatigued. In Nov 2004, at the BIRC, he had adopted a 30sec FES row 30 sec arms only split (seat clamped), to allow the quadriceps to recover yet make good time for 2000m. Typically, the split was progressively staged to 40:20 then 50:10 then non-stop for 2000m. In Sept 2006, in an officially timed marathon, 50,000 meters was achieved in 5hrs 49mins. He now routinely trains non-stop at 3-10,000m. Clearly, there has been profound changes in his physical fitness and stimulated muscle endurance. These changes are now the subject of further studies.

FES rowing is offered at ASPIRE http://www.aspire.org.uk/index.php?id=101 the Steadward Centre at the University of Alberta http://www.steadwardcentre.org/ and the London Regatta Centre http://www.london-regatta-centre.org.uk/ Internet rowing (RowPro http://www.digitalrowing.com/) is used to link participants. FES rowing offers those with SCI a range of work-out intensities and volumes. For many the fun of FES rowing, and the associated social activity, is enough. The competitive element has ensured continuos improvment in performance and technology.

In the BIRC 2006, medals were awarded based on the average time calculated from an individuals previous 10 attempts at 2000m just prior to the championships. If this time was beaten by 10 secs, the rower achieved Gold, between +/-9 secs Silver, and below 10 secs Bronze. In this way the awards were considered fair but competitive across the widely different exercise capacities'.

Acknowledgements

The Henry Smith Charity, the Trusthouse Charitable Foundation, the David Tolkien Trust and SCITCS (Alberta) for their support.

References

Durstine JL, et al. (2001) Blood lipid and lipoprotein adaptations to exercise: a quantitative analysis, Sports Med, 31: 1033-1062.

Hettinga D, Andrews BJ (2007) The feasibility of FES Rowing for High Energy Training and Sport, Neuromodulation 10(3): in-press.

Jacobs PL (2004) Pulling Shoulder Pain Away, Sports n Spokes, July: 38-42.

Manns et al. (1999) Determining the relationship between quality of life, handicap, fitness, and physical activity for persons with SCI, Arch Phys Med Rehabil, Dec;80(12):1566-71

McLean (2002) The London Regatta Centre and ARUP Rowing Tank, The ARUP Journal 1: 21-3. http://www.curlewrowingclub.co.uk/lrctank.pdf

Wheeler G, Andrews BJ, Davoodi R, Nathan K, Weiss C, Jeon J, Bambhani Y, Steadward RD (2002) Functional Electric Stimulation Assisted Rowing, Arch Phys Med Rehabil, 83, 1093-1099.

Verellen J, Andrews BJ, Wheeler GD (2007) cardiorespiratory responses during arm ergometry, FES cycling and two hybrid exercises in SCI, Dis & Rehabil: Assist Technol, 2(2):127-132

Tanasescu M, et al. (2002) Exercise type and intensity in relation to coronary heart disease in men, JAMA, 288:1994-2000.

Figure 2(d) Subject 6 in the adapted Alden 16 shell. The floats mounted below the oarlocks prevent capsize.

Session X

Therapy: Pain, Apnea, Hearing

Chairpersons
Ross Davis (Santa Clarita, CA, USA)
Thordur Helgason (Reykjavik, Iceland)

TRANSCRANIAL ELECTROSTIMULATION OF THE BRAIN ENDORPHINERGIC STRUCTURES FOR EFFECTIVE TREATMENT OF THE SENSORINEURONAL HEARING LOSS: METHOD AND DEVICES

Lebedev V.[1], Malygin A.[1], Ignatov V.[1], Tsirulnikov E.[2], Belimova A.[3], Ponomarenko G.[3], Yanov Y.[4]

[1]TES Center of Pavlov Institute of Physiology of RAS, Saint-Petersburg, Russian Federation
[2]Sechenov Institute of Evolutionary Physiology and Biochemistry of RAS, Saint-Petersburg, Russian Federation
[3]Military Medical Academy, Saint-Petersburg, Russian Federation
[4]Institute of the Ear, Larynx, Nose and Speech, Saint-Petersburg, Russian Federation

Abstract

Earlier we have shown that non-invasive selective transcranial electrostimulation (TES) provides a significant improvement of hearing in almost 50% patients with chronic sensorineuronal hearing loss (SNHL). The goal of the present work consisted in development of method and device to increase efficiency of this non-pharmaceutical therapeutic action. We developed and manufactured "TRANSAIR-07" that combines the TES therapy and simultaneous acoustic effects on auditory receptors in an inverse audiogram mode separately for each ear. The "TRANSAIR-07" device makes audiograms before the session, introduces them into the treatment program, accomplishes the efficiency control and corrects the treatment program during or at the end of the course. An essential efficiency increase of treatment, especially of chronic SNHL, including professional SNHL, was shown. There was revealed a significant whisper speech intelligibility increase and auditory threshold reduction, according to an audiogram up to 35 dB (especially for a speech frequency range), in 60%–90% of chronic SNHL cases. A certain restoration of impulse propagation through auditory nerves was confirmed by recording of the short-latency evoked auditory potentials. For the majority of cases, the level of tinnitus and vertigo either stopped or was considerably reduced. Standard questionnaires showed that quality of life in our patients had also improved significantly.

Introduction

Treatment of sensorineuronal hearing loss is an actual problem of current otorhinolaryngology, as this pathology is characterized by a progressing rise of the patients' population, has tendency for rejuvenation of this pathology, and often involves people of the working ability age. The number of such patients in Russia approaches 12 mln. Acute and chronic SNHL are combined groups of diseases that include lesions of various parts of auditory analizer – hair cells, spiral ganglia cells, auditory nerve, conducting structures, and cerebral cortex [1]. There has been proven efficiency of use of neuropeptides (ultrasonic phonophoresis) in treatment of patients with acute and chronic SNHL by activation of regeneration of central and peripheral nerve conductors, including nerve elements of the hearing organ, normalization of cerebral hemodynamics, microcirculation of inner ear, an increased resistance to hypoxia, and analgetic action [1, 2]. Among current trends in experimental and clinical investigations carried out at the Transcranial Electrostimulation (TES) Center we are studying what impact the brain endorphinergic structures activation has on reparative regeneration in tissues of different types. Our experiments have revealed that a few sessions of the TES accelerate reparative regeneration in injured afferent and efferent somatic nerve fibers [3]. These data have provided ground to explore the TES efficiency for treatment of acute and chronic SNHL caused by acoustical nerve malfunction. The TES therapy has been applied for 20 years with unspecialized "TRANSAIR-02, -03" devices developed by us [4]; it has proved to be an effective method of treatment of acute and chronic SNHL (the positive effect rates are 90% and 45%, respectively) and tinnitus (the positive effect is 45%) [4]. Our goal is to develop a specialized "TRANSAIR-07" device to increase the TES treatment efficiency of SNHL.

Materials and Methods

Device:

The device «TRANSAIR-07» is shown in Fig. 1.
The "TRANSAIR-07" [5] device makes it possible to model personalized tonal acoustic impacts (125 Hz – 8 kHz), according to the inverse audiograms separately for each ear.

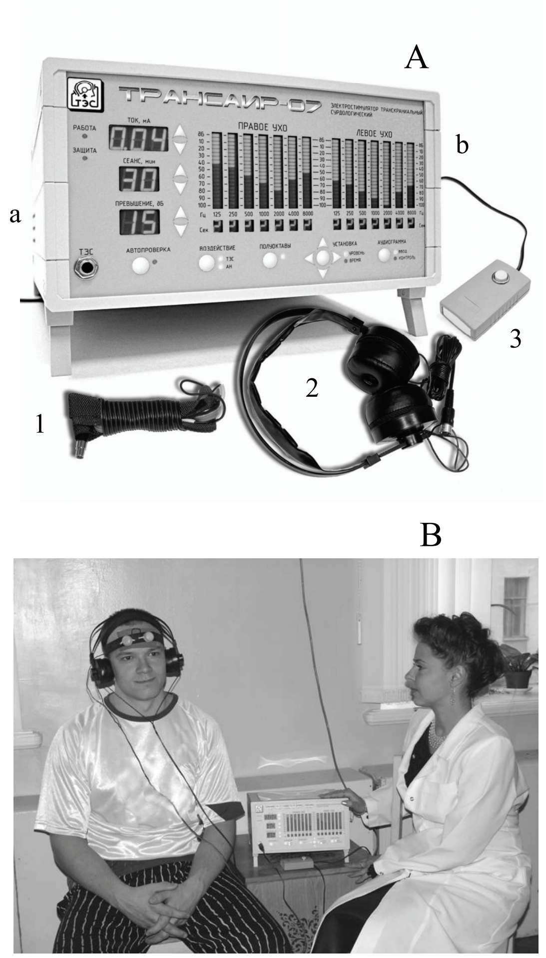

Fig. 1. A – The external appearance of the device with electrodes (1), head-phones (2), and the patient's button (3) used at audiogram output. The left part of the device (a) includes a transcranial stimulator with a socket to plug electrodes , the right part (b) – a block of acoustic loading with indicators of tonal actions corresponding to audiogram frequencies and separate adjustment for each ear. Connection of head-phones – at the back panel of the device. B – Performance of therapeutic procedure.

We may also introduce the data of the patient's previous taped audiograms into the device program, or take audiograms before the session, introduce them into the treatment program, accomplish the efficiency control and correct the treatment program during or at the end of the course.

Patients:

Examined were 81 patients (40 men and 41 women) aged from 22 to 65 years (the mean age – 30 ± 7 years) with different degrees of hearing loss. 29 patients had acute SNHL with duration of anamnesis from 5 days to 3 months. The bone-air interval in this group of patients did not exceed 10 dB. In 20 of them the descending audiogram type was revealed. The hearing loss by air conductivity at the audiogram frequencies (125, 250, 500, 1000, 2000, 3000, 4000, 6000, and 8000 Hz) was from 20 to 60 dB and more. 24 patients with acute SNHL also complained of subjective ear noises. 52 patients had chronic SNHL with the anamnesis duration from 1 to 20 years. Their bone-air interval also did not exceed 10 dB, while the hearing loss at the studied frequencies was from 20 to 70 dB; 41 patients had the descending audiogram type. 38 patients with chronic SNHL complained of subjective ear noises.

By randomization method, all patients were devided into the observation group (19 patients with acute SNHL and 33 patients with chronic SNHL). These patients being treated with TES and acoustic loading. The comparison group (10 patients with acute SNHL and 19 patients with chronic SNHL). These pateints being prescribed only medication therapy (vasodilators of peripheral action, B-group vitamins, biostimulators, anticholinesterase agents). The absence of conductive process in all patiens with SNHL was confirmed by data of acoustic impedansometry. By the degree of expression of complaints, duration of the disease, and characteristics of the hearing loss, the patients of the observation and comparison groups were comparable ($p > 0.05$). Efficiency of treatment was determined by standard assessment of the clinical status, subjective estimation of intelligibility of speech, instrumental studies – tonal threshold audiometry, measurement of noise (with use of an MA-31 audiometer) performed before and after the treatment course. For objective confirmation of dynamic changes of hearing threshold, we used recording of short-latency brainstem acoustic evoked brain potentials (with system «Nikolet Bravo-EP»). Improvement of the auditory function was considered statistically significant at a decrease of the auditory thresholds no less than 10 dB at three frequencies and more or 15 dB at two frequencies and more. To rule out the presence of conductive process in patients with SNHL, acoustic impedansometry was performed (with device «20-2020 Immittance system»). Statistics was performed by methods of variational statistics with use of program package „Statistica 6.0 for Windows". To estimate statistical significance of differences of data, Student's parametric criterion was used ($p < 0.05$).

Treatment procedure:

Patients with SNHL were treated with low-amplitude impulse currents (up to 1 мA), of 3.5 ms duration, with frequency 77.5 imp/s^{-1}. Form of impulses was rectangular, asymmetrical, bipolar, with the total current for the period equal to 0. Eletrodes were placed by the fronto-retromastoidal positions.. The current strength for each patient was selected individually by the appearance of threshold sensations. Acoustical signals were presented during performance of electrostimulation separately into each patient's ear with the aid of head-phones as consecutively generated pure tones at frequencies from 125 to 8000 Hz. Intensity of each tone was regulated automatically with consideration of the decrease of hearing thresholds revealed earlier at the tonal audiogram of a particular patient. The excess of acoustic loading above the hearing threshold at this frequency in the particular ear did not exceed 40 dB. The course of therapy consisted of 10 daily procedures, each 30-min long.

Results

In the observation group, improvement of hearing occurred in 17 patients (89%) with acute SNHL, whereas in the comparison group – in 7 patients (70%). In the observation group a statistically significant ($p< 0.05$) decrease of hearing thresholds was established at all studied frequencies by the air conductivity (125, 250, 500, 1000, 2000, 3000, 4000, 6000, and 8000 Hz) that amounted, on average, to 18.1± 4.8 dB, while by bone conductivity – 134 ± 23 dB. In individual patients the hearing increment reached more significant values – 30-50 dB. In the comparison group the hearing increment amounted, on average, to 12.3±5.8 dB by the air conductivity and 9.6±3.7 dB by the bone conductiviy.

After course of treatment, in patients of the main group with SNHL there was noted improvement of the general feeling and a decrease of accompanying functional disorders (discomfort in the ear, vertigo, headache, incidence of elevation of arterial pressure, total weakness, irritability, an increased fatigue, insomnia, heart pain, emotional suffering due to a decrease of hearing). Clinical symptoms were estimated in scores; the sum of the scores in the main group after treatment decreased from 6.5 ± 0.3 to 1.2 ± 0.1 ($p<0.001$). On the contrary, in the comparison group, a decrease of the sum of the scores was less pronounced – from 6.6 ± 0.2 to 4.8 ± 0.2 ($p<0.05$). In patients with chronic SNHL from the observation group, in the whole diapason of frequencies (from 125 to 8000 Hz) a decrease of hearing thresholds was found in 12 patients, at low frequencies (125–250 Hz) – in 3, at intermedite frequencies (500–1000 Hz) – in 4, and at high frequencies (2000–8000 Hz) – in one patient. Among 13 patiens in whom TES with acoustic loading produced no definite positive effect confirmed by data of threshold tonal audiometry or short-latency auditory evoked potentials, 6 pateints reported subjective feeling of improvement of speech.

A certain restoration of impulse propagation through auditory nerves was confirmed in chronic SNHL by recording of corresponding components of short-latency evoked auditory potentials (Fig. 2).

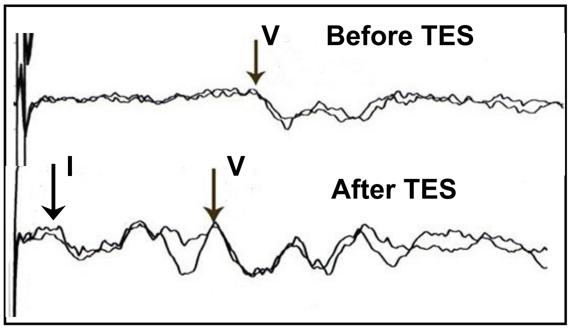

Fig. 2. Examples of the short-latency evoked auditory potentials before and after treatment of a chronic SNHL patient with TES therapy combined with simultaneous acoustic impacts. It is important the appearance of the first wave (1) demonstrating improvement of the nerve impulse propagation through the acoustic receptors and the initial part of the acoustic nerve, increase of amplitude and decrease of V component latency.

The mean data on shortening of latent periods of Vth components of the short latency evoked auditory potentials in acute and chronic SNHL patients are presented in Table 1. For the majority of chronic SNHL cases, the level of tinnitus and vertigo either stopped or were considerably reduced. Our questionnaires show that our patients' quality of life has improved. In the comparison group, changes of auditory thresholds in the whole diapason of frequencies (from 125 to 8000 Hz) were observed in 2 patients,. low frequencies (125-250 Hz) – in 3, at intermediate frequencies (500-1000 Hz) – in 4, and at high frequencies (2000-8000 Hz) – in one potentials after TES and acoustic treatment. intelligibility after treatment.

Table 1.

Changes of latencies and amplitudes of the components V of the short latency evoked auditory potentials.

Type of the SNHL	Dynamix of the Vth comp.	TES therapye	Medicamental treatment
Acute SNHL	Latency, msec	– 1,03±0,24	– 0,56±0,08
	Amlitude, μV	+ 0,82±0,11	+ 0,28±0,05
Chronic SNHL	Latency, msec	– 0,75±0,16	– 0,14±0,03
	Amlitude, μV	+ 0,40±0,07	+ 0,08±0,01

Discussion

The obtained data indicate that positive effects of sound perception in the observation group become evident in the larger number of patients by the air and bone conductivity and that the degree of hearing improvement is higher than in the comparison group patients who were on medication therapy only. The TES therapy, when combined with simultaneous acoustic impacts on acoustic receptors in an inverse audiogram mode, has shown a crucial efficiency increase of treatment, especially of chronic SNHL, including professional SNHL. The study has revealed a significant whisper speech intelligibility increase and auditory threshold reduction, according to the audiogram up to 35 dB (especially for a speech frequency range), in 60%–90% of chronic SNHL cases.

Conclusions

The TES therapy, combined with simultaneous acoustic impacts on acoustic receptors in an inverse audiogram mode, is an effective method for treatment of acute and chronic SNHL. The "TRANSAIR-07" device is easy to operate and profitable.

References

[1].Babiyak VI, Gofman VP, Nakatis AYa, Textbook of Neurootorhinolaryngology, St.-Petersburg., 2002, 728 pp. (in Russian)

[2]. Lebedev VP, Illinsky, Kolosova LI et al. Transcranial electrostimulation of the brain endorphinergic system as an example of the uninvasive functional electrostimulation of the brain homeostatic mechanisms: activation of tissue repair. 4th Annu Conf. of the IFESS, 1999, pp. 216-219.

[3]. Kolosova LI, Akoev GN, Lebedev VP et al. The influence of the transcranial electrostimulation in analgesic regimen on the functional repair of the damaged sciatic nerve. In: Transcranial Electrostimulation. Ed. Lebedev VP. St. Petersburg, 2003, vol. 1, pp. 207-214.(in Russian).

[4].Rosenblum AS, Lebedev VP, Tsirulnikov EM et al. Usage of the transcranial electrostimulation for treatment of the patients with sensorineural hearing loss. J. Ear, Nose and Laryng Diseases.1991, № 1, pp. 31-36 (in Russian).

[5]. Russian Patent № 2214842 (2003 year) "The mode of treatment of the sensorineuronal hearing loss and device for it application". Authors: Tsirulnikov EM, Lebedev VP, Malygin AV, Ignatov VS.

Acknowledgements

This study was partly supported by grant № 01-06-00019a of Russian Humanitarian Scientific Foundation, 2002.

Author's Address

Name - Valery P. Lebedev
Affiliation – TES Center, Pavlov Institute of Physiology, nab. Makarova,6, Saint-Petersburg 199034, Russian Federation
e-mail – lebedev@infran.ru; lebedev.vp@mail.ru
homepage – www.tes.spb.ru

EVALUATION OF HEARING OF PARTIAL DEAFNESS PATIENTS WITH COCHLEAR IMPLANTS BY AUDITORY EVOKED POTENTIALS

Jedrzejczak W. W.[1], Lorens A.[1], Pilka A.[1], Walkowiak A.[1], Piotrowska A.[1], Skarzynski H.[1]

[1] Institute of Physiology and Pathology of Hearing, Warszawa, Poland

Abstract

Partial Deafness Cochlear Implantation (PDCI) is a method of hearing treatment based on a concept of combining electric and acoustic stimulation (EAS). The main subject of this study was to objectively evaluate hearing of patients after such treatment. For this purpose a method of auditory evoked potentials was considered. The advantages and problems of such approach are discussed.

Introduction

For normal hearing people the sound is transmitted by drum membrane through small bones of middle ear to the cochlea. In this structure which resemble snail shell, mechanical vibrations (evoked by sound) are transformed into electrical impulses. These impulses are transmitted to the brain by auditory nerve. The cochlear implant was developed to provide a sense of sound to profoundly deaf persons. It is an electronic device that bypasses the normal hearing mechanism and electrically directly stimulates auditory nerve (Fig. 1).

The internal part of the implant is surgically placed in the mastoid portion of the temporal bone and contains a receiver and an electric stimulator in the same housing with the electrode array. The electrode array extending from the implant housing is inserted into the cochlea. The external part is the speech processor that transforms sound into electric stimuli [1].

There is a large group of patients whose hearing impairment is characterized by normal or slightly elevated thresholds in the low-frequency band, with nearly total deafness in higher frequencies. This type of hearing impairment is described as partial deafness [2]. The patients in this group remain beyond the scope of effective treatment by hearing aids only. Such patients have not been considered before for cochlear implantation, because it was feared that this intervention would damage the functioning part of the cochlea [3].

Partial Deafness Cochlear Implantation (PDCI) is based on a new concept of combining electric and acoustic stimulation (EAS) through High-Tec technologies as cochlear implants [4], [5].

Intraoperative procedure for partially deafened patients [6] allows for preservation of residual hearing after cochlear implantation [7]. In this method the electrode is inserted into cochlea through one of its membranes. This is the least radical way of cochlear implantation which preserves all intracochlear structures. The combination of preserved residual low-frequency, acoustic hearing and high-frequency, electrical stimulation allows a high level of speech understanding, particularly in noise [8] [9].

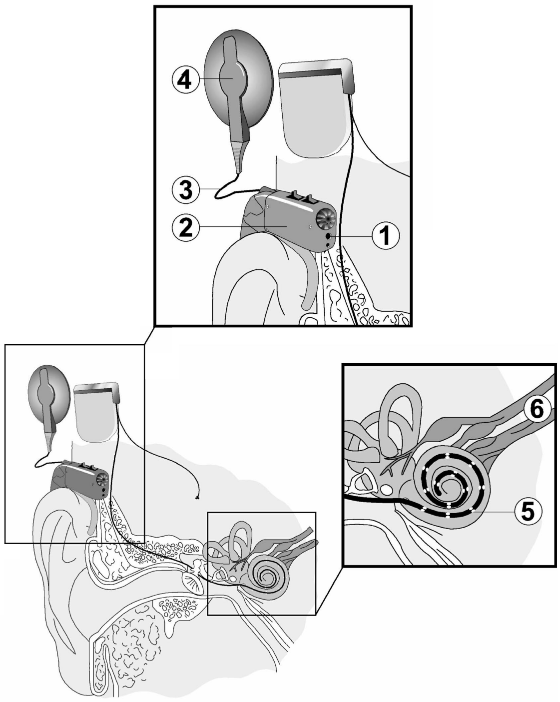

Fig. 1: Scheme of the cochlear implant system. 1 – LED, 2 – speech processor, 3 – connecting cable, 4 – transmitter, 5 – implant electrode (inside cochlea), 6 – auditory nerve.

Recently auditory steady state responses (ASSRs) were used to characterize electrophysiologic response of patients with a cochlear implant [10]. Thresholds estimated in this way demonstrated good agreement with the subjective thresholds.

The main purpose of the present study was to use auditory evoked potentials to evaluate hearing of Partial Deafness patients after Cochlear Implantation.

Material and Methods

PDCI essentially involves 3 challenging aspects. 1) Careful selection of the right candidates most likely to gain substantial benefit from the procedure; 2) Surgical techniques allowing hearing preservation; and 3) transferring the maximum amount of sound information to the patient using an optimised configuration of electrical pulses to the electrodes and acoustic information through a hearing aid. The hearing of PDCI patients was pre- and post-operatively evaluated by audiometric tests, speech discrimination tests and measurement of auditory steady state evoked potentials (auditory steady state responses – ASSRs).

The ASSRs were measured using GSI Audera (Viasys/Grason-Stadler Inc.) at four frequencies, 500 Hz, 1 kHz, 2 kHz and 4 kHz. Typical stimuli with MM type AM/FM modulation were delivered from free field speaker setting. A standard up-and-down procedure, with level increments of ±10 dB, was used to find the threshold of ASSR response. The threshold was defined as the lowest stimulus level at which one observed a statistically significant response, unless no valid response was observed at two consecutive levels above it (Fig. 2).

Results

As a first step the ASSRs were measured with implant switched off, to study the remains of natural hearing of patients. Comparison of ASSR thresholds with pure tone audiogram is shown in Fig. 2. The measured levels were similar to subjective thresholds.

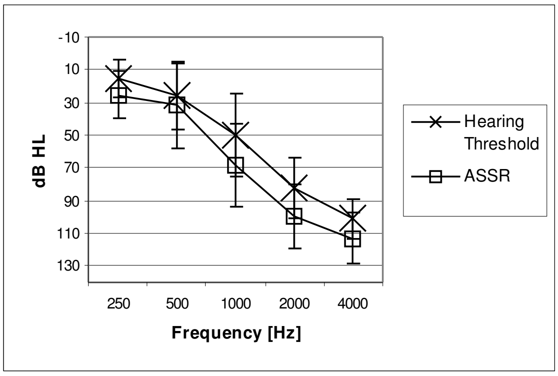

Fig. 2: Mean hearing thresholds for PDCI patients. Mean pure tone audiograms (cross) and mean ASSR (square) thresholds for studied group are shown.

Next the ASSRs were measured when implant was activated. However in this situation a following problem arises. The implant electrode delivers electrical impulses to the auditory nerve and this activity can also be measured as a component of evoked potentials. To test this possibility a person with partial deafness was chosen which had some of her implant channels inactive. This is a usual situation in partial deafness patients. The electrode is inserted only partially to stimulate high frequencies, and leave low frequency area of cochlea intact. Some of the channels at the beginning of electrode are switched off since they do not deliver signal to auditory nerve. This situation can be used to deliver the same activity to channel connected to auditory nerve and then to channel which is normally inactive. In the first situation the subject should hear and in the second should not. ASSRs and subjective thresholds were measured for four settings of cochlear implant: 1) implant switched on, 2) only 2kHz band electrode activated, 3) 2kHz band delivered to electrode which does not deliver sound to auditory nerve, and 4) with implant switched off. The results are presented in Fig. 3. It can be seen that hearing levels evaluated by ASSRs are the same for first three settings.

For first two settings ASSRs levels were similar to behavioural thresholds. Unfortunately when implant was in third setting and the subject does not heard the sound (as can be seen for subjective threshold) ASSR showed the same level as in first two settings. The electric activity of electrode was mistaken for auditory steady response.

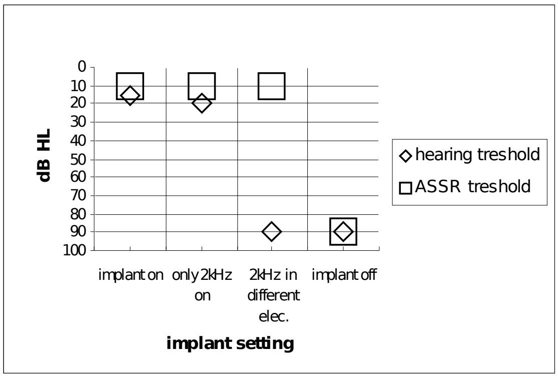

Fig. 3: Hearing thresholds in 2kHz with different cochlear implant setting. Behavioural and ASSR thresholds shown together for comparison. The 90 dB thresholds are marked for situations when subject does not heard the sound or does not had any response.

Discussion

For now only the remains of natural hearing of implanted patients can be tested by ASSRs. Only the partial deafness cochlear implanted patients mark these criteria. In this particular group of implanted patients auditory evoked potentials can provide reasonable and objective measures of hearing levels. The hearing of classically implanted patients must be evaluated by different methods.

When implant is switched on during auditory evoked potentials testing, the electrodes of measuring system are recording an electric artifact caused by implant rather than the response of the brain. The patients with preserved partial hearing can be investigated by auditory evoked potentials when the implant is turned off providing that the stimulation levels are adequately high.

References

[1] Lorens A, Piotrowska A, Skarzynski H, Obrycka A Application of implantable electronic prostheses for patients with hearing impairment. Pol Merkur Lekarski. 19(111):487-9, 2005.

[2] Skarzynski H, Lorens A, Piotrowska A: A new method of partial deafness treatment. Med Sci Monit, 9(4): CS20-24, 2003.

[3] Lorens A, Geremek A, Walkowiak A, Skarżyński H: Residual acoustic hearing in the ear before and after cochlear implantation; in Jahnke K, Fischer M, editors. 4th European Congress of Oto-Rhino-Laryngology Head and Neck Surgery. Bologna, Monduzzi, 1: 135-138, 2000.

[4] von Ilberg C, Kiefer J, Tillien J et al: Electric-Acoustic-Stimulation (EAS) of the Auditory System. New Technology against severe hearing loss. ORL J Otorhinolaryngol Relat Spec, 61(6): 334-40, 1999.

[5] Lorens A Skarzynski H, Piotrowska A, New methods of deafness and partial deafness treatment Biocybernetics and Biomedical Engineering, 26: 75-83, 2006.

[6] Skarzynski H, Lorens A, Piotrowska A, Anderson I. Preservation of low frequency hearing in partial deafness cochlear implantation (PDCI) using the round window surgical approach. Acta Otolaryngol. 127: 41-48, 2007.

[7] Skarżyński H, Lorens A, D'Haese P, Walkowiak A, Piotrowska A, Sliwa L et al.: Preservation of residual hearing in children and post-lingually deafened adults after cochlear implantation: An initial study. ORL J. Otorhinolaryngol. Relat. Spec. 64(4): 247-53, 2002.

[8] Skarzynski H, Lorens A, Piotrowska A, Anderson I.Partial deafness cochlear implantation provides benefit to a new population of individuals with hearing loss. Acta Otolaryngol. 126(9): 934-40, 2006.

[9] Skarżyński H., Lorens A., Piotrowska A., Anderson I. Partial deafness cochlear implantation in children. Jnt J Pediatr Otorhi, 2007, in print.

[10] Menard M, Gallego S, Truy E, Berger-Vachon C, Durrant JD, Collet L. Auditory steady-state response evaluation of auditory thresholds in cochlear implant patients. Int J Audiol. 43 Suppl 1:39-43, 2004.

Author's Address

W. Wiktor Jedrzejczak
Institute of Physiology and Pathology of Hearing ul. Zgrupowania AK "Kampinos" 1
01-943 Warszawa
Poland

w.jedrzejczak@ifps.org.pl

LONG TERM OR SHORT TERM ELECTROMYOSTIMULATION THERAPY IN OBSTRUCTIVE SLEEP APNEA (OSAS)?

Ludwig A[1]

[1] MGK Medical and Cranio-Maxillofacial Hospital Kassel, Germany

Abstract

In two groups an individually shaped mouth floor electrode (IME) had been used for electromyostimulation therapy by patients (n = 16) with OSAS.

The EMS was carried out two times daily for thirty minutes during daytime hours, only. In group I only over a period of eight weeks the EMS was applied and than stopped. In group II the patients used EMS therapy for half a year continuously. Before stimulation and 4, 8, 12 and 26 weeks after starting stimulation 3D-volumetric sonographical measurement of the geniohyoid muscle was carried out.

After four weeks EMS-therapy a volume increase was registered: in group I in median of 19.0 % and after eight weeks of 27.0 %; group II: 19.6 % and 28.2 % (8 weeks). Additionally also in both groups a shortening of the muscle in length of 4.7 % / 4.9 % in median was measurable. In group I after 26 weeks the volume was next to the baseline before stimulation (+ 4.3 %). In the second group, the increase of volume persisted (+ 29.4 %) over the observation period of 12 to 26 weeks.

The EMS-therapy should be carried out as continuous long term therapy or as interval therapy.

Introduction

Many people suffer from an untreated sleeping disorder. They do not know that in most cases they are snoring and have undiagnosed breathing stops also known as sleep apnea. The obstruction is caused in the nose (5 % of the cases), by a relaxation of the soft palate (15 %) or in 80 % in a relaxation of the tongue muscles and muscles of the mouth floor.

During the last years, also innovative muscle stimulation techniques (electromyostimulation = EMS) have became alternatives for therapy of obstructive sleep apnea [1, 2, 3, 4, 5, 6, 7, 8, 9, 10]. The stimulation efficiency and duration are assumed to have influence on the sleeping parameters. There exist different recommendations how long the treatment should be. In most studies an EMS therapy of 4 to 8 weeks is applied [5, 6, 8, 9, 10], but long term follow up does not exist. Therefore it was of interest for how long the EMS therapy has to be applied by patients with OSAS.

Material and Methods

In two groups an individually shaped mouth floor electrode (IME) of the Snorprevent® system (fig. 1) had been used for electromyostimulation therapy. The enoral-cutaneous EMS [11] (fig. 2) was carried out in patients with OSAS (n = 12, RDI < 20, median age 50.1 years) with the low frequency stimulation apparatus I-pulse two times daily for thirty minutes during daytime hours, only. The patients were instructed to choose treatment with maximum intensity. The impulse frequency was 50 Hz, the contraction time 10 s, pause time 20 s, impulse width 250 µs, the ramp time: increase / decrease 1.5 / 1.5 s and the voltage RMS eff. 4.4 V. In group I only over a period of eight weeks the EMS was applied and than stopped. In group II the patients used EMS therapy for half a year continuously.

Fig. 1: EMS-system Snorprevent® with the I-Pulse apparatus (Stimpoint Ltd., Bovenden, Germany).

Diagnostic procedures during EMS

The morphology and volume of the geniohyoid muscle were examined by 2D- and 3D-sonography. By use of a 7.5 MHz linear scanner the muscle was measured in width and from the spina mentalis to the hyoid in length. Moreover, through combination of B-scan-sonography apparatus with a 3D-workstation a three-dimensional demonstration and measurement of the volume of the geniohyoid muscle became possible. Before stimulation and 4, 8, 12 and 26 weeks after starting stimulation 2D-sonographical and also 3D-volumetric measurement of the geniohyoid muscle was carried out.

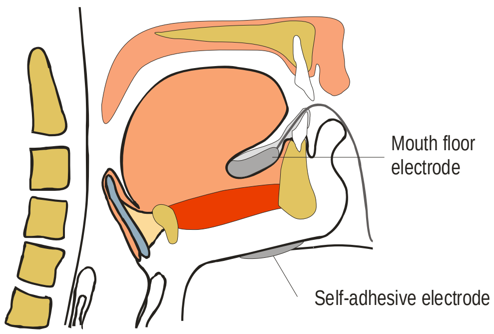

Fig. 2: Cross section of the upper airway with placement of the submental electrode and the intraoral electrode (IME).

Results

After four weeks EMS-therapy a volume increase in both groups was registered: In group I in median of 19.0 % (minimum 9.2 %, maximum 27.6 %) and after eight weeks of 27.0 %. In the second group there exists an increase in medain of muscle volume of 19.0 % and 28.2 % after 8 weeks. There was no significant difference between both groups (fig. 3).

In group I after the end of the stimulation period a decrease of the muscle volume developed in all cases. After 26 weeks the volume was next to the baseline before stimulation (+ 4.3 %).

In group II, the increase of volume persisted (+ 29.4 %) over the observation period of 12 to 26 weeks. No decrease could be found.

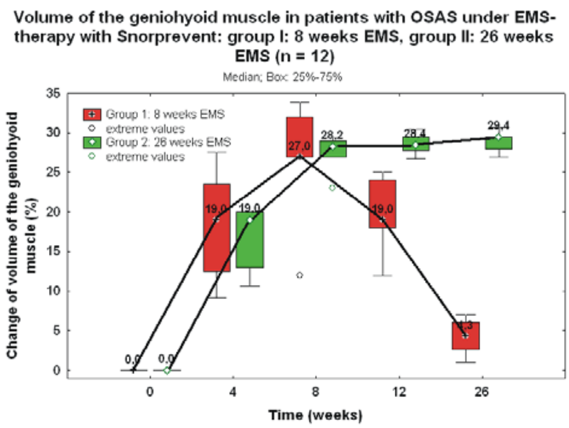

Fig. 3: Diagram of the change of volume of the geniohyoid muscle under EMS therapy.

Additionally also in both groups a shortening (contraction) of the muscle in length of nearly 5 % (4.7 % / 4.9 %) in median was measurable (Fig. 4).

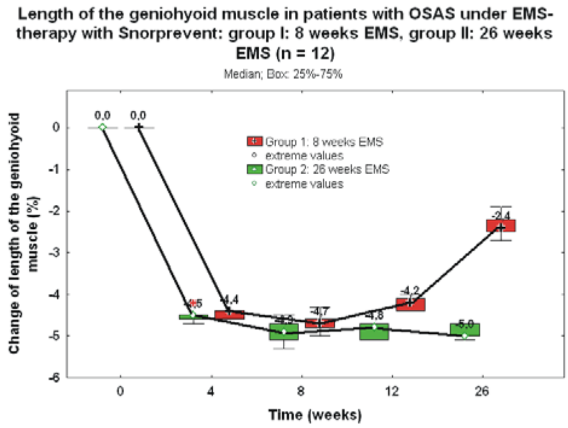

Fig. 4: Diagram of the change of length of the geniohyoid muscle under EMS therapy.

In group 1 after ending the EMS (after 8 weeks) the length of the muscle show an increase nearly to the baseline. Despite of the increase of muscle length snoring and apnea reoccurred only in 50 % of the patients.

Discussion

There exist different recommendations how long the treatment should be. In most studies an EMS therapy of 4 to 8 weeks is applied applied [5, 6, 8, 9, 10, 12].

Under EMS therapy a volume increase in median of 19.0 % (after 4 weeks) and 28 % (8 weeks) was registered. Through the visualization of the muscles in 3D-models the concentric volume increase could be proved which was mainly due to the contraction of the muscles as Oliven et al. in 2004 [13] described. In both groups, a reduction of the muscles in length of 4.7 % was proved. Due to this fact, an opening of the posterior airway was enabled, so that snoring and breathing stops simultaneously were reduced.

In opposite to the opinion, that 8 weeks are enough in treatment, it could be shown that a once again a decrease of the muscle volume after the end of the EMS therapy and a weakness of the muscle occured. Therefore the EMS-therapy with optimized individually adaptable electrodes should be carried out as continuous long term therapy or as interval therapy. As the results show, a pause of stimulation for 4 weeks is possible. After that period stimulation has to be carried out again for maintenance of therapy effect. Despite of the decrease of muscle volume and increase in length in the first group after 8 weeks snoring and apnea reoccurred only in 50 % of the patients.

These results lead to the conclusion that the EMS-therapy should be carried out as continuous long term therapy or as interval therapy.

For controlling efficiency of the EMS, the 2D- and 3D-sonographical demonstration and measuring of the geniohyoid muscle can be used [14].

For evaluation of efficiency in the time course, sonography appears to be a convenient method. The 3D-sonography in this investigation field seems to be superior to the 2D-sonography, because in the former technical procedure the option of volume determination is given.

References

[1] Miki H, Hida W, Inoue H, Takishima T: A new treatment for obstructive sleep apnea syndrome by electrical stimulation of submental region. Tohoku J Exp Med 154, 91 - 92, 1988

[2] Miki H, Hida W, Shindoh C, Kikuchi Y, Chonan T, Taguchi O, Inoue H, Takishima T: Effects of electrical stimulation of the genioglossus on upper airway resistance in anesthetized dogs. Am Rev Respir Dis 140, 1279 - 1284, 1989

[3] Miki H, Hida W, Chonan T, Kikuchi Y, Takishima T: Effects of submental electrical stimulation during sleep on upper airway patency in patients with obstructive sleep apnea. Am Rev Respir Dis 140, 1285 - 1289, 1989

[4] Broniatowski M: The Potential for Neurostimulation in Obstructive Sleep Apnoea. ASAIO Journal 1994, 13 - 16, 1994

[5] Wiltfang J, Klotz S, Jordan W, Cohrs S, Engelke W, Ludwig A, Hajak G: Erste Ergebnisse zum Training der suprahyoidalen Muskulatur bei Probanden und einem Patienten mit obstruktiver Schlafapnoe. Somnologie 1, 160 - 164, 1997

[6] Wiltfang J, Klotz S, Wiltfang J, Jordan W, Cohrs S, Engelke W, Hajak G (1999): First results on daytime submandibular electrostimulation of suprahyoidal muscles to prevent night-time hypopharyngeal collapse in obstructive sleep apnea syndrome. Int J Oral Maxillofac Surg 28, 21 - 25, 1999

[7] Verse T, Schwalb J, Maurer JT, Stuck BA, Hörmann K: Transcutaneous submental electrostimulation therapy for obstructive sleep apnea. First clinical results. Somnologie 6, Suppl 1, 40, 2002

[8] Randerath W: Alternatives/Completions to nasal CPAP. Somnologie 6, Suppl 1, 175, 2002

[9] Randerath, W. J., Galetke, W., Rocholl, C., Rühle, K. H.: Tongue muscle training by electrical stimulation in obstructive sleep apnea. A double-blind, placebo-controlled study. Am J Respir Crit Care Med 167 (7), A 327, 2003

[10] Ludwig, A., Monzavifar, O., Jordan, W.: Results of therapy of sleep apnea syndrome by electromyostimulation. Am J Respir Crit Care Med 167 (7), A 132, 2003

[11] Ludwig, A., Monzavifar, O., Diederich, D.: The individually adapted intraoral electromyostimulation electrode for therapy of sleep apnea. Int J Oral Maxillofac Surg 32, Suppl 1, 122, 2003

[12] Heinrich, F., Käßner, F., Schweisfurth, H.: Elektrisches Zungenmuskeltraining zur Behandlung des habituellen Schnarchens. Eine Kasuistik. 11. Deutscher Kongress für Schlafforschung und Schlafmedizin, Poster 78, Cottbus, 25. – 27.9.2003

[13] Oliven, A., Tov, N., Odeh, M., Geitini L., Steinfeld, U., Oliven, R., Schwartz, A. R.: Effect of genioglossus (GG) contraction on oro- (OP) and naso-pharyngeal (NP) cross-sectional area (CSA) and airflow in patients with obstructive sleep apnea (OSA). Am J Respir Crit Care Med 169 (7), A 435, 2004

[14] Ludwig, A.: Techniken, Methodik, Messverfahren und Ergebnisse der Elektromyostimulation (EMS) zur Therapie schlafbezogener Atmungsstörungen. Abstract-sammlung der 6. Jahrestagung der Norddeutschen Vereinigung für Schlafmedizin (NVSM), 1, 2004

Author’s Address

Priv. Doz. Dr. Dr. Arwed Ludwig
MGK Medical and Cranio-Maxillofacial Hospital
Neue Fahrt 12
D-34117 Kassel, Germany
aludwig@gwdg.de

STIMBELT®: ASSISTIVE SYSTEM FOR THERAPY IN INDIVIDUALS WITH LOW BACK PAIN

Popović D.B.[1], Bijelić G.[2], Schwirtlich L.[3], Vujanić A.[4], Rohrer C.[5], Kanjuh Ž.[3]

[1]Center for Sensory Motor Interaction, Aalborg, Denmark; [2]Center for Multidisciplinary Studies, Belgrade, Serbia; [3]Institute for Rehabilitation "Dr Miroslav Zotović", Belgrade, Serbia; [4]Integrated Microsystems Austria (IMA) GmbH, Wienner Neustadt, Austria, [5]Lohman & Rausher GmbH, Schönau/Triesting, Austria

Abstract

Low Back Pain (LBP) can be caused by the gradual degeneration of joints and soft tissue over time from repetitive microtrauma caused by poor control of spinal structures. The direct rehabilitation goals are to relieve pain, reduce muscle spasms, improve strength and range of motion, and teach patients how to prevent the reoccurrence of LBP. We developed the STIMBELT, a therapeutic stimulation system which interfaces to the user via electrodes embedded in the lumbar belt and allows programmed activation of up to 8 muscle groups in synchrony with the exercise typical for the treatment of LBP. The STIMBELT comprises a sensory system based on accelerometers that can trigger the stimulator to activate appropriate muscle groups to prevent movements that could possibly evoke pain. The STIMBELT was tested in eight subacute and chronic patients. The outcome measures included: a visual analogue scale of pain, the Oswestry LBP disability questionnaire, and an abbreviated version of SF-36 health survey. The results indicate significant benefits with STIMBELT treatment when compared with conventional therapy. Both patients and therapists accepted the new type of treatment with great enthusiasm.

Introduction

Low Back Pain (LBP) is a significant cause of workers' compensation [1]. Between 60% and 90% of the adult population is at risk of developing LBP at some point in their lifetime [2-6]. While the majority of episodes appear to resolve themselves within six weeks, the estimate is that 10% to 20% of affected adults develop symptoms of chronic LBP. Chronic LBP is defined as persistent pain lasting longer than three months and occurring on at least 50% of days. It has a significant impact on functional status, restricting occupational activities with marked socio-economic repercussions [7, 8].

The management of LBP encompasses a range of different interventions including: drug therapy, exercise, patient education, physiotherapy, cognitive-behavioral therapy, alternative therapies and surgery. A multidisciplinary approach founded on the biopsychosocial model has been advocated for some patients with chronic LBP [7]. The treatment goals are to relieve pain, reduce muscle spasms, improve strength and range of motion, promote early return to activity, encourage acting coping strategies and ultimately improve functional status. The risks and benefits of these treatments vary. Acute and chronic LBP warrant separate consideration as they may respond differently to the same intervention [9, 10].

The development of the new instrument for therapy follows recent physiological findings that the central nervous system (CNS) can be reorganized by intensive repetitive exercise, augmented with robots or electrical stimulation. The studies of using electrical stimulation to externally augment movement demonstrated substantial differences between the use of cyclic and task dependent electrical stimulation protocols [11, 12]. The most likely reasons are that electrical stimulation of a motor nerve generates both an orthodromic (towards the muscle) and an antidromic (towards the spinal cord) train of impulses. The antidromic impulses should not be ignored because they facilitate motor learning [13].

Therefore, we developed the STIMBELT, which is an augmentation to the learning of new strategies by means of electrical stimulation (positive feedback) integrated in task oriented exercise. The STIMBELT is a lumbar belt with embedded electrode-arrays which connect to a programmable 8-channel portable battery operated electronic stimulator (UNAFET 8), and a sensory system for assessing trunk movements. In this paper we discuss the operation of the stimulation system only.

STIMBELT for treating Low Back Pain

The STIMBELT allows external activation of the muscles responsible for upper body posture; it contributes to a better biomechanical substrate that could prevent or decrease LBP. The STIMBELT comprises up to 8 pairs of conductive electrode-arrays embedded in the lumbar belt that fits the contours of the lumbar and abdominal regions of the individual using the system. Fig. 1 shows the layout of the electrode-arrays used in this study.

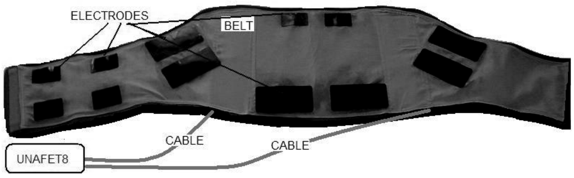

Fig. 1: The inside of the prototype version of the lumbar belt with embedded 6 pairs of matrix electrodes and 2 cables connecting to the UNAFET8® stimulator.

The UNAFET8® stimulator supports several preprogrammed sequences that activate muscles in a timing pattern that is either cyclic or synchronous with the voluntary contractions of agonists or antagonists. Its electrode-arrays allow simple selection of the electrode size, shape, and position with respect to the desired zone on the body of the patient.

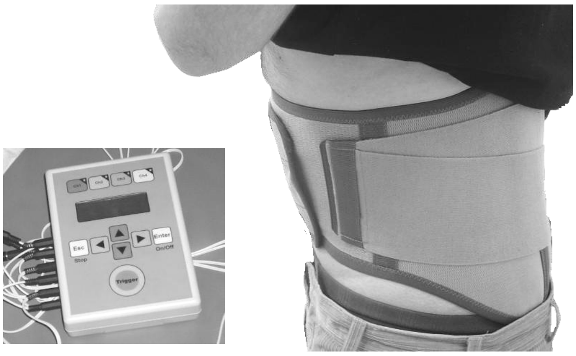

Fig. 2: The eight channel UNAFET8® stimulator (left) and STIMBELT® worn by the subject who participated in this study.

The stimulator (Fig. 2) has push-button switches, and a four line display allowing the therapist or patient to program the timing and set the parameters of stimulation. The stimulator also integrates an infrared (IC) link that allows wireless communication with the host Windows based platform. This IC link allows stimulation programs to be downloaded from the computer, or the stimulation paradigm from the UNAFET8® to be uploaded to the computer.

The stimulation programs allow intermittent, continuous, modulated, low and high frequency modes of activation of sensory-motor systems.

STIMBELT Pilot Study

Subjects. 19 subjects entered to the study; ten out of them were inpatients, and nine outpatients of the Rehabilitation Institute „Dr Miroslav Zotović“, Belgrade with verified lumbar disc herniation and with subacute low back pain confirmed by imaging. All of the subjects participated in the regular physical therapy. Three subjects dropped out of the study: two because they did not like the sensation of being stimulated (both female), whilst one had an acute low back pain attack (not caused by this study). Subjects were randomly divided in two groups. The study was finalized with the following subjects: control group (five male, three female, 39.8±6.3 years), treatment group (six male, two female, 40.9±6.9 years).

Methods. The electrodes (6 pairs) were positioned over the following muscle groups: *Lumbosacral paravertebral bil.*, m. *Obliques Abdominis bil.* and m. *Rectus Abdominis* (lower portions). The individual positioning of the electrodes was facilitated due to the special design of the lumbar belt and the use of a transparent template that was positioned on the skin.

The STIMBELT group exercised in the standing position (Fig. 2) or lying on their back (Fig. 3) with the STIMBELT®. The “on-off” switch was under the control of the subjects themselves. In the first week all muscle groups were stimulated simultaneously - on command. In the second and third weeks, the stimulation was started after an active pelvic tilt and volitional contraction of the m. r*ectus abdominis*.

Subjects were stimulated 30 min. a day for 15 days in addition to their regular Physical Therapy.

Fig. 3: Patient exercising with the STIMBELT activating the appropriate muscle groups in the laying position.

The stimulation parameters were set at: f=50 pulses per second, pulse duration T=500 μs. The stimulation sequences and the rest phases lasted for at least 5 seconds (up to 10 seconds); the rise and fall times were set at 1 second. The maximum intensity was adjusted individually at a level acceptable by the subjects, yet, strong enough to generate muscle contractions.

The control group exercised typical movements with the lumbar belt instrumented with the electrodes with no stimulation.

Assessment and evaluation. The outcomes presented in this paper are the Oswestry Low Back Pain Questionnaire (OLBPQ) and the Visual Analogue Scale (VAS). An assessment was performed at the time of entry in the study and also after three weeks of therapy. The outcomes also included: the reduced version of the SF36® Health Survey, muscle test, and lumbosacral angles (not presented in this paper). At the end of treatment, subjects who were assigned to the STIMBELT group were asked to assess the stimulation effects and their appreciation of the treatment.

Results and discussion.

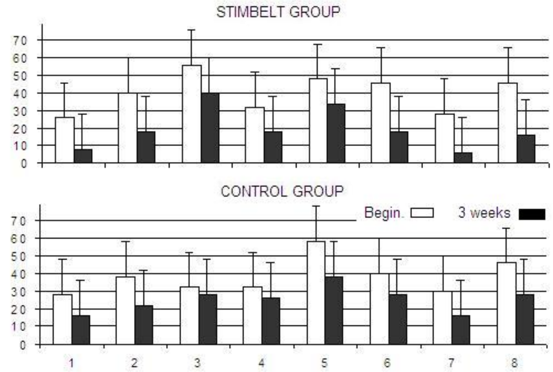

Fig. 4: Oswestry LPB Questionnaire before and after 3 weeks of the study. Maximum is 100% (worst case).

Figure 4 and 5 show individual scores in the VAS and OLBPQ. The maximum in both scores is 100%, related to the major pain and disability.

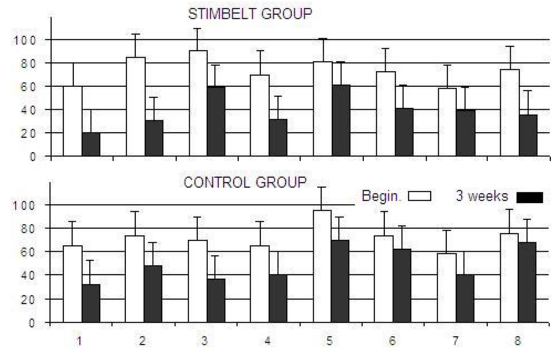

Fig. 5: Visual Analog Scale results before and after 3 weeks of the study. Maximum is 100% (worst case).

The results show the decrease of both scores in both groups as expected. We used the t-test (paired two samples for means) for the analysis of the results. The differences between the groups at the beginning were small with almost identical variances (Fig. 6.). The differences at the end of the treatment (3 weeks) were found to have a significant statistical difference (P=0.04) between the groups in the score of OLBPQ, whilst the VAS (Table 1) scores have close to significant difference (P=0.06).

Both treatments led to substantial improvement in both OLBPQ and VAS scores (P<0.01) although the differences were much bigger in the STIMBELT group compared with the controls.

Table 1: Statistical analysis of the OLBPQ and VAS scores by using t-test.

Comparison between the STIMBELT and CONTROL groups		
	the beginning (day 1)	end of therapy (day 21)
VAS	t STAT = 0.54 P(T<=t)=0.30	t STAT = 1.68 P(T<=t)=0.068
OLBPQ	t STAT = 0.64 P(T<=t)=0.27	t STAT = 2.04 P(T<=t)=0.040

Patients who participated in STIMBELT group, as well as their therapist were very enthusiastic, and most patients asked if they could continue with the treatment in order to further improve their status.

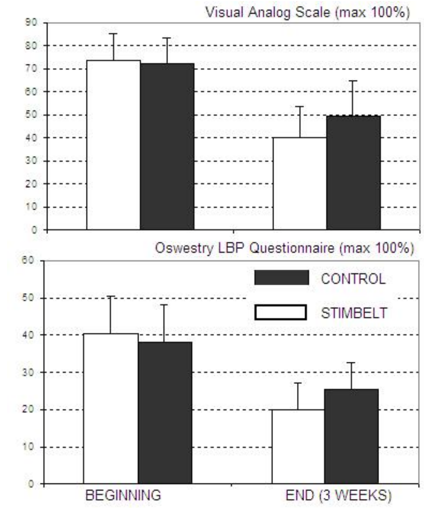

Fig. 6: The averaged VAS and OLBPQ scores at the beginning and at the end of the study

In a satisfaction questionnaire all subjects from the STIMBELT group were asked which treatment they found optimal among the following: 1) Exercise only; 2) Electrical Stimulation only; and 3) STIMBELT, selected the answer N° 3.

The limited size of the group studies did not allow the stratification required for a better understanding of the effects in patients with major pain in comparison with the effects in patients with moderate pain.

The findings from this study provided very valuable improvements in the design of STIMBELT. The positive response of the study participants, therapists, overall reduction of pain and improved OLBPQ score prompted a larger randomized clinical trial to assess the efficacy of this new treatment which will be reported at a later date.

Literature

1. Andersson GBJ. Epidemiologic features of chronic low-back pain. Lancet 1999;354:581–5.
2. Bernard BP, editor. Musculoskeletal disorders and workplace factors. A critical review of epidemiological evidence for work-related musculoskeletal disorders of the neck, upper extremity, and low back. Cincinnati: US Department of Health and Human Service, National Institute for Occupational Safety and Health; 1997.
3. Kerr MS, Frank JW, Shannon HS, Norman RW, Wells RP, Neumann WP, Bombardier C. Biomechanical and psychological risk factors for low back pain at work. Am J Public Health 2001;91:1069-75.
4. Frank JW, Kerr MS, Brooker A, DeMaio S, Maetzel A, Shannon HS, et al. Disability resulting from occupational low back pain. Part I: What do we know about primary prevention? A review of the scientific evidence on prevention before disability begins. Spine 1996;21:2908-17.
5. Bigos SJ, Bowyer OR, Braen GR, Brown K, Deyo R. Acute low back problems in adults: clinical practice guidelines 14. Rockville (MD): Agency for Health Care Policy and Research, Public Health Service, US Department of Health and Health Services; 1994. Pub no 95-0642.
6. Rossignol M, Suissa S, Abenhaim L. Working disability due to occupational back pain: three-year follow-up of 2,300 compensated workers in Quebec. J Occup Med 1988;30:502-5.
7. Deyo RA, Walsh NE, Martin DC, Schoenfield LS, Ramamurthy S. A Controlled Trial of Transcutaneous Electrical Stimulation (TENS) and Exercise for Chronic Low Back Pain. New England J Med 1990;322(23):1627–34.
8. van Tulder M, Koes BW, Bouter LM. Conservative treatment of acute and chronic nonspecific low back pain: a systematic review of randomized controlled trials of the most common interventions. Spine 1997; 22: 2128-56
9. van Tulder MW, Cherkin DC, Berman B, Lao L, Koes BW. The effectiveness of acupuncture in the management of acute and chronic low back pain. Spine 1999; 24(11): 1113-23.
10. van Tulder MW, Malmivaara A, Esmail R, Koes BW. Exercise therapy for low back pain: A systematic review within the framework of the Cochrane Collaboration back review group. Spine 2000; 25: 2784-96.
11. Popović DB, Popović MB, Sinkjær T, Stefanović A, Schwirtlich L. Therapy of Paretic Arm in Hemiplegic Subjects Augmented with a Neural Prosthesis: A Cross-over study, Can J Physio Pharmacol, 2004;82(8/9):749-56.
12. Popović MB, Popović DB, Sinkjær T, Stefanović A, Schwirtlich L. Clinical Evaluation of Functional Electrical Therapy in Acute Hemiplegic Subjects, J Rehab Res Develop, 2003;40(5):443-54.
13. Rushton D.N. Functional Electrical Stimulation and rehabilitation—an hypothesis. Medical Engineering & Physics 2003;25:75–8.

Acknowledgements

The development of the novel apparatus was supported by the companies: Lohman & Rausher, Austria and IMA, Vienna, Austria. The research was partly supported by Danish National Research Foundation, Denmark and Ministry for Science and Environmental Protection, Belgrade, Serbia.

Author's Address

Dejan B. Popović
Aalborg University, SMI, Fredrik Bajers Vej 7 D3, 9220 Aalborg, Denmark
dbp@smi.auc.dk
www.smi.auc.dk/members.dbp

SPINAL CORD STIMULATION FOR CHRONIC PAIN (FAILD BACK SURGERY SYNDROME)

Sabarini M[1]

[1] International Spine Clinic Berlin, Berlin, Germany

Abstract

Introduction:

Innovative procedures such as spinal cord stimulation (SCS) offer a non-destructive and reversible interference for treatment of chronic pain. SCS is minimally invasive procedures that can be effective in cases; where other conventional therapies did not adequately relieve pain. Failed Back Surgery Syndrome (FBSS) is an indication for SCS.

Method:

From 1996 to 2004 we provided SCS to 142 patients with FBSS. All patients had previously undergone spine surgery, 310 surgeries in total.

Results:

In an average of 6,3 years, 142 patients were monitored. Of these patients, 70,4% reported good to very good pain relief of more than 50%; 18,3% patients reported slight pain relief; and 11,3% had no relief. Of the 142 patients, 77,5% take less or no medication. In four cases, the generator was explanted because of unsatisfactory results; in two other cases, the generator was explanted because of infection, but one case received a new generator 6 months later. System defects were observed in two cases and electrode migration was observed in two others. These problems were corrected.

Conclusions:

Spinal cord stimulation is an effective alternative for the treatment of chronic pain, in cases of FBSS, compared with re-operations and destructive treatments. It is a non-destructive, reversible treatment method, and it is cost effective.

MANAGEMENT OF POST STROKE CENTRAL PAIN

Tamaki R, Nonaka J, Hirabayashi H, Nakase H, Sakaki T

Department of Neurosurgery, Nara Madical University, Kashihara, Nara, Japan

Abstract

[Introduction] *Post stroke central pain occurs when spinothalamic tract or thalamocortical tract is injured. It is sometimes intractable, and ADL of such a patient is often limited because of the pain, even if the patient has only mild or no motor weakness. As treatment of central pain, pharmacologic treatment may be effective, but sometimes not. In such a case, electrical stimulation therapy may relief the pain. We retrospectively reviewed our own experience and reviewed the literature to discuss the treatment strategy for post stroke central pain.*

[Clinical material and methods] *30 subjects were included in this study. 18 cases of them underwent surgical intervention. Our treatment strategy was as follows; at first, pharmacologic treatment was attempted with anticonvulsant, antidepressant and so on. If pharmacologic treatment is not effective enough, surgical intervention including motor cortex stimulation, spinal cord stimulation, or deep brain stimulation (VPL or IC) was planned.*

[Conclusion] *As pharmacologic treatment, amitriptyline and clonazepam is sometimes effective, and in two third of the cases with brain motor cortex electrical stimulation therapy, the pain was improved.*

Introduction

Most neurosurgeon and neurologists who has interest in treating brain stroke patient, tend to pay much more energy for acute-stage treatment, but sequelae of stroke is sometimes the most serious problem for such a patient. Central pain is one of the most serious sequelae of stroke. It occurs when spinothalamic tract or thalamocortical tract is injured, but its exact pathophysiology is still unknown.

Numerous approaches for the treatment of post stroke central pain have been reported; pharmacologic treatment with anticonvulsants such as Phenytoin, Lamotrigine, Gabapentin, or antidepressant such as Amitriptyline, and so on. [1] Pharmacologic treatment is sometimes effective, but sometimes not. In such a case, surgical intervention can be the good candidate for treating post stroke central pain. We summarized our own experience for treatment of post stroke central pain and reviewed the literature to discuss the strategy for the treatment.

Clinical material and method

30 patients of post stroke central pain in our institute were included to this study. 6 cases of thalamic hemorrhage, 12 cases of thalamic infarction, 8 cases of putaminal hemorrhage, 2 cases of brainstem infarction, 1 case of brain stem hemorrhage, 1 case of cerebral cortex lesion. 18 cases of them were received surgical intervention.

Strategy for treatment of post stroke central pain

Our strategy for treatment of post stroke central pain is as follows: at first, pharmacologic treatment with anticonvulsant or antidepressant was attempted. If pharmacologic treatment is not effective enough, surgical intervention was considered such as 1) motor cortex stimulation, 2) deep brain stimulation (VPL or IC), 3) spinal cord stimulation. If electrical stimulation is not effective, cingulotomy was considered.

Illustrative cases

Case 1 ; 53 years old woman with subarachnoid hemorrhage due to ruptured right middle cerebral artery aneurysm. She suffered from vasospasm after surgical treatment, and brain CT revealed ischemic damage due to vasospasm in right hemisphere. After 4 years, she presented intractable pain in left side of the body. Pharmacologic treatment didn't relief her pain, and spinal cord stimulation was performed.

Case 2 ; 46 years old woman with left putaminal hemorrhage. After 3 years, numbness and pain appeared and gradually developed. Pharmacologic treatment with clonazepam was effective, and pain was disappeared.

Case 3 ; 48 years old man with right thalamic infarction. Intractable pain of the left side developed after four years, The pain was improved with brain motor cortex stimulation therapy, but it recurred two years later and we performed posterior cervical electrical stimulation therapy.

Case 4 : 58 years old man with left lateral medullary syndrome. Intractable pain appears in right upper extremity one year later. We performed brain motor cortex stimulation therapy two years after onset, and it was effective.

Results

In 12 cases who got enough effect only with pharmacologic treatment, amitriptyline was effective in 7 cases, clonazepam in 7 cases, carbamazepine in 5 cases, mexiletine in 5 cases. Valproate was effective in only 2 of 12 cases. (Table 1)

Drugs	Effective cases
amitriptyline	7
SSRI	0
carbamazepine	5
clonazepam	7
valproate	2
mexiletine	5

Table 1: Number of cases who got enough effect with pharmacologic treatment in 12 cases who underwent only pharmacologic treatment.

In 18 cases who underwent surgical treatment, 15 cases underwent motor cortex stimulation. 10 of 15 cases showed post operative improvement of central pain. Cingulotomy was performed in 3 cases, and 2 of 3 cases showed improvement. Deep brain stimulation underwent in 2 cases, and none of them showed improvement (Table 2)

Surgical intervention	Total (cases)	Effective (cases)
MCS	15	10
CIN	3	2
DBS	2	0

Table 2: Results of surgical intervention: MCS : Motor Cortex Stimulation, CIN : Cingulotomy, DBS : Deep Brain Stimulation.

Discussion

Numerous types of drugs have been tried in the treatment of central pain after stroke, but large controlled trials are still lacking, and the standard of treatment has not established yet. Amitriptyline was the first oral drug to be proved its effect on central pain after stroke in placebo-controlled study. [2] In our series, the effect of each drug is as shown in Table 1. Amityiptyline and clonazepam showed good effect on post stroke central pain patient. For initial treatment for post stroke central pain, NSAIDs is sometimes administered, but we should not use them for long time if they do not have enough effect on the pain. Amirtiptyline or clonazepam is suitable for first choice. Gabapentine, promising drug for treatment of central pain, is also good choice.

And, if pharmacologic treatment is not effective enough, surgical intervention should be considered. Motor cortex stimulation is one of the most promising surgical intervention. It is said that stimulation to motor cortex neuron activates non-nociceptive neurons in the sensory cortex selectively, either through orthodromic activation of neuronal chains to the sensory cortex or antidromic activation of axons projecting from the sensory cortex. [4] Barbiturate sensitivity and opioid insensitivity, response to transcranial magnetic stimulation are reported to be good predictor of patients who likely to benefit from stimulation, but it is still difficult to predict completely. It has been reported approximately 50% of post stroke central pain patients show good response. In our series, 66% (10 of 15 cases) showed improvement. This response rate is comparable to former reports. [3]

Conclusion

As medical treatment, amitriptyline or clonazepam is sometimes effective.

In cases that enough effect is not achieved with pharmacologic treatment, surgical treatment should be attempted, and brain motor cortex stimulation is good candidate for the next treatment.

Everyone who is specialized in stroke treatment should actively take part in not only acute stage treatment, but also chronic stage treatment for post stroke central pain.

References

[1] Frese A et al. Pharmacologic Treatment of Central Post-Stroke Pain. Clin J Pain, vol.22, No.3, 252-260,2006

[2] Leijion G, et al, Central post-stroke pain: a controlled trial of amitriptyline and carbamazepine. Pain 36:27-36, 1989

[3] Carroll D et al, Motor cortex stimulation for chronic neuropathic pain: a preliminary study of 10 cases, Pain, 84;431-437,2000

[4] Tsubokawa T et al, Chronic motor cortex stimulation in patients with thalamic pain. J Neurosurg 78:393-401,1993

Author's Address

Ryo Tamaki

Department of Neurosurgery, Nara Medical University, Kashihara, Nara, Japan

e-mail : rtamaki@naramed-u.ac.jp

TREATMENT OF CHRONICAL NEUROPATHIC PAIN – FIRST CLINICAL EXPERIENCE WITH PERIPHERAL NERVE STIMULATION (PNS)

Girsch W[1], Weigel G[1], Mickel M[1]

[1]Orthropedic Hospital Speising Vienna, Vienna, Austria

Abstract

Introduction:

Central nerve stimulation (CNS) already has proved its efficacy for treatment of chronical severe pain. The aim of our small clinical study was to prove the effectiveness of Peripheral nerve stimulation (PNS) for treatment of neuropathic pain syndrome of the extremities.

Material and Methods:

3 patients, two females (1,2) and one male (3), all suffering from chronic neuropathic pain of one of their extremities were selected for treatment. None of the patients was able to use the extremitiy functionally. In all 3 patients NRS 10, even at rest, required not only psychological treatment but somatical intervention. A stimulation lead was implanted to either the medial fascicle of the brachial plexus (2)(3) or to the sciatic nerve (1) and connected with a Versitrel stimulator (Medtronic Inc), using the system designed for CNS.

Results:

PNS was effective to reduce pain from NRS 10 to 0(3) up to 3(1)(2) and to regain functional use of the extremity. Several technical complications as electrode dislocation (2)(3) and wire breakage (3)had to be noted. Relief from pain occured immediately after onset of stimulation. The positive effect was directly correlated with PNS, and stable over one year.

Discussion:

PNS reduced pain deriving from peripheral nerves reliable and effective. Regarding our follow up periode of one year PNS produced a stable, nearby pain free interval in all three patients. Positioning of the electrodes direct to the brachial plexus and close to the sciatic foramen allowed movement of shoulder and hip to a nearby normal ROM. PNS seems to represent a promising technology for treatment of chronic neuropathic pain in selected cases.

Session XI

Scientific Poster Presentations

INVESTIGATIONS OF SENSORY SIGNALS IN HUMAN PERIPHERAL NERVES – UNDERPINNING PROSPECTS OF FEEDBACK LOOP IMPLEMENTATION IN BCI AND FES DEVICES

Birznieks I[1], Macefield VG[1,2]

[1] Prince of Wales Medical Research Institute, Sydney, NSW 2031 Australia

[2] School of Medicine, University of Western Sydney, NSW 1797, Australia

Abstract

Brain-computer interfaces (BCI) and neuroprosthesis are close to breaking their way beyond the experimental realm and approaching clinical medicine. However, the ambitious long-term goal to regain fine control over human hand function is impossible without meaningful feedback from the periphery. The most comprehensive and accurate source of this information is the patient's own sensory afferents, which retain their capacity to encode mechanical information even below the lesion after spinal cord injury. Accordingly, it should be possible to obtain feedback information by tapping into the sensory signals from peripheral nerves and deliver them directly to the brain, BCI or FES devices controlling the muscles. From this perspective the crucial step towards achieving this goal is to understand how the somatosensory information is encoded, analysed and used by the central nervous system (CNS) to control the motor actions. Using the technique of microneurography – in which a microelectrode is inserted percutaneously into a peipheral nerve of an awake human subject - we recorded signals in human tactile afferents while applying forces to fingertips comparable to those that arise in everyday manipulative tasks. With this technique we are able to analyze tactile neural mechanisms in awake human with a precision and resolution previously available only in experiments on anaesthetized animals, while at the same time the subject can perform motor and psychophysical tasks.

Introduction

Brain-computer interfaces (BCI) and neuroprostheses have showed their potential power in movement restoration after various types of nervous system damage, including stroke and spinal cord injury. Those scientific achievements depend on technologies already available for reading electrical signals from groups of neurons in the brain. Computational models are also available for translating this information into commands controlling artificial limbs or functional electrical stimulation (FES) devices that exploit the patient's own "biological hardware". However, it is clear that the ambitious long-term goal to regain fine control over human hand function is impossible without meaningful sensory input from the periphery. Just imagine how difficult or even impossible it would be to perform even simple everyday tasks without any sensation from the fingers, such as when these afferents are anaestheitzed by cold. It is proposed that sensory information might be accessed by tapping into the afferent signals in peripheral nerves and then delivered to the BCI or FES devices controlling the muscles. Using direct intraneural recordings from patients with spinal cord injury we and our colleagues have demonstrated that peripheral sensory nerve fibres (afferents) below the lesion retain their capacity to encode mechanical information [1]. We have demonstrated the proof-of-principle that flexible platinum-iridium wires can remain within a fascicle of a peripheral nerve on a time scale of days without being dislodged by movements. However, to be able to exploit those signals recorded in peripheral nerves, first of all we must have a thorough understanding of how somatosensory information is encoded, analysed and used by CNS to control the motor actions. To achieve this, the overall goal of our research is to unravel the encoding and processing mechanisms of sensory information endowing humans with their extraordinary ability to manipulate physical objects with their hands. The present account concerns an ongoing investigation of the encoding of manipulative forces by tactile sensors in the fingertips.

Material and Methods

Microneurography

The technique of recording impulses from single nerve fibers in awake human subjects is based on percutaneously inserted specially designed tungsten microelectrodes that impale a peripheral nerve [2], in the present study the median nerve innervating cutaneous receptors in the fingertips

(Fig 1). With this technique it is possible to analyze tactile neural mechanisms in awake human with a precision and resolution previously available only in experiments on anaesthetized animals. During recordings of afferent impulse activity subjects can perform various motor tasks and the subject's experience of the stimuli may be explored with psychophysical methods. Moreover, the microelectrode may also be used for stimulation of single afferent fibers to elucidate the perception induced by a defined series of impulses in an identified sensory unit [3, 4]. Likewise, by stimulating single motor axons contractile properties of single motor units in humans can be analyzed.

Classification of tactile afferents

About 17 000 mechanoreceptive afferent units innervate the glabrous skin of the human hand, i.e., the non-hairy skin of the hand [5]. They are classified into two major categories by the nature of their response to a sustained indentation of the skin. About half of the units are slowly adapting, i.e. they respond with a sustained discharge to a maintained skin deformation. The remaining units “adapt fast”, i.e., they respond only during skin deformation changes. Within each of these two categories, two different types of units can be distinguished on the basis of the properties of their receptive fields: The fast adapting type I units (FA-I) and slowly adapting type I units (SA-I) have small and well-defined fields. A fundamental task of the tactile apparatus is to extract information about spatial details of skin deformations during manual manipulation and exploration. The small receptive fields of the FA-I and SA-I units make them suitable for this task.

In contrast, the fast adapting type II units (FA-II) and the slowly adapting type II units (SA-II) have large receptive fields with obscure borders. SA-II afferents are distinguished by their sensitivity to lateral skin stretch while FA-II afferents are known for their exceptional sensitivity to remote skin tapping. Combined morphological and physiological studies indicate that four functional classes of tactile afferents innervate Merkel-cell-neurite complexes (SA-I afferents), Ruffini end-organs (SA-II afferents), Meissner corpuscles (FA-I afferents) and Pacinian corpuscles (FA-II afferents) [for review see Refs. 6&7].The most common type of afferent in the glabrous skin of the human hand is the FA-I type (43% of the tactile sensors), followed by the SA-I (25%), the SA-II (19%) and the FA-II (13%) types [5].

Special attention was paid to a subpopulation of SA-II afferents classified as “nail units” [8]. SAII-nail units respond to a sustained indentation to the lateral or proximal borders of the nail with a slowly-adapting discharge and have a well-defined “hot spot” dorsolaterally on the distal phalanx, within 2 mm of the borders of the nail. While they share certain features with SA-II endings elsewhere in the skin, such as large receptive fields and a very regular discharge, SAII-nail units respond relatively poorly to skin stretch, unlike the SA-II skin endings. However, each unit responds to remote compression stimuli applied to the centre of the finger pad.

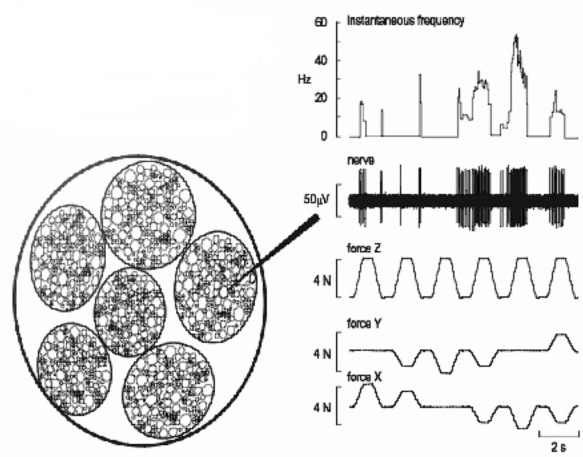

Fig. 1. Unitary recordings from a SA-II cutaneous afferent via a microelectrode inserted percutaneously into the median nerve at the wrist.

Results and Discussion

Sensitivity of the tactile afferents to the direction of force

The sensitivity to direction of force was investigated in SA-I, SA-II and FA-I mechanoreceptive afferents whose receptive fields were located at the distal phalanx of the index middle and ring finger. Because our stimuli did not reliably excite the FA-II afferents due to their sensitivity to mechanical transients, these afferents will not be considered further in the present report.

Superimposed on a 0.2N background normal contact force, stimuli consisted of a force protraction phase lasting for 125 ms, and a plateau phase with constant force (4N) followed by force retraction phase. The test stimuli consisted of parallel increase in normal and tangential force components resulting in a force angle between 0 and 30° relative to the normal. Because of frictional limits between the fingertips and objects, force angles larger than some 30° are rarely compatible with stable grasps in manipulation.

The vast majority of the investigated three afferent types were sensitive to the direction of the tangential force component [9]. For the directionally sensitive afferents typically there was one direction termed “preferred direction” in which the afferent responded most intensely. Regardless of the direction of the strongest response, there was an apparent linear fall in response intensity from stimulation on this direction, to the normal direction, and to the direction opposite to the direction of the strongest response. For individual afferents of each type the preferred directions were distributed around the circumference of the stimulation site, but not uniformly. The directions that dominated differed among the various types of afferents. The directional preference of the afferent was only weakly related to the location of its receptive field on the phalanx.

The majority of SAII-nail afferents also showed a strong responsiveness. Although the stimuli were delivered remote to the receptive fields of the endings, located dorsally around the lateral and distal borders of the nail, the SAII-nail afferents possessed a remarkable capacity to encode forces applied to the volar aspect of the finger. Each ending was directionally specific, responding to compression forces applied to the centre of the finger pad over a narrow range of angles. Moreover, the population of SAII-nail afferents could encode a wide range of forces over a wide range of angles. Because of this, we conclude that nail units are ideally placed to monitor contact and manipulation forces experienced by the finger pad, and may thereby play an important role in the sensorimotor control of the hand. Our results suggest that, owing to the favorable mechanical arrangement of nail units, these receptors are ideally placed to encode the magnitude and direction of forces typically applied to the finger pad during manipulation.

Interaction effects between curvature and force direction on afferent responses

Most objects that we grasp, lift and further manipulate are curved, with curvatures of the same order of magnitude as those of the fingertips. Tactile information pertaining to such ‘gross’ geometrical features of objects are used in the automatic control of fingertip actions. Responses from human tactile afferents were analysed when spherically shaped surfaces were applied to a standard site on the fingertip; the curvatures and force magnitudes and directions used were representative of everyday manipulations [10]. Nearly all SA-I, SA-II and FA-I afferents responded, and for the majority of afferents the response intensity was correlated with curvature. The correlation was positive for about half the afferents and negative for the other half, resulting in a curvature contrast signal within the populations of tactile afferents; afferents terminating at the sides and end of the fingertip tended to show negative correlations. For nearly all afferents, curvature and force direction had interactive effects. Changing the direction of force affected an afferent’s sensitivity to curvature and vice versa. It was concluded that recognition of such shapes takes advantage of signals originating from tactile afferents distributed over the entire terminal phalanx, and that both the direction of fingertip forces and the curvatures of objects contacted during natural manipulations influence the afferents’ responses. Consequently, if humans are able to perceive independently curvature and force direction from signals in tactile afferents, then the CNS must possess mechanisms that disentangle interactions between these and other parameters of stimuli on the fingertips.

Effect of tangential torque loads on tactile afferent responses

Torque loads tangential to the fingertips are common in the majority of natural manipulatory tasks. They develop together with linear loads during self-paced object manipulation to overcome gravitational and inertial forces [11].

Using stimuli that reproduce the cutaneous conditions during dextrous manipulation, we investigated how torque loads applied tangentially to the fingertip skin contacting an object are encoded by the population of human tactile afferents. Torque loads of different magnitudes were applied in clockwise and anticlockwise directions to a standard central site on the fingertip with three contact force levels; these forces correspond to grip forces generated during object manipulation.

The responses of the majority of SA-I, FA-I and SA-II afferents were scaled by the torque loads applied in one or other direction. The majority of FA-I afferents and about half of SA-I afferents showed effects in both directions, while SA-II afferents showed stronger directional preferences. Preliminary analysis did not indicate a robust relationship between type of effect by torque direction or magnitude or by location of receptive field.

Possibility for an ultra fast information coding mechanism

During dexterous manipulation tactile information may be utilized faster than can be explained by codes that require multiple action potentials in the neurones engaged. Therefore it has been scrutinised in detail whether the latency of the first spike elicited in ensembles of tactile afferents may convey information about the fingertip force direction, torque load and shape of contacted surface (curvature). Analyses done by us and our colleagues indicated that indeed the population of tactile afferents has the capacity to provide information about a variety of dynamic mechanical fingertip events using encoding mechanisms based on “first-spike latency”. For example, it was shown that the order by which individual afferents initially discharge to fingertip events effectively represents parameters of fingertip stimulation [12]. This neural code probably represents the fastest possible code for transmission of parameters of fingertip stimuli to the CNS.

Conclusions

Human microneurography is a powerful tool to access afferent input to the brain originating from the fingertip tactile afferents engaged in the sensorimotor control of dexterous manipulation.

Understanding afferent encoding mechanisms and being able to interpret information recorded from the peripheral nerves is an important step towards incorporating sensory-driven control algorithms into BCI and FES devices controlling muscles and human motor actions. Ultimately, this sensory-driven control will be provided by indwelling microwires in human peripheral nerve fascicles.

Acknowledgements

In addition to the authors the following persons have been engaged in the research reported above: Roland S Johansson, Anthony W Goodwin, Heather E Wheat, Goran Westling and Per Jenmalm.

References

[1] Thomas CK and Westling G. Tactile unit properties after human cervical spinal cord injury. Brain, 118: 1547-1556, 1995.

[2] Vallbo Å.B and Hagbarth KE. Activity from skin mechanoreceptors recorded percutaneously in awake human subjects. Exp Neurol, 21: 270-289, 1968.

[3] Konietzny F, Perl ER, Trevino D, Light A and Hensel H. Sensory experiences in man evoked by intraneural electrical stimulation of intact cutaneous afferent fibers. Exp Brain Res, 42: 219-222, 1981.

[4] Vallbo Å.B, Sensations evoked from the glabrous skin of the human hand by electrical stimulation of unitary mechanosensitive afferents. Brain Res, 215: 359-363, 1981.

[5] Johansson RS and Vallbo Å.B. Tactile sensibility in the human hand: relative and absolute densities of four types of mechanoreceptive units in glabrous skin. J Physiol (Lond), 286: 283-300, 1979.

[6] Vallbo Å.B and Johansson RS. Properties of cutaneous mechanoreceptors in the human hand related to touch sensation. Hum Neurobiol, 3: 3-14, 1984.

[7] Darian-Smith I. The sense of touch: Performance and peripheral neural processes, in *Handbook of Physiology*. (Brookhart JM, Mountcastle VB, Darian-Smith I and Geiger SR eds.), American Physiological Society, Bethesda, Maryland, 1984, pp. 739-788.

[8] Johansson RS. Tactile sensibility in the human hand: receptive field characteristics of mechanoreceptive units in the glabrous skin area. J Physiol (Lond), 281: 101-125, 1978.

[9] Birznieks I, Jenmalm P, Goodwin AW and Johansson RS. Encoding of Direction of Fingertip Forces by Human Tactile Afferents. J Neurosci, 21: 8222-8237, 2001.

[10] Jenmalm P, Birznieks I, Goodwin AW and Johansson RS. Influence of object shape on responses of human tactile afferents under conditions characteristic of manipulation. Eur J Neurosci, 18: 164-176, 2003.

[11] Goodwin AW, Jenmalm P and Johansson RS. Control of grip force when tilting objects: effect of curvature of grasped surfaces and of applied tangential torque. J Neurosci, 18: 10724-10734, 1998.

[12] Johansson RS and Birznieks I. First spikes in ensembles of human tactile afferents code complex spatial fingertip events. Nat Neurosci, 7: 170-177, 2004.

Author’s Address

Ingvars Birznieks,
POWMRI, NSW 2031 Randwick, Australia
ingvars.birznieks@unsw.edu.au

MOLECULAR ANALYSIS OF DIFFERENT PHYSICAL APPROACHES IN AGED HUMAN SKELETAL MUSCLE

Pietrangelo T[1], Mancinelli R[1], Toniolo L[2], Reggiani C[2], Fanò G[1]

[1] Dept. of Basic and Applied Medical Science, Center for Excellence on Aging (CeSI), University G d'Annunzio, Chieti, Italy

[2] Dept. of Human Anatomy and Physiology, University of Padova, Padova, Italy

Abstract

Sarcopenia is an physiological status referred to reduction of skeletal muscle strength in older people. Sarcopenia has a multifactorial origin linked to: oxidative damage of fibers (Fulle et al, Exp. Gerontol 40:189, 2005), mitochondrial damage (Brunk UT, Eur J Biochem, 269(8):1996-2002, 2002) reduced levels of GH, IGF-1, steroids and reduced myogenesis (Beccafico et al., ANYAS (270906) 345-352, 2007),

In our study, we analysed the effects of three different physical activity programs (endurance training, resistance training and local vibrational energy application on 65-85 years old people in order to identify the cellular and molecular pathways by which these training projects act against sarcopenia

A nedlee biopsy (50-70 mg) was taken on vastus lateralis muscle before and after the training. We analysed: (i) the specific tension development of single fibers and the expression of myosin heavy chain proteins; (ii) the transcriptional profile and (iii) the regenerative capacity of satellite cells.

The single fiber strength development did not change with any training protocol even if the endurance training significantly increase the cross sectional area of fibers and significantly reduced the myogenicity and fusion index of satellite cells.

Considering the gene expression profiles, each physical activity share a stimulation of a specific metabolic pathway (both endurance and vibrational training increase the aerobic metabolism while the resistance training stimulates the creatine metabolism), it increases the folding of sarcomeric and cytoskeletal proteins and regulates specific responses to reactive oxygen species production. Moreover, endurance and resistance training seemed to silence the Foxo activation due to ageing.

In conclusion, our results suggest that the training protocols have been effective on elderly people because each of them are able to stimulate a specific metabolism. Considering this coherence between exercise typology and metabolisms, we think that also the other results are specific of training type.

THE FIRST INTERNATIONAL FES SPORTS DAY

Donaldson N[1]

[1] University College London, London, UK

Abstract

An event was arranged in June 2006 for spinal cord-injured people who exercise using FES for cycling and rowing. The cyclists used recumbent tricycles: they raced over 100m and 1km to establish new records. The rowers used Concept II ergometers: Robin Gibbons broke is own previous record over 2km. The cyclists played team games. It seems clear that FES Sport can be a real pleasure while exercising the paralysed legs. In my opinion, this should be the popular way to bring the health benefits of FES to SCI people.

Introduction

The phrase Functional Electrical Stimulation (FES) originated at a time when the purpose of these muscle stimulators was seen as substituting for the damaged nervous system to restore normal function. An FES neuroprosthesis was to restore paralysed legs as the pacemaker restored the failing heart. Over the past 20 years, it has become clear to many that this goal is not realistic, at least in the near future, as a treatment for people with complete spinal cord lesions. FES can not compete with wheelchairs for activities of daily living. However, electrical stimulation is the only way that paralysed muscles can be exercised, and attention has shifted to using *FES*[1] for the maintenance of health. Many scientific studies have been performed of the health effects of regular stimulation-exercise [1] and there is no doubt that that this is beneficial. Most studies use cycle ergometers or rowing machines.

However, the number of people with serious spinal cord injury (SCI) who use FES outside research projects is small. Usually, the place where it is done is a hospital or clinic, probably reflecting the size and cost of the machines and that the immediate aims were research goals. Because the exercise was not done at home, the amount of exercise was limited for each person and might not be convenient to them.

A few years ago, we thought that if the benefits of FES-cycling exercise were to benefit many people with SCI, then several developments were necessary:

- the FES exercise must be done at home;
- suitable stimulators had to be available to buy (i.e. CE-marked);
- that cycling should be possible on mobile tricycles so that it could be a sport or recreation.

FES exercise at home

We recently completed a multi-centre trial of FES cycling, with other centres at Glasgow and Nottwill (Swiss Paraplegic Centre). The SCI people trained at home and the target was 1 hour of exercise, five days per week for one year. (The paper by Duffel *et al* [2] describes the results of the muscle study within that project.) This trial showed that it is possible for SCI people to train at home with little supervision. For most training the tricycles were mounted on friction rollers (Fig. 1) but outdoor cycling was also possible (Fig. 2).

CE-marked stimulators

Recently, stimulators for cycling have become available from at several companies[2,3].

Sport or recreation?

Whether mobile cycling is practicable outdoors depends on the available power. Previous studies had found relatively low power was obtained by FES after training. Because the amount of training in our trial, 5 hours/week, was more than in previous investigations and we hoped that this would yield greater power but this was not borne out. But the question remained: was the available power sufficient for enjoyable mobile cycling. In 2005 we arranged the first event at which cyclists from the London and Glasgow centres met for a

[1] The *F* in *FES* is really obsolete but, out of habit, we will continue to use it here.

[2] http://www.berkelbike.nl

[3] http://www.hasomed.de

day of games and races in a sports hall. This was such a success that we then arranged a larger, international meeting in June 2006.

Figure 1: cycle-training at home

Figure 2: outdoor cycling

First International FES Sports Day

We wanted to show show far FES Sport had got by bringing together FES cyclists and FES rowers. With a grant from EPSRC, I was able to invite FES cyclists from all known research groups to come to the event and Professor Andrews invited FES rowers. The venue was the University of Wales stadium in Cardiff.

As it turned out, four Concept II rowing machines were set up and SCI and able-bodied people were invited to try it out. Robin Gibbons, who as an SCI rower himself, is leading the expansion of the number of rowers in London, showed that he can compete with fit AB people, rowing a ‚distance' of 2-5 km.

Thirteen FES cyclists came, two from Sydney, Australia, two from Munich, one from Hasomed (GmbH), two from Glasgow and six from London. We had two aims for them: to establish records for cycling over 100m and 1 km; and to see whether they would enjoy games. The games were a relay race, a slalom race and a game with some similarity to rugby football, played with a cushion.

Pictures from the Sports Day

Figure 3: ready for mobile cycling (London system)

Figure 4: about to start the 1km race

Figure 5: track racing

Figure 6: Carmen Bruck (winner 100m)

Figure 7: Reinhardt Vetter (winner 1km)

Cycle Race Winners

100m: Carmen Bruck, Germany	28.72s
1km: Reinhardt Vetter, Germany	5m 4.43s

Figure 8: FES rowing

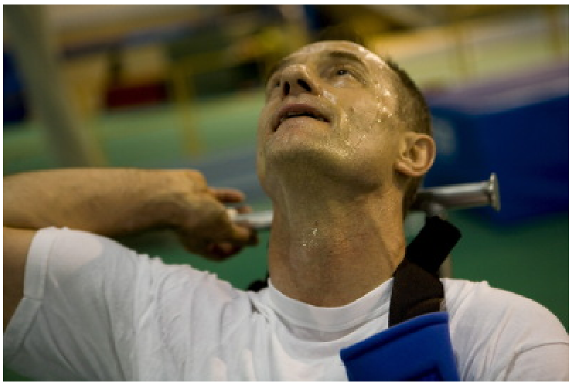

Figure 9: Robin Gibbons after his record-breaking 2km row in 11m 2s.

Figure 10: slalom race

Figure 11: playing the *Cushion Game*

Film

The extent of the cyclists' and rowers' enjoyment can be judged from the film made about the event. This can be downloaded from our website (see below).

Discussion

In my opinion, the three conditions that we thought necessary for the widespread use of FES exercise have been met: it can be done at home, FES systems can be bought, and it can be a pleasurable recreation or sport.

What is now needed are more people with SCI to see that time is right to take it up. My suggestion would be that FES sports clubs should be established with regular meetings in sports halls for games. However, the initiative should come from the FES users. They and the companies will decide whether this becomes widely used or not: it will not, and should not, depend much on academics and medical professionals.

Having said that, it would be good to get these sports recognized as part of the paralympics so that competitions can be used to improve performance. Many improvements should be possible: to the machines, the stimulators, electrodes, stimulator programs [3] and the muscle training.

Understanding why stimulated muscles do not produce more power is perhaps the area where research can make the greatest contribution.

References

[1] Janssen TWJ, Glaser RM, Shuster DB. Clinical efficacy of electrical stimulation exercise training: effects on health, fitness and function. Top. Spinal Cord Inj. Rehab., 3:33-49, 1998.

[2] Duffel LD, Newham DJ, Donaldson N. The effects of a long term programme of functional electrically stimulated cycling on muscle properties and power output in spinal cord injured people. This volume.

[3] Pella A, Ferrante S, Duffell L, Pedrocchi A, Perkins T, Newham D, Donaldson N. Quantitative comparison between different stimulation strategies during cycling on spinal cord injured patients. This volume.

Acknowledgements

We acknowledge the support of The Inspire Foundation and the Engineering & Physical Sciences Research Council. I would particularly like to thank Mr John Gisby who volunteered to help arrange this event.

Author's Address

Prof. Nick Donaldson

Implanted Devices Group

University College London

nickd@medphys.ucl.ac.uk

http://www.medphys.ucl.ac.uk/research/impdev/fits

INTRAORAL ELECTROMYOSTIMULATION FOR THERAPY IN OBSTRUCTIVE SLEEP APNEA

Ludwig A[1]

[1] MGK Medical and Cranio-Maxillofacial Hospital Kassel, Germany

Abstract

Innovative muscle stimulation techniques have become alternatives for therapy of OSAS breathing disorders. In group I an individually shaped mouth floor electrode (IME) and in group II an also individually adaptable multi point silicon electrode (MPE) have been used for electromyostimulation therapy in patients with obstructive sleep apnea. The enoral-cutaneous EMS was carried out with the low frequency stimulation apparatus I-pulse over a period of eight weeks, two times daily for thirty minutes during daytime hours, only. Before and after stimulation treatment 3D-volumetric sonographical measurement of the geniohyoid muscle has been carried out.

All patients (n = 14, average age 51.1 years) totally applied the EMS-therapy. As well under IME as under MPE application after four weeks of EMS-therapy a volume increase in median of 19.6 % (minimum 9.7 %, maximum 27.9 %) was registered, the median after eight weeks IME was 27.6 % and in MPE 24.0 %). No significant difference (ANOVA type: p > 0.05) between both electrodes could be found. In both groups, a reduction of the muscles in length of 4.7 % was proved.

In opposite to so far established stimulation techniques a threefold effectiveness enhancement could be verified by using both individually adaptable electrodes.

Introduction

During the last years muscle stimulation techniques have become alternatives for therapy of OSAS breathing disorders.

In the procedure of electromyostimulation (EMS) the indirect and direct muscle stimulation have to be differentiated. In larger muscle groups, the muscle is stimulated by the nerve which supplies that nerve (indirect muscle stimulation). In case of single muscles which have to be stimulated, 2 electrodes have to be attached to the muscle, if possible at the muscle origin (direct muscle stimulation). Many authors [1, 2, 3, 4, 5, 6, 7, 8] therefore carried out submental stimulation of the suprahyoid muscles. A combined enoral-submental stimulation technique should be prefered [9].

The stimulation efficiency is assumed to have influence on sleeping parameters. In this study, it was of interest whether optimized intraoral electrodes had also influence on efficiency of the EMS-therapy.

Material and Methods

In group I an individually mouth floor electrode (IME) was used for electromyostimulation (EMS) therapy of the tongue and mouth floor muscles in patients with obstructive sleep apnea (Fig. 1). For producing this electrode first a pattern of the lower jaw was produced with special casting of the mouth floor [10]. The lingual frenum was excluded from the electrode surface. The negative form with the attached electrode was additionally stabilized by a biteguard splint.

Fig. 1: Individual mouth floor electrode (IME) in detail of the Snorprevent system.

In group II an individually adaptable multi-point electrode (MPE) made of silicon was applied for EMS-therapy by using the same stimulation parameters as in group I (Fig. 2).

Fig. 2: Multi-point electrode (MPE) in detail of the Snorprevent® *system.* (Stimpoint Ltd., Bovenden, Germany).

In all cases a small self-adhesive electrode was fixed extraorally in the submental area. The EMS apparatus I-pulse was connected with the electrodes. The stimulation intensity in both groups could individually be influenced by the patient himself. For achievement of an efficient recruitment of the muscles, patients were instructed to choose treatment with maximum intensity. The enoral-cutaneous EMS was carried out with the low frequency stimulation apparatus I-pulse over a period of eight weeks, two times daily for thirty minutes during daytime hours, only. The impulse frequency was 50 Hz, the contraction time 10 s, the pause time 20 s and the impulse width 250 µs, the ramp time: increase / decrease 1.5 / 1.5 s and the voltage RMS eff. 4.4 V.

The morphology and volume of the geniohyoid muscle were examined by 2D- and 3D-sonography. By use of a 7.5 MHz linear scanner the muscle was measured in width and from the spina mentalis to the hyoid in length. Moreover, through combination of B-scan-sonography apparatus with a 3D-workstation a three-dimensional demonstration and measurement of the volume of the geniohyoid muscle became possible. After a stimulation phase of 4 and 8 weeks sonographical measures of the muscles were repeated.

Results

All patients (n = 14, average age 51.1 years) totally applied the EMS-therapy. As well under IME as under MPE application after four weeks of EMS-therapy a volume increase in median of 19.6 % (minimum 9.7 %, maximum 27.9 %) was registered, the median after eight weeks IME was 27.6 % and in MPE 24.0 %, Fig. 3). No significant difference (ANOVA type: $p > 0.05$) between both electrodes could be found. Through the visualization of the muscles in 3D-models the concentric volume increase could be proved which was mainly due to the contraction of the muscles. In both groups, a reduction of the muscles in length of 4.7 % was proved. Due to this fact, an opening of the posterior airway was enabled, so that snoring and breathing stops simultaneously were reduced.

The main difference between both electrodes was to be seen in the comfort of application because the IME was fixed like a denture and the MPE electrode had to be fixed by closing the teeth during the 30 minutes stimulation time. The IME could be cleaned like a denture and therefore is especially recommendable for a long time therapy.

The MPE shows the following advantages: the MPE is lower in cost than the IME and no casting of the mouth floor is necessary.

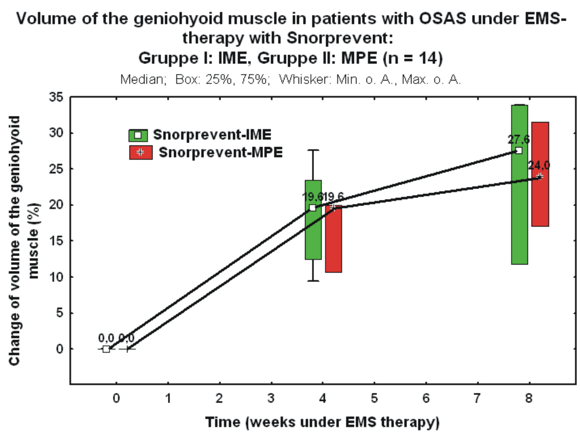

Fig. 3: Diagram of the change of volume of the geniohyoid muscle under EMS therapy.

Discussion

All patients totally applied the EMS-therapy. In all patients the geniohyoid muscle could sonographically be identified and three-dimensionally and in volume be demonstrated. As well under IME as under MPE after four weeks EMS-therapy a volume increase was registered, the median after eight weeks IME was 27.6 % and in MPE 24 %. Through the visualization of the muscles in 3D-models the concentric volume increase could be proved which was mainly due to the contraction of the muscles. In both groups, a reduction of the muscles in length of 4.7 % was proved. The increase of the muscle volume is partly conditioned by a contraction of the muscle leading to an opening of the hypopharyngeal respiratory airway. The proved contraction of the geniohyoid muscle which resulted explains the reduction of the collaps of the posterior airway, so that snoring and breathing stops simultaneously were reduced. The so far observed reduction of in mean 59% ± 30% [11, 12] as well as reduction of breathing stops [13] could be improved through the optimized electrodes, because the contraction of the genioglossus and geniohyoid muscle lead to a greater reduction of the oropharyngeal and naso-pharyngeal collapsibility [9, 13, 14].

The main difference between both electrodes was to be seen in the comfort of application because the IME was fixed like a denture and the MPE electrode had to be fixed by closing the teeth during the 30 minutes stimulation time. The IME could be cleaned like a denture and therefore is especially recommendable for a long time therapy.

The EMS enables a non-invasive therapy of OSAS and snoring whereby this form of therapy should regularly be carried out over a period of at least 8 weeks. In opposite to so far established extraoral stimulation techniques [1, 2, 3, 4, 7], combined intraoral and extraoral electrode techniques and stimulation parameters with this technique [5, 6, 8] a threefold effectiveness enhancement could be verified by using both individually adaptable electrodes (IME as well as MPE) [9]. The optimal fixation, adaptation and size of surface of the intraoral electrode therefore occurred to be essential parameters for an effective EMS-therapy in obstructive sleep related breathing disorders.

Taking the sonographical results into account, an individual adaptable intraoral electrode for EMS should be prefered.

For controlling efficiency of the EMS, the 2D- and 3D-sonographical demonstration and measuring of the geniohyoid muscle can be used. Especially for evaluation of efficiency in the time course, ultrasound appears to be a convenient method.

References

[1] Miki H, Hida W, Inoue H, Takishima T: A new treatment for obstructive sleep apnea syndrome by electrical stimulation of submental region. Tohoku J Exp Med 154, 91 - 92, 1988

[2] Miki H, Hida W, Shindoh C, Kikuchi Y, Chonan T, Taguchi O, Inoue H, Takishima T: Effects of electrical stimulation of the genioglossus on upper airway resistance in anesthetized dogs. Am Rev Respir Dis 140, 1279 - 1284, 1989

[3] Miki H, Hida W, Chonan T, Kikuchi Y, Takishima T: Effects of submental electrical stimulation during sleep on upper airway patency in patients with obstructive sleep apnea. Am Rev Respir Dis 140, 1285 - 1289, 1989

[4] Broniatowski M: The Potential for Neurostimulation in Obstructive Sleep Apnoea. ASAIO Journal 1994, 13 - 16, 1994

[5] Wiltfang J, Klotz S, Jordan W, Cohrs S, Engelke W, Ludwig A, Hajak G: Erste Ergebnisse zum Training der suprahyoidalen Muskulatur bei Probanden und einem Patienten mit obstruktiver Schlafapnoe. Somnologie 1, 160 - 164, 1997

[6] Wiltfang J, Klotz S, Wiltfang J, Jordan W, Cohrs S, Engelke W, Hajak G (1999): First results on daytime submandibular electrostimulation of suprahyoidal muscles to prevent night-time hypopharyngeal collapse in obstructive sleep apnea syndrome. Int J Oral Maxillofac Surg 28, 21 - 25, 1999

[7] Verse T, Schwalb J, Maurer JT, Stuck BA, Hörmann K: Transcutaneous submental electrostimulation therapy for obstructive sleep apnea. First clinical results. Somnologie 6, Suppl 1, 40, 2002

[8] Randerath W: Alternatives/Completions to nasal CPAP. Somnologie 6, Suppl 1, 175, 2002

[9] Ludwig A, Monzavifar O: Comparison of effectivity of enoral-cutaneous and cutaneous submental EMS of the mylohyoideus muscle – Influence on therapy in obstructive sleep apnea? Am J Respir Crit Care Med 167, A 132 (2003)

[10] Ludwig, A., Monzavifar, O., Diederich, D.: The individually adapted intraoral electromyostimulation electrode for therapy of sleep apnea. Int J Oral Maxillofac Surg 32, Suppl 1, 122, 2003

[11] Randerath, W. J., Galetke, W., Rocholl, C., Rühle, K. H.: Tongue muscle training by electrical stimulation in obstructive sleep apnea. A double-blind, placebo-controlled study. Am J Respir Crit Care Med 167 (7), A 327, 2003

[12] Heinrich, F., Käßner, F., Schweisfurth, H.: Elektrisches Zungenmuskeltraining zur Behandlung des habituellen Schnarchens. Eine Kasuistik. 11. Deutscher Kongress für Schlafforschung und Schlafmedizin, Poster 78, Cottbus, 25. – 27.9.2003

[13] Ludwig, A.: Techniken, Methodik, Messverfahren und Ergebnisse der Elektromyostimulation (EMS) zur Therapie schlafbezogener Atmungsstörungen. Abstract-sammlung der 6. Jahrestagung der Norddeutschen Vereinigung für Schlafmedizin (NVSM), 1, 2004

[14] Oliven, A., Tov, N., Odeh, M., Geitini L., Stein-feld, U., Oliven, R., Schwartz, A. R.: Effect of genioglossus (GG) contraction on oro- (OP) and naso-pharyngeal (NP) cross-sectional area (CSA) and airflow in patients with obstructive sleep apnea (OSA). Am J Respir Crit Care Med 169 (7), A 435, 2004

Author's Address

Priv. Doz. Dr. Dr. Arwed Ludwig
MGK Medical and Cranio-Maxillofacial Hospital
Neue Fahrt 12
D-34117 Kassel, Germany
aludwig@gwdg.de

STIMULATION OF HUMAN LUMBAR POSTERIOR ROOT AFFERENTS WITH SURFACE ELECTRODES

Minassian K[1], Hofstoetter U[1], Hofer C[1], Vogelauer M[1], Persy I[1], Rattay F[2], Dimitrijevic MR[3], Kern H[1]

[1] Ludwig Boltzmann Institute of Electrical Stimulation and Physical Rehabilitation, Vienna, Austria

[2] TU-BioMed Association for Biomedical Engineering, Vienna University of Technology, Vienna, Austria

[3] Department of Physical Medicine and Rehabilitation, Baylor College of Medicine, Houston, Texas

Abstract

Leads inserted into the epidural space in close distance to the lumbar cord can stimulate posterior root afferents and affect synaptic action on lower limb motoneurons. In the present work we demonstrate that posterior root afferents can also be depolarized by electrical stimulation delivered transcutaneously at sites corresponding to the longitudinal position of the lumbar cord, based on our recent results derived from healthy humans. We will add supporting evidence for posterior root stimulation with surface electrodes by comparing short-latency reflex responses to transcutaneous and to epidural lumbar posterior root stimulation in a spinal cord injured subject. Motor responses evoked by both methods could be recorded from quadriceps, hamstrings, tibialis anterior, and triceps surae. The segmental reflexes of a given muscle elicited by transcutaneous as well as by epidural stimulation had the same latencies and compound muscle action potential shapes, and similar amplitudes. Thus, the responses elicited transcutaneously were initiated in sensory axons within the posterior roots at their entry into the spinal cord, exactly like it was shown in previous studies for responses to epidural stimulation. Transcutaneous stimulation can depolarize at least a subset of the same neural structures as recruited by implanted epidural leads.

Introduction

In spinal cord stimulation, a lead is inserted into the spinal canal but outside of the spinal cord in the epidural space, and an electric field is applied in the vicinity of the posterior aspect of the spinal cord. Such stimulation of the lumbar cord can evoke a variety of motor effects in the lower limbs, depending on the stimulation parameters [1-3]. In particular, single stimuli and stimulation at low frequencies (e.g. 2 or 5 Hz) elicit monosynaptic reflex responses in the lower limb muscles [1,4]. The neural structures directly depolarized by such epidural lumbar cord stimulation initiating motor responses are large-diameter afferents within the posterior roots [4,5]. The low thresholds of posterior root fibers are not only due to a specific stimulation generated by the epidural electrodes, but are also determined by the anatomy of the posterior roots at their entry into the spinal cord [5,6]. This situation implies that posterior root stimulation even with a non-specific electric field is plausible. Recently we have demonstrated that posterior root afferents can be depolarized by electrical stimulation delivered transcutaneously from the surface of the body with moderate stimulus intensities [7]. For stimulation sites of this transcutaneous technique corresponding to the longitudinal position of the lumbar cord, we have suggested that action potentials are initiated in the most proximal portion of the lumbar posterior root fibers adjacent to the spinal cord. In the present paper we shall first summarize the results derived from transcutaneous spinal cord stimulation in healthy subjects [7]. We will then compare the electromyographic (EMG) characteristics of muscle twitch responses (posterior root-muscle reflexes [4,7]) elicited by transcutaneous spinal cord stimulation (tSCS) with responses to epidural spinal cord stimulation (eSCS) obtained from an incomplete spinal cord injured subject. These data are providing direct evidence that transcutaneous stimulation can depolarize the same afferents at the same sites within the posterior roots as they are stimulated by epidural electrodes.

Material and Methods

Subjects

The study in healthy subjects was conducted on eight men, aged 20–32 years. Additional data was collected from a subject with a chronic, traumatic incomplete spinal cord injury (ASIA C; injury level: C5; aged 24 years; male). The study of tSCS was approved by the local ethics committee.

Transcutaneous spinal cord stimulation

A pair of round electrodes (∅ = 5 cm) was placed over the paravertebral skin, one on each side of the spine and positioned between the T11-T12 spinal processes. A reference electrode pair (8 × 13 cm) was placed over the abdomen. The two electrodes of each pair were connected to function as a single electrode. All electrodes were commercially available self-adhesive transcutaneous electrical neural stimulation electrodes (Schwa-medico GmbH, Ehringshausen, Germany).

A constant-voltage stimulator was used to deliver symmetric, biphasic rectangular pulses with pulse widths of 2 ms. Electrodes were connected to the stimulator such that the paravertebral electrodes acted as the anode during the first phase and as the cathode during the second phase of the biphasic stimulus pulse. For details see [7].

Epidural spinal cord stimulation

EMG-data were collected during the trial phase of SCS before full-implantation of the stimulation system. The subject had a percutaneous electrode placed in the dorsal epidural space at the longitudinal level of the lumbar spinal cord. The electrode was a linear array of four contacts with cylindrical shape (Pisces Quad 3487A lead, Medtronic Inc., Minneapolis, MN) and was connected to an external stimulator (Model 3625 Test Stimulator, Medtronic Inc.) with a lowest available stimulation frequency of 5 Hz.

Recording procedure

The EMG activity of stimulus-evoked compound muscle action potentials (CMAPs) of left and right quadriceps, hamstrings, tibialis anterior, and triceps surae was simultaneously recorded with pairs of silver–silver chloride surface electrodes. The EMG signals were amplified using Phoenix amplifiers (EMS-Handels GmbH, Korneuburg, Austria) with a gain of 502 over a bandwidth of 10–1000 Hz and digitized at 2048 Hz per channel.

Study protocol

The stimulation protocol was conducted with subjects in a relaxed, supine position. In the healthy subjects, muscle responses were elicited by transcutaneous stimulation over the lumbar cord. For a given stimulus intensity, three individual stimuli were triggered at 5-second intervals. Stimulus-evoked muscle responses were tested to determine whether they were of reflex origin by different conditioning-test paradigms [7].

In the spinal cord injured individual, muscle responses elicited transcutaneously were compared with responses to epidural spinal cord stimulation during the same recording session.

Results

Posterior root stimulation in healthy subjects: summary of results

Transcutaneous stimulation of the lumbar cord with single stimuli and a mean intensity of 28.6 V elicited bilateral motor responses in quadriceps (Q), hamstrings (H), tibialis anterior (TA), and triceps surae (TS) simultaneously. The responses were of reflex nature, since they were attenuated when a conditioning stimulus was given 50 ms prior to the test stimulus. Furthermore, the responses were depressed during Achilles tendon vibration. Finally, TS responses were significantly increased by slight plantar flexion and suppressed during voluntary contraction of the antagonistic tibialis anterior, with characteristic modifications of responses also in the other muscles.

Hamstrings responses had the lowest mean thresholds of 23.4 V. The mean common threshold intensity needed to elicit motor responses bilaterally in all studied muscles was 28.6 ± 6.3 V (with the impedance of the stimulation set-up being approx. 1000 Ω). The largest responses were found in TS with EMG amplitudes up to 8974 μV (group average 3637.9 ± 2275.3 μV).

The motor responses had short latencies that were correlated to the subject's height and increased with the distance between the stimulation site and the studied muscle. The latencies amounted to Q, 10.3 ± 1.1 ms; H, 11.2 ± 0.4 ms; TA, 19.1 ± 0.9 ms; and TS, 19.7 ± 1.1 ms.

In one subject, an increase of stimulus intensity resulted in an abrupt shortening of the response latencies as compared with the threshold responses. The range of the discrete shortening was 1.0 – 1.9 ms in the different muscle groups and for different stimulus intensities above 120% of the common threshold intensity. Responses with such reduced latencies demonstrated a less distinct or even absent depression when a prior stimulus was given.

We further compared TS responses to tSCS with the H reflex elicited by tibial nerve stimulation in the popliteal fossa during the same recording session. The responses elicited by tSCS and by peripheral nerve stimulation had same CMAP shapes and widths, with the tSCS–evoked TS responses shifted to shorter latency that was 63.2 ± 1.2% of the H reflex delay.

Posterior root stimulation: comparison of responses elicited by tSCS and eSCS

Motor responses were evoked in all recorded muscles by transcutaneous electrical stimulation over the lumbar cord in the incomplete spinal cord injured subject. Figure 1 shows stimulus-evoked CMAPs in the right Q, H, TA, and TS. Responses to the second pulse of the pair of stimuli applied after 50 ms were depressed in all muscles.

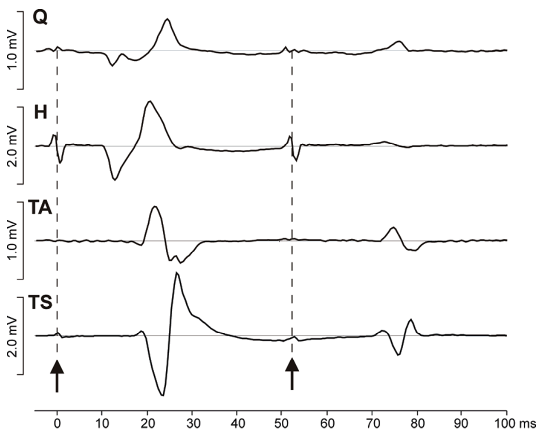

Fig. 1: Q, H, TA, and TS responses to tSCS in a spinal cord injured subject. A pair of stimuli was applied with 55 V. Arrows indicate action potential initiation in the neural target elements, when the function of the paravertebral electrodes abruptly changed from anode to cathode (see stimulus artifacts of the H-trace).

Tibialis anterior and triceps surae were bilaterally recruited at 45 V, whereas 50 V was required to additionally evoke responses in all recorded thigh muscles.

Motor responses with the largest magnitudes were recorded in TS. At the maximum applied stimulus intensity of 55 V, peak-to-peak amplitudes of the responses were: Q, 601.5 ± 169.9 µV; H, 1566.7 ± 581.1 µV; TA, 1021.3 ± 174.9 µV; and TS, 4955.3 ± 664.5 µV (mean of right and left side, three responses each).

During the same recording session, eSCS was applied with a bipolar electrode set-up at a frequency of 5 Hz. With the designated electrode position and polarity, muscle response thresholds were Q, 3.5 V; H, 4.5 V; TA and TS, 7 V.

Applied with intensities above motor threshold, each single pulse of the continuous 5 Hz-stimulation evoked an individual CMAP. The CMAPs elicited with constant stimulation parameters demonstrated modulated amplitudes, but they had short and constant latencies. Maximal peak-to-peak amplitudes of the responses were: Q, 1963.0 ± 1060.4 µV; H, 2015.0 ± 956.9 µV; TA, 762.8 ± 320.8 µV; and TS, 1137.7 ± 1031.5 µV.

Figure 2 compares characteristic CMAPs induced by tSCS with the ones evoked by eSCS. The responses elicited by both methods had the same CMAP shapes and could have similar attainable amplitudes.

An essential result can be seen when comparing the onset latencies and widths of the CMAPs of a given muscle elicited by tSCS and eSCS that had similar amplitudes. Table 1 summarizes these values for the different stimulation techniques. It is evident that the motor responses to tSCS and to eSCS had the same onset latencies and similar CMAP widths.

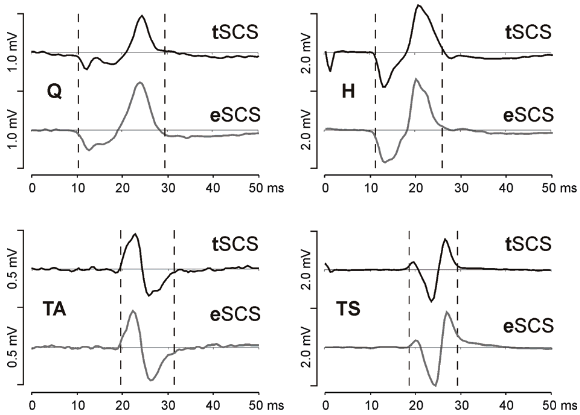

Fig. 2: Q, H, TA, and TS responses to tSCS and eSCS. For comparison in pairs, examples with similar EMG amplitudes were selected. Dashed lines mark on- and offsets of the CMAPs elicited by tSCS.

Muscle	Type of stimulation	Latency (ms)	CMAP width (ms)
Q	tSCS	10.3 ± 0.0	18.7 ± 0.6
	eSCS	10.4 ± 0.2	17.4 ± 0.7
H	tSCS	11.0 ± 0.3	14.7 ± 0.5
	eSCS	11.2 ± 0.0	14.2 ± 0.5
TA	tSCS	19.5 ± 0.0	12.1 ± 0.2
	eSCS	19.7 ± 0.3	12.4 ± 0.5
TS	tSCS	18.3 ± 0.3	10.9 ± 0.3
	eSCS	18.9 ± 0.2	12.9 ± 0.7

Table 1: Comparison of onset-latencies and CMAP widths of Q, H, TA, and TS responses to tSCS and eSCS.

Furthermore, the latencies of the CMAPs elicited by tSCS in the spinal cord injured individual coincide with the group average values of the healthy subjects. The CMAP shapes were characteristic for each muscle and were similar in the spinal cord injured individual and the healthy subjects.

Discussion

In the present work we have shown that electrical stimulation delivered from the surface of the body can elicit bilateral motor responses in several lower limb muscles simultaneously. In a previous study, we demonstrated that the responses were of reflex nature and were most probably transmitted through monosynaptic reflex pathways based on the prolonged refractory period of the responses, suppression by tendon vibration and characteristic modifications during single-joint movements [7].

Information about the initiation sites of the reflex responses elicited by tSCS can be gained from their short latencies. The latency of the tSCS-evoked TS response was about six tenths of the H reflex delay. Considering the lower conduction velocity of α-motoneurons than of group Ia muscle spindle afferents, and that the efferent limb of the H reflex is longer than the afferent one, the latency of the tSCS-evoked TS responses must predominantly consist of the efferent part of the delay. Therefore, responses to tSCS must have been initiated in the most proximal portions of the afferent fibers adjacent to the spinal cord.

In one case, tSCS with increased stimulus intensities resulted in direct activation of efferents in addition to posterior root afferents as was indicated by the different refractory behavior and abrupt latency reduction of the responses. The brief reduction of latency, corresponding to the difference in the delays of the reflex response at threshold and the direct response, coincides with the transit time of monosynaptic reflex pathways through the spinal cord [8]. This finding suggests that the reflex responses were initiated at the posterior root entries into the spinal cord.

In the present manuscript we added new evidence for posterior root stimulation by tSCS gained by comparing the evoked motor responses with responses elicited by eSCS. ESCS was applied at 5 Hz, the lowest available frequency of the utilized external test stimulator. At such rates, responses can be conditioned by the effects of the preceding stimuli, as was reflected by the amplitude-modulations of the successively elicited CMAPs. However, the electrically depolarized target elements will be the same, whether being activated with single stimuli or with 5 Hz-stimulation.

We have previously demonstrated that the neural structures directly excited by eSCS leading to motor effects are large-diameter posterior root afferents [2,4,5]. The individual stimulus-evoked responses were termed posterior root-muscle reflexes (PRM reflexes), according to their initiation and recording site. Responses to 5 Hz-stimulation were shown to be short-latency PRM reflexes, being most probably of monosynaptic nature [2].

The similar morphology and width of CMAPs elicited by tSCS and eSCS suggest that the same afferent structures are stimulated in both cases, resulting in PRM reflexes. Identical latencies of the responses to the two stimulation techniques clearly demonstrate same initiation sites.

The significance of the present study is the demonstration that distinct neural structures within the spinal canal can be depolarized by a rather non-specific electrical stimulation delivered from the surface of the body. The current that flows into the vertebral canal results in a relatively high current density in the well-conducting cerebrospinal fluid. The low thresholds and selective depolarization of posterior root fibers is then a consequence of the anatomical conditions at the terminal cord [4,5,6]. In conclusion, tSCS is a non-invasive method effective to depolarize posterior root afferents and thus at least a subset of the same neural structures as stimulated by epidural electrodes.

References

[1] Murg M, Binder H, Dimitrijevic MR. Epidural electric stimulation of posterior structures of the human lumbar spinal cord: 1. muscle twitches - a functional method to define the site of stimulation. Spinal Cord, 38: 394-402, 2000.

[2] Jilge B, Minassian K, Rattay F, et al. Initiating extension of the lower limbs in subjects with complete spinal cord injury by epidural lumbar cord stimulation. Exp Brain Res, 154: 308-326, 2004.

[3] Dimitrijevic MR, Gerasimenko Y, Pinter MM. Evidence for a spinal central pattern generator in humans. Ann NY Acad Sci, 860: 360-376, 1998.

[4] Minassian K, Jilge B, Rattay F, et al. Stepping-like movements in humans with complete spinal cord injury induced by epidural stimulation of the lumbar cord: electromyographic study of compound muscle action potentials. Spinal Cord, 42: 401-416, 2004.

[5] Rattay F, Minassian K, Dimitrijevic MR. Epidural electrical stimulation of posterior structures of the human lumbosacral cord: 2. Quantitative analysis by computer modeling. Spinal Cord, 38: 473-489, 2000.

[6] Struijk JJ, Holsheimer J, Boom HB. Excitation of dorsal root fibers in spinal cord stimulation: A theoretical study. IEEE Transactions on Bio-medical Engineering, 40: 632-639, 1993.

[7] Minassian K, Persy I, Rattay F, et al. Posterior root-muscle reflexes elicited by transcutaneous stimulation of the human lumbosacral cord. Muscle Nerve, 35: 327-336, 2007.

[8] Troni W, Bianco C, Coletti Moja M, et al. Improved methodology for lumbosacral nerve root stimulation. Muscle Nerve, 19: 595-604, 1996.

Acknowledgements

Wings for Life Spinal Cord Research Foundation. Proj.Nr. WFL-FR-001/06

Medizinisch Wissenschaftlicher Fonds des Bürgermeisters der Bundeshauptstadt Wien. Proj.Nr. 2516.

Author's Address

Karen Minassian
Ludwig Boltzmann Institute of Electrical Stimulation and Physical Rehabilitation,
Wilhelminenspital der Stadt Wien,
Montleartstrasse 37, 1160 Vienna, Austria
karen.minassian@wienkav.at

EXTERNALLY CONTROLLED “CODED” TRAINS OF INPUT TO THE HUMAN LUMBAR CORD CAN ELICIT A VARIETY OF INPUT RELATED FUNCTIONAL AND NON-FUNCTIONAL MOVEMENTS

Persy I[1], Kern H[1], Minassian K[1], Hofstoetter U[1], Hofer C[1], Rattay F[2], Dimitrijevic MR[3]

[1] Ludwig Boltzmann Institute of Electrical Stimulation and Physical Rehabilitation, Vienna, Austria

[2] TU-BioMed Association for Biomedical Engineering, Vienna University of Technology, Vienna, Austria

[3] Department of Physical Medicine and Rehabilitation, Baylor College of Medicine, Houston, Texas

Abstract

The motor nervous system in all mammals including humans develops movements by activating conducting messages through populations of axons. In humans with complete functional isolation of the lumbar cord from brain structure due to accidental injury it is possible to elicit various motor outputs by external electrical stimulation of the human lumbar network, like locomotor-like stepping or standing-like extension, only by changing the stimulation frequency at the same stimulation site. These findings lead us to the present study about signal processing elicited by trains of stimuli of different rates and strengths. There are clearly recognizable repeatable results. One characteristic type of motor-output are responses to low stimulation frequency like 2 Hz, which are segmental, short-latency reflexes in several muscles simultaneously without evident interaction between them, even with increasing stimulus strengths. When changing the frequency to 5–15 Hz with the strength at its maximal level of 10 V and placing the paralyzed lower limb in knee and hip flexion before stimulation is applied, an isotonic contraction leading to an extension movement can be initiated. Applying same stimulation with the limbs initially extended exemplifies an isometric contraction still with the dominating output in the functional extensors. Slightly increasing the frequency characteristically changes the motor output, e.g. at 16 Hz. The dominant part of the extensor muscles is by and by replaced by a flexor motor feature. This alternation of extension towards flexion patterns becomes even more distinct when the frequency is yet incremented to 21 Hz, where also rhythmical patterns start to appear. The nature of neural codes can be based upon two hypotheses; the first upon irregularity, the second upon the changing of rates. This study supports the second hypothesis, where we do apply a regular train, but the difference between the intervals of successive stimuli (frequencies of 2, 10, 16 Hz etc.) is the crucial message for the processor.

Introduction

The nervous system deals with information. That information provided by sense organs impinges in the form of various energies and substances. The impinging events are converted into a form that the nervous system can handle with. Once identified by electrophysiological methods, the train of nerve impulses is recognized as a universal carrier of nervous information over transmission channels [1]. On the other hand in all mammals including humans, motor nervous system develops movements by activity of the conducting messages through shorter and longer large populations of axons coming to the spinal cord and to brain as well as leaving from brain to the spinal cord. The complementary parts involved in generation and control of movements are processing networks of so called ‘pattern generating’ interneurons. Central pattern generators are neuronal ensembles capable of producing the basic spatiotemporal patterns underlying ‘automatic’ movements, e.g. locomotion in the absence of peripheral feedback. Experimental approaches from classical electrophysiological and pharmacological methods to molecular and genetic ones have been used to understand the cellular and synaptic bases of central pattern generator organizations. Recently, it has been shown that the high reliability and flexibility of central pattern generators is determined by the redundant organization. Everything that is crucial for operating a generator is determined by a number of complementary mechanisms acting ‘in concert’. However, various mechanisms are weighted differently in determining aspects of central pattern generator operation [2].

Studies of sustained electrical stimulation of the upper lumbar posterior roots in humans with complete traumatic spinal cord injury (SCI) demonstrated that it is possible to elicit rhythmical, stepping-like movements or sustained, bilateral lower limb extension [3,4,5]. These findings lead us to the present study about signal processing elicited by trains of stimuli of different rates and strengths applied via lumbar posterior roots to the interneuronal population, the interneuronal network situated within the lumbar gray matter. We shall outline our preliminary results extending our previous findings that externally delivered codes – based on the input rate - can communicate with the lumbar interneurons that respond with different configurations of motor outputs and with the generation of a variety of movements.

Material and Methods

Subjects:

We studied recordings obtained in 5 SCI subjects (Table 1), who were neurologically classified as

Subject No.	Sex	Born in	Accident in	Level of SCI
1	m	1978	1996	T7/8
2	m	1977	1994	C5
3	m	1973	1997	C4/5
4	m	1970	1996	C5/6
5	m	1973	1995	C4/5

Table 1: Demographical and clinical data

having a complete spinal cord lesion at the cervical or thoracic level with no motor functions below the lesion. At the time of data collection, the subjects met the following criteria: They were healthy adults with closed, post-traumatic spinal cord lesions; all patients were in a chronic and stable condition; no antispastic medication was being used; stretch and cutaneomuscular reflexes were preserved; there was no voluntary activation of motor units below the level of the lesion as confirmed by brain motor control assessment [6]. To control their spasticity, all subjects had an epidural electrode array implanted. The implantations as well as the clinical protocol to evaluate the optimal stimulation parameters were approved by the local ethics committee. All subjects gave their informed consent.

Stimulation and recording set-up:

All subjects had an epidurally placed electrode for spasticity control. Epidural stimulation within a range of 1–10 V and 2–100 Hz was applied to the posterior lumbar cord. Stimulus evoked electromyographic (EMG) responses were recorded simultaneously with surface electrodes placed over quadriceps, hamstrings, tibialis anterior and triceps surae. The bipolar surface electrodes were placed centrally over the muscle bellies spaced 3 cm apart and oriented along the long axis of the muscles. Subjects were in supine position. The EMG data was analyzed off-line using Windaq Waveform Browser playback software (Dataq Instruments, Akron, OH) and Matlab 6.1 (The MathWorks, Inc., Natick, MA, USA).

Results

There are four clearly recognizable characteristic findings, which are always present and easy repetitive in all studied subjects by stimulating the posterior roots of the lumbar cord epidurally below the level of complete lesion.

A characteristic example of the first finding is shown in Figure 1. Applying repetitive stimulation with low frequency of 2 Hz every stimulus evokes compound muscle action potential (CMAP) responses with short and constant latencies. With low stimulus strength – in this case with the given upper lumbar cord position of the electrode and the stimulation strength of 5 V - CMAPs are only present in thigh muscle groups. When the stimulus strength is increased from 4 to 8V the amplitudes of CMAPs are increasing within the already previously responding thigh muscle groups to 5 V. Moreover, 6 V strength of stimulus activates also short latency CMAPs of leg muscles. Thus, with a repetitive stimulus of low frequency an increasing strength of the stimulus can enlarge the size of a given population of monosynaptically responding spinal motor cells nuclei as well as recruit additional present posterior roots from the first to fifth lumbar segment. All responses are restricted to the stimulation of their associated segmental roots and they do not reveal any interaction between different segments.

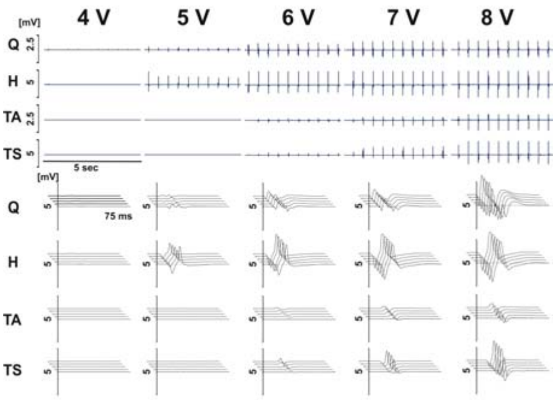

Figure 1: EMG recordings of the lower limb muscle groups (quadriceps, hamstring, tibialis anterior and triceps surae). Compound muscle action potentials (CMAPs) responses with stimulation parameters of 2 Hz and an increasing strength from 4 to 8 Volt recorded for 5 s (top). First five CMAP responses to the train in enlarged time scale of 75 ms (bottom).

Figure 2 describes the outcome of a stimulation adjustment of maximal strength of 10 V and a rate of stimulus repetition of 10 Hz. In the left side of the illustration the paralyzed lower limb is passively placed in knee and hip flexion. The trace of this leg's knee goniometer (referred to as 'KM') reveals that the stimulation of the posterior roots with the above given strength and frequency parameters will immediately extend the flexed paralyzed lower limb. This second finding is demonstrated by the bilateral outcome with a dominant output in the extensor muscle groups. Thus, specific parameters of strength and train of stimuli delivered to the upper portion of the lumbar cord are capable to configurate the output with constant feature, in this case extension of the paralyzed lower limb.

In the right side of Fig. 2 the stimulation is started with an extended paralyzed lower limb. We are proving that the significant motor output of the extensors is generating stiffness of muscles, an isometric contraction and no movement of the limb. In contrast to the above described isotonic contraction, when the paralyzed limb is initially placed in knee and hip flexion (left side of Fig.2).

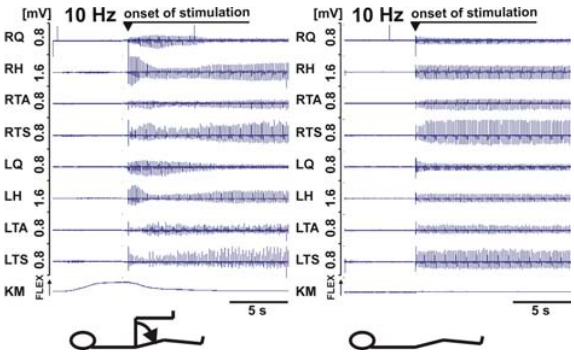

Figure 2: Epidural stimulation with 10 V and 10 Hz. EMGs of the lower limb muscle groups (quadriceps, hamstring, tibialis anterior and triceps surae) and knee goniometer (KM) recorded for 20 s. Left side: The paralyzed lower limb is passively placed in knee and hip flexion before stimulation is started. Right side: The lower limbs are initially extended.

Thus, it is possible to demonstrate clearly a relation between the site of stimulation, the stimulus parameters – strength and frequency of repetition – and their motor response direction, which cannot be modified by changing the initial position of the paralyzed lower limb. The dominant effect in both cases is the extensors EMG activity.

Figure 3 compares responses to stimulation frequencies of 10 Hz (left side) and 16 Hz (right side) with a constant strength of 10 V. This illustration is documenting that the previous induced extensor motor output feature is now modified to a flexor motor feature CMAP activity, only by altering the frequency of the stimulating train. Thus, there is a particular range for the train of stimuli which will elicit particular features of the motor output. So far, these first three illustrations provide evidences that different parameters of stimulation can elicit different features of motor outputs. Moreover, all above shown responses are immediate responses to the particular stimulation and they have ceased when stimulation stopped.

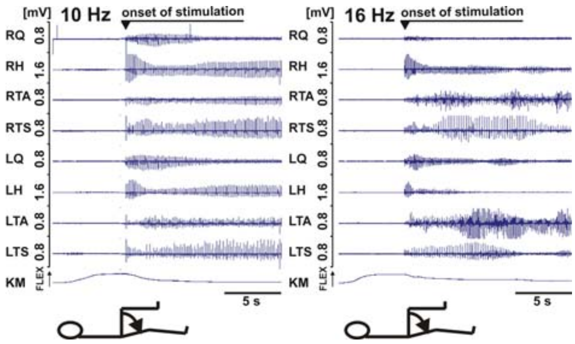

Figure 3: Epidural stimulation with 10 V, 10 Hz (left) and 16 Hz (right). EMGs of the lower limb muscle groups (quadriceps, hamstring, tibialis anterior and triceps surae) and knee goniometer (KM) recorded for 20 s. The paralyzed lower limb is passively placed in knee and hip flexion before stimulation is applied.

In this fourth example the frequency was further increased from 16 to 21 Hz. The begin of the recording illustrated in Figure 4 shows a sustained flexor pattern similar to the one shown in the right side of Figure 3, when the stimulation is applied. But after approximately 20 s this feature is converting to a cyclical and rhythmical activity.

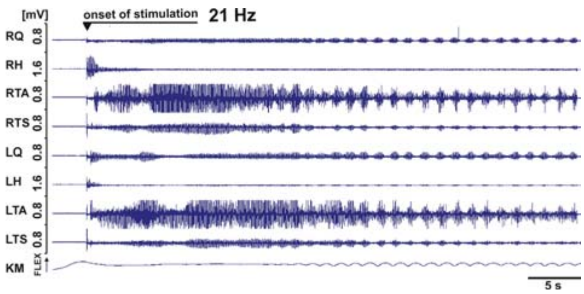

Figure 4: Epidural stimulation with 10 V and 21 Hz. EMGs of the lower limb muscle groups (quadriceps, hamstring, tibialis anterior and triceps surae) and knee goniometer (KM) recorded for 40 s. The initial sustained flexor pattern converts by and by to a cyclical rhythmical activity.

Discussion

In our studies about epidural electrical stimulation of the lumbar posterior structures we have been able to document that it is possible to demonstrate different features of motor output by changing the repetition rate of the trains of stimuli but maintaining constant site of stimulation. Can we consider that sustained series of stimuli of external origin applied in epidural stimulation of lumbar posterior roots is actually mimicking absent biological codes, information for inducing motor outputs like extension or locomotor-like activity of the paralyzed lower limbs? How can we compare these codes – based on the input rates – with biological neural codes?

Actually there are two hypotheses for the nature of neural codes. The time intervals between stimuli can be of constant durations – so called regular – or successive stimuli can have interstimulus intervals of varying durations, i.e. irregular. The first hypothesis states that coding is based on irregularity. This means that each time interval between two successive stimuli is the basic carrier of information for the input code. The underlay of the second hypothesis is the changing of the rates of regular stimuli. Neuronal code of this kind is relatively slow, because many constant intervals need to build up the carrier, in the contrast to the first hypothesis, where the content is already defined by the time between two stimuli.

The conclusions of this study is that the externally coded inputs will be closer to the second hypothesis, since the trains of stimuli are constant and differences between input and output are rather within certain intervals and ranges and they are clearly recognizable. At present we can conclude that the described preliminary findings open a new avenue within the research of responses of the interneurons and microcircuits to externally controlled inputs of coded capabilities.

References

[1] Paillard J. Introductory Lecture: The Functional Labelling of Neural Codes. In Neural Coding and Motor Performance. Massion J, Paillard J, Schultz M, Wiesendanger M (eds). Exp Brain Res, 7: 1-19, 1983.

[2] Arshavsky YI, Deliaina TG, Orlovsky GN. Pattern generation. Curr Opin Neurobiol, 7: 781-789, 1997.

[3] Dimitrijevic MR, Gerasimenko Y, Pinter MM. Evidence for a spinal central pattern generator in humans. Ann NY Acad Sci, 860: 360-376, 1998

[4] Minassian K, Jilge B, Rattay F, Pinter MM. Binder H, Gerstenbrand F, Dimitrijevic MR. Stepping-like movements in humans with complete spinal cord injury induced by epidural stimulation of the lumbar cord: Electromyographic study of compound muscle action potentials. Spinal Cord, 42(7): 401-416, 2004.

[5] Jilge B, Minassian K, Rattay F, Pinter MM, Gerstenbrand F, Binder H, Dimitrijevic MR. Initiating extension of the lower limbs in subjects with complete spinal cord injury by epidural lumbar cord stimulation. Exp Brain Res, 154: 308-326, 2004.

[6] Sherwood AM, McKay WB, Dimitrijevic MR. Motor control after spinal cord injury: Assessment using surface EMG. Muscle Nerve, 19: 966-979, 1996.

Acknowledgements

The authors would like to acknowledge the support of:

The Foundation for Movement Recovery, Oslo, Norway

Wings for Life Spinal Cord Research Foundation. Proj.Nr. WFL-FR-001/06

Author's Address

Ilse Persy
Ludwig Boltzmann Institute for Electrical Stimulation and Physical Rehabilitation,
Montleartstraße 37, 1160 Vienna, Austria
e-mail: ilse.persy@wienkav.at

CHARGEPUMP OUTPUT CIRCUIT FOR BIPHASIC FES

Thorsen R, Ferrarin M

Biomedical Technology Department,IRCCS "S. Maria Nascente", Fond. Don Carlo Gnocchi Onlus

Milano, Italy

Abstract

Surface Functional Electrical Stimulation (FES) requires high stimulation voltages. A step up transformer in the output stage of the stimulation circuit is often used to transfer the entire energy of the stimulation pulse. Transformers are far from ideal as an electronic component, which challenges the precision of stimulation output waveform.

A Voltage Controlled Current Source (VCCS) is presented as an alternative to the transformer coupling. Two (master-slave) coupled trans-conductance amplifiers (OTA) - in series with pre-charged capacitors - are used to drive the output current. After each stimulation pulse the capacitors are recharged by a high-voltage (HV) DC supply. A multiplexer in the output stage is used to provide biphasic output and can be useful for clamping electrodes to ground.

Quiescent power dissipation of the VCCS prototype is 13mW in the low voltage control circuit and less than 1mW in the HV part. Output slew-rate (10-90%) was measured to 6mA/µs and overall efficiency of the VCCS was 70% at 100mA output. The output is charge-balanced within 20µA and virtually separated from ground. The circuit is stable at capacitive loads and is currently used in a clinical trial.

Introduction

Current output stimulator circuits have been dominated by two different principles; either generating the stimulus directly from a high voltage source [1-3, 15] or through a step up transformer [4-14]. The dominating stimulation waveforms are: monophasic [1-3, 4-7] and biphasic [8-16]. Charge balanced stimulation is recommended [16] to minimize the risk of tissue damage when applying FES. Fig. 1 shows a charge balanced biphasic stimulation waveform.

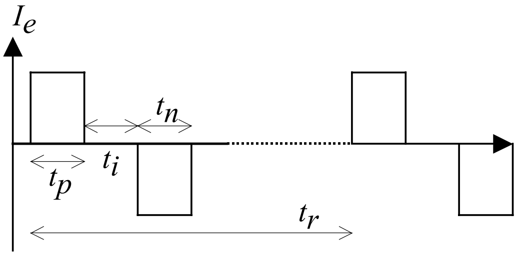

Fig. 1: Electrode current (I_e) for a biphasic stimulation pulse having a repetition interval (t_r), a positive phase duration (t_p), an inter-pulse interval (t_i) and a negative phase duration (t_n).

We have used myoelectric signals (MES) for control of functional electrical stimulation (FES) [17]. In such use, stimulation artifacts (SA) may dominate the recorded MES when the stimulated and the controlling muscle are the same or closely spaced [18]. Utilizing balanced biphasic pulses can reduce the SA, thus leaving minimal charge in the stimulated tissue [18]. The outputs should have high impedance to ground [18] as accomplished by the transformer coupling. However, transformer inductance, parasitic capacitors and skin capacitance [18, 19] may cause transients (in high impedance state) and hence increase SA. Most stimulator designs have not addressed these SA related properties [1 - 16]. Circuits driving the output current directly from a high voltage source using high voltage op-amps (PA85) have been proposed [3], but significant quiescent power consumption (3W) [20] is a problem.

Our objective was to develop an efficient and precise voltage controlled current source (VCCS) without the need for a transformer in the output stage. The VCCS should: produce biphasic stimulation; block DC current, even in a fault condition; provide high output-to-ground impedance, but allow clamping electrodes to ground after the pulse; display minimal quiescent power consumption; and be designed for weight and size minimization.

Material and Methods

Circuit description

Two complementary transconductance amplifiers (OTA) are used for draining and sourcing current in the electrodes through pre-charged capacitors $C_{1\&2}$ and a multiplexer (fig. 2.). The multiplexer determines the polarity of the output current; electrode current can be reversed for the second phase of the biphasic stimulation pulse (fig. 1).

Both between terminal impedance and from terminal to ground impedance are very high; they depend only on impedances of the OTA's FETs.

Stimulation energy is supplied from an isolated switch mode power supply generating an adjustable high voltage ($\pm V_{hv}$) from the battery. The energy is transferred to the capacitors (C_1, C_2) by closing two high voltage switches. The switches are controlled by a logic input signal (*charge control*).

Control & feedback circuits are supplied by a low level (± 3V) voltage. Keeping control & feedback circuits on the low-side has the advantage of causing minimal quiescent power consumption.

A positive analog input signal (V_i) controls output-current size and shape whereas output polarity is determined by two logic inputs (*pc*, *nc*) to the multiplexer.

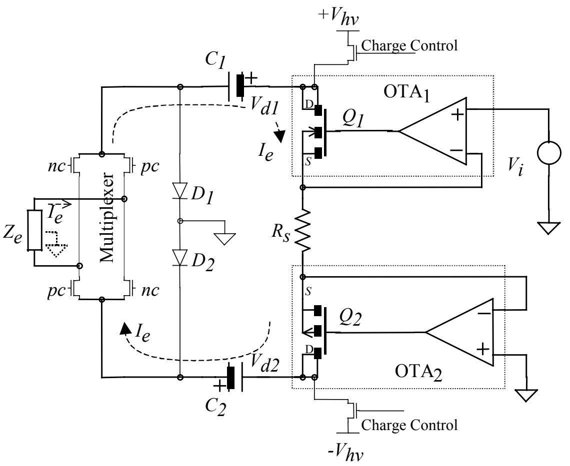

Fig. 2: Block diagram of the VCCS based upon two complementary OTAs; a master OTA_1 and a slave OTA_2. The electrodes are represented by Z_e. The voltage drop $I_e \cdot R_s$ is held equal to V_i by OTA_1 and OTA_2. ***(Patent Pending MI07A00595)***.

The currents in the two OTAs are identical (I_e), since both FET gate currents and op-amp input currents are virtually zero. During stimulation cycle the op-amps will control the FETs such that the potential of the source terminal equals the non-inverting input. Source terminal of Q_2 is held at ground level and source terminal of Q_1 is held at V_i. Hence the inverse transconductance of the VCCS determined solely by the sense resistor (R_s) and stimulation current is determined by (eq. 1).

$$I_e = V_i / R_s \qquad (1)$$

The capacitors must be sufficiently charged to keep the drain-source voltage of the FETs in the active region at all times *(2)* & *(3)*.

$$V_{C1} > V_{ds1,on} + \tfrac{1}{2} I_e Z_e + I_e R_s \qquad (2)$$

$$V_{C2} > -V_{ds2,on} + \tfrac{1}{2} I_e Z_e \qquad (3)$$

Where V_{C1} and V_{C2} are the voltage drops over the capacitors, V_{ds1} and V_{ds2} are the drain-source on-voltage over the transistors Q1 and Q2 respectively. (It is assumed that the electrode potentials are equally positive and negative).

After each biphasic stimulation pulse capacitors are recharged to $V_{C,\max} \approx V_{hv}$ by two switches connecting the drain-terminals to $+V_h$ and $-V_h$ respectively and the 'freewheeling' diodes D_1 and D_2. (Diode and switch voltage drops are negligible). The FETs should be turned off when the capacitors are recharged (break before make) by setting $V_i = 0$. (Op-amps must be biased to ensure both gates are safely below pinch-off when $V_i <= 0$).

The stimulator circuit was realized using: high voltage FETs (Q_1= ZVN2120, Q_2= ZVP2120 having $|V_{ds(on)}|$<1V at 100mA) and high-slew-rate rail-to-rail amplifiers (TLV2772AID). The complete circuit involves components for bootstrapping the FET gates, ensuring stability, switch control etc., but the details of these will be out of the scope for this paper.

The circuit was designed for a maximum current $I_{e,max}$ = 200 mA with the waveform shown in fig. 1., having $t_p = t_i = t_n = 0.3$ *ms and,* t_r = 60 ms.

Calculation of capacitors

By combining *(2)* and *(3)* with the assumption that the capacitors are equal and identically charged, the following condition must hold during the stimulation pulse for the FETs to be in the active region (ref. timing in fig. 1 and the diagram in fig. 2.)

$$V_{C1}(t) + V_{C2}(t) > V_{ds1,\mathrm{on}} - V_{ds2,\mathrm{on}} + I_e(t)\, Z_e + I_e(t)\, R_s \qquad (4)$$

(Electrodes are non-linear but, for simplicity of calculations, Z_e is assumed time invariant and real)

The voltage drop (ΔV_c) over each capacitor after the stimulation pulses (t_p and t_n), provided that I_e is constant for both phases, is (5):

$$\Delta V_c = (t_p + t_n)\, I_e / C_b \qquad (5)$$

The capacitor thus needs to be charged to a level given by *(2) & (3)* plus this voltage drop.

Efficiency

Efficiency (η) of the VCCS is determined by the power loss (P_{FET}) in the FETs, the sense resistor (P_s), the control part (P_c) and the power (P_e) dissipated in the electrodes and tissue.

$$\eta = P_e / P_{tot} = P_e / (P_e + P_{FET} + P_c + P_s) \qquad (6)$$

If the capacitors are of same capacity and charge, the power dissipated in the two FETs is:

$$P_{FET} = \frac{1}{t_r} \int_0^{t_p + t_n} I_e (V_{ds1}(t) - V_{ds2}(t))\, dt$$
$$\approx I_e \frac{t_p + t_n}{t_r} \left(2V_{C,\max} - I_e Z_e - \frac{2(t_p + t_n) I_e}{2C} \right) \qquad (7)$$

It therefore follows that R_s should be little and V_{ds} should be minimized to maximized efficiency.

A sense resistor of $R_s = 10\Omega$ is selected to provide a transconductance of 100mA/1V.

Efficiency is measured at medium current (I_e =100mA) using a load of $Z_{e,r} = 1k\Omega$ [19], realized as two 500Ω resistors in series.

Selecting a capacitor size to $C_{1\&2} = 4.7\mu F$ the voltage drop, according to *(5)* becomes

ΔV_c= (600µs) ·100mA/4.7µF=13V. According to *(2)* this requires: $V_{hv} > \Delta V_c + (V_{ds1} + ½ \cdot I_e Z_e + I_e R_s)$ =13V+1V+½·100mA·1kΩ+100mA·10Ω=65V.

Output characteristics

The quality of the output was measured by slew rate, symmetry and leakage currents at the maximum current $I_{e,max}$ =200mA.

Pulse symmetry was measured with the midpoint of the load grounded through a 100kΩ resistor and controlling that current flow to ground was zero.

DC-leakage to ground was measured by adding a 100nF capacitor in parallel to the 100kΩ reference resistor. A discrepancy in the charge delivered by the two terminals of the stimulator would result in a drift in the voltage over the capacitor away from zero.

The ability to drive a capacitive load was tested by adding a 33nF capacitor in parallel to the resistive load (Z_e = 1kΩ || 33nF) [19].

Results

Quiescent power consumption was below measurable limit (1mW) and the power consumption of the control circuit (the op-amps) was measured 13mW independent of output power.

At 100mA stimulation expected efficiency was *(6)*: $\eta_{theoretical} = 76\%$

A total average power consumption from the high voltage supply was measured to 0.13W, yielding: $\eta_{measured} = 70\%$

At V_{hv} = 130V the maximum output current was I_e= 200mA (see fig. 3.). The slew-rate$_{(10\text{-}90\%)}$ was measured to be 6mA/µs.

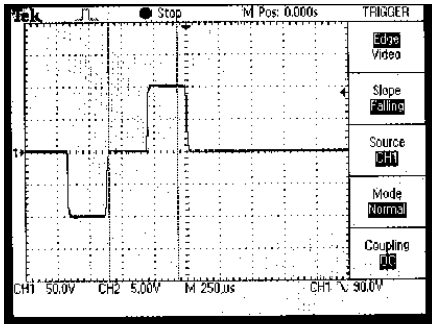

Fig. 3. Oscilloscope (10MΩ) image of the voltage at one terminal of the 1kΩ load @ 100mA. Midpoint of the load is referenced to ground through a 100kΩ resistor, thus half load voltage is seen by the scope.

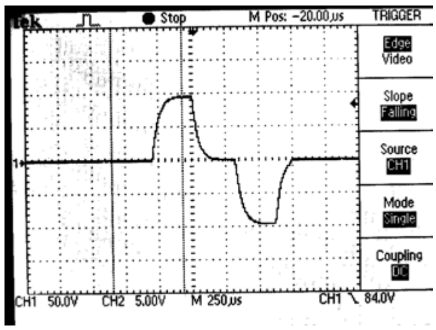

Fig. 4.: Capacitive loading (33nF) of the stimulator output shows stability.

Load-midpoint voltage was measured to be below the noise-floor of the oscilloscope (5mV) at both 100kΩ and 100kΩ||100nF midpoint to ground impedance. Hence the leakage current from the stimulator output to ground is less than 5mV/100kΩ=0.02µA in both cases. Therefore the output demonstrated to be charge balanced within the 20nA precision of the measurement.

Adding a 33nF capacitor in parallel to the 1kΩ load presented stable output with a return to baseline (0V) after stimulation pulse as seen in fig. 4.

Discussion

Some additional losses are caused by parasitic capacitances, voltage drops over multiplexer switches, diodes and charge switches and by reverse currents in diodes and switches accounting for the 6% difference in efficiency.

Optimal efficiency requires an accurate prediction of the electrode impedance charging of the capacitors. In case of insufficiently charged capacitors, the op-amps will drive the output into saturation. Such saturation can then be detected, with the advantage of not connecting to the high voltage side. The detection can be used for impedance prediction for a control scheme for V_{hv}.

Output terminals can be clamped to ground by closing all switches in the multiplexer during re-charging of the capacitors and hence actively discharge the stimulation electrodes.

Duplicating the multiplexer can provide additional time multiplexed outputs thus upgrade the circuit to a multi-channel stimulator.

DC current protection is guaranteed by four components: charge switch, charge pump capacitors, freewheeling diodes and output multiplexer.

Conclusion

The VCCS circuit (patent pending) produces a precise charge balanced biphasic current output with high efficiency and low quiescent power consumption. It is part of a myoelectrically controlled stimulator, currently being tested by patients [21].

References

[1] Malaney J et al., Patent US6493588, 2002

[2] Petrofsky J. Patent US4580569, 1983

[3] Poletto C and Van Doren C. A high voltage, constant current stimulator for electrocutaneous stimulation through small electrodes. IEEE Trans. Biomed. Eng. 1999;46:929-936.

[4] Stanton D, Patent US4392496, 1983

[5] McDonald M, Patent GB1129142, 1968

[6] Johns R and Webb G. A linear current amplifier for stimulation in man. Med. & biol Eng. 1967;405-406.

[7] Cheng KW, Lu Y, et al. Development of a circuit for functional electrical stimulation. IEEE Trans Neural Syst Rehabil Eng 2004;12:43-7.

[8] Roberts W, Patent US4124030, 1978

[9] Fisher W, et al., Patent US6564103, 2003

[10] Dufresne j, et al., Patent US686991, 1987

[11] Alon G, Patent US4690146, 1987

[12] Morawetz P, Patent US4528984, 1985

[13] Bijak M, Mayr W, et al. The Vienna Functional Electrical Stimulation System For Restoration Of Walking Functions In Spastic Paraplegia. Artif Organs 2002;26:224-7.

[14] Ilic M, Vasiljevic D, et.al., Programmable Electronic Stimulator for FES Systems. IEEE Trans. Rehab. Eng. 1994;2:234-238.

[15] Simcox S, Davis G, et al. A portable, 8-channel transcutaneous stimulator for paraplegic muscle training and mobility-A technical note. J Rehabil Res Dev 2004;41:41-52.

[16] Baker L, McNeal D, et al., NeuroMuscular Electrical Stimulation, -A Practical Guide. Los Amigos Res. & Ed. Inst.,California, USA, 2000

[17] Thorsen R, Occhi E, et al., Functional electrical stimulation reinforced tenodesis effect controlled by myoelectric activity from wrist extensors. J Rehabil Res Dev 2006;43:247-56.

[18] McGill K, Cummins K et al., On the nature and elimination of stimulus artifact in nerve signals evoked and recorded using surface electrodes. IEEE Trans. Biomed. Eng. 1982;29:129-137.

[19] Perkins T. Impedances of common surface stimulation electrodes. Proc 9 th Annual Conference of the International FES Society, 2004, England.

[20] www.apexmicrotech.com, PA85 datasheet

[21] Thorsen R, Binda L, et al. First experience of MeCFES for assisting tetraparetic hands in activities of daily living, Proc. XVI Cong. ISEK, Italy, 2006, 176-177.

Acknowledgements

This work has been supported by the Italian Ministry of Health (Ricerca Corrente IRCCS).

Author's Address

Rune Thorsen, Ph.D.
Biomedical Technology Department
IRCCS "S.Maria Nascente" Fond. Don Gnocchi Onlus
Via Capecelatro 66, 20148 Milano,Italy
rthorsen@dongnocchi.it
www.dongnocchi.it/polotecnologico

PHYSIOTHERAPISTS' EXPERIENCES OF USING FES FOR DROPPED-FOOT AFTER STROKE IN IRELAND: A QUALITATIVE STUDY

Roche A, Coote S
Department of Physiotherapy, University of Limerick, Limerick, Ireland

Abstract

Purpose: *Stroke is the most common cause of acquired physical disability in Ireland and many patients present with "dropped-foot" as a result. Studies have shown FES systems to have beneficial orthotic and therapeutic effects on dropped-foot in this population; however clinical utility of FES systems amongst Irish physiotherapists remains low. This study aimed to explore Irish physiotherapists' clinical experience of FES, which it is hoped will help its transfer from research into clinical practice.*

Methods: *A qualitative research design of focus groups was employed with 3 groups held at various locations in Ireland. Sessions were audiotaped, transcribed and subject to thematic analysis.*

Results: *Analysis revealed significant barriers to the successful translation of FES from training into clinical practice, which included time and resource constraints. Therapists reported that improved device user-friendliness would facilitate them adopting FES more in practice.*

Conclusions: *The physiotherapists included in this preliminary study have experienced challenges implementing FES for patients with dropped-foot into their clinical practice. More seamless product transfer relies on continuous exchange of information between engineers, researchers, clinicians and users. Further studies are required to generalise these initial findings to a wider population.*

Introduction

Stroke is the most common cause of acquired physical disability in Ireland [1] and many patients with stroke develop abnormal walking patterns during the recovery period. "Dropped-foot", or the inability to achieve sufficient ground clearance of the foot during the gait cycle, is a deficit which contributes to the development of these abnormal patterns, resulting in a slower, inefficient and less aesthetic form of ambulation. Dropped-foot is most commonly treated using a custom-moulded ankle foot orthosis (AFO) or by using Functional Electrical Stimulation (FES). Both beneficial orthotic [2] and therapeutic [3] effects have been shown in the stroke population as a result of treatment with FES.

Lyons et al [4] conducted an extensive review of portable FES-based neural orthoses for dropped-foot correction, remarking that despite a plethora of Dropped Foot Stimulator (DFS) studies, very few have actually evolved into commercial devices. The authors reason that this "must reflect a fundamental problem either with the technology or with the perception of the technology". Certainly, it would appear that clinical utility of FES systems amongst physiotherapists in Ireland remains low. The majority of more recently published FES clinical trials acknowledge the patient's contribution with some subjective dimension, for example Taylor et al [5] included a questionnaire to explore patient/user's perceptions of the Odstock Dropped Foot Stimulator (ODFS) manufactured in Salisbury, UK; which is the most commonly used FES device in Ireland. However, no published data investigating physiotherapists'/clinicians' views of FES for dropped-foot was retrieved from an extensive literature search.

Hence, the aim of this study is to explore the perceptions, experiences and opinions of physiotherapists working in Ireland who use FES for the correction of post-stroke dropped foot. It is hoped that their contributions will provide insight into the reasons for the low usage of FES in the clinical setting, despite available evidence and recommendations regarding its effectiveness, for example the Royal College of Physicians "National Clinical Guidelines on Stroke" [6].

Methods

The qualitative grounded theory method of focus groups was chosen as it is a particularly useful approach when dealing with a new area of investigation or one which is poorly understood [7]. The focus group technique is often used in studies of an exploratory nature, and thus is appropriate for this preliminary study. As opposed to a questionnaire, focus groups allow participants to clarify and distil ideas during the process, as well as enabling them to voice opinions not previously considered by the researcher.

The University of Limerick (UL) Research Ethics Committee approved the study. Written informed consent was obtained from participants and all data was treated confidentially as per UL research protocol.

Recruitment
Participants were recruited by posting a notice in the January 2007 edition of the Irish Society of Chartered Physiotherapists (ISCP) monthly newsletter "Firsthand", inviting chartered physiotherapists with an interest in FES for dropped-foot to contact one of the investigators (AR). This notice was also distributed via e-mail to members of the special interest group "Chartered Physiotherapists in Neurology and Gerontology" (CPNG), of which both investigators are affiliated. Those who contacted the investigator within a month of the notice being posted/emailed, were forwarded an information leaflet and consent form. From those who consented, three locations and dates of most convenience were decided upon.

Focus Group Structure
The overall structure and question route of each focus group was similar with a series of carefully constructed opening, introductory, transitional, key and ending questions phrased in a conversational manner, as outlined by Kreuger [8]. Participants firstly introduced themselves, with the moderator progressing onto questions regarding training/clinical experience with FES, advantages and barriers to using FES clinically, changes required for participants to use FES more and their perceptions of current FES research.
One of the investigators (AR) acted as moderator for all three sessions. The moderator led the audio-taped sessions and attempted to intervene as little as possible acting only to clarify points and facilitate group interaction where needed. Immediately after each session, the moderator conducted a debriefing session by noting overall group dynamics, significant themes or reactions to particular statements, which would facilitate later analysis.

Data Analysis
A thematic content analysis was conducted using the methods described by Krueger [9]. Firstly, one of the investigators (AR) transcribed the audiotaped group sessions verbatim assigning anonymous codes to each participant. Transcripts were then examined line-by-line and coded by identifying similar concepts. These concepts were then grouped into emerging themes by comparing across all three groups. In addition, the moderator's notes from each debriefing session were used to facilitate this process.
Following thematic analysis of each transcript, a brief descriptive statement, which included key concepts and themes from the discussion, was forwarded to each participant for their respective group. They all responded with full agreement indicating accurate data interpretation, which enhances the trustworthiness of the results.

Results

Group participants
The first (Gr1) and second (Gr2) focus groups were held in February 2007 and were attended by three and four physiotherapists respectively. The third (Gr3) was held in March 2007 consisting of five physiotherapists. All 12 participants were female and the average focus group duration was 60 minutes. Nine participants had received training in the ODFS device.

Focus Group Findings
In all three group discussions, four common themes emerged (See Table 1 for the identified themes and associated concepts). These will be introduced by referring to selected citations from the transcripts. The codes at the end of each citation refer to the focus group session and transcript page number represents the stage of discussion. As is evident from the amount of concepts to emerge with each theme, discussion around barriers to using FES clinically was the most frequent, extensive and emotive across all three groups.

Table 1: Key themes and concepts

Themes	Concepts
Use of FES in the clinical setting	Who & When
	Training
Benefits of FES	Outdoor mobility
	Less effort & falls
Barriers to using FES clinically	Time
	Device issues
	Service issues
	Patient issues
	Translating into practice
Requirements to use FES more	Device user-friendliness
	Resources
	Research

1. Use of FES in the clinical setting

All participants had some experience of using FES, mainly on patients with dropped foot as a result of stroke and multiple sclerosis (MS) Reporting overall mixed results, no therapist used the device regularly. Participants in all three groups generally described not using FES until other interventions had failed;

"I don't tend to go for it as one of the early options" (Gr1, p3).

Whilst some therapists had changed job since training, with a different caseload resulting in less opportunity to use FES, participants still working in the same area echoed the words of this therapist in detailing their overall lack of success in using FES clinically;

> *"We had a spurt of enthusiasm immediately afterwards….it just seemed like more trouble than it was worth"* (Gr1, p6).

The three participants who had not received training were in Group 3 and reported using FES clinically, albeit under the supervision of a trained colleague. These participants argued that reviewing patients with FES was a necessary component of taking over a caseload from an FES-trained colleague who vacates their position;

"It's very much handed down through the ranks so far here" (Gr3, p6).

2. Benefits of FES

For therapists who reported clinical success with FES for patients with drop-foot, benefits were mainly concerned with improved quality of life and a less effortful gait enabling more outdoor mobility;

"They certainly experienced a whole new lease of life outdoors and more confident" (Gr2, p4);

"The advantages of it would be a much longer tolerated walking distance and obviously safety and not tripping or falls" (Gr3, p4).

3. Barriers to using FES clinically

The most cited concept in relation to this theme, which permeated all group sessions, was time;

"I would feel that it takes up an awful lot of department time…it's really time-consuming" (Gr2, p7).

Similarly, because of the time involved in setting up the device, therapists tended to select it less frequently. In turn, they felt additional time was required to familiarise themselves with the device before using it again;

"I was using it so infrequently that I would have to go back and read up on it again every single time before and that's another block of time for me" (Gr1, p9).

These time constraints further sourced to prohibit therapists using FES clinically;

"*You got very frustrated"* (Gr1, p24).

Participants in every group also perceived issues with the device to contribute as a barrier to its clinical utility;

"*We ditched it because of time because of usability it just wasn't user-friendly*" (Gr1, p9);

"The leads were a real nuisance" (Gr3, p25).

Some participants worked in generic rehabilitative/community settings, as opposed to a more specialised neurological service, which they believed influenced their exposure to potential FES candidates;

"We don't have a speciality service like we are jack-of-all-trades to everybody" (Gr1, p10).

In terms of patient issues, one therapist candidly recalled feeling at times, incompetent during a treatment due to difficulties with using the device;

"I think in front of your patient you would often look as though you didn't know what you were doing" (Gr1, p7).

Participants in Group 2 similarly felt pressurised to convince the patient of the device's worth by demonstrate immediate effects;

"The last thing you want to say at the end of 45 minutes is your session is over come back to see me again next week" (Gr2, p8).

Therapists agreed that often the cumulative effect of all these barriers on the patient was that, *"they lose faith in it"* (Gr3, p7).

In all, despite the aforementioned optimism after training, the majority of therapists experienced difficulty in translating FES for dropped foot into their clinical everyday practice, resulting in feelings of frustration and ultimate under-utility of the device;

"It didn't seem to translate when I tried it with people myself" (Gr1, p14);

"In the end it's not worth the reward as far as I can see" (Gr1, p12).

4. Requirements for FES to be used more

The final theme regarding factors that would need to be introduced for these therapists to increase their use of FES clinically, generated the second largest amount of discussion within the groups, with the most common response that of improving the device itself;

"Ideally a more user-friendly device" (Gr1, p22).

One participant in Group 2 believed that more personnel were required in order to construct an appropriate service. However in the absence of this, therapists agreed that funding to purchase devices to be use on a trial basis was a more feasible request;

"You have to have the ability to loan it out and let somebody try it out" (Gr2, p9).

A participant in Group 1 suggested availing of funding to provide more accessible training and retraining or refresher courses;

"A lot more training and back-up like retraining" (Gr1, p22).

Finally, in terms of direction for future research, a therapist in Group 3 believed that independent sources of research would be a welcome addition, which met with agreement from the group;

"*There is a real need for more research from a more independent source*" (Gr3, p26).

Participants would also favour outcome measures focusing more on functional aspects of patients' lives;

"*I suppose function really rather than just gait specifically"* (Gr1, p13);

"Energy cost of walking over a longer distance" (Gr3, p16).

Discussion and Conclusions

This preliminary study aimed to explore the perceptions and experiences of physiotherapists working in Ireland who use FES for the correction of post-stroke dropped foot; the main findings of which are discussed below. As an initial qualitative study, these results have limited external validity; nonetheless methodological rigor and "trustworthy" data were achieved by confirming data interpretation with participants and by using the same moderator and similar questioning routes for each focus group.

The physiotherapists included in this preliminary study have experienced challenges implementing FES for patients with dropped-foot into their practice, despite the majority having received formal training in this field. The time involved in setting up the device on a patient, exposure to potential FES candidates depending on the work setting and overall device user-friendliness were the major barriers perceived by therapists to prohibit their use of FES regularly. Of the patients who were successful in adopting the device, therapists reported improved quality of life in terms of safer, less effortful gait, which enabled more outdoor mobility. Therapists reported that improved device user-friendliness, more accessible training/refresher courses and resources to initially loan patients a device on a trial basis, would facilitate them adopting FES more in practice.

Further studies are required to generalise these initial findings to a wider population and investigate how they may apply to other health care systems. With the advent of wireless devices, physiotherapists' experiences of using these would also be of great interest.

References

[1] Irish Heart Foundation, Council for Stroke. *"Towards excellence in stroke care in Ireland"*. Dublin, Eireann Healthcare Publications, 2003.

[2] Burridge J, Taylor P, Wood D, Swain I. "The effects of common peroneal stimulation on the effort and speed of walking: a randomised controlled trial with chronic hemiplegic patients". *Clin. Rehab*; 11, 201-10, 1997.

[3] Stein RB, Chong S, Everaert DG, Rolf R., Thompson AK, Whittaker M, Robertson J, Fung J, Preuss R, Momose K, Ihashi K. "A multicenter trial of a footdrop stimulator controlled by a tilt sensor". *Neurorehabilitation and Neural Repair*; 20 (3) 371, 2006.

[4] Lyons, G.M., T. Sinkjaer, J.H. Burridge, D.J. Wilcox. "A Review of FES-based Neural Orthosis for the Correction of Drop Foot". *IEEE Transactions on Neural Systems & Rehabilitation Engineering,* 10(4) 260 –279, 2002.

[5] Taylor P, Burridge J, Dunkerley A, Wood D, Norton J, Singleton C, Swain I. "Clinical Audit of 5 Years Provision of the Odstock Dropped Foot Stimulator". *Artificial Organs*, 23 (5) 440-442, 1999.

[6] Royal College of Physicians. "*National clinical guidelines for stroke"*. 2nd edition. Prepared by the Intercollegiate Stroke Working Party. London: RCP, 2004.

[7] Sim, J. and Snell, J. "Focus groups in physiotherapy evaluation and research". *Physiotherapy*, 82 (3), 189-198, 1996.

[8] Krueger, RA. *Developing questions for focus groups*. London: Sage publications, 1998.

[9] Krueger, RA. *Analysing and reporting focus group result.* London: Sage publications, 1998.

Acknowledgements

The authors wish to extend their thanks to all the physiotherapists who participated in this study and to A Roche's research supervisor Prof. Gearóid Ó Laighin, Department of Electronic Engineering, National University of Ireland, Galway, Ireland. A Roche is an Embark Initiative Scholar funded by the Irish Research Council for Science Engineering and Technology (IRCSET).

Author's Address

A Roche is with the Department of Physiotherapy, Health Sciences Building, University of Limerick, Limerick, Ireland (email: aisling.roche@ul.ie).

WIRELESS MOTION-SENSORS DURING FES-INDUCED WALKING IN PARAPLEGIC SUBJECTS.

Russold M[1], Bijak M[2], Rakos M[3], Davis GM[1]

[1] Rehabilitation Research Centre, Discipline of Exercise and Sport Sciences, University of Sydney, Australia

[2] Department of Biomedical Engineering and Physics, Medical University Vienna, Austria

[3] Otto Bock Healthcare GesmbH, Vienna, Austria

Abstract

Walking by paraplegic subjects using functional electrical stimulation (FES) has been a focus of research for several decades. Currently, commercial FES walking systems are not in prevalent clinical or home use. This might be because these systems are difficult to operate, requiring users to control a number of buttons for stepping and stimulation amplitude. While most users prefer to manually initiate stepping via button-pressing, the titration of stimulation amplitude to prevent knee buckle could be automated. We used wireless motion sensors to measure knee angles in two experienced FES walkers, to determine if changes in knee angle could be employed to automatically control stimulation amplitudes. The sensors – mounted on thigh and shank – were integrated into the Vienna FES system and measurements were taken during (at least) two measurements days. We recorded instantaneous knee angles, time-points of step-initiation and changes of stimulation amplitude during FES-gait. Per day, subjects ambulated over level ground and performed a two-minute "warm-up" walk, followed by three walks to maximum stimulation amplitude, with 5-min recovery periods after each task.

The two subjects used different strategies to avert knee buckle. We observed changes in knee angle during stance phase when compared to the knee angle assumed immediately after standing up. S1 increased stimulation-amplitude only after slight changes in knee-angle were observed, while S2 generally increased stimulation amplitude at minor (or no) changes in knee-angle. He also experienced more severe (and faster) knee buckle events requiring him to employ this preventive strategy. These results suggested that changes in knee-angle over a number of stance phases alone might not be adequate to predict a knee-buckle event and increase the stimulation amplitude in time to prevent it.

Introduction

Scientific interest to develop multi-channel stimulation systems for upright mobility in paraplegics has been ongoing since 1977 [1, 2]. Only relatively current innovative developments in biomedical engineering have made small, user-friendly functional electrical stimulation (FES) systems for use after SCI possible [3-5]. Recently, SCI respondents to a survey ranked standing and walking as their top two priorities for using a FES system, with 23% and 66% of individuals who were surveyed requesting these functional outcomes [6]. Most systems for standing and stepping after SCI deploy a "standardized" paradigm of FES-gait using quadriceps muscles, gluteus muscles and the flexor-withdrawal reflex (via common peroneal nerve stimulation) to achieve stance-phase and swing-phase of gait. Generally, gait endurance is limited by fatigue of the quadriceps muscle and consequent knee-buckle of the stance-phase limb.

Despite all the progress made to date, most systems still employ open-loop sequences to control stepping. This means that tempro-spatial information about limb position is not being utilised and unforeseen disturbances during stepping cannot be accounted for. Consequently, patients must manually increase stimulation amplitudes to counteract quadriceps fatigue and to prevent knee-buckle.

In contrast to the developments made so far, (motion-) sensors are already used in a number of applications in everyday life, including air-bag control in automobiles or controllers of game-consoles. This has made these sensors more easily available and affordable for FES-gait applications. Williamson and colleagues used one accelerometer on each shank to determine five phases of gait [7]. Willemsen et al. also demonstrated the ability of a single accelerometer (mounted just below the knee) to distinguish between gait and stance [8]. Other sensors, such as force sensitive resistors have been trialled by Skelly and co-workers to determine gait events [9]. Veltink et al employed a 3-dimensional inertia sensor to automatically balance the output of a two-channel drop-foot stimulator [10]. Several groups have also tried to improve standing and walking by sensing knee angles [11]. Initially goniometers were widely used, but they proved unreliable and difficult to don and doff. Veltink and colleagues measured six different sensor configurations to detect knee unlock [12]. They found that sensors positioned just below and above the knee yielded the most reliable information on knee unlocking.

Based on these results, we deployed a two-sensor array with one sensor located just above and one below the knee in order to investigate which strategies 'experienced' FES-walkers might use to control stimulation amplitude to avert knee-buckle.

Material and Methods

Subjects:

Two sensorimotor complete subjects participated in this study. Both were experienced FES users and had been walking three times a week for at least 6 months prior to this study. Subjects were screened for adequate bone integrity by means of a DEXA scan and underwent a clinical assessment by an experienced physician. The study was approved by the Human Research Ethics Committee of the University of Sydney and all subjects underwent written informed consent prior to their participation.

	Age	Weight	SCI	FES
S1	41	50kg	T4-5	18 mo
S2	54	85kg	T8-9	7 mo

Table 1: Subject characteristics, including FES walking experience for each subject.

Training:

Both subjects had already participated in a previous study in which they progressed from an isokinetic exercise bike via walking between parallel bars to walking on a treadmill [13]. Following an 8-week treadmill training programme and assessments, subjects entered the over-ground walking phase using the Vienna FES system. Stimulation parameters were optimised according to the method described by Bijak et al. [14]. Subjects in this study had participated in the over-ground walking programme for at least 6 month and were able to ambulate with the help of a walking frame.

FES Stimulation system:

Subjects used a modified Vienna functional electrical stimulation system whereby they were able to increase stimulation amplitudes by 10% with a button mounted on their walking-frame. Additional buttons were used to trigger steps and to initiate state changes from sitting to standing. Our experience has shown that an increase in stimulation amplitude of 10% was sufficient to restore knee-lock under most circumstances (unpublished findings).

Measurement system:

Measurements were taken with wireless position sensors (Intersense InertiaCube3, Intersense Inc, Bedford, USA). Each sensor contained a miniature solid-state inertial measurement unit, to sense angular rate of rotation, gravity, and earth magnetic field along three perpendicular axes. The angular rates were integrated within the device to obtain the orientation (yaw, pitch, and roll) of the sensor. Two sensors were positioned on each leg. One on the shank, approximately 5cm below the patella and one on the thigh, approximately 5cm above the patella. Sensors were held in place by means of elastic straps. Custom-designed laboratory software was used to record all gait events (right or left step triggered, stimulation amplitude changes) as well as simultaneous knee angles during these gait events. The knee angles measured during the first two seconds after standing-up were averaged and used as the reference zero-position (full knee-lock).

Measurements:

For each subject, 4 walks were assessed per day and at least 2 measurement days were completed. There was a minimum of one day rest between test days. Subjects walked on level ground with a walking frame at a self-selected pace. The first walk on any given day was a "warm-up" walk of 2-min duration. All other walks were stopped once quadriceps fatigue caused the knee to buckle after maximum stimulation amplitude had been reached. Subjects were provided 5-min recovery between walks.

Results

Table 2 shows the walking performance averaged over the assessment days completed for subject 1 (S1) and subject 2 (S2) respectively. Scores for *safety* and *satisfaction* were extracted using a visual analogue scale with ranges from "not safe" to "very safe" and "not satisfied" to "very satisfied". Higher scores represented improved feeling of safety and satisfaction. S1 walked considerably faster and showed less fatigue during repeated walks. S2 found independent foot-placement difficult and thus walked shorter distances. S2 also demonstrated higher inter-trial fatigue, as revealed by his ambulating for shorter durations during the third and fourth effort.

	#	duration	distance	safety	satisfaction
S1	**1**	128 sec	13.67 m	7.8	8.0
	2	248 sec	26.90 m	8.1	7.9
	3	187 sec	19.23 m	6.6	7.0
	4	173 sec	20.53 m	8.1	7.6
S2	**1**	137 sec	6.15 m	4.0	2.4
	2	253 sec	5.90 m	3.9	3.5
	3	141 sec	5.05 m	3.7	3.7
	4	108 sec	4.80 m	3.6	3.2

Table 2: Walking performance of S1 and S2. Data for S1 were averaged over a total of 12 walks (3 days) and data for S2 were averaged over 8 walks (2 days).

Figure 1 and 2 portray typical recordings from a single walk per subject. Figure 1 shows a slow but marked increase in right knee angle during stance phase in S1 prior to a manual increase in stimulation amplitude.

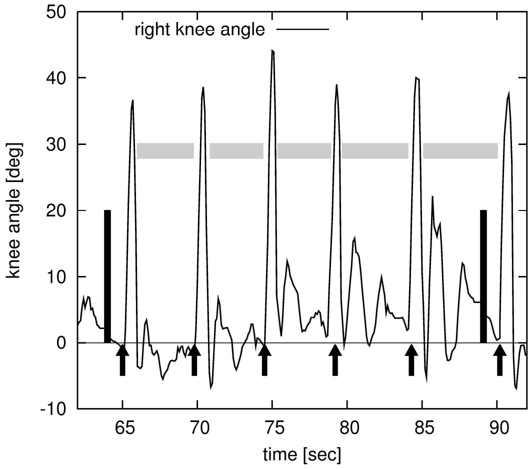

Fig. 1: Typical recording from S1, showing an increase in right knee angle before stimulation amplitude was increased. Vertical bars indicate stimulation increments, arrows represent time-points when steps were trigered and horizontal bars indicate stance phase of the right leg.

In contrast to S1, S2 used a different approach to control the stimulation amplitude. Figure 2 portrays two different incidents of increases in stimulation amplitude. At 81s, S2 increased the stimulation amplitude in response to a knee-buckle of his right knee, while at 98s stimulation amplitude was increased to prevent a possible further knee-buckle. As can be seen from the knee angle chronogram, in either instance there was no previous indication that knee-buckle might soon occur.

In addition to his adopting a highly-risk-averse strategy to prevent knee buckle, S2 scored consistently lower for gait satisfaction and feeling of safety during walking.

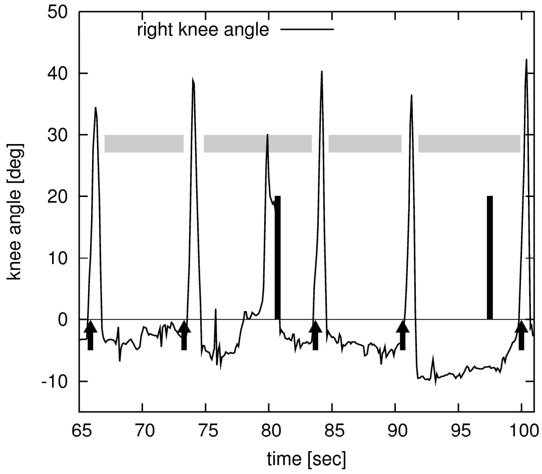

Fig. 2: Typical recording from S2, showing two different causes to increase stimulation amplitude at 81s and 98s. Vertical bars indicate stimulation increments, arrows represent time-points when steps were trigered and horizontal bars indicate stance phase of the right leg.

Discussion

Our results suggest that two different subjects employed different strategies in regards to knee-buckle prevention. S1 seemed to use a *reactive approach* and acted in response with an increase in stimulation amplitude only after (minor) knee-buckle had occurred. Moreover, knee-buckle occurred so slowly that S1 was still able to support his body weight, even with slightly buckled knees. In contrast, S2 used a *preventive strategy* and acted to increase stimulation amplitude well before knee-buckle could occur. This was probably related to the fact that knee-buckle in S2 occurred more quickly and was more severe (eg. Figure 2 at 80s). This could have been related to either body-weight and/or different state of muscle training. It should be noted that overall walking duration and distance for S2 was considerably lower than for S1, and he had poorer stability and less accurate foot placement. But also interpersonal factors might account for differences, as his age was older and he was more conservative in his strategy to avert knee buckle. For these reasons we believe that inter-individual gait-related, physical as well as cognitive differences could also have influenced the lower scores for gait-satisfaction and safety. Although not pointed out to him, S2 would have been aware of the performance of S1 and might have compared his own performance.

Our results suggested that knee-angle alone might be a poor predictor of knee-buckle in some subjects. Knee-buckle may occur at a rapid rate and a FES walking system would have to be able to react to a knee-angle state change in a very short time-frame (generally below 100ms). Although technically feasible, this would demand higher processing power and sampling rates (than a PDA microcontroller might be able to deliver), which could have a negative impact on battery life and device cost.

Additionally, it proved difficult to determine a reliable zero-position after standing up. Not only was full knee-lock not always achieved after standing-up, the position of the sensors could also change during walking. Positioning of the sensors over bony landmarks might be more advised, although this might prove difficult to achieve.

If motion-sensors, or other devices to measure knee angle, were to be incorporated into electrode garments the problem of sensor placement in order to provide a stable recording platform would have to be considered. More elaborate software routines that eliminated slow drift and/or positional changes should be feasible and might be usable to eliminate some of the problems found.

Our results collected to date suggested that some subjects might adopt a *preventive strategy* rather than a *reactive strategy*, especially as this would aid security and stability. The limited ability to mount sensors rigidly enough to prevent signal drift and inaccuracies in our configuration might limit its ability to accurately measure knee angle in a real-world application.

Despite the difficulties encountered we propose to use the developed system to implement a simple feedback control to automatically control knee-angle in the future. We will use the system to investigate the response-time required to avoid knee-buckles even if they are as fast as observed in S2.

References

[1] Kralj A and Vodovnik L. Functional electrical stimulation of the extremities: part 1. J Med Eng Technol, 1(1): 12-15, 1977.

[2] Kralj A and Vodovnik L. Functional electrical stimulation of the extremities: part 2. J Med Eng Technol, 1(2): 75-80, 1977.

[3] Guest R S, Klose K J, Needham-Shropshire B M et al. Evaluation of a training program for persons with SCI paraplegia using the Parastep 1 ambulation system: part 4. Effect on physical self-concept and depression. Arch Phys Med Rehabil, 78(8): 804-7, 1997.

[4] Bijak M, Hofer C, Lanmuller H et al. Personal computer supported eight channel surface stimulator for paraplegic walking: first results. Artif Organs, 23(5): 424-7, 1999.

[5] Bijak M, Mayr W, Rakos M et al. The Vienna functional electrical stimulation system for restoration of walking functions in spastic paraplegia. Artif Organs, 26(3): 224-7, 2002.

[6] Brown-Triolo D L, Roach M J, Nelson K et al. Consumer perspectives on mobility: Implications for neuroprosthesis design. J Rehab Res Develop, 6(39): 659-670, 2002.

[7] Williamson R and Andrews B J. Gait event detection for FES using accelerometers and supervised machine learning. IEEE Trans Rehabil Eng, 8(3): 312-9, 2000.

[8] Willemsen A T, Bloemhof F, and Boom H B. Automatic stance-swing phase detection from accelerometer data for peroneal nerve stimulation. IEEE Trans Biomed Eng, 37(12): 1201-8, 1990.

[9] Skelly M M and Chizeck H J. Real-time gait event detection for paraplegic FES walking. IEEE Trans Neural Syst Rehabil Eng, 9(1): 59-68, 2001.

[10] Veltink P H, Slycke P, Hemssems J et al. Three dimensional inertial sensing of foot movements for automatic tuning of a two-channel implantable drop-foot stimulator. Med Eng Phys, 25(1): 21-8, 2003.

[11] Williamson R and Andrews B J. Detecting absolute human knee angle and angular velocity using accelerometers and rate gyroscopes. Med Biol Eng Comput, 39(3): 294-302, 2001.

[12] Veltink P H and Franken H M. Detection of knee unlock during stance by accelerometry. IEEE Trans Rehabil Eng, 4(4): 395-402, 1996.

[13] Fornusek C and Davis G M. Maximizing muscle force via low-cadence functional electrical stimulation cycling. J Rehabil Med, 36(5): 232-7, 2004.

[14] Bijak M, Rakos M, Hofer C et al. Stimulation parameter optimization for FES supported standing up and walking in SCI patients. Artif Organs, 29(3): 220-3, 2005.

Acknowledgements

This research was jointly supported by Australian National Health and Medical Research Council Project Grant #302013, a NSW MSMR Program Grant and an Outgoing International Fellowship from the European Commission.

Author's Address

Michael Russold
Rehabilitation Research Centre, Discipline of Exercise and Sport Sciences, University of Sydney, Australia
michael@russold.at

THE EFFECT OF MODIFICATION OF THE NANO-TOPOGRAPHY OF IMPLANTABLE SURFACES ON THE PROLIFERATION OF FIBROBLASTS

Sevcencu C [1], Dolatshahi-Pirouz A [2,3], Foss M [2,3], Larsen A N [3], Hansen J L [3], Zachar V [4], Besenbacher F [2,3], Yoshida K [1,5]

[1] Center for Sensory-Motor Interaction (SMI), Aalborg University, Aalborg, Denmark
[2] Interdisciplinary Nanoscience Center (iNANO), University of Aarhus, Aarhus, Denmark
[3] Department for Physics and Astronomy, University of Aarhus, Aarhus, Denmark
[4] Laboratory for Stem Cell Research, Aalborg University, Denmark
[5] Biomedical Engineering Department, Indiana University-Purdue University Indianapolis, Indianapolis, USA

Abstract

Fibrous tissue encapsulation of chronically implantable intraneural electrodes can decrease the performance of the neural interface significantly. This study was performed to investigate if proliferation of fibroblasts – which is correlated to fibrous tissue formation – can be inhibited by changing the nano-topography of the electrodes. In addition, the influence of the surface chemistry on the proliferation of fibroblasts was also investigated. Primary human fibroblasts were cultured on float glass and platinum coated samples with controlled surface nanotopographies. The nanostructures were flat platinum films, and platinum films with 3 types of topographies: Pyramids (P), Huts (H) and Domes (D). The root-mean-square roughnesses of the structures P, H and D were 22.1 nm, 14.9 nm and 9 nm, respectively. Proliferation of fibroblasts was assessed by culturing the cells and quantifying the average cell density daily over a 4 day period. On day 4, the average number of cells counted on P platinum films was by 26% smaller than that found on flat platinum films (329 ± 6 cells/mm^2 vs. 441 ± 5 cells/mm^2, p<0.001). Significant differences were also found between the cell density on flat platinum and those found on the H (383 ± 6 cells/mm^2, p<0.001) and D (365 ± 5 cells/mm^2, p<0.001) platinum films. The average number of fibroblasts counted on glass surface was smaller by 34% than those found on flat platinum films (326 ± 10 cells/mm^2 vs. 495 ± 6 cells/mm^2, p<0.001). In conclusion, proliferation of fibroblasts is influenced by the surface chemistry and can be inhibited by modifying the surface nano-topography.

Introduction

Many functional electrical stimulation therapies rely on the use of chronically implanted electrodes for stimulation and recording. These electrodes may be cuff electrodes placed on peripheral nerves, wire and needle electrodes inserted in various neural structures and muscles. One such peripheral nerve based electrode is the thin-film longitudinal intra-fascicular electrode (tfLIFE) [1]. Independent of their type, shape and size, the implanted electrodes trigger immune reactions leading to their encapsulation in fibrous tissue. Fibrous tissue encapsulation of chronically implantable electrodes can decrease the performance of the neural interface by reducing the selectivity, recording amplitude, and by increasing the stimulation thresholds. This is especially true for selective intraneural devices such as the tfLIFE, whose performance is governed by the proximity of the neural interface to the active tissue [2].

A major role in the formation of the encapsulation tissue around an implanted electrode is played by fibroblasts. These cells adhere and proliferate on the surface of the electrode, and produce the collagen matrix, which is the main component of the capsular wall [3]. Hence, the thickness of the encapsulation tissue growing on the active sites of the electrodes might be reduced if a feasible method to inhibit proliferation of fibroblasts on these sites could be found. Previous studies have shown that the nano-topography of the substrate influences protein adsorption [4], and the adhesive properties, morphology and gene expression of various types of cells [5]. The present experiments have been performed to investigate if proliferation of fibroblasts, which is correlated to fibrous tissue formation, can be inhibited by changing the nano-topography of the electrodes. In addition, proliferation of fibroblasts on substrates with similar topographies, but different chemistry was also investigated.

Material and Methods

Proliferation of fibroblasts was investigated by counting the cells cultured for 4 days on float glass disks and platinum coated samples with 4 types of surface nanostructures.

Preparation of the metalized samples

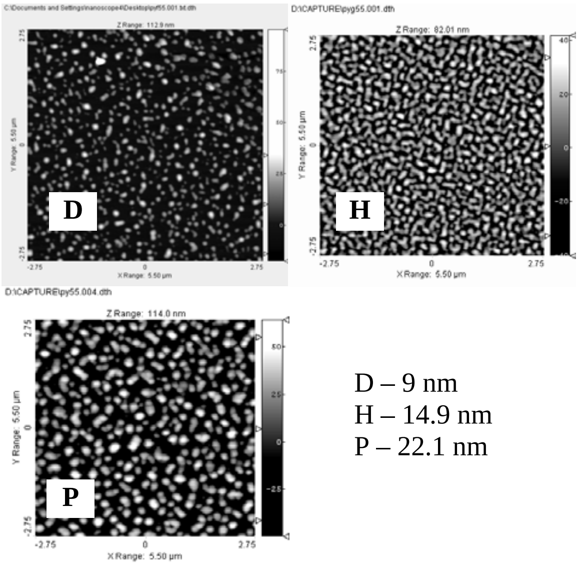

Fig. 1. AFM images (5.5×5.5 μm^2) of the tested nano-rough structures. Average root-mean-square roughness is indicated.

The nanostructures were flat reference platinum films, and platinum films with 3 types of nano-topographies: Pyramids (P), Huts (H) and Domes (D) (Fig. 1). The nanostructures were produced by Si/Ge Molecular Beam Epitaxy (MBE) followed by platinum sputter coating. In brief, a 4” silicon wafer was cleaned by annealing cycles (500º C – 825º C) combined with 600 Å Si-growth. After cleaning, the wafers were coated with Ge films deposited at 550º C. The misfit between the Ge and Si layers gives nanoscale protrusions, typically called huts, pyramids and domes. By change of rate, temperature and composition it is possible to favor the growth of one of them. An alternating deposition of Si and Ge will favor the growth of huts (H), lowering the temperature and deposit more Ge at a higher rate will favor the growth of pyramids (P) and deposition of more Ge without temperature change will favor the growth of domes (D). This was followed by cooling to 300º C, and the deposition of a thin (20 Å) Si surface layer. Finally, a 100 nm thick platinum layer was deposited on the Si/Ge substrate by Physical Vapour Deposition (PVD) sputter coating. The wafers were then broken into approximately 10×10 mm^2 test samples. The nano-topography, including the root-mean-square (RMS) roughness of the resulting structures was characterized by Atomic Force Microscopy (AFM). The RMS roughnesses of the structures P, H and D were 22.1 nm, 14.9 nm and 9 nm, respectively. Prior to seeding them with the investigated cells, the test samples were cleaned by sonication in detergent (Liquinox, PC International Ltd, UK), alcohol and ultra-pure water, and sterilized by steam-sterilization.

Cell culture and counting

Cell culturing was performed in Falcon tissue culture dishes (Becton Dickinson Labware, USA). In a first set of experiments, each culture dish contained 2 float glass disks, one clean and one covered with a flat platinum layer. In a second set of experiments, each culture dish contained 4 silicon samples, one coated with a flat platinum layer and the other 3 with the tested nano-rough platinum layers. In both situations, a total of 20 culture dishes were seeded on Day 0 with primary human fibroblasts (ATCC no. CRL 2429, cell density 8,000 cells/ml). The culture medium consisted of IMDM 21980-032 cell medium (90%), fetal calf serum (10%) and Penicillin/Streptomycin (0.5%). On each of the following 4 days, 5 dishes from each set were selected for counting the cells grown on the tested samples.

Cell counting was performed by fluorescent microscopy (Observer Z1, Zeiss, Brock & Michelsen A/S) and using the Hoechst 33342 nuclear DNA staining technique. After 1 hour of incubation with the fluorescent dye, the cells were fixed for 15 min. with 4% formaldehyde, washed and kept in phosphate buffer solution. Image sampling and counting were performed using a custom-written routine for the AxioVison Rel. 4.6 software. A total of 51 images were collected from each sample. The number of cells was averaged across dishes and sampling days. The means calculated for Day 4 were statistically compared using One-Way ANOVA.

Results

The effect of surface chemistry on the proliferation of fibroblasts

The fibroblasts cultured on flat platinum films proliferated faster than those cultured on uncoated float glass (Fig. 2a). After 4 days in culture, this resulted in 34% smaller number of cells counted on float glass as compared to that found on flat platinum films (326 ± 10 cells/mm^2 vs. 495 ± 6 cells/mm^2, $p<0.001$).

The effect of surface nano-topography on the proliferation of fibroblasts

The fibroblasts growing on flat platinum films had the fastest growth rate, while those growing on P platinum films had the slowest (Fig. 2b). On Day 4, the average number of cells counted on P platinum films was 26% smaller than the count from flat platinum films (329 ± 6 cells/mm^2 vs.

441 ± 5 cells/mm^2, $p<0.001$). Significant differences were also found between the cell density on flat platinum and those found on the H (383 ± 6 cells/mm^2, $p<0.001$) and D (365 ± 5 cells/mm^2, $p<0.001$) platinum films. The differences between the number of cells counted on the nano-rough samples were all statistically significant ($p<0.05$).

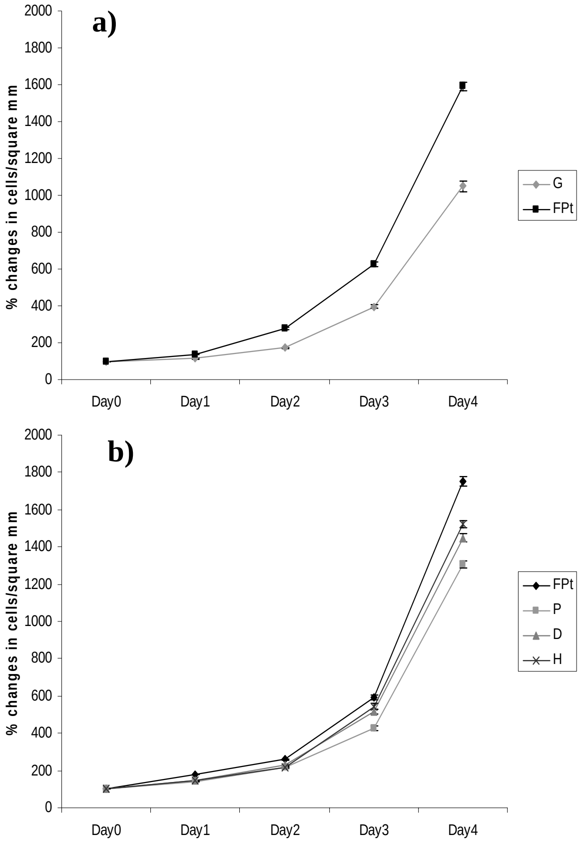

Fig. 2. Effects of surface chemistry (a) and surface nano-topography on the proliferation of fibroblasts (b). FPt – flat platinum; G – glass; D, H and P – the tested nano-structures.

Discussion

In the present study, the number of cells growing on nano-rough platinum films was significantly lower than that counted on flat platinum films and comparable to that found on the surface of glass (Fig. 2). This indicates that the surface nano-topography may be as important as the surface chemistry in driving fibroblasts' proliferation on the surface of an implantable device. While the influence of the surface chemistry on cellular proliferation was extensively studied over the past decades [6], changing the nano-topography of the substrate to manipulate cellular proliferation is a new concept in the field of biocompatibility research.

In our experiments, the number of fibroblasts growing on the surface of glass was significantly smaller than that counted on flat platinum films (Fig. 2a). This is consistent with the results of Raisanen et al and Baharloo et al, who observed that epithelial cells grow better on metallic surfaces than on glass, ceramic and plastic materials [7;8]. As studies have shown, cellular proliferation depends on the ability of the cells to adhere to the substrate, which is strongly influenced by the surface chemistry of the substrate [6]. Hence, our results seem to indicate that platinum has a surface chemistry that facilitates the adhesion of fibroblasts and their proliferation, consequently.

As illustrated in Figure 2b, this property can be modified by changing the nano-topography of the platinum surface. Thus, increasing the nano-roughness of the platinum films significantly reduced the number of fibroblasts growing on these samples (Fig. 2b). Since the minimum number of fibroblasts was found on the roughest surface (P, 22.1 nm), this inhibitory effect seems proportional to the roughness, which was also observed with respect to proliferation of epithelial cells on micro-rough structures [8]. Although the roughness of the H platinum films was larger than that of the D platinum films (14.9 vs. 9 nm), the average number of cells counted on D samples was smaller than that found on H samples (Fig. 2b). This could be explained by a higher density of the nano-protrusions on H platinum films (see Fig. 1), which probably attenuated the observed inhibitory effect.

Regarding the mechanisms supporting the effects of nano-rough structures on cellular proliferation, Dalby et al reported that fibroblasts cultured on a 13 nm-rough polystyrene surface responded to this nano-topography by increasing their cellular surface and the number of focal adhesion contacts [5]. If this was valid for our experiments, too, then the decreased number of fibroblasts per nano-rough surface unit could be an effect of a larger area covered by these cells.

In conclusion, proliferation of fibroblasts on a platinum surface can be inhibited *in vitro* by increasing the nano-roughness of this substrate. Whether or not this is valid *in vivo* and if a smaller number of fibroblasts proliferating on the surface of an electrode can reduce its fibrous tissue encapsulation should be investigated in the future.

Reference

[1] X. Navarro, T. B. Krueger, N. Lago, S. Micera, T. Stieglitz, and P. Dario, "A critical review of

interfaces with the peripheral nervous system for the control of neuroprostheses and hybrid bionic systems", *J. Peripher. Nerv. Syst.*, vol. 10, no. 3, pp. 229-258, Sept.2005.

[2] T. Lefurge, E. Goodall, K. Horch, L. Stensaas, and A. Schoenberg, "Chronically implanted intrafascicular recording electrodes", *Ann. Biomed. Eng*, vol. 19, no. 2, pp. 197-207, 1991.

[3] W. M. Grill and J. T. Mortimer, "Neural and connective tissue response to long-term implantation of multiple contact nerve cuff electrodes", *J. Biomed. Mater. Res.*, vol. 50, no. 2, pp. 215-226, May2000.

[4] B. Müller, M. Riedel, R. Michel, S. M. De Paul, R. Hofer, D. Heger, D. Grützmacher, "Impact of nanometer-scale roughness on contact-angle hysteresis and globulin adsorption", *J. Vac. Sci. Technol. B*, 19(5), pp1715-1720, Sep/Oct2001.

[5] M. J. Dalby, S. J. Yarwood, M. O. Riehle, H. J. Johnstone, S. Affrossman, and A. S. Curtis, "Increasing fibroblast response to materials using nanotopography: morphological and genetic measurements of cell response to 13-nm-high polymer demixed islands", *Exp. Cell Res.*, vol. 276, no. 1, pp. 1-9, May2002.

[6] M. Mrksich, "A surface chemistry approach to studying cell adhesion", *Chemical Society Reviews*, vol. 29, no. 4, pp. 267-273, July2000.

[7] L. Raisanen, M. Kononen, J. Juhanoja, P. Varpavaara, J. Hautaniemi, J. Kivilahti, and M. Hormia, "Expression of cell adhesion complexes in epithelial cells seeded on biomaterial surfaces", *J. Biomed. Mater. Res.*, vol. 49, no. 1, pp. 79-87, Jan.2000.

[8] B. Baharloo, M. Textor, and D. M. Brunette, "Substratum roughness alters the growth, area, and focal adhesions of epithelial cells, and their proximity to titanium surfaces", *J. Biomed. Mater. Res. A*, vol. 74, no. 1, pp. 12-22, July2005.

Acknowledgements

This work was supported by the Danish Technical Research Council (STVF) and the Center for Neural Engineering (CNE). The authors wish to thank Mette Ringgaard for her support during the cell culturing and imaging phases of the study and Jacques Chevallier for sample coating.

Author's Address

Cristian Sevcencu

Center for Sensory-Motor Interaction (SMI), Aalborg University, Aalborg, Denmark

eMail: sevcr@smi.auc.dk

PERSPECTIVES OF FUNCTIONAL MAGNETIC STIMULATION OF THE LEGS OF PARETIC PATIENTS (Comparison of FES with FMS)

J. Szecsi*,**, C. Krewer**, F. Müller** ,A. Straube*, E. Koenig**

*Dept. of Neurology, Ludwig Maximillians University Munich, Germany
**Hospital of Neurology, Bad-Aibling, Germany

Abstract

Since surface magnetic stimulation (FMS) of the leg musculature achieved torques comparable to those achieved by electrical stimulation, but at a lower level of pain, the question arises whether FMS produces more work or improves the smoothness of stimulation-supported or -assisted cycling of paralyzed legs with and without preserved sensibility.

Eight patients with complete SCI and six patients with hemiplegia and preserved sensibility underwent isometric measurement and ergometric cycling experiments using FES and FMS stimulation of the legs. Different patterns of applicability of FMS could be outlined: 1) patients with complete SCI did not benefit from FMS (compared to FES, torque and work did not increase), 2) patients with hemiplegia and preserved sensibility could improve their torque output, and the smoothness of pedaling, and to a lesser extent the ergometric work produced.

Introduction

Recent research has shown [1] that magnetic stimulation of the QF muscle of healthy individuals produced less pain at the same level of isometric torque than surface electrical stimulation (FES) and it was hypothesized that magnetic stimulation is a potential alternative especially for patients with intact or residual sensory function.

FES of the musculature affects not only motor but also sensory and nociceptive fibers. Consequently the use of FES is of limited value for effective muscle training or functional applications (like walking or cycling) in patients with preserved residual sensibility.

Variable electromagnetic fields, however, can be used to stimulate the motor nerves in the muscle, because they bypass the pain receptors located in the skin. Thus, repetitive peripheral magnetic stimulation will probably be increasingly used in the future for neuroprosthetic interventions. First investigations performed on the legs of healthy subjects have shown that magnetic stimulation can achieve isometric forces which are twice as high as those achieved by electric stimulation at the same sensitivity [1]. *The purpose* of the study was to elucidate the prosthetical and therapeutical potential of magnetic stimulation by comparing maximal isometric forces, ergometric work and roughness of pedaling motion using electrical and magnetic stimulation in two groups of paretic (by SCI and stroke) patients with and without preserved sensitivity. It will also be of interest whether electric and magnetic stimulation affect different parts of the muscle (superficial vs. deep).

Material and Methods

Six hemiplegic patients (#1-6) with preserved sensibility (due to stroke) and 8 patients (#7-14) without sensibility (completely paraplegic patients due to SCI, Th4-Th12) participated in the study.

1. In *isometric experiments* the torques evoked by consecutive and simultaneous electrical and magnetic stimulation were measured in the paretic and left m. quadriceps femoris of all patients (#1-14), while they were seated on an isometric test-bed, consisting of a stationary tricycle (OVG-GmbH, Germany) with its front wheel replaced by a torque transducer. An electrical stimulator (maximal current 127 mA, K&T GmbH, Germany) and a magnetic stimulator (maximal induction 1.5 T, Mag&More GmbH, Germany) were used. Starting at the motor threshold, the intensity of electrical and magnetic stimulation was gradually increased in steps of 10 mA and by 20%, respectively, until the maximum tolerable intensity was reached. Combined stimulation was performed at

maximum tolerable electrical stimulation with increasing superimposed magnetic stimulation. In patients with sensibility (#1-6) the maximal isometric voluntary contraction was also recorded.

2. *Ergometric experiments* were performed on the same stationary tricycle with a free-turning front wheel. Electrodes and magnetic coils were consecutively fixed on the quad. muscles bilaterally (patients #7-14, Fig.1) and on the affected side (patients #1-6). First, an

Fig.1. Stationary FMS–cycling (patient with complete SCI Th9). Left and right quad muscles stimulated by M&M PSTIM160 and MAGSTIM Rapid repetitive magnetic stimulators. Annular magnetic coils fixed by polystyrene-brackets were used.

individually appropriate braking resistance was chosen [1]. Electrical and magnetical stimulation were applied in a randomized sequence of 2 minutes of continuous bursts in the case of patients #7-14 and work produced was noted. In the case of patients #1-6, electrical and magnetical stimulation consisted of 3 minutes of 30 sec bursts interrupted by breaks of 30 sec, and the roughness index (RI =1/curvature of cadence) was recorded as a kinematical measure of smoothness of pedaling [2]. Burst durations were chosen by consideration of maximal tolerable coil heating. Subsequently comparisons were performed on isometric torque, work and RI in both FMS and FES conditions at maximum tolerable intensities.To establish whether FMS and FES stimulation affect different parts of the muscle (deep vs. superficial), the sum of simultaneously applied FMS and FES stimulation was considered.

Results

1. *Isometric experiments on plegics with preserved sensibility*(#1-6): Magnetically evoked torque (100%) was typically higher than electrically evoked (70 mA). Fig.2 illustrates the complete protocol

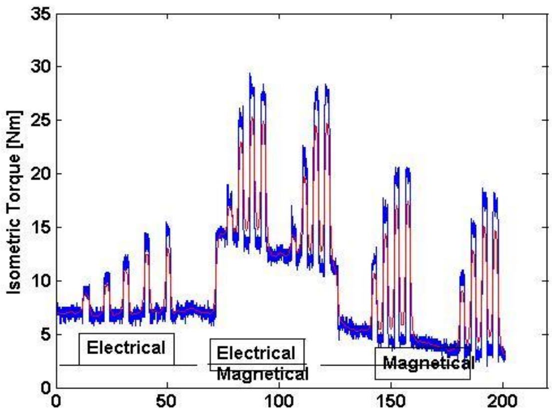

Fig.2. Complete combined stimulation protocol performed on hemiplegic patient #4

(patient #4). FES produced a maximal isometric torque of 8 Nm at a stimulation intensity of 75 mA. Using FMS the torque achieved 14 Nm at 100% intensity. Combined application of FES+FMS evoked 20 Nm torque, i.e. the deviation from the sum of torques (14+8=22 Nm) amounts to only 10%.

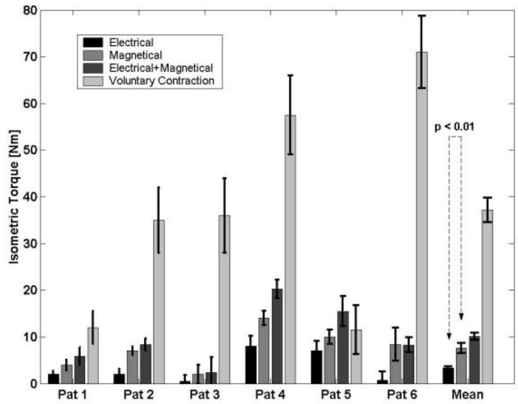

Fig.3.Group comparison of FMS and FES elicited torques in hemiparetic patients.

Group analysis of 6 patients has shown that FMS torque significantly exceeds FES torque (#1-6, Fig.3).

2. Ergometric experiments on hemiplegics with preserved sensibility (#1-6): Work produced during 3 minutes with breaks did not differ in the FMS and FES conditions ($p > 0.04$). In contrast, smoothness of cycling (RI) was significantly improved ($p < 0.05$) by FMS stimulation (illustrated by patient #1 in Fig. 4) and not significantly affected by FES.

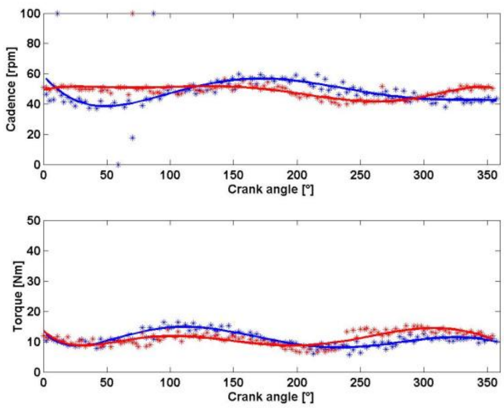

Fig. 4. Improvement of smoothness in the case of a hemiplegic patient (blue; no FMS, red: using FMS).

3. *Isometric experiments on plegics with no sensibility* (#7-14). FMS produced typically less (or equal) isometric torque than FES. While considerable fatigue occured during continuous electrical stimulation, torque pulses evoked by additionally pulsed magnetic stimulation occurred (Fig.5). In the group comparison, the sum of electrical and magnetical evoked torques differs significantly from the combined torque ($p < 0.01$).

4. *Ergometric experiments on plegics with no sensibility* (#7-14). Although cycling by magnetic stimulation is possible (Fig.1), less work is produced during FMS than FES stimulation (N=8, $p < 0.002$). This is in line with the above observation that less torque is generated by FMS than FES stimulation in fresh or moderately exhausted muscle.

Discussion and conclusion

Plegic patients with preserved sensibility (#1-6, hemiplegics): Magnetic stimulation is more effective than electrical stimulation because of preserved sensibility. Torques evoked by magnetic stimulation achieve about ¼ and 1/8 of the maximal voluntary torque of the affected site. Ergometric work did not increase significantly in any stimulation mode, while the roughness index decreased using FMS. From the quantitative kinematical analysis, smoother pedaling was expected with stimulation than without. This expectation could be achieved only with FMS, presumably because of the pain caused by FES. The total effect of combined stimulation could be interpreted as a new, fresh pool of muscle fibers being mobilized by additional magnetic stimulation. Moreover, only a slight decline in electrical and magnetical torque was registered(Fig.2).

Plegic patients without sensibility (complete SCI): Magnetic stimulation is less effective than electrical stimulation in terms of isometric torque and ergometric work produced. Combined stimulation (Fig. 5)shows

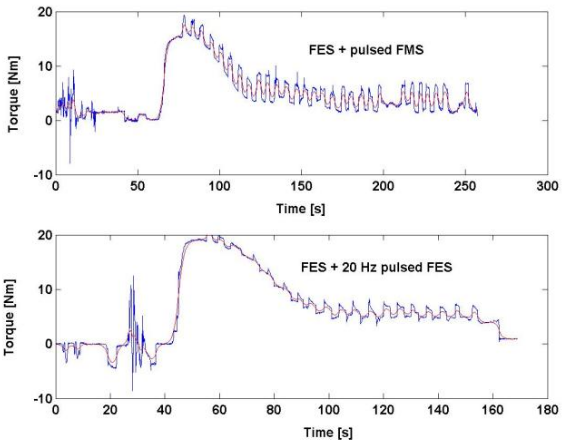

Fig.5. Combined stimulation of complete paraplegic patient

additional torque pulses. These are higher with additional 20 Hz FMS than with 40 Hz FES; therefore we conclude, that deeper parts of the muscle can be additionally mobilized with FMS in the case of paraplegics too.

References

1. Han T-R, Shin H-I, Kim I-S (2006), Magnetic stimulation of the quadriceps femoris muscle; comparison of pain with electrical stimulation. Am. J. Phys. Med. Rehabil.,Vol. 85, pp 593-9.
2. Chen HY, Chen SC, Chen JJ, Fu LL, Wang YL (2005) Kinesiological and kinematical analysis for stroke subjects with asymmetrical cycling movement patterns. J Electromyogr Kinesiol 15: 587-595

Acknowledgements

This work was supported by the Else-Kröner-Fresenius Foundation.

Author's Address

Johann Szecsi, MD
Department of Neurology
University of Munich
D-81377 Munich, Marchioninistr. 23
e-mail: jszecsi@nefo.med.uni-muenchen.de

A METHOD FOR MONITORING KNEE JOINT MECHANICS DURING ELECTRICAL TREATMENT OF DEGENERATED DENERVATED MUSCLES

Vatnsdal B[1], Helgason Þ[1], Pálsdóttir J[1], Ingvarsson P[2], Rafold D[3], Guðmundsdóttir V[2], Knútsdóttir S[2] and Yngvason S[2]

[1]Department of Research and Development, HTS, Landspítali-University Hospital, Reykjavík, Iceland.

[2]Department of Rehabilitation Medicine, Landspitali-University Hospital, Reykjavík, Iceland.

[3]Department of Medical Physics and Biomedical Engineering, Medical University of Vienna, Austria

Abstract

Electrical stimulation therapy of denervated muscles has been under development for several years as a part of the EU project RISE. As the muscles grow in strength and force their mechanical properties alter. This can be utilized to monitor the stimulation treatment.

The purpose of this project was to develop a method to monitor the treatment in a simple, inexpensive, non-invasive and wireless manner.

As a part of the RISE project three patients have received electrical stimulation since 2003. The mechanical properties of the knee joint have been tested regularly with and without the use of stimulation. This is done by capturing the pendular movement of the lower leg with a video camera, this data is fitted to a model and coefficients that describe the mechanical properties extracted from those calculations.

To determine the credibility of the model, the goodness of its fit to the data was examined and this yielded that the model fits the data without considerable error. Furthermore a considerable change could be seen in the mechanical properties when stimulation was applied.

The good fit of the model to the data shows that this method can be used to monitor the mechanical properties of the knee joint in a simple and efficient manner. Error is negligible and the results from each of the patients reflect their physical condition and stimulation compliance. The sensibility of the method must be determined with further comparison with existing methods, and by examining and eliminating some factors which might influence the method.

Introduction

FLACCID paraplegia is accompanied by loss of muscle tone and absence of muscle reflexes in the lowest part of the spinal column after degeneration of the motorneuron. Such an injury concerns about 20 persons per million EU citizens every year. Complications following flaccid paraplegia include: Denervation, severe muscle atrophy, disabled bladder and anus which again cause urinary and feces incontinence, reduced sex ability, deficient blood circulation which again is followed by more muscle atrophy and osteoporosis. A further problem with paraplegics is the development of severe pressure sores. [1]

The EU-funded RISE project has as an aim to use electrical stimulation to restore standing in paraplegics with long-term denervated degenerated muscles [1]. Due to the absence of the neuromuscular junction and decomposition of motor units, muscular contractions can only be elicited by depolarizing the cellular membrane of each single muscle fiber. The application of FES on denervated muscles is strongly inhibited by the high output current required. Using only surface electrodes, to generate usable contractions of a denervated muscle, up to 250 mA are required, which by far exceeds the present standards of maximum output current [2], [3].

Long-term denervation atrophy of skeletal muscles can be reversed if sufficient stimulation therapy is delivered. When starting electrical stimulation the skin gets thicker and more resistant to electrical and mechanical stresses. Therefore, wounds heal faster and the risk of getting pressure sores decrease, the patients can sit longer in their wheel-chairs, which permits activities of daily living and thus a better social reintegration [4].

One of the aims of the RISE project was the development of diagnostic and therapy monitoring methods and equipment for FES of denervated muscles. A direct estimation of force generated in the quadriceps muscles, during electrical stimulation is difficult, due to the cocontraction of antagonists. The elastic properties of the muscles are directly related to the number of molecular contractile actin-myosin cross-bridges, that are active. The stiffness thus decreases as the muscles degenerate. A method that estimates the stiffness and other elastic properties of the muscles, during rehabilitation, would give a good indication of the state of de- and possible regeneration in the muscles.

Material and Methods

Measurement Procedure

During the measurements the patients are sitting on a patient table with their legs in knee flexion position. Ideally the equilibrium state is 90°, but an offset from this state is considered in the measurements. The lower leg is raised to 20° from the equilibrium state and then released to oscillate freely. The oscillation is recorded with a video recorder and the measurement points on the legs are marked with special markers, which can be identified on the recording. To get the parameters needed for calculation, the software KineView is used by tracking the points on the leg (see screen shot in Figure 1). It also calculates the angle between the lower leg and the knee joint, as well as the angular velocity, angular acceleration and the elapsed time of the oscillation.

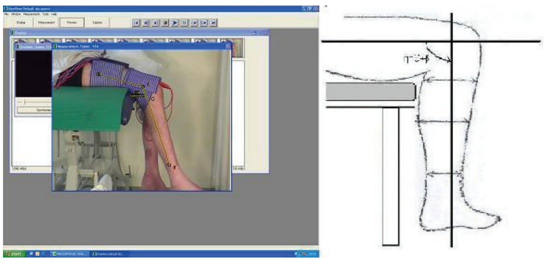

Fig. 1. A screen shot from KineView (left) and diagram of the experimental setup (right).

Figure 1 is a diagram of the experimental setup. It shows how the patient sits on a table. The angle η is composed of the measured angle θ and an offset β from equilibrium position. In equilibrium state, this angle is 90° and the leg is considered to be in rest. With and without stimulation, the leg is made to oscillate and the angle θ is measured. From θ, the angular velocity and angular acceleration is derived. Finally, the parameters of Eq. 1 are calculated and the eleastic properties can be observed.

Mathematical Physiology

The torque-angular velocity ($\tau = J \cdot \alpha = J \cdot d\omega/dt$, where τ is the torque and has the unit [Nm], J is the moment of inertia in [kgm^2] and $d\omega/dt$ is the angular velocity differentiated with respect to time t) relation for the joint is used in a similar manner in place of the force-velocity ($F = m \cdot a = m \cdot dv/dt$) relation of muscle. When a muscle shortens its force decreases as the velocity of shortening increases. This is because the number of actin-myosin cross bridges decreases and each cross bridge produces less force during the period that it is attached in a shortening muscle than an isometric muscle. Part of the decrease in force is also due to shortening of the elastic muscle tissue, i.e., the stiffness decreases. The elastic properties of the soft tissues are of fundamental importance in holding the skeleton together and in providing compliance at joints to modulate the effects of impact forces. Muscles act like springs with a variable spring constant, i.e. their stiffness varies with the level of muscle activation. Muscle stiffness arises from the actin-myosin cross bridges, which are responsible for the generation of muscle force. When a muscle is activated, many cross bridges act in parallel to produce force. The force is proportional to the number of cross bridges, N_p, acting in parallel, i.e. if one cross bridge produces a force f_c then the total force is $F = N_p f_c$. Each cross-bridge acts like a tiny spring with a spring constant k. The stiffness of the cross bridge is defined by the relation between force and displacement for a spring, i.e. $\Delta F = k\Delta x$. When springs act in parallel their stiffness sums. If there are N_p cross bridges acting in parallel then $\Delta F = N_p k \Delta x$. Consequently, muscle stiffness will increase as the number of cross bridges acting in parallel increases, i.e., muscle stiffness increases as muscle force increases [5].

Because the force of a spring changes if it is lengthened or shortened, all muscles acting around a joint must contribute to the joint stiffness. Consequently, the joint can be stiffened by co-contracting the muscles on either side of the joint without having to change the net joint torque. Because the net torque is equal to the difference between torques produced by opposing muscles (quadriceps and hamstrings), while the net stiffness is equal to the sum of the stiffness, it is possible to independently control joint torque and joint stiffness.

Mathematical Model

The mechanical model of the lower limb is composed by two rigid segments: the thigh and the skank-foot complex. Movements of the ankle joint were not considered in order to limit the total number of degree of freedom. The quadriceps and the hamstrings both both are modelled as a spring with an associated spring coefficient K, and a damping device with a damping factor B.

We can model muscle activity using a simple mass/spring/damper rotational system shown in Figure 2. The mass is the lower leg, and the muscles provide the spring and damping forces.

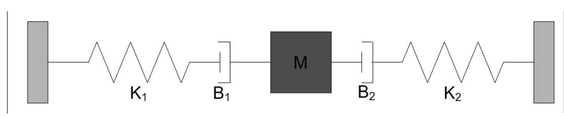

Fig. 2. A simple agonist antagonist system

The basic equation of motion is:

$$J\ddot{\eta} + B\dot{\eta} + K\eta = 0 \qquad \textbf{(1)}$$

where $\eta = \theta + \beta$. θ is the measured oscillation angle and β is the offset from equilibrium position. In an unforced system, $\lim_{t\to\infty}\eta = 0$ which means equilibrium state of the leg. J is the moment of inertia of the leg (dependent on the mass and the center of mass and is therefore a constant for each patient at each time). B is the damping coefficient of the system and K describes the elasticity. K can also be looked at as a spring constant for the system. The kinetic properties of the knee joint changes as the muscle grow and the parameters B and K can be used as a measurement of this change. The parameter K takes into account the acceleration of gravity, i.e. $K = K' + K_g$ where $K_g = m_g l_c$ and l_c is the distance from knee to the center of mass of the leg. Being able to monitor the clinical state of the muscles through the values of B and K is the essence of the evolving method.

Taking the Laplace transform of this expression, with initial conditions, we get the following:

$$J\left[s^2\eta(s) - s\eta(0) - \dot{\eta}(0)\right] + B\left[s\eta(s) - \eta(0)\right] + K\eta(s) = 0 \; \textbf{(2)}$$

Reorganizing the initial conditions to the right side, we get closer to a standard form:

$$\eta(s)\left[s^2 + \frac{B}{J}s + \frac{K}{J}\right] = \dot{\eta}(0) + \eta(0)\left[s + \frac{B}{J}\right] \; \textbf{(3)}$$

where $\eta(0) \neq 0$ and $\dot{\eta}(0) \neq 0$.

Finally, we can make the substitution that $\frac{B}{J} = 2\alpha$ and $\sqrt{\frac{K}{J}} = \omega_n$:

$$\eta(s) = \frac{\eta(0)[s + 2\alpha] + \dot{\eta}(0)}{s^2 + 2\alpha \cdot s + \omega_n^2} \qquad \textbf{(4)}$$

The parameters can described mathematically:

$\alpha = \frac{B}{2J}$ **(6)** , $\omega_n = \sqrt{\frac{K}{J}}$ **(7)** ,. $\omega_d = \sqrt{\omega_n^2 - \alpha^2}$ **(8)**

where $\omega_d = \sqrt{\omega_n^2 - \alpha^2}$ is the damped frequency, $\omega_n = \sqrt{\frac{K}{J}}$ is the natural undamped frequency, α is the exponential decay and β is just a lateralization of the coordinate system needed to get better model fit for the data. [6]

The Mass, and Moment of Inertia

The moment of inertia (J) is one of the factors that are needed for the model estimation of the coefficients of joint stiffness. The moment of inertia of the leg represents its resistance to rotational acceleration about the knee joint. A cylinder is used to approximate the leg rotating about the knee joint and, therefore, the following equation is used to calculate the moment of inerta:

$$J = \frac{1}{3}mL^2 \qquad \textbf{(9)}$$

where m is the mass of the leg in [kg] and L is the length of the leg in [m].

According to [6], the mass of the leg of the patients can be calculated with the following equation:

$$m_{leg} = 0.0226\, m_{body} + 31.33\, l_{leg}\, c_{leg}^2 + 0.016 \qquad \textbf{(10)}$$

where m_{body} is the whole body mass, l_{leg} is the length of the leg and c_{leg} is the legs maximum circumference. For the center of mass, [7] recommends using 42.8% of the distance from the knee to the ankle. This is an estimate for a healthy person and therefore may not apply completely to paraplegic individuals whose muscles have atrophied. However this approach has been used during the project period. It is necessary to estimate the mass and the center of mass during every measurements to be able to follow up the patients precisely (i.e. changes in the parameters). This has not been done yet, and, therefore, the inertia characteristics of the leg was estimated during a visit to Vienna in April 2006 and those measurements and calculations were then used when calculating the other coefficients of (1). Other methods to measure these parameters have been suggested but do all require some additional hardware which could complicate the measurement procedure. To determine if this is necessary, an estimation of the influence of a possible error in the estimation of the mass parameters on the model results will be performed.

Results and Discussion

Figure 3 shows how well the movement is described by the model, compared to the recorded data. It is also apparent from the two figures that the decay of the movement is much faster when electrical stimulation is applied. The mechanical properties extracted from the model also indicate this, as can be seen in Figure 7, where B and K are 0.07 Nms/rad and 5.50 Nm/rad respectively for Patient 1 in March 2007 without stimulation, but 0,52 and 7,93 as stimulation was applied. This was the case for all the patients, although Patient 1 had a much bigger response to the applied stimulation. This was to be expected as the muscle degeneration was more extensive with the other two patients, due to the longer time from their injury. Furthermore Patient's 2 response to stimulation was limited by excess adipose tissue.

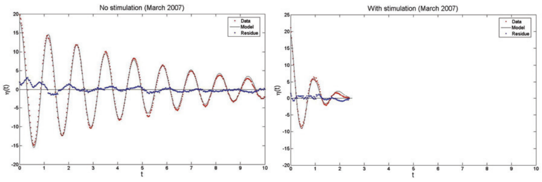

Fig. 3. The model description of the movement compared tothe data recorded with the video camera. Movement without electrical stimulation (left) and with stimulation (right). The red dotted line shows the model description and the black whole line the recorded data. The blue dotted line is the residue. (Patient 1, March 2007)

As Figures 3 shows, the model describes the movement quite well and also the change in the properties due to the applied stimulation. Furthermore changes in the mechanical properties during the course of the therapy can be observed in Figure 4.

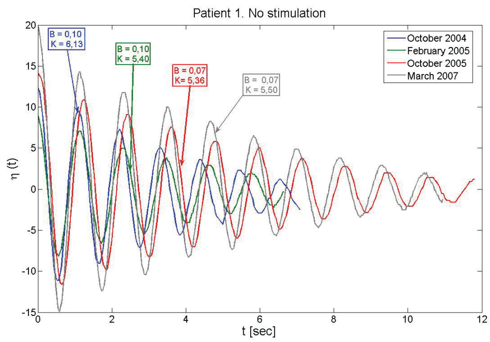

Fig. 4. A comparison of the modeled pendular movement at four different times in the treatment period. The picture shows measurements performed on patient 1 without stimulation in October 2004, February 2005, October 2005 and March 2007.

The stiffness is highest in Oct. 2004 (K = 6.13) and therefore also the frequency of the movement is the highest, as the decay is quicker. The damping factor is the same in Oct. 2004 and Feb. 2004 (B = 0.10) and Oct. 2005 and March 2007 (B = 0.07).

Conclusion

While the model used is a vast simplification of the complicated physiology of muscle mechanical properties, it did fit the data particularly well. The oscillation of the leg is well described by the model and the elastic and damping moments could be calculated from the second order differential equation. The method is simple, inexpensive and patient-friendly.

One possible error source is the mass and center of mass of the lower leg. The moment of inertia and the gravity factor of the elasticity parameter are considered to be a constant. A further uncertainty in this approach is that the method used to estimate the parameters from the body weight is designed for healthy subjects, and not subjects with denervated degenerated muscles. A second possible error sources is the patients posture and position compared to gravity. This factor could be an important part of the parameter estimation, as the behavior of a muscle is dependant on its length and thus will behave differently depending on its posture. A possible approach to control this is suggested in [8]. The equipment described there has two obvious advantages compared to use only of a video camera. Firstly the position of the leg can be held constant in all measurements. Secondly the leg is fixed with regards to oscillating sideways, which is a possible error the video-equipment cannot compensate for. However this method necessitates the use of extensive equipment and thus the ease-of-use element of the monitoring method is lost. There is also a risk of the oscillation being forced into a unnatural perfect oscillation, which could influence the clinical results.

References

[1] Mayr W, Hofer C, Rafolt D, Bijak M, Lanmueller H, Reichel M, Sauermann S and Unger E, “The European Project RISE: General Overview and Engineering Aspects” in Proc. 8th Vienna International Workshop on Functional Electrical Stimulation. pp.24-26.

[2] Salmons S, Ashley Z, Sutherland H, Russold MF, Li F and Jarvis JC, “Functional Electrical Stimulation of Denervated Muscles: Basic Issues”, Artificial Organs, 29 (3), Blackwell Publishing, Inc. 2005, pp. 199-202.

[3] Mayr W, Hofer C, Bijak M, Rafolt D, Unger E, Reichel M, Sauermann S, Lanmueller H and Kern H, “Functional Electricel Stimulation (FES) of Denervated Muscles: Existing and Prospective Technological Solutions”, Basic Applied Myol 12 (6), 2002, pp. 287-290.

[4] Kern H, Hofer C, Mödlin M, Forstner C, Mayr W and Richter W, “Functional Electrical Stimulation (FES) of Long-Term Denervated Muscles in Humans: Clinical Observations and Laboratory Findings”, Basic Applied Myol 12 (6), 2002, pp. 291-299.

[5] Milner T, “Kin301”, 2005. Available at: http://www.sfu.ca/~tmilner/kin301.htm.

[6] Pálsdóttir JL, “Design and Testing of a Method for Monitoring Treatment of Denervated Degenerated Muscles”, Master Thesis, University of Iceland, 2006.

[7] Pavol MJ, Owings TM and Grabiner MD, “Body segment inertial estimation for the general population of older adults”, Journal of Biomechanics 35, 2002, pp. 707-712.

[8] Gallasch E, Rafolt D, Kinz G, Fend M, Kern H and Mayr W, “Evaluation of FES-Induced Knee Joint Moments in Paraplegics with Denervated Muscles”, Artificial Organs 29 (3), Blackwell Publishing, Inc., 2005, pp. 207-211.

Acknowledgements

This work was supported by:
Health Techonlogy Venue - HTV, The Icelandic Center for Research – Rannis, The Research Fund of Landspitali, The Icelandic Student Innovation Fund

Author’s Address

Brynjar Vatnsdal,
Biomedical Engineer
Department of Research and Development
Landspítali-University Hospital
Eiriksgotu 5
101 Reykjavík
Iceland
brynjarp@landspitali.is

Authors